JOURNAL AND PROCEEDINGS

OF THE

ROYAL SOCIETY OF NEW SOUTH WALES

VOLUME
108

PARTS
1-4

1975

PUBLISHED BY THE SOCIETY,
SCIENCE HOUSE, GLOUCESTER AND ESSEX STREETS, SYDNEY

Royal Society of New South Wales

OFFICERS FOR 1975-1976

Patrons

His Excellency the Governor-General of Australia
The Honourable Sir JOHN KERR, K.C.M.G., K.St.J., Q.C.

His Excellency the Governor of New South Wales
Sir RODEN CUTLER, V.C., K.C.M.G., K.C.V.O., C.B.E.

President

E. K. CHAFFER

Vice-Presidents

J. W. PICKETT, M.Sc., Dr.phil.nat.
M. J. PUTTOCK, B.Sc. (Eng.), M.Inst.P.
W. E. SMITH, M.Sc., Ph.D , M.Inst.P.
D. J. SWAINE, B.Sc., Ph.D., F.R.A.C.I.
P. D. TILLEY, B.A., Ph.D.

Honorary Secretaries

J. W. HUMPHRIES, B.Sc., M.Inst.P.
M. KRYSKO v. TRYST (Mrs.), B.Sc., Grad.Dip., A.M. Aust.I.M.M.

Honorary Treasurer

A. A. DAY, Ph.D., F.R.A.S.

Honorary Librarian

W. H. G. POGGENDORFF, B.Sc. (Agr.)

Members of Council

F. C. BEAVIS, B.Sc., Ph.D., F.G.S.
G. S. GIBBONS, M.Sc., Ph.D.
J. L. GRIFFITHS, M.A., M.Sc.
D. K. HUGHES, B.Sc., Dip.Ed.
G. C. LOWENTHAL, B.A., M.Sc., Ph.D., F.A. Inst. P.
D. H. NAPPER, M.Sc. (Syd.), Ph.D. (Cantab.)
L. A. WRIGHT, B.Sc (Eng.), B.A. (Arch.). F.R.I.B.A., M.I.E. (Aust.)
W. B. SMITH-WHITE, M.A.

New England Representative: N. T. M. YEATES, D.Sc. (Agr.), Ph.D. (Cantab.)
South Coast Representative: G. DOHERTY, B.Sc., Ph.D.

Executive Secretary: VALDA LYLE (Mrs.), A.I.P.S.A.

CONTENTS

Parts 1-2

Astronomy:

Biochemistry:

Geology:

Mathematics:

Palaeontology:

Parts 3-4

Chemistry:

Geology:

Contents—*Continued*

Palaeontology :

Plant Physiology :

Journal and Proceedings of the Royal Society of New South Wales

[illegible] 1975 PARTS 1 and 2

[illegible] the Society
[illegible] and Essex Streets, Sydney
[illegible] y, 1975

Royal Society of New South Wales

OFFICERS FOR 1975-1976

Patrons

HIS EXCELLENCY THE GOVERNOR-GENERAL OF AUSTRALIA
THE HONOURABLE SIR JOHN KERR, K.C.M.G., K.St.J., Q.C.

HIS EXCELLENCY THE GOVERNOR OF NEW SOUTH WALES
SIR RODEN CUTLER, V.C., K.C.M.G., K.C.V.O., C.B.E.

President

E. K. CHAFFER

Vice-Presidents

J. W. PICKETT, M.Sc., Dr.phil.nat.
M. J. PUTTOCK, B.Sc. (Eng.), M.Inst.P.
W. E. SMITH, M.Sc., Ph.D., M.Inst.P.
D. J. SWAINE, B.Sc., Ph.D., F.R.A.C.I.
P. D. TILLEY, B.A., Ph.D.

Honorary Secretaries

J. W. HUMPHRIES, B.Sc., M.Inst.P.
M. KRYSKO v. TRYST (Mrs.), B.Sc., Grad.Dip., A.M. Aust.I.M.M.

Honorary Treasurer

A. A. DAY, Ph.D., F.R.A.S.

Honorary Librarian

W. H. G. POGGENDORFF, B.Sc. (Agr.)

Members of Council

F. C. BEAVIS, B.Sc., Ph.D., F.G.S.
G. S. GIBBONS, M.Sc., Ph.D.
J. L. GRIFFITHS, M.A., M.Sc.
D. K. HUGHES, B.Sc., Dip.Ed.
G. C. LOWENTHAL, B.A., M.Sc., Ph.D. F.A. Inst. P.
D. H. NAPPER, M.Sc. (Syd.), Ph.D. (Cantab.)
L. A. WRIGHT, B.Sc (Eng), B.A. (Arch.) F.R.I.B.A., M.I.E. (Aust.)
B. S. WMITH-WHITE, M.A.

New England Representative: N. T. M. YEATES, D.Sc. (Agr.), Ph.D. (Cantab.)
South Coast Representative: G. DOHERTY, B.Sc., Ph.D.

Executive Secretary: VALDA LYLE (Mrs.), A.I.P.S.A.

Journal and Proceedings, Royal Society of New South Wales, Vol. 108, pp. 1-3, 1975

Occultations Observed at Sydney Observatory During 1973

K. P. Sims

The following observations of occultations were made at Sydney Observatory with the 11½-inch telescope. A tapping key was used to record the times on a chronograph. The reduction elements were computed by the method given in the occultation supplement to the *Nautical Almanac* for 1938 and the reduction completed by the method given there. Since the observed times were in terms of coordinated time (UTC), a correction of +0·01190 hour (=42·84 seconds) was applied to these observed times to convert them to ephemeris time with which *The Astronomical Ephemeris for 1973* was entered to obtain the position and parallax of the Moon in terms of the FK_4 coordinate system. The apparent places of the stars of the 1973 occultations were provided by H. M. Nautical Almanac Office. The apparent position of the companion to Z.C. 1110 which was involved in occultation No. 733 was taken to be $7^h\ 18^m\ 32{\cdot}053^s$ in R.A. and +22° 01′ 53″. 85 in Dec.

Table 1 gives the observational material. The serial numbers follow on from those of the previous report (Sims, 1972). The observers

Table 1

Serial No.	S.A.O. or Z.C. No.	Mag.	Date	U.T.C.	Observer
715	0341	6·8	1973 Jan. 13	10 03 23·3	W
716	0647	5·5	1973 Jan. 15	9 21 36·3	S
717	076183	6·7	1973 Mar. 10	8 53 53·0	W
718	076210	8·3	1973 Mar. 10	9 35 22·9	S
719	0557	6·6	1973 Mar. 10	9 42 23·0	S
720	076234	8·3	1973 Mar. 10	10 04 20·8	S
721	0562	6·6	1973 Mar. 10	10 07 17·4	S
722	076237	8·2	1973 Mar. 10	10 21 39·0	S
723	076249	7·3	1973 Mar. 10	10 26 06·9	S
724	076259	7·3	1973 Mar. 10	10 38 11·4	S
725	078963	7·0	1973 Mar. 13	12 15 24·0	R
726	1324	7·2	1973 Mar. 15	9 43 26·8	R
727	1171	6·3	1973 Apr. 10	12 36 35·8	W
728	097955	8·1	1973 Apr. 11	9 05 12·7	S
729	098033	7·8	1973 Apr. 11	12 10 55·9	S
730	1399	6·9	1973 Apr. 12	8 28 15·4	R
731	078236	8·2	1973 May 6	9 19 36·7	W
732	079292	9·1	1973 May 7	7 45 56·8	S
733	—	8·2	1973 May 7	7 52 54·3	S
734	1110	3·5	1973 May 7	7 52 58·8	S
735	097723	8·4	1973 May 8	7 42 08·3	W
736	097745	8·7	1973 May 8	9 21 18·0	W
737	097774	8·5	1973 May 8	10 18 50·5	W
738	1260	7·0	1973 May 8	11 42 49·0	W
739	1378	8·7	1973 May 9	10 26 36·5	S
740	118426	8·6	1973 June 7	8 27 00·3	R
741	1564	6·6	1973 June 7	10 08 12·3	R
742	1662	6·3	1973 June 8	8 01 56·0	S
743	098583	8·5	1973 July 3	8 04 58·2	W
744	118521	8·2	1973 Aug. 1	7 49 28·0	S
745	118558	7·2	1973 Aug. 1	9 16 49·0	S
746	138365	7·2	1973 Aug. 2	9 07 56·3	R
747	138860	9·2	1973 Aug. 3	11 12 24·7	S
748	138633	8·2	1973 Aug. 30	8 28 55·5	R

TABLE 1—*Continued*

Serial No.	S.A.O. or Z.C. No.	Mag.	Date	U.T.C.	Observer
749	2234	8·3	1973 Sep. 3	11 11 33·5	S
750	183683	8·9	1973 Sep. 3	11 45 41·5	S
751	183682	9·4	1973 Sep. 3	11 48 48·9	S
752	185369	8·5	1973 Sep. 5	11 55 12·6	S
753	2510	6·3	1973 Sep. 5	11 55 57·2	S
754	2513	4·3	1973 Sep. 5	12 38 53·8	S
755	2630	5·1	1973 Sep. 6	7 51 39·6	R
756	2778	6·9	1973 Sep. 7	8 37 29·8	R
757	2779	3·9	1973 Sep. 7	8 46 09·5	R
758	2797	3·0	1973 Sep. 7	12 48 43·2	W
759	0880	7·2	1973 Sep. 19	15 58 58·2	R
760	077571	7·9	1973 Sep. 19	15 58 59·5	R
761	077581	8·6	1973 Sep. 19	16 07 25·5	R
762	0882	5·0	1973 Sep. 19	16 22 11·9	R
763	079546	8·3	1973 Oct. 18	16 53 28·2	R
764	187944	8·4	1973 Nov. 1	9 04 53·3	R
765	0160	6·2	1973 Nov. 8	15 46 06·1	R
766	2906	8·7	1973 Nov. 29	10 03 39·2	R
767	163091	8·8	1973 Nov. 29	11 00 44·8	W
768	163780	7·8	1973 Nov. 30	10 14 40·8	S
769	146421	7·7	1973 Dec. 3	10 27 22·1	S

TABLE 2

Serial No.	Lunation No.	p	q	p^2	pq	q^2	Δσ	pΔσ	q	Coefficient of	
										Δα	Δδ
715	619	+22	−98	5	−21	95	−1·1	−0·2	+1·1	+7·0	−0·87
716	619	+87	−49	76	−43	24	+1·4	+1·2	−0·7	+12·4	−0·40
717	621	+98	+22	95	+22	5	+0·2	+0·2	0·0	+12·7	+0·37
718	621	+80	−60	64	−48	36	+0·8	+0·6	−0·5	+12·1	−0·47
719	621	+86	−52	73	−44	27	+2·6	+2·2	−1·4	+12·7	−0·38
720	621	+93	−37	86	−34	14	−0·5	−0·5	+0·2	+13·3	−0·22
721	621	+91	−42	82	−38	18	+1·2	+1·1	−0·5	+13·1	−0·28
722	621	+48	−88	23	−42	77	−0·9	−0·4	+0·8	+8·3	−0·79
723	621	+83	−56	69	−46	31	+1·2	+1·0	−0·7	+12·4	−0·42
724	621	+100	−4	100	−4	0	+0·1	+0·1	0·0	+13·6	+0·11
725	621	+100	+8	99	+8	1	−0·7	−0·7	−0·1	+13·7	−0·11
726	621	+83	−56	69	−46	31	+2·0	+1·7	−1·1	+8·5	−0·81
727	622	+53	−85	28	−45	72	+2·0	+1·1	−1·7	+4·1	−0·96
728	622	+79	+61	63	+48	37	−0·8	−0·6	−0·5	+13·6	+0·32
729	622	+99	+14	98	+14	2	+0·9	+0·9	+0·1	+14·1	−0·20
730	622	+100	+8	99	+8	1	−0·8	−0·8	−0·1	+13·9	−0·30
731	623	+71	+70	51	+50	49	−0·8	−0·6	−0·6	+10·8	+0·61
732	623	+93	+37	86	+34	14	0·0	0·0	0·0	+13·7	+0·16
733	623	+98	−22	95	−22	5	−0·3	−0·3	+0·1	+12·6	−0·42
734	623	+98	−21	96	−21	4	−0·7	−0·7	+0·1	+12·6	−0·42
735	623	+95	+30	91	+29	9	−0·6	−0·6	−0·2	+14·2	0·00
736	623	+98	−22	95	−22	5	+0·4	+0·4	−0·1	+12·3	−0·51
737	623	+98	−20	96	−20	4	+0·7	+0·7	−0·1	+12·4	−0·50
738	623	+59	−81	35	−48	65	+1·9	+1·1	−1·5	+4·5	−0·95
739	623	+75	+66	56	+50	44	−1·3	−1·0	−0·9	+13·7	+0·33
740	624	+84	+55	70	+46	30	−0·7	−0·6	−0·4	+14·8	+0·15
741	624	+92	+40	84	+37	16	+0·1	+0·1	0·0	+15·0	−0·02
742	624	+84	−54	71	−45	29	−0·6	−0·5	+0·3	+8·1	−0·84
743	625	+87	−50	75	−43	25	+1·3	+1·1	−0·6	+9·0	−0·79
744	626	+96	−27	93	−26	7	+1·0	+1·0	−0·3	+11·5	−0·64
745	626	+97	−23	95	−22	5	−0·9	−0·9	+0·2	+11·8	−0·62
746	626	+100	−1	100	−1	0	−0·6	−0·6	0·0	+13·6	−0·42
747	626	+87	−49	76	−43	24	+1·7	+1·5	−0·8	+9·2	−0·79
748	627	+100	+5	100	+5	0	−0·4	−0·4	0·0	+13·9	−0·35

TABLE 2—*Continued*

Serial No.	Lunation No.	p	q	p^2	pq	q^2	Δσ	pΔσ	q	Coefficient of	
										Δα	Δδ
749	627	+100	0	100	0	0	+0·6	+0·6	0·0	+13·7	−0·16
750	627	+96	+28	92	+27	8	−0·8	−0·8	−0·2	+13·8	+0·13
751	627	+81	+59	65	+48	35	+0·6	+0·5	+0·4	+12·4	+0·46
752	627	+67	+74	45	+50	55	−1·1	−0·7	−0·8	+8·9	+0·76
753	627	+84	−54	71	−45	29	−0·5	−0·4	+0·3	+11·7	−0·52
754	627	+86	−51	74	+44	26	−0·4	−0·3	+0·2	+12·0	−0·48
755	627	+73	−69	53	−50	47	+1·7	+1·2	−1·2	+10·9	−0·61
756	627	+91	+42	82	+38	18	−1·5	−1·4	−0·6	+11·3	+0·58
757	627	+88	−48	77	−42	23	−1·4	−1·2	+0·7	+13·3	−0·30
758	627	+85	+53	72	+45	28	−1·0	−0·8	−0·5	+10·1	+0·69
759	627	−97	−24	94	+23	6	+0·3	−0·3	−0·1	−13·4	−0·18
760	627	−94	−34	88	+32	12	−0·2	+0·2	+0·1	−13·1	−0·28
761	627	−64	−77	41	+49	59	−0·8	+0·5	+0·6	−9·3	−0·73
762	627	−70	−72	49	+50	51	−0·8	+0·6	+0·6	−10·1	−0·67
763	628	−97	−24	94	+23	6	+0·7	−0·7	−0·2	−14·1	+0·01
764	629	+52	−85	27	−44	73	−0·6	−0·3	+0·5	+9·8	−0·72
765	629	+54	−84	29	−45	71	+0·8	+0·4	−0·7	+11·8	−0·60
766	630	+85	−52	73	−44	27	−1·5	−1·3	+0·8	+13·7	−0·27
767	630	+25	+97	6	+24	94	+1·1	+0·3	+1·1	−0·2	+1·00
768	630	+37	+93	14	+34	86	−0·3	−0·1	−0·3	+0·6	+1·00
769	630	+97	−25	94	−24	6	−0·8	−0·8	+0·2	+14·8	+0·17

were W. H. Robertson (R), K. P. Sims (S), and H. W. Wood (W). Except for occultations 759, 760, 761, 762, 763, which were reappearances at the dark limb, the phase observed was disappearance at the dark limb. Table 2 gives the results of the reductions which were carried out in duplicate. The Z.C. or S.A.O. numbers given in Table 1 are from the *Catalogue of 3539 Zodiacal Stars for Equinox* 1950·0 (Robertson, 1940) and the *Smithsonian Astrophysical Observatory Star Catalogue.*

References

ROBERTSON, A. J., 1940. *Astronomical Papers of the American Ephemeris Vol. X, Part II.*

SIMS, K. P., 1972. Sydney Observatory Papers No. 69. *J. Proc. Roy. Soc. N.S.W.*, **106**, 81.

(Received 22.10.74)

Journal and Proceedings, Royal Society of New South Wales, Vol. 108, pp. 4-5, 1975

Earth Rotation Related to Net Electric Charge

IRVING MICHELSON

Communicated by M. KRYSKO v. TRYST

Bailey (1960*a*, 1960*b*) postulated a net electric charge on the Sun and thereby explained a number of astrophysical and terrestrial phenomena ; Burman (1969, 1970) showed that Bailey's hypothetical charge value also explains the residual advance of the perihelion of Mercury and similar effects on orbits of minor planets. A hypothetical net electric charge on the Earth, of magnitude determined by an extension of Bailey's premise, is found to be strongly suggestive of a coupling between Earth rotation and electric charge.

Energies of motion in the solar system vary over a wide range of values. Sun-Jupiter orbital energy of order 10^{35} joules and the Moon's rotational kinetic energy of order 10^{23} joules, differing by a factor of a million millions, form bounds within which numerous other planetary energies fall. When two distinct phenomena are found whose energies are within a single order of magnitude of each other, there is enough suggestion of coincidence to justify investigation of possible interrelationships. When agreement is more exact, the implication of underlying physical significance is strengthened.

This is the case with regard to the Earth's rotation and the electrical energy associated with a net charge consistent with Bailey's value of the solar charge. Kinetic energy of Earth rotation, determined by its polar moment of inertia C and its rotational speed ω, is expressed as

$$U_{KE}=\tfrac{1}{2}C\omega^2 \quad \ldots\ldots\ldots\ldots \quad (1)$$

having numerical value $2{\cdot}138\times10^{29}$ joules (Allen, 1963, p. 109). The energy required to bring electric charge Q_E from dispersal at infinite distance to the surface of a conducting sphere of radius a equal to the Earth's radius, is

$$U_{EL}=\tfrac{1}{2}\frac{Q_E^{\,2}}{4\pi\varepsilon_0 a} \quad \ldots\ldots\ldots\ldots \quad (2)$$

where the permittivity constant is represented by $4\pi\varepsilon_0$ when Q_E is given in coulombs, the radius a in meters.

Bailey's choice of solar charge $-Q_S=5\times10^{18}$ coulombs provided approximate equality between the *specific charge* (charge per unit mass) values of the Sun and the five magnetic stars of Blackett's group. If a terrestrial charge is taken on the same hypothesis of equal specific charges for Sun and Earth, the electrical energy U_{EL} is roughly the same in value as the kinetic energy U_{KE} given by (1). Recognizing the approximate character of the values of $-Q_S$ as chosen by Bailey, we choose a value for $-Q_E=1{\cdot}7\times10^{13}$ coulombs, differing by scarcely ten per cent from the value that obtains by strict calculation using known Earth-Sun mass ratio. In this manner near-equality is replaced by exact equality of electrical and kinetic energy forms

$$U_{EL}=U_{KE} \quad \ldots\ldots\ldots\ldots \quad (3)$$

both having the value $2{\cdot}1\times10^{29}$ joules quoted above.

The interest of the fact that the two energies are in close agreement for consistently chosen Earth charge values $-Q_E$, in a hierarchy of energies ranging over not less than twelve orders of magnitude, is twofold. First is the suggestion that equality of U_{EL} and U_{KE} represents an equipartition in a system where mechanical energy of rotation interacts with electrical charge energy. Equality of time-averaged kinetic and potential energies of a simple pendulum motion, or of surface gravity waves, are but two instances among many familiar phenomena in which energies are equally distributed. Second is the support that (3) furnishes for the expectation that Bailey's value (1) is correct. Even if the Earth does not presently hold the charge value $-Q_E$ quoted above, but might at one time when the Earth's rotation was determined, both interpretations would be valid.

It should be recalled that the Earth's rotational speed ω is customarily regarded as one of the independent constants of astronomy, unrelated to other physical magnitudes of the solar system and arbitrary in the sense that a slight change in its value would leave entirely unaffected such quantities as the Earth's orbital distance (astronomical unit), its mass, its distance from the Moon, etc. Relationships have been found, however, linking the rotational motion to these quantities by accurately satisfied simple algebraic relationships (see, e.g., Michelson, 1968). Although it is not possible to affirm a specific mechanism that led to such relationships, or to (3) above, the very existence of such relationships neither explained nor even suspected to exist on the basis of celestial mechanical knowledge is important in suggesting directions for investigation of such phenomena.

Professor of Mechanics,
Illinois Institute of Technology,
Chicago, Illinois, 60616, U.S.A.

References

Allen, C. W., 1963. *Astrophysical Quantities*, Second Edition. Oxford.

Bailey, V. A., 1960*a*. Existence of Net Electric Charges on Stars. *Nature*, **186**, 508

Bailey, V. A., 1960*b*. Net Electric Charges on Stars. Galaxies and "Neutral" Elementary Particles, *J. Proc. Roy. Soc. N.S.W.*, **94**, 77.

Burman, R., 1969. A Solar Charge and the Perihelion Motion of Mercury. *J. Proc. Roy. Soc. N.S.W.*, **102**, 157.

Burman, R., 1970. A Solar Charge and the Perihelion Motion of 1566 Icarus. *J. Proc. Roy. Soc. N.S.W.*, **103**, 1.

Michelson, I., 1968. Nebular Momentum Coupling of the Earth's Rotational and Orbital Motions. *Icarus*, **8**, 265.

(Received 20.2.1974)

Journal and Proceedings, Royal Society of New South Wales, Vol. 108, pp. 6-11, 1975

Potential Antitumour Activity of Some Amino Acid Metal Systems[*]

Alexander J. Charlson, Kevin E. Trainor and Edward C. Watton

Abstract—Copper (II) chelates of L-asparagine and L-glutamine have been prepared. Bis(L-glutaminato)copper(II) shows significant anticancer activity in the KB cell culture test-system, but bis (L-asparaginato)copper(II) is inactive in the same test-system. Induction of filamentous growth in *Escherichia coli* is being used as a preliminary screen for antitumour activity of complex species which cannot be isolated from solution. Using a continuous variation method it is shown that mixtures of L-glutamine and copper(II)sulphate in a molar ratio of 1 : 1, L-glutamine and potassium platinum(II)chloride in a molar ratio of 3 : 2, and L-asparagine and potassium platinum(II)chloride in a molar ratio of 1 : 1 induce filamentous growth in *E. coli*.

Introduction

Takamiya (1960) reported that although dimethylglyoxime (1) did not show antitumour activity in the Ehrlich's carcinoma and Crocker Sarcoma 180 mouse test-systems, the ligand did show antitumour activity in the presence of copper(II) ions. The palladium(II) chelate of 1 shows significant cytotoxicity in the KB cell-culture test-system (Charlson, 1973). Carlsson, Charlson and Watton (1974) have recently reported that, although D-*arabino*-hexosulose-*bis* (thiosemicarbazone) (2) is inactive in the KB cell-culture test-system, the copper(II) chelate of 2 shows significant cytotoxicity in the KB test-system. The copper(II) and palladium(II) chelates of 6-deoxy-L-*arabino*-hexosulose-*bis* (thiosemicarbazone) (3) also show significant antitumour activity in the KB test-system. Copper(II) ions have been implicated (Petering and Van Giessen, 1966 ; Booth and Sartorelli, 1967) in a possible mode of action of the well-known anticancer substance 3-ethoxy-2-oxobutyraldehyde bis (thiosemicarbazone) (KTS) (4). There is thus a certain amount of evidence that metals, such as copper(II) in the chelated form, can " poison " tumour cells[*]. Copper(II) ions can " poison " normal cells. In Wilson's disease, for example, there is an accumulation of copper in brain and liver. It is not surprising, therefore, that Mihich and Mulhern (1965) found that the copper(II) chelate of 4 was more toxic than the ligand to the host animals. At best, the copper(II) chelate of 4 is only partially selective for tumour cells. Palladium(II) chelates are, in all probability, also only partially selective for tumour cells.[†]

The enzyme, L-asparaginase, is known to produce regressions of some rodent and human tumours (Broome, 1963 ; Oettgen *et al.*, 1967). It is believed that the amino acid, L-asparagine (5), must be supplied to L-asparaginase-sensitive tumour cells, because these cells are deficient in L-asparaginase synthetase activity (Horwitz, Old, Boyse and Stockert, 1968). Although the use of L-asparaginase in man can be considered to be selective cancer therapy, the enzyme is now rarely used in the clinic. Patients treated with L-asparaginase develop fatty livers (Wood, 1969). Cooney and Handschumacher (1970) suggested that the catalysis of hydrolysis of L-asparagine by several rare earth metals, particularly lanthanum, might be investigated. It occurred to us that since L-asparagine appears to be a necessary growth factor for certain tumour cells, this amino acid might be able to transport copper(II) ions (or other metal ions) directly into tumour cells. This could, therefore, lead to a selective " poisoning " of tumour cells (Charlson, 1973). Since highly purified

---

[*] Presented in part before the Division of Co-ordination Chemistry at the Broadbeach meeting of the Royal Australian Chemical Institute, February 1974.

[*] There appears to be a controversy as to the exact mode of action of copper(II) KTS. The Yale School (Booth, Johns, Certino and Sartorelli, 1968) claim that the cellular toxicity of the chelate is essentially caused by copper. On the other hand, the Upjohn Group (Van Giessen, Crim, Petering and Petering, 1973) maintain that there is something peculiar about the chemistry of the copper(II) KTS chelate which permits its specific antitumour effects.

[†] Livingstone and Michelson (1970) reported that palladium chelates of dialkyldithiophosphates had anticancer activity in the Walker rat carconoma test-system.

L-glutaminase possesses considerable antitumour activity (Roberts, Holcenberg and Dolowy, 1970), the amino acid, L-glutamine (6), might also be used in conjunction with metal ions to " poison " tumour cells selectively. Baxter and Williams (1974) have also suggested that asparagine and glutamine might be used to direct antitumour metal complexes into tumour cells.

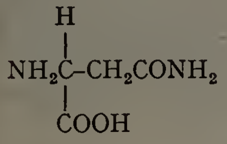

$$\mathrm{NH_2}\overset{\overset{\mathrm{H}}{|}}{\underset{\underset{\mathrm{COOH}}{|}}{\mathrm{C}}}\mathrm{-CH_2CONH_2}$$

(5)

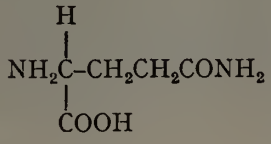

$$\mathrm{NH_2}\overset{\overset{\mathrm{H}}{|}}{\underset{\underset{\mathrm{COOH}}{|}}{\mathrm{C}}}\mathrm{-CH_2CH_2CONH_2}$$

(6)

Results and Discussion

In order to test the hypothesis that metal chelates of 5 and 6 may be selective antitumour substances, our first approach was to prepare the copper(II) chelate of L-asparagine (7)* and the copper(II) chelate of L-glutamine (8), and to have these substances evaluated as potential anticancer compounds. The National Cancer Institute in Bethesda, Maryland, U.S.A., tested 7 and 8. They reported that 7 was inactive in the KB cell-culture test-system (ED_{50}; 100 μg/ml), but 8 showed significant cytotoxicity (ED_{50}; 2·3 μg/ml) in the same test-system.

In addition to the two copper(II) chelates which we isolated, spectral evidence showed that other complex species exist in solution. Since we were unable to isolate these substances, we could not get them evaluated as anticancer substances in conventional test-systems. Accordingly, in an attempt to evaluate the potential antitumour activity of these species we used the continuous variation technique; the variable being the degree of induction of filamentous growth in *Escherichia coli.* We were able to study the full range of a metal chelate system, and thus " pinpoint " ratios to be further evaluated by recommended test procedures. The use of *E. coli* as a preliminary screen for potential antitumour activity of metal chelates is based on the work of Rosenberg and collaborators. These authors showed a correlation between induction of filamentous growth in *E. coli* (Rosenberg *et al.*, 1967) and pronounced anticancer activity in rodent test-systems (Rosenberg *et al.*, 1969) for a number of platinum complexes. Possibly the most spectacular of Rosenberg's compounds is cis-dichlorodiammineplatinum(II), which also shows antineo-plastic activity in man (Conners, 1973).

We tested 5 in the presence of varying amounts of copper(II) ions in the *E. coli* test system, and also mixtures of 6 and copper(II) ions at different metal to ligand ratios. It was shown that mixtures of 6 and copper(II) ions produced maximum filamentous growth in *E. coli* at a molar ratio of 1 : 1 (Figure 1). Mixtures of copper(II) ions and 5 did not show filamentous growth in the bacterial test-system as was the case with pure 5, or 6 or copper(II) ions. It is of interest to compare these results obtained with the *E. coli* test-system and the results of KB testing on chelates 7 and 8 given above. Mixtures of 5 and copper(II) ions showed no filamentous growth, and 7 was inactive in the KB cell-culture test-system. On the other hand, mixtures of copper(II) and 6 showed filamentous growth in *E. coli* and 8 is cytotoxic in the KB test. This does not necessarily mean that there is a direct correlation between the modes of action of these substances in both test-systems, although it should be emphasized that interference with cell growth occurs in both cases.

Since maximum filamentous growth was observed at a molar ratio of 1 : 1 with copper(II) ions and 6, we were interested to determine whether a definite chemical species is produced at this ratio. Using a continuous variation technique similar to that used by Vosberg and Cooper (1941), we obtained evidence that a 1 : 1 species exists in water (Figures 2 and 3). Kirson and Barsily (1959) also reported that asparagine and glutamine can form 1 : 1 complexes with copper ions in solutions of pH less than 4.

We also investigated mixtures of each of the two amino acids with both palladium(II) and platinum(II) ions in the *E. coli* test-system as described above. Mixtures of palladium(II) with either 5 or 6 did not induce filamentous growth in *E. coli.* However, filamentous growth was observed with 5 and platinum(II) ions at a molar ratio of 1 : 1, and extensive production of filaments occurred with a mixture of 6 and platinum(II) ions at a molar ratio of 3 : 2 (Figure 1). It is known that glycine and alanine each form different species with platinum(II) ions (Sidgwick, 1951) and it is likely that platinum(II) ions form different species with both 5 and 6. Morris and Gale (1973) pointed out that amino acids may form complexes with cis-dichloro(di-pyridine) platinum(II), and they suggested that the result of these interactions

---

* The X-ray crystal structure of 7 has been elucidated in this laboratory (Stephens, Vagg and Williams, 1974).

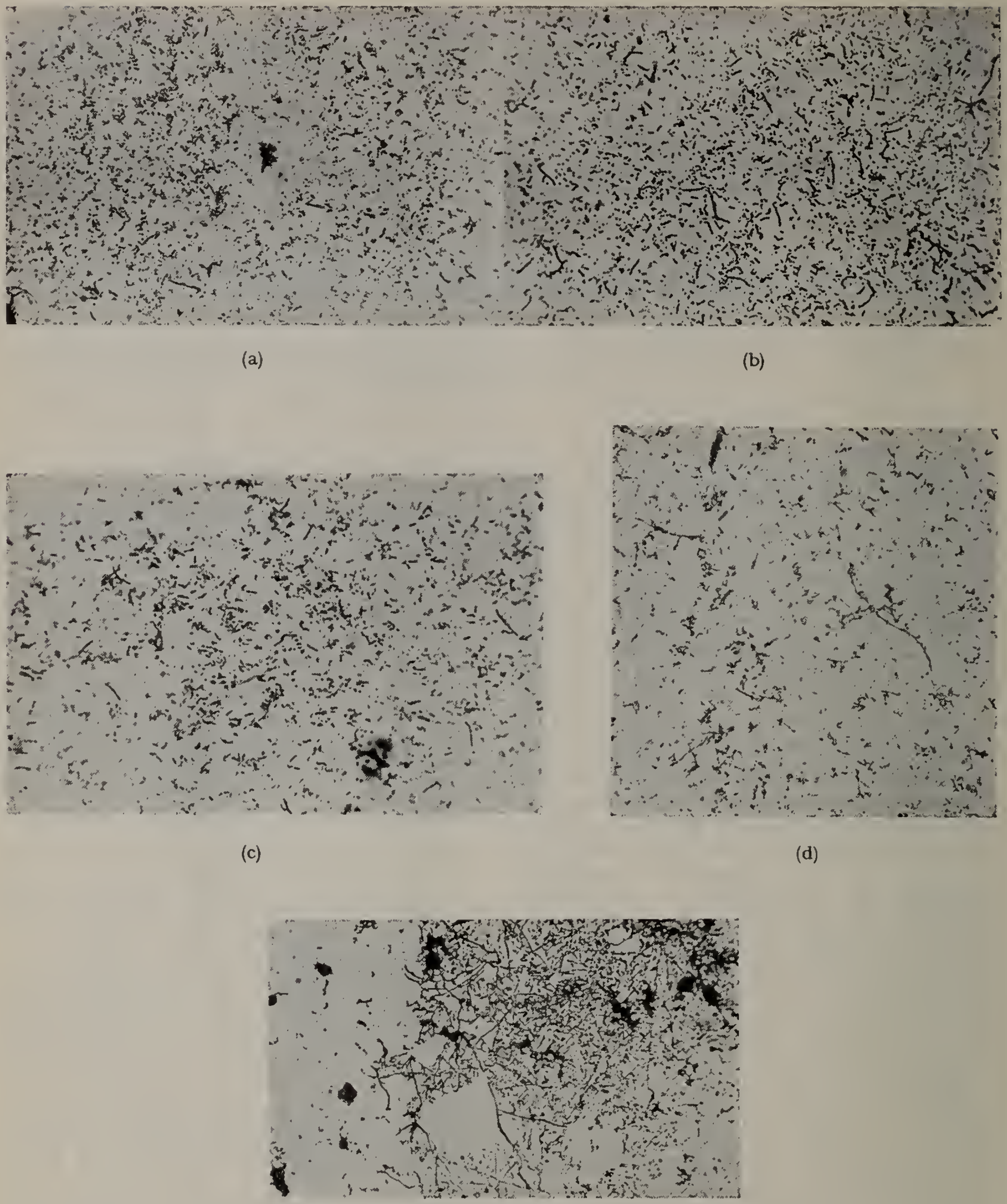

FIGURE 1.—Photomicrographs showing induction of filamentous growth in E. coli by amino acid metal systems.
(a) mixture of 6×10^{-4}M L-glutamine and 4×10^{-4}M copper(II) sulphate.
(b) mixture of 5×10^{-4}M L-glutamine and 5×10^{-4}M copper(II) sulphate.
(c) mixture of 4×10^{-4}M L-glutamine and 6×10^{-4}M copper(II) sulphate.
(d) mixture of 4×10^{-4}M L-asparagine and 5×10^{-4}M potassium platinum(II) chloride
(e) mixture of 1×10^{-2}M L-glutamine and 7×10^{-3}M potassium platinum(II) chloride.

may be of significance in the pharmacological action of this and related platinum compounds.

Our mixtures which show filamentous growth have not been screened for antitumour activity yet.* It is of interest to record that the L-glutamine metal ion mixtures which we have studied, are more effective in producing filamentous growth in *E. coli* than the L-asparagine metal ion mixtures. In a study on the mechanism of inhibition of tumour growth by the enzyme glutaminase, El-Asmar and Greenberg (1966) stated that " it is also possible that the asparaginase activity of the enzyme preparation is a significant factor in the tumour growth inhibition, since asparaginase from guinea pig serum has been reported to retard mouse lymphoma growth. In view of the many known important metabolic functions of L-glutamine and its high requirement in tissue culture media for many mammalian cells, in contrast to asparagine, the action of glutaminase might be anticipated to be the more important factor in tumour growth inhibition observed by the authors ". Our present results would seem to be in accord with the views of El-Asmar and Greenberg.

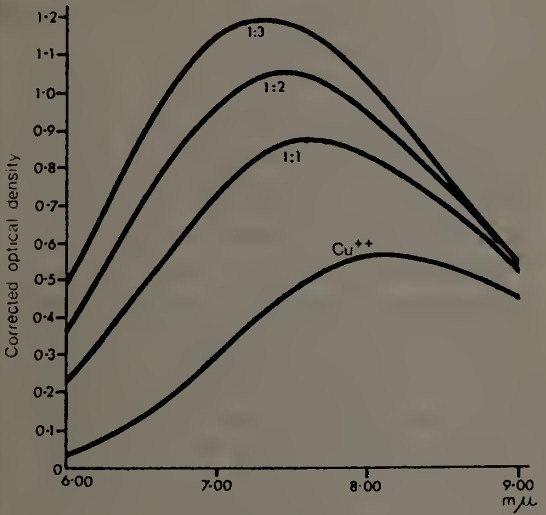

Figure 2.—Absorption spectra of solutions of copper(II) sulphate (0·05 mole/L), and mixtures containing 0·05 mole of copper(II) sulphate and 0·05, 0·10 and 0·15 mole of L-glutamine per L.

Experimental

Preparation of bis(L-asparaginato) copper (II)(7).

Copper(II) sulphate pentahydrate (1·25 g, $0{\cdot}5\times10^{-2}$ mole) in water (10 ml) was added to a vigorously stirred, boiling solution of L-asparagine (1·5 g, $1{\cdot}0\times10^{-2}$ mole) in aqueous (20 ml) sodium hydroxide (0·2 g, $0{\cdot}5\times10^{-2}$ mole). The blue crystalline product which separated (1·6 g) was collected by filtration, washed with ethanol then ether and dried. (*Found*: C, 29·68; H, 4·68; N, 16·89; Cu, 19·52. $C_8H_{14}N_4O_6$ Cu requires C, 29·50; H, 4·33; N, 17·20; Cu, 19·50%). The crystal structure has shown that the two ligands are bonded in a trans planar configuration to the copper atom through the α-nitrogens and carboxylic acids with the fifth and sixth positions occupied by amide oxygen atoms of two adjacent molecules (Stephens, Vagg and Williams, 1974).

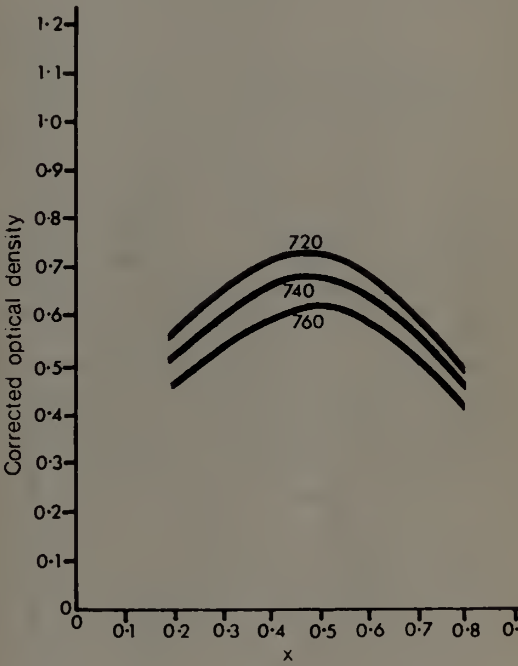

Figure 3.—Continuous variation curves showing a 1 : 1 binary species from L-glutamine and copper(II) sulphate

$$x=\frac{[cu(II)]}{[Cu(II)]+[L\text{-}glutamine]}$$

Preparation of bis(L-glutaminato) copper(II) (8).

L-glutamine (3·0 g, $2{\cdot}0\times10^{-2}$ mole) was dissolved in a hot solution of copper(II) acetate monohydrate (2·0 g, $1{\cdot}0\times10^{-2}$ mole) in water (25 ml). The product, 8, was obtained as very

---

* Mixtures of copper(II) and L-glutamine (1 : 1), platinum(II) and L-glutamine (2 : 3) and platinum(II) and L-asparagine (1 : 1) have been submitted to the National Cancer Institute in Bethesda for anticancer evaluation. The results will be reported at a later date.

fine dark blue needles (3·1 g). (*Found*: C, 33·90; H, 5·22; N, 16·44; Cu, 18·12. $C_{10}H_{18}N_4O_6$ Cu requires C, 33·95; H, 5·13; N, 15·84; Cu, 17·96%). Attempts are being made in this laboratory to obtain single crystals of 8 suitable for an X-ray structural study.

Examination of amino acid metal systems in E-coli.

The B strain of *E. coli* (obtained through the courtesy of Professor P. M. de Burgh, Medical School, Sydney University) was cultured on nutrient agar and subcultured at monthly intervals. All the experiments were performed at 37° in 50 ml ground glass test tubes fitted with fritted glass aeration bubblers. Aerobic conditions were achieved by passing air at a constant rate through flasks containing sterile water (to reduce evaporation in experimental tubes) and then through seven experimental tubes connected in series. Synthetic mineral " C " medium (Roberts *et al.*, 1955) containing 0·2 per cent glucose as energy source (20 ml) was added to each tube and inoculated with *E-coli*. After incubating tubes for 8–12 hr, turbidity of the solutions indicated good bacterial growth. Mineral " C " medium (without glucose), a solution of the amino acid, and (or) a solution of the metal salt were then added to each experimental tube to give a final volume of 30 ml. In a typical experiment using 1×10^{-2}M L-asparagine and 1×10^{-2}M copper(II) sulphate, the first experimental tube contained L-asparagine (10 ml); the second tube contained L-asparagine (8 ml) and copper(II) sulphate (2 ml); the third tube contained L-asparagine (6 ml) and copper(II) sulphate (4 ml); the fourth tube contained L-asparagine (5 ml) and copper(II) sulphate (5 ml); the fifth tube contained L-asparagine (4 ml) and copper(II) sulphate (6 ml); the sixth tube contained L-asparagine (2 ml) and copper(II) sulphate (8 ml) and the seventh tube contained copper(II) sulphate (10 ml). Tubes were again incubated at 37° and samples were withdrawn from each tube every 4–6 hr for microscopic examination (bacteria were stained with a 1 per cent aqueous solution of crystal violet). Experiments were repeated using 1×10^{-3} M L-asparagine and 1×10^{-3}M copper(II) sulphate, and 1×10^{-4}M L-asparagine and 1×10^{-4}M copper(II) sulphate.

No filamentous growth was observed in the twenty-one experimental tubes described above. Mixtures of L-asparagine and potassium palladium(II) chloride and mixtures of L-glutamine and potassium palladium(II) chloride also did not induce filamentous growth in *E. coli*. With a mixture of 5×10^{-4}M L-glutamine and 5×10^{-4}M copper(II) sulphate, filamentous growth was observed (Figure 1*b*). Some filaments were produced by mixtures of 6×10^{-4}M L-glutamine and 4×10^{-4}M copper(II) sulphate (Figure 1*a*) and 4×10^{-4}M L-glutamine and 6×10^{-4}M copper(II) sulphate (Figure 1*c*). Filamentous growth was also observed with mixtures of 4×10^{-4}M L-asparagine and 5×10^{-4}M potassium platinum(II) chloride (Figure 1*d*) and 1×10^{-2}M L-glutamine and 7×10^{-3}M potassium platinum(II) chloride (Figure 1*e*).

In control experiments, synthetic mineral " C " medium, containing 0·2 per cent glucose and different concentrations (1×10^{-2}M, 1×10^{-3}M and 1×10^{-4}M) of copper(II), platinum(II) or palladium(II) ions were inoculated with *E. coli*. In all cases good bacterial growth was observed after incubating tubes for 12 hr at 37°. Similar controls have been carried out for amino acid metal ion mixtures.

Continuous Variation Study on the L-Glutamine Copper(II) Sulphate System

Aqueous solutions containing 0·05 mole of copper(II) sulphate and 0·05, 0·10 and 0·15 moles of L-glutamine were prepared. The optical densities of each solution were measured at a range of wavelengths using a Zeiss PMQ(II) spectrophotometer. The results shown in Figure 2 indicate that one species is formed on mixing solutions of L-glutamine and copper(II) sulphate (Vosberg and Cooper, 1941). Mixtures (10 ml) of 0·17M L-glutamine and 0·17M copper(II) sulphate were made up in the ratios of 2:8, 4:6, 5:5, 6:4 and 8:2. Each solution was diluted with water (5 ml) and optical densities were recorded at 720, 740 and 760 nm. The optical densities of the original solutions were also measured at the above wavelengths. Figure 3 shows the results of molar ratios versus corrected optical densities (Vosberg and Cooper, 1941). All the curves (Figure 3) show a maximum near a molar ratio of 1:1.

Acknowledgement

The authors thank Dr. Harry Wood Jr. of the National Cancer Institute, Bethesda, Maryland, U.S.A. for the results of KB cell-culture testing.

References

Baxter, A. C., and Williams, D. R., 1974. Thermodynamic Considerations in Co-ordination. Part XV. Potentiometric and Calorimetric Study of the Complexes Formed Between Protons, First Transition Series Metal Ions, and Asparaginate and Glutaminate Anions. *J. Chem. Soc. Dalton*, 1117.

Booth, B. A., Johns, D. G., Bertino, J. R., and Sartorelli, A. C., 1968. Sites of Inhibition of DNA Synthesis by Ketoxal Bix (thiosemicarbazone). *Nature*, **217**, 250.

Booth, B. A., and Sartorelli, A. C., 1967. Metabolic Effects of Copper in Intact Cells: Comparative Activity of Cupric Chloride and the Cupric Chelate of Kethoxal Bis(thiosemicarbazone). *Mol. Pharmacol.*, **3**, 290.

Broome, J. D., 1963. Evidence that L-asparaginase of Guinea Pig Serum is Responsible for its Antilymphoma Effects. 1. Properties of L-asparaginase of Guinea Pig Serum in Relation to those of the Antilymphoma Substance. *J. Exptl. Med.*, **118**, 99.

Carlsson, F. H. H., Charlson, A. J., and Watton, E. C., 1974. The Biological Activity of Some Guanylhydrazones and Thiosemicarbazones of Aliphatic Carbonyl Compounds. *Carbohyd. Res.*, **36**, 359.

Charlson, A. J., 1973. The Synthesis of Metal Chelates as Potential Anticancer Substances. Presented at the Second International Symposium on the Use of Platinum Compounds in Cancer Chemotherapy. Wadham College, The University of Oxford.

Conners, T. A., 1973. Platinum Coordination Complexes in Cancer Chemotherapy. *Platinum Metals Rev.*, **17**, 98.

Cooney, D. A., and Handschumacher, R. E., 1970. L-asparaginase and L-asparagine Metabolism. *Ann. Rev. Pharmacol.*, **10**, 421.

El-Asmar, F. A., and Greenberg, D. M., 1966. Studies on the Mechanism of Inhibition of Tumour Growth by the Enzyme Glutaminase. *Cancer Res.*, **26**, 116.

Horwitz, B., Old, L. J., Boyse, A., and Stockert, E., 1968. Asparaginase Synthetase Activity of Mouse Leukaemias. *Science*, **160**, 533.

Kirson, B., and Barsily, I., 1959. The Complexes of Copper with Aspartic Acid, Glutamic Acid, Asparagine and Glutamine. Formation and Composition. *Bull. Soc. Chim. France*, 901.

Livingstone, S. E., and Mikelson, A. E., 1970. Metal Chelates of Biologically Important Compounds. II. Nickel Complexes of Dialkyldithiophosphates and their Adducts with Nitrogen Heterocycles. *Inorg. Chem.*, **9**, 2545.

Mihich, E., and Mulhern, A. I., 1965. Comparative Potency of Kethoxal-Bis(thiosemicarbazone) (KTS) and its Copper(II) Chelate (KTS-Cu) in Rodents. *Fed. Proc.*, **24**, 454.

Morris, C. R., and Gale, G. R., 1973. Interactions of an Antitumour Platinum Compound with Deoxyribonucleic Acid, Histones, L-Amino Acids, Poly-L-amino Acids, Nucleosides and Nucleotides. *Chem. Biol. Interactions*, **7**, 305.

Oettgen, H. F., Old, L. J., Boyse, E. A., Campbell, H. A., Philips, F. S., Clarkson, B. D., Tallal, L., Leeper, R. D., Schwartz, M. K., and Kim, J. H., 1967. Inhibition of Leukemias in Man by L-asparaginase. *Cancer Res.*, **27**, 2619.

Petering, H. G., and Van Giessen, G. J., 1966. The Essential Role of Cupric Ion in the Biological Activity of 3-ethoxy-2-oxobutyraldehyde Bis(thiosemicarbazone). A New Antitumour Agent. *The Biochemistry of Copper.* Acad. Press, New York and London, 197.

Roberts, J., Holcenberg, J. S., and Dolowy, W. C., 1970. Antineoplastic Activity of Highly Purified Bacterial Glutaminases. *Nature*, **227**, 1136.

Roberts, R. B., Abelson, P. H., Cowie, D. B., Bolton, E. T., and Britten, R. J., 1955. Studies of Biosynthesis in *Escherichia coli*. *Carnegie Inst. Wash. Publ.*, 607.

Rosenberg, B., Van Camp, L., Grimley, E. B., and Thompson, A. J., 1967. The Inhibition of Growth or Cell Division in *Echerichia coli* by Different Species of Platinum(IV) Complexes. *J. Biol. Chem.*, **242**, 1347.

Rosenberg, B., Van Camp, L., Trosko, J. E., and Mansour, V. H., 1969. Platinum Compounds: A New Class of Potent Antitumour Agents. *Nature*, **222**, 385.

Sidgwick, N. V., 1951. The Chemical Elements and their Compounds, *Oxford University Press*, **2**, 1596.

Stephens, F. S., Vagg, R. S., and Williams, P. A., 1974. Crystal and Molecular Structure of Bis (L-asparaginato) Copper(II). *Acta Cryst.* In press.

Takamiya, K., 1960. Antitumour Activities of Copper Chelates. *Nature*, **185**, 190.

Van Giessen, G. J., Crim, J. A., Petering, D. H., and Petering, H. G., 1973. Effect of Heavy Metal-on the in Vitro Cytotoxicity of 3-ethoxy-2 oxobutyraldehyde Bis(thiosemicarbazone) and Related Compounds. *J. Natl. Cancer Inst.*, **51**, 139.

Vosberg, W. C., and Cooper, G. R., 1941. Complex Ions. 1. The Identification of Complex Ions in Solution by Spectrophotometric Measurements. *J. Amer. Chem. Soc.*, **63**, 437.

Wood, H. B., 1969. Personal communication.

School of Chemistry,
Macquarie University,
North Ryde, 2113, Australia.

(Received 15.8.74)

Journal and Proceedings, Royal Society of New South Wales, Vol. 108, pp. 12-15, 1975

Bedrock Topography in Northern Jervis Bay

B. D. JOHNSON AND A. D. ALBANI

ABSTRACT—A detailed seismic investigation of the northern part of Jervis Bay, has confirmed the existence of a watershed between Flora Point and Green Point. Additional details have also been obtained on the dendritic drainage pattern.

Introduction

The present study adds detailed information on a more extensive study of Jervis Bay (Albani, Carter and Johnson, 1973) and is part of a larger research project aimed at determining the pre-Pleistocene drainage pattern of the coastal region of New South Wales (Albani, 1973; Albani and Johnson, 1974).

Previous work carried out in Jervis Bay (Albani, Carter and Johnson, 1973) was mainly concerned with the southern portion of the bay. Seismic profiles were made using a low-power marine sparker; from the interpretation of which a system of bedrock channels was defined. These channels, clearly discernable in the entrance region of Jervis Bay, where they reach a depth of 140 m below the present sea level, were seen to form a dendritic drainage pattern extending over the present location of the bay. The quality and sparseness of the profiles in the northern part of the bay did not allow a complete interpretation; however, a drainage watershed was indicated and this was the primary target for the present study.

All these bedrock channels are presently filled by large thicknesses of flat lying sediments in very shallow water, particularly in the northeastern part of the bay.

Sparker Survey and Results

As in similar shallow water investigations (Albani and Johnson, 1974) a low-power (200 joules) marine sparker was used as the seismic source, the arrivals from which are detected by a short hydrophone array. Positioning of the vessel was by theodolite intersections from land-based stations, coordination being achieved by a two-way radio link. The profiles were chosen to run more or less perpendicular to the northern shore, with a few tie lines and passing over some of the available borehole locations for correlation purposes. The locations of these traverses are shown in Figure 1.

The sparker records were interpreted using the seismic velocities determined in the southern part of Jervis Bay (Albani, Carter and Johnson, 1973). A sediment velocity of 1,830 m.p.s. was used which was confirmed by comparing the interpreted depths against the available borehole information.

Profiles of depth to bedrock from water bottom, were prepared and then interpreted in terms of the dendritic drainage pattern observed further south (Albani, Carter and Johnson, 1973). The resulting bedrock contours are shown in Figure 1 and are the most realistic representation of the bedrock configuration subject to the control provided by the previous survey, borehole information and outcropping bedrock on the headlands of Green Point, Red Point and Flora Point.

The presence of the northern end of the dendritic drainage pattern covering most of Jervis Bay is confirmed, one of the bedrock channels apparently originating north of the present coastline west of Flora Point.

Both Flora Point and Green Point have exposed rock platforms and these are apparently joined by a bedrock ridge separating off a minor drainage area to the northeast (see Figure 1). The depth of the ridge is between 12 and 25 metres below present sea level.

A small but very steep drainage channel system is defined in the northeastern part of the area with its outlet northeastwards across the tombolo presently joining the Beecroft Penninsula northwards to the mainland. Geophysical work on land is planned in this region to further define the extent of the bedrock channel. This area is similar to that found in Pitt Water (Albani and Johnson, 1974). Partially consolidated sediments seem to fill these channels, as already noted in the previous survey of Jervis Bay (Figure 2) (Albani, Carter and Johnson, 1973).

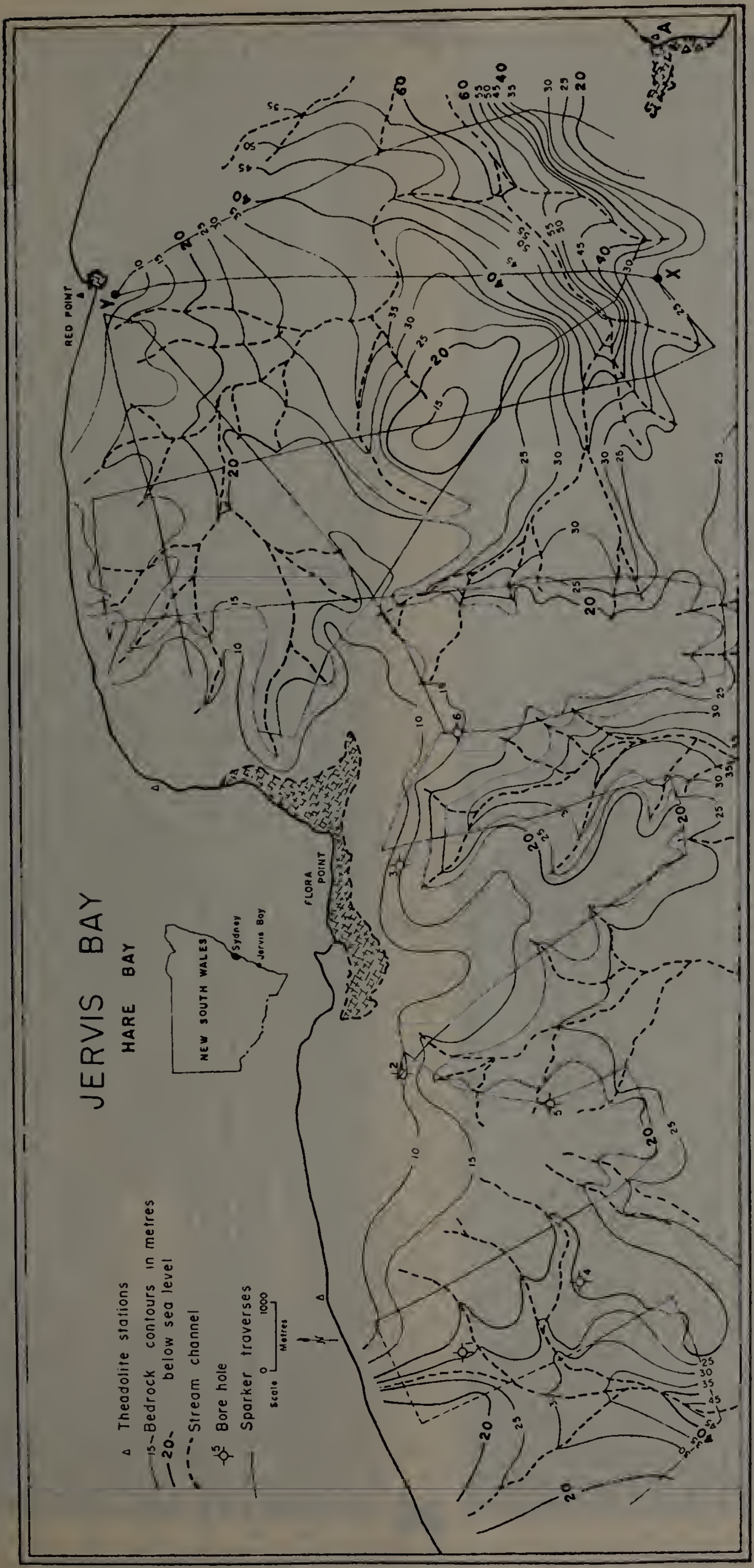

FIGURE 1.—Sparker profile locations and interpreted bedrock topography of northern Jervis Bay. Green Pt. is shown by A in the lower right hand corner of the map. X-Y location of seismic profile illustrated in the paper.

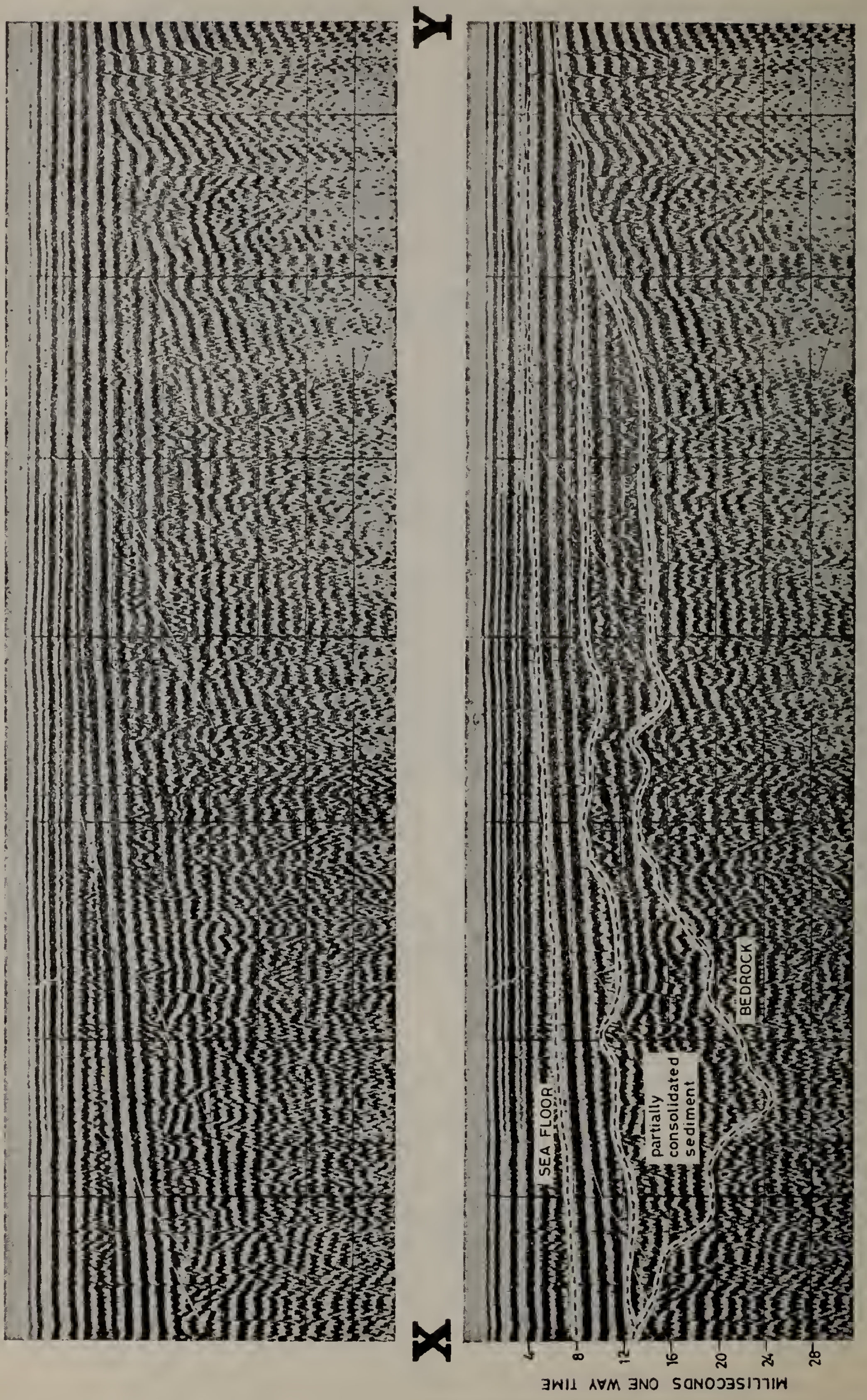

FIGURE 2.—Sparker profile and its interpretation along traverse X-Y.

Conclusion

A sparker survey of the northern part of Jervis Bay has confirmed the northern extent of the dendritic drainage pattern, previously described, and of a minor drainage system which, in the northeastern part of the bay, is separated by a buried bedrock ridge. This latter system has its exit to the sea across the tombolo which presently joins the Beecroft Penninsula, of which Green Point forms the northwesterly projection, to the mainland. It may be reasonably predicted that a steep sided bedrock canyon will be found underlying the tombolo and achieving depths well in excess of 100 metres below present sea level.

The presence of the bedrock channel system confirmed by this survey and the previous work may be interpreted in terms of a drainage pattern cut during the Pleistocene and subsequently filled by sediment after the sea level rise at the end of the Ice Ages (11,000 years ago). It is interesting to note that our studies have shown similar results for both Broken Bay and Jervis Bay. Departures from the above pattern will probably require an interpretation in terms of local movements.

Acknowledgements

The authors are grateful for the assistance of J. Bishop, P. G. Towson and the R.A.N. Training College at Jervis Bay.

References

Albani, A. D., 1973. The Sedimentary Environment and the Distribution of Recent Foraminiferida in Broken Bay, N.S.W. *Ph.D. Thesis, University of New South Wales.*

Albani, A. D., Carter, A. N., and Johnson, B.D., 1973. The Bedrock Topography and Origin of Jervis Bay, N.S.W. *Oceanography of the South Pacific 1972, comp. R. Fraser, N.Z. Nat. Comm. UNESCO, Wellington.*

Albani, A. D., and Johnson, B. D., 1974. The *Evolution of Broken Bay, N.S.W. Jour. Geol. Soc. of Australia*, **21** (2), 209.

B. D. Johnson,
School of Earth Sciences,
Macquarie University,
North Ryde, N.S.W., 2113.

A. D. Albani,
School of Applied Geology,
University of New South Wales,
Kensington, N.S.W., 2033.

(Received 30.4.74)

Journal and Proceedings, Royal Society of New South Wales, Vol. 108, pp. 16-28, 1975

Structure and Jointing in Permian Rocks Near Ravensworth, N.S.W. Northern Sydney Basin

David R. Gray

Abstract—Permian rocks near Ravensworth, New South Wales are part of the northern margin of the Permo-Triassic Sydney Basin. Major structures in the area are open, sub-horizontal, northwest trending non-cylindrical folds. The Bayswater and Glennies Creek Synclines and the Camberwell Anticline are the largest of these structures. The folds are second phase en echelon " pod " folds developed on the eastern flank of the Muswellbrook Anticline.

The main faults near Ravensworth are the Hunter Thrust and the Hebden Fault. The Hunter Thrust is a major border thrust along the northern margin of the Basin which separates Permian and Carboniferous strata. The Hebden Fault is a high angle reverse fault which closes against the Hunter Thrust forming a fault wedge of folded Permian strata.

Four major systematic joint sets (north-northeast, north-west, north-south and east-west) occur in the rocks and appear to have developed independent of folding and faulting. Modification of joints in strata adjacent the Hunter Thrust has taken place because of movements along the Thrust after joint formation.

The deformational history of Permian rocks along the northern margin of the Sydney Basin involves two periods of folding, a protracted period of thrusting and a phase of jointing.

Introduction

This paper describes the structure and jointing in the Ravensworth area, New South Wales and attempts to elucidate the deformational history along the northern margin of the Sydney Basin. It is derived from work undertaken as part of a B.Sc. Hons. degree at the University of Newcastle in 1971.

The Ravensworth area is situated between Singleton and Muswellbrook some 96 km northwest of Newcastle. It contains Late Permian strata in faulted contact with rocks of Carboniferous age (Figure 1). The oldest Permian rocks, the Maitland Group, crop out in a fault wedge between the Hunter Thrust and the Hebden Fault. These consist of fine, medium and coarse grained lithic arenites, pebbly arenites, cobble conglomerates with minor pebble phases (Branxton Formation) and a massive siltstone with minor arenaceous phases (Mulbring Siltstone).

The Maitland Group is conformably overlain by the Singleton Coal Measures which are equivalent in age to both the Tomago and Newcastle Coal Measures. The Singleton Coal Measures consist of three formations, the Saltwater Creek Formation, the Vane Formation and the Goorangoola Formation (Robinson, 1969). The Coal Measure rocks include sandstones, shales, mudstones and coal seams which pass upward into sandstones and conglomerates.

The stratigraphic nomenclature used is dependent on persistent coal seams as formation boundaries. Mapping the outcrop of these coal seams is very difficult because of poor exposure. A stratigraphic and a structural interpretation of the area is also difficult due to the poor outcrop, the poor lateral continuity of the strata and the lack of any distinct marker horizons.

All grid references cited refer to the Camberwell 1 : 63,360 military sheet.

Structure

The Ravensworth area, part of the Dome Belt (Voisey, 1958), is situated in the mildly deformed zone between the Lochinvar and Muswellbrook Anticlines, the two major structural elements in the northern section of the Sydney Basin.

Folding

The area mapped contains a series of folds which are essentially minor warps on the eastern flank of the Muswellbrook Anticline (Figure 2). This structure has an easterly dipping, north-south trending axial plane and plunges at 4·5 degrees to the south (Veevers, 1960).

First phase folds, such as the Muswellbrook and Lochinvar Anticlines are large regional structures with north-south axial plane traces. They have similar trends to fold and fault trends

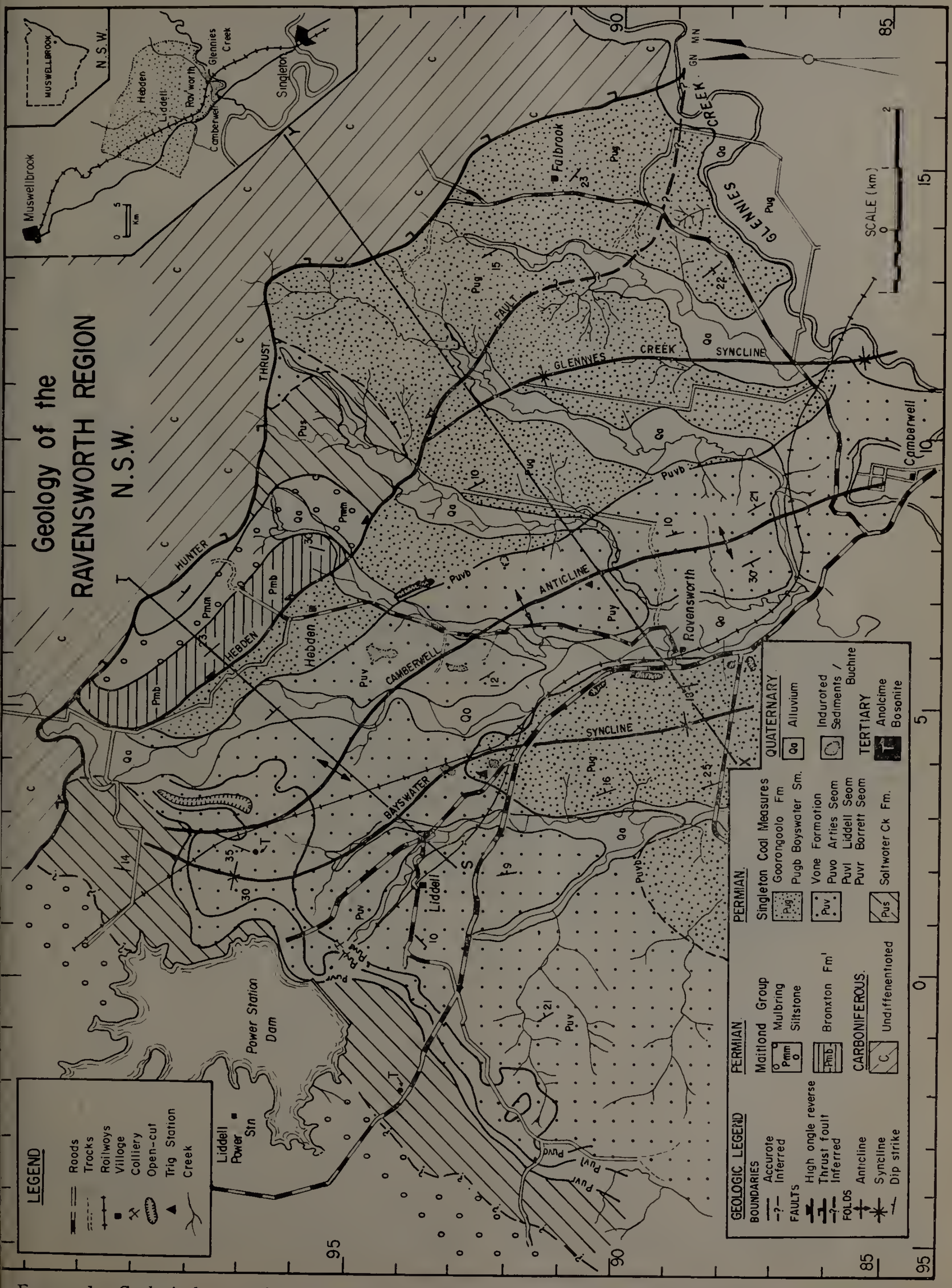

FIGURE 1.—Geological map of the Ravensworth area, New South Wales. All formation boundaries in the Singleton Coal Measures are projected seam outcrops from Booker (1953).

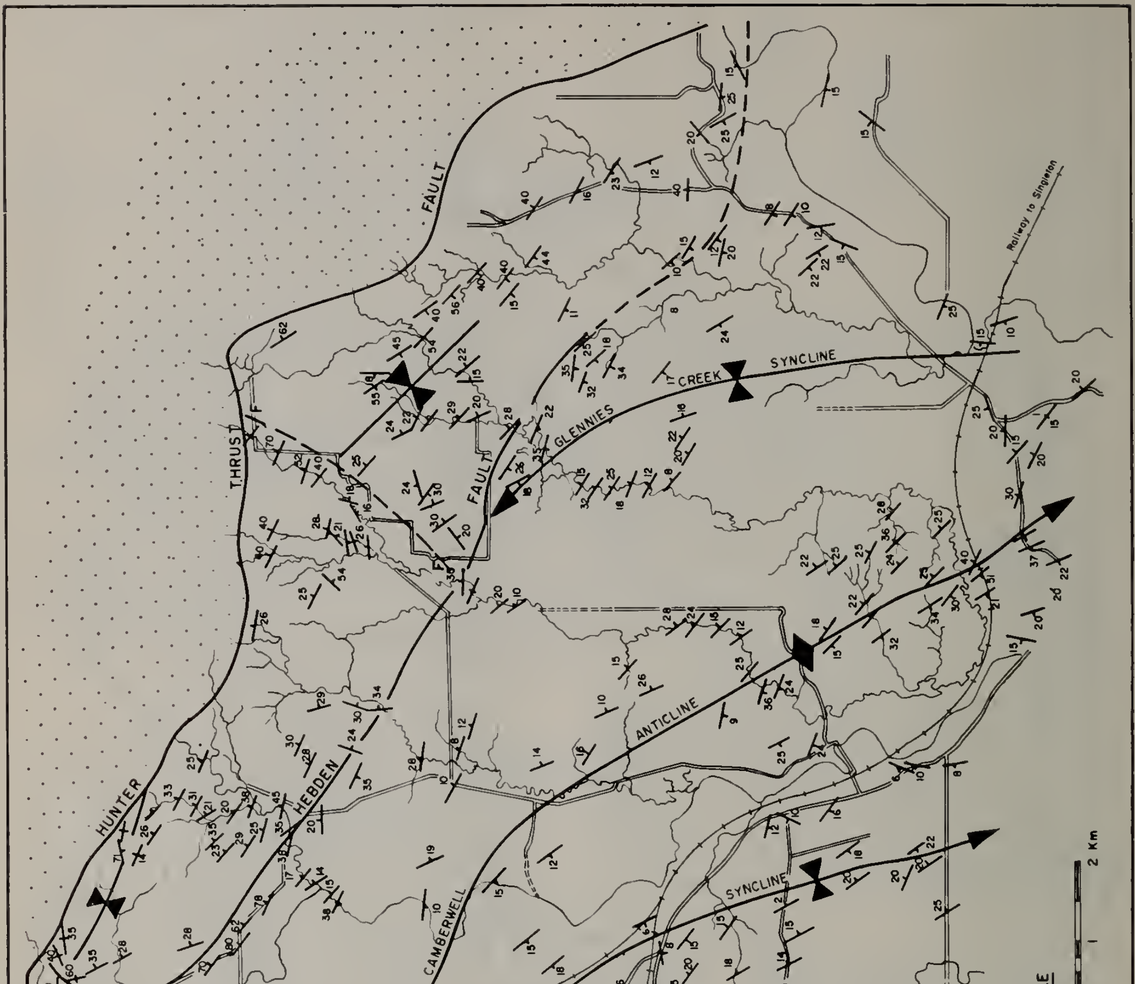

FIGURE 2.—Structure Map of the Ravensworth area.

in the lower and middle Palaeozoic basement rocks underlying the Sydney Basin. This may suggest that the first deformation affecting the Basin was largely manifested by the propagation of basement structure into the overlying sedimentary pile, probably by differential movemovement along existing basement structural anisotropies. Blayden (1971) and Stuntz (1972) consider that the folding of the Lochinvar Anticline was influenced by underlying basement faults. Blayden (*op. cit.*) considers that differential block movement along basement faults has been responsible for many of the structures in the Sydney Basin.

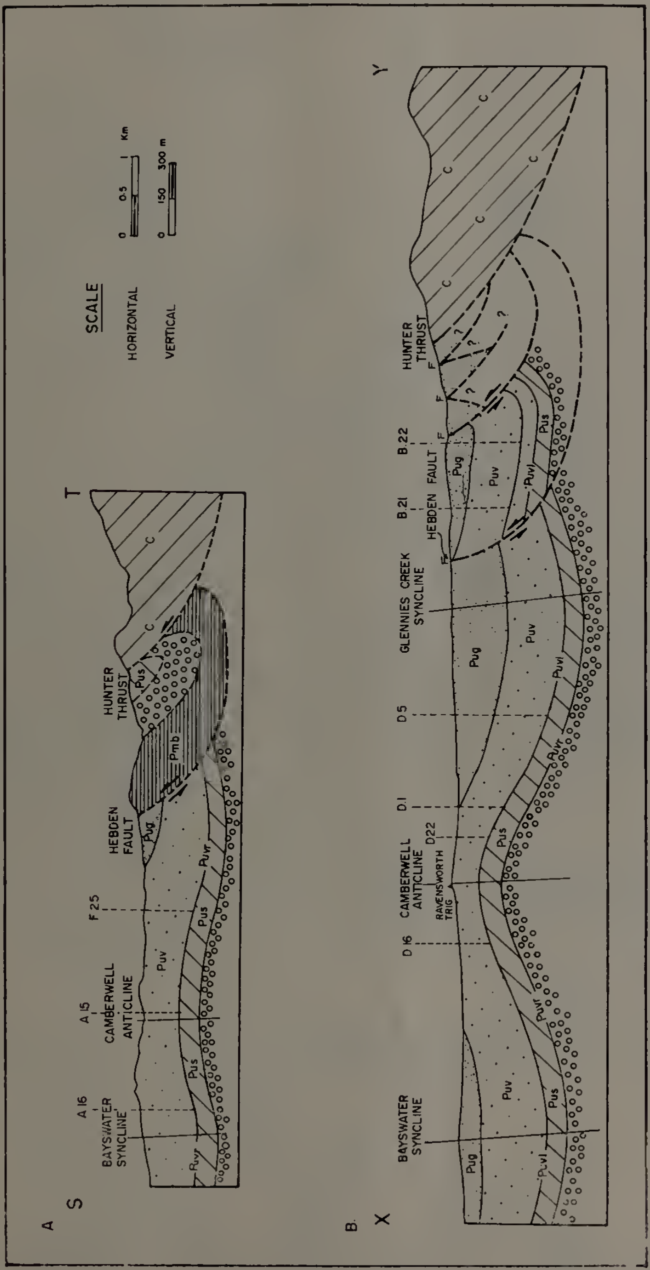

FIGURE 3.—Geologic Cross Sections. A. Section line S–T, Figure 1. B. Section line X–Y, Figure 1.

The open, subhorizontal to gently southeast plunging, north-west trending folds in the

FIGURE 4—See next page for Legend.

Ravensworth area, of which the Camberwell Anticline and the Bayswater and Glennies Creek Synclines are the largest, are non-cylindrical folds whose profiles change progressively from north to south (Figure 3). The folds have amplitudes of 0·2 km and wavelengths of 0·5 km in the north and amplitudes of 0·4 km and wavelengths of 2·5 km in the south.

These local minor folds are probably en echelon " pod " folds which have formed during a second phase of west-northwest folding, associated with thrusting movements along the Hunter Thrust. This second deformation superposed on the first generation folds was at 60° to the first folding compression direction. Buckling experiments on intersecting fold patterns in putty (Gosh and Ramberg, 1966, Plate IIIB, p. 101) show that such a superposed deformation will produce arching of the first phase folds and the development of smaller en echelon " pod " folds on the limbs of these folds. The development of dome and basin structures, such as the Belford and Loder Domes along the northern margin of the Basin reflect the arching of the first generation structures, in this region.

Mapping has shown that the Rixs Creek Syncline (Booker, 1953) is a continuation of the Glennies Creek Syncline. The name Glennies Creek Syncline has been retained for this structure. The Bayswater Syncline plunges approximately at 7° to the south-southwest (154°), whereas the Camberwell Anticline and Glennies Creek Syncline plunge locally to the northwest at 9° and 7° respectively. Subsurface data (recorded in Gray, 1971) indicates a reversal in plunge for the Camberwell Anticline at 052942C ; the plunge changes to 9° to the south-southeast (143°). There is a general tendency for the fold trends to swing from north-northwest to west-northwest northwards through the area. Plunge reversals and curvilinear axial plane traces are due either to differential shortening along the folds during their formation or subsequent modification by later thrusting movements along the Hunter Thrust.

Faulting

The main faults in the Ravensworth area are the Hunter Thrust and the Hebden Fault. The Hunter Thrust, a major border thrust along the northern margin of the Sydney Basin, consists of a series of dislocations separating Permian and Carboniferous rocks. It extends over 80 kms in a northeast direction, from north of Newcastle to Scone. The fault trace, generally covered by soil and alluvium is delineated by the marked physigraphic difference between the Permian and Carboniferous strata. The thrust plane is distinctly nonplanar in places (Osborne, 1929, and Raggatt, 1938) and in the mapped area appears conformable with folded Carboniferous strata in the overthrust block (Gray, 1971). Raggatt (*op. cit.*) considers it is convex to the southwest in section as well as in plan, with a dip varying between 15 and 30°.

The Hebden Fault is a high angle reverse fault which closes against the Hunter Thrust near Falbrook to produce a fault wedge of folded strata. The fault plane strikes approximately northwest and has a calculated minimum dip of 77°. The throw at the northwest end of the fault must be in the order of 1,300 m, whereas drilling data indicate throws of 360 m and 240 m at 102938C and 129918C respectively. Drilling and outcrop data suggest considerable faulting in the southern portion of the fault wedge. Despite poor outcrop it appears likely that the Hebden Fault continues to the south to close against the Hunter Thrust in the vicinity of Falbrook.

FIGURE 4.—Interpreted systematic joint trace pattern in the Ravensworth area ; contoured πS diagrams (poles to joints) designated by upper case letters refer to stereograms designated by the corresponding lower case letter on the diagram. (Contours per 1% area.)

A. creekbed ; 10%, 8%, 6%, 0%
B. creekbed ; 16%, 14%, 12%, 6%, 0%
C. creekbed ; 18%, 16%, 10%, 6%, 0%
D. Foybrook Open Cut ; 20%, 16%, 10%, 8%, 6%, 5%, 0%
E. Liddell Colliery Portal ; 13%, 11%, 8%, 6%, 3%, 0%
F. road cutting ; 20%, 15%, 11%, 9%, 4%, 0%
G. Pukes Gulley Open Cut ; 26%, 22%, 16%, 8%, 0%
H. Elemin Ravensworth Cut ; 13%, 12%, 9%, 7%, 0%
I. creekbed, Bowmans Creek bridge ; 13%, 12%, 9%, 6%, 2%, 0%
J. Hebden Open Cut ; 30%, 22%, 12%, 7%, 0%
K. ridge outcrop ; 10%, 8%, 6%, 5%, 3%, 0%
L. creekbed ; 15%, 10%, 7%, 6%, 3%, 0%
M. disused quarry ; 8%, 7%, 5%, 3%, 0%
K, L, and M are joint measurements from Carboniferous ignimbrites in the overthrust block.

No evidence was found for the York's Creek Fault (Raggatt, 1938, and Booker, 1953), as it is clear from outcrop that the Maitland Group strata terminate against the Hebden Fault. A north-northeast striking fault, however, occurs along the western boundary of the Ravensworth State Forest (110950C) and has an approximate throw of 120 m.

Minor faults with throws less than 15 m are common in the Singleton Coal Measures. These cannot be detected on the surface and are usually exposed in colliery workings and open cut mines (Plate I). This faulting occurs along northeast-southwest (N20E to N40E) and north-south directions. The northeast trending faults are mainly normal faults, with dips ranging from 54 to 76° predominantly to the southeast, together with high angle reverse faults with dips from 82 to 88° to the northwest. The north-south striking faults, more common in the western portion of the area, are generally reverse faults with dips ranging from 30 to 62° to the west.

These minor faults characteristically occur not as isolated faults but in zones, and appear to represent two different sets of faults. The north-south reverse faults are probably related to the compressive Muswellbrook Anticline Phase, whereas the northeast-southwest normal faults are possibly a relaxation phase after the second generation folding. During the Tertiary some of these faults, predominantly the north-northeast normal faults, were opened up by igneous dykes.

Jointing

Jointing is by far the most ubiquitous structure in this area. Two domains of jointing exist, each characterized by the spatial attitude of the joints within it (Figure 4).

Domain A

Domain A geologically corresponds to weakly deformed strata south of the Hunter Thrust. Four essentially vertical " systematic " (Hodgson, 1961) joint sets are developed : (1) north-northeast (N20E to N35E) ; (2) northwest (N45W to N55W) ; (3) east-west ; (4) north-south (Plate II).

Minor variations in the spatial attitude of joints occur across the area and are most probably related to varying lithology and the presence of sedimentary structures. It is well known that fabric and structural anisotropies in a rock body cause re-orientation of stresses responsible for fracture initiation and thereby produce local variations in the attitude of the fractures. Hills (1966) considers that features such as cross-bedding, ripple marks, sole marks, flute casts, concretions, nodules and fossils serve as loci for stress concentration and thus initiate the microfractures which propagate to form joints. Sedimentary fabric must therefore influence the direction and rate of propagation of microfractures, and is predominantly responsible for the irregular and often curviplanar nature of some joint surfaces.

Structures on the joint planes and features associated with joints provide information about the origin and the genetic history of the joints. These include structures such as plume hackle marks and rib markings and features such as displacement indicators (sheared pebbles and fossils) and mineral infilling (Table 1).

Plume hackle marks or plumose patterns are essentially curved striations which fan out from a common origin. They have been found on fracture surfaces identified from other criteria as shear joints (Parker, 1942, and Price, 1966) and also as tension joints (Nadia, 1950 ; Muehlberger, 1961, and Badgley, 1965). Roberts (1961) claimed that plumose patterns typify fractures produced by extremely rapid medium separation, whereas Syme Gash (1972) has shown that they are generally indicative of shear fractures. Bed thickness, grainsize, porosity and the presence of pre-existing structures determine whether they form on joint surfaces (Syme Gash, *op. cit.*).

Rib marking or augen fracture is a series of approximately semi-circular or arcuate ridges along the joint plane. They result from running shear fractures with multiple or continuous shock sources (Syme Gash, *op. cit.*).

The presence of both rib and hackle structures on the north-northeast and northwest joints (Plate III), as well as a variation in dihedral angle between them suggests a shear origin. The dihedral angle between shear joints is a function of the angle of internal friction of the material and consequently varies for differing rock types.

Modification of some of these joints has occurred. Mineral infilling and displacements along north-northeast and northwest joints (Table 1) indicate both tensional and " shear " movements along some joints after their formation. Joints may provide a cumulative record of late tectonic events and therefore lateral displacement along a joint does not necessarily indicate a shear origin, only a phase of shear movement. Similarly, the presence of mineral infilling does not necessarily indicate a tensional origin, only a phase or component of

TABLE 1

Structures Along Joint Surfaces

STRUCTURE OR FEATURE	DOMAIN	JOINT STRIKE	LOCATION	
Plume Hackle Marks	A	N35E	Pykes Gulley Old Cut	980921C
	A	N40W	Pykes Gulley Old Cut	980921C
	A	N20W	Durham No. 2 Cut	026967C
	A	N50W	Hebden Open Cut	071938C
	B	None observed		
Rib Marking	A	N20W	Durham No. 2 Cut	026967C
	B	None observed		
Slickensides	A	None observed		
	B	N20E	Creekbank	096961C
		N20W	Creekbank	096961C
		N20W	Creekbank	096961C
Mineral Infilling	A	N20W	Gravel Quarry	006937C
	A	N55E	Gravel Quarry	006937C
	B	N35W	Creekbed	27960C
	B	N60E (Tension Gashes)	Creekbed	074497C
Displacement	A	N30E (Horizontal Component)	Creekbed	082883C
	A	N25W (Horizontal Component)	Gravel Quarry	006937C
	B	N24E Vertical Component	Creekbed	057992C
	B	N60E	Creekbed	051993C
	B	N55W	Creekbed	113961C

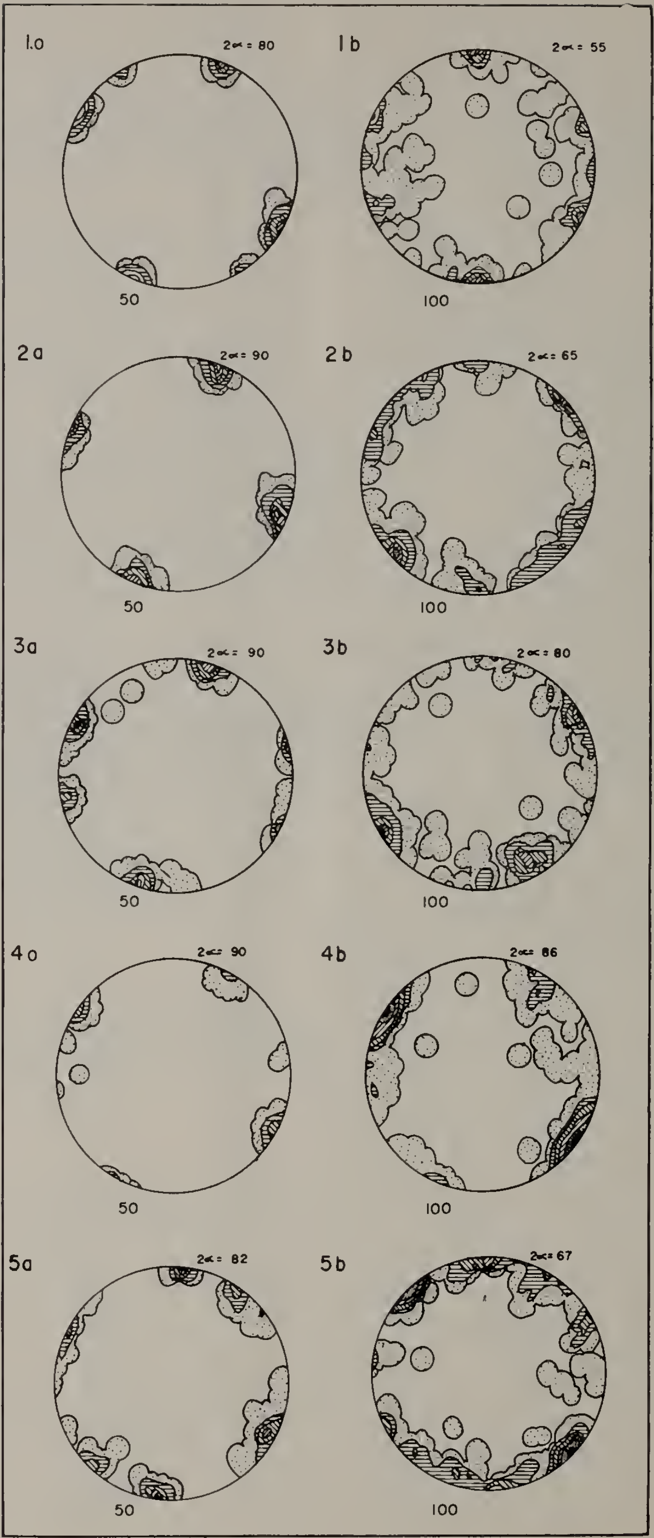

FIGURE 5—See next page for Legend.

tension at some stage in the development of the joint. However, these are probably older than joints without infilling.

The infrequence of hackle and rib markings, and the more uniform orthogonality between the north-south and east-west joints suggests a tensional origin.

Domain B

Domain B corresponds to disturbed Permian strata adjacent the Hebden and Hunter Thrust Faults. Subsets of the four main systematic joints sets of Domain A are present, but are associated with subsidiary joints separated by small dihedral angles. Domain B joints, however, have extremely variable dips and are generally not close to vertical.

Modification of joint sets is marked in Domain B, where slickensides, sheared pebbles (Plate IV), mineral infilling and extremely close joint spacing (down to 1 cm) are more common (Table 1). The general lack of hackle marks, the presence of slickensides and sheared pebbles indicates that movement along joints has predominantly accompanied modification of Domain B joints. An incipient fracture pattern present in a rock mass is accentuated by all subsequent stress conditions (Spencer Jones, 1963). Existing cracks and flaws propagate further before point stress concentration enables new crack formation. This would generally decrease spacing between joints and therefore increase joint frequency. Some zones particularly favourable to stress concentration could develop extremely closely spaced jointing, characteristic of " shear zones ".

Modification of jointing has been associated with thrusting movements along the Hunter Thrust accompanied by subsidiary movements along the Hebden Fault. The complex faulting in the southern portion of this fault wedge reflects the deformational intensity of this zone.

General Observations on Jointing

(i) In both domains there is a definite lithologic control of jointing, since the orientation, planeness and spacing of the joints are dependent on lithology. It is clear that the joints are more closely spaced in shales and siltstones than in sandstones.

Price (1959) suggests that joint spacing is related to the strain energy originally stored in the rock. Different rock materials under the same stress will have different strain energies, depending on the Poisson Ratio and Youngs Modulus of the material and therefore different joint spacing. It has also been theoretically shown that joint frequency is proportional to bed thickness and the inverse of the square root of the shear modulus of the neighbouring beds (Hobbs, 1967).

(ii) The development of jointing appears sporadic as not all joint sets are present at some outcrops (Figure 4).

Surface jointing may not necessarily be representative of the entire joint pattern originally developed in the rock (Chapman, 1958, and Secor, 1962). Incipient jointing in buried rocks undergoes surficial enhancement at the surface, where selective weathering processes and topographic relief may utilize and open up a few favourably oriented joint sets whilst others being unfavourably oriented remain closed. This may explain the absence of some joint sets at the various localities.

(iii) There is an angular difference between the cleat in the coal and the jointing in strata, above and below the coal seams (Figure 5).

FIGURE 5.—S diagrams of cleat and joint measurements (all poles to joints and clear; contours per 1% area).

1. Elemin Ravensworth Cut:
   a. poles to cleat; 36%, 30%, 20%, 10%, 0%
   b. poles to joints; 13%, 12%, 9%, 7%, 0%
2. Newraven No. 2 Cut:
   a. poles to clear; 22%, 20%, 15%, 10%, 5%, 0%
   b. poles to joints; 20%, 15%, 11%, 9%, 4%, 0%
3. Pykes Gulley Old Cut:
   a. poles to cleat; 34%, 32%, 22%, 10%, 0%
   b. poles to joints; 26%, 22%, 16%, 8%, 0%
4. Hebden Open Cut:
   a. poles to cleat; 15%, 10%, 0%
   b. poles to joints; 30%, 22%, 12%, 7%, 0%
5. Foybrook Open Cut:
   a. poles to cleat; 28%, 22%, 16%, 10%, 0%
   b. poles to joints; 20%, 16%, 10%, 8%, 6%, 5%, 0%

2α values are dihedral angles for north-northeast and northwest cleat and joints.

Generally there are only two prominent cleat directions and these correspond to the north-northeast and northwest shear joints.

The angular difference is probably related to the different dihedral angles (2α values, Figure 5) for the cleat and the corresponding joints ; the cleat dihedral angles are clearly larger than those for the joints. Also, Nickelsen and Hough (1967) consider that cleat in coal develops in response to stress differences too small to produce joints in sandstones and shales. Consequently, some of the angular variation could reflect slight changes in stress orientation between cleat and joint formation.

Origin of the Jointing

Joints which develop during the same tectonic cycle as folds and faults usually show well defined relationships to these structures (Nevin, 1949 ; Gilkey, 1953 ; Billings, 1954 ; de Sitter, 1956 and Goguel, 1962), whereas joints in areas where deformation has not been intense may show no definite relationships to the structures present (Parker, 1942 ; Harris, 1960 ; Hodgson, 1961 and Nickelsen and Hough, 1967).

In the Ravensworth area joints show no clear relationships to the structures present. Jointing appears independent of folding as there are no apparent relationships between joint trends and axial plane traces of the folds. Also the joints are essentially vertical and do not remain perpendicular to bedding around the folds. Blayden (1971) in a study of the Macquarie Syncline, near Newcastle also found that jointing developed independent of folding. Jointing also appears genetically unrelated to faulting, although some modification of joints has occurred during subsequent faulting movements.

In other areas where jointing is unrelated to tectonic structures (Parker, *op. cit.* ; Hodgson, *op. cit.*), the joints are systematic over large areas and consistent through considerable vertical extent of rock. Jointing in the Sydney Basin is also systematic over large areas and is similar to the joint pattern in the Ravensworth region (Moelle, *personal communication*, 1971). Two theories have been put forward to explain the formation of such joints ;

(i) Basement Propagation Theory (Kendall and Briggs, 1933 ; Blanchet, 1937, and Hodgson, *op. cit.*), where joints in areas were thick sedimentary piles overlie rigid basement blocks, are considered to propagate upwards due to alternating torsional stresses resulting from gravitational earth tides.

(ii) Uplift-Expansion Theory (Price, 1959, and 1966), where joints result from residual principal stresses reoriented during uplift and unloading such that the mechanics of joint formation are a natural consequence of their physical properties and the sequence of events to which the rocks are subjected, namely burial, compression and subsequent uplift.

The " uplift-expansion " theory is applicable for joint formation along the northern margin of the Sydney Basin since this region approximates the second model proposed by Price (1959, p. 160). Residual northeast compressive stresses probably existed in these rocks after the folding and thrusting movements. This model also satisfactorily explains the observed shear and tension joints in the Ravensworth area as discussed below. Since jointing appears independent of both folding and faulting in this area, joint development must have taken place after folding and during the later stages of thrusting.

The north-northeast and northwest shear joints would have formed first, at a point during uplift where gravitational loading became the intermediate principal stress. The north-south and east-west tension joints developed after further uplift, when the rocks passed into tension in the horizontal direction with gravitational loading the greatest principal stress. Subsequent thrusting movements have resulted in modification of these joints, particularly in strata adjacent the Hunter Thrust.

However, not all joints in the Sydney Basin are post-orogenic. Cook and Johnson (1970) present evidence from jointed " ironstone " intraclasts that some joints in the Basin developed early in the history of the sediments (prior to contemporaneous erosion). These joints would have been reactivated and modified during subsequent folding and faulting episodes.

Another hypothesis put forward by Diessel *et al.* (1967) assumes that distinct vectorial sedimentary features determine the distribution and attitude of the joint pattern in the Sydney Basin. They found that the strike of the major joint set coincided with the direction of deposition. This coincidence in orientation may not necessarily indicate a regional dependence of jointing upon sedimentary anisotropies. It could infer a process-response relationship where the principal basement structural anisotropies control the shape and morphology of the sedimentary basin and thus the regional palaeocurrent trends. Residual basement stresses, which are largely dependent on the basement morphology and the basement anisotropies, strongly influence the regional joint pattern. The jointing would therefore coincide with the regional palaeocurrent trends.

The formation of joints in the Sydney Basin is probably extremely complex and therefore cannot be fully explained by one simple model, such as isostatic adjustment. This model, however, satisfactorily explains the development of joints along the northern margin of the Basin. Even so this does not necessarily preclude the presence of early formed joints (Cook and Johnson, 1970, and Moelle, 1972) and the superimposed effects from upward propagation of basement anisotropies due to basinal subsidence (Blayden, 1971).

Conclusion

The structural history of Permian rocks along the northern margin of the Sydney Basin involves two phases of folding and a protracted period of thrusting. The first phase of folding is probably related to basement movements and a rejuvenation of basement structures in the overlying sediments. The second phase is related to northeast compression associated with thrusting movements along the Hunter Thrust.

The first folding phase produced open, subhorizontal, north-south trending cylindrical folds, characterized by the Lochinvar and Muswellbrook Anticlines. The second phase caused a broad arching of these structures about west-northwest and east-southeast axes producing dome and basin structures, such as the Belford and Loder Domes, and en echelon " pod " folds such as the Camberwell, Bayswater and Glennies Creek folds.

Four systematic joint sets exist in the Permian rocks and appear to have developed independent of both folding and faulting. It is proposed that these are postorogenic joints formed due to lateral expansion associated with isostatic uplift.

The following chronologic tectonic evolution is envisaged for the structural development of the northern margin of the Sydney Basin :

(i) first folding phase producing open north-south cylindrical folds
EARLY PERMIAN

(ii) development of the Hunter Thrust, associated with the second folding phase and the development of the Hebden Fault
LATE PERMIAN

(iii) regional uplift, and the formation of the north-northeast and northwest shear joints, followed by the north-south and east-west tension joints
EARLY TERTIARY

(iv) emplacement of igneous dykes, sills and plugs
LATE TERTIARY

It is possible that some folding accompanied Tertiary uplift, since Blayden (1971) considers that the Macquarie Syncline developed during the Cainozoic. He relates the geometry of the fold to basement faults and to the tilting of underlying basement blocks.

The timing of the Hunter Thrust is uncertain. Since the Permian stratigraphy is different on either side of the Thrust, it must have existed as a major structural weakness in the basement rocks underlying the Sydney Basin before the Early Permian. However, significant movement did not take place along this structure till the Late Permian. Changes in palaeocurrent trends and the nature of sedimentation in the Newcastle Coal Measures (Branagan and Johnson, 1970) and the upper portion of the Singleton Coal Measures (Gray, 1974) reflect the initiation of structural movement associated with the Hunter Thrust. The main period of thrusting which affected the entire Ravensworth stratigraphy, probably followed not long after this initial or embryonic stage.

Acknowledgements

The author acknowledges use of facilities at the University of Newcastle and the assistance given by Dr. K. Moelle, Dr. R. Offler, and Messrs. B. Vitnell and D. Marchoni during the course of the work. Thanks are extended to Liddell Colliery, Hebden Mining Company, Foybrook Open Cut and Liddell State Mine managements for access onto their property.

Finally, the author gratefully acknowledges the helpful discussion and comments by Dr. D. W. Durney in criticism of the various drafts of the paper. Technical assistance during preparation of the paper was provided by Macquarie University.

References

Badgley, P., 1965. *Structural and Tectonic Principles.* Harper, New York.

Billings, M. P., 1954. *Structural Geology.* (Second Edition. Prentice-Hall Inc., Englewood Cliffs.

Blanchet, P. H., 1937. Development of Fracture Analysis as an Exploration Method. *Am. Ass. Pet. Geol. Bull.*, **41**, 1748.

Blayden, I. D., 1971. On the Structural Evolution of the Macquarie Syncline, New South Wales. Ph.D. thesis, University of Newcastle (unpublished).

Booker, F. W., 1953. The Geology and Coal Resources of the Singleton-Muswellbrook Coalfield. Ph.D. thesis, University of Sydney (unpublished).

Branagan, D. F., and Johnson, M. W., 1970. Permian Sedimentation in the Newcastle Coalfield, N.S.W. *Proc. Australas. Inst. Min. Metall.*, **235**, 1.

Chapman, C. A., 1958. Control of Jointing by Topography. *J. Geol.*, **66**, 552.

Cook, A. C., and Johnson, K. R., 1970. Early Joint Formation in Sediments. *Geol. Mag.*, **107**, 361.

Diessel, C. F. K., Driver, R. C., and Moelle, K. H. R., 1967. Some Geological Investigations into a Fossil River System in the Roof Strata of the Bulli Seam, Southern Coalfield, N.S.W. *Proc. Australas. Inst. Min. Metall.*, **221**, 19.

Gilkey, A. K., 1953. Fracture Pattern of the Zuni Uplift. *Rep. Atom. En. Comm.*, R.M.E. 3050.

Goguel, J., 1962. *Tectonics*. W. H. Freeman & Co., San Francisco.

Gosh, S. K., and Ramberg, H., 1968. Buckling Experiments on Intersecting Fold Patterns. *Tectonophysics*, **5**, 89.

Gray, D. R., 1971. The Geology of the Hebden Region, N.S.W. B.Sc. Hons. thesis, University of Newcastle (unpublished).

Gray, D. R., 1974. Sedimentology of Permian Rocks Near Ravensworth, N.S.W., Northern Sydney Basin. *J. Roy. Soc. N.S.W.*, **107**, 17.

Harris, J. F., Taylor, G. L., and Walper, J. L., 1960. Relation of Deformed Fractures in Sedimentary Rocks to Regional and Local Structures. *Am. Ass. Pet. Geol. Bull.*, **44**, 1853.

Hill, P. H., 1966. Joints: Their Initiation and Propagation with Respect to Bedding. *Geol. Mag.*, **103**, 276.

Hobbs, D. W., 1967. The Formation of Tension Joints in Sedimentary Rocks: An Explanation. *Geol. Mag.*, **104**, 550.

Hodgson, R. A., 1961. Classification of Structures on Joint Surfaces. *Am. J. Sci.*, **259**, 493.

Kendall, P. F., and Briggs, H., 1933. The formation of Joints and the Cleat in Coal. *Proc. Roy. Soc. Edin.*, **53**, 164.

Moelle, K. H. R., 1972. On Structural Analyses of Oriented Bore Cores from West Wallsend No. 2 Colliery Holding. *Proc. Aus. I.M.M. Conference*, **43**.

Muehlberger, W. R., 1961. Conjugate Joint Sets of Small Dihedral Angle. *J. Geol.*, **69**, 211.

Nadai, A., 1950. *Theory of Flow and Fracture of Solids*. McGraw-Hill, New York.

Nevin, C. M., 1949. *Principles of Structural Geology* John Wiley & Sons, New York.

Nickelsen, R. P., and Hough, V. N. D., 1967. Jointing in the Appalachian Plateau of Pennsylvania. *Geol. Soc. Am. Bull.*, **78**, 609.

Osborne, G. D., 1929. Some Aspects of the Structural Geology of the Carboniferous Rocks of the Hunter River District between Raymond Terrace and Scone. *Proc. Linn. Soc.*, **54**, 436.

Parker, J. M., 1942. Regional Systematic Jointing in Slightly Deformed Sedimentary Rocks. *Geol. Soc. Am. Bull.*, **53**, 381.

Price, N. J., 1959. Mechanics of Jointing in Rocks. *Geol. Mag.*, **96**, 147.

Price, N. J., 1966. *Fault and Joint Development in Brittle and Semi-Brittle Rock*. Pergamon, Oxford.

Raggatt, H. G., 1938. Evolution of the Permo-Triassic Basin of East Central N.S.W. D.Sc. thesis, University of Sydney (unpublished).

Roberts, J. C., 1961. Feather Fracture and the Mechanics of Rock Jointing. *Am. J. Sci.*, **259**, 481.

Robinson, J. B., 1969. The Singleton Coal Measures. In Packham, G. H. (Ed.), The Geology of New South Wales. *J. Geol. Soc. Aust.*, **16** (1), 350.

Secor, D. J., 1965. Role of Fluid Pressure in Jointing. *Am. J. Sci.*, **263**, 633.

Sitter, L. U. de, 1956. *Structural Geology*. McGraw-Hill, New York.

Spencer-Jones, D., 1963. Joint Patterns and their Relationship to Regional Trends. *Geol. Soc Aust.*, **10**, 279.

Stuntz, J., 1972. The Subsurface Distribution of the "Upper Coal Measures", Sydney Basin, New South Wales. *Proc. Aus. I.M.M. Conference*, **1**.

Syme Gash, P. J., 1972. A Study of Surface Features Relating to Brittle and Semi-Brittle Fracture. *Tectonophysics*, **12**, 349.

Veevers, J. J., 1960. Geology of the Howick Area, Singleton Muswellbrook District, N.S.W. *B.M.R. Report No. 53*.

Voisey, A. H., 1958. Tectonic Evolution of North Eastern New South Wales, Australia. *J. Proc. Roy. Soc. N.S.W.*, **92**, 191.

School of Earth Sciences,
Macquarie University,
North Ryde, N.S.W., 2113.

(Received 21.12.1973)

EXPLANATION OF PLATES

Plate 1.—Fault graben in Hebden Open Cut Mine (072940C); north-northeast trending normal faults typical of the minor faulting in the Singleton Coal Measures.

Plate 2.—Joint trace pattern on bedding plane in creek bed near Bowmans Creek Bridge (063890C); north-northeast and northwest joint sets, with some north-south joints developed near hammer. Hammer oriented approximately north-south.

Plate 3.—Plume hackle marks or plumose pattern, and rib or augen structure along northwest joints, Durham No. 2 Open Cut Mine (026967C).

Plate 4.—Fractured pebble in pebbly arenite, creekbed (051993C); reflects a component of horizontal displacement along a N60E joint.

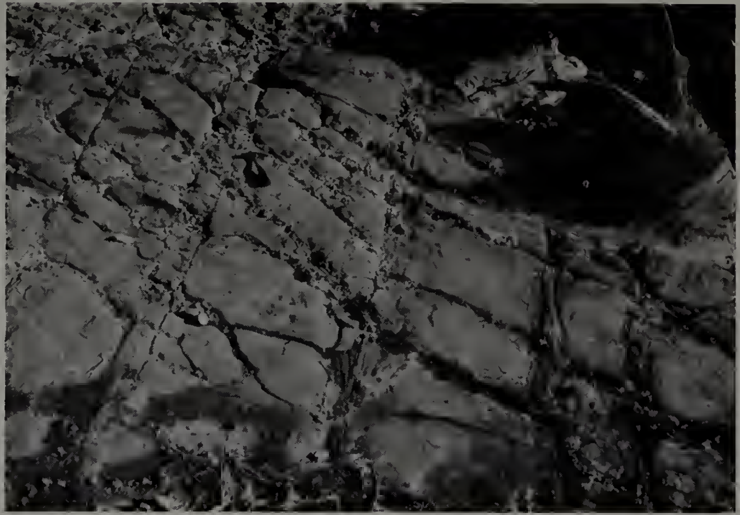

3

4

Journal and Proceedings, Royal Society of New South Wales, Vol. 108, pp. 29-36, 1975

The Geology of the Windellama Area, New South Wales

Ruth Mawson

Abstract—Mapping of some 50 km² in the Windellama area has revealed a sequence of 1,700 m or more of Early Devonian carbonate and terrigenous sediments downfaulted into rocks at least in part of Late Silurian age. The Devonian succession consists of approximately 200 m of terrigenous sediments overlain by about 283 m of carbonates, the Windellama Limestone, overlain in turn by a further 1,200 m or more of sandstones and siltstones. The Windellama Limestone yielded rich macro and micro-faunas of Early Devonian (Lochkovian) age. The overlying terrigenous sediments have yielded a coral-trilobite-brachiopod fauna of Early Devonian (Praguian) age.

Introduction

Windellama is located on the southern tablelands of New South Wales, 40 km S.E. of Goulburn and 224 km S.W. of Sydney. It is an area of primarily rolling terrain, the landforms to the east becoming more rugged where the underlying sediments have proved more resistant to weathering and erosion. The landform pattern tends to be meridional, reflecting regional strike of the rocks.

Previous Investigations

The earliest comment on the geology of the Windellama area appeared in 1834 on the original survey plan drawn up by Robert Hoddle; limestone hills were marked and the occurrence of " fine black marble " noted. Rev. W. B. Clarke (1860), in reporting on the limestone outcrops between Jacqua and Windellama, assumed a relationship between these and the Bungonia limestone.

The commercial potential of the limestone was realized as early as 1874 when John Young opened a small marble quarry on Limestone Creek, Windellama, to provide material for tiling the Great Hall at Sydney University. The curator of the New South Wales Technological Museum, R. T. Baker (1909), regarded the " marble " from Windellama as " the best black marble yet found in New South Wales ".

W. G. Woolnough (1909) was the first to refer to the fossiliferous limestones at Windellama as being Devonian in age and to note the lithologic contrast with Silurian limestones of the Bungonia district. In a detailed study of the limestone, J. E. Carne and L. J. Jones (1919) recognized two belts corresponding to those shown in Figures 3 and 4 of this paper. They considered the limestone to be of Silurian age. M. D. Garretty (1937) accepted this age assignment refining it to Late Silurian on the basis of fossils identified by W. S. Dun; no identifications were listed. He noted that between Bungonia and Windellama the sediments differed considerably from the surrounding Ordovician and Silurian sequences and, on the basis of further fossil identifications by W. S. Dun, dated these as Late Devonian.

G. F. K. Naylor (1949), in summarizing his previous work in the Goulburn district (1935*a*, 1935*b*, 1937, 1939), assigned all the limestone of the area a Silurian age and identified the terrigenous sediments as belonging to either Ordovician or Silurian belts.

It was not until 1970 that J. W. Pickett, in an unpublished report (1970), dated the Windellama limestone as Early Devonian (Siegenian-Emsian) age on the basis of: *Heliolites daintreei* Nicholson and Etheridge, *Favosites* cf. *ovatiporus* Hill and Jones, *Aulopora* sp., *Tryplasma* sp., *Microplasma* sp., and *Trupetostroma* sp.

Pickett and M. B. Huleatt (1971) refined the date to late Siegenian, based on a more complete faunal list. Pickett identified, *inter alia*, *Favosites* cf. *ovatiporus* Hill and Jones, *Heliolites daintreei* Nicholson and Etheridge, *Pseudamplexus princeps* (Etheridge), *Tryplasma* cf. *columnare* Etheridge, *Spathognathodus steinhornensis buchanensis* Philip, *S. inclinatus* (Rhodes), *Hindeodella priscilla* Stauffer, *Ozarkodina denckmanni* Ziegler, *Trichonodella inconstans* Walliser, *T. symmetrica pinnula* Philip, *Plectospathodus alternatus* Walliser.

In a report for the mining exploration firm of Asarco (Australia) Pty. Ltd., R. G. Dingwall and M. Kriewaldt (1972) suggested the sediments underlying the Windellama limestone to be Silurian and those overlying the limestone of

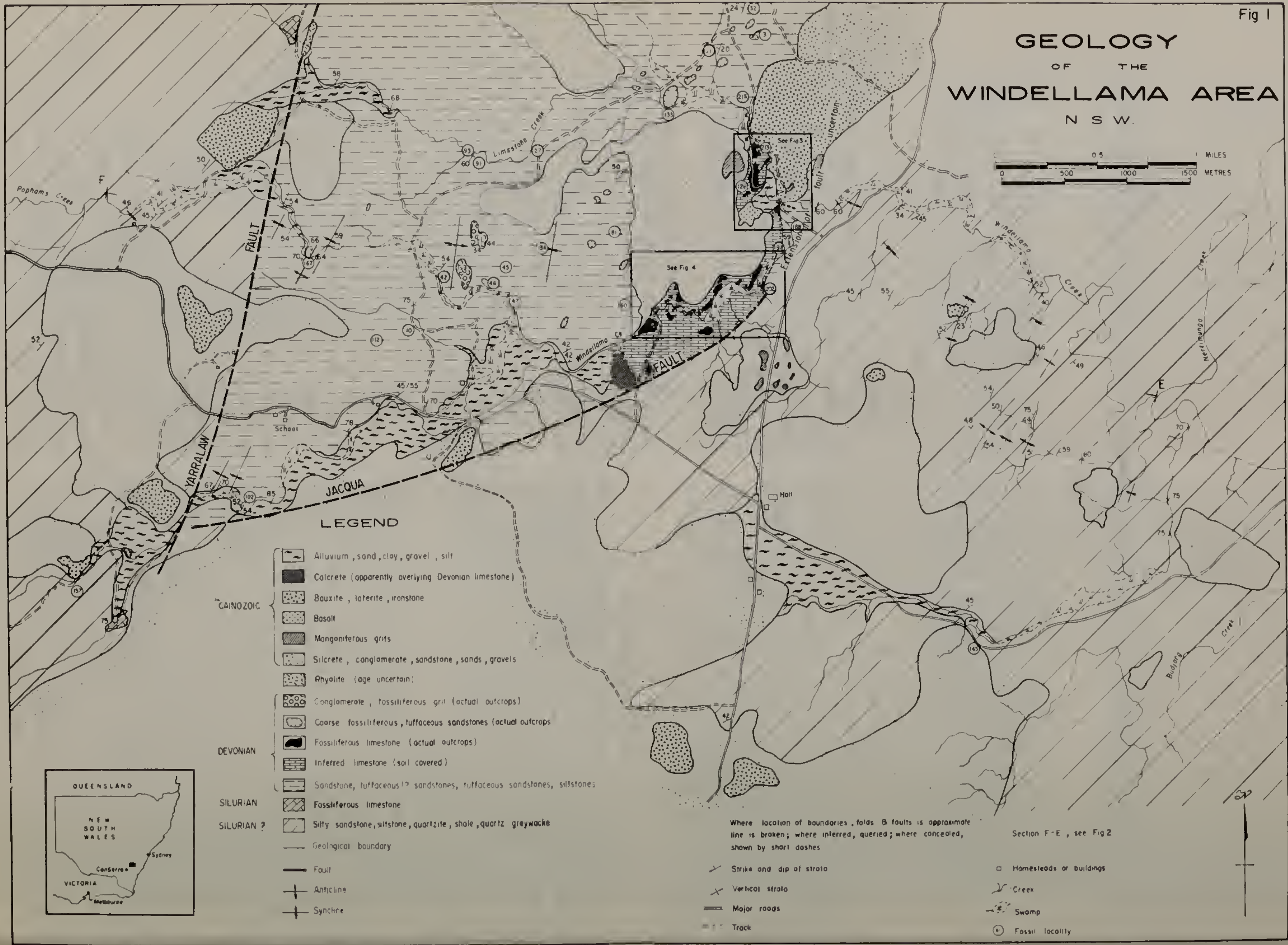
Fig 1
GEOLOGY OF THE WINDELLAMA AREA N S W.
0 0.5 1 MILES
0 500 1000 1500 METRES
LEGEND
CAINOZOIC
Alluvium, sand, clay, gravel, silt
Calcrete (apparently overlying Devonian limestone)
Bauxite, laterite, ironstone
Basalt
Manganiferous grits
Silcrete, conglomerate, sandstone, sands, gravels
Rhyolite (age uncertain)
DEVONIAN
Conglomerate, fossiliferous grit (actual outcrops)
Coarse fossiliferous, tuffaceous sandstones (actual outcrops
Fossiliferous limestone (actual outcrops)
Inferred limestone (soil covered)
Sandstone, tuffaceous (? sandstones, tuffaceous sandstones, siltstones
SILURIAN
Fossiliferous limestone
SILURIAN ?
Silty sandstone, siltstone, quartzite, shale, quartz greywacke
Geological boundary
Fault
Anticline
Syncline
Where location of boundaries, folds & faults is approximate line is broken; where inferred, queried; where concealed, shown by short dashes
Strike and dip of strata
Vertical strata
Major roads
Track
Section F-E, see Fig 2
Homesteads or buildings
Creek
Swamp
Fossil locality
QUEENSLAND
NEW SOUTH WALES
VICTORIA
Sydney
Canberra
Melbourne
YARRALAW FAULT
JACQUA FAULT
FAULT
Extension of fault uncertain
See Fig 3
See Fig 4
Limestone Creek
Windellama Ck
Windellama Creek
Nerrimunga Creek
Bulpong Creek
Pophams Creek
School
Hall
F
E

possible Permian age. The fossils found in the latter, collected northwest of the main body of limestone by Dingwall, were submitted to Dr. J. W. Pickett (1972 unpub. report) who identified: *Fenestella* sp., *Alveolites* sp., *Thamnopora* sp., generically indeterminate ectoprocts and coelenterates, and a small ribbed brachiopod. He suggested possible correlation with early Late Devonian marine sandstones at Goulburn and Nerriga.

Stratigraphy

Sedimentary rocks of Silurian and Devonian age occur within the area (Figures 1 and 2). The Devonian sediments are bounded on the west by a fault (the Yarralaw Fault) trending approximately north-south; a second inferred fault (the Jacqua Fault) marks their eastern and southern boundary. Overlying the Silurian-Devonian sequences is an extensive cover of Cainozoic sediments with, in one area, a minor veneer of loose ?Permian sediments, the latter being too limited in extent to be shown as a separate outcrop on Figures 1 and 3.

Silurian

The limestone that crops out in the south-western corner of the area mapped has been assigned a Late Silurian age on the basis of the presence of *Conchidium* or *Kirkidium* sp. The limestone is massive and jointed, but tends to dip steeply in a westerly direction. It is a compact limestone, somewhat dolomitized, dark grey to grey in colour, with scattered veins of calcite varying in thickness from 5 to 20 mm. Fossils from the limestone include: *Conchidium* or *Kirkidium* sp., and poorly preserved *Favosites* sp., *Heliolites* sp., large rugose corals, nautiloids, and abundant stromatoporoids.

The outcrop of limestone in the northwestern region is of a similar age, as indicated by the presence of *Conchidium* or *Kirkidium* sp., *Favosites* sp., gastropods and stromatoporoids. Despite some alteration owing to its proximity to the Yarralaw Fault, this limestone is of similar lithology to the limestone outcropping in the southeastern corner of the area mapped.

Sediments of Possible Silurian Age

The sediments cropping out in the south and east of the area consist of siltstones, argillaceous siltstones, shales, sandstones, quartzites, and cherts; in places, micaceous siltstone and shale grade into phyllite. The beds are generally from 1 to 30 cm thick and in areas of pronounced folding are strongly cleaved. They form a series of folds, the fold axes being approximately

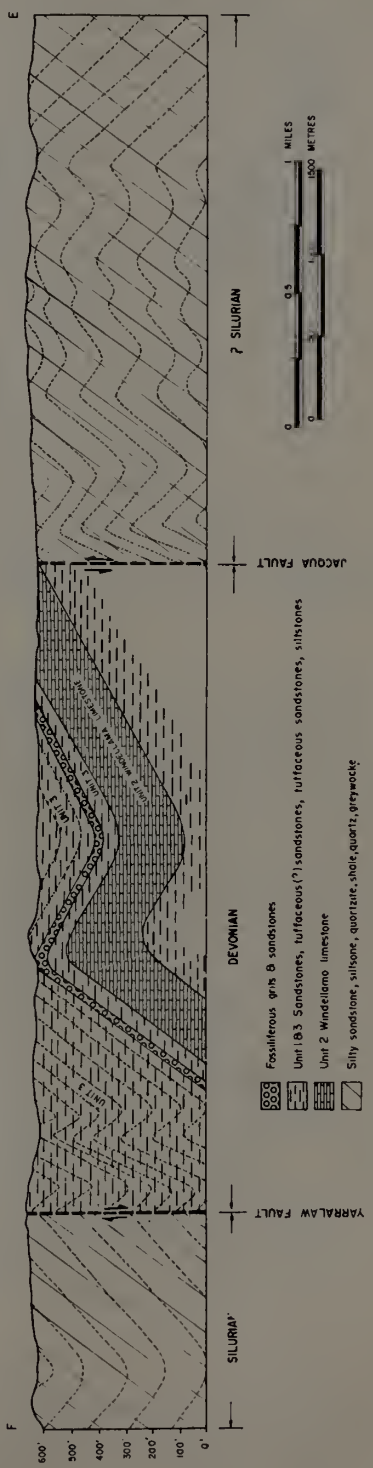

Fig 2 Bedrock Structure from Junction of Windellama and Nerrimunga Creeks 285° to Popham's Creek (F to E - see Fig 1)

meridional, running slightly east of north. Dips generally range from 40° to 52°, but adjacent to the faults, especially the Yarralaw Fault, and in the less competent beds, they steepen considerably. They have been regarded as Silurian or Ordovician by previous workers in the area (Woolnough, 1909 ; Carne and Jones, 1919 ; Garretty, 1937 ; Naylor 1935*a*, 1935*b*, 1937, 1939, 1949 ; Dingwall and Kriewaldt, 1972 unpub.). As no fossils have been recovered from these sediments in the area mapped, a positive age cannot be determined. Two factors suggest a possible Silurian age. Firstly, the limestones cropping out in association with similar terrigenous sediments in the west of the area are Late Silurian (see above). Secondly, the Devonian sediments immediately beneath the basal unit of the Windellama Limestone appear to be conformable with the underlying ?Silurian terrigenous sequence. If the latter were considerably older, one might expect discordance in dips and differing style of deformation. No sequence transitional from these sediments to the Devonian sediments has been observed.

Early Devonian

The lower part of the sequence consists of a series of sandstones, tuffaceous(?) sandstones, and siltstones. These are followed by fossiliferous limestones, and these in turn by fine tuffaceous sandstones, coarser tuffaceous sandstones, grits and conglomerates. These sediments can thus be divided into three units : 1. the sediments underlying the Windellama Limestone ; 2. the Windellama Limestone ; 3. the sediments overlying the Windellama Limestone. A group name could therefore be introduced with three constituent formations, but no formal nomenclature is proposed in advance of more extended regional mapping. Use is however made of the name Windellama Limestone, as the name first introduced formally by Pickett and Huleatt (1971), for the prominent development of highly fossiliferous carbonates.

The beds of the entire sequence strike in a direction a little east of north, and are gently folded. Approaching the Yarralaw Fault the folding becomes more intense, beds dipping at angles up to 70° (Figures 1 and 2).

(i) *The Lower Unit*

South of the junction of the Limestone and Windellama creeks, where the extension of the Jacqua Fault becomes uncertain, is a series of fine-grained thinly bedded sandstones, interbedded occasionally with siltstones. Beds range in thickness from 4 to 24 cm. The sandstones grade into fine tuffaceous(?) sandstones. Fossils found at localities 188, 198, and 202 (loose) consist of *Howellella* sp., other but indeterminate brachiopods, corals, and crinoid stems. The relationship of this lower unit to the ?Silurian sediments to the east is obscure. Because of poor outcrops and abundant soil cover the Jacqua Fault cannot be traced through the area, but the sediments of the lower unit are decidedly more sandy and not so shaly as the underlying ?Silurian sequence. It could be that there was no decided break in sedimentation between the two.

(ii) *The Windellama Limestone*

The Windellama Limestone crops out from the junction of Windellama and Limestone Creeks along the Windellama Creek to Burburba homestead (Figure 4). The major outcrop occurs on Limestone Creek in the vicinity of a disused quarry approximately 200 m north of the junction of Windellama and Limestone creeks (Figure 3).

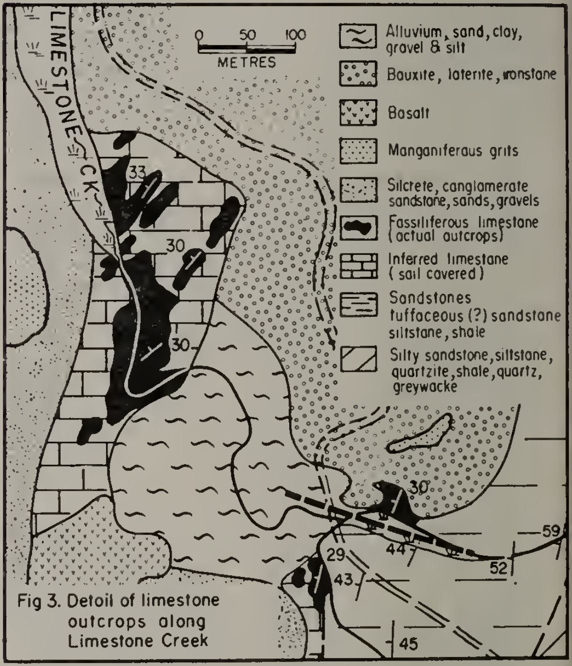

Fig 3. Detail of limestone outcrops along Limestone Creek

As far as one can tell from the limited outcrops, the limestone is conformable with the underlying sediments, but no actual outcrops demonstrate transition to or contact with the lower unit. Such a transition or contact is obscured by a cover of alluvium for a distance of only

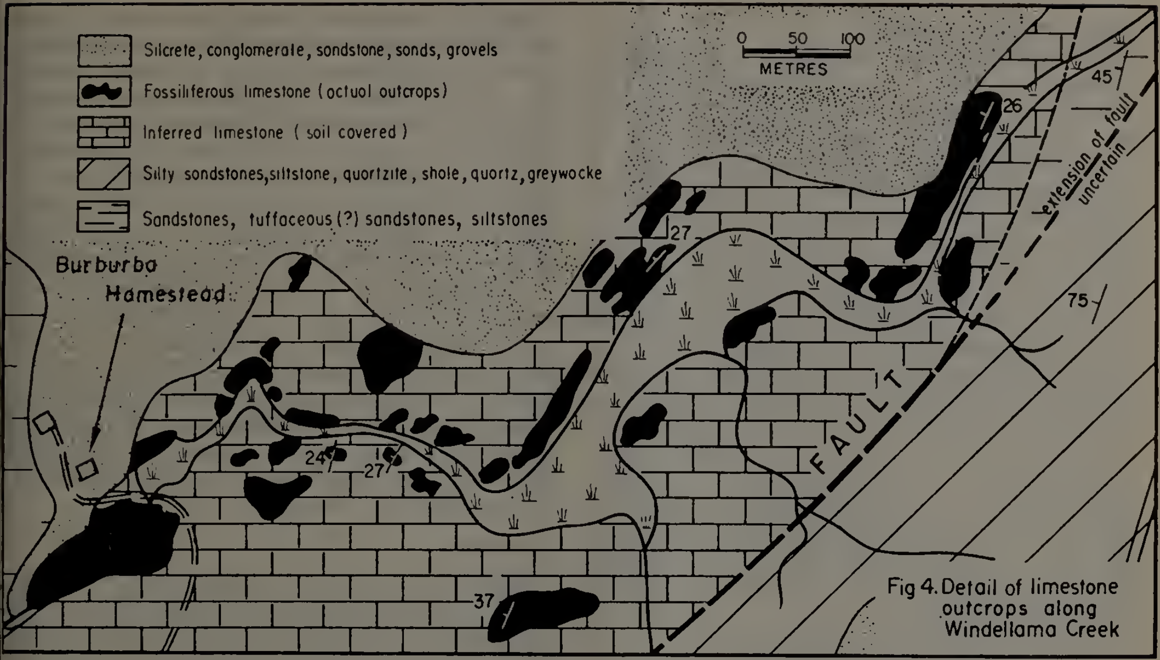

Fig 4. Detail of limestone outcrops along Windellama Creek

from 3·5 to 4 m at the base of the limestone on the north side of Limestone Creek a little to the east of its junction with Windellama Creek.

The total thickness of limestone is at least 283 m. The lowermost limestone is dolomitized and richly fossiliferous. Veins of varying thickness and splashes of calcite are common. Algae and stromatoporoids are the predominant fossils of the limestone at this level, but there is a notable change in fauna up the sequence. Algal material gives way to corals, both tabulate and rugose; brachiopods are also present.

Up the section the limestone becomes less dolomitic, more compact, well-bedded and silicified. This limestone is again richly fossiliferous, but the fauna consists almost entirely of corals, principally tabulates. Some stromatoporoids are to be found, but there is a complete dearth of brachiopods.

Exposures are good in the vicinity of the quarry on Limestone Creek; here well-bedded, highly fossiliferous black micrites in beds from 2 to 20 cm in thickness have three developments of silicification: the lowermost (11·4 m in thickness) occurs 125 m above the base of the limestone, the second (1·4 m in thickness) occurs 171 m above the base of the limestone, and the topmost (4·2 m in thickness) occurs 180 m above the base of the limestone.

The highest beds of the Windellama Limestone appear to be the massive dark grey to black limestones found at the creek crossing at Burburba homestead. These are less richly fossiliferous, and are extensively veined by calcite. North of the Windellama Church, there is a flat with outcrops of calcrete that may be connected with yet higher horizons of limestone not known in outcrop.

The following conodonts have been extracted from the topmost development of silicified beds: *Ambalodus* aff. *galerus*, *Belodella* sp. *devonica*, *Hindeodella equidentata*, *H. priscilla*, *Icriodus woschmidti*, *Ligonodina diversa*, *L. elegans*, *L. salopia*, *L. silurica*, *Lonchodina cristagalli*, *L. greilingi*, *L. walliseri*, *Neoprioniodus bicurvatus*, *N. excavatus*, *N. multiformis*, *Ozarkodina denckmanni*, *O. media*, *O. australis*, *Paltodus acostatus*, *P. unicostatus*, *Plectospathodus alternatus*, *P. extensus*, *P. flexuosus*, *Spathognathodus canadensis*, *S. exiguus philipi*, *S. remscheidensis*, *S. steinhornensis optimus*, *S. wurmi*, *Trichonodella excavatus*, *T. inconstans*, *T. symmetrica*, *T. symmetrica pinnula*. The identifications were kindly checked by Dr. G. C. O. Bischoff, Macquarie University.

The presence of the conodont *Icriodus woschmidti* among the fauna dates at least this part of the section as Lochkovian (cf. Savage, 1973; Link and Druce, 1972). The remainder of the fauna is consistent with this age assignment.

(iii) *The Upper Unit*

No direct contact between the Windellama Limestone and the overlying Devonian terrigenous sediments has been observed because of Cainozoic cover. Approximately 800 m north and slightly to the west of the junction of the Windellama and Limestone creeks (locality 218) there are fine grained fossiliferous siltstones, sandstones and tuffaceous sandstones. Similar lithologies and fossils occur at localities 32, 42, 45, 47, 60, 81, 91, 93, 102, 110, 112, 126, 133, and 167. The fauna of these sediments consists of *Howellella* sp., *Aulacella* sp., and other but indeterminate brachiopods, *Pleurodictyum megastoma*, *Cladopora* cf. *corrigia*, *Syringaxon* sp., *Fenestella* sp. nov. cf. *F. dargoensis*, indeterminate trepostome bryozoan, crinoid stems, *Koneprusites* sp., *Acanthopyge australis*, *Leonaspis* sp., *Cheirurus* (*Crotalocephalides*) *gaertneri* (*Alberti*), *Phacops* sp. and scutelluid trilobites. The presence of *C.* (*C.*) *gaertneri* (Alberti) dates these sediments as Early Devonian (Praguian).

The fine tuffaceous sandstones give way to a series of coarser fossiliferous tuffaceous sandstones that are best exposed in the northeast part of the area. In places, expecially at locality J1, the tuffaceous sediments show spheroidal weathering. Fossils found in this material at localities 3 and 27 include: *Howellella* sp., other orthid, spiriferid and rhynchonellid brachiopods, bryozoans, crinoid stems, rugose and tabulate corals.

Above the coarse tuffaceous sediments a series of poorly cemented, coarse-grained sandstones, grits and conglomerates containing pebbles of quartzite and clasts of clay is found.

Fossils collected earlier by R. G. Dingwall of Asarco (Australia) Pty. Ltd. from coarse weathered sandstones about 1·5 km N.W. of Burburba homestead were thought to be possibly Late Devonian in age (Pickett, 1972) but the presence of the fossils listed above, particularly the trilobites, including *Cheirurus* (*Crotalocephalides*) *gaertneri* (Alberti), from locality 218 where these deposits are *in situ*, confirms an Early Devonian age. Faunas similar to those from locality 218 and those collected by Dingwall have been found at localities 46 and 134.

?*Permian*

Immediately overlying the outcropping limestones on the left bank of Limestone Creek (locality 213) and also to a lesser extent on the right bank (locality 126), are blocky siltstones containing generally fragmentary Devonian trilobites, corals and brachiopods; these blocks are lithologically identical to the fossiliferous Devonian sediments cropping out about locality 218 to the north. This sequence is overlain upslope by laterites here regarded as probably Tertiary in age. The fossiliferous Devonian rocks are however, problematic. Blocks almost a cubic metre in size are present and conceivably still larger blocks may be buried; none of the material whatever shows evidence of rounding —all blocks are angular but much of this angularity is presumably due to breakup along joint planes during weathering. It seems probable that this material has been transported, possibly from the north from the area where outcrops of similar material are known, and spread out as a veneer across the truncated edges of the Devonian limestones, possibly during Permian times.

Cainozoic

Much of the area is capped by Cainozoic rocks: conglomerates, sandstones, grits, laterite and bauxite, silcrete, manganiferous grits and basalt, deep weathered remnants of a formerly vast sheet of sand, gravels and minor basalts.

The Tertiary sandstones are flat-lying, quartz arenite beds consisting predominantly of quartz grains with a few quartzite and shale fragments scattered throughout. Grain size ranges from fine to very coarse sand; sorting is usually poor; sub-rounded grains predominate, Because of poor consolidation, the sandstone readily weathers to sands and gravels. The manganiferous grits consist of sands and gravels cemented by a ferruginous and manganese-rich cement. The grains are predominantly sub-angular to sub-rounded, and are very poorly sorted. Some investigation of these has been made as regards their commercial value. The conglomerate that crops out in two isolated localities, 145 and 157, has angular to rounded clasts of up to 25 cm in diameter set in a fine matrix.

A small outcrop of Tertiary basalt occurs adjacent to a large outcrop of silcrete north-west of the junction of the Windellama and Limestone creeks. In this section it can be recognized as an alkaline olivine basalt containing clusters of olivine phenocrysts. Pinkish mauve titaniferous pyroxene is present, and the plagioclase is arranged subspherulitically. Needles and anhedra of opaque minerals and interstitial zoned plagioclase are also present.

Silcrete, laterite and bauxite deposits, derived from the weathering of older rocks and of Tertiary basalt, crop out frequently in the area.

Red to brown pisolitic ironstone weathers to produce a very distinctive pavement of spherical nodules about 5 mm in diameter. Vermiform laterites are common.

Between the Windellama Church and Burburba homestead there is a large deposit of calcrete, presumably derived from Devonian rocks, possibly the topmost horizons of the Windellama Limestone. Calcrete has also developed on some of the limestone outcropping along Windellama Creek to the northeast.

Structural Features

The fold pattern of the Silurian and Devonian bedrock is shown on Figures 1 and 2. The fold axes strike slightly east of north. Dips average about 46°, but to the west the dip of the thinly-bedded, strongly cleaved shales and fine sandstones increases sharply and in places near vertical bedding can be observed.

The patchiness and paucity of outcrop make the establishment of faults in the area difficult ; two major faults are however, inferred : a NNE trending fault in the west of the area along which the Devonian sequence has been downthrown against a demonstrably Silurian section shown to contain two lenses of fossiliferous limestone of Late Silurian (probably Ludlovian) age. This fault appears to be the southward extension of a fault shown on the Goulburn 1 : 250,000 sheet (Brunker and Offenberg, 1970) as separating Late Devonian sandstones on the east from an Ordovician flysch section to the west ; Brunker and Offenberg (1970) show this fault extending almost to Yarralaw Creek. The presently mapped fault, obviously an extension of Brunker and Offenberg's fault, has been here named the Yarralaw Fault. The Devonian sequence is noticeably more arenaceous than the typically shaly Silurian sequences to the west.

The intrusion of a prophyritic devitrified rhyolite that crops out in the NW corner of the mapped area may have been related to the fault. The rhyolite contains large feldspar fragments, quartz, and very altered spherulitic amphiboles. A very fine-grained red " quartzite ", consisting of at least 90 per cent quartz, lies adjacent to the rhyolite. It is apparently the altered product of the country rock. Large outcrops of quartz near the postulated junction of the two faults give further indication of a fault.

Owing to poor outcrops a second fault, the Jacqua Fault, cannot be picked up with precision on the ground but is inferred from the mapping. Mapping of the Windellama Limestone (Figure 1) shows that southwards along strike the limestones are consistently replaced by unfossiliferous shaly and sandy sediments thought to be of Silurian age, a relationship consistent with NE trending fault in this area. Towards the NW, where it would lie within generally poorly outcropping shales and sandstones (towards the eastern boundary of Figure 1) the position of the fault is uncertain. Similarly, the extension of the fault westward becomes speculative because of the widespread cover of Cainozoic sediments and the virtual absence of outcrop away from Windellama Creek. Almost due east of Burburba homestead, along the line of the fault, a typical fault breccia exhibiting slickenside crops out and can be traced for about 50 to 70 m along the fault line. Loose reef quartz abounds along the line of the fault S and SE of Burburba homestead.

The area about and south of the junction of Limestone and Windellama creeks presents some problems in interpretation. A small, more or less E-W tear fault is evident, deduced from the lateral displacement of the basal beds of the limestones. On the north side of Limestone Creek these are displaced eastwards about 125 m relative to the basal limestone on the south side of the fault ; the limestones on the north side therefore give the appearance of being replaced southward along strike by sandstone. The fault may be a small right lateral wrench fault.

Acknowledgements

I am grateful to Dr. J. W. Pickett of the New South Wales Geological Survey for his practical advice and encouragement, to Asarco (Australia) Pty. Ltd. for making available R. G. Dingwall and M. Kriewaldt's report on the area, to the graziers of Windellama for allowing me access to their properties, and to Dr. J. A. Talent and other colleagues in the School of Earth Sciences, Macquarie University, for their kindness and forebearance when confronted with assorted technical and academic problems.

References

Baker, R. T., 1909. Building and Ornamental Stones of New South Wales. *Technical Education Series No.* 16, *Sydney.*

Brunker, R. L., and Offenberg, A. C., 1970. Goulburn 1 : 250,000 Geological Series Map Sheet SI 55–12, *Geol. Surv. N.S.W.*

Carne, J. E., and Jones, L. J., 1919. The Limestone Deposits of New South Wales. *Min. Res. Geol. Surv. N.S.W.*, **25**, 411.

Clarke, Rev. W. B., 1860. *Researches on the Southern Gold Fields of New South Wales.* Reading and Wellbank, Sydney, 305.

Dingwall, R. G., and Kriewaldt, M., 1972. Final Report on Exploration Licence No. 279, Goulburn, N.S.W. *Asarco* (*Australia*) *Pty. Ltd., Adelaide Office Report No. 60* (*unpub.*).

GARRETTY, M. D., 1937. Geological Notes on the Country Between the Yass and Shoalhaven Rivers. *Jour. Proc. Roy. Soc. N.S.W.*, **70** (2), 364.

LINK, A. G., and DRUCE, E. C., 1972. Ludlovian and Gedinnian Conodont Stratigraphy of the Yass Basin, New South Wales. *Bur. Min. Res., Geol. Geophys. Bull.*, **134**, 136.

NAYLOR, G. F. K., 1935*a*. Note on the Geology of the Goulburn District, with Special Reference to Palaeozoic Stratigraphy. *Jour. Roy. Soc. N.S.W.*, **69**, 75.

NAYLOR, G. F. K., 1935*b*. The Palaeozoic Sediments near Bungonia: Their Field Relations and Graptolite Fauna. *Ibid.*, **69**, 123.

NAYLOR, G. F. K., 1937. Preliminary Note on the Occurrence of Palaeozoic Strata near Taralga, N.S.W. *Ibid.*, **71**, 45.

NAYLOR, G. F. K., 1939. The Age of the Marulan Batholith. *Ibid.*, **73**, 82.

NAYLOR, G. F. K., 1949. A Further Contribution to the Geology of the Goulburn District, N.S.W. *Ibid.*, **83**, 279.

PICKETT, J. W., 1970. Macrofossils from the " Windellama " Limestone. *Rep. geol. Surv. N.S.W., GS 1970/284* (*unpub.*).

PICKETT, J. W., 1972. Marine Fossils from Sandstones at Windellama. *Rep. geol. Surv. N.S.W. Pal. Report No. 72/2* (*unpub.*).

PICKETT, J. W., and HULEATT, M. B., 1971. Age of the Windellama Limestone. *Geol. Surv. Quart. Notes, No.* 2, 1.

SAVAGE, N. M., 1973. Lower Devonian Conodonts from New South Wales. *Palaeontology*, **16** (2), 307.

WOOLNOUGH, W. G., 1909. The General Geology of Marulan and Tallong, N.S.W. *Proc. Linn. Soc. N.S.W.*, **34**, 782.

School of Earth Sciences,
Macquarie University,
North Ryde, N.S.W., 2113.

(Received 5.6.74)

Journal and Proceedings, Royal Society of New South Wales, Vol. 108, pp. 37-51, 1975

The Merrimbula Group of the Eden-Merrimbula Area, N.S.W.

J. Steiner

Communicated by K. A. W. Crook

Abstract—The Upper Devonian Merrimbula Group is divided into three formations and represents a coarse red-bed succession which contains a finer-grained, drab sequence in the middle. The basal 90 m red-beds are termed the Twofold Formation. The middle drab sequence and the upper red-beds are defined as the 350 m Bellbird Creek and 430 m Worange Point Formation respectively. The Twofold Bay Formation records the deposits of a northerly sloping alluvial fan which was built up by a braided stream system and grade into the deposits of small meandering streams at the top. The lower Bellbird Creek Formation represents a marine transgression consisting of barrier island, littoral and shallow marine facies which are overlain by subaqueous deltaic deposits. During Bellbird Creek time the palaeoslope dipped toward the southeast with a southwest-northeast shore-line trend. The upper Bellbird Creek Formation consists of tidal flat deposits with some windblown dunes and lagoon deposits at the top. Average palaeotidal range may have been of the order of 4·6 m. During Merrimbula time palaeowind direction was toward the north. The Worange Point Formation records the deposits of a coastal plain, meandering river belt with the palaeoslope dipping gently toward the south-east. The basal Worange Point rocks probably represent subaerial, top-set deltaic beds. The Worange Point meander belt may have had a width of 2·6 km and the channel depth may have been characterized by a normal low water stage of 4 m and a maximum flood stage of 17 m. Clay mineralogy possibly indicates a palaeoclimatic warming-up trend during Merrimbula time.

Introduction

In the Eden-Merrimbula area Upper Devonian Merrimbula Group rocks outcrop over a large area (Figure 1) (Hall, 1969). The rocks have been folded during the Kanimblan orogeny in early to mid-Carboniferous time (Hill, 1967). The Merrimbula Group is divided into three formations (Table 1), (Steiner, 1972) and represents a coarse red-bed succession which contains a finer-grained, drab sequence in the middle. This report summarizes a detailed stratigraphic and environmental study of the Merrimbula Group (Steiner, 1966) which is based on several sections (Figure 2) recorded

Table 1
Stratigraphy

Brown (1931)	Hall (1957)		Steiner (1966)
" Upper or Lambie Stage "	Merrimbula " Formation " (Upper Devonian)	Merrimbula Group	Worange Point Formation
			Bellbird Creek Formation
			Twofold Bay Formation
	Wolumla Conglomerate Member		Wolumla Conglomerate Member
" Middle or Yalwal Stage "	Lochiel Formation (Upper Devonian)		Lochiel Formation
			Cusack Creek Member
" Lower or Eden Stage "	Eden Rhyolite (Middle Devonian)		Eden Rhyolite (Middle or Upper Devonian)
			Quarantine Bay Member
Un-named (Upper Ordovician)	Un-named (Ordovician ?)		Mallacoota Beds

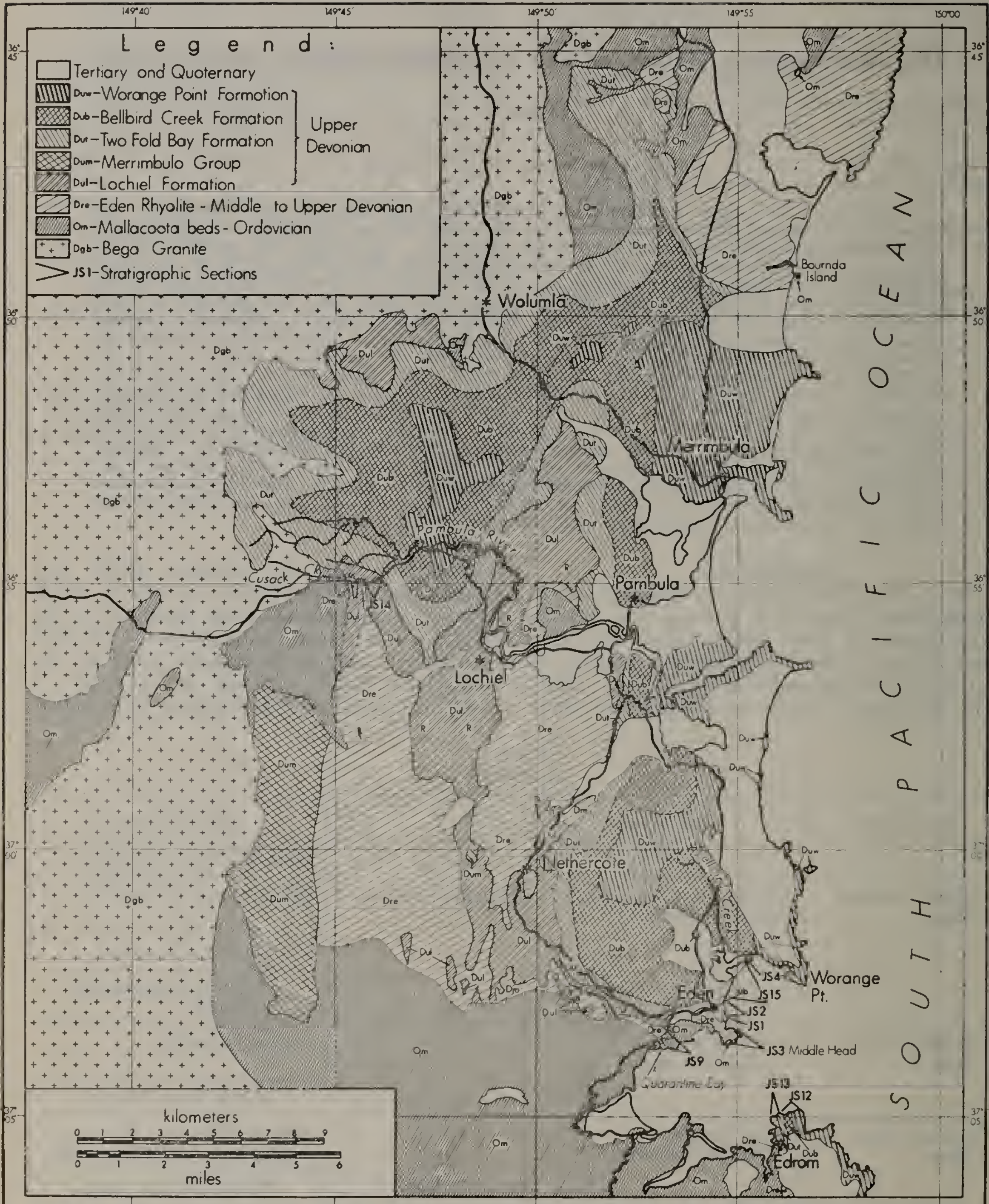

FIGURE 1.—Geological map of the Eden-Merrimbula area, N.S.W.

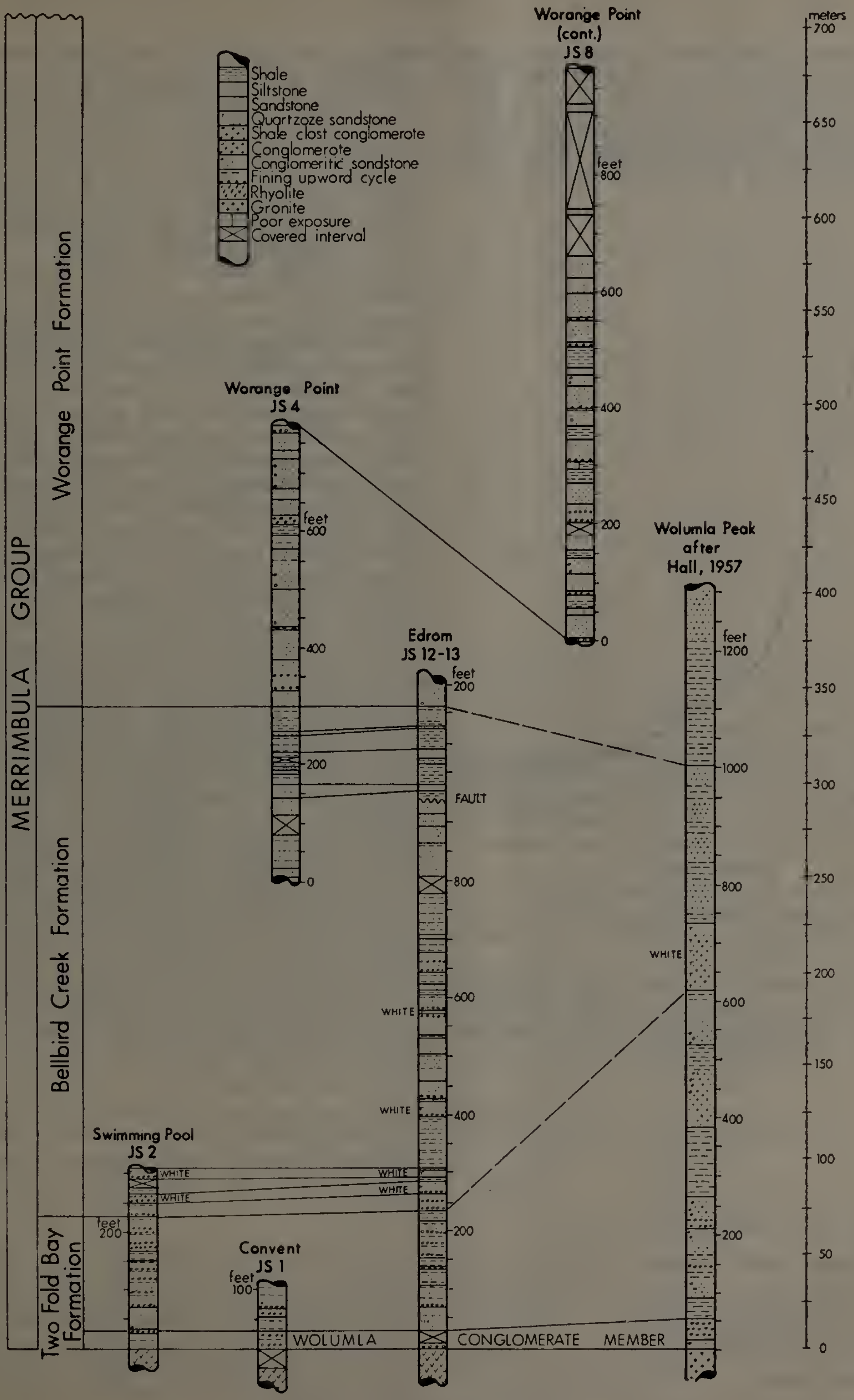

FIGURE 2.—Correlation of Sections.

and measured by the Bouma (1962) method and thin-section analysis. A total of 426 units (Figure 3) and 210 thin-sections have been described in detail, which represent approximately 800 m of the Merrimbula Group. Hill (1967) summarized the macrofauna and age of the Merrimbula Group and a preliminary report on the palynology is included as an appendix here.

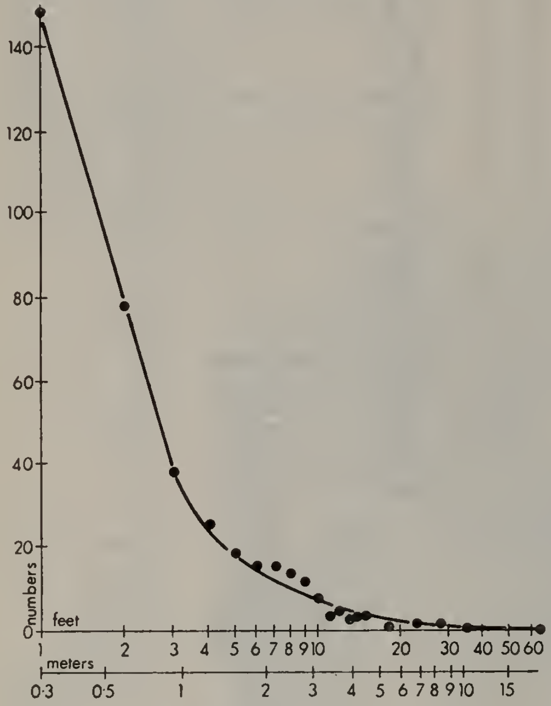

FIGURE 3.—Measured thickness versus number of sedimentation units.

The basal 90 m of red-beds of the Merrimbula Group are designated Twofold Bay Formation which locally unconformably overlies the Eden Rhyolite, the Mallacoota Beds, and the Bega Granite, but appears conformable with the underlying Lochiel Formation (Steiner, 1972). The Wolumla Conglomerate Member, as defined by Hall (1957) is at the base of the Twofold Bay Formation. The section JS1 (Figures 1 and 2) is designated the type section of the Twofold Bay Formation. The top of the Twofold Bay Formation is defined by the uppermost 1 to 1·5 m brick red mudstone horizon.

The middle 350 m of drab beds of the Merrimbula Group are termed the Bellbird Creek Formation, which conformably overlies the Twofold Bay Formation. The base of this Formation is defined by the top of the Twofold Bay Formation or the lowermost green or greyish mudstone or shale in access of 1 m. The transitional contact between these two formations is locally characterized by red, green, and brown mudstone lenses of outcrop scale. The top of the Bellbird Creek Formation and the base of the overlying Worange Point Formation is marked by apparent, multiple erosional contacts which are termed a paraconformity (Dunbar and Rodgers, 1967). This boundary is characterized by a colour change from the drab or green finer-grained beds of the Bellbird Creek Formation to the coarser red or reddish brown beds of the Worange Point Formation. The erosional surfaces are marked by scours and an abundance of nests of cobble and pebble-sized red and green mudstone or shale clasts. In discussing the Bellbird Creek Formation it is convenient to distinguish informally between the upper and lower Bellbird Creek Formation whose type sections are respectively JS12 and JS4 (Figures 1 and 2).

The upper red-beds of the Merrimbula Group (Figure 2) are the 430 m plus of the Worange Point Formation whose base is given by the top of the Bellbird Creek Formation but whose top remains undefined. The sections JS4 and JS8 serve as type section of the Worange Point Formation (Figures 1 and 2).

TABLE 2
Percentage Lithologies—Merrimbula Group

	Conglomerate %	Sandstone %	Siltstone %	Shale %	Cover %
Worange Point Formation	6	70	7	16	1
Upper Bellbird Creek Formation ..	0	48	11	27	14
Lower Bellbird Creek Formation ..	10	57	7	22	4
Twofold Bay Formation..	30	19	10	36	5
Merrimbula Group	11	52	9	23	5

TABLE 3

Colour Statistics of Merrimbula Group

	Lithology	Red Hues		Reddish-Brown %	Drab Hues		
		Purple %	Red %		Brown %	Green %	Grey or Whitish %
Worange Point Formation ..	Conglomerate	39	32	1	27	1	0
	Sandstone	23	23	3	45	6	0
	Sh. and sltst.	2	98	0	0	Trace	0
	Total	19	42	2	33	4	0
Bellbird Creek Formation ..	Conglomerate	0	0	33	4	8	55
	Sandstone	4	3	34	29	21	9
	Sh. and sltst.	0	2	9	12	78	0
	Total	2	2	25	21	39	11
Twofold Bay Formation ..	Conglomerate	48	26	0	11	13	2
	Sandstone	27	45	2	20	2	4
	Sh. and sltst.	40	51	0	1	6	2
	Total	40	41	Trace	8	8	3
Merrimbula Group	Total	14	25	12	25	19	5

Merrimbula Group

Lithology : The sections measured along the coastline (Figure 1 and 2) have 95 per cent outcrop. The percentages of lithologies of the Merrimbula Group are summarized in Table 2. The group is characterized by a high conglomerate (11 per cent) and low shale content (37 per cent). A breakdown of the percentage lithologies by Formation indicates that most of the pebble and boulder conglomerate is contained in the Twofold Bay Formation and its basal Wolumla Conglomerate Member (30 per cent). The poor sorting of Twofold Bay Formation is reflected in its low sandstone content (19 per cent). The conglomerate content of the lower Bellbird Creek Formation (10 per cent) represents granular conglomerate or quartzose grit. The upper Bellbird Creek Formation lacks conglomerate and is nearly evenly split between sandstone and shale plus siltstone. The Worange Point Formation has a high sandstone content (70 per cent) and low content of fine-grained sedimentation units (24 per cent).

Colour : The fresh and weathered colour of each of over 400 sedimentation units was obtained by comparison with the Rock Colour Chart of the Geological Society of America (1951). These fresh colour determinations are tabulated in Table 3. The Merrimbula Group as a whole is characterized by 39 per cent of the sedimentation units of red hues, 12 per cent of reddish-brown, and 49 per cent of drab hues. However, if the breakdown is done by formations and lithologies the following characteristics emerge. In the Twofold Bay Formation, 74 per cent of the conglomerate units, 72 per cent of the sandstone units, and 91 per cent of the shale and siltstone are red (Table 3). With regard to the

TABLE 4

Colour Modes per Lithology of the Merrimbula Group

Unit	Colour Mode	%
Twofold Bay Fm. :		
Conglomerate ..	Red and purple	73
Sandstone ..	Red and purple	71
	Minor brown	22
Shale and siltstone	Red and purple	91
Bellbird Creek Fm. :		
Conglomerate ..	Grey or white	56
	Reddish brown and brown	37
Sandstone ..	Reddish brown and brown	63
	Minor green	21
Shale and siltstone	Green	78
Worange Point Fm. :		
Conglomerate ..	Red and purple	70
	Minor brown mode	27
Sandstone ..	Red and purple	46
	Brown	48
Shale and siltstone	Red	98

Bellbird Creek Formation 67 per cent of the conglomerate units are white or drab, 50 per cent of the sandstone units are drab and 78 per cent of the shale and siltstone units are green. In the Worange Point Formation 71 per cent of the conglomerate units, 46 per cent of the sandstone units, and 100 per cent of the shale and siltstone units are red (Table 3). The colour modes of the Merrimbula Group per lithology are summarized in Table 4 and clearly indicate oxidizing conditions for the deposition of the Twofold Bay and Worange Point Formations and more reducing conditions for the Bellbird Creek Formation.

TABLE 5

Summary of Cross-Stratification Modes

Azimuthal mode 1 .. (aqueous) Twofold Bay Fm.	Vector sum : N359°E, standard deviation 10° Dipmodes : 12·5°, conglomerate, planar, small scale 17·5°, sandstone, simple, large and small scale 22·5°, conglomerate, simple, large and small scale
Aeolian mode .. Merrimbula Group	Approximately due north Dip modes : 32·5°, sandstone, planar, large scale 32·5°, mainly granular conglomerate, planar, small scale
Azimuthal mode 2 .. (aqueous) Bellbird Creek Fm.	Vector sum : N61°E, standard deviation 23° Dip modes : 7·5°, sandstone, simple, small scale 12·5°, conglomerate, planar, large scale 22·5°, granular conglomerate, simple and trough, small and large scale
Azimuthal mode 3 (aqueous) Bellbird Creek and Worange Point Fm.	Vector sum : N133°E, standard deviation 18° Dip modes : 12·5°, sandstone, simple and planar, small and large scale, slumped cross-stratification* 22·5° conglomerate, simple, small scale 25°, sandstone, planar, large scale, slumping*

* 48 cross-stratification reading were taken of slumped cross-laminations.

Cross-stratification : Cross-bedding is common in the Merrimbula Group rocks and a total of 543 cross-bedding directions have been taken. A rose diagram of 217 Merrimbula Group cross-bedding shows three azimuthal modes (Figure 4). Mode 1 is a strong northerly mode, while Modes 2 and 3 are north-easterly and south-easterly respectively. The modal vector sums, modal standard deviations, and cross-bedding characteristics of these modes are summarized in Table 5 which utilizes terminology of McKee and Weir (1953).

The three modes are strongly dependent on stratigraphic position, as shown in a series of 26 cross-bedding rosettes plotted every 30 m for the 800 m of the Merrimbula Group (Figure 5, column 4). The 26 rosettes incorporate twice the cross-stratification readings since a 50 per cent stratigraphic overlap is employed in plotting the rosettes. Cross-bedding rose diagrams for each formation also show that the three modes are characteristic of one or two of the Formation (Figure 6). Mode 1 is typical of the Twofold Bay Formation. The Bellbird Creek Formation is characterized by Modes 2 and 3 and a subsidiary mode 180° from Mode 2 is also present. The trends of ripple marks of the Bellbird Creek Formation are either parallel or perpendicular to Mode 2. The Worange Point Formation yields cross-bedding directions

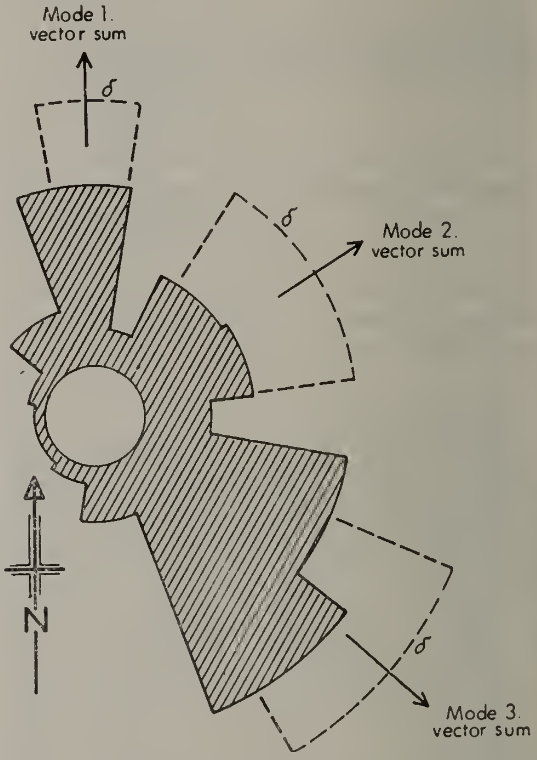

FIGURE 4.—Cross-stratification of Merrimbula Group

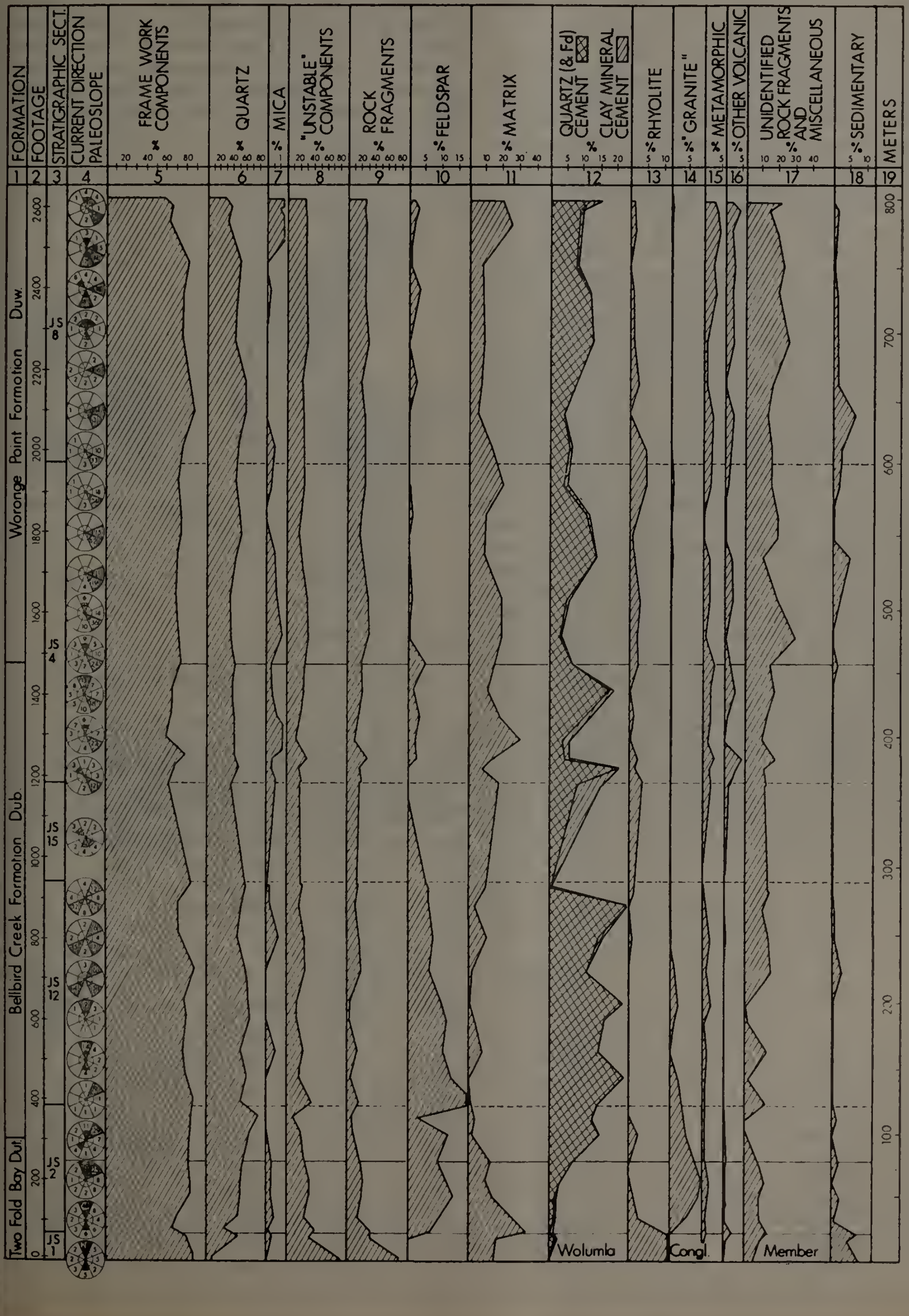

FIGURE 5.—Sedimentary petrology and cross-stratification

of Mode 3 (Figure 6). The cross-stratification data yield the following conclusions:

Paleoslope direction was toward the north during Twofold Bay time and toward the southeast during Worange Point time. During Bellbird Creek time the paleoslope was also dipping toward the southeast with the shoreline trended southwesterly to northeasterly. The details of the cross-bedding and granularmetric analyses (Steiner, 1966) suggest a palaeowind direction from south to north (Table 5). Seventy four per cent of the aeolian strata contain some red pigment and range in colour from purple to red and brown (Table 6). Other directional data such as channel direction (23 readings), directions of thinning and lensing of coarse clastic units (28 readings) and trends of ripple marks (40 readings) are in general agreement with the palaeocurrent conclusions based on cross-stratification. Crook (1967) utilized these palaeocurrent directions in interpreting the regional Upper Devonian palaeogeography.

Direction of transport and colour: For this purpose it is convenient to group purple, red, reddish-brown, and brown interbeds as " red pigmented " strata and green, grey and whitish ones as " neutral " strata of these terrigeneous Merrimbula Group rocks. In the Twofold Bay and Worange Point Formations the vast majority of sedimentation units contain red pigment and therefore the units with down-palaeoslope cross-bedding are also red to brown. However, the colours of the Bellbird Creek Formation has both a terrestrial down-slope and a longshore source (Figure 6), as indicated by equal proportions of red-pigmented (50 per cent) and neutral strata (50 per cent) (Table 6). Colour of the strata is shown to be roughly a function of the colour of the source material, the transportation history, and redox potential of the final environment of deposition (Table 3, 4, 6). Down-palaeoslope current directions are associated with sedimentation units consisting of 75 per cent " red pigmented " strata and 25 per cent of strata of neutral colours. Current direction parallel to the palaeoslope are associated with units comprising 45 per cent " red pigmented " strata and 55 per cent interbeds of " neutral " colour. For the up- and down-palaeoslope directions the proportions are

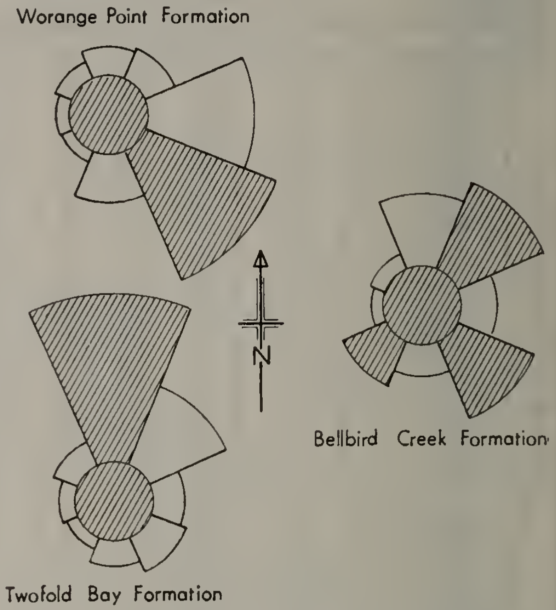

FIGURE 6.—Cross-stratification by Formation.

TABLE 6

Colour Statistics and Current Direction of the Bellbird Creek Formation

Current Direction	Footage of Total %	Red Pigmented Strata			Neutral Strata	
		Red and Purple %	Reddish-brown %	Brown %	Green %	Grey or White %
Down-palaeoslope	30	8	16	51	19	6
Down-and up-palaeoslope	14	0	39	24	37	0
Parallel to palaeoslope	44	0	32	13	26	29
Current direction not known	12	4	4	18	48	26
Total Bellbird Creek Formation ..	100	4	25	21	39	11
Aeolian component	Minor	55		19	26	0

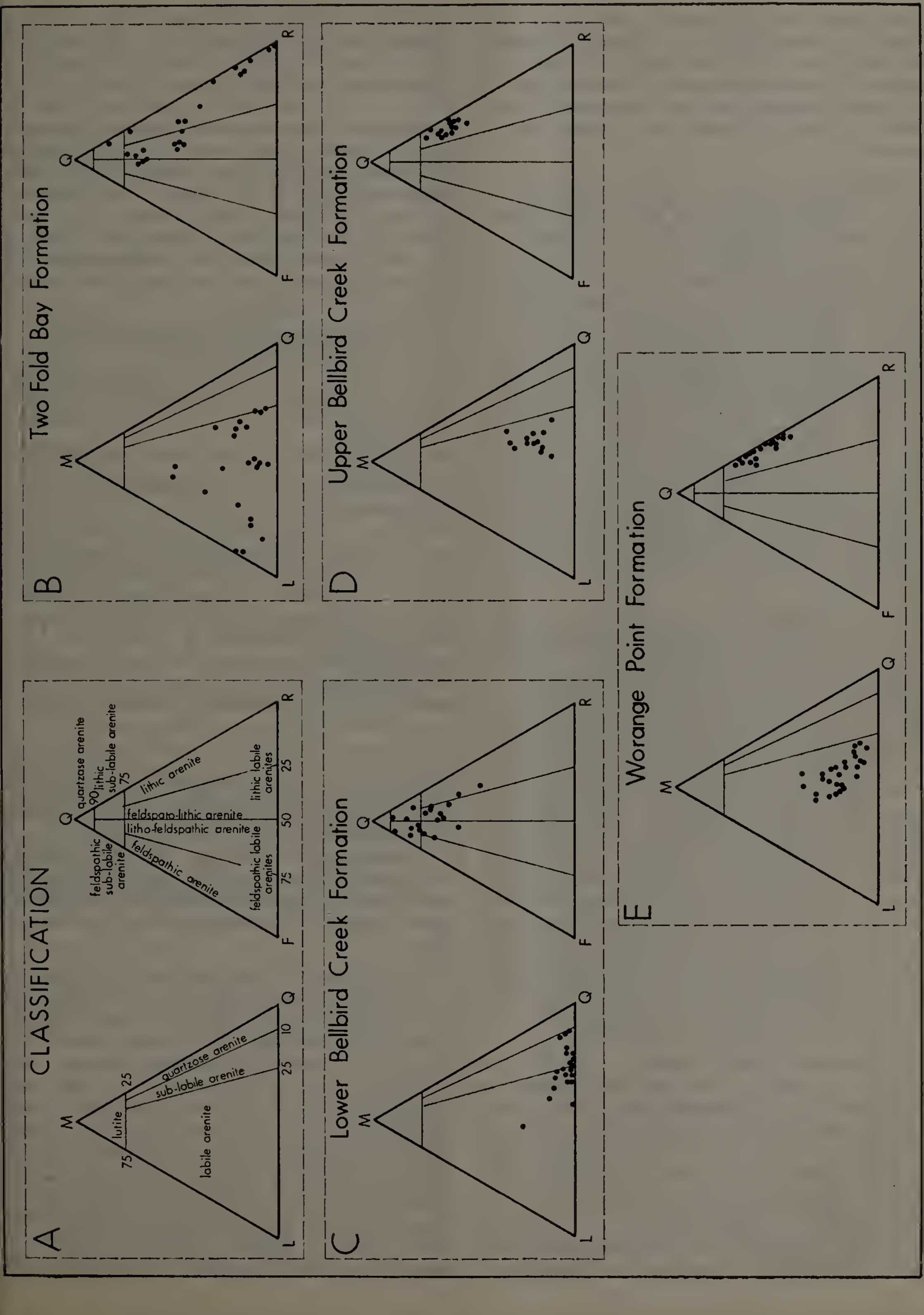

FIGURE 7.—Classification of Merrimbula Group sandstones.

63 per cent "red pigmented" and 37 per cent "neutral" strata (Table 6). These percentages are interpreted to indicate that the red pigment originated up-palaeoslope and after transport to the paralic environment of deposition of the Bellbird Creek formation was progressively reduced.

Sedimentary petrology: The textural details of the sedimentation units of the Merrimbula Group are schematically shown in Figure 2. Crook's (1960) classification of arenites is utilized for the sandstones of the Merrimbula Group (Figure 7*a*). The Lower Twofold Bay Formation, including the Wolumla Conglomerate Member, consists of lithic sandstone, while the upper Twofold Bay Formation units are predominantly feldspatho-lithic sandstones (Figure 7*b*). The lower Bellbird Creek Formation includes two distinct interbedded lithologies which on the QFR diagram (Figure 7*c*) cover areas which are roughly equal to the fields of sublabile sandstone and lithic labile sandstone respectively. The upper Bellbird Creek and Worange Point Formation units consist exclusively of lithic labile sandstone (Figure 7*d* and 7*e*).

The point-count data and the more detailed mineralogical and petrological identifications are also plotted in log form (Figure 5) for the Merrimbula Group and may be summarized as follows. The framework components (phenoclasts), vary between 63 per cent and 88 per cent indicating fair to good sorting (Figure 5, column 5). The extremes of sorting are more typical of the lower Bellbird Creek Formation. The percentage quartz generally varies between 40 per cent and 60 per cent of total (Figure 5, column 6), but quartz content is low in the Wolumla Conglomerate Member (10 per cent–45 per cent) and high in the lower Bellbird Creek Formation (75 per cent). Major unstable components (feldspar and rock fragments) vary around 30 per cent ± 10 per cent and remain fairly constant throughout the Merrimbula Group except in the Wolumla Conglomerate where they reach 80 per cent (Figure 5, column 8).

The matrix content (Figure 5, column 11) is variable according to sorting, but is generally low in the high-energy lower Bellbird Creek units. The silica and clay cement content is summarized in Figure 5, column 12 and silica cement is very high (maxima 25 per cent) in the quartzose granular conglomerates and sandstones of the lower Bellbird Creek Formation.

The clay mineralogy of the fine-grained units of the Merrimbula Group has been determined by the Conolly (1965) method. Kaolinite content varies from zero to 44 per cent and illite content from 56 per cent to 100 per cent. The average kaolinite content is increasing and illite content is decreasing up-section (Table 7). A similar average upsection kaolinite increase can be deduced from Conolly's (1965) data of the Hervey and Cocoparra Groups of the Upper Devonian rocks of the central and western province of New South Wales (Table 7). Although the kaolinite content is largely a function of provenance, the average up-section kaolinite increase may be interpreted as a palaeoclimatic warming-up trend (Van Houten, 1964) during the deposition of the Upper Devonian rocks of New South Wales.

TABLE 7

Clay Mineralogy of Merrimbula Group

	Illite	Kaolinite
Worange Point Fm. .. .. (2 samples)	75·5%	24·5%
Bellbird Creek Fm. .. .. (5 samples)	84·7%	15·3%
Twofold Bay Fm. .. .. (4 samples)	94·5%	5·5%

Clay Mineralogy of Hervey and Cocoparra Group

	Illite	Kaolinite
Worange Point Fm. equivalent (8 samples)	53·7%	46·3%
Bellbird Creek Fm. equivalent (26 samples)	63·8%	36·2%
Twofold Bay Fm. equivalent (2 samples)	70·0%	30·0%

Granularmetric analyses of thin sections employing Friedman's (1961) and Sahu's (1964) methods support the environmental conclusions listed below under formational headings (Steiner, 1966).

Provenance: The feldspar content (Figure 5, column 10) varies between 2 per cent and 17 per cent, but is generally low in the Wolumla Conglomerate Member and the Worange Point Formation. Maximal feldspar content was recorded in the undifferentiated Twofold Bay Formation and in the lower Bellbird Creek Formation where the feldspar is fairly fresh. The feldspar appears cloudy and weathered in the upper Bellbird Creek and Worange Point Formations. Much of this feldspar is probably of granitc origin since the feldspar point counts mimic that of granite fragments (Figure 5, compare columns 10 and 14). The point-count data of other rock fragments (rhyolite, Figure 5, column 13; other volcanic rock, column 16; metamorphic rocks, column 15; and sedimentary rocks, column 18) permit the following provenance conclusions:

The source of the Wolumla Conglomerate near Eden was a rhyolitic volcanic terrain (i.e. Eden Rhyolite). The source of the undifferentiated Twofold Bay and lower Bellbird Creek Formations was a granitic terrain (i.e. Bega granite), and some low-grade metamorphic rocks (i.e. Mallacoota Beds). The source of the upper Bellbird Creek and Worange Point Formation was a general terrain consisting of metamorphic rocks, granite, volcanic rocks, and sedimentary rock (i.e. Mallacoota Beds, Bega granite, Eden Rhyolite, possibly Lochiel basalts, sedimentary rocks, intraformational Merrimbula Group detritus).

Twofold Bay Formation

Wolumla Conglomerate Member, although not always present (Figure 1), consists of massive boulder to pebble purple and red conglomerate and varies in thickness from 1·5 m to 15 m. The well-rounded phenoclast consist of rhyolite, quartz porphyry, granite, sandstone, quartzite, quartz and fine-grained metamorphic rocks. The composition of the phenoclasts is strongly dependent on the lithology of the underlying rocks. Near Eden and at Edrom the phenoclasts are rhyolite pebbles (Figure 5) which tend to be angular and subangular. The coarse-grained units particularly are characterized by high lenticularity and lateral stratigraphic discontinuity. The Wolumla conglomerate member grades transitionally into the overlying undifferentiated strata of the Twofold Bay Formation. The Wolumla conglomerate may be termed a fanglomerate (Dunbar and Rodgers, 1957) and thus represents the deposits of the upper part of an alluvial fan which sloped downward toward the north as indicated by the strong northerly cross-stratification mode (Figure 5). This fan appears to be a continuation of the underlying Lochiel alluvial fan (Steiner, 1972) which was accompanied by basic extrusions.

Undifferentiated Twofold Bay Formation: The red bed sequence of the total Twofold Bay Formation varies in thickness between 70 m near Eden and 180 m in the western part of the map area at Wolumla Peak. The thickness variations can be interpreted as reflecting Eden Rhyolite relief at the time of deposition. Many of the 50–60 units measured are lenticular on the outcrop scale to such an extent that the recorded units represent only one possible vertical profile. Sorting is very poor and the brick red, sandy and silty mudstone units of 1 m to 4 m thickness lack internal stratification. Scour structures, channel-type units, washouts, subaerial desiccation structures, and less common ripple marks have been observed. Isolated shale clasts and nests of shale clasts and some lenses and wedges of shale-clast conglomerates are present throughout the whole sequence. Cross-stratification is common with a strong northerly mode which swings to the north-northeast in the upper part of the Formation (Figures 5 and 6). Only fragmentary plant fossils have been recovered from the formation.

In a vertical profile the units are arranged in fluvial fining-upwards cycles (Allen, 1965). These cycles are less well defined in the Twofold Bay Formation than in the Worange Point Formation or the Old Red Sandstone of Great Britain (Allen, 1962). Particularly in the Wolumla Conglomerate Member and in the lower Twofold Bay Formation the upper fine-grained sub-units of the cycles are missing. The fluvial fining-upward cycles vary in thickness from 1 m or less to 4 m mainly in the upper part of the Twofold Bay Formation. Incomplete coarse-grained fluvial cycles indicate deposition by a braided stream regime (Douglas, 1962; Shelton and Noble, 1974).

It is concluded that the Twofold Bay Formation probably records the deposits of a northerly to north-northeasterly sloping alluvial fan which was built up by the deposits of a small braided stream system which transitionally grade into meandering stream deposits toward the top of the formation. Structureless, brick-red mudstone units are interpreted as occasional mudflow deposits. In general moderately arid to semiarid climate is favourable for the development of alluvial fans (Blissenbach, 1954).

Bellbird Creek Formation

The lower Bellbird Creek Formation includes numerous white granular conglomerate (grit) with less than 5 per cent small pebbles, brown or grey sandstone, and green and brown sandy shale. The overall sorting is considerably better than in the rest of the Merrimbula Group. Individual laminae of the grits are very well sorted and are often truncated at the top by an erosional surface. The grits are usually bimodal, with a major mode in the 2–4 mm size range. Such size modes are generally thought to be very uncommon in sediments around the world (Pettijohn, 1957). Sets of planar cross-stratification of less than 0·3 m thickness are common, but large-scale planar and simple cross-stratification are also present. Current direction is characterized by three modes (Figures 5 and 6) which are 90° and 180° apart. Following Tanner (1955, 1959) these modes have been interpreted as shore-line trend and palaeoslope direction, as discussed above. Small-scale scour structures and sand pockets are interpreted as back shore features (McKee, 1957 ; Soliman, 1964). Shale clasts are present throughout. Organically disturbed or burrowed laminae are not as common as in the upper Bellbird Creek Formation but broken, curled and bent laminae are fairly common and are interpreted as desiccation structures. Many of the disturbed horizons are due to slumping and load casting. The Lower Bellbird Creek Formation contains some graded bedding and reversed graded bedding in the form of coarsening-upward cycles of various magnitude. Coarsening-upward units are typical of barrier island deposits (Straaten, 1961). Sedimentation units are much more laterally continuous than in the Twofold Bay Formation and some thicker sequences (3 to 25 m) can be correlated over a distance of up to 5 km indicating sheet-like sedimentation units. The total Bellbird Creek Formation has yielded a marine fauna.

The basal 75 m of the lower Bellbird Creek Formation record the deposits of a marine transgression in which barrier island, littoral and shallow marine facies have been identified. The overlying 160 m record the deposits of a subaqueous deltaic phase including some littoral and lagoonal or shallow marine deposits.

The Upper Bellbird Creek Formation characteristically consists of medium-grained sandstone and laminated finer sedimentary rocks. The maximum grain size is only slightly larger than the mean grain-size, indicating good sorting. Unstratified, red mudstone units which are typical of the Twofold Bay and Worange Point Formation are not present in the entire Bellbird Creek sequence. In the upper Bellbird Creek Formation units of alternating brown sandy and green, muddy laminae are typical whereby groups of laminae are often lenticular. The types of cross-stratifications are similar to those in the lower Bellbird Creek Formation. Ripple marks of all types are particularly common and are also present in reddish well-laminated shale. Interference ripples and rippled troughs have also been observed. Shale clasts are also common. Ball and pillow structures which have been attributed to quicksand conditions (Shelley, 1964 ; Shearman, 1964) have been observed. Units of burrowed and disturbed laminations are common in specific regular intervals. Broken and curled laminae indicative of desiccation also occur in regular intervals. Rain prints (Hall, personal communication) have been reported and also argue in favour of at least temporary subaerial exposure. Slumping and load casting are present. Sedimentation units are of constant thickness and are laterally continuous facilitating correlation similar to the lower Bellbird Creek Formation. In a vertical profile many of the sedimentation units are grouped into eight tidal flat fining-upward cycles (Klein, 1971). The coarser lower units of these cycles commonly have ripple mark trends perpendicular to the ancient shore-line while in the upper, finer-grained units the ripple mark trends tend to parallel the shoreline. The tidal flat fining-upward sequences range from 3 m to 9 m and average 4·6 m. Granularmetric analysis identified some dune deposits (Steiner, 1966).

The basal 85 m of the upper Bellbird Creek Formation consists of deltaic tidal flat deposits with an average tidal range of 4·6 m neglecting compaction. The upper 25 m are interpreted as transitional facies of lagoon, marsh and coastal stream deposits associated with a few wind-blown units at the top.

The Worange Point Formation

The thickness of the formation is 420 m plus because the top of it is undefined. The formation which has yielded no macrofossils constitutes the upper major red-bed sequence of the Merrimbula Group and due to the presence of well developed fluvial fining-upward cycles it resembles many red-bed sequences around the world (Allen, 1965). The basal 100 m lack conglomerates and are also devoid of sandy red mudstone units in excess of 3 m. In general such units are less common than in the Twofold Bay Formation. Intraformational conglomerate consisting of shale-clast are common and vary in thickness from 15 cm to 2 m. The conglomerate phenoclasts are subrounded to well-rounded. Pebble elongation where measured is roughly perpendicular to current direction. Pebble imbrication with the long axes dipping up-current is present. Conglomeritic sandstones are common and are included in the sandstone statistics discussed above. Planar cross-stratification is present throughout the section but the standard deviation of the azimuthal mode is large (18°, see Table 5) indicating higher variability of palaeocurrent direction than in the Twofold Bay Formation. Oversteepened and slumped cross-stratification is common. Ball and pillow structures are associated with specific sub-units of fining-upward cycles. Units with parallel laminations and small scale cross-stratification occur at specific intervals. Trough-like cross-stratification on the scale of a few feet laterally is much less common than in the Twofold Bay Formation. Load casts and other irregularities at the base of coarser units overlying red mudstone are present. Well developed, in-filled mud cracks are also present. Graded bedding, particularly of maximum grain size, is very common and so are channels, scour structures, shale clasts, and nests of shale clasts. Twelve channel thicknesses (or channel depths) vary from 2·1 to 7·5 m and average 3·7 m. Sedimentation units are laterally much more continuous than in the Twofold Bay Formation, although lensing and wedging has been observed. In correlating the various sections considerable lensing of major units on a scale of 400 m have been noted. The Worange Point Formation measured consists of 16 well-developed fluvial fining-upward cycles plus less frequent finer-grained flood deposits which are associated with non-cyclic sandstone units. The cycles, excluding the flood deposits, range in thickness from 8·3 m to 28 m and average 15 m. Locally these cycles are overlain by mudstones ranging in thickness from 6 to 12 m and average 8·3 m.

The Worange Point Formation records the deposits of a wide meandering river belt situated on a coastal plain with a palaeoslope dipping gently toward the southeast. The basal 100 m of the formation probably represent subaerial top-set deltaic beds. In using the thickness of the fining-upward sub-cycles and the Brazos River, Texas (Bernard and Major, 1963) for comparison the dimensions of the Worange Point river system may have been as follows:

Width of meander belt ..	2·6 km
Normal low water stage ..	4 m
Normal high water stage ..	9·3 m
Average flood stage	13·3 m
Maximum flood stage ..	17 m

Acknowledgements

The author is indebted to K. A. W. Crook for guidance and for suggesting this study which was made possible by an Australian National University Research Scholarship.

Appendix

A Preliminary Report on the Palynology of the Merrimbula Group, N.S.W.

R. Anan-Yorke

A preliminary palynological examination of a few samples of the Upper Bellbird Creek Formation and Worange Point Formation of the Merrimbula Group has been carried out. Neves' and Dale's (1963) method of separation has been employed.

The Upper Bellbird Creek Formation is characterized by a rich association of acritarchs, miospores and rare poorly preserved chitinozoans (ancyrochitinids) particularly in Sample JS4 224. The microfossil assemblage reflects a distinct marine phase. A detailed analysis of the acritarchs shows the following species:

Ammonidium spp.
Ouvernay sphaera radiata Brito
Evittia remota (Deunff) Lister
Estiastria spp.
Leiofusa sp. Brito
Maranhites brasiliensis Form A (Brito) Daemon *et al.*
Maranhites brasiliensis Form P (Brito) Daemon *et al.*
Multiplicisphaeridium ramusculosum (Deflandre) Lister
Multiplicisphaeridium arbusculiferum (Downie) Staplin
Navifusa eisenacki (Brito and Santos) Combaz *et al.*
Navifusa brasiliensis (Brito and Santos) Combaz *et al.*
Pterospermopsis sp.
Stellinium octoaster (Staplin) Jardiné *et al.*
Tunisphaeridium caudatum Deunff and Evitt
Triangulina alargada Cramer
Viliferites tenuimarginatus Brito

Veryhachium europaeum (Stockmans and Willière) Cramer
Veryhachium lairdi (Deflandre) Deunff
Veryhachium trispinosum (Eisenack) Cramer
Veryhachium stelligerum Deunff
Cymatisphaera spp.

The spore assemblage is varied, consisting of *Ancyrospora, Apiculatisporis, Apiculiretusispora, Convulatispora, Contagisporites, Emphanisporites, Hymenozonotriletes, Spinozonotriletes, Reticulatisporites, Retusotriletes, Geminospora, Verrucosisporites* and others.

The occurrence of ancyrochitinids delimits the age of the microfossil assemblage to the pre-Carboniferous age. Several of the acritarchs have been recorded from Lower-Upper Devonian sediments in various localities in Europe, North America, South America and Africa. The varied spore assemblage is consistent with an Upper Devonian age. Characteristic Fammenian elements such as *Hymenozonotriletes lepidophytus* Kedo were not observed.

Several samples processed from the Worange Point Formation were barren. Samples JS4 570–572, JS8 511–516 and JS8 521/TS 199 consist of significant palynofloras, though diagnostic forms were not observed. The architarchs are very rare in the Worange Point Formation. Only a few specimens of the species listed below were observed.

Ammonidium sp.
Cymatiosphaera spp.
Evittia remota (Deunff) Lister
Estiastra sp.
Maranhites brasiliensis Form A (Brito) Daemon *et al.*
Multiplicisphaeridium ramusculosum (Deflandre) Lister
Multiplicisphaeridium arbusculiferum (Downie) Staplin
Navifusa eisenacki (Brito and Santos) Combaz *et al.*
Stellinium octoaster (Staplin) Jardiné *et al.*
Triangulina alargada Cramer
Veryhachium rabiosum Cramer restricted
Veryhachium europaeum (Stockmans and Willière) Cramer
Veryhachium trispinosum (Eisenack) Cramer

The spores are rare in the samples though are more varied and constitute a higher percentage than the acritarchs. The spore assemblage in Sample JS8/511–516 is quite significant. *Emphanisporites, Retusotriletes, Apiculatisporis, Apiculiretusispora, Hymenozonotriletes, Spinozonotriletes, Raistrickia, Granulatisporites, Convulatispora* occur fairly commonly. The playnofloral assemblage is distinctively of Devonian age. The palynofloral assemblage is too poor to suggest a more specific age assignment but the total assemblage suggests very minor marine interbeds stratigraphically high up in the Worange Point Formation.

References

Allen, J. R. L., 1962. Petrology, Origin and Deposition of the Highest Lower Old Red Sandstone of Shropshire, England. *J. Sediment. Petrol.*, **32**, 657.

Allen, J. R. L., 1965. Fining-upward Cycles in Alluvial Successions. *Geol. Journ.*, **4**, 229.

Bernard, H. A., and Major, C. F., 1963. Recent Meander Belt Deposits of the Brazos River: an Alluvial "Sand" Model. *Amer. Ass. Petrol. Geol. Bull.*, **47**, 350.

Blissenbach, E., 1954. Geology of Alluvial Fans in Semi-Arid Regions. *Bull. Geol. Soc. Amer.*, **65**, 175.

Bouma, A. H., 1962. *Sedimentology of Some Flysch Deposits, a Graphic Approach to Facies Interpretations.* Elsevier Publ. Co., Amsterdam.

Brown, I. A., 1931. The Stratigraphy and Structural Geology of the Devonian Rocks of the South Coast of New South Wales. *Proc. Linn. Soc. N.S.W.*, **56**, 461.

Conolly, J. R., 1965. Clay Mineralogy of Some Upper Devonian Sediments from Central New South Wales. *J. Proc. Roy. Soc. N.S.W.*, **98**, 111.

Crook, K. A. W., 1960. Classification of Arenites. *Amer. Journ. Science*, **258**, 419.

Crook, K. A. W., 1967. Upper Devonian Sedimentological Provinces in Eastern Australia and their Controlling Factors, *in* Oswald, D. H. (Ed.), International Symposium on the Devonian System. *Alberta Soc. Petrol. Geol.*, 1335.

Doeglas, D. J., 1962. The Structure of Sedimentary Deposits of Braided Rivers. *Sedimentology*, **1**, 167.

Dunbar, C. O., and Rodgers, J., 1957. *Principles of Stratigraphy.* Wiley, New York.

Friedman, G. M., 1961. Distinction Between Dune, Beach and River Sands from their Textural Characteristics. *J. Sed. Pet.*, **31**, 514.

Geological Society of America, 1951. *Rock Colour Chart.* Boulder, Colorado.

Hall, L. R., 1957. The Stratigraphy, Structure and Mineralization of the Devonian Strata near Eden, N.S.W. *Rept. Dept. Mines, N.S.W.*, **5**, 103.

Hall, L. R., 1969. Quaama-Eden-Cape Howe District *in* Packam *et al.*, *in* Packham, G. H. (Ed.), The Geology of New South Wales. *J. Geol. Soc. Aust.*, **16**, 156.

Hill, D., 1969. Devonian of Eastern Australia, *in* Oswald, D. H. (Ed.), International Symposium on the Devonian System. *Alberta Soc. Petrol. Geol.*, 613.

Klein, G. deV., 1971. A Sedimentary Model for Determining Paleotidal Range. *Geol. Soc. Amer. Bull.*, **82**, 2585.

McKee, E. D., 1957. Primary Structures in Some Recent Sediments. *Bull. Amer. Ass. Petrol. Geol.*, **41**, 1704.

McKee, E. D., and Weir, W., 1953. Terminology for Stratification and Cross-Stratification in Sedimentary Rocks. *Bull. Geol. Soc. Amer.*, **64**, 383.

NAIRN, A. E. H. (Ed.), *Problems in Palaeoclimatology.* Interscience Publ., New York.

NEVES, R., and DALE, B., 1963. A Modified Filtration System for Palynological Preparations. *Nature,* **198**, 775.

PETTIJOHN, F. J., 1949. *Sedimentary Rocks,* 2nd ed. Harper and Bros., New York.

SAHU, B. K., 1964. Depositional Mechanism from the Size Analysis of Clastic Sediments. *Journ. Sed. Pet.,* **34**, 73.

SHEARMAN, D. J., 1964. On Penecontemporaneous Disturbance of Bedding by "Quick Sand" Movement in the Devonian Rocks of North Devon. *Deltaic and Shallow Marine Deposits.* Elsevier, London.

SHELLEY, R. C., 1964. On Penecontemporaneous Deformation of Heavy Mineral Bands in the Torridonian Sandstone of Northwest Scotland. *Deltaic and Shallow Marine Deposits.* Elsevier, London.

SHELTON, J. W., and NOBLE, R. L., 1974. Depositional Features of Braided-Meandering Stream. *Amer. Ass. Petrol. Geol. Bull.,* **58**, 742.

SOLIMAN, S. M., 1964. Primary Structures in a Part of the Nile Delta Sand Beach. *Deltaic and Shallow Marine Deposits.* Elsevier, London.

STEINER, J., 1966. Depositional Environments of the Devonian Rocks of the Eden-Merrimbula Area, N.S.W., Ph.D. Thesis, Australian National University (unpublished).

STEINER, J., 1972. The Eruptive History and Depositional Environment of the Devonian Extrusive Rocks, Eden, N.S.W. *J. Geol. Soc. Aust.,* **19**, 261.

STRAATEN, V. L. M. J. V., 1961. Sedimentation in Tidal Flat Areas. *J. Alberta Soc. Petrol. Geol.,* **9**, 203.

TANNER, W. F., 1955. Paleogeographic Reconstruction from Cross-bedding Studies. *Bull. Amer. Ass. Petrol. Geol.,* **39**, 2471.

TANNER, W. F., 1959. The Importance of Modes in Cross-bedding Data. *J. Sed. Petrol.,* **29**, 221.

VAN HOUTEN, F. B., 1964. Origin of Red Beds—Some Unsolved Problems (see Nairn).

Australian National University,
Canberra, A.C.T. 2600. Australia.

Present Address :
Department of Geology,
University of Alberta,
Edmonton, Alberta, Canada.

(Received 23.9.74)

Journal and Proceedings, Royal Society of New South Wales, Vol. 108, pp. 52–53, 1975

Local Compactness and Free Products of Topological Groups

SIDNEY A. MORRIS

ABSTRACT—It is proved here that a free product (free abelian product) of an infinite family of non-totally disconnected topological groups is never locally compact.

1. Introduction

Definition. Let $\{G_i : i\varepsilon I\}$ be a family of topological groups. Then the topological group F is said to be a *free product* of $\{G_i : i\varepsilon I\}$, denoted by $\prod\limits_{i\varepsilon I}{}^{*}G_i$, if it has the properties:

(*a*) for each $i\varepsilon I$, G_i is a subgroup of F;

(*b*) F is generated algebraically by $\bigcup\limits_{i\varepsilon I} G_i$;

(*c*) if for each $i\varepsilon I$, γ_i, is a continuous homomorphism of G_i into a topological group H, then there exists a continuous homomorphism Γ of F into H such that $\Gamma = \gamma_i$ on G_i, for each i.

Of course a free product is simply the coproduct in the category of all topological groups. Thus, if it exists, it is unique up to (a unique) isomorphism. The *free abelian product* is similarly defined and is the coproduct in the category of all abelian topological groups.

Free products of topological groups were first studied by Graev (1950). He showed that the free product of any family of Hausdorff groups exists and is Hausdorff. (A much simpler—but fallacious—proof of this result appears in Morris (1971). A simple proof of a special case is given in Ordman (1974).

We summarize the other background results in the following

Theorem. Let $\{G_i : i\varepsilon I\}$ be a family of (not necessarily Hausdorff) topological groups.

(i) Morris (1971). $\prod\limits_{i\varepsilon I}{}^{*}G_i$ exists and has as its underlying group structure the free algebraic product of G_i, $i\varepsilon I$.

(ii) Hulanicki (1967) and Morris (1971). If each G_i is maximally periodic, then $\prod\limits_{i\varepsilon I}{}^{*}G_i$ is maximally almost periodic.

(iii) Morris (1971). If each G_i is connected, then $\prod\limits_{i\varepsilon I}{}^{*}G_i$ is connected.

(iv) Ordman (1974). If $\prod\limits_{i\varepsilon I}{}^{*}G_i$ is Hausdorff, then each G_i is a closed subgroup.

(v) Ordman (1974). If at least two G_i are not $\{e\}$, then $\prod\limits_{i\varepsilon I}{}^{*}G_i$ is not compact.

(vi) Ordman (1974). If at least two G_i are not discrete, then $\prod\limits_{i\varepsilon I}{}^{*}G_i$ is not both locally compact and locally invariant.

Note that in our main theorem and in part (vi) of the above theorem a non-triviality condition is assumed. Some such condition is necessary, as the free product of discrete groups is discrete.

2. Results

Lemma. Let $\{G_i : i\varepsilon I\}$ be an infinite family of non-totally disconnected locally compact groups. Let G be the algebraic restricted direct product of $\{G_i : i\varepsilon I\}$ with the finest group topology which will induce the given topology on each G_i. Then G is not locally compact.

Proof. Suppose G is locally compact. Let C_i be the component of the identity in G_i, for each $i\varepsilon I$.

Case 1. There exists an infinite subset J of I such that for each $j\varepsilon J$, C_j has a subgroup R_j isomorphic to the additive group of reals with its usual topology. Of course each R_j has a subgroup Z_j isomorphic to the discrete group of integers.

Let $\prod\limits_{i\varepsilon I}{}^{D}G_i$ denote the restricted direct product of $\{G_i : i\varepsilon I\}$, with the usual topology. Then there is a natural continuous algebraic isomorphism f of G onto $\prod\limits_{i\varepsilon I}{}^{D}G_i$, such that $f|G_i$ is an isomorphism of G_i onto $f(G_i)$, for each $i\varepsilon I$.

Let A be the subgroup of G generated algebraically by $\bigcup\limits_{j\varepsilon J} R_j$. Since R_j is locally compact, $f(R_j)$ is a closed subgroup of $f(G_j) = G_j$.

Thus $f(A)=\prod^D_{j\varepsilon J} f(R_j)$ is a closed subgroup of $\prod^D_{i\varepsilon I} G_i$. Therefore, A is a closed subgroup of G and consequently is locally compact.

Similarly if we define B to be the subgroup of G generated algebraically by $\bigcup_{j\varepsilon J} Z_j$, then B is locally compact. Since B is algebraically isomorphic to $\prod^D_{j\varepsilon J} Z_j$, this implies by Dudley (1961), that B has the discrete topology.

Since each R_j, $j\varepsilon J$, is connected, A is connected. Thus A is a compactly generated locally compact abelian group which has B as a discrete subgroup. By Corollary 1 of Morris (1972), B is finitely generated. This contradicts the definition of B. Thus *Case 1 cannot occur.*

Case 2. There exists an infinite subset K of I, such that each C_k is compact, $k\varepsilon K$.

Let C be the subgroup of G generated algebraically by $\bigcup_{k\varepsilon K} C_k$. Since C_k is compact, $f(C_k)$ is a closed subgroup of $f(G_k)=G_k$. Thus $f(C)=\prod^D_{k\varepsilon K} f(C_k)$ is a closed subgroup of $\prod^D_{i\varepsilon I} G_i$. Therefore C is a closed subgroup of G and consequently is locally compact. Clearly C is also connected.

By §4.13 of Montgomery and Zippin (1955), C has a maximal compact subgroup M. Since C_k is a normal subgroup of C, MC_k is a subgroup of C, for each $k\varepsilon K$. Noting that MC_k is compact and contains M, we see that $MC_k=M$. Thus C_k is a subgroup of M, for each $k\varepsilon K$. The family $\{C_k : k\varepsilon K\}$ generates C algebraically and so $M=C$; that is, C is compact.

However, if C is compact then $f(C)=\prod^D_{k\varepsilon K} f(C_k)$ is compact. This contradicts Theorem 6.2 of Hewitt and Ross (1963) which clearly implies a restricted direct product of an infinite family of non-trivial groups is never compact. This contradiction shows that *Case 2 cannot occur.*

Now, by §4.13 of Montgomery and Zippin (1955) and our assumptions on the family $\{G_i : i\varepsilon I\}$, if G is locally compact then either Case 1 or Case 2 must occur. Hence G is not locally compact.

Department of Mathematics,
University of New South Wales,
Kensington, N.S.W., 2033,
Australia.

Theorem. Let $\{G_i : i\varepsilon I\}$ be an infinite family of non-totally disconnected topological groups. Then $\prod^*_{i\varepsilon I} G_i$ is not locally compact.

Proof. Suppose $\prod^*_{i\varepsilon I} G_i$ is locally compact. Then by part (iv) of our preliminary theorem, each G_i is locally compact. Let G be defined as in the Lemma. Then clearly there is a natural continuous open homomorphism of $\prod^*_{i\varepsilon I} G_i$ onto G. Thus G is locally compact. This contradicts the Lemma. Hence $\prod^*_{i\varepsilon I} G_i$ is not locally compact.

Similarly we obtain the following:

Theorem. Let $\{G_i : i\varepsilon I\}$ be an infinite family of abelian non-totally disconnected topological groups. Then the free abelian products of $\{G_i : i\varepsilon I\}$ is not locally compact.

We conclude by drawing the reader's attention to some work which complements the results obtained here: Morris, Ordman and Thompson (1973) and Morris (1975).

References

DUDLEY, R. M., 1961. Continuity of Homomorphisms. *Duke Math. J.*, **28**, 587.

GRAEV, M. I., 1950. On Free Products of Topological Groups (Russian). *Izv. Akad. Nauk SSSR. Ser. Mat.*, **14**, 343.

HEWITT, E., and ROSS, K. A., 1963. *Abstract Harmonic Analysis, Vol. I.* Springer-Verlag, Berlin, Göttingen, Heidelberg.

HULANICKI, A., 1967. Isomorphic Embeddings of Free Products of Compact Groups. *Colloq. Math.*, **16**, 235.

MONTGOMERY, D., and ZIPPIN, L., 1955. *Topological Transformation Groups.* Interscience, New York.

MORRIS, S. A., 1971. Free Products of Topological Groups. *Bull. Austral. Math. Soc.*, **4**, 17.

MORRIS, S.A., 1972. Locally Compact Abelian Groups and the Variety of Topological Groups Generated by the Reals. *Proc. Amer. Math. Soc.*, **34**, 290.

MORRIS, S.A., 1975. Local Compactness and Local Invariance of Free Products of Topological Groups. *Colloq. Math.*,

MORRIS, S. A., ORDMAN, E. T., and THOMPSON, H. B., 1973. The Topology of Free Products of Topological Groups. *Proc. second. International Conference on Group Theory* (*Canberra*), 1973.

ORDMAN, E. T., 1974. Free Products of Topological Groups with Equal Uniformities. *Colloq. Math.*

(Received 29.4.74)

Journal and Proceedings, Royal Society of New South Wales, Vol. 108, pp. 54-69, 1975

Lower Silurian Rugose Corals from Central New South Wales

R. A. McLean

Abstract—Six species of rugose corals (four new) are described from beds of Upper Llandovery age in central N.S.W. Representative of the family Arachnophyllidae Dybowski are *Arachnophyllum epistomoides* Etheridge, 1909 (Rosyth and Quarry Creek Limestones), *Ptychophyllum auctum* sp. nov. (Rosyth and Quarry Creek Limestones), *P.* cf. *sibiricum* Ivanovskiy, 1963 (Upper limestone horizon, Cobblers Creek, Angullong district), *Cyathactis variabilis* sp. nov. (Rosyth Limestone) and *Stereoxylodes multicarinatus* sp. nov. (Rosyth Limestone). *Strombodes rosythensis* sp. nov. (Rosyth Limestone) has uncertain suprageneric affinities.

Introduction

The rugosans described herein are represented in three major horizons west of Orange in central N.S.W. A summary of the stratigraphy of the correlative Rosyth and Quarry Creek Limestones, together with evidence for their Upper Llandovery age, are given in McLean (1974*a*). Similar data for the Upper Llandovery "upper limestone horizon" in Cobblers Creek, Angullong district, is provided by McLean (1974*b*).

This paper presents the first description of representatives from Australia of the genera *Ptychophyllum* Edwards and Haime, *Cyathactis* Soshkina, *Stereoxylodes* Wang and *Strombodes* Schweigger. In addition, a widely neglected species of *Arachnophyllum* Dana is revised and a lectotype chosen.

Specimen numbers in the University of Sydney Palaeontological Collections bear the prefix SUP and where more than one section has been prepared from the one specimen, they have the suffix a, b etc. Numbers of specimens in the palaeontological collections of the Australian Museum, Sydney, have the prefix AM.F and thin sections in these collections the prefix AM.

Full details of collecting localities within the Rosyth Limestone of the Boree Creek area, south of the Orange-Cudal road are given in McLean (1973).

Systematic Palaeontology

Family Arachnophyllidae Dybowski, 1873
Genus *Arachnophyllum* Dana, 1846

1876 *Strombodes*; Rominger, p. 130.
1901 *Arachnophyllum*; Lambe, p. 180.
1902 *Strombodes*; Počta, p. 176.
1906 *Arachnophyllum* (*Strombodes*); Foerste, p. 318.
1909 *Arachnophyllum*; Etheridge, p. 1.
1933 *Strombodes*; Parks, p. 38.
1939 *Strombodes* (*Arachnophyllum*); Shrock and Twenhofel, p. 25.
?1940 *Zenophila* Hill, p. 414.
1949 *Arachnophyllum*; Amsden, p. 104.
1965 *Arachnophyllum*; Stumm, p. 30.
1965*a* *Arachnophyllum*; Ivanovskiy, p. 114 (*cum syn.*).

Type species: *Acervularia baltica* Schweigger (1819) *sensu* Lonsdale, 1839=*Strombodes murchisoni* Edwards and Haime, 1851. Wenlock Limestone (Upper Wenlock), Shropshire.

Diagnosis: (Based on Hill, 1956, p. F274.) Astreoid corallum with narrow tabularia containing domed, mainly incomplete tabulae. Wide dissepimentarium with numerous small dissepiments. Septa either thickened and complete or each consisting of a network of small trabeculae based vertically on dissepiments but not piercing more than one or two successive dissepiment layers.

Discussion: The great majority of species of *Arachnophyllum* have been described only in terms of their external morphological features, or from very inadequate sectioned material. Detailed revision of the genus is badly needed and a great number of species may prove to be synonymous, this being particularly so for the numerous described species from North America.

It appears that two main morphological groups are represented in *Arachnophyllum*. One group, characterized by the type species, *A. murchisoni* (Edwards and Haime, 1851) and also *A. pentagonum* (Goldfuss, 1826), possesses prominent ridges on the distal surface of the corallum, subdividing it into "corallites" and corresponding to upflexing of dissepimental layers. The other group, characterized by *A. diffluens* (Edwards and Haime, 1851), lacks these surface ridges. Lang and Smith (1927) considered *A. diffluens* to be merely a variant of *A. murchisoni*, but the upflexing of dissepimental layers forming surface ridges in the latter seemed to them a significant enough feature to warrant distinction of the two species, despite gradational forms between them. Ivanovskiy (1965*a*) considered *A. diffluens* to be a synonym of *A. murchisoni* since the two forms are highly variable and similar in features other than the development of the surface ridges. In the N.S.W. species, *A. epistomoides* Etheridge, 1909, described below, no specimens have been seen in which surface ridges and upflexing of dissepimental layers occur. Hence, it seems useful at present to recognize the two species groups, although it is evident they are very closely related and future work may well show there are all gradations between the two extremes.

In redescribing the type material of the species *A. murchisoni* (Edwards and Haime), *A. diffluens* (Edwards and Haime) and *A. typum* M'Coy from the Wenlock Limestone of Shropshire, Lang and Smith (1927) discussed the detailed structure of the septa. According to them the septa became restricted to trabeculae in the dissepimentarium, these trabeculae being based on dissepimental crests, also, these " septal crests " developed vertical and horizontal series of spines, which, when thickened with secondary tissue, tended to form a " three dimensional rectilinear meshwork " (Lang and Smith, 1927, p. 466). Such a feature has apparently been described in only one other species of *Arachnophyllum*, namely *A. pentagonum* (Goldfuss), Amsden (1949, p. 105) mentioning septa degenerating into " vertical plates or crests resting upon the dissepimental floor " with " transverse vertical plates between the septal crests " in material from the Brownsport Formation (Ludlow) of Tennessee.

However, from the illustrations of Lang and Smith and Amsden, while it seems evident that the continguous septa of the inner parts of the corallite have broken down to isolated vertical spines, probably linked by lamellar schlerenchymal tissue, the presence of connecting vertical plates and spines between septa is not clear. It is suggested that secondary thickening of the dissepimental crests, between septa, possibly to lend greater strength to the septal structure, could also give the appearance of connecting plates between septa, and oblique intersections of dissepiments and septa could also lead to this impression. It is felt here that distinction of specimens apparently lacking this feature into a different genus is not justified, considering the generally poor state of knowledge of most material hitherto ascribed to *Arachnophyllum.*

Hill (1940, p. 414), described a new genus (*Zenophila*, type species *Z. walli* (Etheridge, 1892), from the " Barrandella Shales " and Hume Limestone (Ludlow) of the Yass district, N.S.W.. Hill distinguishes this genus from *Arachnophyllum* on the basis of its lack of the " trabecular meshwork " described by Lang and Smith (1927) and its septa not reaching the corallite axis. Since the septa in *Arachnophyllum* need not reach the axis (Lang and Smith, 1927, p. 466 ; Lambe, 1901, p. 184), although they commonly do, and the validity of the " trabecular meshwork " structure is not certain, it seems likely that *Zenophila* is probably synonymous with *Arachnophyllum.* This has already been suggested by Ivanovskiy (1965*a*) and the type species *Z. walli* was listed as a species of *Arachnophyllum* by Ivanovskiy (1965*b*).

Range : Upper Llandovery of Gotland, Estonia, Siberian Platform, north-east America and N.S.W. ; Wenlock of Britain, Urals and north-east America ; Ludlow of Czechoslovakia, Tennessee, Indiana-Kentucky and ?N.S.W..

Arachnophyllum epistomoides Etheridge, 1909

Plate I, Figures 1–6 ; Plate II, Figure 1.

1909 *Arachnophyllum* (?) *epistomides* Etheridge, p. 1, Plates 44–46.

Material : Lectotype (here designated) AM 4866, Paralectotype AM 4343, Quarry Creek Limestone, most easterly outcrop (" Bed A ") in Quarry Creek. Topotypes SUP 45228–45229.

Additional material : SUP 45230–45233, Quarry Creek Limestone, Spring Creek ; SUP 45234, Quarry Creek Limestone, middle outcrop (" Bed B ") in Quarry Creek ; SUP 27150, 45235–45241, Rosyth Limestone, Boree Creek area. Upper Llandovery.

Diagnosis : Large *Arachnophyllum* lacking surface ridges and corresponding upflexing of dissepiment layers. Septa ranging from 38–54 in number, major septa not extending far into tabularium. Tabulae strongly convex with broad central arch corresponding to boss in calicular pit. Dissepiments very elongate in central portion of intertabularial space.

Description : Corallum large and tabular, reaching dimensions of 75 cm in width and 45 cm in height. Coralla astreoid, with septa of adjoining corallites occasionally confluent. Corallite walls entirely lacking. Distal surface of corallum shows slight swelling surrounding calical pits, which have dimensions of 5–6 mm in width and 3 mm in depth. Broad calical boss 1–2 mm in height occurs in calical pits.

Septa vary in number from 36 to approximately 54 in material studied. Septa short, not extending far into tabularium where it is generally possible to distinguish slightly shorter and thinner minor septa. However, isolated septal lamellae may be present in tabularium (see Plate I, Figures 4, 6). Between tabularia it is difficult to observe any continuity along plane of septum (see lectotype, Plate I, Figure 1) and it appears septa break down into isolated trabeculae, of indeterminate type, strongly coated in sclerenchymal thickening in most cases. Trabeculae probably pierce several dissepimental layers, although angle of longitudinal section in relation to direction of trabecular growth cannot be determined exactly. Plate I, Figure 6 illustrates possible irregularity of alignment of trabeculae.

Tabularia range in diameter from about 5–7 mm, with spacing, while quite variable, generally in range of about 15–25 mm. Tabulae complete and incomplete, strongly convex with broad axial arch and slightly concave lateral zone. Common spacing of tabulae of 0·2–0–4 mm with average of 0·3 mm. Dissepiments globose adjacent to tabularia, layers steeply inclined in that region, average dimensions ranging from 0·3–0·4 mm in height and 0·5–0·6 mm in width. In central portion of inter-tabularial space dissepiments strongly elongate, in flat, moderately arched or slightly sagging series, with height of 0·1–0·2 mm.

Remarks: In the original description of *Arachnophyllum epistomoides* by Etheridge (1909) no mention was made of either type specimens or where the material was housed. Location of the syntype material, however, at the Australian Museum, Sydney, showed that of the specimens figured by Etheridge, only a transverse and longitudinal section (possibly from different specimens) could be found and the three silicified specimens (Etheridge 1909, Plate 44, Figure 1, AMF 7613; Plate 45, Figures 1, 2) have been misplaced or lost. Hence the transverse section (Etheridge 1909, Plate 46, AM 4866) has been designated here as lectotype and the longitudinal section (Etheridge 1909, Plate 44, Figure 2, AM 4343) a paralectotype.

Lack of surface ridges in *A. epistomoides* allies this species to the *A. diffluens* group, other members of this group appearing to be *A. mamillare* (Owen, 1844), *A. approximatum* (Parks, 1933) and *A. speciosum* (Dybowski, 1873), although the last two species require further study and may be synonymous with *A. diffluens*. *A. diffluens* (*sensu stricto*) has been recorded from the Jupiter-Chicotte Formations (Upper Llandovery-Wenlock) of Anticosti Island, Pike Arm Formation equivalents (Upper Llandovery) of Newfoundland, Wenlock Limestone of England and localities of un-named horizons in Ontario and Quebec (Lambe, 1901). This species may be distinguished from *A. epistomoides* by having a narrower tabularium, longer septa extending into the tabularium, smaller, more globose dissepiments as compared to the very elongate type in *A. epistomoides*, and completely contiguous septa between " corallites ", a feature not commonly visible in *A. epistomoides*. Lang and Smith (1927) described the " trabecular meshwork " structure discussed above as being present in the British (Wenlock) specimens of *A. diffluens*, but no mention has been made of this in descriptions of material ascribed to this species from other localities (Lambe, 1901; Shrock and Twenhofel, 1939). As mentioned previously, this structure has not been clearly observed in any material of *A. epistomoides*.

A. mamillare (Owen, 1844) from late Llandovery—Lower Ludlow strata of North-Eastern United States (Manistique Dolomite, Louisville Limestone and Hopkinton Dolomite-Stumm, 1965) also appears to lack prominent surface ridges, but may be distinguished from *A. epistomoides* by possessing very prominent swelling of dissepimental layers around the calical pits to give cone-shaped protruberances on the distal surface. This specimen also lacks the elongate dissepiments of *A. epistomoides*. A related form described by Foerste (1906) as *A. mamillare distans* occurs in strata of Upper Llandovery age in Kentucky (Waco Limestone).

A. approximatum, described by Parks (1933) from the La Vieille Formation (Upper Llandovery—Wenlock) of Quebec, also appears to lack surface ridges but absence of figured sections make any close comparisons with *A. epistomoides* impossible. It seems, however, that closer spacing of tabularia would distinguish it from *A. epistomoides* in any case.

The material described by Hill (1940) as *Zenophila walli* (Etheridge, 1892), from the Ludlow of the Yass district of N.S.W. (see discussion above) differs from *Arachnophyllum epistomoides* in having smaller tabularia with sagging, incomplete tabulae, closer spacing of tabularia (5–10 mm) and fewer septa (20–24), with major septa extending well into tabularia and minor septa reduced to isolated spines. It also has more globose dissepiments in the central area of the dissepimentarium and lacks abundant sclerenchymal coating of septa and dissepiments.

In general, *A. epistomoides* may be distinguished from all described species by the extremely elongate dissepiments in the central area of the intertabularial spaces.

Genus *Ptychophyllum* (Edwards and Haime, 1850).

?1876 *Vesicularia* Rominger, p. 135.
?1890 *Ptychophyllum*; Foerste, p. 342.
?1903 *Ptychophyllum*; Foerste, p. 713.
1926 *Ptychophyllum*; Lang, p. 431.
1949 ?*Ptychophyllum*; Amsden, p. 112.
1962 *Ptychophyllum*; Stumm, p. 3.
1962 *Ptychophyllum*; Norford, p. 41.
1963*b* *Ptychophyllum*; Ivanovskiy, p. 78 (*cum syn.*)
1965*a* *Ptychophyllum*; Ivanovskiy, p. 76.

Type species: *P. stokesi* Edwards and Haime, 1850, " Lockport Dolomite " (Upper Wenlock—Lower Ludlow), Drummond Island, Lake Huron, Michigan.

Diagnosis (based on Smith, 1945, p. 51): Solitary, cylindrical, turbinate or patellate rugose coral having typically moderately deep calical pit with prominent axial boss. Major septa reach axis, becoming twisted into axial vortex. Small, arched tabellae and incomplete tabulae form convex series and wide dissepimentarium contains small, elongate to globose dissepiments.

Discussion: The genus *Ptychophyllum* Edwards and Haime has been generally poorly studied in the past and thorough descriptions have been given only by Smith (1945), Amsden (1949) and Ivanovskiy (1965*b*). The characteristic feature of the genus is development by the major septa of an axial vortex, which may produce an axial boss in the calice. Development of minor septa is variable, some species having long forms extending at least half the corallite radius, as exemplified by the type species, *P. stokesi* Edwards and Haime, whereas in others minor septa are vestigial, as in *P. auctum* sp. nov. In the doubtful Upper Devonian species *P.? kindlei* Smith, the minor septa are apparently lacking (Smith, 1945).

The nature of the septa in the peripheral parts of the corallite is noteworthy. In the type species, *P. stokesi* Edwards and Haime, the septa in this region tend to break down and give the appearance of being composed of twisted strands which appear to become united with the dissepiments between the septa. This feature has also been described by Smith (1945) in his species *P.? kindlei* and *P.? whittakeri*, and by Amsden (1949) in *P.? cliftonense*. Despite poor preservation it may also be seen to a small extent in specimens of *P. auctum* sp. nov. described below.

The genus *Vesicularia* Rominger, 1876, from the Upper Wenlock—Lower Ludlow of Michigan and Ontario (" Lockport Dolomite ") and Iowa (Hopkinton Dolomite) has been interpreted by Smith (1945, p. 52) and in the faunal lists of Bassler (1950) as a synonym of *Ptychophyllum*. However, it is a compound form and there is no mention by Rominger in describing the three species *V. major*, *V. minor* and *V. variolosa* spp. nov. of any axial vortex of the septa. There are even " spinulose projections " (Rominger, 1876, p. 136) on the septal ridges of *V. minor*. Unfortunately, the type material of Rominger apparently has not been studied in thin section and Rominger's figures are inadequate and hence the designation of the genus remains in doubt. It appears the form may be most clearly related to *Arachnophyllum* Dana and Rominger also noted (p. 125) similarities to *Cystiphyllum*, *Vesicularia* supposedly differing only in its compound growth form.

Range: Upper Llandovery of Siberian Platform, ? China, ? British Columbia, and N.S.W.; Wenlock of Siberian Platform; Wenlock—Ludlow of Ontario, Michigan and Wisconsin.

Ptychophyllum auctum sp. nov.

Plate II, Figures 2–7, 11, 12; Plate III, Figures 1, 2

Derivation of name: Latin *auctus*=enlarged, referring to peripherally dilated septa.

Material: Holotype SUP 45204, Quarry Creek Limestone, " Bed A ", Quarry Creek, Paratypes SUP 45205–45207 Quarry Creek Limestone " Bed A ", Quarry Creek. SUP 45208, Rosyth Limestone Boree Creek area, is doubtfully included in this species. Upper Llandovery.

Diagnosis: Cylindrical *Ptychophyllum* with a maximum diameter of at least 33 m. Septal number average 60–70, major septa strongly dilated in the dissepimentarium but tapering rapidly in tabularium, forming a prominent axial vortex. Minor septa short, often lonsdaleoid, not extending axially as far as tabularium. Dissepiments small, weakly elongate, very steeply inclined; tabularium consisting of arched series of globose and elongate tabellae.

Description : Corallum solitary, cylindrical and elongate with maximum observed length of approximately 12 cm. True diameter difficult to estimate as all specimens have suffered abrasion and epitheca is not preserved. Most complete specimen, doubtfully included in this species (SUP 45208, from the Rosyth Limestone), shows maximum diameter of 33 mm and smaller, more incomplete forms from the Quarry Creek Limestone show common diameter of 20–25 mm. Detail of calice is not available but a depth of at least 6–7 mm. in the smaller specimens is probable. Septa show maximum numbers of 74 at a diameter (incomplete) of 24 mm. (SUP 45204*a*) and 72 in the largest specimen.

Major septa are strongly dilated in dissepimentarium and in some of the better preserved specimens (e.g. Plate II, Figures 11, 12) there is splitting of septa in this region into " strands " that appear contiguous with dissepiments adjacent to septa (see discussion above). Septa in this zone may reach a diameter of about 0·7 mm. In tabularium, major septa become thinner, most continuing to axis to form prominent axial vortex and septa in this region have common width of approximately 0·15 mm. Minor septa short, although total length cannot be determined owing to incomplete preservation of corallites. However, none reach axially as far as dissepimentarial-tabularial boundary. Where minor septa can be observed in sections they are thin and in the specimen from the Rosyth Limestone (SUP 45208), their discontinuous nature can be seen (Plate II, Figures 8, 10). Dissepiments very steeply inclined and elongate adjacent to tabularium. Towards periphery, dissepiments slightly less inclined and more globose ; generally they are small in size (av. 1–1·5 mm in width, 0·5–0·6 mm in height, although the Rosyth Limestone specimen is slightly larger). Tabularium composed of moderately arched series of mainly elongate tabellae, which tend to be more globose towards margin of dissepimentarium. Average height of tabellae reaches 0·5–0·8 mm.

TABLE 1

Dimensions of Ptychophyllum auctum *sp. nov. Values of septal number (n) marked with an asterisk (*) refer to incomplete specimens in which minor septa are not preserved.*

SUP	Dc (mm)	n
45204a (calice) ..	24	74
45204b	>22·5	74
45204c	23	74
45204d	>22	62
45205a (calice) ..	>17·5	60
45205b	>18	60
45205c	>15	?58
45205d	>15	56
45205e	>15	?31
45206a (calice) ..	>16·5	32*
45206b	18·5	34*
45206c	18	34*
45206d	18	33*
45206e	?14	33*
45206f	?10	?25*
45207	23	60
45208a (calice) ..	>29	72
45208b	33	70

Remarks : The only species of *Ptychophyllum* to show any strong similarities to *P. auctum* sp. nov. is *P. sibiricum* Ivanovskiy, 1963*b*, from the Upper Llandovery of the Siberian Platform. Comparable features include the predominantly cylindricum growth form, corallite diameter (20–30 mm), broad axial vortex of major septa, steeply inclined rows of small, slightly elongate dissepiments and the size, shape and disposition of the tabellae. *P. sibiricum* may be distinguished, however, by having much weaker dilation of the major septa in the dissepimentarium and comparable widths of the major and minor septa in this region. It also has longer minor septa, reaching apparently to the tabularial boundary and a proportionately wider tabularium (approx. 15 mm at corallite diameter 21 mm, compared to 13 mm at an approximate diameter of 25 mm in *P. auctum*). Ivanovskiy (1963*b*, p. 79) (Plate XXI, Figure 1*a*) made no mention of peripheral breakdown of septa in his description of *P. sibiricum* and there is none evident in his illustration although the specimen may be incomplete (epitheca not visible). It is evident, however, that the two species are related closely, owing to the dilation of septa in the dissepimentarium and their thinning into a broad axial vortex.

The specimen (SUP 45208) from the Rosyth Limestone is included in *P. auctum* with reservation, since it is larger than the Quarry Creek Limestone material and appears to generally have longer minor septa, slightly more globose dissepiments and, in the more distal transverse section (Plate II, Figure 10), the septa appear far more discontinuous peripherally than is normally shown in the Quarry Creek material. However, in the more proximal transverse section (Plate II, Figure 8), the septa are more similar to the typical *P. auctum*. The strong dilation of the major septa in the dissepimentarium links this form to the representatives of the species from Quarry Creek and until more material from the Rosyth Limestone can be located, it appears best included as *P. auctum* ? .

Ptychophyllum cf. *sibiricum* Ivanovskiy, 1963

Plate III, Figures 3–9

Material: SUP 20111, 45209–45215. Upper limestone horizon, Cobblers Creek, Angullong district. Upper Llandovery.

Diagnosis: Cylindrical *Ptychophyllum* with corallite diameter up to 19 mm. Septa range in number from 48 to 66, major septa forming axial vortex of variable intensity. Both major and minor septa thickened in dissepimentarium. Dissepiments small, moderately elongate, steeply inclined; tabellae elongate and in arched series.

Description: Probably cylindrical coralla with corallite diameter ranging from 10 to 13·5 mm in material available although corallites are abraded as in *P. auctum* sp. nov. Calice moderately deep (depth at least 8 mm in SUP 45214) with steep walls and convex-upward base.

TABLE 2

Dimensions of Ptychophyllum *cf.* sibiricum *Ivanovskiy*

Slide No. (SUP)	Dc (mm)	n
20111a	16	62
45209a	18	58
45210	15	56
45211	18·5	58
45212a (calice) ..	18·5	56
45212b	19	56
45212c	17·5	56
45213a	15·5	62
45215a	13·5	48

Septal number ranges from 48 in smallest specimen to 66, with an average of 56 to 58. Septal number and corallite diameters for specimens available are listed in Table 2. Both major and minor septa are dilated in dissepimentarium, the major septa being slightly wider than the minor septa. Major septa taper axially, forming a generally prominent axial vortex (e.g. SUP 45210, 45212, Plate III, Figure 8). Owing to the incomplete nature of the material, however, this variation in axial vortex could be due to sections cut at different ontogenetic stages—there was material available for only one transverse and longitudinal section in most cases. It is notable, however, that in one specimen, SUP 45212, there is quite a variation in the intensity of the axial vortex, although it is uncertain at what position in the corallite the original sections were made. Minor septa are long, extending axially to margin of tabularium. Preservation insufficient to confirm any peripheral breakdown of septa.

Dissepiments small, weakly elongate and steeply inclined, average height 0·4 mm, width 0·8 mm. Tabularium composed of moderately arched series of elongate tabellae, usually somewhat flattened marginally but becoming more domed in arched axial region. Average height of tabellae 0·8–1 mm. Diameter of tabularium commonly 8–10 mm, i.e. slightly more than half diameter of corallite.

Remarks: The above described material bears closest resemblance to the Upper Llandovery species *Ptychophyllum sibiricum* Ivanovskiy, 1963*b*, from the Siberian Platform. Similarities may be seen in the septa being thickened in the dissepimentarium and tapering axially in a broad axial vortex, together with the minor septa extending axially as far as the tabularium and being thickened almost equally with the major septa in the dissepimentarium. Also the dissepiments are of comparable size, shape, and inclination to the axis and the tabellae are of similar size and disposition. The Siberian material differs somewhat in being generally larger (corallite diameter commonly 21–22 m, max. 32 mm, compared to a maximum of 19 mm observed in the Angullong specimens). They also show a proportionally larger number of septa (92, n/Dc=4·38 as compared to generally 56 to 58, n/Dc 3·2–4·0). However, the close relationship to *P. sibiricum* is evident in all other features.

P. cf. *sibiricum* may be distinguished from *P. auctum* sp. nov., by having much less pronounced thinning of the major septa in the tabularium as well as minor septa extending axially to the tabularium and thickened almost equally with the major septa in the dissepimentarium. No evidence of peripheral breakdown of the septa in *P.* cf. *sibiricum* can be confirmed, although the state of preservation is poorer than in the material of *P. auctum* from the Quarry Creek Limestone.

Genus *Cyathactis* Soshkina, 1955

1901 *Cyathophyllum* (*part.*) ; Lambe, p. 133.
1928 *Cyathophyllum* (*part.*) ; Twenhofel, p. 117.
1939 *Cyathophyllum* (*part.*) ; Northrop, p. 141.
1955 *Cyathactis* (*part.*) Soshkina, p. 122.
1963*b* *Cyathactis* (? *part.*) ; Ivanovskiy, p. 75 (*cum syn.*).
1965*a* *Cyathactis* ; Ivanovskiy, p. 76.
1965*c* *Cyathactis* ; Ivanovskiy, p. 25.
1971 *Cyathactis* ; Lavrusevich, p. 62.
1972 *Cyathactis* ; Merriam, p. 33.

Type species : *C. typus* Soshkina, 1955 ; Upper Llandovery, Siberian Platform.

Diagnosis : Solitary corallum with generally straight, thin septa of two orders, the major septa usually reaching or nearly reaching the axis. Dissepiments numerous, mainly globose ; tabularium composed of complete and incomplete tabulae, with or without tabellae.

Discussion : The genus showing greatest resemblances to *Cyathactis* is *Ptychophyllum* Edwards and Haime, as discussed by Ivanovskiy (1965*c*). The features that distinguish it from *Cyathactis* are its development of an axial vortex of the major septa, together with the presence of numerous tabellae.

The following species are regarded herein as probable representatives of the genus *Cyathactis* : *C. typus* Soshkina, 1955 ; *C. tenuiseptatus* Soshkina, 1955 ; *C. balticus* Kaljo, 1958 ; *C. longiseptatus* Lavrusevich, 1971 ; *C. gazellensis Merriam*, 1972 ; *C. euryone* (Billings, 1862) ; *C. anticostiense* (Billings, 1862) ; *C. interruptus* (Billings, 1862) and *C. cormorantense* (Twenhofel, 1928).

Range : Lower Llandovery of Estonia ; Middle Llandovery of Tadzhikistan ; Middle—Upper Llandovery of Siberian Platform and Anticosti Island ; Upper Llandovery of Estonia, ? Urals, ? south-west Siberia, north-east U.S.S.R., Quebec (Gaspé) and N.S.W. ; Wenlock of Siberian Platform, Tadzhikistan, Anticosti Island, Quebec (Gaspé) and ? Nevada ; Ludlow of Quebec (Gaspé) and ? California.

Cyathactis variabilis sp. nov.

Plate III, Figures 10–12 ; Plate IV, Figures 1, 2

Derivation of name : Latin *variabilis*=variable, referring to the differences in dissepimental size and shape.

Material : Holotype SUP 46181. Paratypes SUP 46182, 46183. Rosyth Limestone, Boree Creek area. Upper Llandovery.

Diagnosis : *Cyathactis* having a deep calice ; relatively few septa, somewhat thickened in the dissepimentarium ; numerous dissepiments of very variable size ; and arched, closely spaced, incomplete tabulae and tabellae.

Description : Corallum incomplete but probably turbinate with corallite diameter of at least 45 mm. at base of calicular pit. Total mature height of corallum not less than 45 mm. Epitheca and peripheral parts of dissepimentarium not preserved in any of available material. Calice deep, not completely preserved in any specimens, but at least 10 mm in depth with maximum width of approximately 25 mm at base of calicular pit, the base being slightly arched.

Septa long, major septa extending to axis where they may be weakly curved (see Plate IV, Figure 2). Minor septa at least half length of major septa. Total number of septa not certain due to incomplete nature of material but probably about 80 are present. Septa show mild thickening in dissepimentarium but become abruptly thinner in tabularium (see Plate III, Figure 12).

Tabularium broad, with maximum diameter of approximately 25 mm in largest specimen (SUP 46182) and approximately 18 mm in smallest (SUP 46183). Tabulae moderately arched, mainly complete in axial region, with zone of elongate tabellae in peripheral area. Tabular spacing commonly 0·3–0·6 mm. Dissepiments small, moderately inclined to axis, becoming steep closer to tabularium. At least 12 rows of dissepiments present, but material is incomplete. Dissepiments commonly small and weakly elongate, size variable, average 0·5–1 mm wide and 0·3–0·8 mm high, but often larger, elongate forms are present, ranging up to 3·3–5 mm wide and 1–1·5 mm high.

Remarks : Although only three very incomplete specimens have been found, enough material is present to build up a reasonable picture of the form and compare it with other described species. None of these species bear any close resemblance to *C. variabilis* sp. nov. in all features, but some similarities are evident.

The only forms to show a comparable number of septa to *C. variabilis* are *C. cormorantense* (Twenhofel, 1928) and *C. longiseptatus* Lavrusevich, 1971. *C. cormorantense* appears comparable in septal number and corallite size, but may be distinguished in having widely spaced, flattened tabulae and a narrower dissepimentarium. It also appears to lack septal dilation and has shorter major septa (see Twenhofel, 1928, Plate III, Figures 3–4).

C. longiseptatus occurs in Horizon G to Horizon K (Middle Llandovery-Lower Wenlock) of Tadzhikistan and is similar to *C. variabilis* in septal number and length and tabularial size and form. However, it differs in lacking dilation of septa in the dissepimentarium, having a much smaller corallite size and smaller, more uniformly sized dissepiments (see Lavrusevich, 1971, Plate VIII, Figures 2–4).

The North American forms *C. anticostiense* (Billings, 1862) and *C. interruptus* (Billings, 1862) are both large forms like *C. variabilis*, but have a greater number of septa (more than 100) and much narrower tabularium together with more uniformly sized dissepiments (see Lambe, 1901, Plate X, Figure 6 and Plate XI, Figure 3).

In general, *C. variabilis* is distinguished from other described species of *Cyathactis* by having peripheral dilation of septa and dissepiments of variable size.

Genus *Stereoxylodes* Wang, 1944

1894 *Cyathophyllum* (*Heliophyllum*); Weissermel, p. 591.
1902 *Cyathophyllum* (*part.*); Počta, p. 87.
1927 *Xylodes* (*part.*) Lang and Smith, p. 475.
1929 *Xylodes* (*part.*); Smith and Tremberth, p. 362.
1939 *Xylodes* (*part.*); Weissermel, p. 47.
1940 *Xylodes* (*part.*); Prantl, p. 6.
1944 *Entelophyllum* (*Stereoxylodes*) Wang, p. 24.
?1951 *Entelophyllum* (*part.*); Schouppé, p. 244.
1956 *Entelophyllum* (*part.*); Hill, p. F275.
?1956 *Ptychophyllum* (*Nanshanophyllum*) Yü, p. 612.
?1960 *Stereoxylodes*; Zheltonogova, p. 77.
1962 *Stereoxylodes*; Soshkina *et al.*, p. 319.
1964 *Stereoxylodes*; Strelnikov, p. 57.
?1964 *Carinophyllum* Strelnikov, p. 59.
1964 *Ramulophyllum* (? *part.*) Nikolaeva, p. 52.
?1964 *Ornatophyllum* Nikolaeva, p. 57.
1965*a* *Stereoxylodes*; Ivanovskiy, p. 71.
?1965*a* *Carinophyllum*; Ivanovskiy, p. 71.
1966 *Ramulophyllum*; Sytova and Ulitina, p. 241.
1968 *Ramulophyllum*; Sytova, p. 62.
?1968 *Carinophyllum*; Shurygina, p. 129.
1970 *Stereoxylodes*; Sytova, p. 70.
?1971 *Carinophyllum*; Strelnikov, p. 78.

Type species: Cyathophyllum (*Heliophyllum*) *pseudodianthus* Weissermel, 1894. Wenlock or Ludlow. Germany (drift.)

Diagnosis: Phaceloid or solitary corallum with septa typically dilated peripherally and strongly carinate. Dissepiments numerous and tabulae commonly show differentiation into axial and periaxial series.

Discussion: *Stereoxylodes* was originally described as a subgenus of *Entelophyllum* Wedekind, 1927 by Wang (1944) and was erected to include those forms previously included in *Entelophyllum* but which possess strongly carinate, peripherally dilated septa. Hill (1956) listed *Stereoxylodes* as a synonym of *Entelophyllum* but subsequent authors have considered it as a full genus, this seeming reasonable on the basis of *Stereoxylodes* having typically strongly carinate and dilated septa. However, their views on the nature and interpretation of the genus have varied. Zheltonogova (1960, p. 77) considered *Stereoxylodes* as a mainly solitary form with rare budding, and described a solitary species, *S. carinatum*, from the Chagyr Suite (Upper Wenlock) of South-west Siberia. This form, however, has only weakly developed carinae and little dilation of the septa and so is only doubtfully considered as a representative of *Stereoxylodes*, being perhaps more likely to be a representative of *Entelophyllum*. Strelnikov (1964), p. 57) considered the genus contained only solitary forms and Ivanovskiy (1965*a*), p. 71) suggested that the name *Stereoxylodes* be reserved for solitary forms with the morphology of that genus, compound representatives being included in the genus *Carinophyllum* Strelnikov, 1964. This latter form is discussed below. Sytova (1970, p. 70) modified *Stereoxylodes* still further, considering it contained forms either solitary or rarely forming a " pseudocolony ". She also stated that the primary septa consisted of a fan-shaped arrangement of radiating trabeculae. This latter feature could represent a vertical section intersecting the carinae, such a structure being typical of carinate forms (e.g. *Heliophyllum* Hall; Smith, 1945, Plate 33, Figure 3*b*). Sytova considered also that a peripheral zone of dilated septa and sclerenchymal tissue was confined to the early growth stages only, and this is generally found in described species, although *S. pseudodianthus sinense* Wang, 1944 has a prominent peripheral stereozone in mature stages. Wang's material is probably atypical of the genus but there does not seem sufficient evidence at this time to exclude his subspecies from the genus, although this was suggested by Sytova (1970, p. 71). The form described by Sytova (1970, p. 71) as *S. minimus* is mainly a solitary form, but does occur as branching colonies.

The genus *Ramulophyllum* Nikolaeva, 1964, was originally described (Nikolaeva, 1964, p. 52) as a solitary form, with thick, carinate septa and a dissepimental and tabular structure similar to that described for *Stereoxylodes*. The form described by Sytova (1968, p. 62) as *R. explicatum* from the Skala Horizon (Upper Ludlow—Lower Pridoli) of Podolia has thinner, more complete septa than is typical of *Ramulophyllum*. Nikolaeva (1964) described six new species of *Ramulophyllum* from the Aynasuy Horizon of Central Kazakhstan (considered Upper Silurian by Ivanovskiy, 1965*b* and basal Devonian by Hill, 1967). Of the species, *R. heterozonale* (type species), *R. heliophylloides* and *R. parvum* in particular appear to show very similar structure to that of *Stereoxylodes*. The major difference appears to lie in the more degenerate peripheral septal structure shown in *Ramulophyllum*. The septa appear to break down into separate " strands " with irregularly oriented septal lamellae, giving the appearance of rather large, randomly inclined carinae. Very small globose dissepiments appear to be " clustered " around the septal lamellae in forms showing greatest breakdown of septa. These features are shown especially in the Czechoslovakian " *R.*" *prosperum* (Počta, 1902) (see Prantl, 1940, Figures 6–8). This species was listed as a possible synonym of *Stereoxylodes* by Ivanovskiy (1965*b*), and considered congeneric with *S. pseudodianthus* by Prantl (1940). However, this feature appears to be a further development of the formation of dilated, carinate septa found in representatives of *Stereoxylodes*, the specimens of *Stereoxylodes pseudodianthus* figured from the Wenlock of England by Lang and Smith (1927, p. 475, Figure 15) and Lower Ludlow of Estonia (Ivanovskiy, 1965*a*, Plate XIX, Figure 2) showing some peripheral septal breakdown of this type. Hence it seems reasonable to include *Ramulophyllum* as a synonym of *Stereoxylodes*, although forms with more degenerate septa should perhaps be included as a subgenus of *Stereoxylodes*. For the present, however, *Ramulophyllum* is included with reservations as a synonym.

Nikolaeva (1964) also described the new genus *Ornatophyllum* from the same horizon as *Ramulophyllum*. According to Nikolaeva the distinguishing features of the former were the major septa being longer than in *Ramulophyllum*, forming an axial complex. The length of septa in described species of *Stereoxylodes* is variable although they generally extend to near the axis, but the presence of septal lamellae which may form a weak axial complex may be enough to distinguish the genus. In all other respects, particularly the dilated, strongly carinate septa, *Ornatophyllum* seems comparable to *Stereoxylodes*. Its position is unresolved.

The position of the genus *Carinophyllum* Strelnikov, 1964, is not certain. It was originally described as a solitary form (Strelnikov, 1964, p. 59), but the type species then designated, *Cyathophyllum confusum* Počta, 1902 from the Upper Silurian (Budnany) of Czechoslovakia, is colonial (see Počta, 1902, Plate 99, Figure 3–11). *C. confusum* was considered congeneric with *S. pseudodianthus* by Prantl (1940). In internal morphology the genus is very similar to *Stereoxylodes*, differing in having very strongly dilated septa that are greatly thickened with schlerenchyme. As mentioned above, Ivanovskiy (1965*a*) suggested that the name *Carinophyllum* be used for compound forms having the internal morphology of *Stereoxylodes* and subsequent workers have recognized colonial representatives of *Carinophyllum* only (see Shurygina, 1968, p. 78). Whether the presence of abundant sclerenchymal thickening of the septa in *Carinophyllum* is due to environmental factors or is a feature peculiar to that particular genus and is thus of taxonomic importance is not certain. If the latter is the case, then subgeneric status seems the most useful classification of " *Carinophyllum* ".

Range : Upper Llandovery of N.S.W. ; Wenlock of England, Germany (drift), Czechoslovakia and ? China ; Upper Silurian of Estonia, Czechoslovakia, ? Poland, Podolia, ? Turkey, Urals, Subpolar Urals, Vaygach Island and Kazakhstan.

Stereoxylodes multicarinatus sp. nov.

Plate IV, Figures 3–10 ; Plate V, Figure 2

Derivation of name : After the strongly carinate nature of the septa, particularly in the axial zone.

Material : Holotype SUP 46184, Paratypes SUP 46185–46187. SUP 46188 is doubtfully included in the species. Rosyth Limestone, Boree Creek area. Upper Llandovery.

Diagnosis : Solitary, trochoid *Stereoxylodes* with septa strongly carinate with spinose projections, particularly in tabularium in late growth stages, and marked peripheral breakdown of septa.

Major septa reach axis. Tabulae divided into strongly arched axial series and concave periaxial series; dissepiments numerous, small and slightly elongate.

Description: Solitary, trochoid corallum with diameter ranging from approximately 30–45 mm Corallum height of approximately 40 mm in small relatively incomplete specimen (SUP 46188). Epitheca generally not preserved, but where present (in probable representative of *S. multicarinatus*, SUP 46188) it is mainly smooth with faint horizontal wrinkles and pronounced septal grooves. Calice shows a pit with depth of about 18 mm in largest specimen (SUP 46185), with diameter 15 mm at base and 25 mm at rim, where overall corallite diameter is 45 mm. Sides of calical pit steep, with slight development of broad boss at base of pit. Wide calicular platform present which is flat or slightly arched.

Maximum septal number of approximately 90 in largest specimen (incomplete, SUP 46185), and generally ranges from 80–86 in smaller forms. Septa of two orders, major septa extending or almost extending to corallite axis, where weak twisting of septal ends may occur. Major septa withdrawn from axis in earlier growth stages (see Plate IV, Figure 6). Carinae generally strongly developed, particularly on major septa, and in longitudinal section (e.g. Plate IV, Figure 10) can be seen to consist of spines or denticles, at least on their outer edges. Carinae generally almost perpendicular to septal lamellae in axial region but usually more oblique in dissepimentarium, forming typical zig-zag carinae. Septa strongly thickened in dissepimentarium but major septa taper towards axis. However, towards outer margin of dissepimentarium, septa lose their solid structure and break down to give retiform appearance, consisting of thin septal lamellae and carinae with occasionally clusters of small dissepiments around these elements. This structure is illustrated in Plate IV, Figure 3. Minor septa are thinner than major septa and approximately 0·3–0·4 of length of major septa.

Tabularium wide, at least half diameter of corallite, composed of narrow periaxial series of strongly concave, incomplete tabulae and strongly arched axial series consisting of large, globose tabellae at margin and slightly sagging incomplete tabulae and tabellae in the centre (see Plate IV, Figure 9). Dissepiments small, globose or weakly elongate, very steeply inclined so as to be almost parallel to corallite wall. Average dimensions 0·8–1·0 mm wide and 0·4 mm high.

Ontogeny: Although only a few specimens are available for study and the material is very incomplete preserved, some comments may be made on the morphological changes during growth of the form, owing to the different growth stages preserved in different specimens.

The earliest stage preserved (? early neanic) is represented in SUP 46187*a* (Plate IV, Figure 6) where at a corallite diameter of 13 mm, 68 septa are present. At this level, the major septa are somewhat withdrawn from the axis, although a few isolated, wavy septal lamellae extend into this zone. The septa are quite strongly dilated, especially near the periphery and carinae are well developed though widely spaced. Peripheral breakdown of the septa can be detected but the material is incomplete in this region. Minor septa are very short although periphery of specimen is not preserved.

A late neanic or early ephebic stage is represented in SUP 46184*a* (Plate IV, Figure 9) where at a corallite diameter of 25 mm, 84 septa are developed. At this stage the major septa reach the axis and are slightly twisted. The major septa are moderately dilated and solid near the inner margin of the dissepimentarium, tapering towards the axis and remaining dilated but breaking up into the retiform condition towards the periphery. Septa are moderately carinate throughout and minor septa extend up to half length of major septa.

A late ephebic stage is represented in SUP 46185*b* (Plate IV, Figure 5), sectioned just below the calical pit where the corallite diameter is 36 mm and septal number 90. Major septa are strongly dilated, tapering only near the axis, where they meet. Carinae are very numerous and septa are broken down to a retiform condition in most of the dissepimentarium. Where the septa are " solid " (near dissepimentarial—tabularial boundary) they appear to be thickened with sclerenchyme which decreases towards the periphery, exposing the retiform condition. Minor septa are at least half the length of the major septa.

Remarks: None of the described species of *Stereoxylodes* show any very close similarities to *S. multicarinatus* sp. nov. It is a larger species than any described, the only species approaching it in dimensions being *S. prosperus* (Počta, 1902) from the Upper Silurian (Budnany) of Czechoslovakia. Other similarities to this species include the strongly carinate, dilated septa breaking down into a reticulate structure peripherally and the shape and disposition of dissepiments and tabulae. It may, however, be clearly distinguished from *S. multicarinatus* by possessing offsets and shorter major septa and lacking carinae in the axial region.

The type species, *S. pseudodianthus* (Weissermel, 1894), has long septa as in *S. multicarinatus* and very strong development of carinae, although this is not as pronounced as in *S. multicarinatus* in the axial zone, but the septa are not as strongly dilated in the dissepimentarium and peripheral breakdown of septa is not as pronounced (see particularly Lang and Smith, 1927, p. 475, Figure 15).

Specimens of *Strombodes rosythensis* sp. nov., described below, may show development of carinae similar to those of *Stereoxylodes multicarinatus*, but they are generally more weakly developed in the former (see Plate VI, Figure 3). The N.S.W. occurrence of *Stereoxylodes* is apparently the oldest recorded at present. The genus first appears overseas in the Wenlock of Europe and is most common in the Upper Silurian of Eastern Europe and Central Asia.

? *Stereoxylodes* sp.

Plate IV, Figure 11 ; Plate V, Figure 1

Material : SUP 46189 Rosyth Limestone, Boree Creek area, Upper Llandovery.

Description : Solitary, trochoid corallum with maximum corallite diameter of 42 mm. Calice similar to that in *S. multicarinatus* sp. nov. Septal number 86 at corallite diameter 32 mm. just below base of calice. Major septa long, reaching axis, where they show marked twisting, Septa strongly dilated in dissepimentarium, tapering towards axis and showing marked peripheral breakdown as in *S. multicarinatus*. Carinae only weakly developed, particularly on axial side of peripheral breakdown of septa. Minor septa approximately 0·3 length of major septa.

Tabularium incompletely preserved but there appears to be less strong differentiation into an axial and periaxial series of tabulae. Strongly arched series of tabellae at least are present. Dissepimentarium only partly present in imperfect longitudinal section, but size and disposition appears similar to that in *S. multicarinatus* sp. nov.

Remarks : This specimen differs from *S. multicarinatus* sp. nov. only in the prominent twisting of the axial ends of the major septa and the weak development of carinae. It shows similarities to *Ptychophyllum* Edwards and Haime, 1850, in possessing an axial vortex and the dilated septa, but the presence of carinae, although weak, and the much more pronounced peripheral breakdown of the septa serve to distinguish it. It may represent an aberrant form of *S. multicarinatus*, but until the species can be studied in more detail with a larger number of specimens, its taxonomic position remains unresolved.

Family Uncertain

Discussion : The suprageneric status of *Strombodes* Schweigger, 1819, is at present uncertain. Previous authors have included it as a representative of various families of the suborder Columnariina Rominger, 1876 (e.g. Chonophyllidae Holmes : Hill, 1956 ; Kaljo, 1958 ; Spongophyllidae Dybowski : Ivanovskiy, 1965*a*). However, *Strombodes* shows very close similarities to the genus *Entelophyllum* Wedekind, 1927, a representative of the Arachnophyllidae (suborder Streptelasmatina). *Entelophyllum*, as defined by Sytova (1952) and Ivanovskiy (1963*a* and *b*) is taken to include massive, fasciculate and solitary coralla with lamellar septa, horizontal convex or convexo-concave, often incomplete tabulae and usually small, globose dissepiments that may be exceptionally lonsdaleoid. Hence the only significant difference between this genus and *Strombodes* seems to be that the latter has typically well-developed lonsdaleoid dissepiments that are elongate rather than globose. Therefore it does not appear justified to separate *Strombodes* and *Entelophyllum* into separate suborders. Equally, however, the view of Ivanovskiy (1965*a*) whereby *Arachnophyllum* and *Entelophyllum* were grouped in the Columnariina (family Arachnophyllidae) together with *Strombodes* (family Spongophyllidae), while typical Arachnophyllid forms *Ptychophyllum* and *Cyathactis* were included in the Streptelasmatina (family Ptychophyllidae), does not appear acceptable. A restudy of these and related forms would appear essential before this taxonomic problem can be resolved.

Genus *Strombodes* Schweigger, 1819

?1927 *Kyphophyllum* Wedekind, p. 19.
?1937 *Kyphophyllum* ; Soshkina, p. 27.
?1927 *Tenuiphyllum* (*part.*) Soshkina, p. 31.
?1944 *Kyphophyllum* ; Wang, p. 26.
?1949 *Cyathophyllum* (*part.*) ; Amsden, p. 108 (*non* Goldfuss, 1826).
1955 *Evenkiella* (*part.*) Soshkina, p. 126.
?1958 *Kyphophyllum* ; Kaljo, p. 107.
1962 *Tabulophyllum* ; Ivanovskiy, p. 120 (*non* Fenton and Fenton, 1924).
1963*a* *Evenkiella* ; Ivanovskiy, p. 80.

1963*b* *Evenkiella*; Ivanovskiy, p. 88.
?1963*b* *Tenuiphyllum*; Ivanovskiy, p. 90.
?1965 *Strombodes*; Stumm, p. 47.
1965*a* *Strombodes*; Ivanovskiy, p. 116 (*cum syn.*).
1965 *Kyphophyllum*; Strelnikov, p. 40.
1966 *Strombodes*; Sytova and Ulitina, p. 233.
?1968 *Evenkiella*; Lavrusevich, p. 115.
?1970 *Strombodes* (*Kyphophyllum*); Flügel and Saleh, p. 281.
?1970 *Tenuiphyllum*; Flügel and Saleh, p. 284.
1971 *Strombodes*; Strelnikov, p. 79.
?1972 *Kyphophyllum*; Merriam, p. 36.
1973 *Strombodes*; Strelnikov, p. 49.
non 1960 *Evenkiella*; Zheltonogova, p. 86.

Type species: Madrepora stellaris Linnaeus, 1758, Slite Beds (Wenlock), Gotland.

Diagnosis: Fasciculate, massive or ? solitary corallum. Septa of two orders, usually thin, characteristically lonsdaleoid near periphery of corallite. Tabulae complete and incomplete, commonly domed. Dissepiments usually elongate.

Discussion: The genus *Kyphophyllum* was erected by Wedekind (1927) and subsequently revised by Sytova (1952). Wedekind's material consisted of both solitary and compound forms (Wedekind, 1927, p. 19). However, Sytova (1952) included only compound forms, with the following diagnosis (summarized): " fasciculate colonies, with thin, sometimes discontinuous septa, strongly convex tabulae and large, flattened, often lonsdaleoid dissepiments ". On such a basis, there seems little reason to doubt that *Kyphophyllum* is synonymous with *Strombodes*, a view held by Smith (1945), Wang (1950) and Ivanovskiy (1965*a*). Flügel and Saleh (1970) suggested that *Kyphophyllum* be considered a subgenus of *Strombodes* on the basis of *Kyphophyllum* being a solitary form. There has been no consistency in the past as to how forms with similar internal morphology, but having both solitary and compound coralla, should be classified. In the main, both solitary and compound forms have been grouped in the one genus, so until a definitive statement is made on this subject, it seems best to follow this viewpoint. Accordingly *Kyphophyllum* is here included as a probable synonym of *Strombodes*.

The genus *Evenkiella* Soshkina, 1955, was erected to include forms having colonial coralla, thin lamellar septa, flattened convex tabulae which are usually incomplete, together with large, lonsdaleoid dissepiments (Soshkina, 1955 and Ivanovskiy, 1963*a* and *b*). On the basis of the variability within the similar genus *Entelophyllum*, as described by Sytova (1952) and Ivanovskiy (1963*a* and *b*), it seems reasonable to regard *Evenkiella* as a junior synonym of the genus *Strombodes*, as defined above. Ivanovskiy (1965*a*, p. 85) recognized a relationship between *Strombodes* and *Evenkiella* by placing the latter in the family Spongophyllidae as well, but still considered them separate genera.

To the genus *Tenuiphyllum* Soshkina, 1937, as redefined by Ivanovskiy (1963*b*, p. 90), were assigned forms having massive coralla, occasionally lonsdaleoid septa, convex tabulae and numerous, rather small dissepiments. The characteristic feature was development of an " internal wall " from lamellar sclerenchymal thickening of the septa to make them laterally contiguous at some part of their length. Wang (1950) considered *Tenuiphyllum* a synonym of *Entelophyllum* but the genus shows similarities to both cerioid *Strombodes* and *Entelophyllum*, and probably is closer to *Strombodes* in rather commonly showing elongate lonsdaleoid dissepiments. Soshkina *et al.* (1962, p. 319) considered *Tenuiphyllum* synonymous with *Kyphophyllum* and Sytova (1952) included the species *T. flexuosum* Soshkina, 1937 in *Kyphophyllum*. However, Flügel and Saleh (1970, p. 284) believed *Tenuiphyllum* constituted a distinct genus. The " internal wall " may distinguish it as an aberrant form of *Strombodes* but the described species need to be studied in more detail before their true taxonomic status is clarified.

The systematic position of the genus *Micula* Sytova, 1952, is uncertain. The name was proposed for forms having solitary, cylindroconical coralla; long septa of two orders; arched, incomplete tabulae and small globose dissepiments. The lack of budding in this form was used to distinguish it from *Entelophyllum*. However, lonsdaleoid septa may be present in some specimens (Sytova, 1952) and it seems the genus may represent an intermediate between true *Entelophyllum* and *Strombodes*. Sytova (1952) suggested that the solitary species, " *Kyphophyllum primaevum* " described by Wang (1944), belongs to either *Micula* or an intermediate between *Micula* and *Kyphophyllum*. It is possible that forms apparently possessing solitary coralla and previously included in " *Kyphophyllum* " (*K. cylindricum* Wedekind, 1927; *K. conicum* Wedekind, 1927; *K. tenue* Wedekind, 1927; *K. multiseptatum* Soshkina, 1937 ; *K. primaevum* Wang, 1944 ; *K. schmidti* Kaljo, 1958), could perhaps be included in *Micula*, if one considers that solitary and compound forms should not be grouped in the one genus although this does not seem a useful distinction. The systematic position of these species and of *Micula* itself for the moment remains unresolved.

Range : Upper Ashgill of Estonia ; Llandovery of Estonia and ? north-east Iran ; Upper Llandovery of Siberian Platform and N.S.W., Wenlock of Gotland, northern Urals, Subpolar Urals and Siberian Platform ; Upper Silurian of Estonia, northern Urals, Arctic U.S.S.R. (Chernov Ridge), Kazakhstan, ? California and ? Nevada.

Strombodes rosythensis sp. nov.

Plate V, Figure 3–6 ; Plate VI, Figure 1–5

Derivation of name : After the type horizon, the Rosyth Limestone.

Material : Holotype SUP 45217, Paratypes SUP 25165, 45218–45227, Rosyth Limestone, Boree Creek area, Upper Llandovery.

Diagnosis : Phaceloid or partially cerioid *Strombodes* with parricidal and non-parricidal calicinal increase. Average corallite diameter of 13 mm., septa commonly showing dilation and weak ? carinae in dissepimentarium. Dissepiments in broad zone, with at least five rows.

Description : Corallum colonial, both phaceloid and cerioid. Corallites commonly fasciculate immediately after budding. Adjacent corallite walls usually in contact, or periodically so, giving cerioid transverse section during later ontogeny. Epitheca thin, with faint vertical septal striations and horizontal imbricating rings, representing impressions of dissepiments. Transverse wrinkling and rejuvenescence frequently shown. Corallites cylindrical, showing polygonal transverse section when cerioid. Colonies may reach size of 60 cm or more in width and 30 cm in height. Corallite diameter may increase gradually from very narrow initial stage (1–2 mm) with sudden increase in mature dimensions (average 13 mm) or may never reach normal maximum size owing to crowding by adjacent larger corallites. Maximum diameter observed, 18 mm.

Growth commonly ceases at a particular level in adjacent corallites, some then sending out buds. Increase invariably calicinal, usually from outer rim of calice, although occasionally from central pit (in this case it is probably simple rejuvenation). At least six offsets observed from one calice during ontogeny in corallites showing rejuvenescence (Plate V, Figures 3, 4). Increase is mostly non-parricial since rejuvenescence almost always occur at time of budding. Calice deep, with broadly flaring, flattened margin, average diameter of calicular pit 7 mm, depth 4–5 mm. Axial boss in pit average 4 mm wide, with height 1–2 mm.

Septa usually lonsdaleoid, average number 52 (maximum observed 62). Major septa reach almost to axis. In late ontogeny weak axial vortex may occur, with septa reaching almost to axis. Major septa generally thickened in dissepimentarium and may show weak zig-zag ? carinae. Minor septa generally weakly developed, strongly lonsdaleoid, rarely extending into tabularium. Minor septa do not appear to be distinguishable until a diameter of approximately 7 mm is reached (although silicification tends to obscure most detail in immature stages). In longitudinal section (Plate V, Figure 6), possible trabecular nature of septa shown by short spines arising from dissepiments (including also oblique intersections of septa). Being perpendicular to dissepimental surface, they are gently inclined towards corallite axis.

Tabulae incomplete mainly, strongly distally arched in axial region with sagging lateral margins. Central area flattened, with slight axial depression, or composed of imbricating subsidiary tabellae. Tabularium average diameter 4·5–5 mm, tabular spacing 0·3–0·5 mm. Dissepiments mainly elongate, tending to be more globose in inner area of dissepimentarium. In peripheral area, maximum width of dissepiments reaches approximately 2·5 mm, decreasing axially to more globose types of width 0·5 mm. Average dissepimental height 0·4–0·5 mm. Dissepiments commonly in 5–6 rows, gently inclined towards axis, becoming steeper near tabularial margin.

Remarks : Only three species of *Strombodes* show much similarity to the Rosyth form. *S. socialis* (Soshkina, 1955), from the Upper Llandovery of the Siberian Platform and the Lower Wenlock of the Urals is comparable to the local species in its phaceloid growth form and non-parricidal increase, strongly lonsdaeloid septa and elongate dissepiments and tabular form (see Soshkina, 1955 ; Ivanovskiy, 1965*a* ; Strelnikov, 1971). In particular the longitudinal section figured by Soshkina (1955, Plate XII, Figure 2) is very similar to that of the Rosyth species. However, *S. socialis* may be distinguished by much larger dimensions (up to 30–40 mm corallite diameter) a larger number of much thinner septa (70) and a greater number of dissepiments (10–15 rows).

S. elkinense (Sytova, 1952), from the Wenlock of the Northern Urals shows strong similarities to *S. rosythensis* in its manner of increase, with formation of offsets from the rim of the old calice at the time of rejuvenescence (Sytova, 1952). It is also comparable to the Rosyth form in corallite dimensions, septal number and septal form. However, it may be distinguished by having thinner septa, a wider tabularium with more widely spaced tabulae and fewer, more globose and more steeply inclined dissepiments.

Acknowledgements

The writer is grateful to Dr. B. D. Webby for critical review of the manuscript. The project was partly supported by a Commonwealth Postgraduate Studentship at the University of Sydney.

References

In order to save costs some publications have not been cited in the bibliography. These are included in Cotton, G. (1973).

Amsden, T. W., 1949. Stratigraphy and Paleontology of the Brownsport Formation (Silurian) of Western Tennessee. *Bull. Peabody Mus. nat. Hist.*, **5**, 1.

Bassler, R. S., 1950. Faunal Lists and Descriptions of Paleozoic Corals. *Mem. geol. Soc. Am.*, **44**, 1.

Cotton, G., 1973. *The Rugose Coral Genera*, Elsevier, Amsterdam.

Etheridge, R. Jr., 1909. *Arachnophyllum* from the Halysites Limestone of the Mount Canobolas District, New South Wales. *Rec. geol. Surv. N.S.W.*, **8**, 304.

Flügel, H. W., and Saleh, H., 1970. Die paläozoischen Korallenfaunen Ost-Irans. I. Rugose Korallen der Niur-formation (Silur). *Jb. geol. Bundesant*, **113**, 267.

Foerste, A. F., 1890. Notes on Clinton Group Fossils, with Special Reference to Collections from Indiana, Tennessee and Georgia. *Proc. Boston Soc. nat. Hist.*, **24**, 263.

Foerste, A. F., 1903. Silurian and Devonian Limestones of Western Tennessee. *J. Geol.*, **11**, 544, 679.

Foerste, A. F., 1906. The Silurian, Devonian and Irvine Formations of East-Central Kentucky, etc., *Bull. Ky geol. Surv.*, **7**, 1.

Hill, D., 1940. The Silurian Rugosa of the Yass-Bowning District, N.S.W. *Proc. Linn. Soc. N.S.W.*, **65**, 388.

Hill, D., 1956. Rugosa; *in* Moore, R. C. (Ed.), *Treatise on Invertebrate Paleontology. Part F. Coelenterata.* Lawrence, Kansas, F233.

Hill, D., 1967. The Sequence and Distribution of Ludlovian, Lower Devonian and Couvinian Coral Faunas in the Union of Soviet Socialist Republics. *Palaeontology*, **10**, 660.

Ivanovskiy, A. B., 1962. Elementi devonskoy fauni v silure Sibirskoy Platformi. *Trudy sib. nauchno-issled. Inst. Geol. Geofiz. miner. Syr.*, **23**, 120.

Ivanovskiy, A. B., 1963*a*. Razvitnie i geneticheskie svyazi predstaviteley rodov siluriyskikh rugoz *Entelophyllum* Wdkd i *Evenkiella* Soshk. *Geol & Geofiz. 1963*, **11**, 80.

Ivanovskiy, A. B., 1963*b*. *Rugozy ordovika i silura Sibirskoy Platformi.* 160pp. Moscow. Nauka (Akad. Nauk SSSR, Sib. Otd. Inst. Geol. Geofiz.).

Ivanovskiy, A. B., 1965*a*. *Drevneyshie rugozy.* 152pp. Moscow. Nauka. (Akad. Nauk SSSR, Sib. Otd. Inst. Geol. Geofiz.).

Ivanovskiy, A. B., 1965*b*. *Stratigraficheskie i paleobiogeograficheskie obzor rugoz ordovika i silura.* 120pp. Moscow. Nauka (Akad. Nauk SSSR, Sib. Otd. Inst. Geol. Geofiz.).

Ivanovskiy, A. B., 1965*c*. Filogeniya semeystva Ptychophyllidae Dybowski; *in* Sokolov, B. S., and Ivanovskiy, A. B. (Eds.), Rugozy paleozoya SSSR. *Trudy I Vsesoyuznogo simpoziuma po izucheniyu iskopaemykh korallov*, **2**. Moscow. Nauka (Akad. Nauk SSSR, Sib. Otd. Inst. Geol. Geofiz.), 25.

Kaljo, D. L., 1958. Nekotorie novie i maloizvestnie rugozy Pribaltiki. *Eesti NSV Tead. Akad. geol. Inst. Uurim.*, **3**, 101.

Lambe, L. M., 1901. A Revision of the Canadian Palaeozoic Corals; the Madreporaria aporosa and the Madreporaria rugosa. *Contr. Can. Palaeont.*, **4** (2), 97.

Lang, W. D., 1926. *Naos pagoda* (Salter), the Type of a New Genus of Silurian Corals. *Q. J. geol. Soc. Lond.*, **82**, 428.

Lang, W. D., and Smith, S., 1927. A Critical Revision of the Rugose Corals Described by W. Lonsdale in Murchison's "Silurian System". *Q. J. geol. Soc. Lond.*, **83**, 448.

Lavrusevich, A. I., 1968. Rugozy postludlovskikh otlozheniy doloniny r. Zeravshan. (Tsentralny Tadzhikistan); *in* Sokolov, B. S., and Ivanovskiy, A. B. (Eds.), *Biostratigrafiya pogranichnykh otlozheniy silura i devona.* Moscow. Nauka (Akad. Nauk SSSR, Sib. Otd. Inst. Geol. Geofiz.), 102.

Lavrusevich, A. I., 1971. Rugozy rannego silura Zeravshano-Gissarskoy gornoy oblasti; *in* Lavrusevich, A. I. (Ed.), Paleontologiya i stratigrafiya. 3. *Trudy Uprav. geol. Sov. Minist. Tadzhik. SSR*, 38.

McLean, R. A., 1973. Studies of Lower-early Middle Silurian Rugose Corals from Central New South Wales. Unpubl. Ph.D. Thesis, Univ. of Sydney.

McLean, R. A., 1974*a*. Chonophyllinid Corals from the Silurian of New South Wales. *Palaeontology*, **17** (3), 655 *in press.*

McLean, R. A., 1974*b*. Cystiphylliade and Goniophyllidae (Rugosa) from the Lower Silurian of New South Wales. *Palaeontographica.* Abt. A., 147, *in press.*

Merriam, C. W., 1972. Silurian Rugose Corals of the Klamath Mountains Region, California. *Prof. Pap. U.S. geol. Surv.*, **738**, 1.

Nikolaeva, T. V., 1964. Noyve rugozy semeystva Ramulophyllidae iz silura tsentralnogo Kazakhstana. *Trudy vses. nauchno-issled. geol. Inst.* (*N.S.*), **9**, 49.

Norford, B. S., 1962. The Silurian Fauna of the Sandpile Group of Northern British Columbia. *Bull. geol. Surv. Can.*, **78**, 1051.

Parks, W. A., 1933. New Species cf Stromatoporoids, Sponges and Corals from the Silurian Strata of Baie des Chaleurs. *Univ. Toronto Stud. geol. Surv.*, **33**, 1.

Počta, P., 1902. Anthozoaires et Alcyonaires; *in* Barrande, J. (Ed.), *Systême Silurien du Centre de la Bohême*, **8** (2), 1.

Prantl., 1940. Výskyt rodu *Xylodes* Lang and Smith (Rugosa) v českén siluru. *Rozpr. Ceské Akad. Věd Umění*. Tr. II, **49** (14), 1.

Rominger, C., 1876. Lower Peninsula 1873–1876. Palaeontology, Fossil Corals. *Geol. Surv. Mich.*, **3** (2), 1.

Schouppé, A., 1951. Kritische Betrachtungen und Revision des Genusbegriffes *Entelophyllum* Wdk. nebst einegen Bemerkungen zu Wedekind's "Kyphophyllidae" und "Kodonophyllidae". *Sber. öst. Akad. Wiss.* Abt. I, **160**, Bd 3 and 4, 243.

Shrock, R. R., and Twenhofel, W. H., 1939. Silurian Fossils from Northern Newfoundland. *J. Paleont.*, **13**, 241.

Shurygina, M. V., 1968. Pozdnesilurieskie i rannedevonskie rugozy vostochnogo sklona severnogo i srednogo Urala; *in* Ivanovskiy, A. B. (Ed.), *Korally pogranichnikh silura i devona Altae—Sayanskoy gornoy oblasti i Urala*. Moscow. Nauka (Akad. Nauk SSSR, Sib. Otd., Inst. Geol. Geofiz.), 117.

Smith, S., 1945. Upper Devonian Corals of the Mackenzie River Region, Canada. *Spec. Pap. geol. Soc. Am.*, **59**, 1.

Smith, S., and Tremberth, R., 1929. On the Silurian Corals *Madreporites articulatus* Wahlenberg and *Madrepora truncata* Linnaeus. *Ann. Mag. nat. Hist.* Ser. 10, **3**, 362.

Soshkina, E. D., 1937. Korally verkhnego silura i nizhnego devona vostochnogo i zapadnogo sklonov Urala. *Trudy paleozool. Inst.*, **6** (4), 1.

Soshkina, E. D., 1955. Fauna ordovika i gotlandiya nizhnego techeniya r. Podkamennaya Tunguska, ee ekologiya i stratigraficheskoe znachenie. *Trudy paleont. Inst.*, **56**, 93.

Soshkina, E. D., Dobrolubova, T. A., and Kabakovich, N. V., 1962. Podklass Tetrakoralla; *in* Sokolov, B. S. (Ed.), *Osnovy Paleontologii, 2. Gubki, Arkeosiaty, Kishechnopolostnye, Chervi*. Moscow. (Akad. Nauk SSSR), 286.

Strelnikov, S. I., 1964. Ob obeme semeystva Kodonophyllidae (Rugosa). *Paleont. Zh. 1964*, **4**, 49.

Strelnikov, S. I., 1965. Ordovikskie i siluriyskie rugozy ostrovov Vaygacha i Dolgogo. *Uchen. Zap nauchno-issled. Inst. Geol. Arkt.* (*Paleont. Biostratigr.*), **8**, 24.

Strelnikov, S. I., 1971. Znachenie rugoz dlya stratigrafii siluriyskikh otlozheniy Pripolyarnogo Urala i Gryady Chernysheva; *in* Ivanovskiy, A. B. (Ed.), Rugozy i stromatoporoidei paleozoya SSSR. *Trudy II Vsesoyuznogo simpoziuma po izucheniyu iskopaemykh korallov SSSR. 2.* Moscow. Nauka (Akad. Nauk SSSR, Sib. Otd. Inst. Geol. Geofiz.), 71.

Strelnikov, S. I., 1973. Rugozy iz siluriyskikh otlozheniy podnyatiya chernova i polyanogo Urala. *Paleont. Zh. 1973*, **2**, 46.

Stumm, E. C., 1962. Silurian Corals from the Moose River Synclinorium, Maine. *Prof. Pap. U.S. geol. Surv. 430–A*, 1.

Stumm, E. C., 1965. Silurian and Devonian Corals of the Falls of the Ohio. *Mem. geol. Soc. Am.*, **93**, 1.

Sutherland, P. K., 1965. Rugose Corals of the Henryhouse Formation (Silurian) in Oklahoma. *Bull. Okla. geol. Surv.*, **109**, 1.

Sytova, V. A., 1952. Korally semeystva Kyphophyllidae iz verkhnego silura Urala. *Trudy paleont. Inst.*, **40**, 127.

Sytova, V. A., 1968. Tetrakorally skalskogo i borshchovskogo gorizontov Podolii; *in* Balashov, Z. G. (Ed.), *Siluriyskogo—devonskaya fauna Podolii*. Leningrad Univ., 51.

Sytova, V. A., 1970. Tetrakorally grebenskogo gorizonta Vaygacha; *in* Cherkesov, C. B. (Ed.), *Stratigrafiya i fauna siluriyskikh otlozheniy Vaygacha* (*sbornik statey*). Nauchnoissled. Inst. Geol. Arkt. minist. Geol. SSSR.—Leningrad, 65.

Sytova, V. A., and Ulitina, L. M., 1966. Rugozy isenskoy i biotarskoy svit.; *in* Chetverikova, N. P., *et al.*, Stratigrafiya i fauna siluriyskikh i nizhnedevonskikh otlozheniy Nurinskogo Sinklinoriya. *Materiali po geologii Tsentralnogo Kazakhstana*, **6**, 198.

Twenhofel, W. H., 1928. Geology of Anticosti Island. *Mem. geol. Surv. Can.*, **154**, 1.

Wang, H. C., 1944. Silurian Rugose Corals from Eastern and Northern Yunnan. *Bull. geol. Soc. China*, **24**, 21.

Wang, H. C., 1950. A Revision of the Zoantharia Rugosa in the Light of their Minute Skeletal Structures. *Phil. Trans. R. Soc.* ser. B, **234** (611), 175.

Wedekind, R., 1927. Die Zoantharia Rugosa von Gotland (bes Nordgotland). *Sver. geol. Unders. Afh.* ser. Ca., **19**, 1.

Weissermel, W., 1894. Die Korallen der Silurgeschiebe Ostpreussens und des östlichen Westpreussens. *Z. dt. geol. Ges.* **46**, 580.

Weissermel, W., 1939. Neue Beitrage sur Kenntnis der Geologie, Palaeontologie und Petrographie der Umgegend von Konstantinopel. 3. Obersilurische und devonische Korallen, Stromatoporoiden und Trepostome von der Prinzeninsel Antirovitha und aus Bithynien. *Abh. preuss. geol. Landesamt.*, **190**, 1.

Yü, C. M., 1956. Some Silurian Corals from the Chiuchuan Basin, Western Kansu. *Acta palaeont. sin.*, **4**, 499.

Zheltonogova, V. A., 1960. Siluriyskaya sistema. Podklass Tetracoralla (Rugosa). Tetrakorally; *in* Khalfin, L. L. (Ed.), Biostratigrafiya paleozoya Sayano—Altayskoy gornoy oblasti. Tom 2. Sredniy Paleozoy. *Trudy sib. nauchno-issled. Inst. Geol. Geofiz. miner. Syr.*, **20**, 74.

Department of Geology and Geophysics,
University of Sydney,
Sydney, N.S.W.

(Received 10.12.73)


1

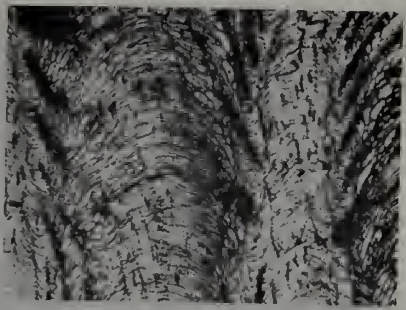
2

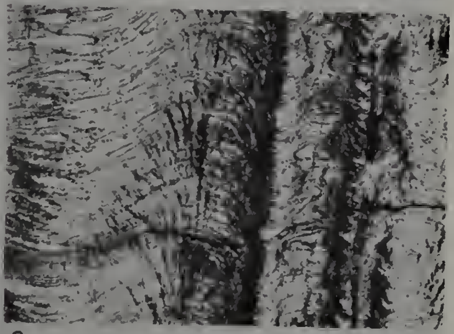
3


4


5

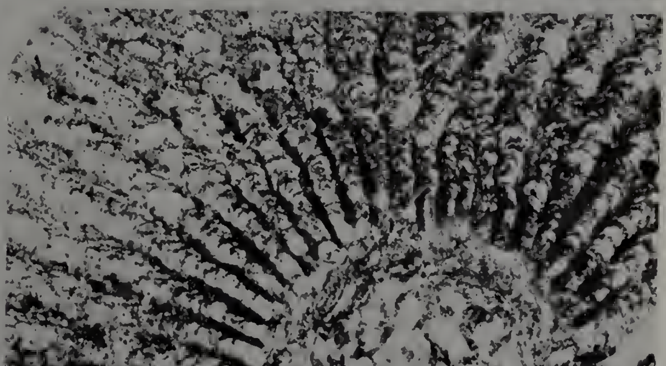
6


1

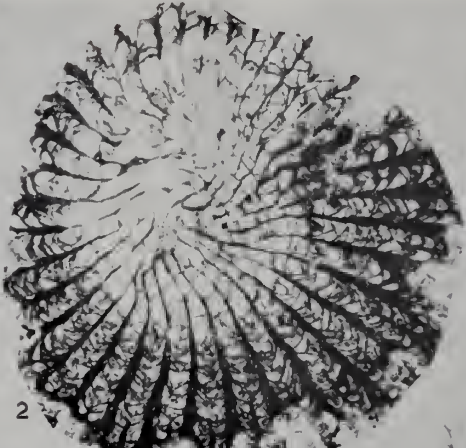
2


3


4

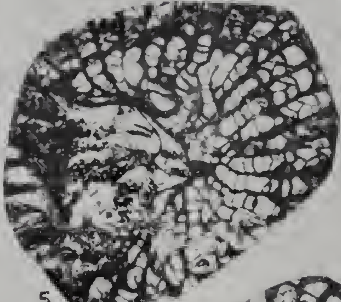
5


7

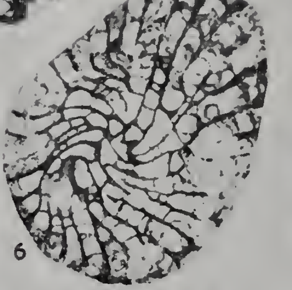
6

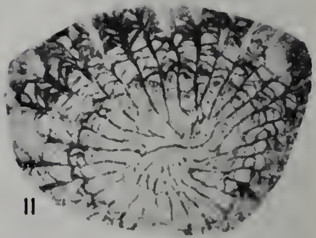
11

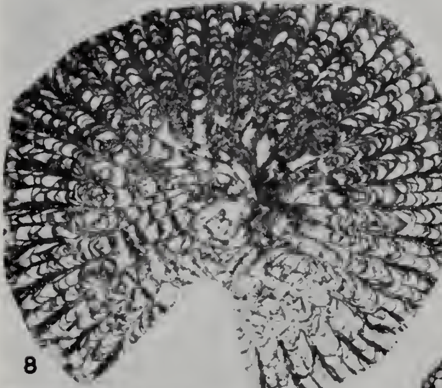
8

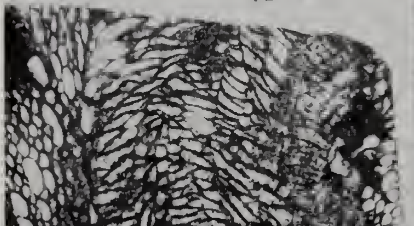
9

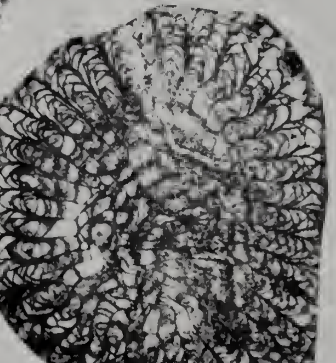
10

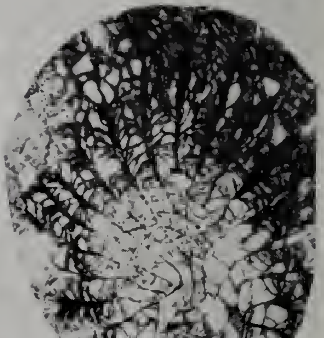
12

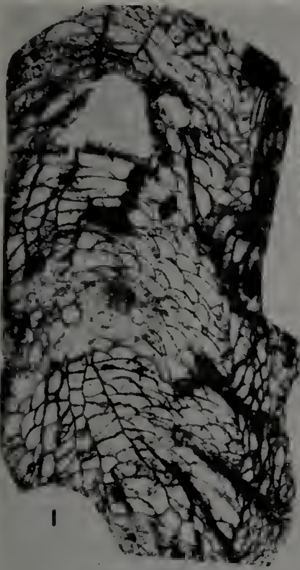
1

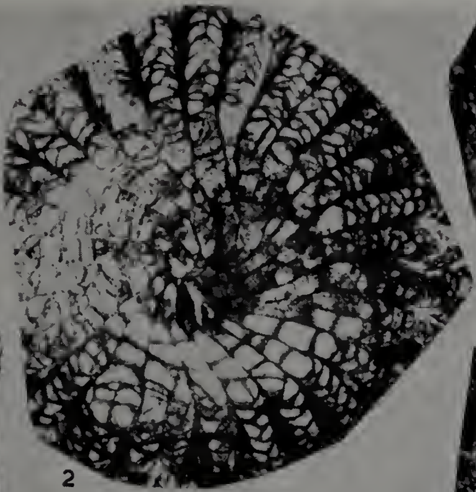
2

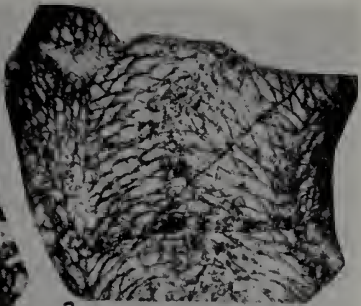
3

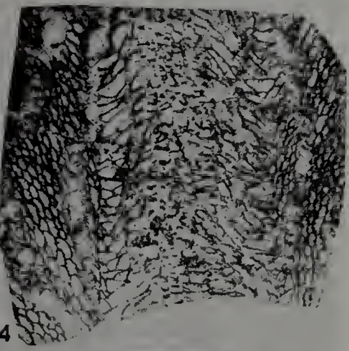
4

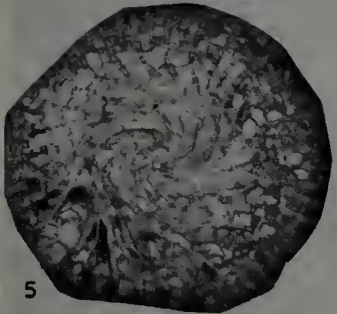
5

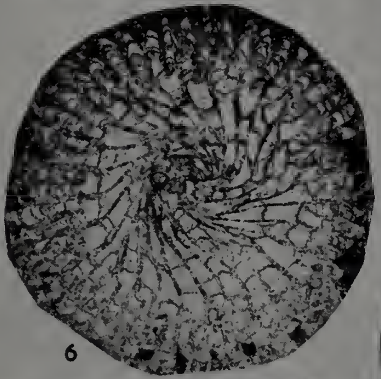
6

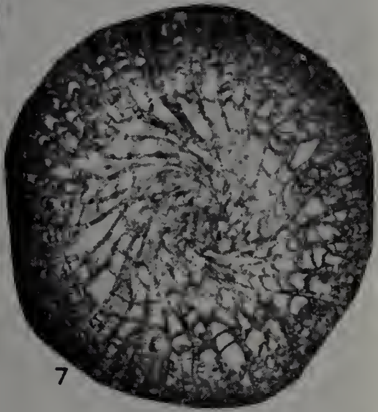
7

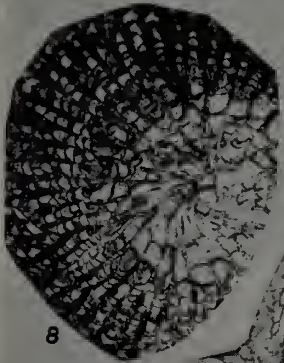
8

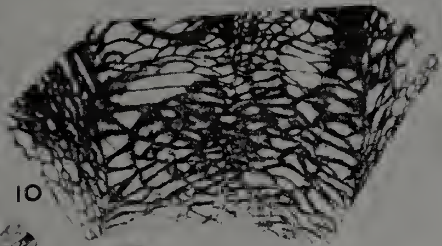
10

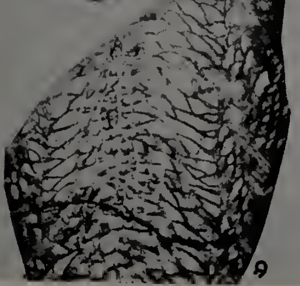
9


11


12

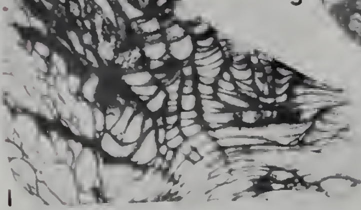

1

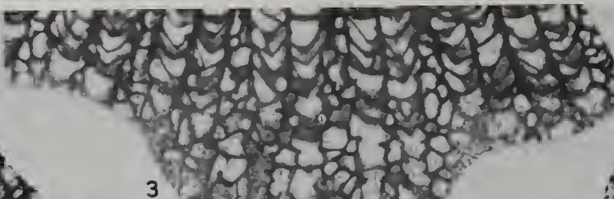

3

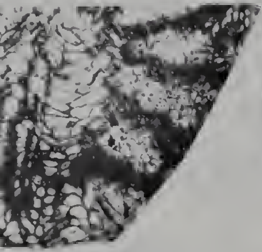

4

5

2

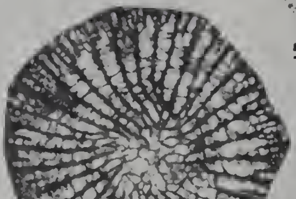

6

7

11

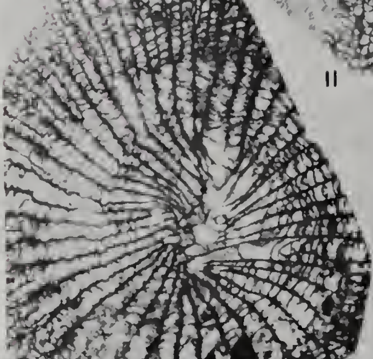

8

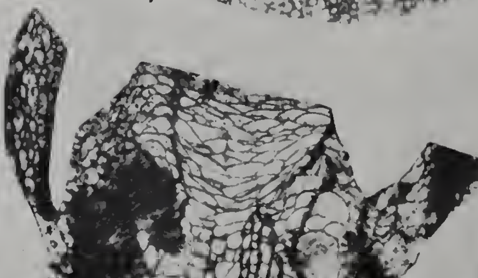

9

10


1

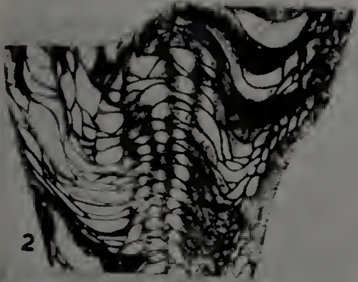
2


3

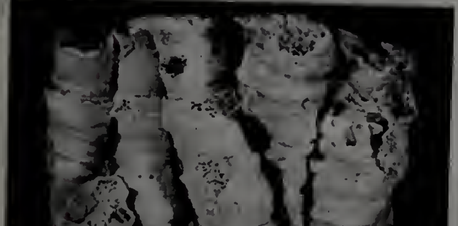
4


5


6

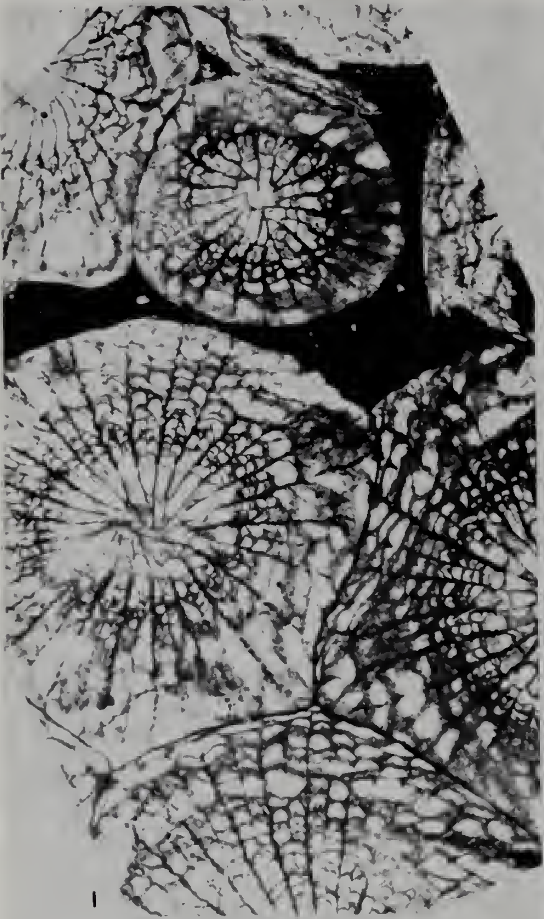
1

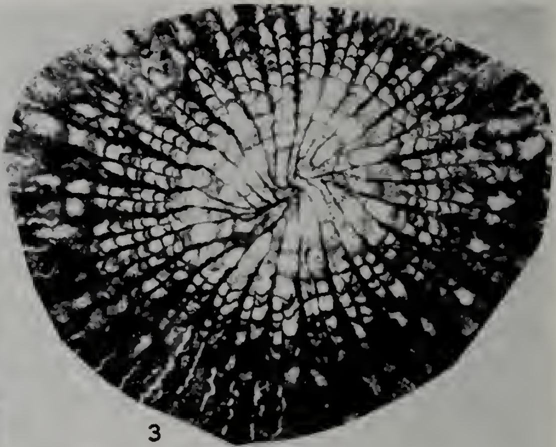
3

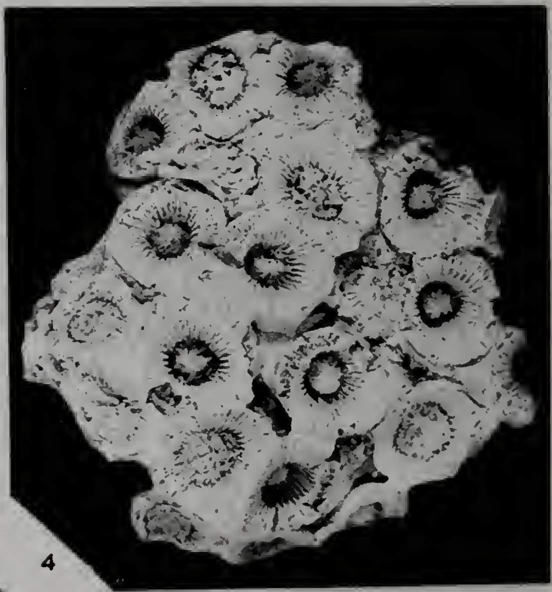
4


2


5

EXPLANATION OF PLATE I

Figures 1–6.—*Arachnophyllum epistomoides* Etheridge, Quarry Creek Limestone. 1, AM 4866, lectotype, longitudinal section, ×2. 2, SUP 45230, longitudinal section, ×2. 3, AM 4343, paralectotype, longitudinal section, ×2. 4, SUP 45228, topotype, transverse section showing septal lamellae in tabularium, ×4. 5, AM 4866, lectotype, transverse section of portion of dissepimentarium showing breakdown of septa and ? lamellar sclerenchymal coating of septal elements, ×4. 6, AM 4866, lectotype, transverse section showing breakdown of septa in dissepimentarium, ×4.

EXPLANATION OF PLATE II

Figure 1.—*Arachnophyllum epistomoides* Etheridge, Rosyth Limestone, ×4. SUP 27150b, longitudinal section of tabularium.

Figures 2–7, 11, 12.—*Ptychophyllum auctum* sp. nov., Quarry Creek Limestone, ×3. 2, SUP 45204a, holotype, transverse section. 3–6, SUP 45206b–e, paratype, transverse sections (Figure 3 shows most distal section, others are in order). 7, SUP 45204e, holotype, longitudinal section. 11, SUP 45205e, paratype, transverse section. 12, SUP 45205d, paratype, transverse section.

Figures 8–10.—*Ptychophyllum auctum* ? sp. nov., Rosyth Limestone, ×2. 8, SUP 45208b, transverse section. 9, SUP 45208c, longitudinal section. 10, SUP 45208a, transverse section.

EXPLANATION OF PLATE III

Figures 1, 2.—*Ptychophyllum auctum* sp. nov., Quarry Creek Limestone, ×3. 1, SUP 45205f, paratype, longitudinal section. 2, SUP 45207, paratype, transverse section.

Figures 3–9.—*Ptychophyllum* cf. *sibiricum* Ivanovskiy, Upper limestone horizon, Cobblers Creek, Angullong district, ×3. 3, SUP 45213b, longitudinal section. 4, SUP 20111b, longitudinal section. 5, SUP 45210, transverse section. 6, SUP 45212c, transverse section. 7, SUP 45211, transverse section. 8, SUP 45209a, transverse section. 9, SUP 45215c, longitudinal section.

Figures 10–12.—*Cyathactis variabilis* sp. nov., Rosyth Limestone, ×2. 10, SUP 46183a, paratype, longitudinal section. 11, SUP 46182b, paratype, longitudinal section. 12, SUP 46182a, paratype, transverse section.

EXPLANATION OF PLATE IV

Figures 1, 2.—*Cyathactis variabilis* sp. nov., Rosyth Limestone, ×2. 1, SUP 46181b, holotype, longitudinal section. 2, SUP 46181a, holotype, transverse section.

Figures 3–10.—*Stereoxylodes multicarinatus* sp. nov., Rosyth Limestone. 3, SUP 46184a, holotype, transverse section showing septal structure in dissepimentarium (note carinae), ×9. 4, SUP 46184b, holotype, longitudinal section showing tabularium, ×3. 5, SUP 46185b, paratype, transverse section at base of calice, ×3. 6, SUP 46187a, paratype, transverse section of early growth stage, ×3. 7, SUP 46185a, paratype, transverse section above base of calice, ×3. 8, SUP 46184a, holotype, transverse section, ×3. 9, SUP 46187b, paratype, longitudinal section, ×3. 10, SUP 46185c, paratype, longitudinal section showing dissepimentarium above base of calice (note carinae), ×3.

Figure 11.—?*Stereoxylodes* sp., Rosyth Limestone, ×2. SUP 46189b, longitudinal section showing tabularium.

EXPLANATION OF PLATE V

Figure 1.—?*Stereoxylodes* sp., Rosyth Limestone, ×2. SUP 46189a, transverse section.

Figure 2.—*Stereoxylodes multicarinatus* sp. nov., Rosyth Limestone, ×3. SUP 46186, paratype, longitudinal section showing part of tabularium and margin of dissepimentarium at right.

Figures 3–6.—*Strombodes rosythensis* sp. nov., Rosyth Limestone. 3, SUP 45226, paratype, lateral view of silicified specimen showing calicinal buds, ×1·5. 4, SUP 45221, paratype, lateral view of silicified specimen showing non-parricidal offset from old level of calice, ×1. 5, SUP 45217a, holotype, transverse section, ×5. 6, SUP 45217d, holotype, longitudinal section showing calice, ×5.

EXPLANATION OF PLATE VI

Figures 1–5.—*Strombodes rosythensis* sp. nov., Rosyth Limestone. 1, SUP 45217b, holotype, transverse section, ×5. 2, SUP 45217d, holotype, longitudinal section, ×5. 3, SUP 45219a, paratype, transverse section, ×5. 4, SUP 45227, paratype, distal surface of silicified specimen, ×1. 5, SUP 45226, paratype, lateral view of specified specimen showing single calicinal offset, ×1·5.

Journal and Proceedings, Royal Society of New South Wales, Vol. 108, pp. 70-74, 1975

A Note on the Fossil Megafloras of the Nymboida and Red Cliff Coal Measures, Southern Clarence-Moreton Basin, N.S.W.

J. C. E. Flint and R. E. Gould

Abstract—The Nymboida and Red Cliff Coal Measures of the southern Clarence-Moreton Basin, N.S.W., have yielded Triassic *Dicroidium* megafloras. The Nymboida flora comprises at least 26 species and is correlated with the Middle Triassic flora of the Esk and Neara Beds of Queensland. The Red Cliff flora comprises 15 species and is equated with the Queensland Upper Triassic Ipswich flora.

Introduction

The Nymboida and Red Cliff Coal Measures occur at the base of the Mesozoic sequence in the southern part of the Clarence-Moreton Basin in north-eastern New South Wales, unconformably overlying the Palaeozoic Fitzroy or Coffs Harbour Beds (McElroy, 1963, 1969; Voisey, 1969). The Nymboida Coal Measures occur in the south-western portion of the basin around Nymboida, about 35 km south-west of Grafton, and are mined for coal at Nymboida Colliery. The Red Cliff Coal Measures outcrop on and near the coast about 40 km east-north-east of Grafton (Figure 1). Both units contain *Dicroidium* megafloras which are typical of the Triassic of Gondwanaland.

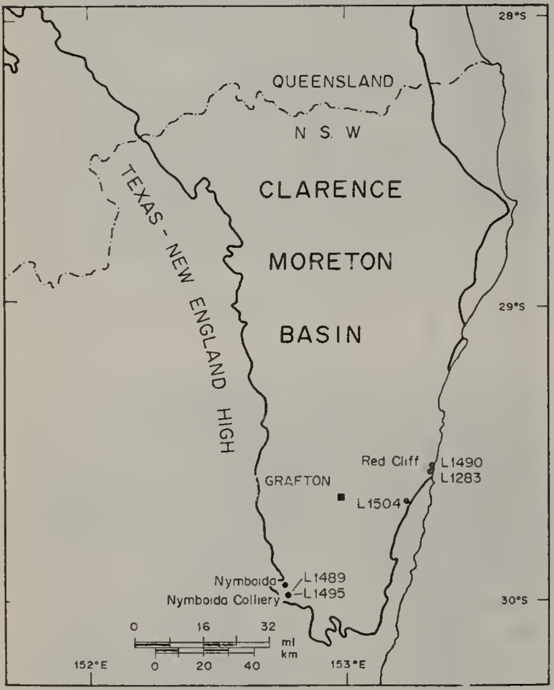

Figure 1.—Locality Map.

McElroy (1963, 1969) considered that the Red Cliff and Nymboida Coal Measures were stratigraphic equivalents, and correlated them with the Ipswich Coal Measures of Queensland in the north of the basin. However, he also suggested that correlation with the Queensland Esk Beds was a possibility on the basis of palaeobotanical evidence determined by de Jersey (1958).

Numerous plant megafossils have been collected from the Basin Creek Formation which is the uppermost unit of the Nymboida Coal Measures, and less numerous specimens were obtained from the Red Cliff Coal Measures. No major taxonomic revision has been attempted here, the fossils merely being identified by comparison with known forms, especially those described from other formations in the Clarence-Moreton Basin and Esk Trough.

Nymboida Coal Measures

Specimens were obtained from shales overlying Farquhars Creek Seam in the No. 2 and No. 3 workings of Nymboida Colliery (UNEL1459), and from an open-cut section (UNEL1489) on the ridge just to the west of the underground workings. All localities are in the Basin Creek Formation. Determinations from this formation include:

Neocalamites carrerei (Zeiller) Halle 1908.

Phyllotheca sp.

Asterotheca hillae Walkom 1924. Some specimens appear to grade into *A. fuchsii* (Zeiller) Kurtz 1921. [Plate I, Figures 1, 2.]

Dictyophyllum davidii Walkom 1917. [Plate I, Figure 3.]

Cladophlebis australis (Morris) Seward 1904.

C. concinna (Presl) du Toit 1927, *sensu* Jones and de Jersey (1947); referred to *C. mesozoica* Kurtz 1947, by Jain and Delevoryas (1967). [Plate I, Figures 7, 8.]

C. lobifolia (Phillips) Seward 1900, *sensu* Walkom (1924); includes ? *Hoegia* sp. of de Jersey (1958, Figure 4). [Plate I, Figures 4–6.]

C. cf. *johnstonii* Walkom 1925.

Lepidopteris madagascariensis Carpentier 1935. [Plate II, Figures 1, 2.]

Dicroidium odontopteroides (Morris) Gothan 1912; includes *D. lancifolium* (Morris) Gothan 1912. [Plate III, Figure 11.]

D. feistmantelii (Johnston) Gothan 1912; includes forms that could be referred to *Dicroidium* intermediate sp. B of Anderson and Anderson (1970).

D. dubium (Feistmantel) Anderson and Anderson 1970; "*T. talbragarensis*" of Jones and de Jersey (1947).

D. eskense (Walkom) Townrow 1957. [Plate II, Figure 3.]

D. narrabeenense (Walkom) Jacob and Jacob 1950.

Hoegia papillata Townrow 1957. [Plate II, Figures 4, 5.]

Anthrophyopsis grandis Walkom 1928. [Plate II, Figure 9.]

Pterophyllum cf. *nathanii* Walkom 1924.

Nilssonia cf. *princeps* (Oldham and Morris) Seward 1917.

Pseudoctenis eathiensis (Richards) Seward 1911. [Plate II, Figure 9.]

Taeniopteris crassinervis (Feistmantel) Walkom 1917. [Plate II, Figures 7, 8.]

T. lentriculiforme (Etheridge) Walkom 1917. [Plate III, Figures 8, 9.]

Ginko digitata (Brongniart) Heer 1877.

Ginkgoites bidens (Tenison-Woods) Florin 1936.

Phoenicopsis elongatus (Morris) Seward 1903. [Plate II, Figure 6*b*.]

Rissikia media Townrow 1967. [Plate II, Figure 6*a*.]

Various fruiting bodies.

Red Cliff Coal Measures

Specimens from the Red Cliff Coal Measures were obtained from shales and fine sandstone lenses in the basal conglomerate (UNEL1283), and from just below the lower coal seam on the shoreline at Red Cliff (UNEL1490); a few specimens were obtained from 13·5 km inland to the south-west (UNEL1504).

Determinations include:

Cladophlebis australis (Morris) Seward 1904.

Fertile *C. australis sensu* Walkom (1917*a*) and Hill, Playford, and Woods (1965); cf. *Asterotheca falcata* de la Sota and Archangelsky 1962. [Plate III, Figure 5.]

Dicroidium odontopteroides (Morris) Gothan 1912.

D. feistmantelii (Morris) Gothan 1912.

D. dentatum (Walkom) Anderson and Anderson 1970. [Plate III, Figure 1.]

Xylopteris elongata (Carruthers) Frenguelli 1943. [Plate III, Figure 2.]

Pachypteris cf. *austropapillosa* Douglas 1969. [Plate III, Figure 3.]

Yabeiella brackebuschiana (Kurtz) Oishi 1931, *sensu* Jones and de Jersey (1947); probably *Y. spatulata* Oishi 1931, of Jain and Delevoryas (1967). [Plate III, Figure 4.]

Y. mareyesiaca (Geinitz) Oishi 1931. [Plate III, Figure 6.]

Pterophyllum multilineatum Shirley 1897. [Plate III, Figure 7.]

Taeniopteris cf. *lata* Oldham and Morris 1863.

Linguifolium denmeadii Jones and de Jersey 1947.

Ginkgoites cf. *magnifolius* du Toit 1927.

Phoenicopsis elongatus (Morris) Seward 1903.

Chiropteris sp.; superficially like *Ginkgo digitata* (Brongniart) Heer 1877.

Conclusions

Comparison of the fossil megafloras of the Nymboida and Red Cliff Coal Measures with those of the Esk and Neara Beds (Jell, 1969) and Ipswich Coal Measures is given in Table 1. Data on the Esk and Ipswich floras were for the most part obtained from Walkom (1915, 1917*a*, *b*, 1924, 1928), Hill (1930, 1960), Jones and de Jersey (1947), Hill, Playford, and Woods (1965), and Townrow (1966). At least 80% of Nymboida species are present in the Esk flora, while 54% are represented in the Ipswich flora; 45% of the Red Cliff flora are present in the Esk flora and at least 87% in the Ipswich Coal Measures.

The presence of the typically Esk species *A. hillae*, *D. davidii*, *C. lobifolia*, *L. madagascariensis*, *D. eskense*, *A. grandis*, *P. eathiensis*, and *T. crassinervis* in the flora of the Nymboida Coal Measures indicates a close correlation with the Esk flora. *Asterotheca hillae* is not known in, and is apparently older than, the flora of the Ipswich Coal Measures (Hill, 1960). *Lepidopteris madagascariensis* is also not found in the Ipswich Coal Measures and ranges from Early to Middle Triassic (Townrow, 1966). The Esk Beds are considered to be of Middle Triassic age on stratigraphic, radiometric, and palynological evidence (Whitaker, 1972 ; de Jersey, 1972).

The species *X. elongata*, *Y. brackebuschiana*, *Y. mareyesiaca*, and *P. multilineatum* in the Red Cliff Coal Measures suggest that the flora is equivalent to that of the Ipswich Coal Measures ; *P. multilineatum* is restricted to the Ipswich flora (Jones and de Jersey, 1947). The Ipswich Coal Measures are considered to be Late Triassic (Karnian) age on palynological evidence (de Jersey, 1971).

Thus on megafloral evidence the Nymboida Coal Measures are correlated with the Middle Triassic Esk and Neara Beds, while the Red Cliff Coal Measures are equated with the Upper Triassic Ipswich Coal Measures.

TABLE 1

Comparison of Nymboida and Red Cliff Megafloras

Species	Nymboida	Red Cliff	Esk	Ipswic
Equisetales:				
Neocalamites carrerei	+	o	o	+
Phyllotheca sp.	+	o	o	o
Filicinae:				
Asterotheca hillae	+	o	+	o
A. fuchsii	+	o	o	+
Dictyophyllum davidii	+	o	+	o
Cladophlebis australis	+	+	+	+
Fertile 'C. australis'	o	+	+	+
C. concinna	+	o	o	+
C. lobifolia	+	o	+	o
C. cf. johnstonii	+	o	+	+
Pteridospermales:				
Lepidopteris madagascariensis	+	o	+	o
Dicroidium odontopteroides	+	+	+	+
D. feistmantelii	+	+	+	+
D. dubium ('T. talbragarensis')	+	o	+	+
D. dentatum	o	+	o	+
D. eskense	+	o	+	o
D. narrabeenense	+	o	?+	+
Hoegia papillata	+	o	+	+
Xylopteris elongata	o	+	?o	+

Pachypteris cf. *austropapillosa*	o	+	o	o
Incertae sedis:				
Anthrophyopsis grandis	+	o	+	o
Yabeiella brackebuschiana	o	+	o	+
Y. mareyesciaca	o	+	o	+
Bennettitales:				
Pterophyllum multilineatum	o	+	o	+
P. cf. *nathanii*	+	o	+	o
Cycadales:				
Nilssonia cf. *princeps*	+	o	+	o
Pseudoctenis eathiensis	+	o	+	o
Taeniopterids:				
Taeniopteris crassinervis	+	o	+	o
T. lentriculiforme	+	o	+	+
T. cf. *lata*	o	+	?o	+
Linguifolium denmeadii	o	+	o	+
Ginkgoales:				
Ginkgo digitata	+	?+	+	+
Ginkgoites bidens	+	o	+	+
Ginkgoites cf. *magnifolius*	o	+	+	+
Phoenicopsis elongatus	+	+	+	+
Incertae sedis:				
Chiropteris sp.	o	+	?+	?+
Coniferales:				
Rissikia media	+	o	+	?+

Acknowledgements

The cooperation of the management and staff of Nymboida Colliery is gratefully acknowledged. The authors wish to thank Mr. Keith Holmes for assistance in the collection of specimens, and Mr. Greg Retallack for discussion. J.C.E.F. was supported by a Commonwealth Scholarship.

References

ANDERSON, H. M., and ANDERSON, J. M., 1970. A Preliminary Review of the Biostratigraphy of the Uppermost Permian, Triassic and Lowermost Jurassic of Gondwanaland. *Palaeontologia Africana*, **13**, supplement, 1.

HILL, D., 1930. The Stratigraphical Relationship of the Shales About Esk to the Sediments of the Ipswich Basin. *Proc. R. Soc. Qd*, **41**, 162.

HILL, D., 1960. The Upper Brisbane Valley Fault Trough. In Hill and Denmead (1960), 269.

HILL, D., and DENMEAD, A. K. (Eds.), 1960. The Geology of Queensland. *J. geol. Soc. Aust.*, **7**.

HILL, D., PLAYFORD, G., and WOODS, J. T., 1965. *Triassic Fossils of Queensland. Qd. Palaeontogr. Soc., Brisbane.*

JAIN, R. K., and DELEVORYAS, T., 1967. A Middle Triassic Flora from the Cacheuta Formation, Minas de Petroleo, Argentina. *Palaeontology*, **10**, 564.

Jell, P. A., 1969. The Geology of the Linville District *Qd Govt Min. J.*, **70**, 97.

De Jersey, N. J., 1958. Macro- and Micro-Floras of North-eastern New South Wales. *J. Proc. R. Soc. N.S.W.*, **92**, 83.

De Jersey, N. J., 1971. Triassic Miopores from the Tivoli Formation and Kholo Sub-Group. *Publs geol. Surv. Qd*, 353.

De Jersey, N. J., 1972. Triassic Miospores from the Esk Beds. *Publs geol. Surv. Qd*, 357.

Jones, O. A., and De Jersey, N. J., 1947. The Flora of the Ipswich Coal Measures—Morphology and Floral Succession. *Pap. Dep. Geol. Univ. Qd* (n.s.), **3** (3).

McElroy, C. T., 1963. The Geology of the Clarence-Moreton Basin. *Mem. geol. Surv. N.S.W., Geology*, 9.

McElroy, C. T., 1969. The Clarence-Moreton Bsain in New South Wales. *J. Geol. Soc. Aust.*, **16** (1), 457.

Packham, G. H. (Ed.), 1969. The Geology of New South Wales. *J. Geol. Soc. Aust.*, **16** (1).

Townrow, J. A., 1966. On *Lepidopteris madagascariensis* Carpentier (Peltaspermaceae). *J. Proc. R. Soc. N.S.W.*, **98**, 203.

Voisey, A. H., 1969. New England Region. Lower Palaeozoic Systems. *J. Geol. Soc. Aust.*, **16** (1), 229.

Walkom, A. B., 1915. Mesozoic Floras of Queensland. Part I. *Publs geol. Surv. Qd*, 252.

Walkom, A. B., 1917*a*. Mesozoic Floras of Queensland. Part I—continued. *Publs geol. Surv. Qd*, 257.

Walkom, A. B., 1917*b*. Mesozoic Floras of Queensland. Part I—concluded. *Publs geol. Surv. Qd*, 259.

Walkom, A. B., 1924. On Fossil Plants from Bellevue, near Esk. *Mem. Qd Mus.*, **8**, 77.

Walkom, A. B., 1928. Fossil Plants from the Esk District, Queensland. *Proc. Linn. Soc. N.S.W.*, **53**, 458.

Whitaker, W. G., 1972. A Note on the Occurrence of Phenoclasts of Lower Palaeozoic Oolitic Arenite in the Upper Triassic Kholo Sub-Group. *Qd Govt Min. J.*, **73**, 149.

Department of Geology,
University of New England,
Armidale, N.S.W., 2351.

(Received 5.4.1974)

EXPLANATION OF PLATE I

Figures 1, 2.—*Asterotheca hillae* Walkom. 1, UNEF13396, ×1·1. 2, UNEF13401 (counterpart of part of Figure 1), ×2·2.

Figure 3.—*Dictyophyllum davidii* Walkom. UNEF13416, ×1·1.

Figures 4–6. *Cladophlebis lobifolia* (Phillips) Seward *sensu* Walkom. 4, UNEF14102, X 0.6. 5, UNEF14104, ×1·1. 6, UNEF14103, ×1.

Figures 7–8. *Cladophlebis concinna* (Presl) du Toit *sensu* Jones and de Jersey. Note fertile pinnules on lower portions of pinnae. 7, UNEF14122, ×1·1. 8, UNEF14123, ×1.

Figure 9.—*Anthrophyopsis grandis* Walkom. UNEF13528, ×1·2. All from Nymboida Coal Measures

EXPLANATION OF PLATE II

Figures 1, 2. *Lepidopteris madagascariensis* Carpentier. 1, UNEF14119, ×1. 2, UNEF13609, ×1.

Figure 3.—*Dicroidium eskense* (Walkom) Townrow. UNEF13334, ×0·5.

Figures 4, 5. *Hoegia papillata* Townrow. 4, UNEF14120, ×0·9. 5, UNEF13340, ×0·6.

Figure 6.—a. *Rissikia media* Townrow. b. *Phoenicopsis elongatus* (Morris) Seward. UNEF13465, ×0·6.

Figures 7, 8.—*Taeniopteris crassinervis* (Feistmantel) Walkom. 7, UNEF14126, ×0·7. 8, UNEF14125, ×0·7

Figure 9.—*Pseudoctenis eathiensis* (Richards) Seward. UNEF13451, ×0·7.

All from Nymboida Coal Measures.

EXPLANATION TO PLATE III

Figure 1.—*Dicroidium dentatum* (Walkom) Anderson and Anderson. UNEF13559, ×1·1.

Figure 2.—*Xylopteris elongata* (Carruthers) Frenguelli. UNEF12640, ×1.

Figure 3.—*Pachypteris* cf. *austropapillosa* Douglas. UNEF13393, ×1·1.

Figure 4.—*Yabeiella brackebuschiana* (Kurtz) Oishi. UNEF13583, ×2.

Figure 5.—Fertile pinnae of *Cladophlebis australis* (Morris) Seward. UNEF13608, ×1·5.

Figure 6.—*Yabiella mareyesiaca* (Geinitz) Oishi. UNEF13533, ×1·5.

Figure 7.—*Pterophyllum multilineatum* Shirley. UNEF13571, ×0·75.

Figures 8, 9. *Taeniopteris lentriculiforme* (Etheridge) Walkom. UNEF13454, ×1·2.

Figure 10.—Unusual specimen of ? *Dicroidium* showing double dichotomy. UNEF13359, ×1.

Figure 11.—*Dicroidium odontopteroides* (Morris) Gothan. UNEF13455, ×0·7.

Figures 1–7.—From Red Cliff Coal Measures.

Figures 8–11.—From Nymboida Coal Measures.


1


2

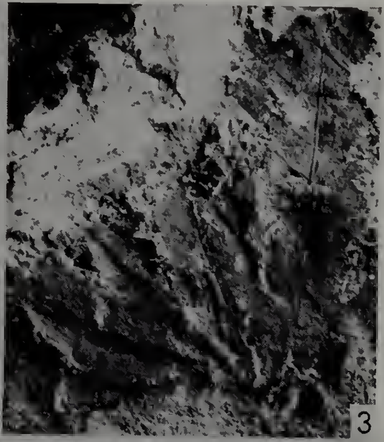
3

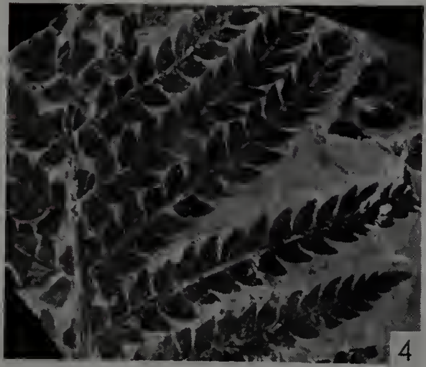
4


5

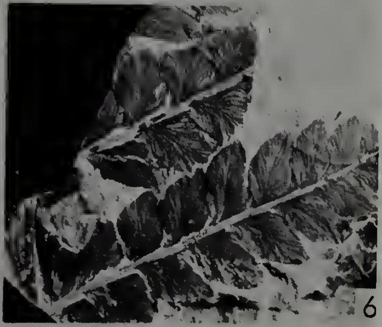
6

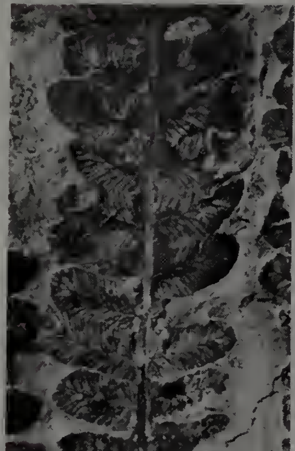
7


8

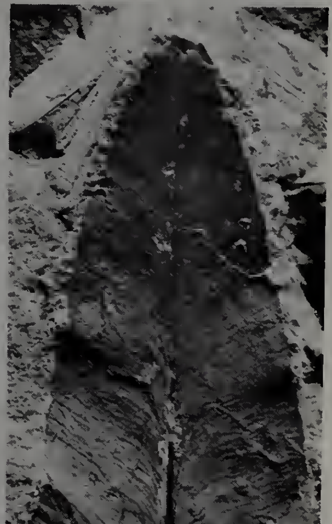
9

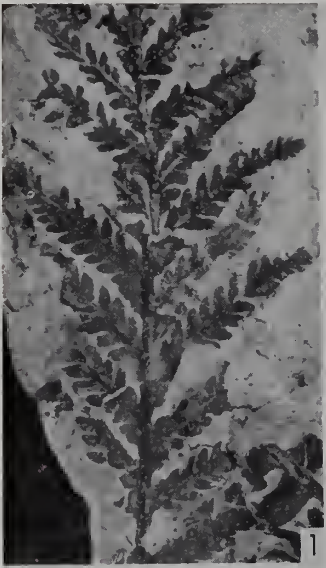
1

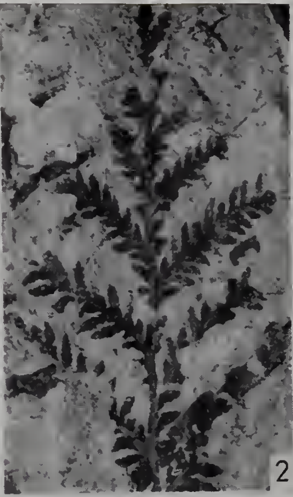
2

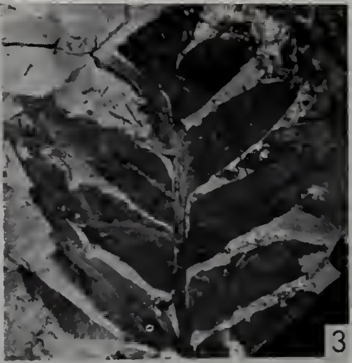
3

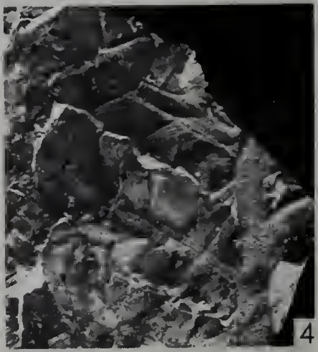
4


5

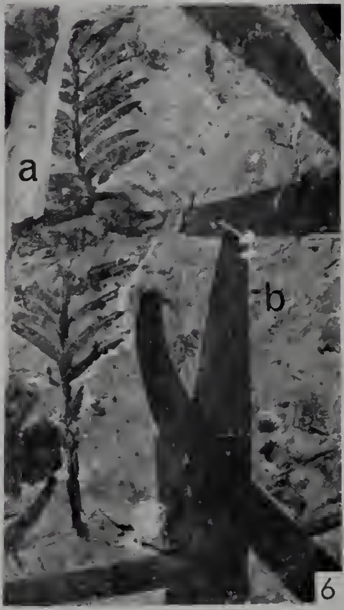

6

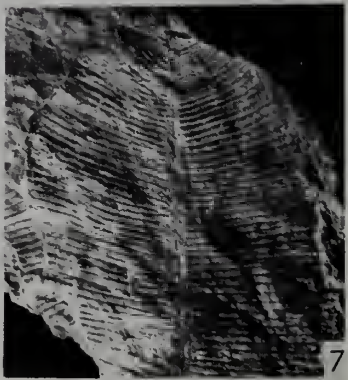
7

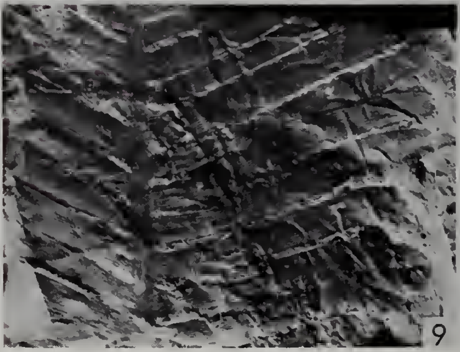
9

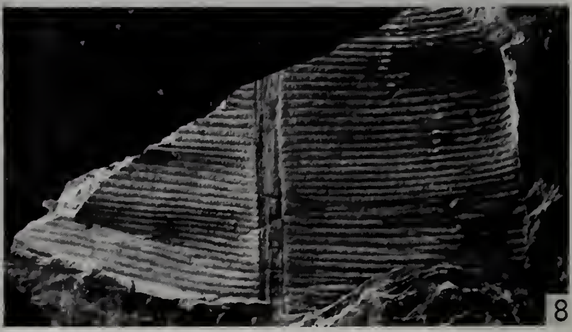
8


1


2


3


4

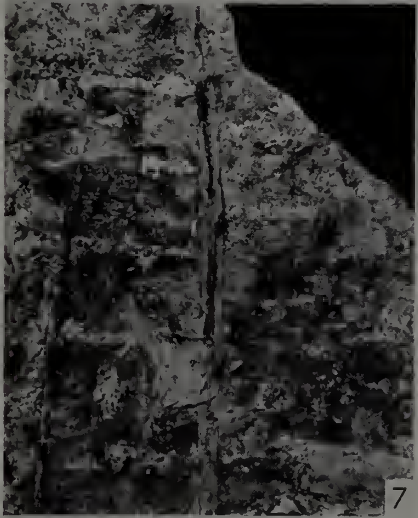
7


6


5


8


9


10


11

Journal and Proceedings, Royal Society of New South Wales, Vol. 108, pp. 75-93, 1975

Late Ordovician Coral Faunas from North-Eastern New South Wales

RUSSELL L. HALL

Communicated by B. D. WEBBY

ABSTRACT—The first Ordovician coral faunas described from north-eastern New South Wales occur in two widely separated fault blocks in the Peel Fault System: the Trelawney Beds south-east of Tamworth and the Uralba Beds north of Attunga. The latter is a new stratigraphic unit. The faunas are rich in heliolitids, halysitids, favositids and members of the early rugosan genera *Palaeophyllum, Cyathophylloides* and *Crenulites.* New taxa described are the rugose corals *Palaeophyllum bothroides* sp. nov., *P. trelawneyense* sp. nov., *Cyathophylloides sinuata* sp. nov., *C. juncta* sp. nov., *Crenulites australis* sp. nov., *C. australis minor* sp. et subsp. nov. and the tabulate corals *Plasmoporella bacilliformis* sp. nov., *P. contigua* sp. nov., *Plasmopora circumflexa* sp. nov., *Palaeofavosites magnus* sp. nov., *P. crassus* sp. nov., *P. spinimarginatus* sp. nov., *P. varispinulatus* sp. nov., *Catenipora flexa* sp. nov., *C. spatiosa* sp. nov. and *Falsicatenipora stricta* sp. nov. These faunas are of Eastonian or early Bolindian age and are tentatively correlated with Fauna IV of Webby (1972) in the Ordovician sequences of central western New South Wales.

Introduction

The oldest strata known in the New England area of north-eastern New South Wales are fossiliferous limestones found within the imbricate zone of the Peel Fault System south-east of Tamworth (the Trelawney Beds) and north-east of Attunga (the Uralba Beds). These are unique exposures brought to the surface by complex faulting within the Peel Fault System; elsewhere in northern New South Wales Ordovician rocks presumably are deeply buried. Corals and conodonts from these limestones indicate they are Upper Ordovician (Eastonian or early Bolindian) in age.

The Peel Fault System is a major crustal fracture separating Lower Palaeozoic rocks of the " Central Complex " of New England from the Middle and Upper Palaeozoic strata of the " Western Belt of Folds and Thrusts " (Voisey, 1959). The rocks east of this break are slates, phyllites, cherts and massive red jaspers that show a high degree of deformation and silicification. Small limestone lenses within this sequence have yielded coral faunas of Silurian age (descriptions to be published elsewhere). To the west are younger banded radiolarian cherts, limestones, sandstones and conglomerates which have been gently folded.

The outcrop of the Peel Fault System is marked by lenses of schistose serpentinite and fault blocks caught up along the many subsidiary faults. These blocks are composed of rocks ranging in age from Lower Ordovician (Packham, 1969) through Upper Ordovician (Philip, 1966; and this paper), Silurian (Hall, 1963), Lower Devonian (Johnston, 1968), Lower Carboniferous (Pickett, 1966) and Permian (Crook, 1961; Hall, 1963; Runnegar, 1970). Further search for Lower Palaeozoic strata in New England might best be directed to this zone.

The Uralba Beds (see Text Figure 1*c*):

Name Derivation: After Mr. E. Gallagher's property, " Uralba ", on which the outcrop occurs. Grid Reference 884895, Attunga 1 : 63,360 topographic sheet.

Lithology: Massive green cherts, buff coloured mudstones and grey, fine-grained limestones.

Thickness: Over 130 metres; neither the base nor the top of the sequence is known due to faulting.

Type Section: as exposed at Grid Reference 884895, Attunga 1 : 63,360 topographic sheet; bounded by fault planes of the Peel Fault System.

Age and Relations: Upper Ordovician (late Eastonian or early Bolindian); faulted against Woolomin Beds to the east, south and west, and against serpentinite to the north (see Text Figure 1*c*).

Discussion: The several limestone lenses included in this sequence were first mapped by Chappell (1961). He recorded them as a single lens (L6) from which he reported *Halysites, Favosites* and *Heliolites,* indicating an Ordovician-Silurian age for the limestone which he placed

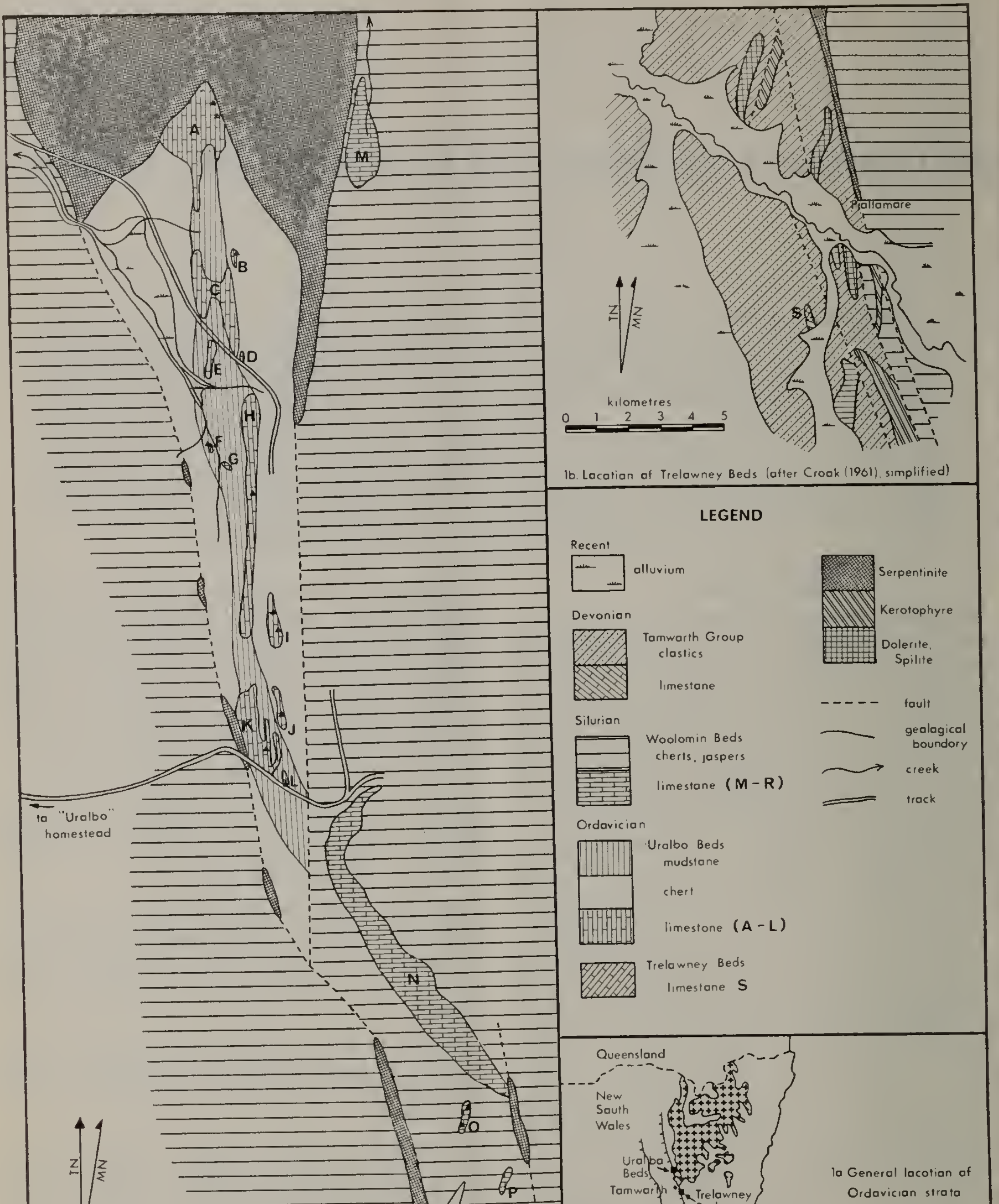
A
B
C
D
E
F
G
H
I
J
K
L
M
N
O
P
Q
R
to "Uralba" homestead
TN
MN
0 25 50 75
metres
▲ fossil locality
1c Location of Uralba Beds
Pallamare
S
TN
MN
kilometres
0 1 2 3 4 5
1b. Location of Trelawney Beds (after Crook (1961), simplified)
LEGEND
Recent
alluvium
Devonian
Tamworth Group clastics
limestone
Silurian
Woolomin Beds cherts, jaspers
limestone (M – R)
Ordovician
Uralba Beds mudstone
chert
limestone (A – L)
Trelawney Beds limestone S
Serpentinite
Kerotophyre
Dolerite, Spilite
fault
geological boundary
creek
track
Queensland
New South Wales
Uralba Beds
Tamworth
Trelawney Beds
1
2
Newcastle
area of map above
1a General location of Ordovician strata
1 Mooki Fault
2 Peel Fault System
New England Granite Complex

FIGURE 1.

in the Woolomin Beds. The outcrop of the Uralba Beds runs approximately north-south within the Peel Fault System; any indication of bedding planes has been obscured by a well-developed cleavage which is persistent throughout the limestones and mudstones. Following are faunal lists for each of the fossiliferous lenses at this locality (see also Text Figure 1*c*):

Lens A	*Palaeophyllum* sp. cf. *P. rugosum* Billings; *Palaeophyllum* sp. cf. *P. thomi* (Hall); *Cyathophylloides sinuata* sp. nov; *Crenulites australis* sp. nov.; *Palaeofavosites magnus* sp. nov.; *Catenipora spatiosa* sp. nov. and *Plasmopora circumflexa* sp. nov.
Lens B	*Palaeophyllum* sp. cf. *P. rugosum* Billings; *Palaeophyllum* sp. cf. *P. thomi* (Hall); *Catenipora flexa* sp. nov and indeterminate streptelasmatids.
Lens F	*Falsicatenipora stricta* sp. nov. and *Favosites* sp.
Lens H	Favositids.
Lens I	*Palaeophyllum* sp. cf. *P. rugosum* Billings; *Palaeophyllum bothroides* sp. nov.; *Cyathophylloides sinuata* sp. nov.; *Calapoecia* sp. cf. *C. canadensis* Billings; *Palaeofavosites crassus* sp. nov.; *Palaeofavosites rarispinulatus* sp. nov.; *Palaeofavosites* sp.; *Plasmoporella inflata* Hill; *Plasmoporella* sp. cf. *P. inflata* Hill; *Cyrtophyllum* sp. and *Catenipora flexa* sp. nov.
Lens J	Deformed specimens of a small species of *Palaeophyllum.*
Lens K	*Quepora* sp.; *Halysites* sp. and indeterminate streptelasmatids.
Lens L	*Palaeophyllum* sp. cf. *P. rugosum* Billings.

Brachiopods, gastropods and polyzoa have also been found in some lenses as well as some fragmented conodonts.

A biostratigraphic scheme for the fossiliferous Ordovician sequences of the central west of New South Wales, based on corals and stromatoporoids, was proposed and later expanded by Webby (1969, 1972). The faunas of the Uralba Beds may be most closely compared with Webby's Fauna IV which is "typified by the abundant favositids, *Favistina*-like forms and the first appearance of *Catenipora*" (1972, p. 150). Webby's Fauna III has many elements in common with the fauna from the Uralba Beds, particularly *Favistina* (=*Cyathophylloides* of this paper) and *Plasmoporella inflata* Hill but the abundance of *Catenipora flexa* sp. nov. and other halysitids suggests closer correlation with the younger Fauna IV. *Catenipora* is also reported from the upper part of the Gordon Limestone in Tasmania (Etheridge, 1900; Banks, 1962) and Webby suggests (1969, p. 358) that these beds may be Bolindian in age (=uppermost Caradoc-Ashgill or Maysville-Richmond).

The coral faunas from the Uralba Beds and the Trelawney Beds are similar at the generic level and have four species in common. The abundance of halysitids in several of the lenses of the Uralba Beds suggests that they may represent a slightly younger horizon than that of the Trelawney Beds, from which no halysitids are known. Conodonts from the two localities are also similar (Philip, 1966 and personal comment).

The green to green-grey cherts weather to a reddish-brown colour and form large boulders on the surface of the outcrop; they are very hard and apparently unbedded. Associated more intimately with the limestone lenses is a belt of massive buff to brown mudstones having a well-developed cleavage. Adjacent to the limestones these strata become darker in colour and more shaley with fine partings. A lengthy search of these beds has failed to reveal further fossils, particularly graptolites, which might be of value in more accurately determining the age of the coral faunas.

The Trelawney Beds (see Text Figure 1*b*):

Name Derivation: Mr. R. Kilborn's property, "Trelawney"; the outcrop occurs at Grid Reference 171299, Map Sheet No. 1, "Tamworth", (Crook, 1961).

Lithology: Ranges from pale grey bioclastic limestone to nodular, buff coloured, argillaceous limestone.

Thickness: Unknown due to faulted boundaries.

Age and Relations: Upper Ordovician (possibly late Eastonian); faulted against various formations of Devonian and Silurian age.

Discussion: Benson originally mapped this outcrop as part of the Nemingha Limestone of Lower Middle Devonian age; Crook placed the outcrop in his Drik-Drik Formation (Crook, 1961, pp. 182–3) and assumed it to be Lower Devonian in age.

Philip (1966) first determined the Ordovician age of this outcrop and proposed the name, Trelawney Beds. He compared the conodont fauna of the Trelawney Beds with faunas from strata of Trentonian to Maysvillian age in North America (pp. 112–3) and suggested correlation with the Upper Carodoc or the Eastonian stage of the Victorian Ordovician succession. The coral fauna from the Trelawney Beds described in this paper includes: *Palaeophyllum* sp. cf. *P. thomi* (Hall); *Palaeophyllum trelawneyense* sp. nov.; *Cyathophylloides sinuata* sp. nov.; *Cyathophylloides juncta* sp. nov.; *Crenulites australis* sp. nov.; *Crenulites australis minor* sp. et subsp. nov.; *Palaeofavosites magnus* sp. nov.; *Palaeofavosites spinimarginatus* sp. nov.; *Plasmopora circumflexa* sp. nov.; streptelasmatids; *Reuschia* sp.; *Plasmoporella bacilliformis* sp. nov. and *Plasmoporella contigua* sp. nov. This fauna is closely comparable with Webby's Fauna III (Webby, 1969). Although *Plasmoporella inflata* Hill, which Webby refers to as "diagnostic" for his Fauna III, is absent from the Trelawney Beds, *Plasmoporella bacilliformis* sp. nov. is a very closely related species. The fauna is notable in lacking halysitids.

Material and Methods

All material described in this paper is lodged in the fossil collections at the Geology Department, University of New England, Armidale (subsequently abbreviated UNE F). The locality numbers refer to the catalogue of localities kept in the same Department, as follows: Locality 841, Uralba Beds; Locality 842, Trelawney Beds. Lens numbering within the Uralba Beds sequence is shown in Text Figure 1*c*. The area of outcrop of the Uralba Beds was mapped by the writer using plane table techniques at a scale of 1 inch to 100 feet. All material from the Trelawney Beds was collected by Prof. G. M. Philip and kindly made available to me for study.

Systematic Descriptions:

Phylum	Coelenterata
Order	Rugosa Milne-Edwards and Haime, 1850
Suborder	Columnariina Rominger, 1876
Family	Stuariidae Milne-Edwards and Haime, 1850
Genus	*Palaeophyllum* Billings, 1858

Type Species: *Palaeophyllum rugosum* Billings, 1858

Palaeophyllum rugosum Billings 1858

1858 *Palaeophyllum rugosum* Billings; Plate I, Figures 6*a*, *b*.
1901 *Palaeophyllum rugosum* Billings; Lambe, p. 101.
1950 *Palaeophyllum rugosum* Billings; Bassler, Plate 18, Figures 15, 16.
1959 *Palaeophyllum rugosum* Billings; Hill, Plate I, Figures 6*a*, *b*.
1960 *Palaeophyllum rugosum* Billings; Pestana, p. 868; Plate 109, Figure 5.
1961 *Palaeophyllum rugosum* Billings; Strusz, pp. 341–2; Plate 42, Figures 7, 8, 15; Text-fig. 3.
1961 *Palaeophyllum rugosum* Billings; Hill, pp. 1, 2; Plate 1, Figures 1–6.

Palaeophyllum sp. cf. *P. rugosum* Billings 1858
Plate Ia–e, Figure 2

Material: Twenty specimens, UNE F11555–71 and UNE F11578–80, from which numerous thin sections were cut; seven transverse and eight longitudinal sections catalogued. From Locality 841, lenses A, I and L, Uralba Beds.

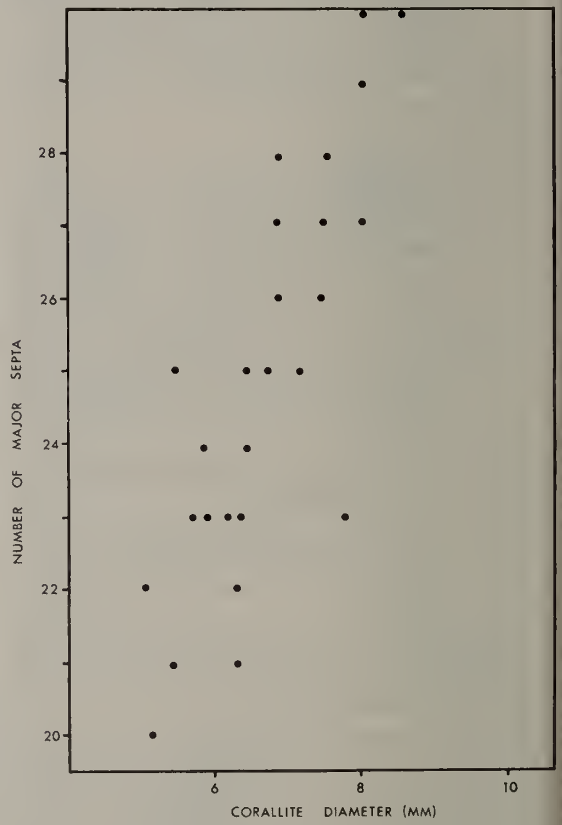

FIGURE 2.—*Palaeophyllum* sp. cf. *P. rugosum* Billings. Scatter diagram of number of major septa × diameter.

Description: Phaceloid colony, corallites cylindrical, free for greater part of length, cerioid for a short distance after budding. Increase lateral and non-parricidal.

Corallites circular in cross-section; 5–8 mm in diameter, commonly 6·5 mm, with thick peripheral stereozone averaging 0·65 mm in mature corallites. Major septa number 22–28, rarely 30, reaching about three-quarters of the distance to the axis, often with tips fused in groups of two or three. Septa thicken slightly towards periphery, then thicken abruptly within stereozone; in some sections the bases of major septa are seen to be embedded in the stereozone layer and do not reach the epitheca. Numbers of major septa at various corallite diameters are: 5 mm, 20–22; 7 mm, 25–28; 8 mm, 27–30 (see Figure 2). Minor septa very short, often incompletely developed, rarely extending more than 0·1 mm beyond the peripheral stereozone as blunt spines.

Tabulae very thin, generally flat or gently domed with edges strongly downturned; axial zone may show broad depression; occasionally incomplete. Spacing regular, 8–12 in a length of 5 mm.

Remarks: The present material resembles *P. rugosum* Billings as redescribed by Hill (1959) in most features, but has a thicker stereozone and more closely spaced tabulae. Tabulae in specimens described by Pestana (1960) show the same spacing as these specimens. The "somewhat funnel-shaped" tabulae, described but not figured by Hill (1961), are not seen.

Palaeophyllum bothroides sp. nov.

Plate If–j7, Figure 3

Name Derivation: Greek *bothros*=trench; *-oides*=in the form of. A reference to the form of the tabulae in longitudinal section.

Material: Six specimens, UNE F11572-7 (holotype UNE F11575), from which five transverse and four longitudinal sections were cut. From Locality 841, lens I, Uralba Beds.

Description: Phaceloid corallum of large, branching corallites; increase by lateral budding, non-parricidal. Corallite diameters between 6·0 and 9·5 mm, with a thick peripheral stereozone ranging between 0·6 and 0·9 mm.

Major septa range in number between 20 and 26 in mature corallites, straight, withdrawn from the axis or extending almost to the axis where they are fused in irregular groups of two or three; thin axially and thickening gradually approaching the stereozone. Numbers of major septa at various diameters are: 6 mm, 20–22; 8 mm, 22–23; 9 mm, 26 (see Figure 3). Minor septa regularly developed in some sections but entirely absent in others; appear as short, blunt spines extending just beyond the stereozone.

Tabulae very thin, usually meeting the walls at right angles or with slight upturning; horizontal. Axial sections, however, show development of a pronounced axial trough with almost vertical sides and horizontal floor, 1·5–2·0 mm wide and 0·5–0·7 mm deep. Tabulae complete, evenly spaced with 6–9 in a length of 5 mm except in rare crowded zones where there may be 13; highly arched tabellae occasionally developed at periphery.

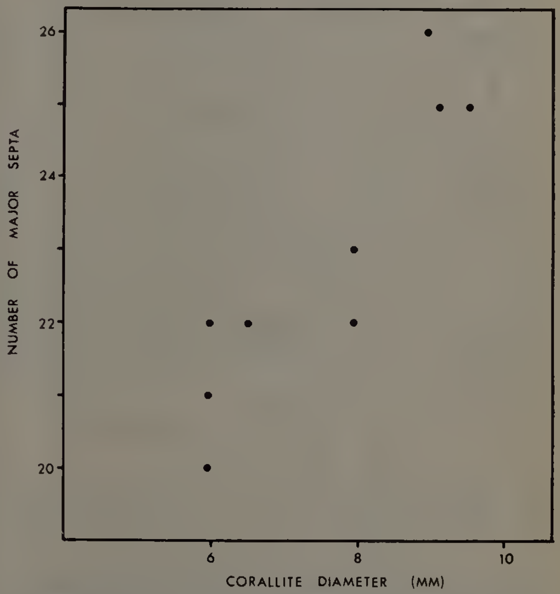

FIGURE 3.—*Palaeophyllum bothroides* sp. nov. Scatter diagram of number of major septa × diameter.

Remarks: This species differs from *P.* sp. cf. *P. rugosum* in having larger diameters with fewer septa at corresponding diameters, tabulae with strongly depressed axial regions and wider spacing of tabulae.

Palaeophyllum thomi (Hall) 1857

1857 *Columnaria thomi* Hall; *in* Emory, Plate 20, Figures 1*a–d*.
1903 *Cyathophylloides thomi* Walcott; Plate 29.
1915 *Columnaria* (*Palaeophyllum*) *thomi* Bassler; p. 26.
1950 *Palaeophyllum thomi* (Hall); Bassler, p. 275; Plate 18, Figures, 12–14; Plate 19, Figure 12.
1959 *Palaeophyllum thomi* (Hall); Hill, p. 4; Plate I, Figures, 1, 2.
1961 *Palaeophyllum thomi* (Hall); Flower, pp. 91, 92; Plate 47, Figure 9; Plate 51; Plate 52.

Palaeophyllum sp. cf. *P. thomi* (Hall) 1857

Plate Ik–n, Figure 4

Material: Eleven specimens, UNE F11581–91, from which ten transverse and ten longitudinal sections were prepared, from Locality 841, lenses A and B, Uralba Beds. Two transverse and two longitudinal sections, UNE F11791–2, cut from material no longer extant, from Locality 842, Trelawney Beds.

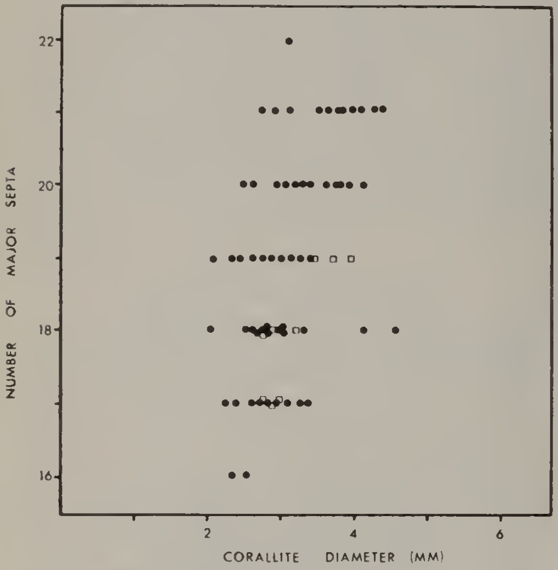

FIGURE 4.—*Palaeophyllum* sp. cf. *P. thomi* (Hall). Scatter diagram of number of major septa × diameter. ☐ from Trelawney Beds; ● from Uralba Beds.

Description: Corallum of phaceloid, cylindrical corallites of small diameter; corallites free for greater part of length, sometimes twisting but generally subparallel. Adjacent corallites may be in contact for short distances where outgrowths from the epitheca connect the walls; in transverse section this produces what appear to be short, cateniform chains of up to four corallites. However, connecting tubes, as seen in *Syringopora*, are not seen. Increase by lateral budding, non-parricidal.

Corallite diameters range from 2·1 to 4·6 mm with a thick peripheral stereozone from 0·2–0·4 mm thick. Major septa range in number from 16 to 22; long, straight, of even thickness, reaching almost to the axis where the tips of groups of septa may be fused. Septal counts at various diameters are: 2·5 mm, 16–18; 3·0 mm, 17–21; 4·0 mm, 20–21 (see Fig. 4). Minor septa incompletely developed, with only a few seen in any section, and often completely absent; when present appear as short, blunt spines extending just beyond the stereozone.

Tabulae closely spaced, 9–12 in a length of 5 mm; complete; highly arched with axial notch, or flat and gently depressed axially with strongly downturned edges.

Remarks: The present material agrees closely with the descriptions and figures of the holotype given by Hill (1959). Flower (1961) describes *P. thomi* from New Mexico in which the tabulae show wide variations in form, as described for the present material.

Palaeophyllum trelawneyense sp. nov.

Plate Io–q; Figure 5

Name Derivation: Named after the Trelawney Beds from which the type material was collected.

Material: Five transverse and three longitudinal sections, numbered UNE F11744/1–8, cut from the holotype, of which hand-specimen material is no longer extant. From Locality 842, Trelawney Beds.

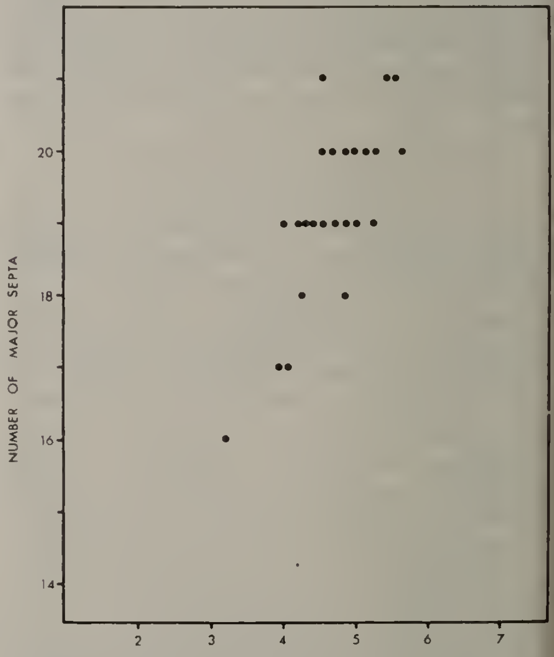

FIGURE 5.—*Palaeophyllum trelawneyense* sp. nov. Scatter diagram of number of major septa × diameter.

Description: Phaceloid; corallites cylindrical with lateral, non-parricidal increase. Corallites circular in cross-section; 3·0 to 4·6 mm in diameter with a peripheral stereozone 0·4–0·5 mm wide. Major septa long, thin, extending almost to the axis where the tips are fused in irregular groups; number of major septa 16–21. Minor septa have not been observed. Tabulae variable in form: gently arched or sagging axially, with edges turned upwards or downwards; 10 to 15 in a length of 5 mm.

Remarks: Compared with the other species of this genus from the Uralba Beds and Trelawney Beds, this species is most closely allied with *P.* sp. cf. *P. rugosum* but is distinct from that species in having smaller average corallite diameters with fewer septa, in lacking the development of minor septa altogether and in having more closely spaced and variable tabulae. In general dimensions, number of major septa and spacing of tabulae this species is very similar to *P. macrocaule* Webby, but the relatively long minor septa of that species are not developed. Webby also describes the frequent elongation of one septum to form "an axial, columella-like structure" (1972, p. 154); this feature is not seen in *P. trelawneyense* where all the major septa are long, extending almost to the axis.

Ontogeny in Palaeophyllum: Serial section examination of the budding in two species (*P.* sp. cf. *P. rugosum* and *P. bothroides*) shows that in both increase is lateral and non-parricidal. Only a single daughter corallite is formed, though in one case two were observed to form simultaneously. The daughter corallite is formed almost entirely external to the normal edge of the parent calyx by an outward swelling of the parent wall. The partition dividing the parent from the daughter corallite is formed by the swelling of the peripheral ends of about four of the septa in the parent corallite. After an early aseptate stage the long cardinal septum is the first of the protosepta to appear and may later extend right across the daughter corallite. Bulges on the wall representing the alar septa appear next. Insertion of metasepta in the cardinal quadrants is usually accelerated, these often appearing before the counter septum is finally developed. The daughter corallite usually remains in contact with the parent for a length of 3–4 mm, separating just before the maximum number of septa is formed.

Genus: Cyathophylloides Dybowski 1873.

Type Species: Cyathophylloides kassariensis Dybowski 1873.

Discussion: The genus *Favistella* Dana 1846 was based on the genotype *Columnaria alveolaris* Van Cleve, but Van Cleve's description was never published. Later workers generally used the genus as *Favistella* Hall 1847 which had as its type species *Favistella stellata*. Bassler redefined the genus *Favistella*, accepting *F. alveolata* Goldfuss as the type species, but Flower (1961, p. 76) points out that the original description of this species was so general that much confusion arose in subsequent species identification. He thus proposed the new name *Favistina*, based on *F. undulata* Bassler, for the group of Ordovician corals formerly included under the name *Favistella* Bassler.

Spjeldnaes (1964) described *Cyathophylloides kiaeri* with characters intermediate between those of *Cyathophylloides* and *Favistella*. Simmons and Oliver (1967, p. 10) suggested that the name *Favistina* Flower ought to be utilized for such intermediate forms, as it is based on a well known type species, whereas the type species of *Cyathophylloides* is not well known. Browne (1965, p. 1186) described species of *Favistina* Flower which possessed features in common with both *Favistella* Dana and *Cyathophylloides* Dybowski. She then proposed enlarging the scope of the genus *Cyathophylloides* Dybowski to include *Favistella* Dana (=*Favistina* Flower). This usage is followed here.

Cyathophylloides sinuata sp. nov.

Plate IIa, b

Name Derivation: Latin *sinuatus*=waved. A reference to the form of the corallite walls.

Material: Twenty-two specimens: UNE F11610–23 from Locality 841, lenses A and I, Uralba Beds; UNE F11696–9 from Locality 842, Trelawney Beds. From this material fifteen transverse and sixteen longitudinal sections were cut. UNE F11698 designated holotype.

Description: Corallum massive, corallites cerioid with thick walls (0·15 to 0·5 mm) which are generally crenulate in cross-section, with a dark axial plane present; wall segments curved. Corallite diameters variable within each corallum, ranging from 2·1 to 5·3 mm. Major septa long and thin, 11–15 in mature corallites, reaching almost to the axis where the tips may be fused in irregular groups or interfinger, becoming twisted; occasionally withdrawn. Minor septa well developed, ranging in appearance from short, blunt spines extending just beyond the stereozone, to thin spines up to half the length of the major septa.

Tabulae broadly domed, often with axial depression and edges strongly downturned; rarely incomplete; spacing varies between 9 and 18 in a length of 5 mm, though crowded zones are not developed.

Remarks: This species is similar to that described as *Cyathophylloides* cf. *C. burksae* Flower by Browne (1965, pp. 1189-9), but differs in having tabulae twice as closely spaced and lacking crowded zones. *C. neminghensis* (Etheridge) 1918 differs from the present species in having fewer septa (only 7–10 major) and tabulae more widely spaced, with 6 in a length of 5 mm, generally horizontal.

Cyathophylloides juncta sp. nov.

Plate IIc, d; Figure 6

Name Derivation: Latin *junctus*=united. A reference to the fusing of the tips of the septa.

FIGURE 6.—*Cyathophylloides juncta* sp. nov. (A) UNE F11701/2 (holotype), T.S., ×3; (B) UNE F11701/1 (holotype), L.S., ×3.

Material: Four specimens, UNE F11700-3, from which four transverse and five longitudinal sections were cut. From Locality 842, Trelawney Beds. Holotype is UNE F11701.

Description: Corallum massive, corallites cerioid with thick walls (0·2–0·5 mm); wall segments curved; walls crenulate with a dark axial plane. Corallites polygonal in cross-section, 5 to 7 sided, varying in diameter between 1·7 and 3·0 mm. Major septa long, usually extending to the corallite axis where the tips are twisted together and fused to form a loose, " columella "-like structure; the number of major septa varies from 10 to 14 in mature corallites. Minor septa consistently developed, thin, varying from short spines which extend only about 0·1 mm beyond the peripheral stereozone to those extending half the distance to the axis.

Tabulae strongly arched and tent-shaped, rising to a maximum height at position of " columella " where they are frequently disrupted; unevenly spaced with 10–22 in a length of 5 mm.

Remarks: This species differs from *C. sinuata* in the presence of the loose " columella " formed by the fusion and twisting of the tips of the major septa at the axis and also in the more strongly inclined tabulae. Average diameter of the corallites in this species is smaller than in *C. sinuata*.

Genus: Crenulites Flower 1961.

Type Species: Crenulites duncanae Flower 1961.

Crenulites australis sp. nov.

Plate IIe, f

Name Derivation: Latin *australis*=southern, referring to the first occurrence of this North American genus in Australia.

Material: Five specimens, UNE F11624-28, from Locality 841, lens A, Uralba Beds; eight specimens, UNE F11704-11, Locality 842, Trelawney Beds. From this material twenty-two transverse and twenty longitudinal sections were cut. UNE F11705 designated holotype.

Description: Corallum massive, broad and flattened, up to 10 cm across and reaching 5 cm in height. Cerioid, corallites slender and radiating slightly from the base. Corallites polygonal, with diameters between 1·4 and 2·4 mm, with straight or slightly wavy wall segments showing a dark axial plane. Walls 0·06–0·2 mm thick. Septa amplexoid, of variable appearance in cross-section; 14–16 in each corallite. Close to anterior surface of tabulae the eight or nine major septa reach almost to the corallite centre, being straight and of even thickness. Minor septa are invariably present in such sections as very short stubs. In other sections two orders of septa are not able to be distinguished, all appearing as short stubs; in some sections septa are not seen.

Tabulae widely and evenly spaced, 6–9 in a length of 5 mm; horizontal or gently arched, with downturned edges; in some transverse sections the scalloped nature of the tabulae near the walls can be seen as they pass in and out of the plane of section. Longitudinal sections passing close to the walls show the tabulae with short prolongations on their upper surfaces (representing the cut ends of amplexoid septa) which do not reach the tabulum next above, though become longer as the wall is approached.

Remarks: C. australis differs from the six known species belonging to this genus (all described from North America) in having smaller corallites. It is most closely allied to *C. duncanae* Flower in size, but differs from that species in regularly possessing eight or nine septa and in having more widely spaced tabulae which lack any zones of crowding.

Crenulites australis minor sp. et subsp. nov.

Plate IIg, h

Material: One specimen, UNE F11712 (holotype), from which two transverse and two longitudinal sections were cut. From Locality 842, Trelawney Beds.

Remarks: This form is very similar in most aspects to *C. australis* sp. nov. and so is not fully described. It differs from that species in having corallites of consistently smaller diameters, being 1·0 to 1·5 mm across.

Suborder: Streptelasmatina Wedekind 1927.

Family: Streptelasmatidae Nicholson in Nicholson and Lydekker 1889.

" Streptelasmatid gen. et sp. indet "

Plate IIi–l

Remarks: Two fragments from Locality 842, Trelawney Beds and one from Locality 841, lens K, Uralba Beds (thin sections numbered UNE F11687–9 and UNE F11738 respectively).

The form from the Uralba Beds is a large solitary corallite which has been compressed; smaller diameter is 11·4 mm. Septa wavy, thin, withdrawn from the axis, numbering 70, with two orders distinguishable; axial structure not apparent. Wall thin, averaging 0·4 mm (Plate IIk).

There are two forms present in the material from the Trelawney Beds. The first is a solitary corallite 9·6 mm in diameter with 29 major septa which extend only two-thirds of the distance to the axis and thicken markedly towards the wall. Corallite wall thick, up to 1·5 mm, and the minor septa appear as short stubs on the inner surface of the stereozone. Tabulae apparently domed and incomplete (Plate IIi, l). The second form from the Trelawney Beds is a solitary corallite 10·6 mm in diameter with thin wall (up to 0·5 mm) and 35 long, thin major septa which extend almost to the axis where the tips may be fused in small groups. Minor septa well developed, up to one fifth the length of the major septa (Plate IIj).

Order: Tabulata Milne-Edwards and Haime 1850.

Family: Syringophyllidae Pocta 1902.

Subfamily: Syringophyllinae Pocta 1902.

Genus: *Calapoecia* Billings 1865.

Type Species: *Calapoecia anticostiensis* Billings 1865.

Calapoecia canadensis Billings 1865

1865 *Calapoecia canadensis* Billings, p. 426.

1957 *Calapoecia* aff. *canadensis* Billings; Hill, p. 101; Plate III, Figures 14*a*, *b*.

(For a complete synonymy see Cox, 1936, p. 7.)

Calapoecia sp. cf. *C. canadensis* Billings 1865

Plate IIIa, b; Figures 7, 8

Material: Four silicified specimens, UNE F11592–5, from which three transverse and two longitudinal sections were prepared. From Locality 841, Uralba Beds, lens I.

Description: Corallum massive, 15 cm high by 20 cm wide and 5 cm thick. Corallites radiating from base, polygonal or rounded in cross-section, 2·0–2·5 mm in diameter and closely spaced, with centres never more than 3·0 mm apart. Corallites separated by a wall 0·2 to 0·5 mm thick, being wider at the corners between corallites to produce the rounded appearance of the corallites in cross-section. Short spines, reaching only about one fifth the distance to the axis, arranged in vertical rows down the inner wall of each corallite, project upwards from a broad base; as many as 20 in a cycle, though full number usually not seen due to silicification. Where common wall between corallites is continuous, spines alternate; frequently spines appear as discrete units in transverse sections separated by pores.

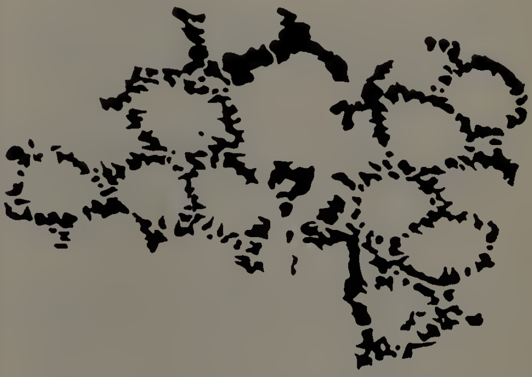

FIGURE 7.—*Calapoecia* sp. cf. *C. canadensis* Billings. UNE F11592/1, T.S., ×5.

Tangential sections down a wall show strongly perforate or cribriform appearance, pores being 0·2–0·3 mm in diameter, developed in vertical and horizontal rows; those in vertical rows spaced 10–12 in a length of 5 mm. In oblique sections across corallite walls anastomosing pores are seen with highly irregular outlines.

Tabulae very variable in form: complete, horizontal or sagging axially, occasionally arched, rarely incomplete; may be continuous in adjacent corallites, passing through the pores in the walls. Spacing irregular, 7–10 in a length of 5 mm. New corallites appear between adjacent corallites.

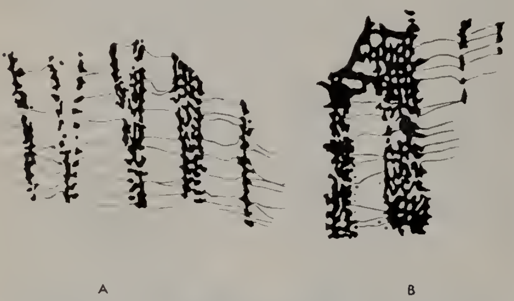

FIGURE 8.—*Calapoecia* sp. cf. *C. canadensis* Billings. (A) UNE F11592/2, L.S., ×3·5; (B) same specimen, L.S., ×3·5.

Remarks: This material agrees very closely with that described as *C. canadensis* by Cox (1936) except that the tabulae in his description are more closely spaced. The small, vertical tubes which he described as " disruptive canals " and attributed to the presence of commensal organisms have not been observed in the present material. Hill (1957) noted the first Australian occurrence of this genus from Cudal, N.S.W.

Family: Heliolitidae Lindstrom 1876.

Subfamily: Plasmoporinae Wentzel 1895

Genus: *Plasmoporella* Kiaer 1897.

Type Species: *Plasmoporella convexotabulata* forma *typica* Kiaer 1899.

Plasmoporella inflata Hill 1957
Plate IIIc, d

1957 *Plasmoporella inflata* Hill, p. 104; Plate IV, Figures 26*a*, *b*; Figures 28*a*, *b*.

Material: Two specimens, UNE F11597–8, from which one transverse and one longitudinal section were cut. From Locality 841, lens I, Uralba Beds.

Description: Corallum hemispherical with tabularia 1·2–1·6 mm in diameter, with centres between 1·5 and 2·0 mm apart, though some may be in contact. Tabularia circular in cross-section, with 12 short, thick septal ridges projecting into the tabularia, and usually extending beyond the wall into the coenenchyme. The septa are connected by curved wall segments, usually unthickened.

Tabulae typically complete and gently domed; spacing variable, usually 16–19 in a length of 5 mm, but where incomplete and highly arched tabellae are developed this number may be as high as 22. The coenenchyme consists of globose dissepiments of variable size and form; new tabularia arise from the coenenchyme.

Remarks: The present material is almost identical with that described by Hill (1957) and differs only in having slightly smaller tabularia.

Plasmoporella sp. cf. *P. inflata* Hill 1957
Plate IIIe, f

Material: Three specimens, UNE F11596, UNE F11693 and UNE F11729 from Locality 841, lens I, Uralba Beds. Two transverse and three longitudinal sections were cut from this material.

Description: Coralla small, about 3 cm high, with corallites radiating from the base. Tabularia circular in cross-section, ranging from 1·3 to 1·9 mm in diameter, averaging 1·5 mm; spacing of tabularia in coenenchyme variable, centres from 1·8 to 2·2 mm apart, with adjacent tabularia sometimes almost in contact. Walls of tabularia curved, usually thickened (up to 0·15 mm thick), but may be entirely absent, leaving discrete septal ridges around margin of tabularium. Septal apparatus present in the form of 12 thickened septal ridges (up to 0·2 mm thick) with blunt protrusions extending only about 0·1 mm into the tabularia but up to 0·25 mm into the surrounding coenenchyme.

Tabulae horizontal or broadly arched upwards, evenly spaced with 20–24 in a length of 5 mm. Incomplete tabellae, usually more strongly arched, frequently present. Coenenchyme consists of small, arched dissepiments, usually 0·3 to 0·5 mm wide and in approximately horizontal layers between tabularia.

Remarks: This form shows close similarities with *P. inflata* Hill in having greatly thickened septal ridges which protrude both into the tabularia and the surrounding coenenchyme; *P. inflata* has more widely spaced and less consistently arched tabulae; the tabularia in that species are more evenly distributed throughout the coenenchyme and are of slightly smaller diameter. The septal ridges in *P. bacilliformis* sp. nov. extend much further into the coenenchyme and the wall segments are much thinner; the coenenchymal tissue is more compact and the tabulae more strongly arched in that species.

Plasmoporella bacilliformis sp. nov.

Plate IIIg, h ; Figure 9

Name Derivation : Latin *bacilliformis*=rod-shaped. A reference to the prominent longitudinal septal ridges.

Material : Four specimens, UNE F11717–9 (holotype UNE F11719) from which five transverse and eight longitudinal sections were cut. Locality 842, Trelawney Beds.

Description : Tabularia circular in cross-section, consistently 1·5 to 1·7 mm in diameter and regularly spaced at intervals of 2·0 to 2·5 mm through the coenenchyme. Septa number 12, being thick, blunt ridges which extend 0·2 mm into each tabularium but as much as 0·4 mm into the surrounding coenenchyme ; wall segments between these thick septal ridges smoothly curved, 0·05 mm thick.

Tabulae smoothly arched, complete, closely spaced, 15–20 in a length of 5 mm ; incomplete tabellae often present down the margins of tabularia. Coenenchyme consists of small, arched dissepiments, 0·2–0·4 mm wide and up to 0·2 mm in height ; some dissepiments broad and flattened, or sagging in the centre.

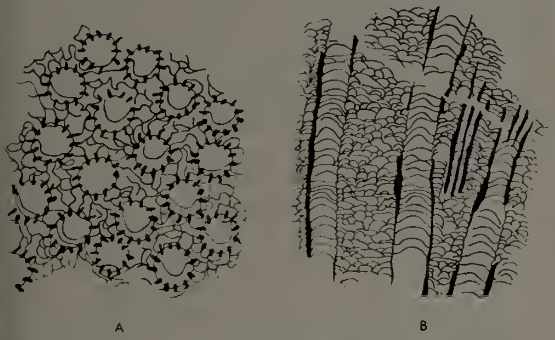

FIGURE 9.—*Plasmoporella bacilliformis* sp. nov. (A) UNE F11719 (holotype), T.S., ×3 ; (B) UNE F11719 (holotype), L.S., ×3.

Remarks : This species bears closest resemblance to *P. inflata* Hill but differs from it in that the septal ridges are thicker and project further beyond the walls of the tabularia into the surrounding coenenchyme ; the coenenchyme of *P. bacilliformis* is more compact, consisting of smaller, arched dissepiments. The tabulae of the present species are more strongly arched and more closely spaced.

Plasmoporella contigua sp. nov.

Plate IIIi, j ; Figure 10

Name Derivation : Latin *contiguus*=bordering. A reference to the tabularia being in contact.

Material : Three specimens, UNE F11720–22, from which two transverse and four longitudinal sections were cut. UNE F11720 designated holotype. From Locality 842, Trelawney Beds.

Description : Corallum 9·5 cm across, with corallites radiating from the base. Tabularia of constant size, 1·2 to 1·4 mm in diameter, with walls 0·06–0·1 mm thick. Where corallites in contact, cross-sectional form is polygonal, becoming circular only where coenenchyme present. Septal apparatus consists of continuous ridges which in transverse section vary in appearance from sharp, spine-like protrusions up to 0·2 mm long to blunt, rounded protrusions. Number of ridges seen in each corallite varies, commonly 11, maximum 12. Tabulae strongly arched upwards, evenly spaced with 13 to 16 in a length of 5 mm ; incomplete and strongly arched tabellae present.

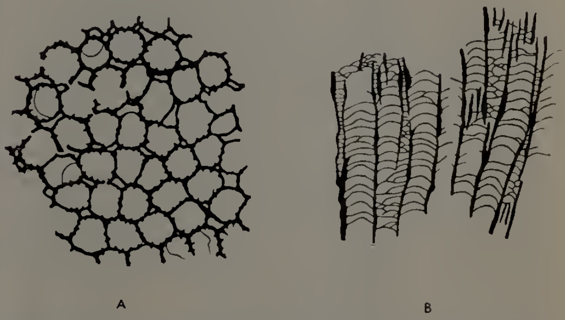

FIGURE 10.—*Plasmoporella contigua* sp. nov. (A) UNE F11720/1 (holotype), T.S., ×3 ; (B) UNE F11720/2 (holotype), L.S., ×3.

Small, irregular patches of coenenchyme occur between many corallites, being 0·2 to 0·7 mm across and containing small, arched dissepiments.

Remarks : *P. contigua* is apparently unique for this genus in having coenenchyme only irregularly developed, with walls of most tabularia in contact. This produces a very close resemblance to *Proheliolites* Kiaer in transverse sections, but the vertical series of downwardly directed septal spines so characteristic of that genus are lacking. The horizontal elements of the coenenchyme are globose dissepiments rather than horizontal solae as in *Proheliolites*.

Genus : *Plasmopora* Milne-Edwards and Haime 1849.

Type Species : *Porites petalliformis* Lonsdale 1839.

Plasmopora circumflexa sp. nov.

Plate IIIk, l

Name Derivation : Latin *circumflexus*=arched. A reference to the form of the tabulae.

Material : One specimen, UNE F11694, from Locality 841, lens A, Uralba Beds ; and four specimens, UNE F11723–6, from Locality 842, Trelawney Beds. UNE F11723 designated holotype.

Description : Tabularia circular in cross-section, ranging between 0·8 and 1·2 mm in diameter ; distance between centres of adjacent tabularia from 1·1 to 3·0 mm (mostly 1·3–1·6 mm) ; tabularia separated by one to four rows of tubules which are between 0·15 and 0·3 mm across. Twelve tubules surround each tabularium, their walls usually being continuous with the septa ; in some instances narrow extensions from surrounding tubules may reach the tubularium walls. Tubules immediately surrounding tabularia do not differ in size or form from those in the remainder of the reticulum. Walls of tabularia circular in cross-section, rarely crenulate ; not thickened relative to walls of tubules ; spines blunt and of even thickness, ranging up to 0·24 mm in length, 12 in each tabularium.

Tabulae smoothly arched, evenly spaced ; usually 14–16 in a length of 5 mm, though this number may vary between 10 and 20. Occasionally tabulae may be flat or sagging where they are more unevenly spaced ; some incomplete tabellae. Coenenchyme consists of slender tubules, polygonal in cross-section, with horizontal solae which are spaced 20 to 30 in a length of 5 mm.

Remarks : This species is characterized by the constantly arched tabulae and well developed septal spines.

Genus : Cyrtophyllum Lindstrom 1882.

Type Species : Cyrtophyllum densum Lindstrom 1882.

Cyrtophyllum sp.

Plate IVa, b

Material : One transverse and one longitudinal section cut from material no longer extant, UNE F11695. From Locality 841, lens I, Uralba Beds.

Description : Tabularia of even size, ranging from 0·7 to 1·0 mm in diameter, circular in cross-section, with strongly crenulate walls. Distances between the centres of adjacent tabularia vary between 1·0 and 1·5 mm ; commonly separated by one, though occasionally as many as three, rows of tubules. Walls of tabularia slightly thickened relative to those of tubules, being from 0·04 to 0·1 mm thick. Twelve septa, ranging in form from blunt, rounded protrusions of the crenulated walls to definite ridges projecting up to 0·1 mm into the tabularium.

Tubules rounded to subangular in cross-section, usually 0·2–0·3 mm in width and often with discontinuous walls. Tabulae smoothly concave upwards and evenly spaced with 20–25 in a length of 5 mm ; pairs of tabellae are common, being inclined towards axis to rest on tabulum next below. Solae horizontal, closely spaced, 40–45 in a length of 5 mm, sometimes continuous across several tubules.

Remarks : This form is characterized by depressed and closely spaced tabulae, with frequent incomplete tabellae. The transverse section is characterized by frequent discontinuities in the tubule walls.

Family : Favositinae Dana 1846

Genus : Palaeofavosites Twenhofel 1914.

Type Species : Favosites aspera d'Orbigny 1850.

Discussion : Palaeofavosites was separated from *Favosites* on the basis of having mural pores largely or completely confined to the wall angles or corallites ; septal spines may or may not be present. Flower (1961) regarded the genus *Foerstephyllum* as including Ordovician cerioid corals with fairly thick walls and numerous septal ridges or rows of septal spines, commonly 20 or more in number, some in two series. In advanced species the fibrous sclerenchyme of the common walls between adjacent corallites becomes separated by a thin, dark " axial plate ". Mural pores are lacking in the older species but occur in younger species.

Flower (1961) described as *Palaeofavosites sparsus* a form with wall structures and tabulae resembling those of *Foerstephyllum vacuum*, but lacking septal spines ; mural pores were present in the wall angles. Intermediate forms, possessing mural pores but with the septal apparatus represented by a series of spines were placed by Flower in the genus *Foerstephyllum* (*F. minutum*, p. 70 and *F. porosum*, p. 71), though he recognized the transitional nature of these forms. It seems preferable to retain in the genus *Palaeofavosites* all those forms possessing mural pores in the wall corners, rather than posing the difficulty of distinguishing members of this genus from species of *Foerstephyllum* on the basis of combinations of such variable characters as the degree of development of spines or septal ridges and microstructure of the walls.

Palaeofavosites magnus sp. nov.

Plate IVc, d.

Name Derivation: Latin *magnus*=large. A reference to the many corallites of unusually large diameter.

Material: A single corallum, UNE F11728 (holotype), from Locality 841, Uralba Beds, from which four transverse and three longitudinal sections were cut. Four specimens, UNE F11713–6, from Locality 842, Trelawney Beds; from this material two transverse and five longitudinal sections were cut.

Description: Corallum massive, cerioid, corallites radiating from the base; polygonal in cross-section, reaching 4·6 mm in diameter, but averaging between 2·0–3·0 mm. Wall segments typically curved, but may be straight or wavy; 0·05 to 0·15 mm thick, with a distinct dark, axial plane bounded by sclerenchyme.

Tabulae thin, complete, gently sagging or domed in centres, with edges turned up or down; spaced evenly, 5–9 in a length of 5 mm. Pores averaging 0·1 mm in diameter observed very close to wall angles.

Remarks: *P. sparsus* Flower and *P. mccullochae* Flower from North America have the same average dimensions as the present species, but lack the large diameter corallites. Both these species have tabulae rather more widely spaced.

Palaeofavosites crassus sp. nov.

Plate IVe, f

Name Derivation: Latin *crassus*=thick. A reference to the very thick walls in some parts of the corallum.

Material: A single corallum (the holotype), UNE F11599, from which two transverse and two longitudinal sections were cut. From Locality 841, lens I, Uralba Beds.

Description: Corallum massive, cerioid; corallites polygonal, varying in diameter between 1·8 and 3·8 mm. Wall segments straight or wavy, of variable thickness with a dark axial plane. In those parts of corallum where walls thickened (up to 0·2 mm), 16–20 thick, blunt septal ridges are observed which in adjacent corallites may be opposite or alternate to give the walls a strongly crenulate appearance in cross-section. Where corallite walls are thin (0·02–0·1 mm) the septal ridges are narrow and pointed. Two series of septa not observed.

Tabulae straight and complete, or wavy with edges turned up or down; evenly spaced with 6–10 in a length of 5 mm. Mural pores clearly seen in transverse and longitudinal sections very close to the wall angles.

Remarks: This species is characterized by the continuous, vertical septal ridges, especially in those parts of the corallum where the walls are thickened. The thin, dark axial plane is frequently obscured in such zones. The septal ridges appear as continuous vertical elements in longitudinal sections passing close to the corallite wall, suggesting that their distal edges are smooth rather than serrated as in *P. spinimarginatus*. The mural pores are found in vertical rows down either side of the wall angle, being round, 0·1 mm in diameter and about 0·4 mm apart.

Palaeofavosites spinimarginatus sp. nov.

Plate IVg, h; Figure 11

Name Derivation: Latin *spina*=spiny; Latin *marginatus*=margined. A reference to the spines on the inner edges of the septal ridges.

Material: A single specimen, UNE F11727 (holotype), from which one transverse and one longitudinal section were cut. From Locality 842, Trelawney Beds.

Description: Corallum massive, corallites polygonal, five to seven, but usually six-sided; mature corallites range in diameter from 1·7 to 2·2 mm. Walls straight with a dark axial plane always present, 0·05–0·1 mm thick, with very short, sharp spines up to 0·1 mm in length. Spines number up to 18 in a cycle, but usually fewer than this observed in one section. Septal

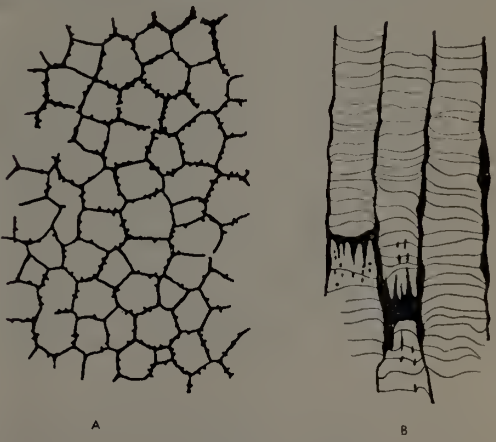

FIGURE 11.—*Palaeofavosites spinimarginatus* sp. nov. (A) UNE F11727/1 (holotype), T.S., ×2·5; (B) UNE F11727/2 (holotype), L.S., ×2·5.

apparatus consists of lamellar ridges which are produced into short, sharp spines along their inner edge; in oblique longitudinal sections they appear as continuous vertical lines which break up into a series of dots as they pass out of the plane of section.

Tabulae horizontal, gently sagging or wavy, with edges usually turned up or down approaching wall; evenly spaced, with 8–14 in a length of 5 mm. Mural pores located at wall corners, 0·05–0·1 mm in diameter.

Remarks: Comparison of the septal apparatus in the present material with that in *P. crassus* and *P. rarispinulatus* suggests that the present species is transitional, having continuous lamellar septal ridges which break into discrete spines along their inner edge. This species has generally smaller corallite diameters than the other species of the genus described in this paper, lacks wall thickening and has more closely spaced tabulae.

Palaeofavosites rarispinulatus sp. nov.

Plate IVi, j

Name Derivation: Latin *spinula*=small thorn; Latin *rarus*=scarce. A reference to the infrequent small spines.

Material: Nine specimens, UNE F11601–9, from Locality 841, lens I, Uralba Beds. Five transverse and five longitudinal sections were prepared. Holotype is UNE F11608.

Description: Corallum massive, cerioid; corallites polygonal, varying in diameter between 1·3 and 3·8 mm, most in the range 1·9-2·6 mm. Wall segments may be straight, wavy or curved in transverse section, varying in thickness between 0·05 and 0·2 mm, with a thin, dark axial plane. Septal spines usually present, but variable in development with 2–16 in any one corallite, arising from wall crenulations where these are present; spines short and pointed. Mural pores occasionally seen, very close to wall corners.

Tabulae evenly spaced, 6–8 in a length of 5 mm; complete, horizontal or wavy, with edges turned up or down near walls; in some corallites tabulae extremely variable in form and spacing becomes irregular.

Remarks: P. rarispinulatus differs most noticeably from *P. crassus* in having the septal elements reduced to discrete spines; a maximum of 16 spines has been counted in one corallite but in most only a few are seen, suggesting that they are widely spaced in vertical rows.

Palaeofavosites sp.

Plate IVk, l

Material: A single specimen, UNE F11600, from which two transverse and three longitudinal sections were cut. From Locality 841, lens I, Uralba Beds.

Description: Corallites polygonal, four to seven sided, with very thick walls (0·1–0·4 mm) which are often crenulate in both transverse and longitudinal sections, with a dark axial plane. Corallites large, from 3·0 to 4·1 mm in diameter. Septa or septal spines lacking. Round mural pores, 0·15–0·24 mm in diameter, located in wall corners, but rare.

Tabulae evenly spaced, 7–8 in a length of 5 mm, usually wavy with edges turned up or down near walls. In transverse sections many small, curved lines adjacent to the walls indicate the crenulate nature of the edges of the tabulae.

Remarks: This species is characterized by the large corallites with thick walls, lacking septa, and particularly by the crenulate tabulae.

Family: Auloporidae Milne-Edwards and Haime 1851.

Subfamily: Syringoporinae Nicholson 1879.

Genus: Reuschia Kiaer 1930.

Type Species: Reuschia aperta Kiaer 1930.

Reuschia sp.

Plate Va

Material: Part of a single colony from Locality 842, Trelawney Beds, from which one thin section was cut, UNE F11743.

Description: Corallum phaceloid, with corallites in contact for 2–3 mm after branching, often forming cerioid patches; corallites branch outwards from axis of colony and are not parallel. Corallites circular in cross-section, 1·5–2·5 mm in diameter, averaging 2·3 mm, with thick walls and a very narrow lumen. Typical corallite of 2·2 mm diameter having a central lumen of 0·5 mm in diameter surrounded by a thick wall (0·85 mm) consisting of two distinct layers. The outer layer, 0·25 mm thick, separated from the thick (0·6 mm) inner layer by a dark line. Inner surface of wall may have occasional broad undulations. In longitudinal sections tabulae not seen; calyx expanded.

Remarks: Kaljo and Klaaman (1965) list occurrences of this genus from the Upper Ordovician of Norway (Hill, 1953) and China (Yu, 1960); Hill (1959) also describes a species from Arizona, *R. subparallelus*. The present form is similar to this last species in general dimensions but differs in having corallites that diverge from the central axis of the colony.

Family : Halysitidae Milne-Edwards and Haime 1850.

Subfamily : Halysitinae Milne-Edwards and Haime 1850.

Genus : Halysites Fischer von Waldheim 1813.

Type Species : Tubipora catenularia Linnaeus 1767.

Halysites sp.

Plate Vb, c ; Figure 12

Material : A single specimen, UNE F11752, from Locality 841, lens K, Uralba Beds. Two transverse and two longitudinal sections were prepared.

Description : Corallum of slender corallites, up to 9 cm tall ; ranks of one to five, usually three, macrocorallites bounding compact lacunae of polygonal or somewhat elongated cross-sectional form, e.g. 3·0×6·0 mm ; 4·0×7·0 mm ; 2·2×10·3 mm ; 5·5×2·0 mm. Macrocorallites oval in cross-section, averaging 1·4–1·7 mm× 0·8–1·0 mm in size, with smoothly convex walls 0·1–0·13 mm thick. Septal spines absent. Walls constricted between macrocorallites ; ratio of diameters at end and midlength positions respectively being 5 : 9.

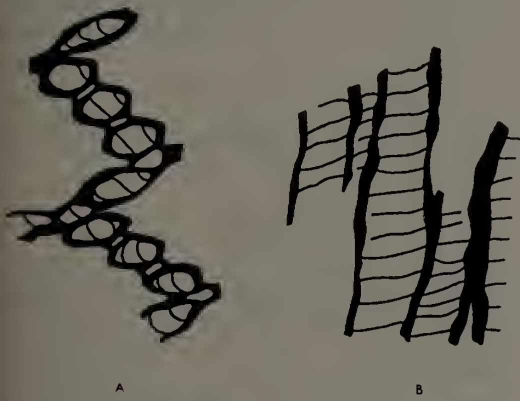

FIGURE 12.—*Halysites* sp. (A) UNE F11752/1, T.S., ×5; (B) UNE F11752/2, L.S., ×5.

Rectangular microcorallites, averaging 0·2× 0·6 mm in size and with their greater length transverse to the rank, occupy the constrictions between macrocorallites. Mesocorallites at the junction of ranks are triangular to polygonal in cross-section and about 0·5 mm across.

Tabulae in the macrocorallites are straight, horizontal and evenly spaced with 9–12 in a length of 5 mm ; those in microcorallites are more closely spaced.

Remarks : The single specimen of this species is silicified and has been compressed so that accurate measurements of corallite diameters proved difficult to obtain. Webby and Semeniuk (1969) have described the only true *Halysites* previously known from Ordovician rocks : *H. praecedens* from the upper parts of the Bowan Park Limestone and the Canomodine Limestone in the central west of New South Wales. These strata have been correlated with the Upper Eastonian. The present form differs noticeably from *H. praecedens* in having compact lacunae with frequent junctions between ranks which contain only a few macrocorallites ; no lacunae are known in the material representing *H. praecedens* which has long, open ranks of corallites. The specimen from the Uralba Beds has more elongated macrocorallites, with less marked constrictions in the walls and narrower microcorallites in comparison with *H. praecedens*.

Subfamily : Cateniporinae Hamada 1957.

Genus : Catenipora Lamarck 1816.

Type Species : Catenipora escharoides Lamarck 1816.

Catenipora flexa sp. nov.

Plate Vd–g

Name Derivation : Latin *flexus*=bending. A reference to the form of the ranks.

Material : Eleven specimens, often silicified, UNE F11644–54, from which nine transverse and eleven longitudinal sections were cut ; UNE F11650 designated holotype. From Locality 841, lenses B and I, Uralba Beds.

Description : Lacunae variable within each colony, ranging from medium, oval in cross-section (1·0×0·5 cm) formed by ranks containing 4–6 corallites, to curved, labyrinthine (5·0×1·0 cm) with ranks containing 2-13 corallites. Macrocorallites oval in cross-section with thin, dark holotheca ; average size 1·8× 1·3 mm, with walls smoothly convex, giving a ratio of 2 : 3 for the width at constrictions and corallite midlengths respectively. In cross-section chambers vary from oval with smoothly rounded ends to subquadrate with ends flattened along common wall between corallites. Microcorallites absent ; mesocorallites absent.

Walls range in thickness between 0·2 and 0·4 mm ; in corallites where greatest wall thickness is developed three distinct wall layers (holotheca, midwall and peripheral stereozone) are seen. Spines are developed in well-defined vertical rows, with as many as ten rows in each corallite ; development of spines down length of any corallite apparently not continuous, many chambers showing from two to four horizontal rows between adjacent tabulae, with none in adjacent chambers. Spines thick at base, projecting upwards and usually pointed; deposits of poikiloplasm frequently obscure or completely replace spines. Tabulae complete, horizontal, gently arched or sagging; spacing uneven down length of each corallite ranging from 7 to 10 in a length of 5 mm.

Remarks: This species closely resembles *C. workmanae* Flower (1961) from the Second Value Formation, New Mexico but differs in having larger, more open lacunae bounded by curved ranks of corallites. Australian representatives of this genus are known from a limestone breccia at the top of the Malachi's Hill Beds (Webby and Semeniuk, 1969, p. 357) and the upper beds of the Gordon Limestone of Tasmania (Etheridge, 1900; Banks, 1962). *C. flexa* is readily distinguished by the ranks of uniform, oval corallites forming elongated, labyrinthine lacunae and the frequent development of spines.

Catenipora spatiosa sp. nov.

Plate Vh, i; Figure 13

Name Derivation: Latin *spatiosus*=roomy. A reference to the wide spacing of the ranks.

Material: Five specimens, UNE F11639–43; UNE F11640 designated holotype. Three transverse and two longitudinal sections were cut from this material, from Locality 841, lens A, Uralba Beds.

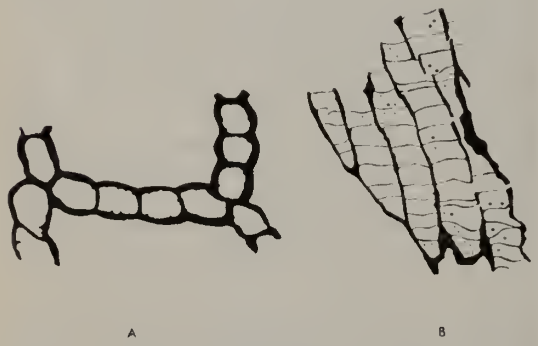

FIGURE 13.—*Catenipora spatiosa* sp. nov. (A) UNE F11640/2 (holotype), T.S., ×3·5; (B) UNE F11640/1 (holotype), L.S., ×3·5.

Description: Lacunae large, elongated, often labyrinthine, up to 1·0 cm wide and often exceeding 3·5 cm in length. Walls 0·3 mm thick, with thin, dark holotheca and in places a third layer can be seen in the wall structure. Macrocorallites large, ranging from 1·6 to 2·6 mm in length and 1·5 to 1·8 mm in width; end of chambers flattened, with thin, straight walls between adjacent corallites. External walls only slightly convex, giving a ratio for the diameters at the end and midlength of corallites respectively of 7 : 8.

Septa only occasionally seen in transverse sections as short spines up to 0·1 mm long; in tangential longitudinal sections the cut ends of these spines are seen in vertical rows, with three or four horizontal rows between adjacent tabulae. Tabulae thin, complete, horizontal or slightly sagging; evenly spaced with 6–8 in a length of 5 mm.

Remarks: This species resembles *Falsicatenipora chillagoensis* (Etheridge) but definitely lacks mesopores at the junctions of ranks. In his original description Etheridge makes no mention of gonopores (=mesopores) but refers to " feeble gonopores " in material from the Gordon Limestone in Tasmania which he believed to be conspecific with the material from Chillagoe, Queensland.

Genus: *Quepora* Sinclair 1955.

Type Species: *Halysites catenularia* var *Quebecensis* Lambe 1900.

Quepora sp.

Plate V j–l

Material: Four specimens, UNE F11739–42, from which four transverse and four longitudinal sections were cut. From Locality 841, lens K, Uralba Beds.

Remarks: The material representing this form has been deformed and only broken fragments of the ranks have been preserved; no lacunae have been seen. However, the material represents an undoubted *Quepora*. Corallites are rounded to slightly oval in cross-section; the longer diameter ranges from 1·3 to 1·6 mm, the shorter diameter from 0·7 to 1·1 mm. Septal spines absent; microcorallites and mesocorallites absent. Tabulae horizontal, straight and evenly spaced, 6–8 in a length of 5 mm.

Subfamily: Schedohalysitinae Hamada 1957.

Genus: *Falsicatenipora* Hamada 1958.

Type Species: *Halysites japonicus* Sugiyama 1940.

Falsicatenipora stricta sp. nov.

Plate Vm, n; Figure 14

Name Derivation: Latin *strictus*=straight. A reference to the straight walls of the macrocorallites.

Material: Four specimens, silicified, UNE F11734–7; UNE F11734 designated holotype. From Locality 841, lens F, Uralba Beds.

Description: Corallum tall, up to 9·0 cm high; corallites radiating from the base to form hemispherical surface. Lacunae compact, with smooth outlines, polygonal or elongated in cross-section; sizes 7·5×2·5 mm; 3·2×2·2 mm; 3·5×1·5 mm. Ranks moniliform, consisting of one or two macrocorallites which are elongated parallel to the rank, narrow, with straight walls (0·08–0·1 mm thick) which are not constricted at corallite junctions. Macrocorallites 1·1×0·5 mm, 1·4×0·4 mm. Septal spines absent. Microcorallites entirely absent; mesocorallites occasionally present at junction of ranks, triangular to rounded in cross-section with internal diameter of 0·02 mm. Tabulae in macrocorallites thin, straight, evenly spaced with 17–25 in a length of 5 mm.

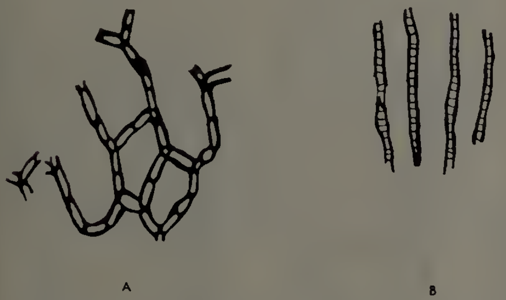

FIGURE 14.—*Falsicatenipora stricta* sp. nov. (A) UNE F11734/1 (holotype), T.S., ×3·5; (B) UNE F11734/2 (holotype), L.S., ×3·5.

Remarks: This species is easily recognized in hand specimen by the long narrow macrocorallites with straight sides which lack septal spines. The compact, polygonal and smooth-sided lacunae give this species a superficial resemblance to *Halysites lithostrotonoides* Etheridge, but the shape of the macrocorallites is again distinctive. The rectangular form of the macrocorallites is similar to those of *F. hillae* (Hamada) but in the present species they are more elongated and the lacunae are larger.

Acknowledgements

I wish to express my gratitude to Professor G. M. Philip who encouraged the beginning of this study and who made available for description material he collected from the Trelawney Beds. Dr. B. Runnegar, Professor Dorothy Hill and Dr. B. Webby provided valuable advice and discussion on taxonomic and biostratigraphic considerations, literature and preparation of the manuscript for publication. Assistance in preparing the illustrations was given by Mr. B. Whan, Mr. J. Whorwood and Dr. D. Ellenor.

References

BANKS, M. R., 1962. Ordovician System. The Geology of Tasmania. *J. geol. Soc. Aust.*, **9**, 147.

BASSLER, R. S., 1915. Bibliographic Index of American Ordovician and Silurian Fossils. *U.S. Nat. Mus. Bull.*, 92.

BASSLER, R. S., 1950. Faunal Lists and Descriptions of Palaeozoic Corals. *Mem. geol. Soc. Am.*, 44.

BILLINGS, E., 1858. Report for the year 1857. *Rep. geol. Surv. Can.*, for 1857, 142.

BILLINGS, E., 1865. Notice of Some New Genera and Species of Palaeozoic Fossils. *Canadian Naturalist*, new ser., **2**, 425.

BROWNE, R. G., 1965. Some Ordovician Colonial Corals of North-Central Kentucky. *J. Paleont.*, **39**, 1177.

CHAPPELL, B. W., 1961. The Stratigraphy and Structural Geology of the Manilla-Moore Creek District, N.S.W. *J. Proc. R. Soc. N.S.W.*, **95**, 63.

COX, I., 1936. Revision of the Genus *Calapoecia* Billings. *Canada nat. Mus. Bull.*, **80**, 1.

CROOK, K. A. W., 1961. Stratigraphy of the Tamworth Group (Lower and Middle Devonian), Tamworth-Nundle District, N.S.W. *J. Proc. R. Soc. N.S.W.*, **94**, 173.

DYBOWSKI, W. N., 1873. *Monographie der Zoantharia sclerodermata rugosa aus der silurformation Estlands*, Nord-Livlands und der Insel Gotland.

ETHERIDGE, R., 1900. A Tasmanian Species of *Halysites*. *Pap. Proc. R. Soc. Tasm. for* 1898–99.

ETHERIDGE, R., 1918. Two Remarkable Corals from the Devonian of New South Wales. *Rec. Aust. Mus.*, **12**, 49.

FLOWER, R. H., 1961. Part I. Montoya and Related Colonial Corals. *Mem. Inst. Min. Technol. New Mex.*, **7**, 1.

HALL, R. L., 1963. Geology of an Area North-east of Attunga, New South Wales. *Univ. New England, B.Sc. Hons. Thesis (unpubl.)*.

HILL, D., 1953. The Middle Ordovician of the Oslo Region, Norway. 2. Some Rugose and Tabulate Corals. *Norsk. Geol. Tidsskr.*, **31**, 143.

HILL, D., 1957. Ordovician Corals from New South Wales. *J. Proc. R. Soc. N.S.W.*, **91**, 97.

HILL, D., 1959. Some Ordovician Corals from New Mexico, Arizona and Texas. *Bull. Inst. Min. Technol. New Mex.*, **64**, 1.

HILL, D., 1961. On the Ordovician Corals *Palaeophyllum rugosum* Billings and *Nyctopora billingsii* Nicholson. *Bull. geol. Surv. Can.*, **80**, 1.

JOHNSTON, D. A., 1968. The Geology of the Halls Creek-Oaky Creek District, South of Bingara, N.S.W. *Univ. New England, B.Sc. Hons. Thesis (unpubl.)*.

KALJO, D., and KLAAMAN, E., 1965. The Faunas of the Portrane Limestone, III The Corals. *Bull. Br. Mus. nat. Hist., Geology*, **10**, 422.

KIAER, J., 1899. Den Korallenfaunen der Etage 5 des norwegischen Silursystems. *Palaeontographica*, **XLVI**, 1.

KIAER, J., 1930. Den fossilforende ordovicisk-siluriske lagrekke pa Stord og bemerkninger om de ovrige fossilfun i Bergens feltet. *Bergens Mus. Arbok. Naturv. rekke*, **II**, 1.

LAMBE, L. M., 1901. A Revision of the Genera and Species of Canadian Palaeozoic Corals. The Madreporaria Aporosa and the Madreporaria Rugosa. *Geol. Surv. Canada, Contrib. Canadian Palaeont.*, **IV**, 97.

LINNAEUS, C., 1767. Systema Naturae I: 533–1327 and (37). *Edito Duodecima Reformata.*

LONSDALE, W., 1839. See Murchison, R. I.

MURCHISON, R. I. The Silurian System. Pts. 1, II, 657.

D'ORBIGNY, A., 1850. Prodrome de Palaeontologie.

PACKHAM, G. H., 1969. The Geology of New South Wales. *J. geol. Soc. Aust.*, **16** (1).

PESTANA, H. R., 1960. Fossils from the Johnson Springs Formation, Middle Ordovician, Independence Quadrangle, California. *J. Paleont.*, **34**, 862.

PHILIP, G. M., 1966. The Occurrence and Palaeogeographic Significance of Ordovician Strata in Northern New South Wales. *Aust. J. Sci.*, **29**, 112.

PICKETT, J., 1966. Lower Carboniferous Coral Faunas from the New England District of New South Wales. *Mem. geol. Surv. N.S.W. Palaeontology*, **15**, 1.

RUNNEGAR, B. N., 1970. The Permian Faunas of Northern New South Wales and the Connection Between the Sydney and Bowen Basins. *J. geol. Soc. Aust.*, **16**, 697.

SIMMONS, G. C., and OLIVER, W. A., 1967. Otter Creek Coral Bed and its Fauna, East-Central Kentucky. *Bull. U.S. geol. Surv.*, 1244F.

SPJELDNAES, N., 1964. Two Compound Corals from the Tretaspis Beds of the Oslo-Asher District. *Institutt. for Geologi, ard. C. Blindern.*

STRUSZ, D. L., 1961. Lower Palaeozoic Corals from New South Wales. *Palaeontology*, **4**, 334.

SUGIYAMA, T., 1940. Stratigraphical and Palaeontological Studies of the Gotlandian Deposits of the Kitakami Mountainland. *Sci. Rep. Tohoku Univ.*, ser. 2, Geology, 21.

VOISEY, A. H., 1959. Tectonic Evolution of North-Eastern New South Wales, Australia. *J. Proc. R. Soc. N.S.W.*, **92**, 191.

WEBBY, B. D., 1969. Ordovician Stromatoporoids from New South Wales. *Palaeontology*, **12**, 637.

WEBBY, B. D., 1972. The Rugose Coral *Palaeophyllum* Billings from the Ordovician of Central New South Wales. *Proc. Linn. Soc. N.S.W.*, **97**, 150.

WEBBY, B. D., and SEMENIUK, V., 1969. Ordovician Halysitid Corals from New South Wales. *Lethaia*, **2**, 345.

YU, CH., 1960. Pozdneordovikskije korally Kitaja. *Acta palaeont. sin*, **8**, 65.

University of New England,
Armidale, N.S.W.

Present address:
McMaster University,
Hamilton, Ontario, Canada.

(Received 30.9.74)

EXPLANATION OF PLATE I

FIGURES a–e.—*Palaeophyllum* sp. cf. *P. rugosum* Billings. (a) UNE F11560, T.S., ×6, showing major septa fused in small groups and weakly developed minor septa; (b) and (c) UNE F11570, T.S., ×3; (d) UNE F11555/6, L.S., ×4; (e) UNE F11555/3, L.S., ×4.

FIGURES f–j.—*Palaeophyllum bothroides* sp. nov. (f) UNE F11573/1 (paratype 1), T.S., ×4; (g) and (h) UNE F11573/1, T.S., ×2; (i) UNE F11575/4 (holotype), L.S., ×3, showing deep trench-like structure in tabulae; (j) UNE F11575/3 (holotype), L.S., ×3.

FIGURES k–n.—*Palaeophyllum* sp. cf. *P. thomi* (Hall). (k) and (m) UNE F11590/1 and UNE F11791/2 respectively, L.S., ×5; (l) UNE F11586/2, T.S., ×6; (n) UNE F11588/3, T.S., ×3.

FIGURES o–q.—*Palaeophyllum trelawneyense* sp. nov. (o) enlargement of part of (p), T.S., ×6; (p) UNE F11744/1 (holotype), T.S., ×2; (q) UNE F11744/8 (holotype), L.S., ×4.

EXPLANATION OF PLATE II

FIGURES a, b.—*Cyathophylloides sinuata* sp. nov. (a) UNE F11698/1 (holotype), T.S., ×3; (b) UNE F11698/2 (holotype), L.S., ×3.

FIGURES c, d.—*Cyathophylloides juncta* sp. nov. (c) UNE F11701/2 (holotype), T.S., ×6; (d) UNE F11701/1 (holotype), L.S., ×6.

FIGURES e, f.—*Crenulites australis* sp. nov. (e) UNE F11705/1 (holotype), T.S., ×4; (f) UNE F11706/2 (paratype 2), L.S., ×4. Note amplexoid septa and crenulated margins of tabulae.

FIGURES g, h.—*Crenulites australis minor* sp. et subsp. nov. (g) UNE F11712/1 (holotype), T.S., ×4; (h) UNE F11712/2 (holotype), L.S., ×4.

FIGURES i–l.—Indeterminate streptelasmatids. (i) and (l) UNE F11687, L.S., ×2 and UNE F11689, T.S., ×1·5, respectively; (j) UNE F11688, T.S., ×1·5; (k) UNE F11738, T.S., ×1·5.

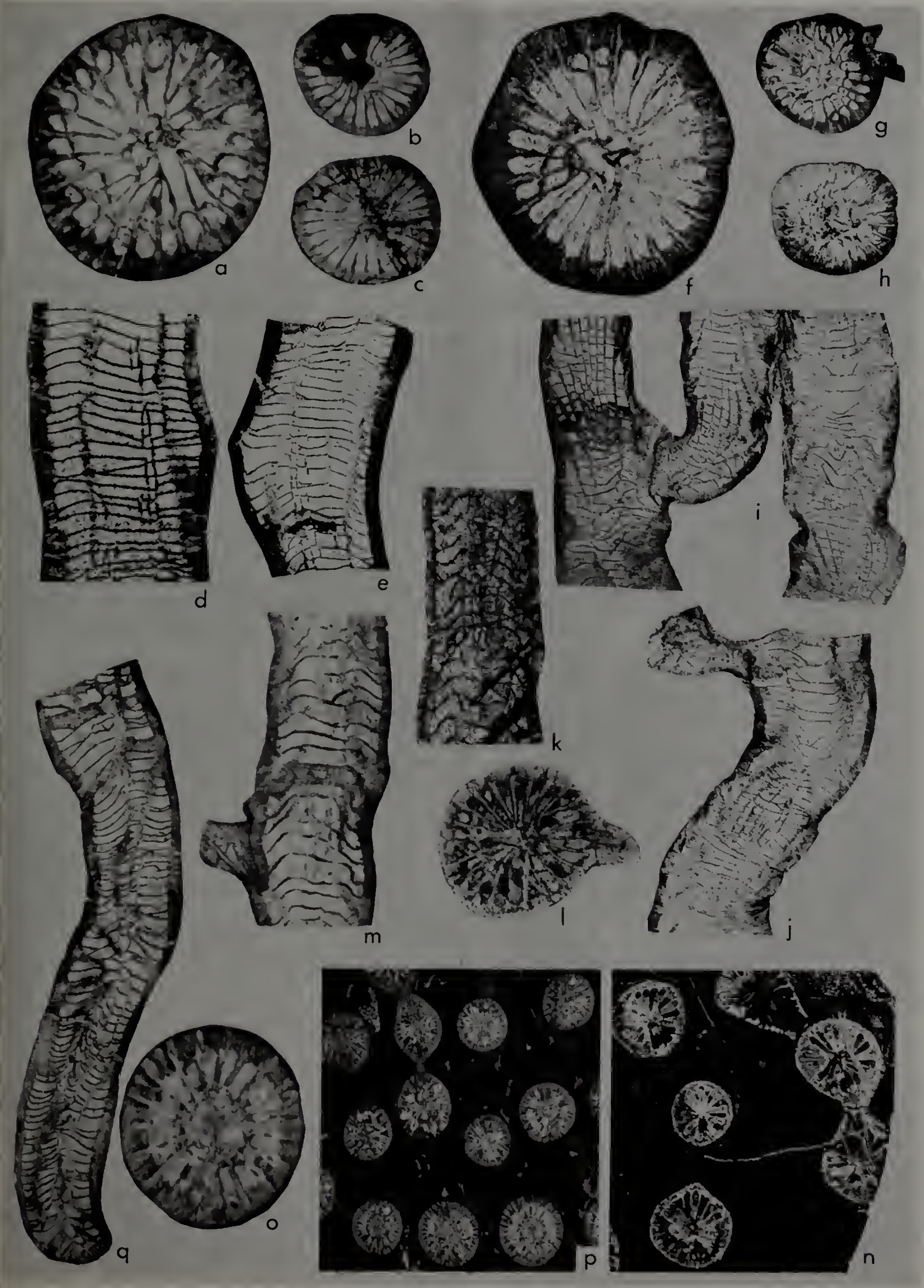
a
b
c
f
g
h
d
e
i
k
m
l
j
q
o
p
n

HALL PLATE II

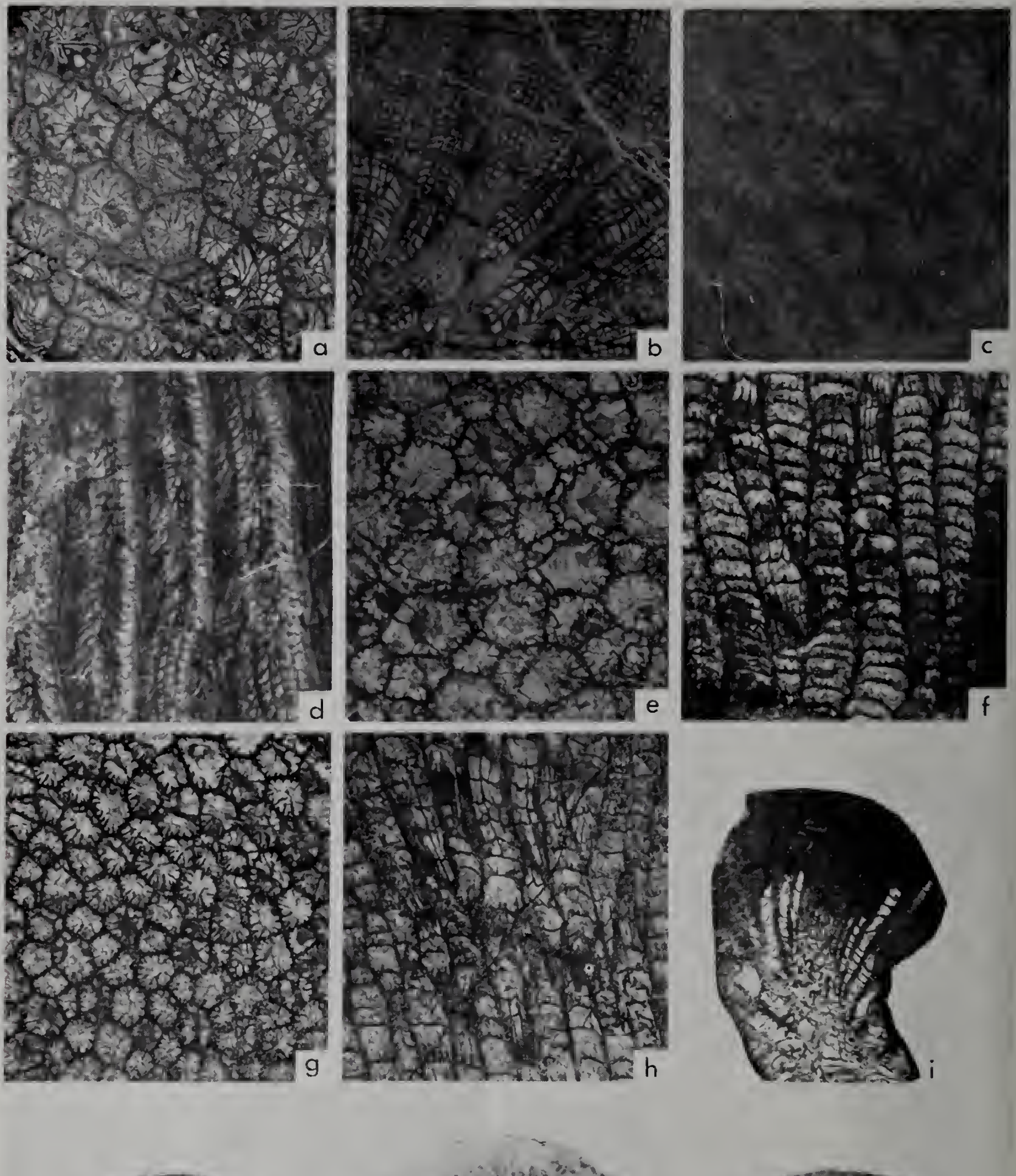

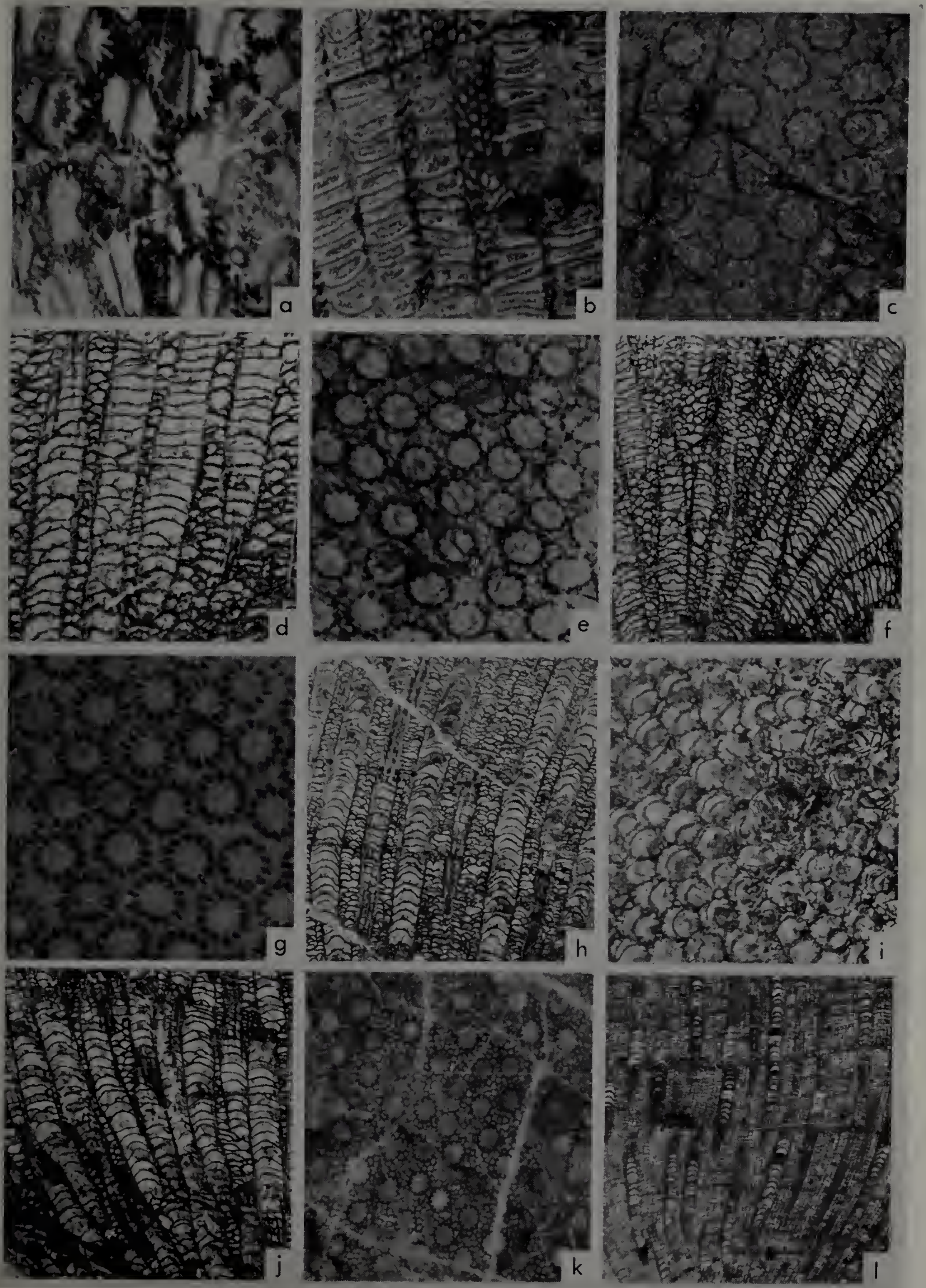
a
b
c
d
e
f
g
h
i
j
k
l

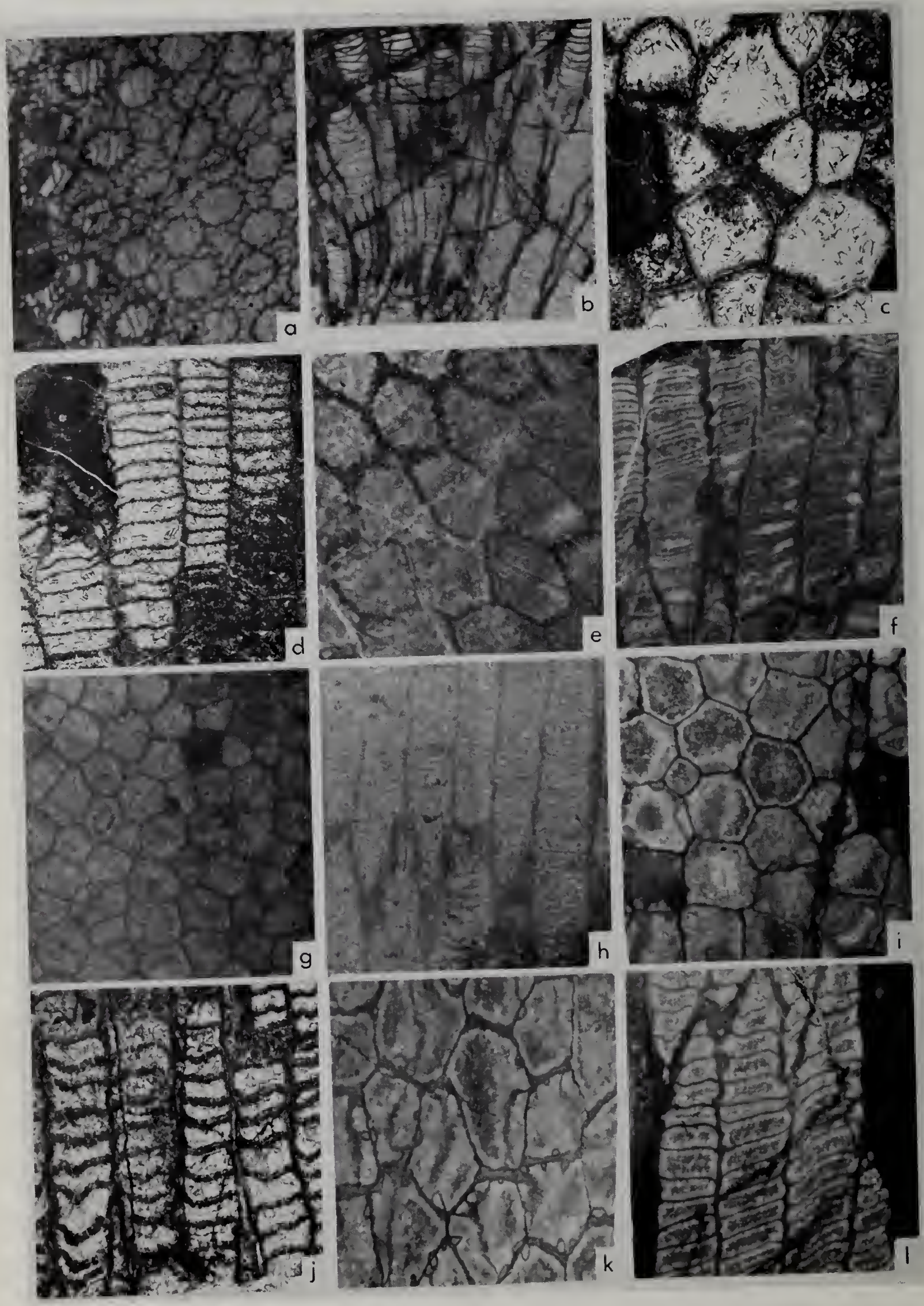
a
b
c
d
e
f
g
h
i
j
k
l

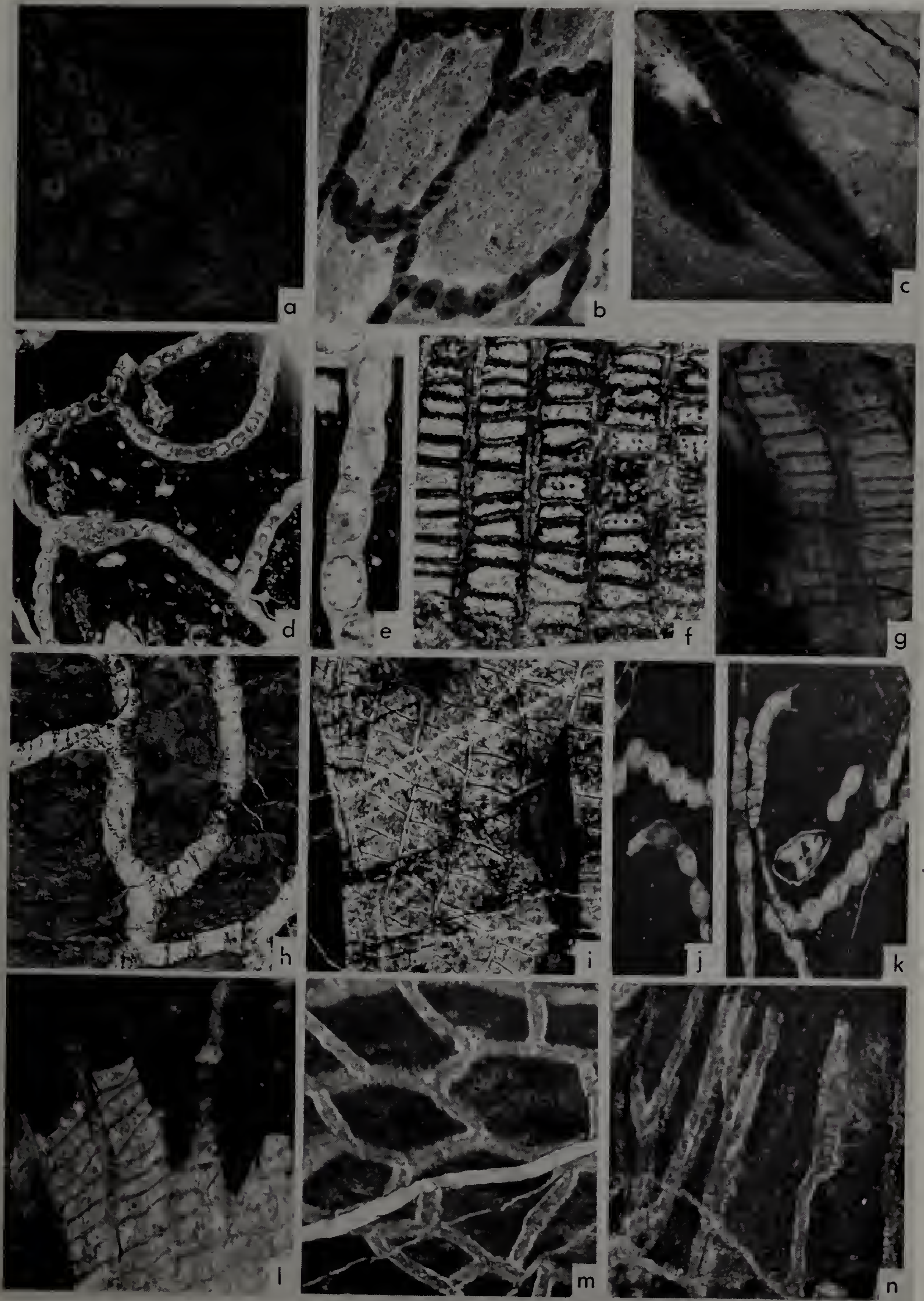
a
b
c
d
e
f
g
h
i
j
k
l
m
n

EXPLANATION OF PLATE III

FIGURES a, b.—*Calapoecia* sp. cf. *C. canadensis* Billings. (a) UNE F11592/1, T.S., ×4; (b) UNE F11592/2, L.S., ×4. Showing spinose septa and cribriform wall structure.

FIGURES c, d.—*Plasmoporella inflata* Hill. (c) UNE F11598/2, T.S., ×4, showing septal spines extending into coenenchyme; (d) UNE F11598/1, L.S., ×4, showing arched tabulae.

FIGURES e, f.—*Plasmoporella* sp. cf. *P. inflata* Hill. (e) UNE F11693/3, T.S., ×4, showing thickened septal ridges and in places absence of wall; (f) UNE F11729/1, L.S., ×4.

FIGURES g, h.—*Plasmoporella bacilliformis* sp. nov. (g) UNE F11718/1, paratype 2, T.S., ×4, showing thickened septal ridges and absence of corallite walls; (h) UNE F11719/2 (holotype), L.S., ×4, showing thick, continuous septal ridges and strongly arched tabulae.

FIGURES i, j.—*Plasmoporella contigua* sp. nov. (i) UNE F11720/1 (holotype), T.S., ×4, showing septal ridges and small patches of coenenchyme developed at corners of adjacent corallites; (j) UNE F11720/2 (holotype), L.S., ×4.

FIGURES k, l.—*Plasmopora circumflexa* sp. nov. (k) UNE F11723/1 (holotype), T.S., ×4; (l) UNE F11724/1 (paratype 1), L.S., ×4.

EXPLANATION OF PLATE IV

FIGURES a, b.—*Cyrtophyllum* sp. (a) UNE F11659/1, T.S., ×4, showing tubules with discontinuous walls; (b) UNE F11695/2, L.S., ×4.

FIGURES, c. d.—*Palaeofavosites magnus* sp. nov. (c) UNE F11728/1 (holotype), T.S., ×4; (d) UNE F11728/2 (holotype), L.S., ×4.

FIGURES e, f.—*Palaeofavosites crassus* sp. nov. (e) UNE F11599/2 (holotype), T.S., ×4, showing thickened walls with dark axial line, pores in wall angles; (f) UNE F11599/3 (holotype), L.S., ×4, showing pores near wall angles and continuous septal ridges.

FIGURES g, h.—*Palaeofavosites spinimarginatus* sp. nov. (g) UNE F11727/1 (holotype), T.S., ×4; (h) UNE F11727/2 (holotype), L.S., ×4, showing cut ends of spines grading into continuous septal ridge.

FIGURES i, j.—*Palaeofavosites varispinulatus* sp. nov. (i) UNE F11608/1 (holotype), T.S., ×4, showing rare septal spines and pores in wall angles; (j) UNE F11603/3 (holotype), L.S., ×4.

FIGURES k, l.—*Palaeofavosites* sp. (k) UNE F11600/2, T.S., ×4; (l) UNE F11600/4, L.S., ×4.

EXPLANATION TO PLATE V

FIGURE a.—*Reuschia* sp. UNE F11743, tangential section through colony, ×1·5, showing thick walls and narrow central lumen.

FIGURES b, c.—*Halysites* sp. (b) UNE F11752/1, T.S., ×4, showing form of ranks and lacunae, with microcorallites visible in bottom centre; (c) UNE F11752/2, L.S., ×4.

FIGURES d–g.—*Catenipora flexa* sp. nov. (d) UNE F11650/2 (holotype), T.S., ×2, showing curving ranks of macrocorallites with spines; (e) enlargement of part of Figure (d) showing septal spines, ×5; (f) UNE F11650/10 (holotype), L.S., ×8, showing ends of septal spines; (g) UNE F11650/7 (holotype), L.S., ×6, showing vertical rows of septal spines.

FIGURES h, i.—*Catenipora spatiosa* sp. nov. (h) UNE F11640/2 (holotype), T.S., ×2, general view showing large macrocorallites; (i) UNE F11640/1 (holotype), L.S., ×5.

FIGURES j–l.—*Quepora* sp. (j) UNE F11740, T.S., ×4; (k) UNE F11742, T.S., ×4; (l) UNE F11742, L.S., ×5.

FIGURES m, n.—*Falsicatenipora stricta* sp. nov. (m) UNE F11734/1 (holotype), T.S., ×6, showing compact lacunae and macrocorallites with straight sides; (n) UNE F11734/2 (holotype), L.S., ×6.

AUSTRALASIAN MEDICAL PUBLISHING CO. LTD.
71-79 ARUNDEL ST., GLEBE, N.S.W., 2037
1975

THE ROYAL SOCIETY OF NEW SOUTH WALES

The Society originated in the year 1821 as the Philosophical Society of Australasia. Its main function is the promotion of Science through the following activities : Publication of results of scientific investigation through its Journal and Proceedings ; the Library ; awards of Prizes, and Medals ; liaison with other Scientific Societies ; Monthly Meetings ; and Summer Schools for Senior Secondary School Students. Special Meetings are held for the Pollock Memorial Lecture in Physics and Mathematics, the Liversidge Research Lecture in Chemistry and the Clarke Memorial Lecture in Geology.

Membership is open to any interested person whose application is acceptable to the Society. The application must be supported by two members of the Society, to one of whom the applicant must be personally known.

Membership categories are :

- Ordinary Members : $15.00 per annum plus $3 application fee.
- Absentee Members : $10.50 per annum plus $3 application fee.
- Associate Members (spouses of members and persons under 25 years of age) : $3.00 per annum plus $2.00 application fee.
- Associate Members (with Journal) : $10.50 per annum plus $2 application fee.

Subscription to the Journal, which is published in four Parts per year, issued twice yearly in May and November, for non-members is $A17 p.a. plus postage.

For application forms for membership and enquiries *re* subscriptions, write to :

The Executive Secretary,
The Royal Society of New South Wales,
Science House,
157 Gloucester Street,
Sydney, 2000, N.S.W.

The Society welcomes manuscripts of research (and occasional review articles) in all branches of science, art literature and philosophy, for publication in the Journal and Proceedings.

Manuscripts will be accepted from both members and non-members, though those from the latter should be communicated through a member. A copy of the Guide to Authors is obtainable on request and manuscripts may be addressed to the Honorary Secretary (Editorial) at the above address.

THE ROYAL SOCIETY OF NEW SOUTH WALES SYDNEY
FOUN. 1821. INC. 1881

Contents

Astronomy :

Biochemistry :

Geology :

Mathematics :

Palaeontology :

AUSTRALASIAN MEDICAL PUBLISHING CO. LTD.
71-79 ARUNDEL ST., GLEBE, N.S.W., 2037
1975

Journal and Proceedings of the Royal Society of New South Wales

[illegible] 1975 PARTS [illegible] and [illegible]

[illegible]

Journal and Proceedings, Royal Society of New South Wales, Vol. 108, pp. 95–110, 1975

Wool Research in the Division of Protein Chemistry, CSIRO*

W. G. Crewther and F. G. Lennox

Abstract—Research in the Division of Protein Chemistry, CSIRO., relating to the biosynthesis, structure and chemistry of the wool fibre and to the mechanisms involved in chemical processing of wool has been reviewed. In some instances it has been necessary to refer to related studies in other laboratories.

Introduction

Owing to the importance of the sheep industry in the Australian economy, research on wool production and utilization has been given considerable support by the Australian Wool Industry and the Australian Government. This research includes a substantial amount of work on the structure of wool and on its constituent proteins, thus providing an ever broadening foundation for developing new wool processes and for dealing with some of the more serious technical problems facing the industry in the future. Together with other aspects of wool research, advances in research on the wool proteins and their organization to form the wool fibre have been critically surveyed at the International Wool Textile Research Conferences initiated in Australia in 1955 (Int. Wool Text. Res. Conf., 1st, 1955) and held subsequently at Harrogate (Int. Wool Text. Res. Conf., 2nd, 1960), Paris (Int. Wool Text. Res. Conf., 3rd, 1965) and San Francisco (Int. Wool Text. Res. Conf., 4th, 1970). Such advances have also been surveyed in recent reviews (Crewther *et al.*, 1965 ; Fraser *et al.*, 1972 ; Bradbury, 1973).

In the following brief account, some aspects of present knowledge on wool proteins are discussed in relation to current trends and future needs. Reference is made to studies of the intact fibre and its constituent cellular and ultra-structure, to the derivatization of the wool proteins and their separation into fractions representing the major groups of proteins present in the fibre, to the further fractionation of these groups to yield individual protein chains and to the determination of amino acid sequences of some of these purified proteins. Attention is also drawn to what may well prove to be the most challenging and difficult aspects of the overall programme. This is to ascertain the location of covalent crosslinkages in the native wool fibre, how the sequences of the individual proteins determine their conformation within the fibre, to investigate their location and interaction with other proteins in the structure and their accessibility to, and interaction with, chemicals used in wool research and in wool processing. The ultimate goal is to know the location within the fibre of all the protein chains and the positions of their constituent amino-acid side-chains in relation to the histological and fine structural detail. Such studies may have to await the development of better experimental methods than those available at present. Meanwhile our expanding knowledge of the chemistry and structure of the wool fibre is providing new insights and new incentives to wool technologists who are endeavouring to develop new or improved processes in the wool textile industry.

Biosynthesis and the Structure of the Wool Fibre

The wool fibre is composed of a cortex containing elongated spindle-shaped cells covered by a cuticle comprising flat overlapping scale cells. These originate in separate layers of germinal cells situated just above the papilla at the base of the wool follicle in the skin of the sheep. The blood supply to the papilla is believed to be the source of the amino acids which are assembled into the wool proteins on polyribosomes located in the cells of the wool root. As the cortical and cuticle cells stream up the follicle they elongate or flatten respectively and, at a level corresponding to about one third of the height of the follicle, they lose their capacity to react with compounds used for detecting thiol groups, such as sodium nitroprusside, due to the oxidative conversion of thiol groups to disulphide groups. This reaction, which is the most significant feature of the fibre-hardening or keratinization process, is delayed if copper is deficient in the diet of the animal

---

* Invited paper.

(Marston, 1946) and since no copper-containing oxidative enzyme has been detected in the follicle it is possible that the cupric ion itself is responsible for catalyzing the crosslinking reaction.

More recent studies using the electron microscope have shown that the cortical cells contain oriented filaments known as macrofibrils and that these consist of much smaller filaments known as microfibrils (Birbeck and Mercer, 1957 ; Rogers, 1959). The microfibrils are about seven nm in diameter and their centres are spaced about nine nm apart, the intermicrofibrillar spaces being filled with an apparently amorphous matrix (see Fraser, MacRae and Rogers, 1972). The heavier staining of the matrix as compared with the microfibrils following partial reduction and treatment with osmic acid has led to the suggestion that the matrix has a higher cystine content than the microfibril (Birbeck and Mercer, 1957 ; Rogers and Filshie, 1962). Post-staining with lead salts after staining with osmic acid shows that the inner core of the individual microfibrils differs from the outer annulus. Evidence for this annular structure has been obtained also from X-ray diffraction and electron microscope studies (Bailey *et al.*, 1965 ; Millward, 1970 ; Fraser *et al.*, 1971). Attention is currently being directed to the determination of the more detailed structure of the microfibril through studies of fibrillar material extracted from the pre-keratin of rat vibrissae follicles (Whitmore, 1972*a*, *b* ; Jones, unpublished).

Another interesting feature of the wool follicle is that the unusual amino acid citrulline occurs in the inner root sheath, where it appears to be associated with the proteins not incorporated in the so-called trichohyaline droplets. It also occurs in the medulla which is present as a central structure in coarse wool fibres and in hair (Rogers, 1963). Presumably citrulline is derived from arginine but the significance of its location in the follicle and fibre has yet to be determined. The protein of the medulla is insoluble in solutions containing reducing agents and protein disaggregating agents apparently due to the presence of ε–(γ–glutamyl)–lysine crosslinks (Harding and Rogers, 1971).

It has also been shown that the proteins comprising α–keratin can be synthesized in a cell-free system containing messenger RNA. During protein synthesis the ribosomes are grouped to form polyribosomes of three sizes and it has been suggested that the size of the polyribosome is directly related to the molecular weight of the protein being synthesized, each ribosome corresponding with about 30 amino acid residues (Steinert and Rogers, 1971*a*, *b*). Additional information on the biosynthesis of the fibre has been derived from an extension of earlier studies (Hardy, 1949, 1951 ; Hardy and Lyne, 1956) on the development of embryonic mouse hair and sheep skin in tissue culture. In the more recent studies hair from a young mouse was grown in tissue culture using a collagen gel containing mouse embryonic digest as the culture medium (Frater and Whitmore, 1973).

The cortical cells in the wool fibre appear to be of two different types which differ in their sub-cellular structure, in their uptake of stains such as with methylene blue or osmic acid and in their reaction with chemicals. In Merino fibres these cells have a bilateral distribution (Horio and Kondo, 1953 ; Mercer, 1953) and constitute two adjacent strands known as the ortho and para segments which twist around one another along the length of the fibre so that the ortho segment is always found on the outside of each crimp wave (Fraser and Rogers, 1955 ; Fraser and MacRae, 1956). It has been suggested that the formation of crimp in fine wools is due to the differential effect of moisture on these two types of cell. In coarser, less-crimped wool fibres the two types of cell are not distributed bi-laterally. The reason for the difference in properties between the two types of cells is not known with any certainty, but electron micrographs of fibre cross sections show that in the ortho cortex the microfibrils are frequently arranged in whorls whereas in the paracortex hexagonal packing is more common (Rogers, 1959 ; Rogers and Filshie, 1962). In addition, the paracortical cells appear to contain more high-sulphur matrix proteins between the microfibrils than the orthocortex (Leach *et al.*, 1964).

The measurement of electron micrographs of stained sections of α–keratin may give erroneous data as a result of changes in dimensions during staining. X-ray diffraction measurements on the other hand are capable of providing more precise information. Nonetheless, values for the microfibrillar diameter (7·2 nm) and distance between centres of microfibrils (8·7 nm) obtained from X-ray diffraction studies on porcupine quill (Fraser *et al.*, 1971) are similar to values obtained for other α–keratins by electron microscopy.

Synthetic polypeptides which adopt the α–helical conformation give reflections corresponding to a pitch of 0·54 nm and an axial rise per residue of 0·15 nm. The high-angle diffraction pattern from α–keratin on the other hand contains meridional arcs of spacing 0·515 and 0·149 nm. Crick (1952) and Pauling and Corey (1953) suggested independently that groups of α–helices were distorted to form two or three stranded coiled-coils which enable the residues on the inside of the assembly to pack together more neatly. The pattern obtained from α–keratin agrees closely with that predicted for an α–helical coiled-coil rope (Fraser *et al.*, 1964).

Recent studies of the low-angle meridional and near-meridional low-angle pattern (Fraser and MacRae, 1971, 1973) suggest that in the microfibril, the low-sulphur proteins are arranged on a helix with a unit height of 6·7 nm and pitch of 22 nm which is subject to a periodic axial distortion of period 23·5 nm.

With progressive stretching of α–keratins, such as wool and hair fibres, in steam the characteristic 0·51 nm spacing along the fibre is gradually replaced by a 0·34 nm spacing which characterizes β–keratin, a different ordered arrangement in which the polypeptide molecular chains have been shown to be almost fully extended (Astbury and Woods, 1933 ; Fraser and Suzuki, 1970). This new meridional spacing is attributed to the mean axial distance between individual amino acid residues in the polypeptide chain. New reflections appearing in the equatorial pattern at 0·47 nm and 0·97 nm are ascribed to interchain and intersheet spacings respectively in pleated-sheet structures which are formed during mechanical extension of the fibre (Astbury and Sisson, 1935 ; Fraser *et al.*, 1969).

Extraction and Isolation of Wool Proteins

In parallel with biophysical studies of the intact fibre, investigations have been directed to the extraction of wool proteins and to their subsequent identification, fractionation, purification and characterization. The studies to be described here were based on the earlier work of Goddard and Michaelis (1934, 1935) which showed that a high proportion of the proteins comprising α–keratins can be extracted at pH 11–12 after reduction of the disulphide bonds by reagents such as thioglycollic acid or mercaptoethanol. Alternatively 6–8 M urea can be used as a disaggregating solvent thus permitting extraction at lower pH values (Jones and Mecham, 1943). The thiol groups in the wool proteins are then alkylated, preferably with iodoacetate to form *S*–carboxymethyl derivatives of kerateine, which have greater solubility than those obtained with alternative reagents. In our early research some fractionation of the proteins was obtained by a process of preferential extraction (Gillespie and Lennox, 1953, 1955*a*, *b*) but in recent studies the objective has been to obtain maximum extraction of the proteins and subsequently to fractionate the protein mixture (Gillespie, 1972*a*). The present procedures have been developed in a series of studies (see Crewther *et al.*, 1965 ; Bradbury, 1973 ; Fraser *et al.*, 1972) which show that the extractable proteins of the wool fibre are of three types differing greatly in structure and properties. As a result of these differences in properties it is possible to separate the three types of protein by fractional precipitation from solution. An outline of the procedure used and an indication of the approximate proportion of the wool proteins in each main fraction is shown in Figure 1. The largest protein fraction obtained by this procedure, which is designated the low-sulphur protein fraction because it contains only about 1·7% sulphur as compared with about 3·5% sulphur in the original fibre, consists of protein chains with molecular weights in the range 46,000–56,000 (Jeffrey, 1972 ; O'Donnell and Woods, 1956). The high-sulphur protein fraction, with a sulphur content of 4·5–6·5% depending on the breed and nutritional status of the sheep, contains protein chains with molecular weights between 10,000 and 25,000. On very good pastures, or when pen fed on a diet supplemented with formaldehyde-protected proteins, sheep may produce wool yielding a high-sulphur protein fraction containing as much as 7·0% sulphur containing chains with molecular weights as high as 30,000. The half-cystine content in such wool proteins is about 30 residues/100 residues. Proteins comprising the third type of extractable proteins are rich in glycine (up to 40 residues/100 residues) and tyrosine (up to 22 residues/100 residues) and contain 1·4 to 30% sulphur. They contain no methionine and usually relatively small proportions of lysine, histidine and isoleucine. These proteins all have molecular weights less than 10,000 and can be classified as Type I or Type II high-tyrosine proteins according to their solubility properties (see Figure 1).

There are a variety of alternative procedures available for rupturing the disulphide bonds of wool and producing soluble derivatives of the proteins. For example, tributyl phosphine (Maclaren *et al.*, 1968) has been shown to give virtually complete reduction of the disulphide bonds in a variety of solvents but after alkylation the amount of protein extracted is less than that obtained by reduction with a thiol, alkylation, and extraction with similar solvent systems. Alternatively the disulphide groups can be oxidized to produce two sulphonic acid groups. Thompson and O'Donnell (1962) have shown that performic acid is preferable to peracetic acid (Alexander and Earland, 1950) for this purpose in that oxidation of the disulphide groups with performic acid is virtually complete without significant peptide hydrolysis.

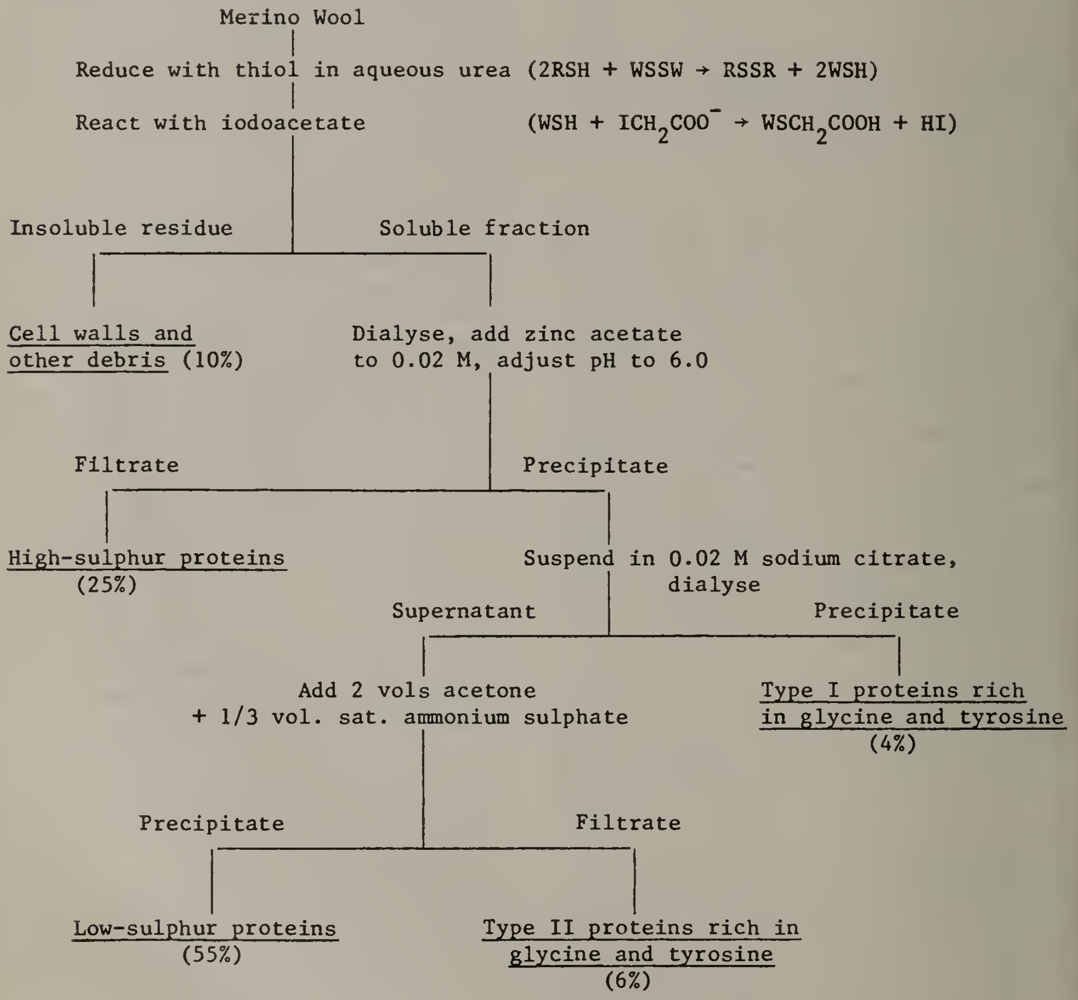

FIGURE 1.—Basic procedures used in separating the main protein constituents of wool.

In addition, a number of different alkylating agents have been tested following reduction with 2–mercaptoethanol or mercaptoacetic acid in the presence of 8 M urea. *S*–Cyanoethyl, *S*–hydroxyethyl, *S*–carbamidomethyl kerateines have been produced but in each case the high-sulphur protein fraction is virtually completely insoluble in aqueous buffers. As a result, these protein derivatives form a floccular precipitate when solutions of the kerateine derivatives in 8 M urea are dialysed against distilled water, the low-sulphur proteins remaining in solution (Gillespie, 1963*b*; Bhatnagar and Crewther, 1969).

After separating the wool proteins into fractions containing the major protein types it is necessary to identify the individual proteins present in each fraction and to isolate each in a pure homogeneous state so that its chemical structure, including the sequence of the constituent amino acids, can be established. As recently stressed by Sparrow (1972) this has proved to be a most difficult problem with keratins for several reasons. Firstly solubilized wool proteins have no known biological activity, such as enzymic or hormonal activity, that could be used to identify the chains and to follow the course of purification. Secondly, they show a marked tendency to aggregate, and disaggregating agents such as urea must be present at high concentration during fractionation. Thirdly, each major protein type comprises a complex mixture of closely-related chains which, although apparently highly effective in conferring the desired mechanical properties on the fibre, greatly complicate the task of isolating pure protein species. Finally the *S*–carboxymethyl or other charged groups introduced into the structure to confer chemical stability and solubility tend to mask charge differences present on individual proteins prior to derivatization and so accentuate the difficulty of isolation.

The greatest difficulty in fractionation and purification has been encountered with solutions of the low-sulphur proteins and this may be associated with the presence in these chains of α–helical regions which are stabilized by interaction with α–helical regions in other chains as shown by measurements of the optical rotatory dispersion of their solutions (Harrap, 1963 ; Crewther *et al.*, 1968). The rupture of these interchain associations is a necessary prerequisite to the isolation of the individual chain species. Usually 8 M urea has been used as a disaggregating solvent for this purpose. The problem is exacerbated by the presence of several different chains in the low-sulphur fraction with large but similar molecular weights and similar amino acid compositions.

When the *S*-carboxymethyl kerateines are subjected to starch-gel electrophoresis in 8 M urea several protein bands are produced, the most deeply-stained when numbered in order from the origin being bands seven and eight. These major bands are also present in electrophoretograms of the low-sulphur protein fraction. Fractions enriched in the proteins corresponding with each of these two bands have been prepared in 8 M urea by stepwise elution from DEAE-cellulose columns at pH 8·6 and gel filtration of suitable fractions on Sephadex G–200 (O'Donnell and Thompson, 1964 ; Thompson and O'Donnell, 1965). Techniques have also been devised for the fractionational precipitation of " component 7 " and " component 8 " from solutions of the low-sulphur protein fraction in aqueous *n*–propanol or 4 M LiBr to yield relatively pure preparations of both " components " (Dowling and Crewther, 1975). Amino acid sequence studies on the *N*–terminal section of " component 8 " showed it to consist of a mixture of closely-related proteins (Thompson and O'Donnell, 1967 ; O'Donnell and Thompson, 1968 ; O'Donnell, 1969).

Immunodiffusion studies (Frater, 1968) and electrophoresis of the low-sulphur protein fraction on acrylamide gel slabs (Sparrow and Crewther, 1972) have recently shown that both " component 7 " and " component 8 " comprise several different proteins which have been designated components 7a, b and c and components 8a, b, cl, c2 and c3 (Sparrow, McKern, Dowling and Crewther, private communication). By using shallow salt gradients on DEAE-cellulose combined with ion-exchange chromatography on SP–Sephadex it has been possible to resolve the low-sulphur protein complex into a number of fractions, some of which contain virtually pure components identifiable as 7c, 8a, 8b and 8c3.

An alternative method of studying the low-sulphur protein complex has been by partial proteolysis, thereby excising most of the non-helical regions of the protein chains and permitting the precipitation of helix-enriched fragments at pH 4·0 in the form of triple chain particles 160 Å in length, about 20 Å in diameter and of molecular weight about 40,000 (Crewther and Harrap, 1967 ; Crewther and Dowling, 1971 ; Dobb *et al.*, 1973 ; Suzuki *et al.*, 1973). There is evidence for at least three types of α–helical segments in the low-sulphur proteins and two of these have been identified as individual chain segments of about 100 residues in the triple-chain particle and prepared in a state of considerable purity. The complete amino acid sequence of one such chain segment has been elucidated (Hogg, Dowling, Crewther, Inglis and McKern, unpublished) and sequence studies on the other helical segments are in progress (Gough, Inglis, Dowling and Crewther, unpublished).

The high-sulphur wool proteins, which remain in solution when the low-sulphur and high-glycine-tyrosine proteins are precipitated with zinc acetate at pH 6, have been fractionated by several methods including ammonium sulphate precipitation and chromatography on DEAE-cellulose, cellulose phosphate and SE–Sephadex. The extreme heterogeneity of the unfractionated high-sulphur wool protein preparation compared with other protein systems has been clearly demonstrated by the electrophoretic mobility of their protein constituents (Joubert *et al.*, 1968), by their behaviour during ion exchange chromatography and gel filtration

(Joubert *et al.*, 1968 ; Gillespie, 1963*b* ; Darskus *et al.*, 1969 ; Darskus, 1972) and by immunodiffusion techniques (Frater, 1969). One high-sulphur protein preparation from wool, designated SCMK–B2, was originally believed to be a single protein (Gillespie, 1963*a*) but was later shown to consist of a family of closely-related proteins all lacking lysine, histidine and methionine from which four different protein chains were recovered in a sufficiently pure state for sequence studies (Lindley and Elleman, 1972).

Some of the high-tyrosine proteins are very easily extracted from wool with alkaline thioglycollate solution (Gillespie and Lennox, 1955*a* ; Simmonds and Stell, 1955 ; DeDeurwaerder *et al.*, 1964). They are also readily recoverable from wool by extraction with 50% formic acid (Zahn and Biela, 1968*a*, *b*). In the studies of Gillespie and Darskus (1971) these proteins were precipitated together with the low-sulphur proteins at pH 6·0 by the addition of zinc acetate and ammonia. After solution of the precipitate in 0·02 M sodium citrate and dialysis against deionized water the high-tyrosine proteins could be divided into two types on the basis of their solubility in deionized water (Figure 1). The insoluble Type I proteins were then collected and dissolved in aqueous ammonia, presumably by ionization of phenolic side-chains of tyrosine residues. The soluble Type II proteins were recovered from the low-sulphur protein fraction, by utilizing their greater solubility in aqueous acetone in the presence of ammonium sulphate.

The identification and fractionation of this family of proteins has been greatly facilitated by the use of electrophoresis on cellulose acetate (Blagrove *et al.*, 1975). The proteins rich in glycine and tyrosine are characterized by relatively low molecular weights (<10,000) and by the restricted range of amino acid residues constituting individual chains. In many instances glycine and tyrosine residues constitute about 50% of the residues in the molecule. All chains are devoid of methionine and some contain little or no lysine, histidine, isoleucine or glutamic acid (Gillespie, 1972 ; Gillespie and Frenkel, 1974*b*). One Type II high-tyrosine chain has been shown by Gillespie and Frenkel (unpublished) to contain only 11 different amino acid residues. Approximately 80% of the molecule was found to consist of glycine, tyrosine, serine and cystine. Ion exchange chromatography and isoelectric focussing of the Type I family of high-tyrosine proteins have shown the presence of thirty to forty different protein species belonging to about ten families. The significance of this heterogeneity, like that of the high-sulphur and low-sulphur proteins, is not yet understood (Gillespie and Frenkel, 1974*b*, *c*).

Attention has been focussed mainly on the proteins extractable from wool because methods are available for studying their structures. There is an equal need, however, to know the molecular structure of proteins located in the membranes isolated from wool. In preliminary studies on the composition of the epicuticle, a chemically inert and very thin membrane which is released from the surface of wool fibres by treatment with chlorine and vigorous agitation, it was shown to be rich in serine, glycine, cystine and glutamic acid (King and Bradbury, 1968). The membranous residue from wool obtained by oxidation with performic acid and extraction with ammonia or urea (Bradbury *et al.*, 1971) closely resembles the epicuticle in amino acid composition. It is also desirable to learn more about the lipid in wool of which about 1% is released when the fibre is treated with formic acid (Bradbury *et al.*, 1965 ; Bradbury and King, 1967). Lipid is also released during prolonged extraction with alkaline thioglycollate (Lennox, unpublished). This material appears to be relatively inaccessible and may well have an important influence on the penetration of chemicals into the fibre.

Influence of Breed and Nutrition of Sheep on Wool Proteins

Before rapid methods for estimating amino acids and techniques for solubilizing and fractionating wool proteins became available, intact wool was frequently subjected to chemical analysis for particular elements, such as nitrogen and sulphur, and on account of the relative constancy of the values obtained wool was assumed to have a constant composition (Marston, 1946). However, it is now known that even wool from a single sheep can vary in composition to a considerable degree. For example, the rate of growth and the cystine content of wool are increased by abomasal infusion of cystine or sulphur-rich proteins (Reis and Schinkel, 1963) and there are other major changes in the overall amino acid composition of the wool (Gillespie, 1965 ; Gillespie and Reis, 1966 ; Gillespie and Darskus, 1971). This change was found to be associated with a variation in the proportions of the constituent low-sulphur, high-sulphur and high-glycine-tyrosine proteins. Variations in the content of high-sulphur proteins in wool between 18% and 34% have been attributed to both genetic and dietary factors (Gillespie and Reis, 1966; Campbell *et al.*, 1972). The role of the former is evidenced by the differences observed between fleeces produced by different sheep in the one flock grazing on the same pasture. The importance of diet is seen in the effects of changes in the nutrition of individual sheep on the composition of the wool produced. One conspicuous feature of the wool from sheep fed on a high-protein diet containing adequate amounts of the sulphur-containing amino acids is the increase in the proportion of a group of proteins in the wool designated "ultra-high-sulphur" proteins which contain some 30 residues per cent of half-cystine residues (Lindley *et al.*, 1971).

Similarly it has been shown that variations in the tyrosine content of wool between about 2·3 and 4·3% of the amino acid residues are associated with changes in the content of the proteins rich in glycine and tyrosine (Gillespie and Darskus, 1971; Gillespie and Frenkel, 1974*a*; Frenkel *et al.*, 1974). As with variations in cystine content, these variations also can be related to dietary and genetic changes in the sheep. Experimentally a reduction in the content of proteins rich in glycine and tyrosine in the wool can be readily induced by infusions of zein, maize gluten, wheat gluten or an amino acid mixture corresponding in composition to zein, into the abomasum of the sheep. Interference with the metabolism of the aromatic amino acids has been suggested to explain the effect.

Other treatments of the sheep causing a similar inhibition of the synthesis of the high-tyrosine proteins, such as intravenous infusion of mimosine, intravenous injection of the synthetic steroid, opticortenol, or abomasal infusion of methionine to sheep maintained on a wheat diet, result in weak wool and in some cases defleecing of the animal occurs. The relationship between the synthesis of high-tyrosine proteins and defleecing is not understood (Frenkel, Gillespie and Reis, unpublished).

Amino Acid Sequences in Wool

The relative proportions of the various amino acids and the sequence in which they are linked together in the peptide chain or chains of a protein exert a profound effect on its properties. They largely determine the conformation the protein will assume in a particular environment, how it will interact with other proteins in the vicinity with chemicals, how it is affected by irradiation of all types, and in the case of a fibrous protein, how the fibre behaves when subjected to mechanical stress. The amino acid sequences and the architecture of the proteins of wool also determine the resistance of the fibre to digestion by proteolytic enzymes and its susceptibility to digestion in the gut of the clothes moth larva and the carpet beetle. It is therefore important to ascertain the amino acid composition and sequence of those proteins which can be isolated from wool in a sufficiently pure state. This has been facilitated by the construction of an automatic amino acid sequenator and the improvement of existing methods for the identification of amino acid derivatives and for the determination of the sequences of small peptides using the machine (Crewther and Inglis, unpublished; Inglis and Nicholls, unpublished; Inglis *et al.*, 1974).

The family of low-sulphur wool proteins known as component 8, has been cleaved with cyanogen

1 2 3 4 5 6 7 8 9 10 11 12 13 14 15 16 17 18
GLN–ASN–ARG–GLN–CMC–CMC–GLU–SER–ASN–LEU–GLU–PRO–LEU–PHE–SER–GLY–TYR–ILE–

19 20 21 22 23 24 25 26 27 28 29 30 31 32 33 34 35 36
–GLU–THR–LEU–ARG–ARG–GLU–ALA–GLU–CMC–VAL–GLU–ALA–ASP–SER–GLY–ARG–LEU–SER–

37 38 39 40 41 42 43 44 45 46 47 48 49 50 51 52 53 54
–SER–GLU–LEU–ASN–LEU–VAL–GLN–GLU–VAL–GLU–GLU–CMC–TYR–GLU–ARG–ARG–TYR–GLU–

55 56 57 58 59 60 61 62 63 64 65 66 67 68 69 70 71 72
–GLU–GLU–ILE–ALA–LEU–ARG–ALA–THR–ALA–GLU–ASN–GLU–PHE–VAL–ALA–LEU–LYS–LYS–

73 74 75 76 77 78 79 80 81 82 83 84 85 86 87 88 89 90
–ASP–VAL–ASP–CMC–ALA–TYR–LEU–ARG–LYS–SER–ASP–LEU–GLU–ALA–ASN–VAL–GLU–ALA–

91 92 93 94 95 96 97 98 99 100 101 102 103 104 105 106 107 108 109
LEU–ILE–GLN–GLU–THR–ASP–PHE–LEU–ARG–ARG–LEU–TYR–GLU–GLU–GLU–ILE–ARG–VAL–LEU

FIGURE 2.—The amino acid sequence of the Type II helical peptide segment recovered from the helical fragments produced by partial proteolysis of the low-sulphur wool protein SCMK–A, with chymotrypsin. *S*–Carboxymethylcysteine residues are indicated by CMC.

bromide and a 77-residue peptide from the *N*–terminus has been partly sequenced (Hosken *et al.*, 1968) and more recently partial sequences have been determined (Figure 2) for helical peptides isolated from the mixed low-sulphur proteins of wool (Hogg *et al.*, 1971; Inglis, McKern and Crewther, unpublished; Gough, Inglis and Crewther, unpublished). These sequences show a clear pattern in which hydrophobic residues occur at positions 1, 4 or 5, 8, 11 or 12, 15, 18 or 19, and so on (Figure 2), thus producing a band of hydrophobic side-chains when the sequence is arranged in the form of a 3·6 residue/turn helix. This could be considered diagnostic for a coiled-coil structure of the form proposed by Crick (1952, 1953) and Pauling and Corey (1953).

Among the high-sulphur proteins three individual structures, each containing about 100 residues, have been isolated and sequenced in South Africa (Haylett and Swart, 1969; Haylett *et al.*, 1971) and three other high-sulphur proteins belonging to another family and having 171, 156 and 151 residues per molecule (Figure 3) have been sequenced in Australia (Elleman, 1971; Dopheide and Elleman, 1972). As will be noted from Figure 3, these three proteins are highly homologous and a large part of each is made up of variant repetitions of the decapeptide sequence Thr–Ser–Cys–Cys–Glu–Pro–Thr–Cys–Ile–Glu.

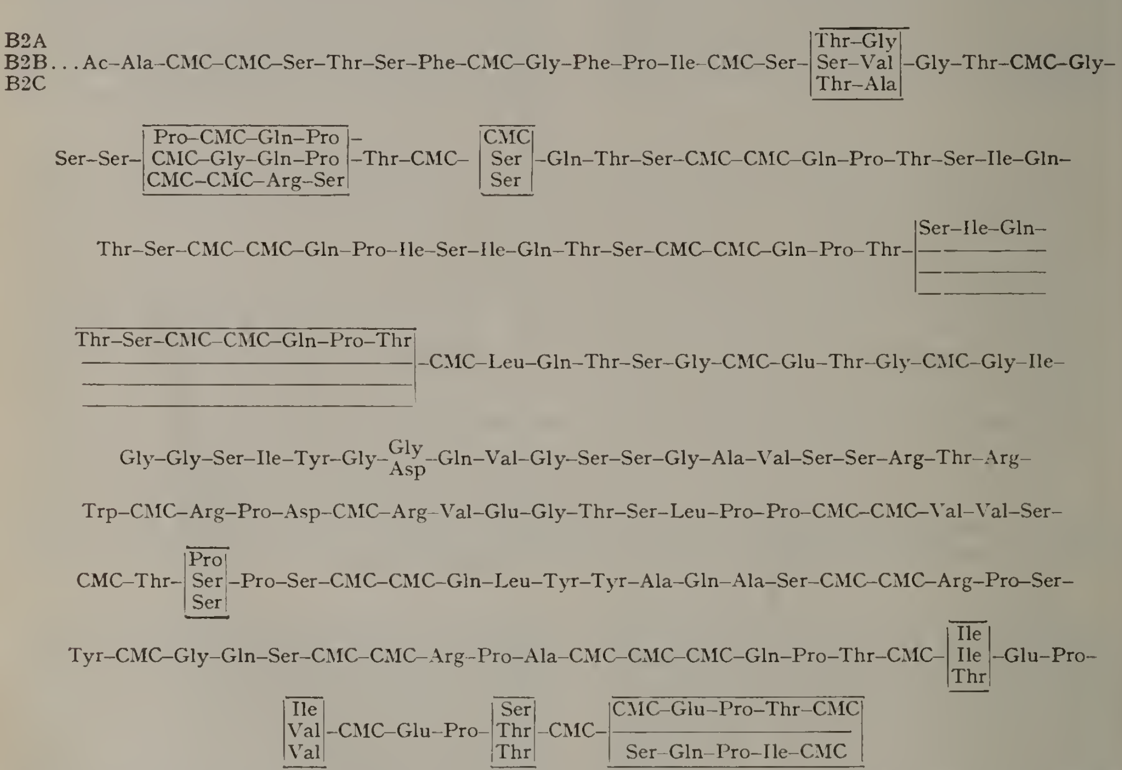

FIGURE 3.—Comparison of the amino acid sequences of high-sulphur wool proteins SCMK–B2A and SCMK–B2C with that of SCMK–B2B. Sequence differences are enclosed in boxes. Sequence deletions are indicated by lines.

An interesting feature of the high-sulphur and low-sulphur protein sequences studied so far is that in most instances the *N*–terminal amino acid residues were found to be acetylated. In the former the terminus is acetyl-alanine (Figure 3) and in component 8, the only low-sulphur chain for which the *N*–terminal sequence is known, it is acetyl-serine (O'Donnell and Thompson, 1968). By contrast, in the high-tryosine proteins examined so far, the *N*–terminal amino groups are free (Dopheide, 1973, unpublished data; Marshall, unpublished data). Other important features of these sequences are that many of the residues occur in pairs, and also, especially in the high-sulphur proteins, there are many examples of the same or closely similar sequences of amino acid residues being repeated in the same molecule. This suggests that the genes for these proteins have arisen from the duplication of smaller genes with subsequent mutations arising in most instances from single base changes in the codons specifying certain amino acids (Elleman *et al.*, 1973). Many of the proteins in wool appear to have been derived from common ancestors.

The high-glycine-tryosine proteins, being of low molecular weight, are readily extracted from wool by a variety of solutions, and the individual protein species are somewhat easier to separate from one another during fractionation than those of the low-sulphur and high-sulphur groups. The sequence of a member of the Type I subgroup of high-tryosine proteins (Dopheide, 1973) is shown in Figure 4. The amino acid sequence of this protein is necessarily dominated by the glycine residues. However, no pattern is apparent in the arrangement of the glycine residues and it will be necessary to determine the sequences of other related proteins to determine which residues, if any, play an essential role before any structure for these proteins can be postulated. However if certain deletions or insertions are accepted it is conceivable that portions of these chains show a decapeptide "repeat" which may be related to the "repeat" in the high-sulphur protein sequences (Lindley, unpublished). On the other hand the high content of relatively few amino acids in this chain gives a high probability of such repeats at intervals of 10 residues assuming a random distribution of residues and further information is needed before the decapeptide-repeat hypothesis can be tested.

Ser–Tyr–CMC–Phe–Ser–Ser–Thr–Val–Phe–Pro–Gly–CMC–Tyr–Trp–Gly–Ser–Tyr–Gly–Tyr–Pro–
Leu–Gly–Tyr–Ser–Val–Gly–CMC–Gly–Tyr–Gly–Ser–Thr–Tyr–Ser–Pro–Val–Gly–Tyr–Gly–Phe–
Gly–Tyr–Gly–Tyr–Asp–Gly–Gly–Ser–Ala–Phe–Gly–CMC–Arg–Arg–Phe–Trp–Pro–Phe–Ala–Leu–Tyr

FIGURE 4.—Amino acid sequence of the high-tyrosine protein, component 0·62.

Once the amino acid sequence of each major constituent of wool has been determined it will be possible to collect information about the positions of interchain and intrachain disulphide linkages in the fibre. As yet little is known about the distribution of disulphide bonds in wool. Lindley and Cranston (1974) have shown that the reactivity of these bonds with thioglycollate, and hence the ease with which they can be ruptured is greatly affected by the nature of the adjacent amino acid residues. Disulphide groups in proximity to polar residues appeared to be more reactive than those associated with non-polar residues. This work is being extended to determine which protein chains are preferentially liberated as the disulphide bonds are progressively converted to *S*–carboxymethyl groups. This study may give preliminary information about the distribution of reactive and less reactive disulphide bonds.

Location of Proteins in the Intact Fibre

While it is essential in the determination of the complete structure of wool to know the sequence of the amino acid residues in each protein, it is likewise important to know the location and conformation of the proteins in the wool fibre and their interrelationship with one another.

Electron micrographs of cross sections of wool fibres reduced and stained with osmium tetroxide suggest that the low-sulphur proteins comprise the microfibrils whereas the high-sulphur proteins are located in the matrix. Initially the proteins rich in glycine and tryosine were believed to be located in the inter-cellular regions in the wool fibre (DeDeurwaerder *et al.*, 1964) but the amount extractable from Merino wool (up to 12%) is too large to be wholly accommodated at this site. The current view (Fraser *et al.*, 1973) is that α–keratins contain a variable proportion of these proteins located in the matrix with associated high-sulphur proteins. This is based on the observation that the volume ratio, matrix/microfibril, as determined by X-ray diffraction measurements approximates closely the mass ratio, high-sulphur protein + high-tryosine protein/low-sulphur protein. An alternative means of determining the location of the proteins is to isolate the individual histological components of the fibre by methods involving minimum damage to the constituent proteins. These can then be extracted by conventional methods and individual proteins identified by chromatographic and electrophoretic techniques developed for the proteins of the intact fibre. Mechanical disruption of fibres swollen in formic acid appears to be the most acceptable method at present available for preparing sufficient cuticle and cortical cells for amino acid analysis (Bradbury *et al.*, 1965; Bradbury *et al.*, 1966) and both types of cell have now been prepared in sufficient quantity for protein fractionation (Ley, unpublished).

An alternative approach for locating various types of protein in the wool follicle is now being explored. Antibodies to purified wool proteins are prepared by injecting them into rabbits and the antibodies are then labelled with a fluorescent dye or the enzyme peroxidase. The binding sites of these labelled antibodies in sections of skin are then determined using fluorescence microscopy (Frater, unpublished) or by the production of a coloured product when peroxidase constitutes the label. Earlier studies on the preparation of antibodies to wool proteins for studies on the homogeneity of wool protein preparations (Frater, 1968, 1969) suggested that such methods are feasible.

Chemical Reactivity in Relation to the Utilization of Wool

The effects of chemicals, physical deformation, heat and various types of radiation on wool reflect the susceptibility to modification by these treatments of the terminal and side-chain groups, the main chain peptide bonds and crosslinks such as disulphide groups. The rate at which the wool fibre is modified in this way is a function of both the reactivity and the accessibility of the various reactive sites. Accessibility to chemical reagents may be increased, for example, by swelling in water or by mechanical, biological or other forms of damage or pre-treatment.

As with other protein materials, wool is very susceptible to damage by highly alkaline solutions, especially at elevated temperatures. Hydrolysis of the amide bonds in glutamine and asparagine residues is liable to occur with liberation of ammonia, also peptide bonds in the main chain and disulphide crosslinks are liable to be broken. The hydrolytic products formed from cystine residues in this way can be further degraded to form α–aminoacrylic acid residues which then react with cysteine residues, another major product from the hydrolysis of cystine, to form lanthionine residues.

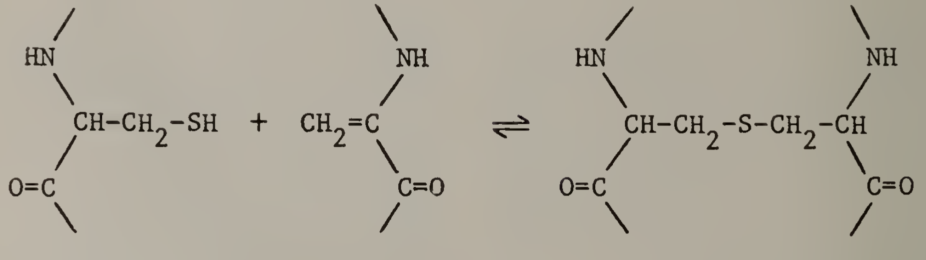

The extent of this reaction is determined by the activity of hydroxyl ions within the wool fibre and this in turn is dependent on the pH and ionic strength of the liquor surrounding the fibre (Crewther and Dowling, 1965). Yellowing of the fibre is also a problem if wool is heated in solutions at pH values greater than seven (Lennox, 1960) and the underlying chemical changes are more complicated than the hydrolytic reactions referred to above. Thus in the process of scouring greasy wool to remove wax, suint and dirt, discoloration and tendering are liable to occur if the pH and the temperature of the scouring liquor are not carefully controlled. Such difficulties are more likely to be encountered with the older method of soap-soda scouring than the newer methods employing synthetic detergents which are effective in neutral solutions.

At pH values less than seven, damage to wool is less likely partly because the "isoelectric point" of the fibre lies in the vicinity of pH 5 so that swelling of the fibre is minimal in dilute acid and partly because disulphide groups are more stable to acid than to alkali. For this reason the dyeing of wool with acid dyes, which carry sulphonic acid groups to render them soluble, normally produces little appreciable damage even though it may involve boiling in dilute acid solution for prolonged periods. Similarly wool can be dyed without apparent damage in cold concentrated formic acid (Harrap, 1959 ; Milligan, 1961), a process that laid the foundations of modern methods for the cold dyeing of wool in aqueous solvents. The method of choice for the removal of vegetable matter from clean wool involves a more severe acid treatment. The wool is soaked in dilute sulphuric acid and hot air is forced through the wool to evaporate the water and concentrate the acid. The wool is then baked at a temperature frequently greater than 100°C to char and embrittle the burr and other vegetable matter which can then be powdered and shaken out from the wool. Damage can be minimized during carbonizing by the addition of certain wetting agents to the acid bowl used for soaking (Crewther, 1955 ; Crewther and Pressley, 1958). Reaction with excess concentrated sulphuric acid causes sulphation of the serine and threonine residues in the wool proteins and virtually eliminates the affinity of wool for acid dyes (Maclaren and Kirkpatrick, 1970), an effect that is sometimes observed when wool is carbonized under excessively severe conditions. Since acids degrade wool by hydrolysis to its constituent amino acids the conditions of exposure to acid solutions must be carefully controlled. As with alkaline treatments, the ionic strength of the acid solutions has a major effect on the hydrogen ion activity within the fibre and hence on the extent of fibre damage at a particular pH of the external solution. Peptide bonds adjacent to aspartic acid residues are particularly susceptible to hydrolysis in dilute acid solutions (Leach, 1955).

The proteins of wool are also susceptible to damage by light, especially in the presence of moisture. This is evidenced by chemical changes in the wool, loss in strength and discoloration. These changes are associated with the photooxidation of the cystine residues through a series of partial oxidation stages to the formation of two cysteic acid residues (Sweetman *et al.*, 1965). Such breakdown contributes to loss in strength of the fibre and to the production of negatively charged centres which change its affinity for dyes and other ionic compounds. Accompanying the loss in strength, and usually apparent at an earlier stage, yellowing discoloration is observed which appears to be associated with the photooxidation of the tryptophan residues in the wool (Lennox and Rowlands, 1969). The tips of wool fibres in the animal's fleece are particularly susceptible to chemical changes of this type and because of the concomitant loss in strength much of this damaged fibre is lost during processing.

Much attention has been given to the chemistry of the photodegradation of tryptophan which proceeds through several intermediates giving rise to formyl kynurenine. Intermediates not previously recognized have been isolated and identified in the course of this work (Savige, 1971), but the chemical nature of the yellow product or products resulting from the photooxidation of wool remains unknown. Evidence for the formation of polymerized yellow products from tryptophan residues has been obtained (Holt and Milligan, 1973) but so far these have resisted attempts at identification. A further complication is that fluorescent whitening agents, which are applied to textiles to enhance their brightness and whiteness, catalyze the yellowing of wool by light. This is a major problem for the industry and a considerable amount of research has been directed to elucidating its nature and to minimizing its effects. Whereas the photoyellowing of untreated wool becomes more pronounced the further the radiation extends into the ultra-violet region and is a significant problem only in summer, that of a fluorescently whitened wool fabric occurs most rapidly at the absorption maximum of the fluorescent whitening agent employed and occurs in all seasons (Leaver and Ramsay, 1969). Also by treatment of wool with a stilbene or pyrazoline fluorescent whitening agent containing a radioactive marker prior to irradiation it has been shown that the whitening agent becomes covalently bound to the wool during exposure (Milligan and Holt, 1973). Currently attention is being given to the synthesis of new fluorescent whitening agents and to new methods of application to the fibre in order to understand the mechanism of the yellowing processes, and eventually to achieve a better performance on wool.

It has been shown that partial protection against photoyellowing can be conferred by impregnating wool fabric with thiourea and formaldehyde (Milligan and Tucker, 1964) but this treatment is not completely fast to washing and the residual protective effect following laundering is not sufficient to justify widespread adoption of the treatment. The protective action of these chemicals is probably associated firstly with the restriction of conformational changes due to the introduction of methylene bridges by reaction of formaldehyde with side-chain groups and secondly to the reductive bleaching effect of the thiol groups of the thiourea. It has recently been shown (Gee, unpublished) that a wide range of thiols or other reducing agents (Holt *et al.*, 1974) give similar beneficial effects.

The setting of wool fabrics to assist retention of creases or pleats is known to involve chemical changes in the cystine residues of the wool proteins. Reagents such as bisulphite or thioglycollate which increase the thiol content of the wool are widely used commercially as setting agents for wool fabrics, for example, to impart permanent creases. It has been shown that the increase in thiol content facilitates thiol-disulphide exchange reactions within the fibres. This reaction in turn allows mechanical stress to be relieved within the fibre as the proteins take up new conformations (Caldwell *et al.*, 1964).

Many shrink-proofing treatments for wool fabrics also involve the chemical modification of disulphide groups. Oxidizing treatments which convert the disulphide bonds to sulphonic acid groups confer shrink resistance on wool presumably by softening the scale edges and roughening the surface of the scales. This greatly decreases felting which is due, at least in part, to the ratchet action between adjacent fibres as the unidirectional scales of one fibre slide over their counterparts in the other, thus preventing them from returning to their original positions after each distortion of the fabric brought about by mechanical agitation during laundering. It has been shown that when permanganate solutions containing common salt are used as a wet chlorination process for shrinkproofing wool a subsequent treatment with sodium sulphite greatly enhances the shrinkproofing effect (McPhee, 1963). This observation finds a ready explanation in a study on the intermediates formed during oxidation of disulphide groups in proteins and simpler compounds. Intermediate oxidation states of the form $-SO.S-$ or $-SO_2S-$ were shown to be formed with a variety of oxidizing agents, including halogens. When these intermediates were reacted with sulphite the products of the reaction were shown to contain sulphonate groups and thiosulphate groups. The reaction of oxidized disulphide groups with sulphite is probably as follows :

$$WS\text{–}SO.W + SO_3^{2-} \rightarrow WS\text{–}SO_3^- + WSO^-$$
$$WSO^- + SO_3^{2-} + H^+ \rightarrow WS^-SO_3^- + OH^-$$
$$WS\text{–}SO_2.W + SO_3^{2-} \rightarrow WS\text{–}SO_3^- + WSO_2^-$$

and the rupture of crosslinkages together with the consequent solution of proteins, accounts for the greatly increased shrinkproofing effect following treatment with sulphite (Sweetman and Maclaren, 1965). An investigation of the mechanism of the chlorination reaction which is unique in its shrinkproofing effect has shown (Gordon, unpublished data) that chlorine attacks not only disulphide bonds but also peptide bonds adjacent to certain amino acid residues. It is therefore effective in producing soluble sections of peptide chain which can then exert a large osmotic effect and cause extensive surface damage to the wool fibres.

The traditional dyeing procedures used for wool fabrics depend on electrostatic attractions between ionic groups on the dye molecule and those on the wool proteins for binding of the dye by the fibre. Negatively-charged sulphonate groups on acid dyes interact with the positively-charged groups of lysine and arginine residues in the fibre and these attractions are supplemented by hydrogen bonding and hydrophobic bonding between the proteins and appropriate regions of the dye structure. That the ionic effect is preeminent is shown by the fact that the number of ionizable basic groups in the fibre can be assessed by determining the amounts of acid dyes bound by the wool (Maclaren, 1960).

Greater washfastness of dyes is achieved by the use of chrome dyes which rely for their effectiveness on the formation *in situ* of a very large complex between chromic ions and the dyestuff which is too large to diffuse out of the fibre (Hartley, 1969). The normal electrostatic and hydrophobic binding of acid dyes are operative in the older and cheaper process of chrome dyeing during which the chrome salts and the dye are applied to the wool in separate treatments. In the meta-chrome process the two reagents are applied simultaneously. The great advantages of chrome dyeing are the high levels of washfastness and lightfastness achieved. On the other hand the shades obtained are relatively dull and it is partly for this reason and the need for high levels of washfastness and bright shades in certain end uses that the so-called reactive dyes, which form covalent bonds with wool, have been developed and are growing in popularity.

The reactive dyes interact principally with the lysine, histidine, serine, tryosine or cysteine residues in the wool proteins by displacement or addition reactions. In general, they display excellent fastness to washing and cover a very wide range of shades. However the lightfastness is sometimes poor compared with the chrome dyes. One widely used class of reactive dyes carries a sulphuric acid ester grouping which is converted to a vinyl sulphone on treatment with alkali. In weakly acid solution these groups interact readily with the lysine and *N*–terminal amino groups in wool to produce a covalent bond. Although the main purpose of inserting reactive groups on dyes is to increase washfastness it has been observed for example with a particular Astrazon dye (Gale and Wilshire, 1974*a*, *b*) that the insertion of the reactive groups, N–2, 3–dibromopropionyl and *N*–chlorodifluoropyrimidyl, into the dye can also impart improved lightfastness to the dye after reaction with the wool fibre.

The Thiolan dyes which carry isothiuronium groups have been developed as a new class of reactive dyes for wool (Guise and Stapleton, 1973). After the dye has been distributed evenly throughout the wool, the pH of the dyebath is raised to decompose the isothiuronium groups to thiol groups. Some of these react with cystine residues in the wool thereby binding the dye by a bisulphide linkage. Other thiol groups are oxidized by the air to form disulphide groups which link dye molecules together so trapping them within the fibre.

An area awaiting further development lies in the more extensive application of polymers, both internally and at the surface of the fibre, to confer additional properties supplementing those of the untreated fibre. A preliminary study of the mode of attachment of a polyurethane polymer to the surface of the fibre (Kriegler, 1971) suggested that combination between isocyanate groups of the polymer and the ε–amino groups of the lysine residues is not essential for shrink-resist and permanent-press effects although interaction with other groups may be involved.

Undoubtedly the attitudes of scientists and technologists to the wool fibre and its industrial potentialities are changing as new information concerning the structure, chemistry and physics of the fibre is made available. We are becoming much more aware that the tissue constituting the wool fibre has a highly organized native structure hiding many chemical and biological subtleties yet to be uncovered.

References

Alexander, P., and Earland, C., 1950. Structure of Wool Fibres: Isolation of an α– and β–Protein in Wool. *Nature, Lond.*, **166**, 396.

Australia, CSIRO, Division of Protein Chemistry, Parkville, 1972. Protein Chemistry: Review and Abstracts, 1971.

Astbury, W. T., and Sissons, W. A., 1935. X-Ray Studies of the Structure of Hair, Wool, and Related Fibres III. The Configuration of the Keratin Molecule and its Orientation in the Biological Cell. *Proc. Roy. Soc., Lond.*, **150A**, 533.

Astbury, W. T., and Woods, H. J., 1933. X-Ray Studies of the Structure of Hair, Wool, and Related Fibres II. The Molecular Structure and Elastic Properties of Hair Keratin. *Roy. Soc. Lond. Phil. Trans.*, **232A**, 333.

Bailey, C. J., Tyson, C. N., and Woods, H. J., 1965. The Equatorial Scattering of X-Rays by Keratin and Its Relation to an Annular Microfibril Model. *Proc. Int. Wool Text. Res. Conf., 3rd, Paris, 1965*, Section 1, 105.

Bhatnagar, G. M., and Crewther, W. G., 1969. The Conformation of the High-Sulphur Proteins of Wool. 1. Preparation and Properties of a Water-Soluble Metakeratin. *Int. J. Protein Res.*, **1**, 199.

Birbeck, M. S. C., and Mercer, E. H., 1957. The Electron Microscopy of the Human Hair Follicle. 1. Introduction and the Hair Cortex. *J. biophys. biochem. Cytol.*, **3**, 203.

Blagrove, R. J., Frenkel, M. J., and Gillespie, J. M., 1975. The Electrophoresis of the High-Tyrosine Proteins of Keratins on Cellulose Acetate Strips. *Comp. Biochem. Physiol.*, In press.

Bradbury, J. H., 1973. The Structure and Chemistry of Keratin Fibres. *Advanc. Protein Chem.*, **27**, 111.

Bradbury, J. H., Chapman, G. V., Hambly, A. N., and King, N. L. R., 1966. Separation of Chemically Unmodified Histological Components of Keratin Fibres and Analyses of Cuticles. *Nature, Lond.*, **210**, 1333.

Bradbury, J. H., Chapman, G. V., and King, N. L. R., 1965. The Chemical Composition of Wool. III. Analysis of Cuticle, Skin Flakes and Cell Membrane Material. *Proc. Int. Wool. Text. Res. Conf., 3rd, Paris, 1965*, Section 1, 359.

Bradbury, J. H., and King, N. L. R., 1967. The Chemical Composition of Wool. IV. The Quantity of Each Histological Component. *Aust. J. Chem.*, **20**, 2803.

Bradbury, J. H., Leeder, J. D., and Watt, I. C., 1971. The Cell Membrane Complex of Wool. *Appl. Polym. Symp.*, No. 18, 227.

Caldwell, J. B., Leach, S. J., Meschers, A., and Milligan, B., 1964. The Role of Thiol Groups in the Setting of Wool. *Text Res. J.*, **34**, 627.

Campbell, M. E., Whiteley, K. J., and Gillespie, J. M., 1972. Compositional Studies of High and Low-Crimp Wools. *Aust. J. biol. Sci.*, **25**, 977.

Crewther, W. G., 1955. Carbonizing Investigations III. A New Method for Protecting Wool During Carbonizing. *Proc. Int. Wool Text. Res. Conf. Australia, 1955, E*, 408.

Crewther, W. G., Dobb, M. G., Dowling, L. M., and Harrap, B. S., 1968. The Structure and Aggregation of Low-Sulphur Proteins derived from Alpha Keratins. In W. G. Crewther (Ed.,), *Symposium on Fibrous Proteins Australia, 1967*. Butterworths (Australia), Sydney, 329.

Crewther, W. G., and Dowling, L. M., 1965. The Effects of Salts on the Formation of Lanthionine in Wool. *Proc. Int. Wool Text. Res. Conf., 3rd, Paris, 1965*, Section II, 431.

Crewther, W. G., and Dowling, L. M., 1971. The Preparation and Properties of Large Peptides from the Helical Regions of the Low-Sulphur Proteins of Wool. *Appl. Polym. Symp.*, No. 18, 1.

Crewther, W. G., Dowling, L. M., Gough, K. H., Inglis, A. S., and McKern, N. M., 1973. Comparative Studies on the α Helical Segments of Wool Proteins Using the Sequenator. *Proc. Aust. biochem. Soc.*, **6**, 4.

Crewther, W. G., Fraser, R. D. B., Lennox, F. G., and Lindley, H., 1965. The Chemistry of Keratins. *Advanc. Protein Chem.*, **20**, 191.

Crewther, W. G., and Harrap, B. S., 1967. The Preparation and Properties of a Helix-Rich Fraction Obtained by Partial Proteolysis of Low-Sulphur *S*–Carboxymethylkerateine from Wool. *J. biol. Chem.*, **242**, 4310.

Crewther, W. G., and Pressley, T. A., 1958. Carbonizing Investigations. Part IV: Industrial Carbonizing Trials to Assess the Protection of Wool by Surface Active Agents Added to the Acid. *Text. Res. J.*, **28**, 67.

Crick, F. H. C., 1952. Is α–Keratin a Coiled Coil. *Nature, Lond.*, **170**, 882.

Crick, F. H. C., 1953. The Packing of α–Helices: Simple Coiled Coils. *Acta crystallogr.*, **6**, 689.

Darskus, R. L., 1972. Electrophoretic and Chromatographic Characterization of Sulphur-Rich Proteins from Wool. *J. Chromat.*, **69**, 341.

Darskus, R. L., Gillespie, J. M., and Lindley, H., 1969. The Possibility of Common Amino Acid Sequences in High-Sulphur Protein Fractions from Wool. *Aust. J. biol. Sci.*, **22**, 1197.

DeDeurwaerder, R. A., Dobb, M. G., and Sweetman, B. J., 1964. Selective Extraction of a Protein Fraction from Wool Keratin. *Nature, Lond.*, **203**, 48.

Dobb, M. G., Millward, G. R., and Crewther, W. G., 1973. Examination in the Electron Microscope of *S*–Carboxymethylkerateine–A and the Helix-Rich Fraction Obtained from it by Partial Proteolysis. *J. Text. Inst.*, **64**, 374.

Dopheide, T. A. A., 1973. The Primary Structure of a Protein, Component 0·62, Rich in Glycine and Aromatic Residues, Obtained from Wool Keratin. *Eur. J. Biochem.*, **34**, 120.

Dopheide, T. A. A., and Elleman, T. C., 1972. Repetitive Sequences Implying Gene Duplication in a Group of High-Sulphur Proteins from Wool Keratin. *Proc. Aust. biochem. Soc.*, **5**, 3.

Dowling, L. M., and Crewther, W. G., 1974. Isolation of Components from the Low-Sulphur Proteins of Wool by Fractional Precipitation. *Prep. Biochem.*, **4**, 203.

Elleman, T. C., 1971. Amino Acid Sequence of a High-Sulphur Protein from Wool. *Nature New Biol., Lond.*, **234**, 148.

Elleman, T. C., Lindley, H., and Rowlands, R. J., 1973. Periodicity in High-Sulphur Proteins from Wool. *Nature, Lond.*, **246**, 530.

Fraser, R. D. B., Gillespie, J. M., and MacRae, T. P., 1973. Tyrosine-Rich Proteins in Keratins. *Comp. Biochem. Physiol.*, **44**B, 943.

Fraser, R. D. B., and MacRae, T. P., 1956. The Distribution of Ortho- and Para-Cortical Cells in Wool and Mohair. *Text. Res. J.*, **26**, 618.

Fraser, R. D. B., and MacRae, T. P., 1971. Structure of α–Keratins. *Nature, Lond.*, **233**, 138.

Fraser, R. D. B., and MacRae, T. P., 1973. *The Structure of* α*–Keratin. Polymer*, **14**, 61.

Fraser, R. D. B., MacRae, T. P., and Miller, A., 1964. The Coiled-Coil Model of α–Keratin Structure. *J. molec. Biol.*, **10**, 147.

Fraser, R. D. B., MacRae, T. P., Millward, G. R., Parry, D. A. D., Suzuki, E., and Tulloch, P. A., 1971. The molecular Structure of Keratins. *Appl. Polym. Symp.*, No. 18, 65.

Fraser, R. D. B., MacRae, T. P., Parry, D. A. D., and Suzuki, E., 1969. The Structure of β–Keratin. *Polymer*, **10**, 810.

Fraser, R. D. B., MacRae, T. P., and Rogers, G. E., 1972. *Keratins : Their Composition, Structure and Biosynthesis.* Charles C. Thomas, Springfield, Ill., U.S.A.

Fraser, R. D. B., and Rogers, G. E., 1955. The Bilateral Structure of Wool Cortex and its Relation to Crimp. *Aust. J. biol. Sci.*, **8**, 288.

Fraser, R. D. B., and Suzuki, E., 1970. A Quantitative Study of the Amide I Vibrations in the Infra-Red Spectrum of β–Keratin. *Spectrochim. Acta*, **26**A, 423.

Frater, R., 1968. Immunological Studies on Wool Proteins. *Aust. J. biol. Sci.*, **21**, 815.

Frater, R., 1969. Heterogeneity in a High-Sulphur Protein from Wool. *Aust. J. biol. Sci.*, **22**, 1087.

Frater, R., and Whitmore, P. G., 1973. *In Vitro* Growth of Post-Embryonic Hair. *J. invest. Derm.*, **61**, 72.

Frenkel, M. J., Gillespie, J. M., and Reis, P. J., 1974. Factors Influencing the Biosynthesis of the Tyrosine-Rich Proteins of Wool. *Aust. J. biol. Sci.*, **27**, 31.

Gale, D. J., and Wilshire, J. F. K., 1974*a*. Fibre-Reactive Basic Dyes. I. Polymethine Dyes Containing the N–Chloroacetyl Group. *J. Soc. Dyers Colour.*, **90**, 97.

Gale, D. J., and Wilshire, J. F. K., 1974*b*. Fibre-Reactive Basic Dyes. II. Polymethine Dyes Containing the N–2, 3–Dibromopropionyl and N–Chlorodifluoropyrimidyl Groups. *J. Soc. Dyers Colour.*, In press.

Gillespie, J. M., 1963*a*. The Isolation and Properties of Some Soluble Proteins from Wool. V. The Isolation of the High-Sulphur Protein SCMKB2. *Aust. J. biol. Sci.*, **16**, 241.

Gillespie, J. M., 1963*b*. The Isolation and Properties of Some Soluble Proteins from Wool. VII. The Heterogeneity of the High-Sulphur Proteins. *Aust. J. biol. Sci.*, **16**, 259.

Gillespie, J. M., 1965. The High-Sulphur Proteins of Normal and Aberrant Keratins. In A. G. Lyne and B. F. Short (Eds), *Biology of the Skin and Hair Growth.* Angus and Robertson, Sydney, 377.

Gillespie, J. M., 1972*a*. Proteins Rich in Glycine and Tyrosine from Keratins. *Comp. Biochem. Physiol.*, **41**B, 723.

Gillespie, J. M., 1972*b*. The Use of Quaternary Ammonium Ethyl Cellulose in the Fractionation of Tyrosine-Rich Proteins from Wool. *J. Chromat.*, **72**, 319.

Gillespie, J. M., and Darskus, R. L., 1971. Relation Between the Tyrosine Content of Various Wools and their Content of a Class of Proteins Rich in Tyrosine and Glycine. *Aust. J. biol. Sci.*, **24**, 1189.

Gillespie, J. M., and Frenkel, M. J., 1974*a*. The Diversity of Keratins. *Comp. Biochem. Physiol.*, **47**B, 339.

Gillespie, J. M., and Frenkel, M. J., 1974*b*. The Macroheterogeneity of Type I Tyrosine-Rich Proteins of Merino Wool. *Aust. J. biol. Sci.*, **27**, 616.

Gillespie, J. M., and Frenkel, M. J., 1974*c*. Heterogeneity of Tyrosine-Rich Proteins of Wool. *Proc. Aust. biochem. Soc.*, **7**, 4.

Gillespie, J. M., and Lennox, F. G., 1953. Preparation of an Electrophoretically-Homogenous Keratin Derivative from Wool. *Biochem. Biophys. Acta*, **12**, 481.

Gillespie, J. M., and Lennox, F. G., 1955*a*. Keratin Derivatives Extracted from Wool with Alkaline Thioglycollate Solutions. *Aust. J. biol. Sci.*, **8**, 97.

Gillespie, J. M., and Lennox, F. G., 1955*b*. An Electrophoretic Study on "Component 2" Extracted from Wool with Alkaline Thioglycollate Solutions. *Aust. J. biol. Sci.*, **8**, 378.

Gillespie, J. M., and Reis, P. J., 1966. The Dietary-Regulated Biosynthesis of High-Sulphur Wool Proteins. *Biochem. J.*, **98**, 669.

Goddard, D. R., and Michaelis, L., 1934. A Study on Keratin. *J. biol. Chem.*, **106**, 605.

Goddard, D. R., and Michaelis, L., 1935. Derivatives of Keratin. *J. biol. Chem.*, **112**, 361.

Guise, G. B., and Stapleton, I. W., 1975. New Approaches to Fast Dyes for Wool. I. Isothiuronium Salts as Protected Dye Reactive Groups. *J. Soc. Dyers Colour.*, In press.

Harding, H. W. J., and Rogers, G. E., 1971. The ε–(γ–Glutamyl) Lysine Cross-Linkage in Citrulline Containing Protein Fractions from Hair. *Biochemistry*, **10**, 624.

Harding, H. W. J., and Rogers, G. E., 1972. Formation of the ε–(γ–Glutamyl) Lysine Cross-Link in Hair Proteins. Investigation of Transamidases in Hair Follicles. *Biochemistry*, **11**, 2858.

Hardy, M. H., 1949. The Development of Mouse Hair *in vitro* with Some Observations on Pigmentation. *J. Anat.*, **83**, 364.

Hardy, M. H., 1951. The Development of Pelage Hairs and Vibrissae from Skin in Tissue Culture. *Ann. N.Y. Acad. Sci.*, **53**, 546.

Hardy, M. H., and Lyne, A. G., 1956. Studies on the Development of Wool Follicles in Tissue Culture. *Aust. J. biol. Sci.*, **9**, 559.

Harrap, B. S., 1959. Dyeing Wool at Room Temperature. *J. Soc. Dyers Colour.*, **75**, 106.

Harrap, B. S., 1963. The Conformation of a Soluble Wool Keratin Derivative. *Aust. J. biol. Sci.*, **16**, 231.

Hartley, F. R., 1969. The Chemistry of Chrome Mordanting of Wool. *J. Soc. Dyers Colour.*, **85**, 66.

Haylett, T., and Swart, L. S., 1969. Studies on the High-Sulphur Proteins of Reduced Merino Wool III. The Amino Acid Sequence of Protein SCMKB-IIIB2. *Text. Res. J.*, **39**, 917.

Haylett, T., Swart, L. S., Parris, D., and Joubert, F. J., 1971. The Primary Structure of Some High-Sulphur Proteins of Reduced Wool. *Appl. Polym. Symp.*, No. 18, 37.

Hogg, D., Dowling, L. M., and Crewther, W. G., 1971. Sequence Studies on a Large Peptide from the Helical Regions of the Low-Sulphur Proteins of Wool. *Proc. Aust. Biochem. Soc.*, **4**, 16.

Holt, L. A., and Milligan, B., 1973. The Application of Enzymic Hydrolysis and Tritium Labelling to a Study of the Modification of Tryptophyl Residues in Proteins. *Aust. J. biol. Sci.*, **26**, 871.

Holt, L. A., Milligan, B., and Wolfram, L. J., 1974. Fluorescent Whitening Agents. V. The Use of Reducing Agents for Retarding the Yellowing of Fluorescently Whitened Wool by Sunlight. *Text. Res. J.*, **44**, 846.

Horio, M., and Kondo, T., 1953. Crimping of Wool Fibres. *Text. Res. J.*, **23**, 373.

Hosken, R., Moss, B. A., O'Donnell, I. J., and Thompson, E. O. P., 1968. Methionyl Sequences in Low-Sulphur Proteins of Wool. *Aust. J. biol. Sci.*, **21**, 593.

Inglis, A. S., Nicholls, P. W., and Sparrow, L. G., 1974. Detection of Sub-Nanomole Amounts of Phenylthiohydantoins of Amino Acids. *J. Chromat.*, **90**, 362.

International Wool Textile Research Conference, 1st, Australia, 1955. Proceedings. Published by CSIRO, Melbourne, 1956.

International Wool Textile Research Conference, 2nd, Harrogate, 1960. Proceedings. Published in the Journal of the Textile Institute, Transactions, 1960, Volume 51, No. 12.

International Wool Textile Research Conference, 3rd, Paris, 1965. Proceedings. Published by L'Institut Textile de France, Paris, 1965.

International Wool Textile Research Conference, 4th, Berkeley, California, 1970. Proceedings. Published in Applied Polymer Symposia No. 18, 1971.

Jeffrey, P. D., 1972. The Molecular Weights of the Low-Sulphur Proteins from Wool. *J. Text. Inst.*, **63**, 91.

Jones, C. B., and Mecham, D. K., 1943. The Dispersion of Keratins. II. Studies on the Dispersion of Keratins by Reduction in Neutral Solutions of Protein Denaturants. *Archs Biochem. Biophys.*, **3**, 193.

Joubert, F. J., de Jager, P. J., and Swart, L. S., 1968. Studies on the High-Sulphur Proteins of Reduced Merino Wool. In W. G. Crewther (Ed.), *Symposium on Fibrous Proteins Australia, 1967*. Butterworths (Australia), Sydney, 343.

King, N. L. R., and Bradbury, J. H., 1968. The Chemical Composition of Wool. V. The Epicuticle. *Aust. J. biol. Sci.*, **21**, 375.

Kriegler, A. B., 1971. Covalent Bonding Between Polymers and Wool Proteins: The Extent of Covalent Bonding Between Wool and a Polyurethane Prepolymer Containing Isocyanate Groups. *J. Text. Inst.*, **62**, 411.

Leach, S. J., 1955. The Kinetics and Mechanism of Aspartic Acid Liberation from Proteins. *Proc. Int. Wool Text. Res. Conf. Australia, 1955, C*, 181.

Leach, S. J., Rogers, G. E., and Filshie, B. K., 1964. The Selective Extraction of Wool Keratin with Dilute Acid. I. Chemical and Morphological Changes. *Archs Biochem. Biophys.*, **105**, 270.

Leaver, I. H., and Ramsay, G. C., 1969. Studies in Wool Yellowing. Part XXVI. Photoyellowing of Fluorescent-Brightened Wools—Wavelength Dependence and ESR Studies. *Text. Res. J.*, **39**, 722.

Lennox, F. G., 1960. A Spectrophotometric Study of Yellowing in Wool Fabric. *J. Text. Inst.*, **51**, T1193.

Lennox, F. G., and Rowlands, R. J., 1969. Photochemical Degradation of Keratins. *Photochem. Photobiol.*, **9**, 359.

Lindley, H., Broad, A., Damoglou, A. P., Darskus, R. L., Elleman, T. C., Gillespie, J. M., and Moore, C. H., 1971. The High-Sulphur Protein Fraction of Keratins. *Appl. Polym. Symp.*, No. 18, 21.

Lindley, H., and Cranston, R. W., 1974. The Reactivity of the Disulphide Bonds of Wool. *Biochem. J.*, **139**, 515.

Lindley, H., and Elleman, T. C., 1972. The Preparation and Properties of a Group of Proteins from the High-Sulphur Fraction of Wool. *Biochem. J.*, **128**, 859.

Maclaren, J. A., 1960. The Estimation of Basic Groups in Wool by Dye Uptake Measurements. *Archs Biochem. Biophys.*, **86**, 175.

Maclaren, J. A., and Kilpatrick, D. J., 1970. Sulfation of Wool as a Dye-Resist Process. *Text. Res. J.*, **40**, 880.

Maclaren, J. A., Kilpatrick, D. J., and Kirkpatrick, A., 1968. Reduced Wool Fibres, their Preparation and Alkylation. *Aust. J. biol. Sci.*, **21**, 805.

McPhee, J. R., 1963. Shrinkproofing of Wool with Peracetic Acid Followed by Sodium Sulfite. *Text. Res. J.*, **33**, 755.

Marston, H. R., 1946. Nutrition and Wool Production. In C. L. Bird (Ed.), *Fibrous Proteins*. Proc. Symp. Leeds, 1946. Society of Dyers and Colourists, Bradford, 207.

Mercer, E. M., 1953. The Heterogeneity of Keratin Fibres. *Text. Res. J.*, **23**, 388.

Milligan, B., 1961. Investigations into the Continuous Dyeing of Wool. *J. Soc. Dyers Colour.*, **77**, 106.

Milligan, B., and Holt, L. A., 1973. The Photochemical Binding of Fluorescent Whitening Agents to Proteins. In *Fluorescent Whitening Agents*. Proc. Symp. Stockholm, Sweden, 1973. NFR (Swedish Natural Science Research Council), Stockholm, MVC–Report 2, 63.

Milligan, B., and Tucker, D. J., 1964. Studies in Wool Yellowing. Part VII. Processes for Retarding Yellowing by Sunlight. *Text. Res. J.*, **34**, 681.

Millward, G. R., 1970. The Substructure of α-Keratin Microfibrils. *J. Ultrastruct. Res.*, **31**, 349.

Moffitt, W., and Yang, J. T., 1956. The Optical Rotatory Dispersion of Simple Polypeptides. I. *Proc. natn. Acad. Sci. USA*, **42**, 596.

O'Donnell, I. J., 1969. Studies on Reduced Wool. IX. The N–Terminal Sequence of a Fragment Produced by Cleavage of Component 8 with Cyanogen Bromide. *Aust. J. biol. Sci.*, **22**, 471.

O'Donnell, I. J., and Thompson, E. O. P., 1964. Studies on Reduced Wool. IV. The Isolation of a Major Component. *Aust. J. biol. Sci.*, **17**, 973.

O'Donnell, I. J., and Thompson, E. O. P., 1968. Studies on Reduced Wool. VIII. N–Acetyl Peptides Isolated from a Major Component. *Aust. J. biol. Sci.*, **21**, 385.

O'Donnell, I. J., and Woods, E. F., 1956. The Size and Configuration of Some Soluble Wool Keratins. *J. Polym. Sci.*, **21**, 397.

Pauling, L., and Corey, R. B., 1953. Compound Helical Configurations of Polypeptide Chains: Structure of Proteins of the α–Keratin Type. *Nature, Lond.*, **171**, 59.

Reis, P. J., and Schinckel, P. G., 1963. Some Effects of Sulphur-Containing Amino Acids on the Growth and Composition of Wool. *Aust. J. biol. Sci.*, **16**, 218.

Rogers, G. E., 1959. Electron Microscope Studies of Hair and Wool. *Ann. N.Y. Acad. Sci.*, **83**, 378.

Rogers, G. E., 1963. The Localization and Significance of Arginine and Citrulline in Proteins of the Hair Follicle. *J. Histochem. Cytochem.*, **11**, 700.

Rogers, G. E., and Filshie, B. K., 1962. Electron Staining and Fine Structure of Keratins. In S. S. Breese (Ed.), *International Congress for Electron Microscopy, 5th, Philadelphia, 1962.* Vol. 2. Academic Press, New York, 0.

Savige, W. E., 1971. Isolation and Identification of Some Photo-oxidation Products of Tryptophan. *Aust. J. Chem.*, **24**, 1285.

Simmonds, D. E., and Stell, I. G., 1955. The Amino-Acid Composition of Protein Fractions Extracted from Wool. *Proc. Int. Wool Text. Res. Conf. Australia, 1955, C*, 75.

Sparrow, L. G., 1972. Some Recent Advances in the Chemistry of Wool Proteins. *Wool Sci. Rev.*, No. 43, 2.

Sparrow, L. G., and Crewther, W. G., 1972. Further Resolution of the Low-Sulphur *S*–Carboxymethylkerateine Fraction from Wool by Acrylamide-Gel Electrophoresis. *J. Text. Inst.*, **63**, 629.

Steinert, P. M., and Rogers, G. E., 1971*a*. Protein Biosynthesis in Cell-Free Systems Prepared from Hair Follicle Tissue of Guinea Pigs. *Biochim. Biophys. Acta*, **232**, 556.

Steinert, P. M., and Rogers, G. E., 1971*b*. The Synthesis of Hair Keratin Proteins *in Vitro*. *Biochim. Biophys. Acta*, **238**, 150.

Suzuki, E., Crewther, W. G., Fraser, R. D. B., MacRae, T. P., and McKern, N. M., 1973. X-Ray Diffraction and Infrared Studies of an α–Helical Fragment from α–Keratin. *J. molec. Biol.*, **73**, 275.

Sweetman, B. J., Eager, Joan, Maclaren, J. A., and Savige, W. E., 1965. A Study of Partial Oxidation of the Disulphide Groups in Wool. *Proc. Int. Wool Text. Res. Conf., 3rd, Paris, 1965*, **2**, 85.

Sweetman, B. J., and Maclaren, J. A., 1965. Chemical Reactions Involved in the Shrinkproofing of Wool by Oxidation-Sulfite Processes. *Text. Res. J.*, **35**, 315.

Thompson, E. O. P., and O'Donnell, I. J., 1962. Studies on Oxidized Wool. V. Comparison of Protein Fractions Extracted from Wool by Peptide Mapping of Enzymic Digests. *Aust. J. biol. Sci.*, **15**, 552.

Thompson, E. O. P., and O'Donnell, I. J., 1965. Studies on Reduced Wool. V. A Comparison of the Two Major Components. *Aust. J. biol. Sci.*, **18**, 1207.

Thompson, E. O. P., and O'Donnell, I. J., 1967. Studies on Reduced Wool. VII. The Complexity of one of the Major Components. *Aust. J. biol. Sci.*, **20**, 1001.

Whitmore, P. G., 1972*a*. Isolation of Microfibrils from Rat Vibrissal Follicles. *J. Cell Biol.*, **52**, 174.

Whitmore, P. G., 1972*b*. Microfibrillar Material from Various Sources of Keratin. *Aust. J. biol. Sci.*, **25**, 1313.

Zahn, H., and Biela, M., 1968*a*. Über die Isolierung tyrosinreicher Proteine aus Wolle. *Text.–Prax.*, **23**, 105.

Zahn, H., and Biela, M., 1968*b*. Tyrosinreiche Proteine im Ameisensäure–Extrakt von reduzierter Wolle. *Eur. J. Biochem.*, **5**, 567.

Division of Protein Chemistry, CSIRO,
Parkville (Melbourne), Victoria 3052

(Received 7.3.75)

Journal and Proceedings, Royal Society of New South Wales, Vol. 108, pp. 111–118, 1975

The Garra Formation (Early Devonian) at Wellington, N.S.W.

Brian D. Johnson

Abstract—Andesitic volcanics, often regarded as Ordovician, but here referred to the Early Devonian Cuga Burga Volcanics, out-crop in a much faulted, north plunging anticline in the Wellington Caves area. The volcanics are overlain by the Garra Formation. The latter commences with an apparently transgressive sequence of volcanically derived sediments grading from conglomerates and siltstones through to marine shales and these in turn into limestones at the base of a carbonate sequence some 970 metres in thickness. It is contended that a complete sequence of the Garra Formation exists in the Wellington area and that this can be informally divided into 20 units. After the initial transgressive phase, subtidal marine carbonates were deposited on a shallow platform ; the upper half of the formation is characterized by extensive sabkha style deposition on intertidal and supratidal flats. Conodonts indicate correlation of the basal Garra limestones with the limestones at the base of the Mandagery Park Formation (late Lochkovian-early Praguian).

Introduction

Richly fossiliferous horizons have long been known to occur in the limestones of the Garra Formation near the Wellington Caves, south of Wellington, N.S.W., but their stratigraphic sequence and faunal composition have not been detailed ; with the exception of the corals, (Strusz, 1965*b*, 1966, 1967*b*, Strusz and Jell, 1970) the diverse invertebrate faunas have received little attention. Mapping of the Wellington Caves area was undertaken to determine the field relationships of the Garra Formation to contiguous units and to establish the stratigraphic and lithologic sequence as a basis for palaeoecological analysis of the faunas.

The area (Figure 1) forms part of the eastern flank of the Molong High. The oldest outcrops in the region are Ordovician spilites and graptolitic shales (Oakdale Formation) overlain by fossiliferous Silurian limestones (Narragal Limestone) and graptolitic shales (Barnby Hills Shale). Andesitic vulcanism, with extensive intermediate lavas and detrital deposits, commenced at or about the close of the Silurian and continued into the Early Devonian (Cuga Burga Volcanics). All the above outcrop typically along the Oakdale Anticline (Strusz, 1960) to the east of the Caves area.

The oldest outcrops within the area mapped are lavas, herein assigned to the Cuga Burga Volcanics. These are overlain by a thick sequence of Early Devonian limestones representing an eastward extension from a major meridional belt of limestones, the Garra Formation (Strusz, 1965*a*), and physically separated from it by a synclinal belt of Late Devonian quartz rich clastics, the Catombal Group (Conolly, 1963 ; Roberts *et al.*, 1972). There is no further sedimentary record of events until the late Cainozoic when the various alluvials of the present drainage system accumulated.

Stratigraphy

Cuga Burga Volcanics

Andesitic lavas, tuffs and detrital sediments of volcanic derivation, previously regarded as Ordovician in age (e.g. Adrian, 1971) and so indicated on the Dubbo 1 : 250,000 geological sheet (Offenburg *et al.*, 1968), are here assigned to the Cuga Burga Volcanics as defined by Strusz (1960) ; this assignment has been implied previously by Strusz (1967*a*), Savage (1968) and Druce (1970). Correlation is indicated by the close petrographic similarities to the typical Cuga Burga outcrops mapped by Strusz (1960) and, more important, by field relationships in the area north of Newrea (south east of the Wellington Caves) where these volcanics are seen to be underlain by the Late Silurian Barnby Hills Shale.

Owing to the weathered nature and lack of stratification in most outcrops, precise relationships and thicknesses are not clear. The better exposures to the south (' Camelford Ridge ') are massive and strongly jointed, making bedding difficult to determine. The lowest outcrops are a suite of breccias with coarse angular, andesitic clasts and minor red lithic tuffs. They are overlain by green andesites grading into dark red and purple andesites with quartz veins and disseminated copper.

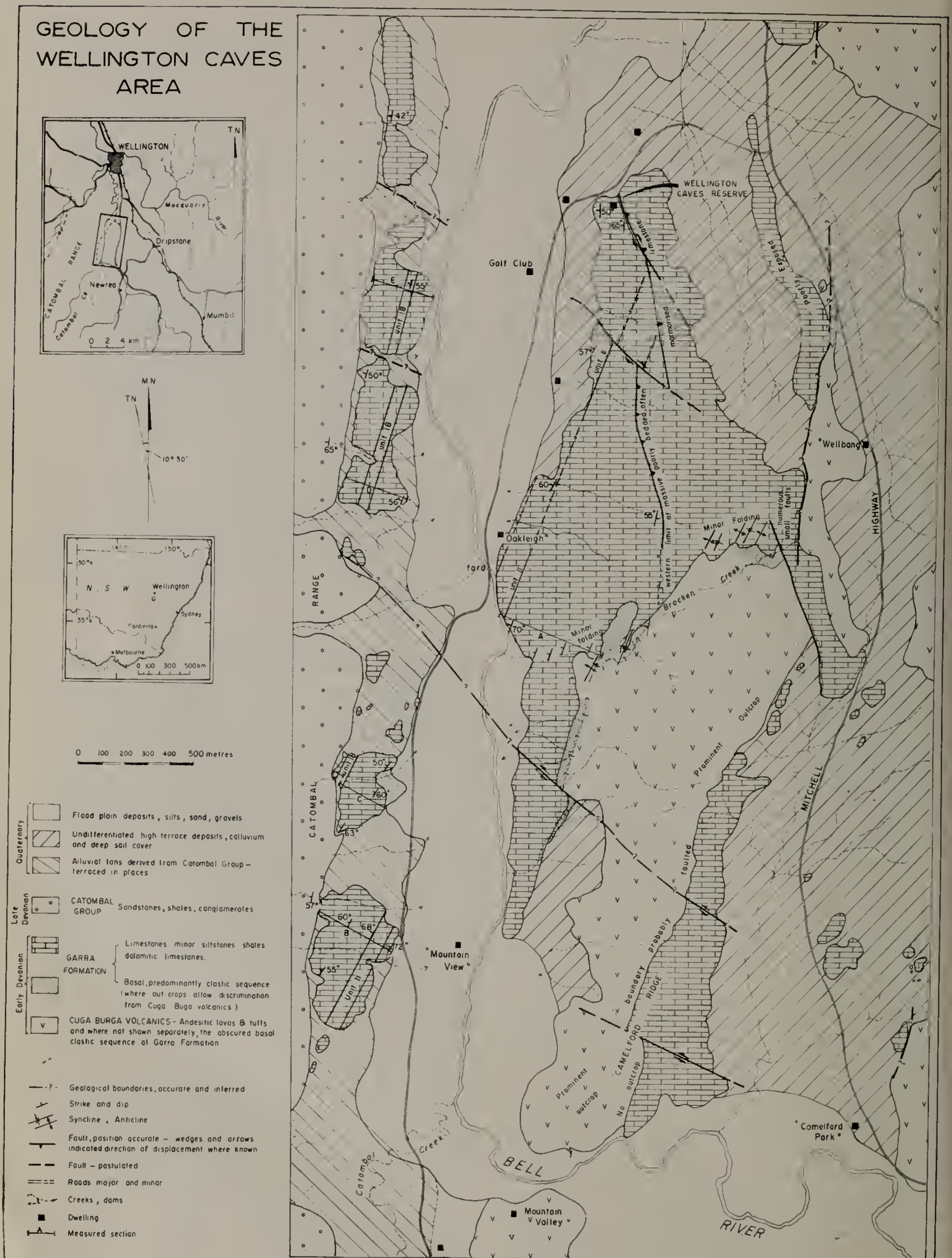
GEOLOGY OF THE WELLINGTON CAVES AREA
WELLINGTON
TN
Macquarie River
Dripstone
CATOMBAL RANGE
Newrea
Catombal Ck
Mumbil
0 2 4 km
MN
TN
10° 30'
145° 150°
30°S
N. S. W.
Wellington
Sydney
35°S
Canberra
Melbourne
0 100 300 500km
0 100 200 300 400 500 metres
Quaternary
Flood plain deposits, silts, sand, gravels
Undifferentiated high terrace deposits, colluvium and deep soil cover
Alluvial fans derived from Catombal Group - terraced in places
Late Devonian
CATOMBAL GROUP Sandstones, shales, conglomerates
Early Devonian
GARRA FORMATION
Limestones minor siltstones shales dolomitic limestones.
Basal, predominantly clastic sequence (where out-crops allow discrimination from Cuga Buga volcanics)
CUGA BURGA VOLCANICS - Andesitic lavas & tuffs and where not shown separately, the obscured basal clastic sequence of Garra Formation
Geological boundaries, accurate and inferred
Strike and dip
Syncline, Anticline
Fault, position accurate - wedges and arrows indicated direction of displacement where known
Fault - postulated
Roads major and minor
Creeks, dams
Dwelling
Measured section
WELLINGTON CAVES RESERVE
Golf Club
limestone
marmorised
poorly bedded, often
limit of massive poorly
western
unit II
unit III
unit IB
Exposed
poorly
Wellbang
HIGHWAY
MITCHELL
Oakleigh
ford
Minor folding
Minor folding
numerous small faults
Brocken Creek
Prominent outcrop
faulted
probably
boundary
CAMELFORD RIDGE
No outcrop
Prominent outcrop
CATOMBAL RANGE
Mountain View
Mountain Valley
Camelford Park
Catombal Creek
BELL RIVER
A
B
C
D
E
42°
55°
50°
65°
56°
60°
57°
70°
63°
68°
72°

FIGURE 1.

Garra Formation

The above, essentially volcanic unit (approx. 200 metres), is overlain by 30–50 metres of polymictic conglomerates, siltstones and shales, compositionally consistent with derivation from earlier erupted lavas. These sediments are best exposed in deeply weathered, discontinuous outcrops along Bracken Creek. The conglomerate has well rounded clasts, imbricated in part, in a claret coloured siltstone matrix. Alternating siltstones and shales overlie the conglomerate ; these grade into approximately 10 metres of fine silty shales with discontinuous, thin, contorted laminae of limestone and several recessive biostromes composed of abundant rugose and tabulate corals, stromatoporoids and crinoid columnals, with interstitial mudstone. The first laterally persistent limestone bed of the Garra Formation occurs approximately two metres above the highest of these biostromes.

Definition of the top of the Cuga Burga Volcanics and the base of the Garra Formation is open to variant interpretation. The cessation of vulcanism and subsequent deposition of detritus from the reworked lavas and tuffs in an apparently transgressive sequence of basal conglomerate, siltstone, shale, limestone, may be regarded as either representing the close of ' Cuga Burga ' or the commencement of ' Garra ' events ; the latter is suggested here. Formal naming of this member has been deferred pending accumulation of data over a wider area. The appearance of marine biota and the transition to a carbonate sequence indicates an important change in depositional environment ; this horizon has been used as the base for measurement of the stratigraphic column (Figure 2). As both the conglomerate and biostromes outcrop very poorly, the first laterally persistent limestone bed has been used, for the purposes of mapping (Figure 1), as an approximation to the base of the Garra Formation.

Strusz (1965*a*), in describing the Garra Formation, estimated its thickness to be between 915 and 1,200 metres, but due to sporadic outcrop, rapid facies changes, thickness variations and an apparent absence of a complete sequence at any locality, did not propose formal subdivision. It is here suggested that a complete sequence is developed in the Wellington Caves area.

Within the mapped area, five sections were measured (see locations Figure 1) ; close lithological and faunal correlation has enabled compilation of a stratigraphic column (Figure 2). This correlation demonstrates that faulting and/or folding has caused offsetting and some apparent increases in thickness between the marker horizons—Units 11 and 18 of Figure 2.

The composite section is nevertheless considered to be complete (*cf.* Strusz 1965*a*) ; there are 970 metres of carbonates in this area, but an additional 45 metres occurs in outcrops 2·5 km to the north of Section E on the west bank of the Bell River. Still younger units eroded from the area in post-Praguian, pre-Fasnian times, prior to the onset of deposition of the Catombal Group arenites, may occur elsewhere.

Within the western part of the area distinctive horizons, especially the biostromes, may be mapped and correlated with confidence and thus the sequence has been informally subdivided into 20 units based on lithological, sedimentological and faunal data.

Analysis of the nature, composition, grain size and structures of the sediments and the aspect of the autochthonous fauna has enabled the depositional environment of each unit to be inferred (Figure 3). The depositional history of the Garra Formation in this area may be summarized as follows :

1. Initial transgressive phase ; reworking of volcanics ; onset of carbonate deposition and appearance of marine biota (Units 1–2).
2. Period of fluctuating, predominantly subtidal carbonate deposition on a shallow platform ; variable terrigenous influx continues (Units 3–9).
3. Period of gradual carbonate build-up ; cessation of terrigenous influx ; quiet environment with highly diverse fauna, shallowing and decreasing in diversity towards close (Units 10–11).
4. Development of sabkha-style, tidal and desiccated supratidal flats (Units 12–17).
5. Brief subtidal episode ; quiet environment with diverse fauna (Unit 18).
6. Further development of tidal and supratidal flats (Units 19–20).
7. Cessation of deposition ; uplift and erosion.

Relationships in the eastern half of the area are difficult to determine as much of the limestone is massive and apparently marmorized ; almost all bedding, fossils and original textures have been lost. The boundary of this massive limestone may well be faulted, juxtaposing massive, structureless units characteristic of the upper part of the sequence against the well bedded lower units (e.g. in the Fault Wall of the Cathedral Cave).

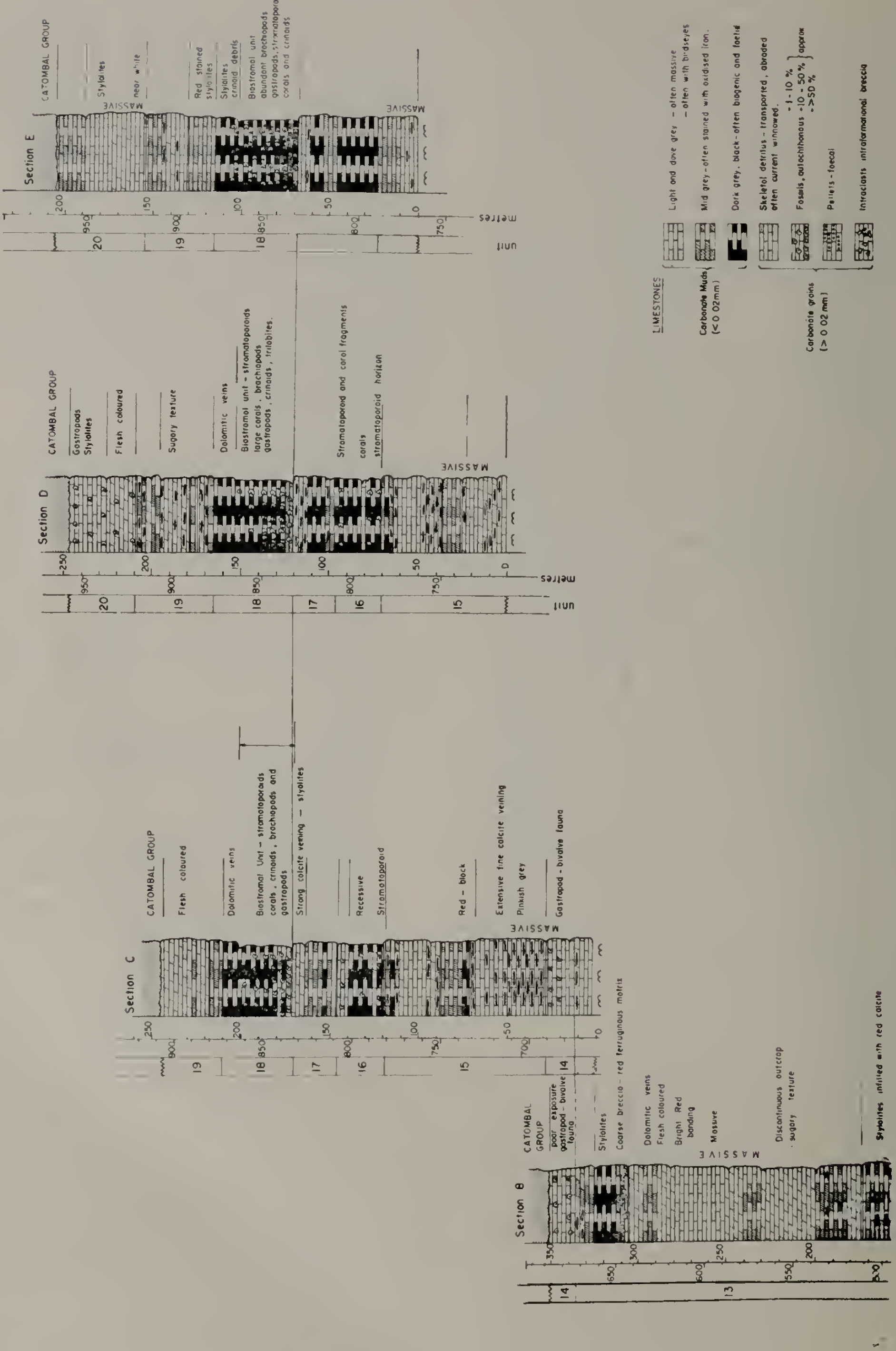
Section E
CATOMBAL GROUP
Stylolites
near white
Red stained stylolites
Stylolites crinoid debris
Biostromal unit abundant brachiopods gastropods, stromatoporoids corals and crinoids
MASSIVE
Section D
CATOMBAL GROUP
Gastropods
Stylolites
Flesh coloured
Sugary texture
Dolomitic veins
Biostromal unit - stromatoporoids large corals, brachiopods gastropods, crinoids, trilobites.
Stromatoporoid and coral fragments
corals
stromatoporoid horizon
Section C
CATOMBAL GROUP
Flesh coloured
Dolomitic veins
Biostromal Unit - stromatoporoids corals, crinoids, brachiopods and gastropods
Strong calcite veining - stylolites
Recessive
Stromatoporoid
Red - block
Extensive fine calcite veining
Pinkish grey
Gastropod - bivalve fauna
Section B
CATOMBAL GROUP
poor exposure gastropod - bivalve fauna
Stylolites
Coarse breccia - red ferruginous matrix
Dolomitic veins
Flesh coloured
Bright Red banding
Massive
Discontinuous outcrop
sugary texture
Stylolites infilled with red calcite
metres
unit
LIMESTONES
Carbonate Muds (< 0 02mm)
Light and dove grey - often massive - often with birdseyes
Mid grey - often stained with oxidised iron.
Dark grey, black - often biogenic and foetid
Carbonate grains (> 0 02 mm)
Skeletal detritus - transported, abraded often current winnowed.
Fossils, autochthonous - 1 - 10 % - 10 - 50 % - > 50 % approx
Pellets - faecal
Intraclasts intraformational breccia

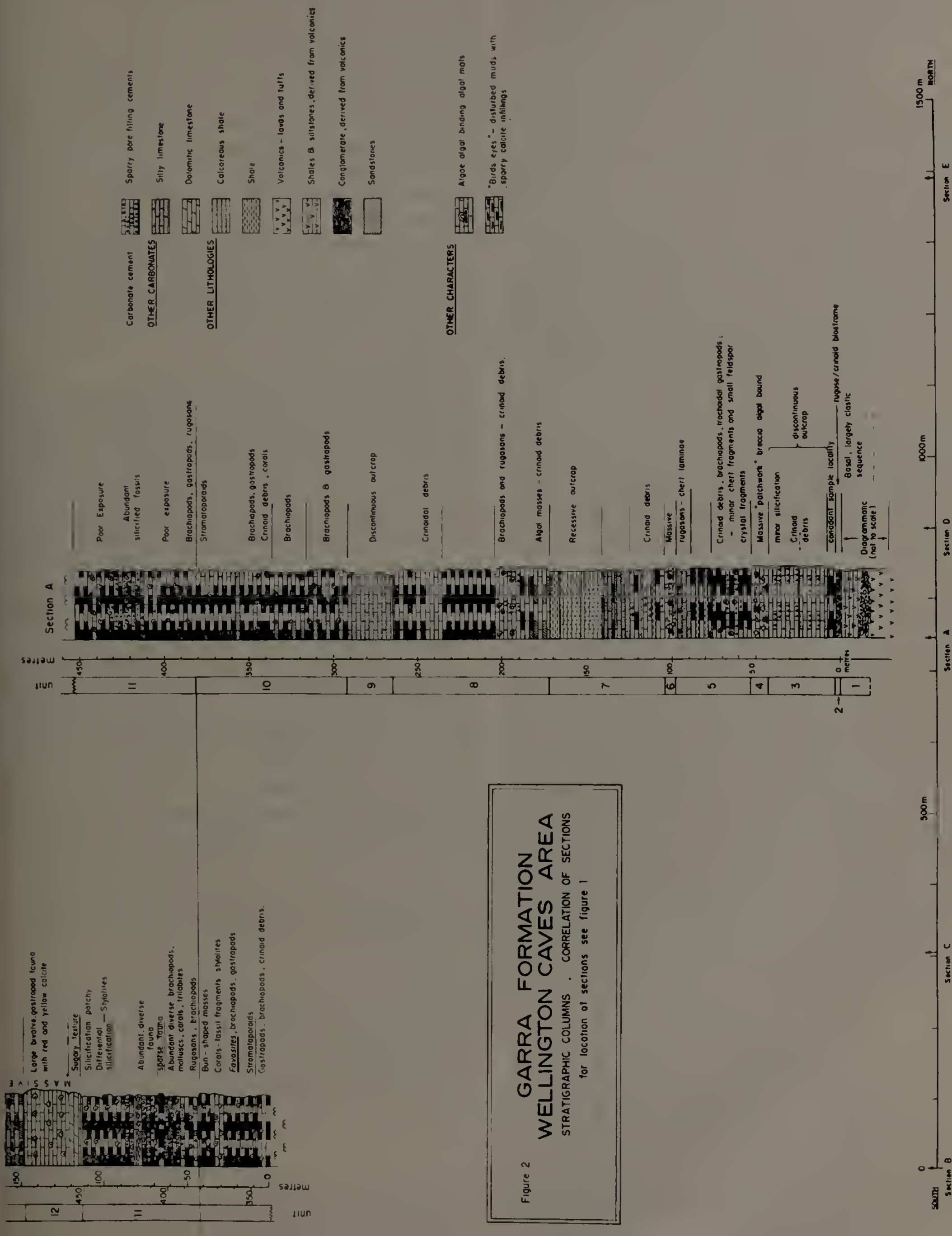
Figure 2
GARRA FORMATION
WELLINGTON CAVES AREA
STRATIGRAPHIC COLUMNS . CORRELATION OF SECTIONS
for location of sections see figure 1
Section A
unit
metres
Carbonate cement
Sparry pore filling cements
OTHER CARBONATES
Silty limestone
Dolomitic limestone
OTHER LITHOLOGIES
Calcareous shale
Shale
Volcanics - lavas and tuffs
Shales & siltstones, derived from volcanics
Conglomerate, derived from volcanics
Sandstones
OTHER CHARACTERS
Algae algal binding algal mats
"Birds eyes" - disturbed muds with sparry calcite infillings
Poor Exposure
Abundant silicified fossils
Poor exposure
Brachiopods, gastropods, rugosans
Stromatoporoids
Brachiopods, gastropods
Crinoid debris, corals
Brachiopods
Brachiopods & gastropods
Discontinuous outcrop
Crinoidal debris
Brachiopods and rugosans - crinoid debris.
Algal masses - crinoid debris
Recessive outcrop
Crinoid debris
Massive
rugosans - chert laminae
Crinoid debris, brachiopods, trochoidal gastropods, - minor chert fragments and small feldspar crystal fragments
Massive "patchwork" breccia algal bound
minor silicification
Crinoid debris
discontinuous outcrop
conodont sample locality
rugose/crinoid biostrome
Basal, largely clastic sequence
Diagrammatic (not to scale)
Large bivalve, gastropod fauna with red and yellow calcite
Sugary texture
Silicification patchy
Differential silicification — Stylolites
Abundant, diverse fauna
sparse fauna
Abundant diverse brachiopods, molluscs, corals, trilobites
Rugosans, brachiopods
Bun-shaped masses
Corals - fossil fragments stylolites
Favosites, brachiopods, gastropods
Stromatoporoids
Gastropods, brachiopods, crinoid debris.
12
11
10
9
8
7
6
5
4
3
2
1
0
50
100
150
200
250
300
350
400
450
0
500 m
1000 m
1500 m
SOUTH
NORTH
Section B
Section C
Section A
Section D
Section E

FIGURE 2.

Limestones along the eastern flank of ' Camelford Ridge ' are marmorized and dolomitized but retain some of their primary character. The outcrops to the volcanics in the south are rich in rugosans and crinoid debris, set in a red ferruginous calcite matrix ; these horizons may be equivalent to the lowest units exposed in Bracken Creek. Creamy dolomitic limestones with abundant rugose and tabulate corals occur in the north of this block. Breccias of limestone fragments in bright orange and red ' terra rossa ' are common.

Limestone outcropping immediately beside and to the east of the Mitchell Highway have been completely recrystallized and heavily veined with black and white calcite.

Age of the Garra Formation

Correlation with northern hemisphere Early Devonian sequences has been somewhat problematic (Strusz, 1967*a*). Druce (1970), on the basis of conodonts considered the Garra Formation to be Middle Siegenian in its lower part. Combining this information with information from corals and brachiopods, Strusz (in Strusz *et al.*, 1972) considers the Garra Formation as extending from the latest Lochkovian or earliest Praguian at the base, through Praguian, probably into Zlichovian.

Additional support for the late Lochkovian—early Praguian age of horizons low in the Garra Formation comes from a conodont fauna from the lowest bed of Unit 3 in Bracken Creek (base of Section A, Figure 2). The forms have been kindly identified by Dr. G. C. O. Bischoff as : *Belodella* sp, *Hindeodella priscilla*, H. *equidentata*, *Icriodus pesavis*, *Lonchodina detorta*, *L. cristagalli*, *L. greilingi*, *Neoprioniodus bicurvatus*, *N. excavatus*, *N.* cf. *multiformis*, *Ozarkodina typica*, *O. denckmanni*, *O. media*, *Paltodus* sp., *Plectospathodus flexuosus*, *P. extensus*, *Spathagnathodus remcheidensis*, *S. inclinatus wurmi*, *S.* aff. *asymmetricus*, *Trichonodella excavata*. (Slide No. MU 7277). Dr. Bischoff considers the age to be late Lochkovian-early Praguian.

A conodont fauna from Unit 11, 410 metres above the base of the sequence (70 metres above the base of Section B, Figure 2) includes the forms : *Icriodus pesavis*, *Ozarkodina denckmanni*,

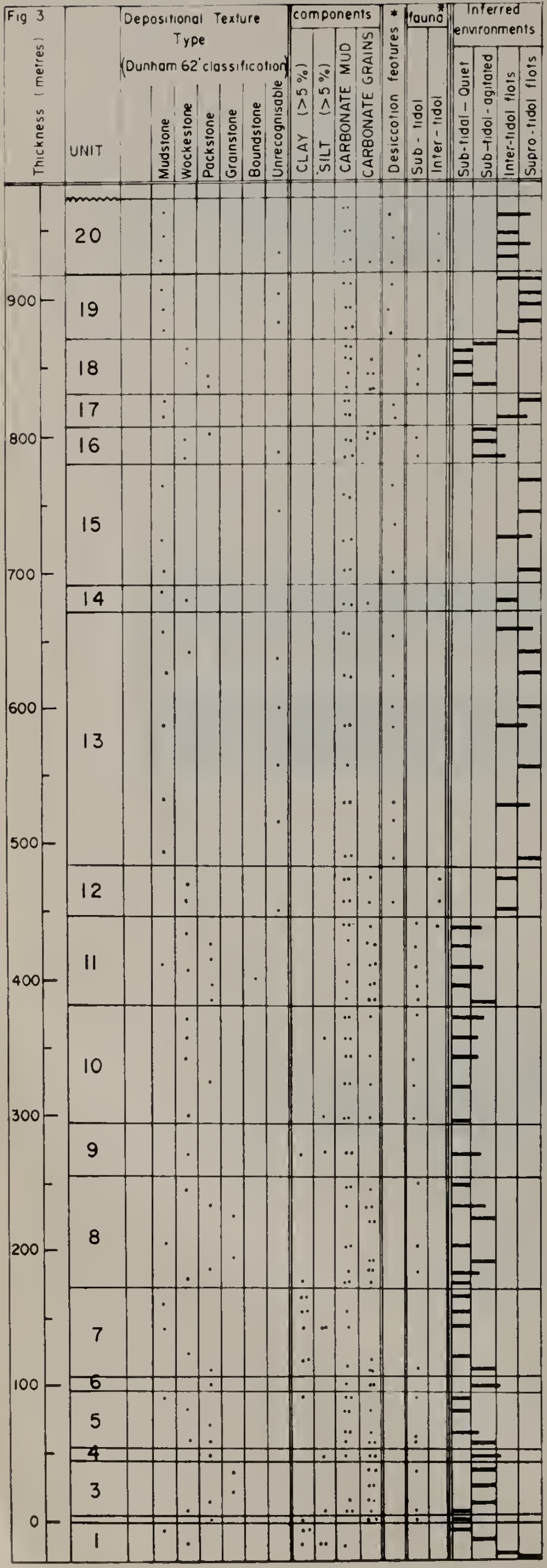

FIGURE 3.

(*a*) Dessication features :—' bird's eyes ', mud cracks, algal mats, vadose silts ; for distribution of dolomites see Figure 2.

(*b*) Discrimination of faunal aspect based on the generalization that brachiopods, corals, bryozoans, crinoids, stromatoporoids were unable to survive subaerial desiccation in the intertidal zone.

Spathagnathodus exiguus philipi, *S. optimus*, *S. sulcatus*. (Slide No. MU 7278). Dr. Bischoff considers the age of this fauna to be early Praguian. Interestingly, the fauna includes *Spathagnathodus sulcatus* and *Icriodus pesavis*, shown by Savage (1973*a*, *b*) as having mutually exclusive ranges.

Units higher than Unit 11 have so far failed to yield conodonts in the mapped area though conodonts are abundant in samples from roadside outcrops of dark grey, highly fossiliferous limestones underlain and overlain by light grey massive algal limestones on the Mitchell Highway 19 km NNE of Wellington (the fauna and lithological sequence suggest probable correlation with Unit 18). *Spathagnathodus exiguus philipi*, *S. optimus*, *Ozarkodina denckmanni*, *O. typica australis*, *Plectospathodus extensus* are prominent (Slide No. MU 7279) but in spite of quite high yields *S. sulcatus* and definitive younger forms such as *S. exiguus exiguus* or species of *Polygnathus* were not obtained.

On the similarity of the conodont faunas and regional relationships, I suggest correlation of the basal Garra Formation with the basal limestones of the Mandagery Park Formation (Savage, 1968, 1973*a*, *b*) ; the latter is interpreted as a tongue of Garra extending out into the Cowra Trough.

According to my analysis, previously listed coral, conodont and brachiopod faunas from the Wellington area have come from the following horizons :

Strusz, (1965*b*, 1966, 1970) rugose corals, Localities Cr 103, 106, BR^3/200, BR^3/214, = Unit 11. Localities Cr 100, 94, 89, 111, 113, BR^1/177 = Unit 18.

Also assignable to this unit are localities Cr 1, 2, and 77, just outside the mapped area.

Druce, (1970) conodonts, Locality WC5 = Unit 10.

Strusz, (in Strusz *et al.*, 1972) Brachiopods Locality Wellington Golf Course = Unit 10, 11

Unpublished details of Dr. Strusz's sections are given in his Ph.D. thesis (Strusz, 1963), (his BR^3 = Section B, BR^2 = Section D, BR^1 = Section E).

Catombal Group

The lowest units of the Catombal Group in the area are red to white, medium grained sandstones (orthoquartzites) of the Brymedura Sandstone (Conolly, 1963). There is a marked angular discordance of strike between the Garra limestones and Catombal clastics in the south of the area, the angle of discordance gradually decreasing northwards.

There is no evidence of Middle Devonian sedimentation, either in the Wellington area or for that matter in central N.S.W. (Pickett, 1972).

Structure

The broad structure appears to be a much faulted, north-plunging anticline. The western limb of the antiform is well preserved in uniformly dipping, well bedded limestones. The boundary of the marmorized limestones angularly transgresses the strike of the well bedded limestones and may be a fault. Many of the boundaries between volcanics and limestone could be faulted but this cannot be determined with certainty due to poor outcrops ; an unfaulted boundary nevertheless occurs in Bracken Creek.

Small tight minor folds are common in the basal limestone units (i.e. near the Cuga Burga Volcanics) but are absent from the remainder of the sequence. Evidence of faulting has been inferred from the measured sections more often than from direct field observation. Faulting prior to deposition of the Catombal Group produced a number of fault slices causing offsetting ; either faulting or undetected folding has increased the apparent thicknesses (Figure 1) between the distinctive biostromes and in addition has resulted in minor discordances in strike direction between sequences in the blocks.

The difference in orientation between basal sediments of the Catombal Group and the Garra Formation indicates that in this area the Garra Formation was dipping at about 15° north-easterly when deposition of the Catombal Group commenced ; this is evidence for mild tectonism and erosion having occurred during the Middle Devonian. Following the cessation of deposition of the Catombal Group, the region underwent major deformation, presumably during the Carboniferous.

Acknowledgements

I am indebted to Dr. John A. Talent for supervision of the project and to him and Dr. D. L. Strusz and Dr. C. McA. Powell for criticism of the manuscript ; to Dr. G. C. O. Bischoff for identifying and dating the conodont faunas, and to Mr. Dean Oliver for drafting the diagrams under the supervision of Mr. Rod Bashford.

Addendum

The stratigraphic position of limestones along the eastern flank of Camelford Ridge is currently under review; conodonts recently discovered indicate a pre-Garra age. A paper discussing these findings and their significance is in preparation.

References

ADRIAN, J., 1971. Stratigraphic Units in the Molong District, New South Wales. *Rec. Geol. Surv. N.S.W.*, **13** (4), 179.

CONOLLY, J. R., 1963. Upper Devonian Stratigraphy and Sedimentation in the Wellington-Molong District, N.S.W. *J. Proc. Roy. Soc. N.S.W.*, **96**, 73.

DRUCE, E. C., 1970. Conodonts of the Garra Formation (Lower Devonian), N.S.W. *Bull. Bur. Min. Res., Geol. Geophys.*, **116**, 29.

KLAPPER, G., 1969. Lower Devonian Conodont Sequence, Royal Creek, Yukon Territory, and Devon Island, Canada. *J. Paleontology*, **43**, 1.

OFFENBURG, A. C., ROSE, D. M., PACKHAM, G. H., 1968. 1 : 250,000 Geological Series, Sheet SI–55–4 Dubbo, N.S.W. *Geol. Surv. N.S.W.*

PICKETT, J. W., 1972. Correlation of the Middle Devonian Formations of Australia. *J. Geol. Soc. Aust.*, **18**, 457.

ROBERTS, J., *et al.*, 1972. Correlation of the Upper Devonian Rocks of Australia. *J. Geol. Soc. Aust.*, **18**, 467.

SAVAGE, N. M., 1968. The Geology of the Manildra District, N.S.W. *J. Proc. Roy. Soc. N.S.W.*, **101**, 159.

————, 1973*a*. Lower Devonian Conodonts from New South Wales. *Palaeontology*, **16**, 307.

————, 1973*b*. Lower Devonian Biostratigraphic Correlation in Eastern Australia and Western North America. *Lethaia*, **5**, 341.

STRUSZ, D. L., 1960. The Geology of the Parish of Mumbil, near Wellington, N.S.W. *J. Proc. Roy. Soc. N.S.W.*, **93**, 127.

————, 1963. Studies in the Palaeontology, Petrography and Stratigraphy of the Garra Beds. Unpubl. Ph.D. thesis, University of Sydney.

————, 1965*a*. A Note on the Stratigraphy of the Devonian Garra Beds of N.S.W. *J. Proc. Roy. Soc. N.S.W.*, **98**, 85.

————, 1965*b*. Disphyllidae and Phacellophyllidae from the Devonian Garra Formation of N.S.W. *Palaeontology*, **8**, 518.

————, 1966. Spongophyllidae from the Devonian Garra Formation of N.S.W. *Palaeontology*, **9**, 544.

————, 1967*a*. Lower and Middle Devonian of the Molong Geanticline, N.S.W., Australia. In: Oswald, D. H., (ed.). *International Symposium on the Devonian System*. Vol. 2, 123. Alberta Society of Petroleum Geologists, Calgary, Canada.

————, 1967*b*. *Chlamydophyllum, Iowaphyllum* and *Sinospongophyllum* (Rugosa) from the Devonian of N.S.W. *Palaeontology*, **10**, 426.

————, *et al.*, 1972. Correlation of the Lower Devonian Rocks of Australia. *J. Geol. Soc. Aust.*, **18**, 427.

————, and JELL, J. S., 1970. *Cyathophyllum* (*Radiophyllum*) from the Devonian of Eastern Australia. *Bull. Bur. Min. Resour. Geol. Geophys. Aust.*, **116**, (*Palaeont. Pap.* 1968), 119.

School of Earth Sciences,
Macquarie University,
North Ryde, N.S.W., 2113.

(Received 15.1.75)

Journal and Proceedings, Royal Society of New South Wales, Vol. 108, pp. 119–130, 1975

Hydrothermal Ca-Al Silicates in Ophiolitic Rocks Near Coolac, N.S.W.

H. G. Golding and A. S. Ray

Abstract—The modes of occurrence and diagnostic properties of hydrothermal grossular, chrome grossular, vesuvianite, prehnite and monoclinic and orthorhombic epidote minerals, from Coolac ophiolites are described. The Fe content of the prehnite and chemical analyses of zoisite concentrates, are reported. Differential thermograms of the Coolac vesuvianite and prehnite differ from those of the same minerals from other geologic environments. A distinctive habit of zoisite is recorded. Most of the observed garnet and vesuvianite occur in rodingitic enclosures within serpentinized peridotite. The prehnite and most of the zoisite occur in segregations at junctions of ultramafic with other rocks. The formation of these minerals may partly pre-date emplacement of the ophiolites at a continent margin. Additionally, the mineral sequence : epidote→clinozoisite→ orthorhombic epidote group minerals→grossular and/or vesuvianite apparently registers increasing stratigraphic depth in the mafic part of the ophiolite suite and may indicate sub-sea-floor metamorphism.

Introduction

Occurrences of hydrothermal garnet, vesuvianite, prehnite and minerals of the epidote group in the Coolac ultramafic belt were briefly noted by Golding (1969, 1971). The purpose of this paper is to record new data on these minerals from occurrences in the Mt. Lightning–Mooney Mooney Range sector of the belt. A sheet of serpentinized harzburgite dips steeply eastward throughout the sector. In the Mooney Mooney Range the harzburgite is flanked on the west by successive masses of pyroxenitic, gabbroic and basaltic rocks or by mafic rocks and serpentinite. Brown (1973) additionally delineated a zone of predominant keratophyre (Figure 1). The authors regard this rock succession as an ophiolite sequence in which the harzburgitic member forms the stratigraphic base. The distribution of the hydrothermal minerals with respect to this proposed sequence is considered.

The minerals under review commonly occur as fine-grained aggregates in which, although one phase may predominate, several phases are intimately admixed and some are poorly crystallized. These features hamper optical study and the preparation of material for chemical analyses, and in some instances result in broad X-ray reflections. The application of combined techniques, however, yields diagnostic data. Field work was shared by both authors. The senior author (H.G.G.) is responsible for most of the petrography, the second author (A.S.R.) for the X-ray and chemical analyses except where otherwise acknowledged.

Modes of Occurrence

The investigated minerals tend to occur in specific sub-environments as follows :

Gp. 1 rodingites : Tabular bodies, 1–15 m long and <1 m wide, with characteristic jointing (Plate I, A) completely enclosed within serpentinite or partly serpentinized harzburgite along North and Central Mooney Ridges (Figure 1) and at Mt. Lightning (Figure 2). The constituents are garnet and/or vesuvianite + chlorite ± diopside ± minor tremolite. Relict undeformed microtextures indicate a gabbroic or doleritic precursor for some examples, but are commonly lacking. Garnetite and vesuvianite rock are essentially monomineral variants of the group.

Gp. 2 rodingites : Diverse rocks, including segregations of zoisite and of prehnite up to 1 m wide, at junctions of serpentinized harzburgite and variolitic spilite at Haystack Creek, Mt. Lightning (Figure 2). Associated rocks include gneissic garnet-chlorite rock, trondhjemite, albitite and tremolite rock.

Northern zoisitites : Apparently independent masses of zoisite-rich rock encountered as blocks, 10–20 cm wide, and similar material completely replacing feldspars, 3–4 cm wide, in gabbro pegmatite. Both occur at or close to the junction of clinopyroxenite and gabbro at North Mooney Ridge (Figure 1).

Easterly reaction selvedges : Sporadic tabular masses, ~50 cm wide, of prehnite ± garnet at junctions of harzburgite and granodiorite along South Mooney Ridge (Figure 1).

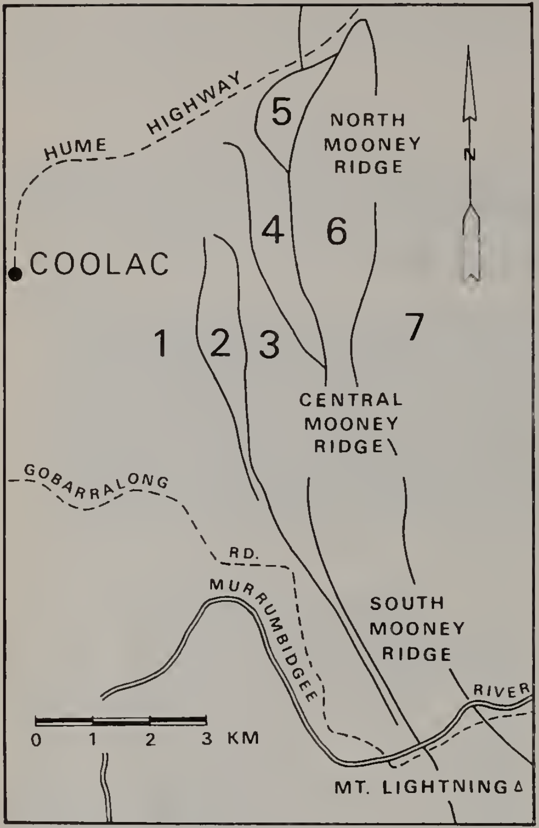

FIGURE 1.—Sketch map of the north of the Coolac ultramafic belt showing principal lithologic subdivisions.

1 : Silurian volcanic and sedimentary rocks.
2 : Keratophyres.
3 : Basalts and metabasalts with some serpentinite.
4 : Gabbros and metagabbros.
5 : Clinopyroxenite and wehlite.
6 : Harzburgite and serpentinite.
7 : Silurian granodiorite.

Veinlets in ultramafic rocks : Mainly of Gp. 1 rodingite, garnet or vesuvianite, in chromitite, at Mt. Lightning.

Other sub-environments : Keratophyres, metabasites and associated epidosite veins flanking harzburgite in the Mooney Mooney Range (Figure 1) and at Mt. Lightning (Figure 2) and sporadic lenses of albitite and trondhjemite in harzburgite or serpentinite. The hydrothermal Ca-Al silicates are principally members of the epidote group. Micro-veinlets of prehnite additionally occur in some albitite.

Garnet

Garnet-rich portions of Gp. 1 rodingites, and garnetites (70 to 95% garnet), are finely granular to dense, and white or pale grey in hand specimens. Thin sections reveal aggregates of moderately clear, colourless, polygonal grains, 0·1 to 0·3 mm wide, which are optically isotropic, or more commonly, pale brown turbid aggregates in which the grain boundaries are indistinct. In the turbid material isotropism is modified by milky internal reflections due to dispersed impurities. Garnet euhedra are uncommon but the crystal form is expressed against chlorite. In gneissic Gp. 2 rodingites, augen of granular garnet are aligned within a matrix of chlorite. Much Coolac garnet appears to have crystallized from a paste. This is inferred from the dispersed impurities, turbid cores to numerous grains, variable crystallinity, relict colloform texture (Plate I, B) and (?) dehydration pores lined with chlorite Plate I, C).

Chrome garnet, emerald green in thin section, is associated with chlorite in veinlets penetrating chromite. The grains are commonly zoned (Plate II, A). In some grains there is a chromite core, a median zone of green isotropic garnet and a rim of pale pink, anisotropic garnet. Wider veins of colourless garnet in chromite display a selvedge of green garnet at contacts with chromite.

The terminology for garnets used in this paper follows Deer *et al.* (1962*a*). These and other authors have recorded hydrogrossular as a constituent of rodingite. Hydrogrossular, a member of the series $3CaO.Al_2O_3.3SiO_2$–$3CaO.Al_2O_3.6H_2O$, exhibits decreasing refractive index and increasing cell size with increasing substitution of Si by 4H. Provided that no significant substitution of Ca^{2+} by Fe^{2+}, Mg^{2+} or Mn^{2+} or of Al^{3+} by Fe^{3+} has occurred the position of a garnet in the series may be estimated from the curves of Hutton (1943) and Yoder (1950). On this basis data obtained from very small sub-samples of clear Coolac garnet (Samples 3, 5, 6, 7 ; Table 1) suggest a composition close to that of anhydrous grossular but the material tested may not be representative. Dispersed impurity, approaching vesuvianite in composition, may be responsible for the low-index material (Zabinsky, 1964) in Samples 2, 4 and 5 (Table 1).

Differential thermal curves of Coolac garnetites containing <10% of chlorite or vesuvianite lack peaks (Figure 3). Thermograms of strongly hydrous grossulars are reported to show endothermic peaks at 650–690°C and exothermic peaks at 870° and 940°C (Deer *et al.*, 1962*a*). A moderately hydrous grossular from South Africa exhibits an endothermic reaction at ∼1100°C but the

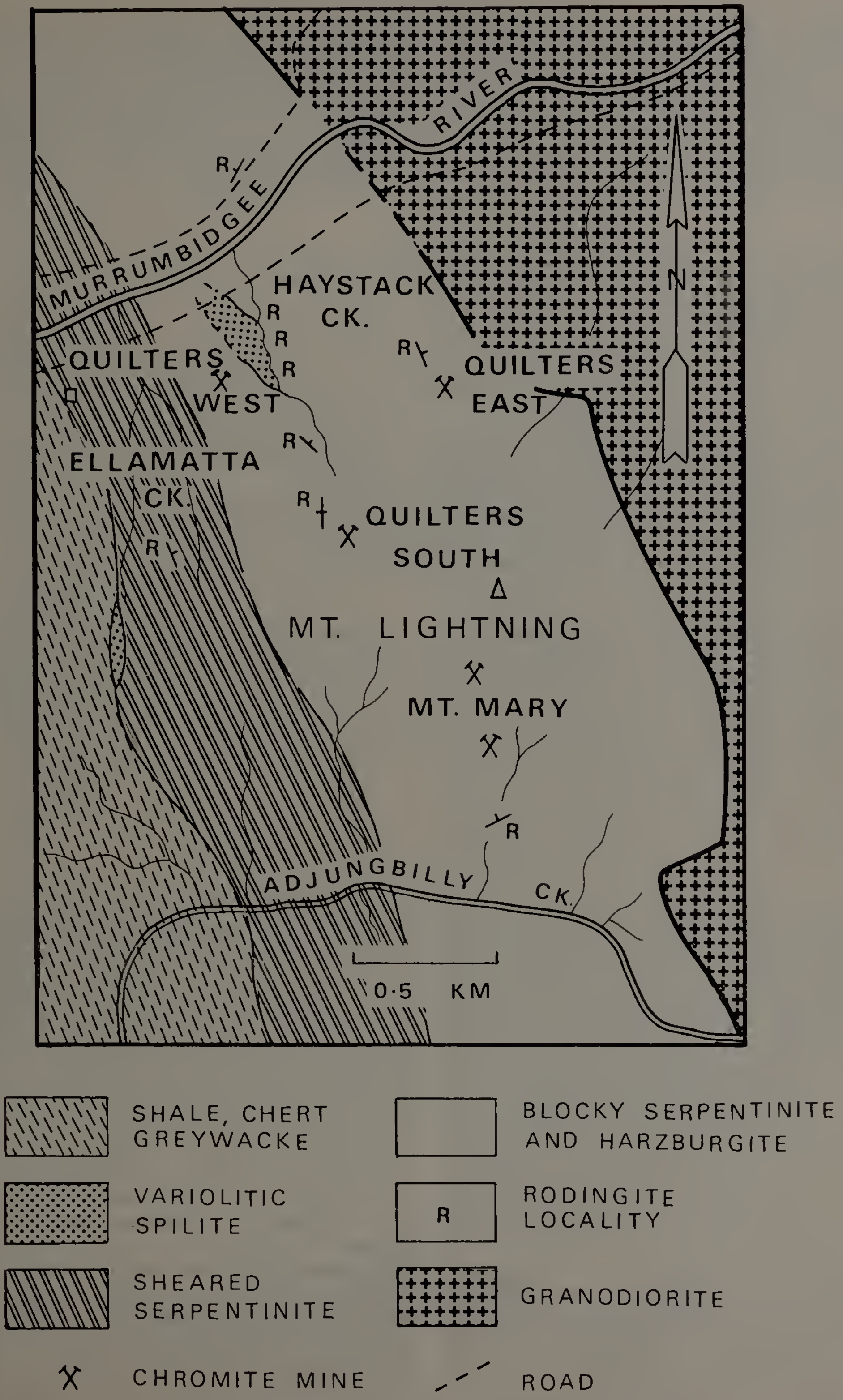

Figure 2.—Geological sketch map of Mt. Lightning.

curve begins to descend at ~1080°C (Frankel, 1959). There is no indication of this reaction in the low index Coolac material (Sample 2). These data tend to confirm the view that the non-chromiferous Coolac garnets are variably crystallized, impure grossulars and/or only slightly hydrous grossulars.

colours but in some specimens shows normal low first order polarization colours. In some specimens the mineral is uniaxial, in others it is biaxial. Lamellar twins and patchy zoning are common. In rare veinlets the vesuvianite crystals are 1 mm wide and enclose garnet crystals 0·1 mm wide.

TABLE 1

Data on Garnets from Mt. Lightning.

Sample	Location	Host Material	n ±0·002	a Å ±0·005
1	Quilters East	White Gp. 1 garnetite (D=3·37). Garnet (90%)+chlorite	1·734	—
2	Quilters East	White chert-like patches (D=3·39) of dense, impure garnet in rodingite-serpentine breccia	1·693–1·700	—
3	Above Haystack Creek	Pink and green Gp. 1 rodingite. Garnet (60%), vesuvianite (20%)+diopside	1·733	11·855
4	Haystack Creek	Mottled grey and cream Gp. 2 rodingite. Garnet (85%), zoisite (10%)+sphene	1·723–1·726	11·860
5	Haystack Creek	Pink and grey gneissic Gp. 2 rodingite. Garnet (60%), chlorite (20%)+zoisite	1·734 (clear) + 1·699 (turbid)	11·862
6	East Ellamatta Creek	Pinkish-white Gp. 1 garnetite. Garnet (90%)+chlorite	1·732–1·733	11·853 11·849
7	East Ellamatta Creek	As Sample 6. Garnetite with relict colloform texture	1·730 1·729 1·732	11·856 11·851 11·854
8	Quilters West	Veinlets of zoned garnet+chlorite in chromite	*1·82 (green) 1·79 (pink)	— —

* ±0·01.

Vesuvianite

Vesuvianite commonly forms patches, streaks and veinlets surrounded by grossular and chlorite. The ratio of vesuvianite to grossular increases toward the centres of some Gp. 1 rodingite bodies. In other Gp. 1 rodingite bodies vesuvianite occurs to the exclusion of grossular. Some vesuvianite-rich rodingites (up to 95% vesuvianite) are megascopically pink and finely saccharoidal, others are brownish grey, brittle rocks with greasy lustre and conchoidal fracture. The pink variety is common in chromite-rodingite breccia. Megascopically pale green vesuvianite forms rare veinlets in some chromitite.

Thin sections of vesuvianite-rich rodingite reveal aggregates of polygonal and rectangular grains. The grains, up to 0·5 mm wide, are euhedral against chlorite and less turbid than most grossular. The vesuvianite commonly shows anomalous yellow and brown polarization

The refractive indices, cell sizes and D.T.A. data for selected examples of Coolac vesuvianite have been compared (Table 2) with samples collected by one of the authors (H.G.G.) from other ophiolite environments. According to Tröger (1956) $\omega<1{\cdot}720$ indicates $<5\%$ $TiO_2+Fe_2O_3+FeO$ but data in Deer *et al.* (1962*a*) show some departures from this rule. Maximum indices of Coolac vesuvianites do not exceed 1·717, but vesuvianites from Chrome Hill, Nundle and Radusa, Macedonia (Table 2) register higher indices, and a value of 1·729 was recorded by Miles (1950) for vesuvianite from Eulaminna, Western Australia. The extensive possibilities for ionic substitution in vesuvianites (Ito and Arem, 1970) preclude simple correlations between optics, cell dimensions and compositions for the group as a whole. There is a suggestion (Table 2), however, that the higher index vesuvianites from Chrome Hill and Radusa have the smaller cell dimensions.

Differential thermograms of the Coolac vesuvianites show a characteristic endothermic peak at ~1050°C. Continued heating gives an exothermic peak at ~1090°C (Figure 3). According to Peters (1961) the first reaction registers lattice disruption and dehydration, the second reaction registers recrystallization to garnet, melilite and doubtful anorthite. The thermal behaviour of the Coolac samples accords with that of vesuvianite from the Totalp-Serpentinmasse, near Davos, Switzerland (Peters, *ibid.*). The Chrome Hill and Radusa material react at slightly lower temperatures possibly due to the presence of admixed phases. Brown vesuvianite from a contact metamorphic aureole near Marulan, N.S.W., tested for comparison, and vesuvianite from Vesuvius (Peters, *ibid.*), exhibit distinctly lower temperature endothermic reactions (Figure 3). The low refringence and the refractory thermal behaviour of the ophiolitic vesuvianite, particularly the Coolac samples, may indicate a relative deficiency of Fe and Ti, volatiles or other constituents.

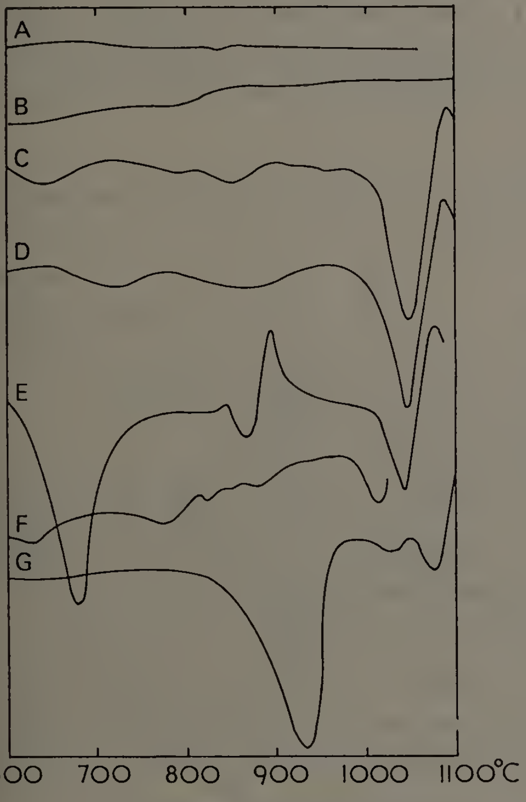

FIGURE 3.—Differential thermograms (600–1,100°) of garnetiferous and vesuvianite-rich materials.

A : Garnetite (Sample 6, Table 1).
B : Chert-like garnetite (Sample 2, Table 1).
C : Vesuvianite rock (Sample 1, Table 2).
D : Vesuvianite-rich rodingite (Sample 2, Table 2).
E : Gp. 1 rodingite containing grossular, vesuvianite, chlorite and pyroxene, Ellamatta Creek, Mt. Lightning.
F : Vesuvianite-bearing vein material, Radusa (Sample 8, Table 2).
G : Brown vesuvianite from calc-silicate rock, near Marulan, N.S.W.

Patches of vesuvianite in a matrix of grossular may indicate compositional variations from domain to domain in the original rocks. Veinlets of vesuvianite, and vesuvianite-rich centres of rodingite bodies, possibly delineate the passage of late magmatic fluids.

Prehnite

Prehnite is a minor constituent of the northern zoisitites but forms prehnitites (70 to >95% prehnite) at Haystack Creek and at peridotite-granodiorite contacts. The prehnitites are of medium grain size (0·5–2·0 mm) but appear to be porcellanous in hand specimens. Most are white and massive, but grey bands of chlorite+sphene occur in some samples and grey or cream-coloured zoisitic patches occur in others. Interstitial prehnite in the northern zoisitites is pellucid but most prehnite is slightly turbid. Euhedra are absent. Grain aggregates exhibit diverse textures which include radiating, banded columnar, polygonal granular (? columns viewed transversely) and sutured (Plate II, B). The grains show two cleavages, normal second order polarization colours and pronounced undulose or mosaic extinction.

Coleman (1961) noted that the distinction of fine-grained prehnite and pectolite may be uncertain if based solely on refractive indices and strong X-ray reflections. The relatively coarse-grained textures of the Coolac prehnitites and other prehnite-bearing rocks, however, are usually diagnostic and optical and X-ray powder determinations have been confirmed by D.T.A. and a partial chemical analysis of one of the Haystack Creek prehnitites. The latter, estimated to contain <5% impurities (zoisite, chlorite and sphene), was analysed by Dr. P. Bayliss, using atomic absorption spectroscopy and gave the following wt% values : SiO_2 : 44·0, Al_2O_3 : 23·5, CaO : 24·7 and H_2O : 4·6 (Sub-total : 96·8%).

The D.T.A. of the Coolac prehnite accords with that reported for prehnite by McLaughlin (1957). The curve shows double endothermic peaks corresponding to dehydration in two stages at ~780° and ~870°±20°C (Figure 4) and is usually diagnostic despite considerable variation in the position and intensity of the two peaks depending mainly on the amounts and kinds of other phases present. The presence of substantial chlorite, however, is confusing. In view of the occurrence of prehnite and zoisite in various proportions in chlorite-poor Gp. 2 rodingites at Haystack Creek, reference curves for artificially prepared mixtures of the two minerals in the proportions 3 : 1, 1 : 1 and 1 : 3 have been compared (Figure 4). A thermogram of deuteric prehnite from the Prospect alkali dolerite intrusion near Sydney, obtained for comparison, differs notably from that of the Coolac prehnite but accords with that reported for prehnite elsewhere by Norin (see Deer *et al.*, 1962*b*). The two patterns of thermal behaviour may indicate two structural varieties of the mineral.

TABLE 2

Data on Vesuvianite from the Mooney Mooney Range (Samples 1, 2), Mt. Lightning (Samples 3–6) and from Other Ophiolites Samples 7, 8).

Sample	Locality	Host Material	D.T.A. C	n ±0·002	Cell Edge Å a±0·005 c±0·01
1	North Mooney Ridge	Pink vesuvianite rock in chromite-rodingite breccia	*En 1050 Ex 1090	ε 1·712 ω 1·715	—
2	Central Mooney Ridge	Grey Gp. 1 rodingite containing 80% vesuvianite which shows normal polarization colours	En 1050 Ex 1090	—	—
3	Quilters South	Brownish grey, Gp. 1 rodingite containing 95% vesuvianite which is biaxial	En 1050 Ex 1085	min 1·710 max 1·716	15·595 11·80
4	Upper Haystack Creek	Vein of vesuvianite in garnetized dolerite	En > 1030	—	15·602 11·85
5	Ellamatta Creek	Centre of Gp. 1 rodingite. Vesuvianite (30%), grossular (30%) +chlorite+diopside	Chlorite peaks+ En 1041 Ex 1075	—	—
6	Quilters East	Vein of green biaxial vesuvianite in chromite	—	min 1·713 max 1·717	15·590 11·84
7	Chrome Hill, Nundle	Vein of green vesuvianite+grossular in serpentinite	En > 1020	max 1·720	15·570 11·84
8	Radusa, Macedonia	Vein of green vesuvianite+diopside+grossular in rodingite	En > 1015	max 1·721	15·583 11·84

* En : Endothermic peak. Ex : Exothermic peak.

Prehnite is regarded as a solid solution of ideal aluminian and ferrian end-members: $Ca_2Al_2Si_3O_{10}(OH)_2$ and $Ca_2Fe_2^{3+}Si_3O_{10}(OH)_2$ respectively. The refractive indices increase with increasing substitution of Fe^{3+} for Al^{3+} (Tröger, 1956 ; Hashimoto, 1964) and $\gamma \leqslant 1{\cdot}640$ indicates Al prehnite ($<1{\cdot}5$ mole per cent of the ferrian end-member, and $<1{\cdot}0$ wt% Fe_2O_3). Refractive indices of prehnites from three occurrences at Haystack Creek are $\gamma = 1{\cdot}637$–$1{\cdot}640 \pm 0{\cdot}002$ (av: 1·638) and $\alpha = 1{\cdot}613$–$1{\cdot}614 \pm 0{\cdot}002$ (av: 1·614). These values indicate a low Fe content. Determinations of Fe by means of wet chemical and X.R.F. methods gave values for total Fe as Fe_2O_3 from 0·2 to 0·3 wt% in Haystack Creek prehnitites. Most prehnites from diverse geologic environments apparently contain <10 mole per cent of the ferrian end-member (Hashimoto, *ibid.*) but electron probe studies of prehnite from rocks in the prehnite-pumpellyite metagreywacke facies (Surdam, 1969) and from a contact metamorphic environment (Robinson, 1973) show these prehnites to be highly variable with some grains containing up to 30 mole per cent of the ferrian end-member. Similar studies are desirable for the Coolac prehnites but the mineral in the Haystack Creek sub-environment may be uniformly Fe-poor.

An occurrence of zoisite replaced by veinlets of prehnite in Newfoundland (Watson, 1942) may imply that prehnite is related retrogressively to zoisite (Liou, 1971 ; Holdaway, 1972). One of the Haystack Creek rocks contains prehnite pseudomorphs of zoisite crystals but in most of the prehnite-zoisite associations near Coolac the prehnite occupies spaces between un-replaced zoisite euhedra (Plate II, C).

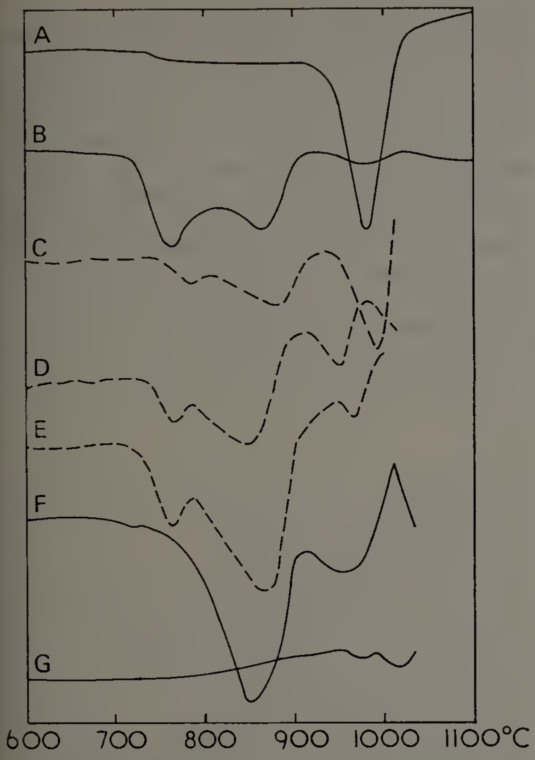

FIGURE 4.—Differential thermograms (600–1,100°C) of prehnite-rich, zoisite-rich and related materials.

A : Zoisitite (>95% zoisite), Haystack Creek.
B : Prehnitite (>95% prehnite+a little zoisite), Haystack Creek.
C, D, E : Mixtures of A and B in the respective proportions 3 : 1, 1 : 1 and 1 : 3.
F : Prehnite from the Prospect Intrusion, N.S.W.
G : Green epidote from the Harts Range, Central Australia.

Epidote Minerals

Terminology and Identification

The Al-Fe epidote minerals may be referred to a series with the ideal end-members $Ca_2Al_3Si_3O_{12}(OH)$ or zoisite (Ps_0) and $Ca_2Fe^{3+}_3Si_3O_{12}(OH)$ or pistacite (Ps_{100}). They may also be conveniently subdivided into two orthorhombic groups : zoisite ($Ps_{0-2\cdot5}$) and ferrian zoisite ($Ps_{2\cdot5-5}$) and two monoclinic groups : clinozoisite (Ps_{5-10}) and epidote (Ps_{10-35}) (see Deer *et al.*, 1962*a* ; Holdaway, 1972).

In the present study orthorhombic members have been distinguished from monoclinic members using the X-ray criteria of Seki (1959), zoisite has been distinguished from ferrian zoisite on the basis of optics and Fe content (Myer, 1966), and epidote has been arbitrarily distinguished from clinozoisite on the basis of colour and pleochroism.

Because intimate intergrowths of epidote minerals have been frequently reported elsewhere (see Ackermand and Raase, 1973) X-ray powder patterns of samples have been checked for the possible presence of both orthorhombic and monoclinic members. The diagnostic X-ray reflections for the zoisites (absent for clinozoisite) are at d=3·67, 3·62, 3·15, 3·08, 2·72 and 2·33 Å, and those for clinozoisite (absent for zoisite and ferrian zoisite) at d=3·47, 3·40, 3·20, 2·59, 2·45, 2·16 and 1·57 Å. The absence of X-ray reflections for vesuvianite which, in some of its occurrences, resembles zoisite in thin section, was also checked.

Myer (1966) drew attention to the widespread confusion of terminology for the orthorhombic epidote minerals, and proposed that the terms α-zoisite and β-zoisite be discarded in favour of ferrian zoisite and zoisite respectively. Myer distinguished zoisite with up to 0·14 atoms of Fe^{3+} (on the basis of 25 oxygens), O.A.P. $\perp$ to the cleavage (100) and dispersion $r>v$ from ferrian zoisite with $>0\cdot14$ atoms of Fe^{3+}, O.A.P. $\parallel$ cleavage (100) and dispersion $r<v$. Reference to published analyses and formulae of orthorhombic epidote minerals (Deer *et al.*, 1962*a* ; Seki and Kuriyagawa, 1962 ; Seki *et al.*, 1963 ; Myer, 1966) suggests that total Fe as $Fe_2O_3<1\cdot2$ wt% indicates zoisite and values $>1\cdot3$ wt% indicate ferrian zoisite. In several Coolac samples Fe content inferred from the optics of selected grains has been confirmed by bulk chemical analyses of concentrates (Table 3) by means of X-ray fluorescent spectrometry.

Because some epidote minerals retain hydroxyl after heating at 1,000°C (Deer *et al.*, *ibid.*), the loss on ignition of analysed zoisite concentrates was determined at 1,400°C. A repeat determination made at 1,000°C on one sample, and consistent strong endothermic peaks at 975°±15°C in differential thermograms (Figure 4), however, suggest that heating at 1,000°C may in fact suffice for the determination of water in Fe-poor zoisite. No reference to the D.T.A. of zoisite was encountered in the literature but the dry decomposition of zoisite to a mixture of anorthite, gehlenite and pseudowollastonite at or above 810°C is reported by Deer *et al.* (*ibid.*). Differential thermograms of clinozoisite-rich material from Mooney Mooney Range epidosites are similar to those of analysed zoisite concentrates. Zoisite and clinozoisite therefore cannot be distinguished by D.T.A. Once zoisite has been determined by other methods, however, the D.T.A. curve provides a useful guide to the proportions of phases present, at least in zoisite-prehnite assemblages. A thermogram of green epidote from the Harts Range, Central Australia, tested for comparison, exhibits a weak endothermic peak at $\sim$975°C followed by a stronger peak at $\sim$1,015°C (Figure 4) suggesting water loss in two stages. The second peak accords with that for epidote recorded by McLaughlin (1967).

Zoisite

At North Mooney Ridge zoisitite contains zoisite (70–80%)+diopside and prehnite. Similar material in the gabbro pegmatite contains zoisite (70–80%)+grossular and prehnite. At Haystack Creek zoisitites contributing to Gp. 2 rodingites contain zoisite (60–95%)+prehnite, chlorite, albite and sphene. Hand specimens of these rocks are pink to pale grey and commonly indistinguishable from some Gp. 1 rodingites. In the best-crystallized material the zoisite forms felted aggregates of decussate, euhedral crystals up to 1·0×0·5×0·2 mm with a tabular, bladed habit. Prehnite, chlorite or grossular occupies the interstices. In some Haystack Creek specimens zoisite forms turbid masses of interlaced prisms or plumose acicular aggregates. Diffractograms confirm the presence of orthorhombic members of the epidote group, and the absence of monoclinic members, in all these segregations.

The habit of the well-crystallized zoisite (Figure 5 ; Plate II, C) results in three principal kinds of grain sections : (i) narrow, elongate, length-fast sections || cleavage (100), (ii) broader plates || (001) giving Bx_a interference figures and showing length-slow cleavage traces and (iii) doubly terminated, length-fast sections || O.A.P. (010). This distinctive habit and optic orientation is not described in texts available to the authors, but doubly terminated sections are known in metamorphic rocks (e.g. Joplin, 1968, p. 206). The optic orientation indicates zoisite as distinct from ferrian zoisite. All the segregated Coolac zoisite displays normal low first order interference colours, and lacks zoning and multiple twins. Cross fractures are common in all elongated sections irrespective of orientation. Other optical data and chemical analyses of zoisite concentrates (Table 3) preclude the presence of significant amounts of ferrian zoisite in the segregations.

Epidote Minerals in the Ophiolite Sequence

Green epidote forms micro-veinlets comprising 5–15% of the rock in quartz keratophyres of the Mooney Mooney Range and accompanies clinozoisite in metabasalts flanking Mt. Lightning on the west. Colourless clinozoisite is the common epidote mineral in metabasalts and metagabbros of the Mooney Mooney Range. The metabasalts contain variable amounts of calcic plagioclase, albite, augite, actinolite, chlorite and clinozoisite. The metagabbros contain variable amounts of calcic plagioclase, saussurite, albite, augite, hornblende, actinolite, tremolite, chlorite and clinozoisite and are veined by epidosites containing predominant clinozoisite. The veins, $\sim$1 cm wide, are pink and finely saccharoidal in appearance. They sharply penetrate or merge with the metagabbros that are mottled pink and green.

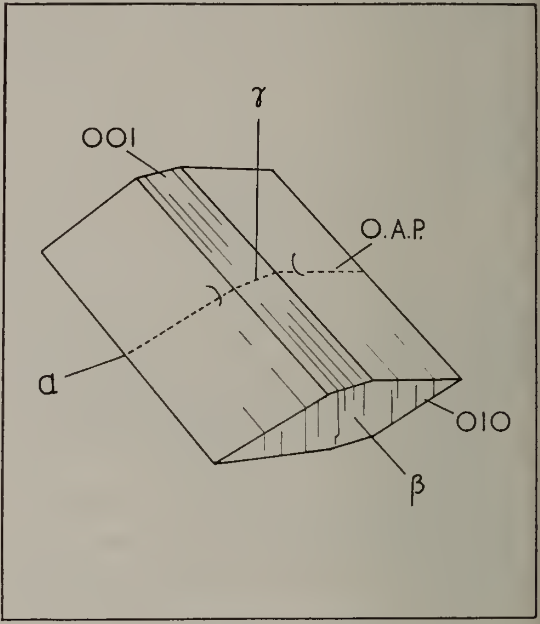

FIGURE 5.—Habit and optic orientation of zoisite from segregations at North Mooney Ridge and Haystack Creek.

The clinozoisite of the metagabbros and veins occurs in polygonal granular aggregates or clusters of prismatic crystals. Individual crystals attain a maximum width of 0·5 mm. Doubly terminated sections are absent. Most grain sections show anomalous polarization colours, blues predominating. Lamellar twins and patchy zoning are common. Grains with regular zoning occur in some specimens. This heterogeneity on the scale of vein widths, microdomains and single grains is characteristic. Diffractograms indicate predominant clinozoisite±minor amounts of zoisite or ferrian zoisite as revealed by weak reflections at d=3·68 and d=3·15 Å.

Some metagabbros ~100 metres west of the harzburgite contain diopsidic augite, chlorite, grossular (10–20%), in some samples vesuvianite (5%), together with members of the epidote group (10–20%). Grossular, vesuvianite and epidote group minerals are segregated in respective micro-domains. The epidote group minerals display some doubly terminated sections, predominantly first order polarization colours, minor zoning and twins. The status of this material as zoisite, ferrian zoisite, a mixture of both, or of one or both of these with minor clinozoisite (see Ackermand and Raase, *ibid.*) has not been determined.

TABLE 3

Chemical Analyses of Zoisite Concentrates from Segregations at North Mooney Ridge (Sample 1) and Haystack Creek, Mt. Lightning (Samples 2, 3 and 4). Impurities : Sample 1 contains ~10% of Diopside + Prehnite. Samples 2, 3 and 4 ~5% of Prehnite + Chlorite + Sphene ± Albite. Analyst : A. S. Ray.

	1	2	3	4	Formula of Sample 4 on the Basis of 25 (0)		
SiO_2	39·84	39·67	39·40	39·85	Si	6·100	6·137
TiO_2	0·07	0·07	0·15	0·09	P	0·037	
Al_2O_3	31·85	32·67	32·79	31·54	Al	—	
*Fe_2O_3	0·69	0·44	0·39	0·43	Al	5·689	5·753
MnO	0·02	0·07	0·00	0·07	Fe	0·055	
MgO	1·79	0·70	0·33	0·83	Ti	0·009	
CaO	23·40	23·29	23·02	23·36			
K_2O	0·01	0·15	0·55	0·15	Mn	0·009	
P_2O_5	0·13	0·31	0·16	0·31	Ca	3·837	4·057
SO_3	0·04	0·04	0·01	0·04	Mg	0·184	
†Loss	3·30	3·60	2·50	3·60	K	0·036	
Total ..	101·14	101·01	99·30	100·27			

Optical Data

β ± 0·002	1·695	1·697	1·695	1·700
2V+ (meas) ..	42°	36°	33°	20°
Dispersion	r>v	r>v	—	r>v

* Total Fe as Fe_2O_3.
† Loss on ignition.

In the harzburgitic member of the rock association metabasites are represented principally by the enclosures of Gp. 1 rodingite which are devoid of minerals belonging to the epidote group.

A broad trend of variation in the secondary Ca-Al silicates from west to east across the mafic-ultramafic association is suggested as follows : green epidote→clinozoisite→orthorhombic epidote group minerals→grossular and vesuvianite. This trend is one of increasing stratigraphic depth in the proposed ophiolite sequence (Figure 6). It may broadly reflect hydrothermal alteration of mafic rocks in conditions of increasing temperature and/or decreasing oxygen fugacity with increasing stratigraphic depth (see Coombs *et al.*, 1970 ; Holdaway, 1972 ; Liou, 1973) together with variations induced in proximity to ultramafic contacts. The influence of initial rock composition, the proximity of some samples to former channels of enhanced fluid mobility or metasomatic activity, and other factors, also require consideration in future studies.

Discussion

Rodingite has been variously defined and interpreted (Coleman, 1967 ; Aumento and Loubat, 1971 ; Aumento, 1972 ; De, 1973 ; O'Brien and Rogers, 1973). The term has been used for diverse rocks the relationships of which to ophiolite sequences (Church, 1972 ; Page, 1972 ; Moores, 1973 ; and Gass and Smewing, 1973) require re-appraisal. An adequate description of the rodingitic rocks near Coolac must await studies of the complete mineral assemblages and of the petrochemistry of associated variants. Present observations, however, suggest that the qualifier " rodingitic " is appropriate for those members of the ophiolite suite that contain substantial amounts of relatively well-crystallized, Fe-poor, secondary Ca-Al silicates. Saussuritic rocks and most epidosites are thereby excluded. Near Coolac rodingitic rocks are characterized by grossular, vesuvianite, prehnite and "zoisitic" minerals. Grossular may accompany each of the others, but intimate associations of prehnite and vesuvianite have not been encountered and associations of orthorhombic epidote minerals and vesuvianite are uncommon. Free silica and carbonates are absent from rodingitic assemblages except at junctions with trondhjemite, albitite or granodiorite.

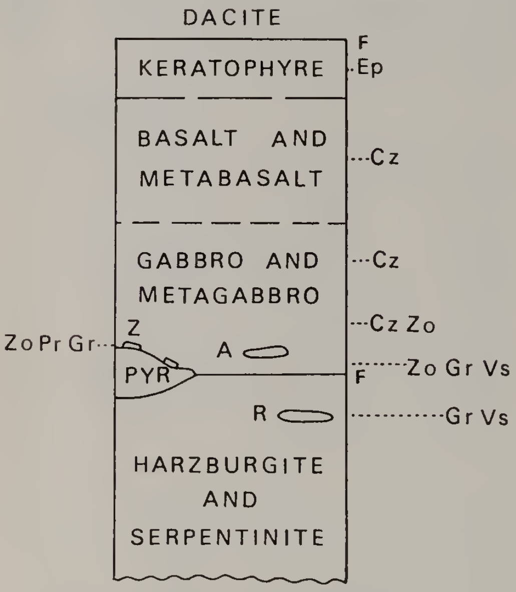

FIGURE 6.—Schematic ophiolite sequence in the Mooney Mooney Range showing trend in the distribution of the secondary Ca-Al silicates.

Z : zoisitite.
PYR : clinopyroxenite.
A : amphibolite.
R : Gp. 1 rodingite.
F : proposed fault.
Ep : epidote.
Cz : clinozoisite.
Zo : zoisite and/or ferrian zoisite.
Gr : grossular.
Vs : vesuvianite.
Pr : prehnite.

The Coolac rodingitic rocks include a wide range of products that may have formed in different ways and at different times. For example, Gp. 1 rodingites apparently represent mafic dykes or pockets of trapped mafic magma. Metasomatism may have merged with the consolidation of some of these rocks but succeeded consolidation of others. Gp. 2 rodingites apparently belong to reaction zones (Coleman, 1967) that formed at junctions of contrasted rock types. Zoisitized gabbro pegmatite may have been altered as a result of magmatic or external fluid attack or may have resulted from contact metamorphism that involved the recrystallization of saussurite (Olsen, 1961).

Several formerly problematic features of the rock association in the Mooney Mooney Range may be interpreted as logical consequences of ophiolite generation and modification according to current concepts (Bonatti *et al.*, 1971; Aumento, 1972; Moores, 1973; Gass and Smewing, 1973; Spooner and Fyfe, 1973). Ophiolites are regarded as segments of former sub-oceanic lithosphere generated at rifts beneath oceans or marginal seas, modified by faulting, intrusion, differentiation and complex metamorphism that included hydrothermal processes, prior to emplacement at margins of continents or island arcs.

The status of the rock association in the Mooney Mooney Range as a partly preserved ophiolite sequence is suggested by an assemblage of features. These features include (i) the tectonic setting between granodiorite and chert-bearing sedimentary and volcanic rocks, (ii) a rock sequence ranging from deformed harzburgite (with enclosures of podiform chromitite, Gp. 1 rodingite and trondhjemite) through essentially undeformed diopside-rich cumulates or through amphibolite to altered gabbro, basalt and keratophyre, (iii) diverse gabbroic rocks that are sporadically veined with epidosite, (iv) basaltic rocks that exhibit a variety of relict igneous textures and are closely associated with serpentinite in some areas, (v) metabasite assemblages that are similar to those of the greenschist, and transitional greenschist to amphibolite, facies of metamorphism, (vi) mafic dykes and apophyses displaying apparently conflicting age relationships and (vii) a trend in the distribution of hydrothermal Ca-Al silicates that may correlate with "sub-sea-floor metamorphism".

"Sub-sea-floor metamorphism" incorporates "dynamothermal –", "background –" and "geothermal system metamorphism" (Spooner and Fyfe, 1973). Geothermal system metamorphism involves the circulation of hot brines that become increasingly reducing with depth prior to upward discharge. Such fluid circulation may have promoted the formation and influenced the variation of the epidote minerals and may have induced some types of rodingitization. It might be conjectured that the rock association in the Mooney Mooney Range incorporates an ophiolite sequence generated at a rift and an intrusion, represented by the pyroxenite, that was generated above a subduction zone (see Stevens *et al.*, 1974). Irrespective of such conjectures, metasomatism doubtless occurred at various times in the complex history of the association and prehnite and grossular at peridotite-granodiorite contacts may have resulted from the post-emplacement passage of fluids that were meteoric in origin.

ACKNOWLEDGEMENTS

The authors thank Dr. P. Bayliss for the partial analysis of prehnite, Mr. G. Melville for drafting and Professor J. J. Frankel for helpful suggestions.

References

Ackermand, D., and Raase, P., 1973. Coexisting Zoisite and Clinozoisite in Biotite Schists from the Hohe Tauern, Austria. *Contr. Mineral and Petrol.*, **42**, 333.

Aumento, F., 1972. The Oceanic Crust of the Mid-Atlantic Ridge at 45°N., *In* Irving, E (Ed.), *The Ancient Oceanic Lithosphere*, Dpt. Energy, Mines, Res., Ottawa, 49.

Aumento, F., and Loubat, H., 1971. The Mid-Atlantic Ridge near 45°N. XVI. Serpentinized Ultramafic Intrusions. *Can. J. Earth Sci.*, **8**, 631.

Bonatti, E., Honnorez, J., and Ferrara, G., 1971. Peridotite-Gabbro-Basalt Complex from the Equatorial Mid-Atlantic Ridge. *Phil. Trans. Roy. Soc. Lond. A*, **268**, 385.

Brown, P., 1973. Ophiolites of the Central Mooney Mooney Ranges, a Portion of the Coolac-Goobarragandra Ultramafic Belt, N.S.W. Hons. B.Sc. thesis, Univ. of N.S.W. (unpublished).

Church, W. R., 1972. Ophiolite: its Definition, Origin as Oceanic Crust and Mode of Emplacement in Orogenic Belts, with Special Reference to the Appalachians, *In* Irving, E. (Ed.), *The Ancient Oceanic Lithosphere*, Dpt. Energy, Mines, Res., Ottawa, 71.

Coleman, R. G., 1961. Jadeite Deposits of the Clear Creek Area, New Idria District, San Benito County, California. *J. Petrology*, **2**, 2.

Coleman, R. G., 1967. Low Temperature Reaction Zones and Alpine Ultramafic Rocks of California, Oregon and Washington. *U.S. geol. Surv. Bull.*, **1247**, 1.

Coombs, D. S., Horodyski, R. J., and Naylor, R. S., 1970. Occurrence of Prehnite-Pumpellyite Facies Metamorphism in Northern Maine. *Am. J. Sci.*, **268**, 142.

De, A., 1972. Petrology of Dikes Emplaced in the Ultramafic Rocks of Southeastern Quebec and Origin of Rodingite. *Geol. Soc. Amer. Mem.*, **132**, 489.

Deer, W. A., Howie, R. A., and Zussman, J., 1962*a*. *Rock-Forming Minerals.* Vol. 1, *Ortho- and Ring Silicates.* Longmans, London.

Deer, W. A., Howie, R. A., and Zussman, J., 1962*b*. *Rock-Forming Minerals.* Vol. 3, *Sheet Silicates.* Longmans, London.

Frankel, J. J., 1959. Uvarovite Garnet and South African Jade (Hydrogrossular) from the Bushveld Complex, Transvaal. *Amer. Mineral.*, **41**, 565.

Gass, I. G., and Smewing, J. D., 1973. Intrusion, Extrusion and Metamorphism at Constructive Margins: Evidence from the Troodos Massif, Cyprus. *Nature*, **242**, 26.

Golding, H. G., 1969. The Coolac-Goobarragandra Ultramafic Belt, N.S.W. *J. Proc. Roy. Soc. N.S.W.*, **102**, 173.

Golding, H. G., 1971. Local and Regional Trends of Serpentinization and Metaserpentinization in the Coolac-Goobarragandra Ultramafic Mass, New South Wales. *Geol. Soc. Aust. Spec. Publs.*, **3**, 321.

Hashimoto, M., 1964. The Chemistry and Optics of Prehnite. *J. Geol. Soc. Japan*, **70**, 180.

Holdaway, M. J., 1972. Thermal Stability of Al-Fe Epidote as a Function of fO_2 and Fe Content. *Contr. Mineral and Petrol.*, **37**, 307.

Hutton, C. O., 1943. Hydrogrossular, a New Mineral of the Garnet-Hydrogarnet Series. *Trans. Roy. Soc. N.Z.*, **73**, 174.

Ito, J., and Arem, E. J., 1970. Idocrase: Synthesis, Phase Relations and Crystal Chemistry. *Amer. Mineral.*, **55**, 880.

Joplin, G. A., 1968. *A Petrography of Australian Metamorphic Rocks.* Angus and Robertson, Sydney.

Liou, J. G., 1971. Synthesis and Stability Relations of Prehnite, $Ca_2Al_2Si_3O_{10}(OH)_2$. *Amer. Mineral.*, **56**, 507.

Liou, J. G., 1973. Synthesis and Stability Relations of Epidote, $Ca_2Al_2FeSi_3O_{12}(OH)$. *J. Petrology*, **14**, 381.

McLaughlin, R. J. W., 1967. Thermal Techniques. *In* J. Zussman (Ed.), *Physical Methods in Determinative Mineralogy*. Academic Press, London.

Miles, K. R., 1950. Garnetized Gabbros from the Eulaminna District, Mt. Margaret Goldfield. *Bull. geol. Surv. W. Aust.*, **103**, 108.

Moores, E. M., 1973. Geotectonic Significance of Ultramafic Rocks. *Earth Sci. Rev.*, **9**, 241.

Myer, G. H., 1966. New Data on Zoisite and Epidote. *Am. J. Sci.*, **264**, 364.

O'Brien, J. P., and Rodgers, K. A., 1973. Xonotlite and Rodingites from Wairere, New Zealand. *Mineral. Mag.*, **39**, 233.

Olsen, E. J., 1961. High Temperature Acid Rocks Associated with Serpentinite in Eastern Quebec. *Am. J. Sci.*, **259**, 329.

Page, B. M., 1972. Oceanic Crust and Mantle Fragment in Subduction Complex near San Luis Obispo, California. *Bull. geol. Soc. Am.*, **83**, 957.

Peters, T., 1961. Differential thermoanalyse von Vesuvian. *Schweiz. Min. Petr. Mitt.*, **41**, 325.

Robinson, D., 1973. Prehnite from the Contact Metamorphic Aureole of the Whin Sill Intrusion, Northern England. *Amer. Mineral.*, **58**, 132.

Seki, Y., 1959. Relation Between Chemical Composition and Lattice Constants of Epidote. *Amer. Mineral.*, **44**, 720.

Seki, Y., and Kuriyagawa, S., 1962. Mafic and Leucocratic Rocks Associated with Serpentinite of Kanasaki, Kanto Mountains, Central Japan. *Jap. J. Geol. Geogr.*, **33**, 15.

Seki, Y., Kuriyagawa, S., and Horikoshi, T., 1963. Mafic and Leucocratic Rocks Associated with Serpentinite in the Sasaguri and Omi-Kotaki Areas in the Sangun Metamorphic Belt of Japan. *Sci. Rpts. Saitama Univ.*, B, **4**, 193.

Spooner, E. T. C., and Fyfe, W. S., 1973. Sub-Sea-Floor Metamorphism, Heat and Mass Transfer. *Contr. Mineral and Petrol.*, **42**, 287.

Stevens, R. K., Strong, D. F., and Kean, B. F., 1974. Do Some Eastern Appalachian Ultramafic Rocks Represent Mantle Diapirs Produced Above a Subduction Zone ? *Geology*, **2**, 175.

Surdam, R. C., 1969. Electron Microprobe Study of Prehnite and Pumpellyite from the Karmutsen Group, Vancouver Island, British Columbia. *Amer. Mineral.*, **54**, 256.

Tröger, W. E., 1956. *Optische Bestimmung der Gesteinsbildenden Minerale.* Teil 1, *Bestimmungstabellen.* Schweizerbart'sche Verlagsbuchhandlung, Stuttgart.

Watson, K. D., 1942. Zoisite-Prehnite Alteration of Gabbro. *Amer. Mineral.*, **27**, 638.

Yoder, H. S., 1950. Stability Relations of Grossularite. *J. Geol.*, **58**, 221.

Zabinski, W., 1964. On the Occurrence of a Dispersed Vesuvianite Phase in some so-called Hydrogrossulars. *Bull. Acad. Polon. Sci., Ser. Sci. Geol. Geogr.*, **12**, 149.

School of Applied Geology,
University of New South Wales,
Kensington, N.S.W., 2033.

(Received 27 September 1974)

EXPLANATION OF PLATE I

A : Gp. 1 rodingite dyke in massive, partly serpentinized harzburgite. Southern slope of Mt. Lightning near Adjungbilly Creek.

B : Gp. 1 garnetite showing relict colloform texture. East Ellamatta Creek, Mt. Lightning. Thin section, ordinary light. Frame length 1·3 mm.

C : Porous Gp. 1 garnetite with clusters of euhedral to sub-hedral garnet crystals separated by pores lined with chlorite. Quilters East, Mt. Lightning. Thin section, ordinary light. Frame length 1·9 mm.

EXPLANATION OF PLATE II

A : Chromite-cored, uvarovitic garnet crystals associated with chlorite (white) and chromite (black) in veinlet penetrating chromitite. Quilters West, Mt. Lightning. Thin section, ordinary light. Frame length 0·6 mm.

B : Prehnitite with sutured texture from junction of serpentinized harzburgite and granodiorite. North bank of the Murrumbidgee River near Mt. Lightning. Thin section, polars crossed. Frame length 3·5 mm.

C : Zoisite euhedra (high relief) separated by prehnite (white) in Gp. 2 rodingite, Haystack Creek, Mt. Lightning. Thin section, polars partly crossed. Frame length 1·6 mm.

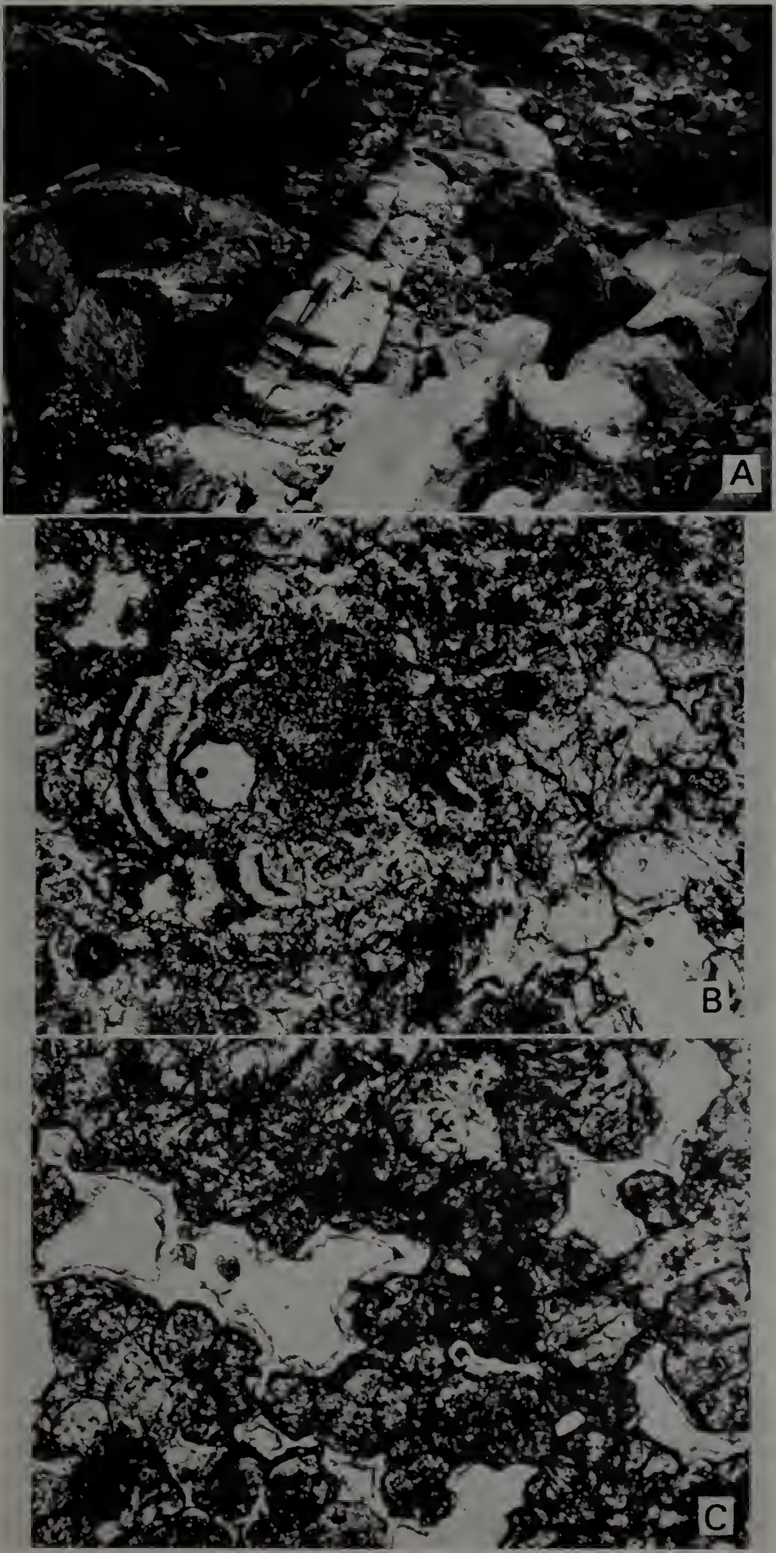
A
B
C

GOLDING AND RAY PLATE II

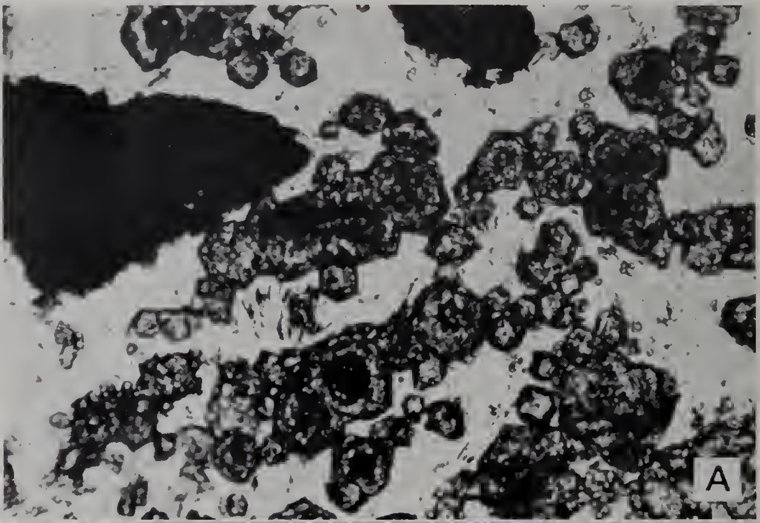

Journal and Proceedings, Royal Society of New South Wales, Vol. 108, pp. 131–146, 1975

Petrology and Petrochemistry of Igneous Rocks in the Mullaley Area of New South Wales

JUDITH M. BEAN

ABSTRACT—Division of igneous rocks in the Mullaley area into six groups (Bean, 1974), is further supported by petrological, mineralogical and chemical data. The Garrawilla Volcanics comprise a mildly alkaline, low-K, high-Fe lineage, similar to the mildly alkaline Hawaiian lineage, except for higher $Fe_2O_3 : FeO+Fe_2O_3$ ratios. The latter reflect a build up of volatiles in the more felsic Garrawilla lavas with the result that all rocks more evolved than hawaiites are either vesicular or pyroclastic.

The Nombi Extrusives are moderately strongly undersaturated, low-K rocks which differ markedly from Hawaiian basanites in their low-Al values.

The Glenrowan Intrusive lineage is a mildly undersaturated, moderately high-K, low-Al, low $Fe_2O_3 : FeO$ lineage. The range in chemistry of the rocks is proposed as the result of fractionation, initially deep within the crust ($P \leqslant 9$ kb), and finally *in situ* within the sills.

The Napperby Limburgite, by virtue of its strong degree of undersaturation and high-K content, is a unique rock type in the area. The mildly undersaturated Tambar Trachybasalt is also unique in its high-K, low-Na, high-Al composition.

The Bulga Complex is comprised of the more evolved members of a mildly undersaturated, moderately high-to high-K, low $Fe_2O_3 : FeO$ lineage. The phonolites and phonolitic trachytes represent dual differentiation trends—one towards strong Na- and *ne*-enrichment, the other towards K-enrichment; similar trends have been observed in the alkaline sequences of Gough Island (Le Maitre, 1962) and Nandewar Volcano (Abbott, 1969).

Factors which may have been significant in genesis of the lineages are briefly discussed.

Introduction

Field relationships, distribution and general petrography of rock types found in the Mullaley area of New South Wales have previously been outlined by Bean (1974). Six groups of igneous rocks are recognized: the Garrawilla Volcanics, the Nombi Extrusives, the Glenrowan Intrusives, the Napperby Limburgite, the Tambar Trachybasalt and the Bulga Complex. The present paper presents the petrography, mineralogy and chemistry of these rocks and includes discussion on some aspects of petrogenesis.

Petrography and Mineralogy

Garrawilla Volcanics (Table 1)

(*a*) Alkali olivine basalt and alkali basalt have only positively been identified as non-vesicular flows. Alteration of both phenocrystal and groundmass olivine is extensive and excludes the rocks from bulk chemical study. In the alkali olivine basalts a significant proportion of the olivine occurs as microphenocrysts with core compositions ranging from Fa_{22} to Fa_{24}.[1]

Both the alkali olivine basalts and alkali basalts consist of laths of labradorite, and rarely bytownite (An_{78} to An_{70}[2]), euhedral grains of mauve brown titanaugite and olivine, and grains of a faintly pinkish brown homogeneous titanomagnetite. Primary interstitial analcime (clear, isotropic, $n=1{\cdot}488–1{\cdot}489$) is minor in some flows. At least two thick flows contain up to 40 modal percent of a brown glass charged with fine dendrites of opaque oxide.

TABLE 1

Modal Analyses of Garrawilla Volcanics

All modal values are in volume percent

Rock Type	Alkali Olivine Basalt		Hawaiite		
Specimen No. . .	716	925	917	843	837
Olivine	16	17	6	11	10
Clinopyroxene . .	38	33	16	17	16
Feldspar (predominantly plagioclase) . .	27	39	27	53	53
Opaques . .	8	6	7	8	12
Glass	—	—	42	—	—
Altered felsic minerals . .	11	5	2	11	9

---

[1] Olivine compositions, unless otherwise stated, are based on β refractive index measurements ($\pm 0{\cdot}002$) and the data of Bowen and Schairer (1935).

[2] Plagioclase compositions quoted as a percentage An are based on β refractive index measurements ($\pm 0{\cdot}002$) and the data of Chayes (1952).

(*b*) Hawaiite occurs dominantly as non-vesicular flows. The average grainsize of less than 0·1 mm limits detailed petrography and mineralogy.

The rocks are dominated by laths and anhedral grains of plagioclase, ranging in composition from An_{67} to An_{25}. These contrast with larger strongly zoned crystals, with a core composition of An_{48} to An_{33}, which are tentatively interpreted as having crystallized at moderately high P/T conditions.

Microphenocrysts of olivine range from Fa_{22} to Fa_{30}. Groundmass olivine in hawaiite 723[1] has an average composition of Fa_{38} ($\Delta 2\theta\ \text{olivine}_{131}-2\theta\ \text{silicon}_{111}=4{\cdot}24^{\circ}$; Yoder and Sahama, 1957). Pyroxene occurs as minute euhedral grains of colourless augite or rarely as ophitic plates of mauve brown titanaugite.

Cubes of titanomagnetite are optically homogeneous and contain a significant ulvöspinel component ($a_0=8{\cdot}427$ Å in hawaiite 723 and 8·458 Å in hawaiite 716). Lamellae of ilmenite are rare in titanomagnetite 757 ; $a_0=8{\cdot}428$ Å. A strongly pleochroic red brown to light straw biotite occurs as anhedral grains adjacent to olivine or, rarely, as euhedral crystals.

(*c*) Mugearite is a minor rock type in the non-vesicular flows. Despite extensive weathering of the vesicular flows and pyroclastic units, which prevents confirmation by analysis, it is proposed that many of these porous rocks are also mugearites.

Confirmed mugearites are characterized by abundant small cubes of Fe-Ti oxide, minor very small (less than 2 μ in length) prisms of colourless augite, and abundant feldspar, dominantly oligoclase. Microphenocrysts of olivine elongated parallel to *c* are minor and biotite is accessory.

(*d*) Soda trachyte has been identified positively only as massive non-scoriaceous lapilli tuffs and volcanic agglomerates. The majority of pyroclastic units and perhaps some of the vesicular flows also appear to be of soda trachyte. Volcanic agglomerate 845 consists of lithic fragments dominated by small laths of alkali feldspar ; cubes of opaque mineral and an interstitial felsic phase are minor. Na_2O and K_2O values of 8·10 and 2·82 weight percent, respectively (partial analysis of specimen 845), are interpreted as approximating the values of these oxides in the alkali feldspar ; thus the mineral is lime anorthoclase or anorthoclase.

(*e*) Megacrysts occur in at least 84 percent of the non-vesicular basalts and hawaiites. The percentage in the mode is commonly less than one, but in the Twin Peaks type lava of the small lava domes the percentage is as high as 30. All crystals are less than 6 mm in diameter and most are less than 1 mm. All display marginal resorption and/or reaction with the liquid in which they were enclosed.

The most abundant megacryst phase is a pale mauve brown clinopyroxene ($\beta=1{\cdot}694$ to $1{\cdot}698$) featuring a marginal zone of spongy pyroxene rimmed by clear titanaugite. Olivine with core composition ranging from Fa_{12} to Fa_{24} is next in abundance. The resorbed crystals of olivine are consistently richer in forsterite, by 9 to 18 molecular percent, than microphenocrysts of olivine in the host rock. An iron titanium oxide phase, a dark green spinel ($n=1{\cdot}775$) and a grey to green brown spinel ($n\simeq 1{\cdot}77$) are also represented. Orthopyroxene ($\gamma=1{\cdot}692$), and a mineral altered to an aggregate of clinopyroxene, (?) rhönite, opaque mineral and feldspar, are very rare. The latter aggregate is interpreted as the alteration product of kaersutitic amphibole. Inclusion-filled apatites (cf. Le Maitre, 1962 ; Wilshire and Standard, 1963 ; Wright, 1968) are common ; in hexagonal cross sections the grey brown inclusions are aligned parallel to the prism faces, and in tabular longitudinal sections (commonly 1·5 mm in length) they form lines parallel to the *c* axis. Pyramidal terminations of the crystals display a narrow zone devoid of inclusions. The very rare occurrence of other breakdown products of amphibole in the Garrawilla lavas tends to exclude the origin for inclusion-filled apatites proposed by Edwards (1938) and Benson (1939).

" Xenocrystal material of peridotitic origin ", as reported by Wilshire and Standard (1963) in the Mullaley basalts, was not found in the Garrawilla rocks.

(*f*) Secondary analcime occurs in vesicles and pore spaces throughout the Garrawilla volcanic sequence. Generally the mineral is feebly anisotropic and displays uneven extinction ; occasionally it is multiply twinned. The refractive index is low ($n=1{\cdot}483$ to $1{\cdot}484$) and measurements of the cell dimension a_0 yielded 13·709, 13·695 and 13·688 Å ($\Delta 2\theta\ \text{analcime}_{639}-2\theta\ \text{silicon}_{331}=1{\cdot}825^{\circ}$, $1{\cdot}929^{\circ}$ and $1{\cdot}972^{\circ}$, respectively ; Cu/Ni radiation). These values are significantly lower than refractive indices and cell dimensions of many igneous analcimes and indicate relatively Si-rich compositions. Similar cell dimensions have been measured on

---

[1] Specimen numbers used in this paper consist of the final three digits of University of New England, Geology Department, Rock Museum numbers.

analcime formed by burial metamorphism (Wilkinson and Whetten, 1964 ; Coombs and Whetten, 1967) and slightly smaller dimensions on analcime formed in a playa lake by diagenetic processes (Ross, 1928 ; 1941). Analcime with similar properties was attributed by Bradley (1929) to be the product of precipitation at low temperatures following the interaction of Na salts in lake waters with the dissolution products of volcanic ash.

In considering the origin of the secondary analcime at Mullaley it is important to note that—

(i) no zonation of the mineral could be detected in either a horizontal or vertical direction ; and
(ii) even if one allows for removal of a thickness of 150 metres of rock from the top of the present maximum erosion level of the Jurassic sedimentary units, the maximum possible depth of burial of the highest development of the analcime must have been less than 300 metres.

In the light of these factors it is proposed that the analcime was precipitated from ground waters percolating through, or stationary in, the volcanic sequence. It is expected that, during deposition of the Jurassic Purlawaugh and Pilliga Beds, the porous Garawilla sequence would have been saturated with ground water. The deposits of unlithified volcanic ash and lapilli at the base of the sequence could well have provided the Al, Si and Na required for precipitation of the analcime. Nashar and Davies (1960) have demonstrated that solutions, which have derived their constituents by weathering of basalt at atmospheric temperatures, can precipitate secondary minerals including zeolites.

Nombi Extrusives (Table 2)

(*a*) Basanite of the Nombi Extrusives consists of small euhedral grains of olivine (Fa_{22}), titansalite and opaque oxide, poikilitically enclosed in coarse grained plates of analcime and nepheline ; poikilitic grains of plagioclase (An_{58} to An_{40}) are essential in some specimens. Apatite and strongly pleochroic biotite are accessory. The opaque oxide is an optically homogeneous titanomagnetite with some alteration to titanomaghemite ; for titanomagnetite 720 $a_0=8\cdot420$ Å. Analcime is clear, isotropic and $n\simeq1\cdot488$; for analcime 718 $\Delta2\theta$ $\text{analcime}_{639}–2\theta\ \text{silicon}_{331}=1\cdot684°$.

(*b*) Xenocrysts of peridotitic origin are rare. Olivine (Fa_{11}) with deformation bands, and orthopyroxene ($\beta=1\cdot672$, $\gamma=1\cdot678$) surrounded by a well-defined reaction rim (consisting of oriented olivine granules and an unidentified interstitial green phase) have been identified.

(*c*) Megacrysts. Crystals of resorbed olivine (Fa_{18} to Fa_{23}) and faintly mauve brown clinopyroxene constitute up to 10 volume percent of the basanites. Each pyroxene crystal is surrounded by a spongy aggregate of optically continuous clinopyroxene, opaque mineral and unidentified phases ; one weakly birefringent phase stains with methylene blue (Shand, 1939) and may be nepheline. The spongy aggregate is separated from the host basanite by a rim of titansalite optically similar to that of the basanite.

TABLE 2

Modal Analyses of Nombi Extrusives

All Modal Values are in volume percent

Rock Type	Basanite				
Specimen No.	747	721	743	749	720
Olivine	16	18	18	16	11
Clinopyroxene	42	42	40	36	45
Opaque	6	6	7	6	9
Plagioclase	4	5	12	14	7
Nepheline	15	29	23	28	27
Analcime	9				
Altered felsic mineral	8	—	—	—	—
Biotite	tr	tr	tr	tr	1

Glenrowan Intrusives (Table 3)

(*a*) Alkali dolerite. Crystals of Mg–rich olivine (Fa_{12} to Fa_{20} ; average Fa_{14}) and glomeroporphyritic aggregates of slightly titaniferous clinopyroxene constitute approximately 15 volume percent of the alkali dolerites. These may be products of crystallization at moderate pressures.

The remainder of the rock consists of phenocrysts of olivine (Fa_{21} to Fa_{26}), randomly oriented laths of plagioclase (An_{68} to An_{52}) and prisms of titanaugite ($\beta=1\cdot701$). The latter tend to group around the large crystals of Mg-rich olivine. Interstitial areas are filled with plagioclase, rarely alkali feldspar or partly devitrified glass, and minor analcime. A secondary zeolite is probably thomsonite. Approximately 40 percent of the grains of opaque oxide contain one or more lamellae of ilmenite.

Extensive alteration of olivine renders the alkali dolerites unsuitable for chemical analysis.

(*b*) Microsyenodolerite (denotes a medium grained intrusive rock equivalent to trachyandesite as defined by Coombs and Wilkinson, 1969). Three textural types of microsyenodolerite are recognized (*cf.* three textural types proposed by Walker, 1923 for teschenites from Scotland) each type representing a different degree of evolution of the Glenrowan magma.

TABLE 3

Modal Analyses of Glenrowan Intrusives

All Modal Values are in volume percent

Rock Type	Specimen No.	Olivine*	Clinopyroxene*	Opaques	Feldspar	Analcime	Altered felsic	Mesostasis	Felsic Evolved Phase
Alkali dolerite	889	16	36	6	35	7	—	—	—
	725	17	27	6	47	—	3	—	—
	934	16	20	4	55	—	5	—	—
	934	16	21	5	55	—	3	—	—
Basalt-type microsyenodolerite	906	18	21	7	50	4	—	—	—
	894	25	21	7	30	2	—	15	—
	884	21	17	4	55	2	—	—	1
	932	17	19	6	58	tr	—	—	tr
Dolerite-type microsyenodolerite	930	16	22	5	53	2	—	—	2
	891	12	23	5	46	14	—	—	—
	909	13	19	4	55	9	—	—	—
	905	11	16	5	56	12	—	—	—
Gabbro-type microsyenodolerite	857	10	13	9	68	—	—	—	—
	848	5	18	5	57	9†	—	6	—
	893	2	19	5	48	8	—	18	—

* Includes large resorbed crystals.
† Includes zeolites.

The most basic type, the *basalt-type microsyenodolerite*, differs from alkali dolerite in the absence of phases which may have crystallized at moderate pressures, and in the presence of an evolved felsic phase in interstitial portions of some specimens. Olivine ranges in core composition from Fa_{26} to Fa_{31}. Detailed work on the feldspar of specimen 884 indicates a continuous zoning in the laths from a core of labradorite (Or_3 Ab_{40} An_{57} weight percent[1]), through potash andesine (Or_9 Ab_{49} An_{42}) and lime anorthoclase, to rims of soda sanidine (Or_{44} Ab_{50} An_6).

More differentiated microsyenodolerites are characterized by an ophitic relationship between plagioclase and titanaugite. Olivine in these *dolerite-type microsyenodolerites* ranges in core composition from Fa_{26} to Fa_{31}. Interstitial portions of the rock typically contain small prisms and hook-shaped crystals of pyroxene, elongate grains of olivine (composition not determined) and cubes and dendritic crystals of opaque mineral, all included in a base of analcime ($n=1{\cdot}488$ to $1{\cdot}489$, clear, isotropic) and/or sanidine. In some specimens the interstitial phase is comprised solely of analcime and small laths and tabular crystals of sanidine.

The most evolved rocks of the Glenrowan Intrusives are *gabbro-type microsyenodolerites*. In these olivine (Fa_{36} to Fa_{66}) is minor and the more Fa-rich grains are markedly elongate parallel to *c*. Titanaugite grains display up to four oscillatory zones of varying titania content and a marginal rim of green soda salite. Feldspar 857 consists of twinned microphenocrysts, rarely of bytownite—An_{78} and commonly labradorite (average Or_6 Ab_{44} An_{50} weight percent), zoned to potash andesine, and joined abruptly by a ragged margin of untwinned sanidine. Groundmass feldspar includes small laths of plagioclase, equant crystals of anorthoclase and anhedral grains of soda sanidine (Or_{49} Ab_{45} An_6).

As in all the microsyenodolerites the opaque mineral is dominantly titanomagnetite with fine lamellae of ilmenite. In addition numerous small cubes and tabular crystals of ilmenite build skeletal grains and pyrite occurs as cubes either included in the titanomagnetite or as isolated grains.

Interstitial felsic-rich phases are prominent. Acicular crystallites of opaque mineral, spherulites of alkali feldspar, euhedral grains of a brown amphibole and acicular crystals (grouped in parallel arrangement) of an unidentified mafic mineral are present in some interstitial portions of the rocks. Rims of green soda salite on titansalite and discrete grains of soda salite or aegirine augite/aegirine are evident.

Labradorites of the Glenrowan Intrusives are high temperature, structurally disordered types. Values of $2\theta_{(131)}-2\theta_{(1\bar{3}1)}$ (Smith and Yoder, 1956) and $\Gamma 2\theta_{(220)}+2\theta_{(131)}-4\theta_{(1\bar{3}1)}$ (Smith and Gay, 1958) for labradorites 884 (An_{59}) and 857 (An_{54}) are $1{\cdot}99$ and $1{\cdot}96$, and $0{\cdot}92$ and $0{\cdot}86$, respectively.

---

[1] Feldspar compositions quoted as percentages of Or, Ab, An were calculated from values of CaO, Na_2O and K_2O determined by partial analysis of density fractions. On calculation of the An, Ab and Or contents, the total of feldspar components was greater than $98{\cdot}12$ weight percent in eight of the analyses, and equal to $97{\cdot}42$ in the ninth analysis. To evaluate the range of composition in each density fraction X-ray diffraction traces were run across the $(\bar{2}01)$ peak of each concentrate.

Napperby Limburgite (Table 4)

(*a*) Limburgite. Apart from the nodules and olivine xenocrysts, the limburgite consists of small euhedral grains of olivine (Fa_{17}) and titansalite, cubes of Fe-Ti oxide (a_0=8·376 Å), small laths of alkali feldspar and glass.

TABLE 4

Modal Analyses of the Napperby Limburgite (943 and 944) and Tambar Trachybasalt (936)

All Modal Values are in volume percent

Rock	943	944	936
Olivine	26	23	13
Clinopyroxene	38	35	23
Glass	31	35	—
Alkali feldspar	0	3	—
Opaque mineral	5	4	4
Feldspar zeolites	—	—	60

(*b*) Dunite nodules. Olivine of the nodules ranges in composition from Fa_9 to Fa_{14}; deformation bands subparallel to (100) and undulose extinction are evident. $\Delta 2\theta$ $olivine_{131}-2\theta$ $silicon_{111}$ equals 4·5° (Cu/Ni radiation), indicating an average composition of Fa_{10}. Olivine xenocrysts, broken from the nodules, constitute approximately 20 volume percent of the limburgite.

Tambar Trachybasalt (Table 4)

The trachybasalt is characterized by a high percentage of feldspar, including alkali feldspar. Partly resorbed crystals of olivine (Fa_{16}, Fa_{17}) are minor. Laths of labradorite, euhedral grains of titanaugite and ophitic and skeletal grains of Fe-Ti oxide are the essential constituents.

Bulga Complex (Table 5)

(*a*) Trachyandesite 946 contains minor resorbed and partly replaced intratelluric crystals of olivine (Fa_{35}, Fa_{36}), titaniferous augite, labradorite (An_{61} to An_{57}) and opaque mineral.

The remainder of the rock consists of titaniferous augite, laths of feldspar (labradorite An_{55-53} and potash andesine/potash oligoclase—β=1·551, 1·548), cubes of titanomagnetite (a_0=8·462 Å) with lamellae of ilmenite, minor olivine Fa_{49} and accessory apatite.

(*b*) Tristanite 941 contains minor intratelluric crystals of olivine (Fa_{52} to Fa_{61}) and inclusion-filled apatite. Apart from these, the rock consists of phenocrystal (Fa_{57}) and groundmass olivine, skeletal grains of acmitic titaniferous augite or salite and cubes of titanomagnetite (a_0=8·466 Å) with some lamellae of ilmenite. Alkali feldspar, consisting of equidimensional cores of lime anorthoclase (Or_{15} Ab_{59} An_{26} weight percent, β=1·540 to 1·536) surrounded by a sharply delineated rim of homogeneous sanidine (Or_{44} Ab_{50} An_6; β=1·532), is the predominant mineral. Isotropic analcime occurs interstitially; n=1·492, $\Delta 2\theta$ $analcime_{639}$ -2θ $silicon_{331}$=1·652°. Secondary zeolite, dominantly natrolite, is minor.

(*c*) Phonolitic trachyte and microsyenite. Microsyenite, in Old Bando Ridge and Mount Mullaley, is medium grained and hypidiomorphic granular. It consists of alkali feldspar (showing incipient exsolution and some complex twinning), colourless salite or light green soda salite (specimen 990—$Z \wedge c$=44 to 45°; β=1·710), opaque mineral, and very minor olivine. Pegmatoidal phases consist of alkali feldspar, aegirine augite, nepheline and isotropic analcime. Adjacent to these phases, magnetite is altered along {111} planes.

TABLE 5

Modal Analyses of Rocks from the Bulga Complex

All Modal Values are in volume percent

Rock Type	Trachy-andesite	Trist-anite	Phonolitic Trachyte			Phono-lite
Specimen No.	946	941	990	999	104	065
Olivine . .	6	11	—	4	3	—
Clinopyroxene	20	8	6	11	13	12
Opaque mineral . .	9	5	3	5	3	7
Feldspar . .	65	}76	91	80	81	}81*
Analcime . .	—		—	—	—	
Nepheline . .	—	—	—	—	—	

* Nepheline⩾20%.

By contrast, in phonolitic trachytes the alkali feldspar is optically homogeneous and dominantly sanidine (β=1·531, 1·530). Microphenocrysts, probably of lime anorthoclase (β=1·542 to 1·535), are prominent in porphyritic types such as Coogal Mountain. The rocks can be subdivided on the basis of the pyroxene.

Phonolitic trachyte 999 (Mount Talbareeya) consists of soda sanidine (Or_{42} Ab_{55} An_3 and Or_{47} Ab_{51} An_2 weight percent), soda salite (X-pale grass green, Y-pale grass green, Z-pale brown green; $Z \wedge c$=45 to 47°; β=1·715) rarely with cores of titaniferous salite, fayalitic olivine (microphenocrysts Fa_{86} and Fa_{87}) and an optically homogeneous magnetite or titanomagnetite (a_0=8·414 Å).

Phonolitic trachyte 104 (The Billies) is a soda sanidine–soda ferrosalite (X-green, brown green, Y-intense green, Z-brown, $Y>X>Z$; $Z\wedge c=51$ to 54° ; $\alpha=1\cdot719$, $\gamma=1\cdot745$; $2V\gamma=62$ to 63°)—fayalitic olivine rock. The olivine is distinctly yellow, $DR\approx0\cdot05$, well developed cleavage parallel to (010) ; value of $\Delta2\theta$ $\text{olivine}_{131}-2\theta$ silicon_{111} is beyond the value given by Yoder and Sahama (1957) for Fa_{100}.

Phonolitic trachytes constituting Mundry Hills and Mount Baloola are exceptionally fine grained and consist of sanidine, soda hedenbergite ($Z\wedge c=56$ to 62° ; $\beta=1\cdot750$), yellow Fa-rich olivine, minor nepheline and opaque oxide.

(*d*) Phonolite. The phonolites consist essentially of slender laths of sanidine ($\beta=1\cdot528$) and minor lime anorthoclase ($\beta=1\cdot534$, $1\cdot532$), and smaller tabular grains of nepheline euhedral towards aegirine augite (X–brown, Y–green brown, Z–intense green, $Z>Y=X$; $\beta=1\cdot770$, $\gamma=1\cdot789$ Ratz Castle 065 and Mount Nombi ; $\gamma-\alpha<0\cdot04$; $Z\wedge c$ increasing from 53° to at least 74° as the acmite component increases[1]). Aegirine (faint brown to near colourless ; $Z\wedge c=79°$ to 90°, commonly 88° to 90° ; $\gamma-\alpha>0\cdot045$) occurs as very small tabular crystals adjacent to interstitial analcime. Magnetite is partially altered along {111} planes to hematite. Preferential replacement of either the alkali feldspar or the nepheline by natrolite is widespread.

Analcime syenite, consisting of alkali feldspar, analcime and minor soda pyroxene, occurs as schlieren in the phonolite of Carthian Hill. Analcime syenite also constitutes the core of the Mount Bulga plug dome. The latter rock (069) is hypidiomorphic granular and comprised essentially of alkali feldspar, analcime (isotropic ; $n=1\cdot488$ to $1\cdot490$; $\Delta2\theta$ $\text{analcime}_{639}-2\theta$ $\text{silicon}_{331}\simeq1\cdot680°$) and soda salite (X–light green, very dark green, Y–light brownish green, brownish green, Z–brown, light brown, dark brown, $Z=Y>X$; $\beta=1\cdot713$, $1\cdot714$; $Z\wedge c=47$ to 53°). The latter mineral varies in colour intensity irregularly within and between grains. Marginal zones with $\beta=1\cdot729$ and small discrete grains occurring adjacent to analcime are aegirine augite. Nepheline and apatite are minor and natrolite of late magmatic origin is prominent as the replacement product of the felsic minerals.

Phonolite 078 from Mount Bulga, which is regarded as the final liquid in the differentiation process, consists of irregular laths of alkali feldspar and euhedral grains of nepheline ($\simeq35$ volume percent). A green pyroxene occurs in the lens-shaped zones in the rock. Magnetite virtually lacks any alteration to hematite.

(*e*) Intratelluric crystals in the phonolitic trachytes and phonolites. Intratelluric crystals of alkali feldspar, olivine, amphibole, inclusion-filled apatite and opaque oxide are rare in the phonolitic trachytes. By contrast, crystals of alkali feldspar ($\beta=1\cdot533$ to $1\cdot528$; extensively altered to kaolinite and/or zeolites and showing incipient exsolution) constitute up to 35 volume percent of some specimens of phonolite (e.g. The Pinnacle phonolite) ; minor quantities of kaersutite, opaque oxide and inclusion-filled apatite occur in the majority of specimens.

Single crystals of kaersutite measure up to 4 mm in length, are strongly pleochroic (X–light yellow to pink brown, Y–intense reddish brown, Z–greenish brown, $Y>Z>X$), $\alpha=1\cdot683$, $\beta=1\cdot699$, $2V_\alpha=75\pm5°$, $Z\wedge c=0°$ and $\gamma-\alpha<0\cdot04$. Compositional zoning is indicated by marked changes in colour. The majority of the crystals are completely pseudomorphed by an aggregate of aegirine augite and magnetite altering to hematite. By contrast, aggregates of similar origin in the phonolitic trachytes consist of soda salite or soda ferrosalite and magnetite.

Chemistry

Chemical analyses and norms of igneous rocks from the Mullaley area are listed in Tables 6 to 8. As noted previously some rock types are too altered for meaningful analysis. In distinguishing the different groups of rocks, the significant parameters are found to be K_2O, $Fe_2O_3 : FeO+Fe_2O_3$ and Al_2O_3.

In distinguishing lineages the present author regards it as important that K_2O and Na_2O levels be considered separately ; on the commonly used plot of K_2O versus Na_2O the distinctive feature of a particular lineage is often masked by the level of the other oxide. It is surely genetically significant that in the ten alkaline lineages plotted on Figures 1 and 2, the range of K_2O in the basic rocks is greater than the range of Na_2O in the same rocks. This difference in the behaviour of K_2O and Na_2O during genesis of a parental basic magma is evident in the Mullaley rocks where all groups, except the Tambar Trachybasalt, are average-Na types (definitions of terms low-, average-, moderately high- and high- are given in captions of Figures 1 and 2). The K_2O values of the rock

---

[1] From study of the optical properties of a number of analysed specimens of aegirine augite it is concluded that $Z\wedge c$ and $\gamma-\alpha$ can be valid indicators of the percentage acmite component in a soda pyrexene ; the Bulga aegirine augites are generally too fine grained for measurement of 2V and sign.

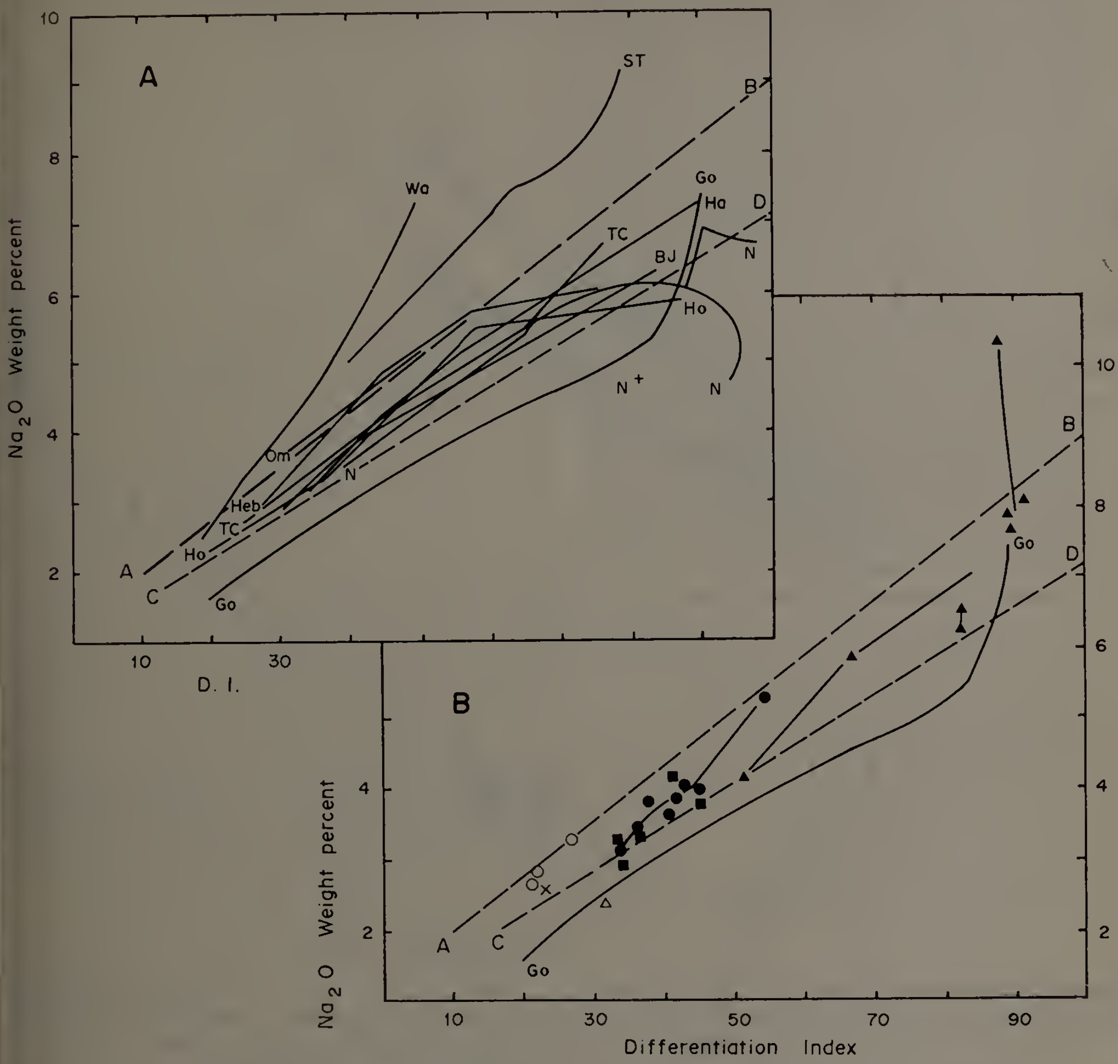

Figure 1A.—Generalized trend lines for Na_2O values versus differentiation index in ten alkaline and mildly alkaline lineages. Wa—theralites from Lake Waihola, East Otago (Coombs and Wilkinson, 1969); ST—Square Top intrusion, Nundle, N.S.W. (Wilkinson, 1965); Om—nepheline basanites and associated pegmatoids from Omimi, East Otago (Coombs and Wilkinson, 1969); Heb—Hebridean alkaline province (Tilley and Muir, 1962, Table 2, Nos. 1 and 2; Muir and Tilley, 1961, Table 4, Nos. 1, 2 and 10); TC—lavas from Tristan da Cunha (Baker *et al.*, 1964); Ha—Hawaiian mildly alkaline province (averages; Macdonald and Katsura, 1964, Table 10); Ho—alkali basalt→hawaiite→mugearite→trachyte lineage from the Hocheifel province (Huckenholz, 1965*a*); N—Nandewar Volcano (Abbott, 1969); BJ—Black Jack sill near Gunnedah (Wilkinson, 1958); Go—lavas from Gough Island (Le Maitre, 1962). Line AB constructed through points $Na_2O=9\%$, D.I. = 100 and $Na_2O=2\%$, D.I. = 10. Line CD constructed through points $Na_2O=5\cdot35\%$, D.I. = 70 and $Na_2O=2\cdot25\%$, D.I. = 20. Lineages with Na values falling in area A-B-C-D are regarded as average-Na lineages, those plotting below CD as low-Na lineages, and those above AB as high-Na lineages.

Figure 1B.—Plot of Na_2O values versus differentiation index for analysed specimens from the Mullaley area. Solid circles—Garrawilla Volcanics; open circles—Nombi Extrusives; solid squares—Glenrowan Intrusives; cross—Napperby Limburgite; open triangle—Tambar Trachybasalt; solid triangles—Bulga Complex. Lines AB and CD and Go as in Figure 1A.

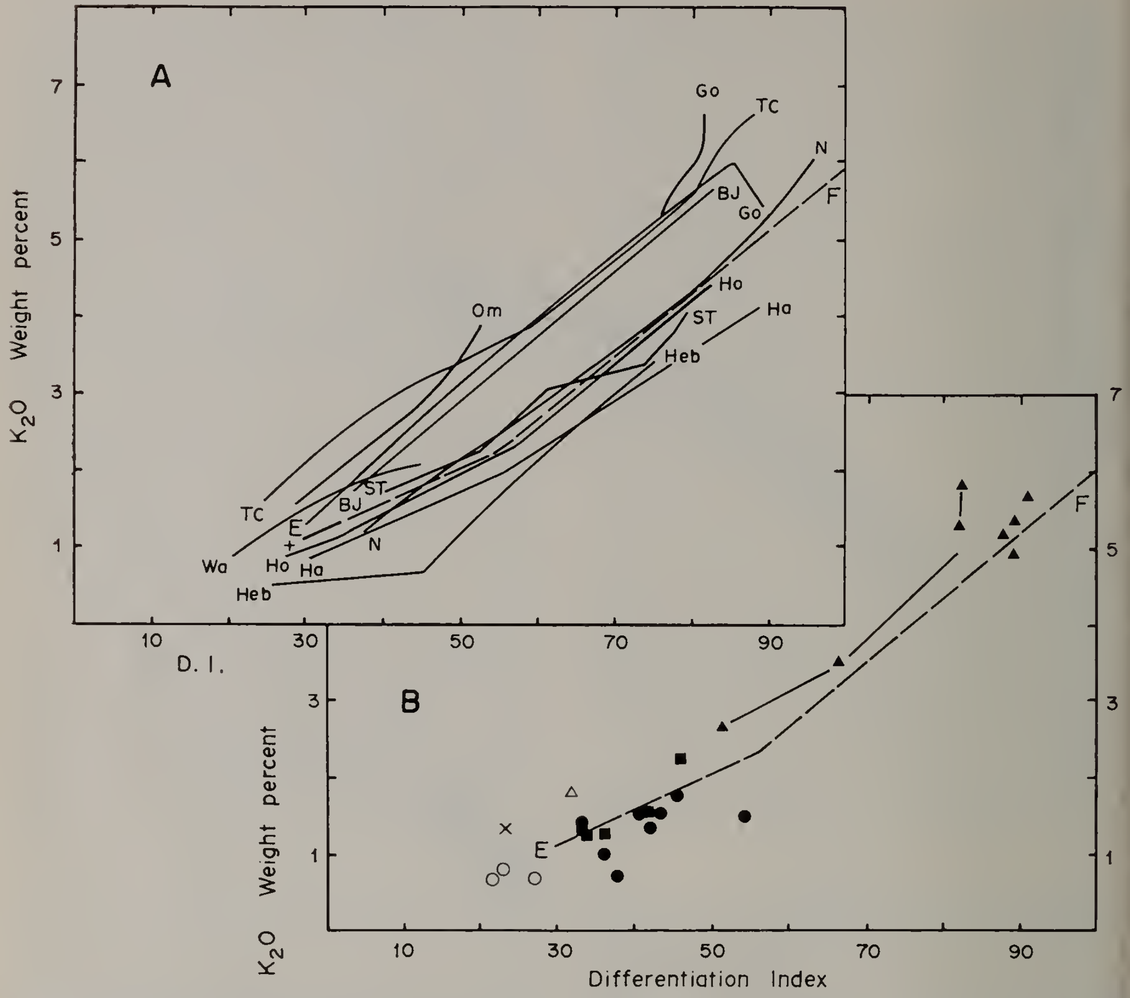

FIGURE 2A.—Generalized trend lines for K_2O values versus differentiation index in ten alkaline and mildly alkaline lineages. Cross—Hawaiian basanite (average; Macdonald and Katsura, 1964, Table 10). Other symbols as in Figure 1A. Line EF constructed to separate lineages regarded as low-K lineages (below) from those regarded as moderately high- and high-K lineages (above EF).

FIGURE 2B.—Plot of K_2O values versus differentiation index for analysed specimens from the Mullaley area. Symbols as in Figure 1B. Line EF as in Figure 2A.

groups range from low in the Garrawilla Volcanics and Nombi Extrusives, to moderately high in the Glenrowan Intrusives and possibly the Bulga complex, to high in the Napperby Limburgite and Tambar Trachybasalt.

The distinction between low–K and moderately high–K lineages at the line EF in Figure 2 correlates with the feldspar mineralogy of the rocks. Lineages classified as low–K lineages correspond to those of Coombs and Wilkinson (1969) in which $Na_2O : K_2O$ ratios exceed 2 : 1; the rocks are one feldspar types, there is generally a continuous range in composition from labradorite in the basalts to anorthoclase in the trachytes; sanidine is absent. By contrast, lineages which plot above line EF feature intermediate rocks which are two feldspar types—plagioclase in association with sanidine, and more evolved rocks in which sanidine is the sole feldspar.

In evaluating Fe in the Mullaley lineages a plot in an AFM diagram is not distinctive; all three lineages are high-Fe types. By contrast, $Fe_2O_3 : FeO + Fe_2O_3$ plotted against D.I. (Figure 3) is significant; the high $Fe_2O_3 : FeO + Fe_2O_3$ ratios of the Garrawilla lineage distinguish

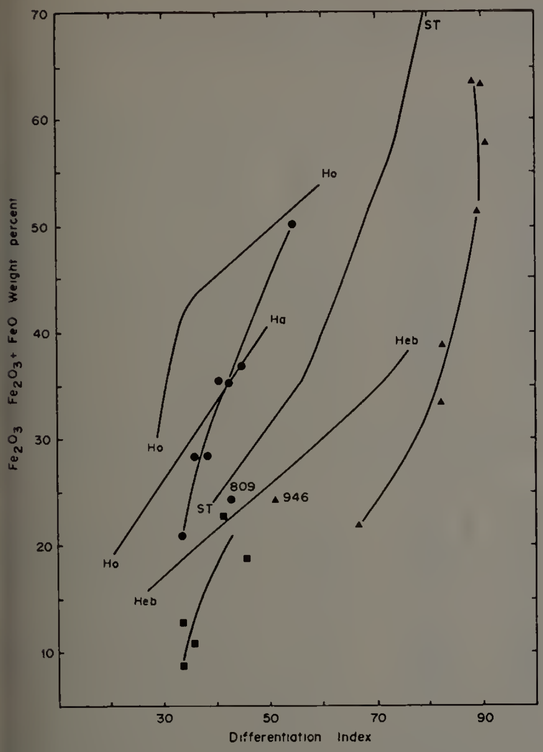

FIGURE 3.—Plot of $Fe_2O_3 : FeO+Fe_2O_3$ against differentiation index for analysed specimens from Mullaley. Symbols as in Figure 1B. Hawaiite 809 and Trachyandesite 946 are anomalous. Generalized trend lines for Hocheifel (Ho), Hawaiian mildly alkaline (Ha), Square Top (ST) and Hebridean alkaline (Heb) lineages included for comparison.

these rocks from those of the Glenrowan Intrusives and Bulga Complex which possess low ratios.

A third parameter found to be critical in assessing the Mullaley rocks is Al_2O_3 plotted against D.I. As seen in Figure 4 the Garrawilla Volcanics can be regarded as average-Al rocks, the Tambar Trachybasalt as a high-Al rock and the Nombi Extrusives, Napperby Limburgite and Glenrowan Intrusives as low-Al rocks.

Garrawilla Volcanics

From the limited range of rock types suitable for chemical analysis (Table 6), it is proposed that the Garrawilla Volcanics constitute a mildly alkaline (Coombs, 1963), low-K, average-Na, average-Al, high-Fe lineage.

This lineage differs from the mildly alkaline lineage at Hawaii (Macdonald and Katsura, 1964) only in its $Fe_2O_3 : FeO+Fe_2O_3$ ratios (Figure 3). The high and rapidly increasing $Fe_2O_3 : FeO+Fe_2O_3$ ratio of the lavas is regarded as a primary magmatic feature reflecting a build up of volatiles in the lavas with increasing evolution. The high percentage of modal magnetite in the hawaiites and mugearites, and the tendency of the lavas, particularly the felsic types, to be vesicular or to erupt explosively, support the proposal that the high Fe_2O_3 was a magmatic feature and not the result of post crystallization oxidation. Also pyroxene is minor and biotite constitutes up to 1·5 volume percent of the hawaiites and mugearites.

In the absence of chemical analyses of the soda trachytes, it is proposed that these rocks may be Si-saturated types containing *hy*. In accord with Osborn (1959, 1960), it is probable that the extensive precipitation of titanomagnetite in the hawaiites and mugearites would have allowed a build-up of Si in the more evolved lavas. If so, the delicate balance of the Garrawilla lineage astride the thermal ridge (located experimentally at low pressures along

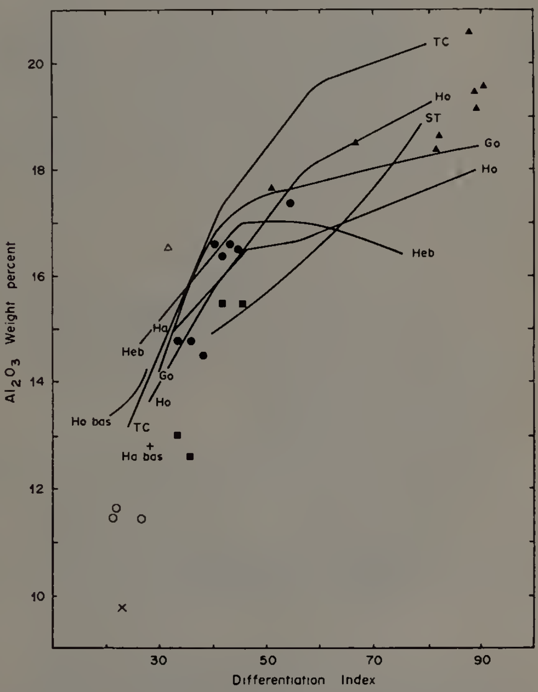

FIGURE 4.—Generalized trend lines for Al_2O_3 values against differentiation index for six alkaline and mildly alkaline lineages. Ho bas—basanites from the Hocheifel province (Huckenholz, 1965*b*); Ha bas—Hawaiian basanite (average; Macdonald and Katsura, 1964, Table 10). Other symbols as in Figure 1A. Analysed specimens from Mullaley plotted as individual points. Note low-Al values of the Napperby Limburgite (cross), Nombi Extrusives (open circles) and Glenrowan Intrusives (solid squares), and the high-Al value of the Tambar Trachybasalt (open triangle).

TABLE 6

Analyses of Rocks from the Garrawilla Volcanics and Nombi Extrusives, Mullaley Area, N.S.W.

	1	2	3	4	5	6	7	8	9	10	11	11a	12	12a
SiO_2 ..	45·91	46·58	47·89	47·84	48·23	47·33	48·03	48·90		41·75	41·01	41·01	43·43	43·43
TiO_2 ..	2·40	2·15	2·05	3·03	2·40	2·95	3·10	2·33		2·45	2·30	2·30	2·50	2·50
Al_2O_3 ..	14·80	14·80	14·53	16·60	16·40	16·60	16·50	17·38		11·62	11·46	11·46	11·42	11·42
Fe_2O_3 ..	2·78	3·31	3·23	4·52	3·97	2·86	4·73	6·48		3·20	5·72	3·00	4·17	3·00
FeO ..	10·37	8·32	8·03	8·17	7·27	8·86	8·03	6·41		9·50	8·27	10·72	8·35	9·40
MnO ..	·17	·14	·14	·15	·13	·13	·15	·14		·14	·14	·14	·17	·17
MgO ..	8·39	7·83	7·60	4·90	6·00	4·50	4·90	3·51		11·60	11·70	11·70	10·53	10·53
CaO ..	8·60	8·80	8·70	7·75	7·95	8·60	7·00	5·65		11·56	10·68	10·68	10·75	10·75
Na_2O ..	3·14	3·50	3·87	3·66	3·90	4·05	3·97	5·33	8·10	2·85	2·70	2·70	3·30	3·30
K_2O ..	1·39	·98	·73	1·55	1·40	1·55	1·80	1·52	2·82	·70	·80	·80	·70	·70
P_2O_5 ..	·65	·79	·75	·50	·70	1·26	·52	·82		·82	·56	·56	·66	·66
H_2O^+ ..	1·59	2·06	1·76	1·41	1·27	1·01	·50	1·18		2·93	3·72	3·72	2·66	2·66
H_2O^- ..	·12	·61	·57	·19	·41	·21	·40	·22		·56	·94	·94	·99	·99
Total ..	100·31	99·87	99·85	100·27	100·03	99·91	99·63	99·87		99·68	100·00	99·73	99·63	99·51
					Norms							Norms		
Or ..	8·21	5·79	4·31	9·16	8·27	9·16	10·64	8·98		4·14	4·73	4·73	4·14	4·14
Ab ..	22·74	28·97	32·74	30·97	33·00	31·61	33·59	43·83		8·14	10·09	6·74	15·80	14·37
An ..	22·19	21·78	20·13	24·30	23·12	22·55	21·90	19·02		16·85	16·79	16·79	14·29	14·28
Ne ..	2·07	·35	—	—	—	1·44	—	·69		8·66	6·91	8·73	6·57	7·34
Di ..	13·23	13·51	14·66	8·83	9·47	9·77	7·64	2·93		28·25	25·89	26·29	27·78	27·99
Hy ..	—	—	1·13	5·30	1·71	—	1·87	—		—	—	—	—	—
Ol ..	20·06	16·08	14·23	6·65	10·84	11·49	9·15	7·31		18·97	16·97	21·78	15·08	17·11
Mt ..	4·03	4·80	4·68	6·55	5·75	4·15	6·86	9·39		4·64	8·29	4·35	6·04	4·35
Ap ..	1·52	1·84	1·75	1·17	1·63	2·94	1·21	1·91		1·91	1·31	1·31	1·54	1·54
Il ..	4·56	4·08	3·89	5·75	4·56	5·60	5·89	4·43		4·65	4·37	4·37	4·75	4·75
Total ..	100·32	99·87	99·85	100·28	100·03	99·93	99·65	99·89		99·70	100·01	99·75	99·64	99·52
D.I. ..	33·5	36·1	38·0	40·7	42·0	42·8	44·8	54·3		21·8	22·8	21·2	27·6	27·0
Normative $\frac{An \times 100}{Ab+An}$	49·4	42·9	38·1	44·0	41·2	41·6	39·5	30·3		67·4	62·5	71·4	47·5	49·9

1. Garrawilla hawaiite transitional to basalt (924)
2. Garrawilla hawaiite transitional to basalt (724)
3. Garrawilla hawaiite transitional to basalt (723)
4. Garrawilla hawaiite (716)
5. Garrawilla hawaiite (758)
6. Garrawilla hawaiite (809)
7. Garrawilla hawaiite (717)
8. Garrawilla hawaiite transitional to mugearite (757)
9. Non-scoriaceous buff coloured lapilli tuff/volcanic agglomerate (845)—soda trachytic composition.
10. Nombi basanite (721)
11. Nombi basanite (748). Analyst G.I.Z. Kalocsai.

11a. Nombi basanite (748) recalculated with Fe_2O_3 equal to 3 weight percent.

12. Nombi nepheline hawaiite (720).

12a. Nombi nepheline hawaiite (720) recalculated with Fe_2O_3 equal to 3 weight percent.

Analyses 1–10 and 12 by J. M. Bean.

the plane of critical undersaturation in the basalt tetrahedra) would have been lost and Si-saturated liquids evolved.

Nombi Extrusives

The Nombi basanites are moderately strongly undersaturated, low-K, low-Al, low total alkalis rocks (Table 6). They differ significantly from the basanites of Hawaii (Macdonald and Katsura, 1964) and Hocheifel (Huckenholz, 1956*b*) in their low-Al and low total alkalis. It is proposed that this unusual chemistry could be the result of accumulation in a basanitic magma of crystals of olivine and clinopyroxene, fractionated from a larger body of basanitic magma at pressures of ≈9 kb. In fact, if 10 weight percent of olivine and clinopyroxene, in a ratio of either 1 : 1 or 1 : 2 (compositions used are those of olivine and clinopyroxene which precipitated from an alkali olivine basalt

TABLE 7

Analyses of Glenrowan Intrusives, the Napperby Limburgite and the Tambar Trachybasalt from the Mullaley Area, N.S.W.

	1	2	3	4	5	6	7	8
SiO_2		46·65	46·73	47·55	48·90	47·36	42·23	45·74
TiO_2		2·60	2·40	2·45	2·23	2·80	2·45	2·00
Al_2O_3		13·00	13·00	12·60	15·50	15·50	9·80	16·55
Fe_2O_3		1·68	1·10	1·25	2·16	2·61	3·56	4·16
FeO		11·45	11·84	10·22	9·18	8·86	8·68	7·06
MnO		·20	·20	·14	·13	·15	·15	·17
MgO		9·05	9·75	8·45	5·70	4·30	16·40	7·20
CaO	9·40	8·30	8·10	9·30	7·30	9·30	9·70	9·70
Na_2O	2·24	2·98	3·26	3·36	3·83	4·17	2·60	2·38
K_2O	1·15	1·32	1·27	1·30	2·24	1·55	1·33	1·81
P_2O_5		·57	·58	·82	·77	·50	·71	·71
H_2O^+		1·72	1·26	2·47	1·35	2·41	1·28	2·06
H_2O^-		·44	·28	·29	·38	·45	·65	·67
Total		99·96	99·77	100·20	99·67	99·96	99·54	100·21
				Norms				
Or		7·80	7·51	7·68	13·24	9·16	7·86	10·70
Ab		24·87	23·39	25·53	30·34	26·12	5·42	20·14
An		18·20	17·09	15·47	18·49	19·01	11·15	29·14
Ne		·19	2·27	1·57	1·12	4·96	8·98	—
Di		15·74	15·79	20·67	10·43	19·69	25·71	11·52
Hy		—	—	—	—	—	—	3·14
Ol		22·31	24·68	18·16	15·17	7·90	27·03	11·38
Mt		2·44	1·59	1·81	3·13	3·78	5·16	6·03
Ap		1·33	1·35	1·91	1·79	1·17	1·66	1·66
Il		4·94	4·56	4·65	4·24	5·32	4·65	3·80
Total		99·98	99·77	100·21	99·68	99·97	99·55	100·24
D.I.		33·6	33·8	35·7	45·6	41·4	22·8	31·6
Normative $\frac{An \times 100}{Ab+An}$		42·3	42·2	37·7	37·9	42·1	67·3	59·1

1. Glenrowan alkali dolerite (725)
2. Glenrowan basalt-type microsyenodolerite (932)
3. Glenrowan basalt-type microsyenodolerite (884)
4. Glenrowan dolerite-type microsyenodolerite (930)
5. Glenrowan gabbro-type microsyenodolerite (857)
6. Glenrowan gabbro-type microsyenodolerite (848)
7. Napperby Limburgite (944)
8. Tambar Trachybasalt (936)

Analyses 1–8 by J. M. Bean.

composition at 9 kb and 1,220°C ; Green and Ringwood, 1967), is subtracted from the Nombi basanite average composition the resulting composition is very close to that of the average Hawaiian basanite. To test the feasibility of this proposal detailed microprobe work on the megacrysts of olivine and clinopyroxene in the basanites is required.

Both the complete isolation of some outcrops of basanitic rock from all outcrops of Garawilla Volcanics, and the greater than five percent *ne*, suggest that it is unlikely that the basanitic magma was derived from the Garrawilla magma by any direct fractionation process (Green and Ringwood, 1967).

Glenrowan Intrusives

The alkali dolerites and microsyenodolerites of the Glenrowan Intrusives constitute a mildly undersaturated, moderately high- to high-K, low-Al, low total alkalis, low-Fe_2O_3 : FeO lineage (Table 7). The low Fe_2O_3 : FeO+Fe_2O_3 ratios indicate a low oxygen fugacity in the magmas. A low percentage of titanomagnetite (relative to that in Garrawilla lavas of similar D.I.) and continued crystallization of olivine into evolved rock types are in accord with such conditions. Evolved phases of the microsyenodolerites, containing analcime, aegirine augite and no olivine, indicate a higher oxygen fugacity in the final stage of fractionation.

TABLE 8

Analyses of Rocks from the Bulga Complex, Mullaley Area, N.S.W.

	1	2	3	4	5	6	7	8	9	10
SiO_2	49·35	52·15	57·62	57·89		59·28	57·53	56·40	57·90	
TiO_2	1·20	·74	·48	abs		abs	abs	abs	abs	
Al_2O_3	17·65	18·52	18·39	18·67		19·19	19·58	19·48	20·60	
Fe_2O_3	2·76	2·20	2·32	2·68		3·32	2·69	2·26	2·05	
FeO	8·60	7·81	4·61	4·21		1·91	1·94	2·12	1·17	
MnO	·13	·15	·15	·15		·13	·09	·17	·16	
MgO	3·43	1·76	·18	·02		·07	·12	·25	·02	
CaO	6·58	4·07	2·30	2·36		1·52	1·25	1·30	1·15	
Na_2O	4·17	5·85	6·55	6·27	6·45	7·70	8·10	8·87	10·40	9·17
K_2O	2·66	3·52	5·30	5·83	5·50	5·33	5·68	4·95	5·18	5·22
P_2O_5	1·03	1·05	·19	·09		abs	abs	abs	abs	
H_2O^+	2·12	1·89	1·39	1·74		1·58	2·46	3·41	·95	
H_2O^-	·33	·29	·41	·17		·30	·22	·33	·16	
Total	100·01	100·00	99·89	100·08		100·33	99·66	99·54	99·74	
					Norms					
Or	15·72	20·80	31·32	34·45		31·50	33·57	29·25	30·61	
Ab	32·99	38·46	42·06	39·01		46·50	38·87	36·57	31·56	
An	21·59	13·33	5·14	5·59		2·07	·30	—	—	
Ne	1·24	5·98	7·24	7·61		10·10	16·07	19·55	24·69	
Cor	—	·20	—	—		—	—	—	—	
Ac	—	—	—	—		—	—	2·11	5·93	
Na met.	—	—	—	—		—	—	—	·96	
Di	3·61	—	4·44	4·92		2·27	3·48	5·59	4·71	
Wo	—	—	—	—		1·20	·79	—	·17	
Hy	—	—	—	—		—	—	—	—	
Ol	13·73	12·02	3·18	2·49		—	—	·51	—	
Mt	4·00	3·19	3·36	3·88		4·81	3·90	2·22	—	
Ap	2·40	2·45	·44	·21		—	—	—	—	
Il	2·28	1·41	·91	—		—	—	—	—	
Total	100·01	100·02	99·89	100·07		100·33	99·66	99·54	99·74	
D.I.	51·2	66·7	82·2	82·6		89·5	91·3	89·1	88·1	
Normative $\frac{An \times 100}{Ab+An}$	39·6	25·7	10·9	12·5		4·3	0·8	0·0	0·0	

Analyses 1–10 by J. M. Bean.

1. Trachyandesite (946), small dome east of Wyuna homestead.
2. Tristanite (941), Bullomins Knob on Bando Station.
3. Phonolitic trachyte (999), Mount Talbareeya.
4. Phonolitic trachyte (104), The Billies.
5. Phonolitic trachyte (031), small quarry east of Kyndalyn homestead.
6. Phonolite (065), Ratz Castle.
7. Phonolite (074), Mount Bulga.
8. Analcime syenite (069), Mount Bulga.
9. Fine grained phonolite (078), Mount Bulga.
10. Fine grained phonolite (079), Mount Bulga.

The composition of the Glenrowan magmas, prior to their *in situ* differentiation in sills at shallow depths, may be the result of fractionation of the magmas deep within the crust ($P \leqslant 9$ kb). The low-Al, low total alkalis and low normative plagioclase values of the rocks correlate with the high percentage of large crystals of Mg-rich olivine and slightly titaniferous clinopyroxene seen in the alkali dolerites. In the more differentiated Glenrowan rocks similar crystals are not visible, but the chemical character of the rocks suggests that such crystals may have been present; with the longer time required for fractionation the crystals could have been completely assimilated by the magma.

Napperby Limburgite

The Napperby Limburgite, with its high content of dunite nodules, strong degree of undersaturation and high-K value (Table 7) is unique in the Mullaley area.

Calculations (Table 9, No. 2) using the composition of olivine from a dunite (atomic ratio Mg : Fe^{2+}=91·1 : 8·9 ; Deer, Howie and Zussman, 1962) and an alkali olivine basalt composition (Green and Ringwood, 1967), indicate that O'Hara's (1968) proposal (that lherzolite fractionation can produce crystal/liquid mixtures with strongly undersaturated compositions) is not an acceptable mechanism for genesis of the Napperby Limburgite.

By contrast, the limburgitic composition may have been derived by the inclusion, in a basanitic magma derived at depth by partial melting, of ≈20 weight percent residual mantle material (Table 9, No. 3). However, the high-K value excludes a direct genetic link between the Nombi basanitic magma and a basanite able to produce the Napperby Limburgite.

Tambar Trachybasalt

As indicated in Table 7 the Tambar Trachybasalt is a mildly undersaturated[1], high-K, low-Na, Al-rich rock. It is almost identical in major element chemistry to the high alumina liquid obtained by Green and Ringwood (1967, Table 15) by fractionation in an alkaline basaltic liquid at 9 kb and 1,220°. In the Tambar rock, the presence of very minor resorbed crystals of olivine and a low TiO_2 content (removal of titaniferous clinopyroxene) suggest the operation of a similar fractionation process in derivation of the Al-rich magma. The initial alkaline olivine basalt magma would need to have possessed a high-K value.

Bulga Complex

From the limited range of rock types found in outcrop it is proposed that rocks of the Bulga Complex constitute a mildly undersaturated moderately high-K, average-Na, high-Fe lineage (Table 8), similar to lineage F as proposed by Coombs and Wilkinson (1969).

Both the dominance of evolved rock types and the restricted areal extent of outcrop of the Complex, suggest that a " cupola " or " high " in a large magma chamber existed beneath the area of outcrop. Fractionated liquids from throughout the large chamber could have migrated to such a " high " prior to their extrusion.

The phonolitic trachytes and phonolites represent dual fractionation trends. The phonolites crystallized from liquids fractionating towards strong Na-enrichment, and increasing degree of undersaturation ; by contrast, the phonolitic trachytes crystallized from liquids fractionating towards K-enrichment at a fairly constant degree of undersaturation. The former trend occurred under hydrous, peralkaline conditions and oxygen fugacities either higher than, or at least decreasing at a slower rate than, those under which the phonolitic trachyte trend occurred (supported by occurrence, composition and modal percentage of olivine, pyroxene, magnetite and analcime). The phonolitic trachytes crystallized in anhydrous conditions with oxygen fugacities, either lower than or decreasing at a more rapid rate than in the phonolitic trend (*cf.* Nash and Wilkinson, 1970). It may be significant that the phonolites occur in endogenous lava domes within which the volatiles were contained during crystallization ; by contrast, the phonolitic trachytes occur as flows and exogenous domes.

TABLE 9

Calculated Compositions Relevant to Genesis of the Napperby Limburgite

	1	2	3
SiO_2	43·3	44·6	42·9
TiO_2	2·5	2·0	2·1
Al_2O_3	10·0	11·8	10·1
Fe_2O_3	3·6	1·5	2·7
FeO	8·9	11·6	10·2
MnO	·2	·2	·2
MgO	16·8	18·2	18·5
CaO	9·9	7·3	9·7
Na_2O	2·7	2·1	2·4
K_2O	1·4	·6	·7
P_2O_5	·7	·2	·6
Or	8·3	3·5	3·9
Ab	5·2	15·7	5·8
An	11·0	21·0	14·7
Ne	9·5	1·1	8·0
Di	26·7	11·2	23·7
Ol	27·7	41·1	34·7
Mt	5·2	2·2	3·9
Il	4·8	3·8	4·0
Ap	1·6	·5	1·3
D.I.	23	20	18

1. Napperby Limburgite calculated anhydrous.
2. Alkali olivine basalt composition as used by Green and Ringwood (1967) in experimental runs, plus 25 weight percent of olivine. Olivine composition No. 6, Table 2. Deer *et al.* (1962).
3. Average Nombi basanite plus 20 weight percent olivine. Composition of olivine as for 2.

---

[1] The small percentage of *hy* in this rock is very probably the result of post-magmatic oxidation. The modal percentage of opaque mineral is low (3·9) and thus it is unlikely that the high percentage of Fe_2O_3 (4·16) in the chemical analysis, represents magmatic Fe_2O_3.

A plot of the phonolites in Petrogeny's Residua System at $P_{H_2O}=1{,}000$ bars (Fudali, 1963) indicates that the rocks plot in the thermal deep in the undersaturated portion of the system (Figure 5). The most evolved phonolite 078 plots close to the minimum melting composition at 750±7°C. As there is no thermal deep in a similar portion of this system under anhydrous conditions (Schairer, 1957) the trend in the phonolitic trachytic liquids towards the Or-Ks side of the system (K-enrichment trend) is as expected.

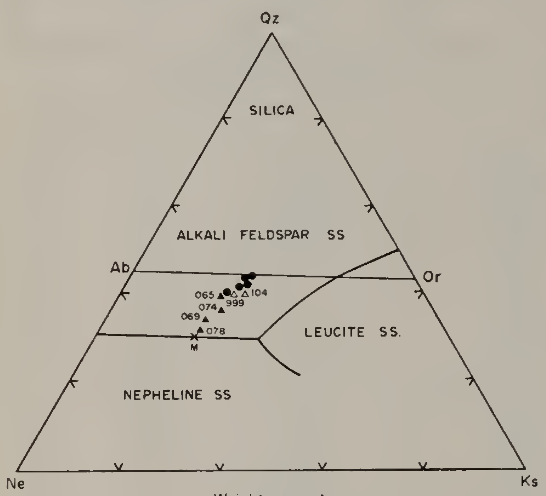

Figure 5.—Plot of normative salic constituents (less anorthite) of the Bulga Complex phonolitic trachytes (open triangles), the Bulga Complex phonolites (solid triangles) and the Gough Island aegirine augite trachytes (solid circles) (Le Maitre, 1962) in the system Ne-Ks-Qz (weight percent). The boundary curves, M—minimum on the liquidus surface along the nepheline-alkali feldspar boundary curve, are taken from Fudali (1963, Figure 1). Liquidus relationships were determined in part of the Ne-Ks-Qz-H_2O system at P_{H_2O} of 1,000 bars and the data projected onto the anhydrous base of the tetrahedron.

A similar divergence of fractionation trends in the late stage of fractionation of an alkaline magma is evident in the Gough Island (Le Maitre, 1962) and Nandewar (Abbott, 1969) sequences (Figures 5 and 6). In all three lineages a strong Na-enrichment trend only occurs under hydrous conditions.

Conclusions

Division of igneous rocks cropping out in the Mullaley area into six groups is further validated by detailed petrography, mineralogy and chemistry.

1. The Garrawilla Volcanics, of late Triassic/early Jurassic age, constitute a mildly alkaline, low-K, high $Fe_2O_3:FeO$ lineage; the alkali olivine basalts, alkali basalts, hawaiites and mugearites are characterized by one feldspar—a plagioclase, and the soda trachytes by anorthoclase; titanomagnetite is abundant in intermediate rock types and the tendency to erupt explosively increased markedly with increasing evolution of the lavas.

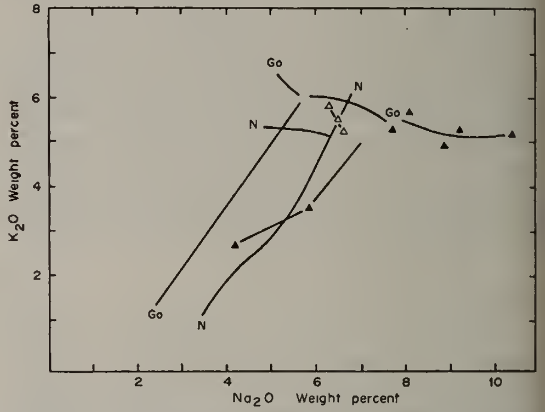

Figure 6.—Generalized trend lines for variation of K_2O against Na_2O for rocks from Gough Island (Go), Nandewar Volcano (N) and the Bulga Complex, Mullaley (triangles). Bulga phonolitic trachytes—open triangles.

2. The Nombi Extrusives, of similar late Triassic/early Jurassic age, are moderately strongly undersaturated, low-K, low-Al, low total alkalis basanites; analcime and nepheline are prominent constituents.

3. The Glenrowan Intrusives are distinguished as mildly undersaturated, moderately high- to high-K alkali dolerites and microsyenodolerites, with low-Al, low total alkalis and low $Fe_2O_3:FeO+Fe_2O_3$ ratios; sanidine is prominent in the microsyenodolerites, in association with plagioclase, and occurs as the sole feldspar in the evolved felsic phases. The modal percentage of opaque mineral is lower than in the Garrawilla Volcanics and olivine ranges continuously in composition to at least Fa_{66}.

4. The Napperby Limburgite is a unique rock type characterized by high-K and a strong degree of undersaturation. Xenocrystic olivine is prominent.

5. The Tambar Trachybasalt is distinguished by high-K, low-Na, mild degree of undersaturation, high-Al and high total alkalis.

6. The Bulga Complex is dominated by the evolved rock types phonolitic trachyte and phonolite; trachyandesite and tristanite are minor. It is proposed that the parental magma possessed a mild degree of undersaturation and

a moderately high- to high-K value. The phonolites and phonolitic trachytes represent dual differentiation trends, one towards Na- and *ne*-enrichment and the other towards K-enrichment. The former trend was effected under hydrous, peralkaline conditions with oxygen fugacities either higher than, or at least decreasing at a slower rate than, those under which the K-enrichment trend was effected.

Critical chemical parameters in distinguishing the Mullaley lineages are Al, K and $Fe_2O_3:FeO+Fe_2O_3$. The levels of Al (and total alkalis) may correlate with fractionation of Mg-rich olivine and clinopyroxene in the parental magmas at pressures of ≈ 9 kb (*cf.* Green and Ringwood, 1967).

Levels of K vary without relation to other major or minor elements; the only correlation is that the K content may increase with a decrease in the age of the igneous activity; this may in turn correlate with increasing stability of the Mullaley area.

The parameter $Fe_2O_3:FeO+Fe_2O_3$ (when reflecting magmatic $Fe_2O_3:FeO+Fe_2O_3$) is taken as an indicator of the oxygen fugacity in the magma. In rocks in which the ratio is high, olivine is minor or absent, the modal percentage of magnetite is high, and hydrous phases such as biotite and analcime appear; the tendency of the lavas to erupt explosively increases as the ratio increases.

Acknowledgements

The author is grateful for a Commonwealth Postgraduate Scholarship. Helpful discussions and guidance from members of staff of the University of New England Geology Department, and in particular Professor J. F. G. Wilkinson, are gratefully acknowledged. Assistance was received from the Geology Department, Newcastle University in the production of maps and diagrams.

References

ABBOTT, M. J., 1969. Petrology of the Nandewar Volcano, N.S.W., Australia. *Contr. Mineral. and Petrol.*, **20**, 115.

BAKER, P. E., GASS, I. G., HARRIS, P. G., and LE MAITRE, R. W., 1964. The Volcanological Report of the Royal Society Expedition to Tristan da Cunha, 1962. *Phil. Trans. R. Soc.*, **256**, 439.

BEAN, JUDITH M., 1974. The Geology and Petrology of the Mullaley Area of New South Wales. *J. geol. Soc. Aust.*, **21**, 63.

BENSON, W. N., 1939. " Kaersutite and Other Brown Amphiboles in the Cainozoic Igneous Rocks of the Dunedin District ". Mineralogical notes from the University of Otago, N.Z., No. 3. *Trans. R. Soc. N.Z.*, **69**, 283.

BOWEN, N. L., and SCHAIRER, J. F., 1935. The System $MgO-FeO-SiO_2$. *Am. J. Sci.*, **29**, 151.

BRADLEY, W. H., 1929. The Occurrence and Origin of Analcite and Meerschaum Beds in the Green River Formation of Utah, Colorado and Wyoming. *Prof. Pap. U.S. geol. Surv.*, **158A**, 1.

CHAYES, F., 1952. Relations Between Composition and Indices of Refraction in Natural Plagioclase. *Am. J. Sci. Bowen Volume*, 85.

COOMBS, D. S., 1963. Trends and Affinities of Basaltic Magmas and Pyroxenes as Illustrated on the Diopside-Olivine-Silica Diagram. *Min. Soc. Am. Spec. Pap. No. 1*, 227.

COOMBS, D. S., and WHETTEN, J. T., 1967. Composition of Analcime from Sedimentary and Burial Metamorphic Rocks. *Bull. geol. Soc. Am.*, **78**, 269.

COOMBS, D. S., and WILKINSON, J. F. G., 1969. Lineages and Fractionation Trends in Undersaturated Volcanic Rocks from the East Otago Volcanic Province (New Zealand) and Related Rocks. *J. Petrol.*, **10**, 440.

DEER, W. A., HOWIE, R. A., and ZUSSMAN, J., 1962. *Rock-forming Minerals*, Vol. 1. Longmans.

EDWARDS, A. B., 1938. The Tertiary Volcanic Rocks of Central Victoria. *Q. Jl. geol. Soc. Lond.*, **94**, 243.

FUDALI, R., 1963. Experimental Studies Bearing on the Origin of Pseudoleucite and Associated Problems of Alkalic Rock Systems. *Bull. geol. Soc. Am.*, **74**, 1101.

GREEN, D. H., and RINGWOOD, A. E., 1967. The Genesis of Basaltic Magmas. *Contr. Mineral. and Petrol.*, **15**, 103.

HUCKENHOLZ, H. G., 1965*a*. Der Petrogenetische Werdegang der Klinopyroxene in der Tertiären Vulkaniten der Hocheifel. I Die Klinopyroxene der Alkaliolivinbasalt-Trachyt-assoziation. *Beitr. Miner. Petrogr.*, **11**, 138.

HUCKENHOLZ, H. G., 1965*b*. II Die Klinopyroxene der Basanitoide. *Beitr. Miner. Petrogr.*, **11**, 415.

LE MAITRE, R. W., 1962. Petrology of Volcanic Rocks, Gough Island, South Atlantic. *Bull. geol. Soc. Am.*, **73**, 1309.

MACDONALD, G. A., and KATSURA, T., 1964. Chemical Composition of Hawaiian Lavas. *J. Petrol.*, **5**, 82.

MUIR, I. D., and TILLEY, C. E., 1961. Mugearites and their place in Alkali Igneous Rock Series. *J. Geol.*, **69**, 186.

NASH, W. P., and WILKINSON, J. F. G., 1970. Shonkin Sag Laccolith, Montana I. Mafic Minerals and Estimates of Temperature, Pressure, Oxygen Fugacity and Silica Activity. *Contr. Mineral. and Petrol.*, **25**, 241.

NASHAR, B., and DAVIES, M., 1960. Secondary Minerals of the Tertiary Basalts, Barrington, New South Wales. *Mineralog. Mag.*, **32**, 480.

O'HARA, M. J., 1968. The Bearing of Phase Equilibria Studies in Synthetic and Natural Systems on the Origin and Evolution of Basic and Ultra-basic Rocks. *Earth-Sci. Rev.*, **4**, 69.

OSBORN, E. F., 1959. Role of Oxygen Pressure in the Crystallization and Differentiation of Basaltic Magma. *Am. J. Sci.*, **257**, 609.

OSBORN, E. F., 1962. Reaction Series for Subalkaline Igneous Rocks Based on Different Oxygen Pressure Conditions. *Am. Miner.*, **47**, 211.

ROSS, C. S., 1928. Sedimentary Analcite. *Am. Miner.*, **13**, 195.

ROSS, C. S., 1941. Sedimentary Analcite. *Am. Miner.*, **26**, 627.

Schairer, J. F., 1957. Melting Relations of the Common Rock-forming Silicates. *Am. Ceramic Soc. J.*, **40**, 215.

Shand, S. J., 1939. On the Staining of Feldspathoids and on the Zoned Structure in Nepheline. *Am. Miner.*, **24**, 508.

Smith, J. R., and Yoder, H. S., 1956. Variations in X-ray Powder Diffraction Patterns of Plagioclase Feldspars. *Am. Miner.*, **41**, 632.

Smith, J. V., and Gay, P., 1958. The Powder Patterns and Lattice Parameters of Plagioclase Feldspars. *II. Mineralog. Mag.*, **31**, 744.

Tilley, C. E., and Muir, I. D., 1962. The Hebridean Plateau Magma Type. *Trans. Edinb. geol. Soc.*, **19**, 208.

Walker, F., 1923. The Igneous Geology of the Dalmeny District. *Trans. R. Soc. Edinb.*, **53**, 361.

Wilkinson, J. F. G., 1958. The Petrology of a Differentiated Teschenite Sill near Gunnedah, New South Wales. *Am. J. Sci.*, **256**, 1.

Wilkinson, J. F. G., 1965. Some Feldspars, Nephelines and Analcimes from the Square Top Intrusion, Nundle, N.S.W. *J. Petrol.*, **6**, 420.

Wilkinson, J. F. G., and Whetten, J. T., 1964. Some Analcime-bearing Pyroclastic and Sedimentary Rocks from New South Wales. *J. Sed. Petr.*, **34**, 543.

Wilshire, H. G., and Standard, J. C., 1963. The History of Vulcanism in the Mullally District, New South Wales. *Proc. R. Soc. N.S.W.*, **96**, 123.

Wright, J. B., 1968. Oligoclase Andesine Phenocrysts and Related Inclusions in Basalts from part of the Nigerian Cenozoic Province. *Mineralog. Mag.*, **36**, 1024.

Yoder, H. S., and Sahama, Th. G., 1957. Olivine X-ray Determinative Curve. *Am. Miner.*, **42**, 475.

Department of Geology,
University of New England,
Armidale, N.S.W., 2351.

(Received 19 November 1974)

Journal and Proceedings, Royal Society of New South Wales, Vol. 108, pp. 147–156, 1975

Continental Reconstructions and the Distribution of Coral Faunas During the Silurian*

JOHN PICKETT

Introduction

Modern theories of sea-floor spreading have given tremendous impetus to the elaboration of proposals for past configurations of continental masses ; palaeomagnetic studies have resulted in the production of an increasing number of palaeogeographic maps. This paper takes three of these maps and examines them in relation to the distribution of coral faunas of the Silurian period, with a view to both pointing out possible deficiencies in the reconstructions and to determining possible regional distribution patterns or faunal provinces.

The continental reconstructions used are those of Creer (1973) ; Rickard and Belbin (MS) ; and Smith, Briden and Drewry (1973). The latter is distinctively different from the others in the separation of Europe and Asia at the Urals. The configuration of Rickard and Belbin proposes a very close fit of all the continental masses, without a conspicuous gap between Gondwanaland and Asia. The basis for producing this model differs slightly from the others, in that in addition to palaeomagnetic information, it draws on simple geometric fit ; the aim behind its production was to arrive at a condensed Pangaea. A probable result of this is a greater proximity of many areas to the equator than is achieved by other methods. All three reconstructions point to a substantial southern landmass, with a considerable number of very much smaller land areas in the north.

The distribution of hermatypic corals in present-day seas is controlled by two major constraints ; minimum temperature of the ocean waters and the availability of sunlight. Other restrictions (e.g. turbidity, salinity) tend to be more local. Reef corals will not thrive in waters in which the temperature falls to 18°C for any length of time. The optimum temperature is in the range 25°–29°C. They are thus effectively restricted to a zone within the latitudes 30°N and 30°S.

A most important feature of hermatypic corals is the presence of symbiotic algae within the tissues of the polyp. It is their presence which causes the restriction of hermatypic corals to the photic zone. Most coral polyps, which are carnivorous, feeding on plankton, are expanded only at night. This, coupled with the dependence of the polyps on their photosynthetic symbionts, produces a very marked diurnal cycle in the physiological functions of the coral animals. It has been shown (Goreau and Goreau, 1959) that the uptake of calcium is greatest under clear, sunny conditions, and is reduced to 50% of this on a cloudy day, falling to 10% under conditions of total darkness. Because of this daily cycle, the skeletons of corals show tiny laminae corresponding to the daily skeletal increments. It is possible to observe these tiny growth lines on extremely well preserved fossil corals, the growth lines indicating that the rugose corals of the Palaeozoic era also enjoyed the benefits of symbiotic zooxanthellae. By detailed analysis of these daily increments on a Devonian coral, one colleague (Scrutton, 1965) concluded that the Devonian year consisted of 13 lunar months each of 30½ days. Fossil calcareous algae, indicative of well-lit waters, are frequent associates of corals. It thus seems unlikely that the environmental constraints to which Palaeozoic corals were subject varied greatly from those governing present coral distribution.

Geographical Distribution

Initially, simply to examine the spread of occurrences, known localities for corals during Llandovery, Wenlock and Ludlow times were plotted on the reconstruction of Smith, Briden and Drewry (1973) (Figures 1–3). Since the distribution of corals is virtually identical for all three epochs, the information was grouped for the other two projections (Figures 4, 5).

Reconstructions specifically based on Silurian palaeomagnetic data are almost unobtainable, since the data for this period seem particularly unreliable. The titles of the three selected for

---

* Presidential Address delivered to the Royal Society of New South Wales at Science House, Gloucester Street, Sydney, on April 2, 1975.

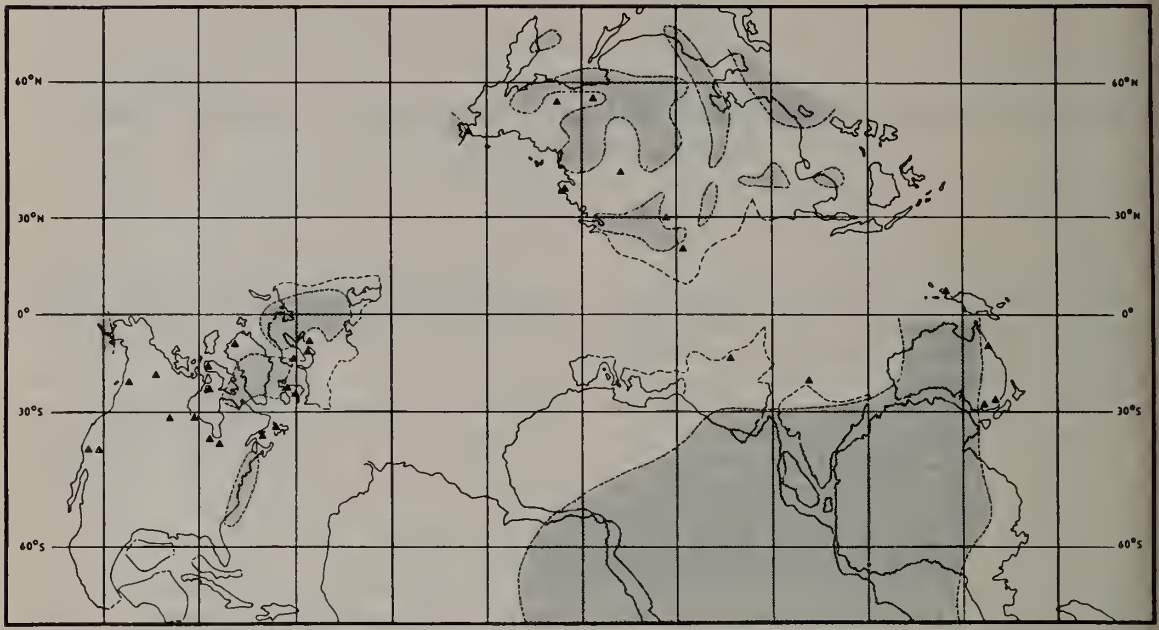

FIGURE 1.—Distribution of corals during the Llandovery. Reconstruction of Smith, Briden and Drewry, 1973. For all maps, stippling indicates probable land areas.

FIGURE 2.—Distribution of corals during the Wenlock. Reconstruction of Smith, Briden and Drewry, 1973.

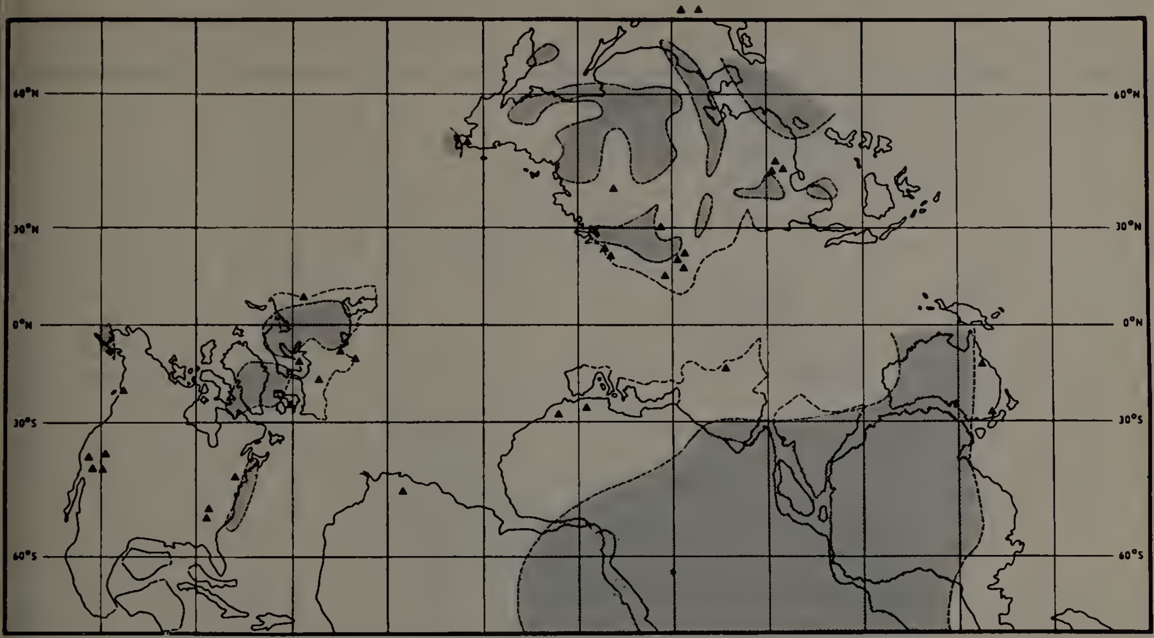

FIGURE 3.—Distribution of corals during the Ludlow. Reconstruction of Smith, Briden and Drewry, 1973.

depicting the present data are "Lower Devonian" (Smith, Briden and Drewry), "Silurian and very early Devonian" (Creer), and "Pangaea" (Rickard and Belbin). The latter was re-drafted for this paper using a polar position in present-day Angola, and covers a time interval including the Silurian. To facilitate appreciation of the differences between the three reconstructions, all have been presented on a Mercator projection, which, although not ideal for illustrating distribution of land masses, is useful when considering equatorial distribution such as might be expected with the corals. The distribution of corals during the early Devonian is rather similar to that during the Silurian, the disparity in age is not great, and the credibility of the reconstructions is greater than for the Ordovician. For these reasons the early Devonian palaeomaps have been selected as more nearly representing the Silurian situation.

The most immediately obvious disparity in distribution is shown by the Japanese occurrences. In all three reconstructions, the islands of Japan occupy an extreme northerly position, varying from about 75°–90°N for the models of Creer and Smith *et al.*, to 40°–48°N for that of Rickard and Belbin. Occurrences in Asia, especially northwestern USSR, China and the Indo-Chinese area are in fairly high latitudes, certainly more northerly latitudes than those in which corals occur at present.

The southern distribution is surprisingly consistent for the three reconstructions considered. The coral occurrences all fall north of 40°S, with two exceptions, namely the Venezuelan localities of Scrutton (1971) and those in Algeria on the projection of Rickard and Belbin. The occurrence of *Favosites argentina* (Clarke, 1913; Hill, 1958) at Cerro del Fuerte in Argentina has been shown to be Devonian (Baldis, 1971). The report of *Favosites niagarensis* from the Amazon Valley (Ruedemann in Maury, 1929) was regarded by Hill (1959) as doubtful; it was not substantiated by Lange (1972), and certainly seems out of place in the succession he describes for the Trombetas Formation. In view of the fairly tropical situation of northern Africa on most reconstructions and the known occurrences of Silurian rocks in the region, the relative paucity of the faunas of that area seems somewhat anomalous. It may be that this is due to insufficient documentation rather than a real paucity of the faunas, however.

The maps show no pronounced equatorial distribution of corals on any of the reconstructions examined. There is no immediate reason for assuming that the latitudinal distribution of Silurian corals was the same as that of the present ones. Relatively minor changes in either ocean temperatures or temperature-tolerance of the organisms could be responsible for substantial differences in

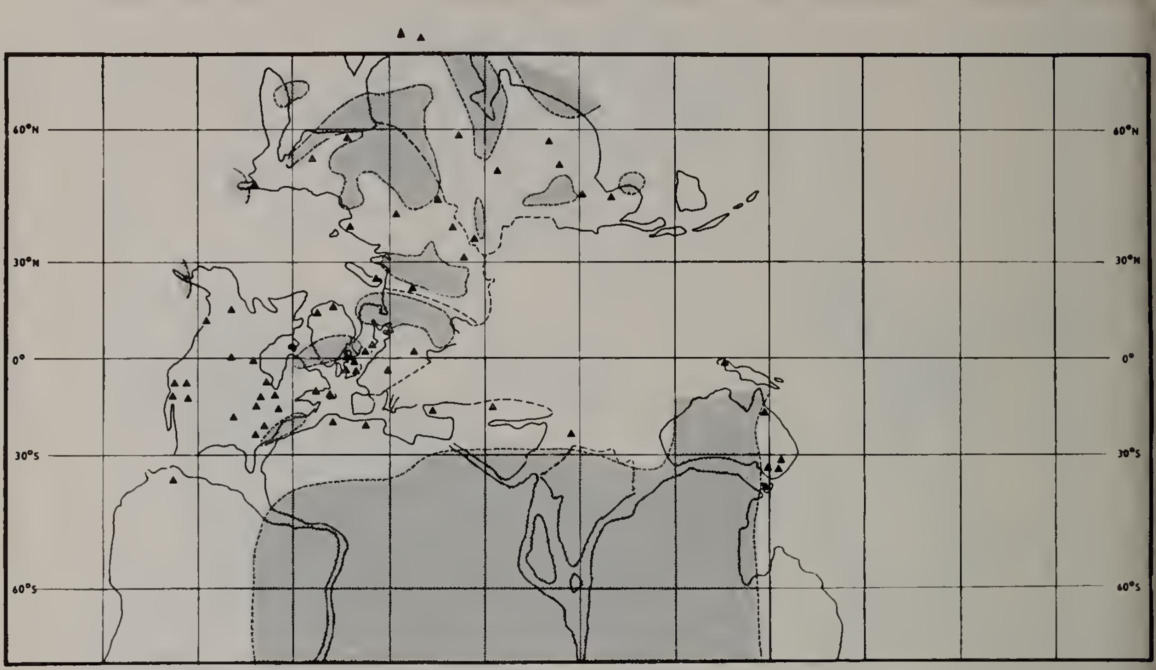

FIGURE 4.—Distribution of corals during the Silurian. Reconstruction of Creer, 1973.

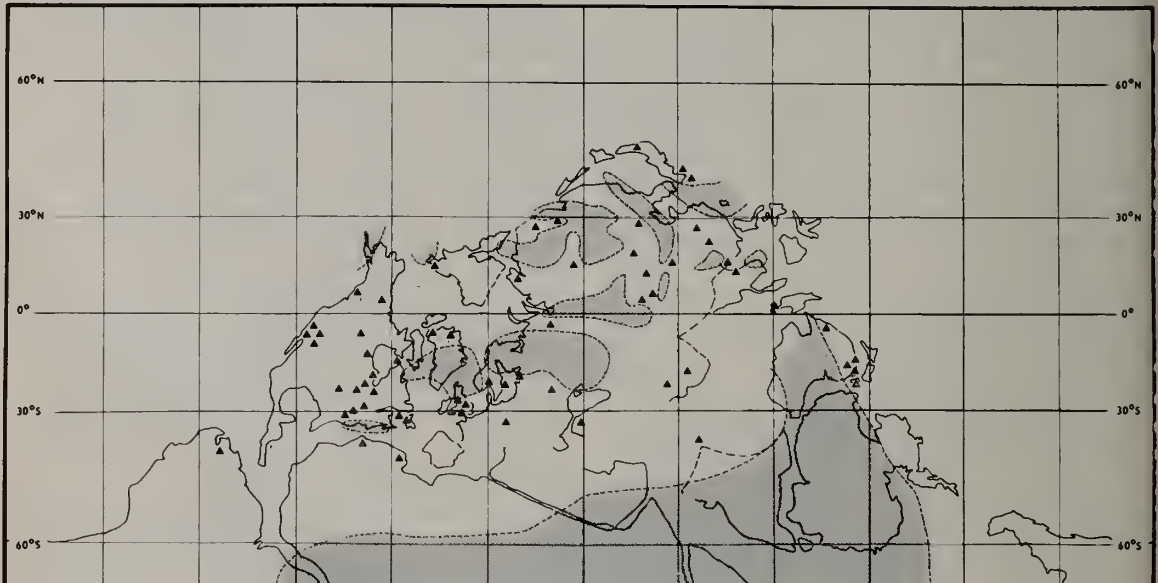

FIGURE 5.—Distribution of corals during the Silurian. Reconstruction of Rickard and Belbin, MS.

distribution patterns. It is the *unequal* distribution which is worthy of note ; this will be further discussed later.

Provincialism

The unevenness of information available from the many areas from which corals are known makes it very difficult to be quite positive about faunal provinces. The first step was to draw up a list of coral genera which are recognized within the Silurian, deleting those which are synonyms or whose validity is suspect. Even then the list presented here is not exhaustive, as some genera with very restricted distribution, which are probably still to be recognized elsewhere, have not been included. This applies to a number of the Russian tabulate genera, since taxonomists in countries outside the USSR have not devoted similar attention to this group. Table 1 shows those genera considered within this study. No discussion of synonymies is incorporated here ; the list is however not conservative.

Table 1 shows the distribution of genera in various areas. Ideally, a geographical analysis would be accompanied by a determination of the area in which each taxon originated, to determine migration directions. To do this for over 200 genera would be an unrealistic undertaking using present knowledge of stratigraphic ranges ; the genera are therefore designated according to the country from which the type species was described, as follows :

O	Europe (Old World)
N	North America (New World)
A	Asia
V	Australia (Van Dieman's Land)
J	Japan
S	South America

In addition, those genera which occur in the four continents O, A, N, V are considered to form part of a *universal fauna* and are designated U. These genera are most characteristic of Silurian coral assemblages throughout the world.

The aim of this operation was to derive a formula for composition of the various local faunas (e.g. for Australia $O_{16}N_3A_6V_8J_1U_{28}$). While the formulae so derived do reflect to a certain extent the affinities of the fauna, their usefulness is very much a reflection of the amount of work done in this area (e.g. Africa O_2U_1) or simply of the abundance of its faunas. A further disadvantage of this approach is that there is no indication of what groups make a local fauna distinctive. The gross unevenness of the data precludes any possibility of a useful result using computer or other statistical techniques (*cf.* Leleshus, 1972). For these reasons this approach was abandoned, and the data ultimately evaluated by setting out the genera geographically (Table 2), then examining each genus individually for its usefulness as a provincial index. For this kind of analysis those genera which are known from a single locality, or are only recently described, may assume an exaggerated importance. Consequently it was desirable to use a number of criteria to determine the validity of the various genera in provincial analysis. The following are considered appropriate : (a) the genus should be both distinct and distinctive ; (b) it should form a reasonable component of the fauna ; (c) it must show some restriction in its distribution. In Table 2 those genera which are potentially significant according to these requirements are shown in italics.

A chiefly western and northern province can be defined in broad terms, characterized by the genera *Cystihalysites*, *Syringolites*, the acervulariids *Diplophyllum* and *Acervularia*, *Ditoecholasma*, *Entelophylloides*, *Chonophyllum*, *Goniophyllum*, *Holophragma*, *Mesofavosites*, *Palaeofavosites* and *Porpites*. This province includes North America, Europe, and probably also northern USSR. A southern and eastern province including Australia, Japan, central and southeast Asia and India is less well-defined, characterized chiefly by the halysitids *Schedohalysites* and *Falsicatenipora*. Also important in this province are *Mucophyllum*, the chonophyllid *Yassia*, and possibly *Holmophyllia*. Not all reported occurrences of the Australian *Mucophyllum* are true representatives of that genus, those from the Baltic and possibly also elsewhere being much-thickened chonophyllids. Another Australian genus which, on a literature survey, would appear characteristic of the province, is *Hattonia*. This genus was recently shown to be exclusively Australian (Pickett and Jell, 1974) ; the central Asian species referred to the genus by various authors are probably a species group of the otherwise characteristically Devonian genus *Dictyofavosites*. It is also possible that *Sparsisolenia* Stasinska from Norway may prove to be a synonym of *Hattonia*.

Although the southern and eastern province is less well-defined generically, a number of species which are common to Australia and parts of Asia offer evidence of faunal affinity : the Australian species *Halysites cratus* Etheridge fil. and *Halysites sussmilchi* Etheridge fil. in Japan ; *Acanthohalysites pycnoblastoides yabei* in China ;

TABLE 1

Distribution of Silurian coral genera. Column numbers : 1, Europe ; 2, western North America ; 3, eastern North America ; 4, Arctic North America ; 5, southeastern and eastern Asia ; 6, central Asia ; 7, northern Asia ; 8, Japan ; 9, Australia ; 10, Africa ; 11, South America. For further explanation see text.

DISTRIBUTION OF SILURIAN CORAL GENERA

		1	2	3	4	5	6	7	8	9	10	11
Acanthocyclus	O	●		●			●					
Acanthohalysites	U	●		●		●		●	●	●		●
Acervularia	O	●		●	●							
Adaverina	O	●										
Agetolites	A						●					
Alleynia	O	●					●					
Allotropiophyllum	H			●								
Altaja	A						●					
Alveolites	U	●		●		●	●	●		●		
Amplexoides	A					●						
Amsdenoides	N			●								
Angopora	O	●					●	●		●		
Angullophyllum	V									●		
Anisophyllum	N			●								
Antherolites	A						●					
Aphyllum	A	●						●				
Arachnophyllum	U	●	●	●			●	●		●		
Araeopoma	O	●										
Aulocystella	A						●	●		●		
Aulopora	U	●		●			●			●		
Auloporella	N			●								
Australophyllum	V	●	●							●		
Barrandeolites	A	●					●					
Barrandeophyllum	O						●					
Bogimbailites	A						●					
Briantelasma	N			●								
Calostylis	O	●				●	●			●		
Camptolithus	N			●								
Cannipora	N			●								
Cantrillia	O	●										
Capnophyllum	N			●								
Carinophyllum	A							●				
Catenipora	U	●	●	●	●	●	●	●	●	●		
Ceriaster	A					●	●					
Chavsakia	A						●					
Chonophyllum	O	●	●	●	●		●					
Circophyllum	O	●	●				●	●				
Cladopora	U	●	●	●			●	●		●		
Coenites	U	●		●			●	●	●	●		●
Columnaxon	S											●
Contortophyllum	A							●				
Coronoruga	V						●			●		
Corrugopora	H			●								
Cosmiolithus	O	●										
Crassilasma	A	●					●					
Craterophyllum	N	●		●			●					
Cyathactis	U	●	●	●			●	●		●		
Cyathophylloides	O	●	●				●	●	●			
Cylindrostylus	A						●					
Cymatelasma	O	●										●
Cymatella	A							●				
Cystihalysites	A	●	●	●	●			●				●
Cystilasma	A						●	●				
Cystipaliphyllum	A						●					
Cystiphyllum	U	●	●	●	●	●	●		●	●		
Daljanolites	A						●					
Dalmanophyllum	O	●	●	●						●		
Denayphyllum	N		●									
Densiphyllum	O	●										
Dentilasma	A	●						●		●		
Desmidopora	O	●					●			●		
Dinophyllum	A	●		●		●		●				
Diplochone	O							●				
Diploepora	O	●								●		
Diplophyllum	N		●	●								
Disphyllum	O				●	●				●		
Ditoecholasma	H			●								
Dokophyllum	O	●					●	●				
Duncanella	N			●								
Endophyllum	O	●										
Entelophylloides	N		●	●								
Entelophyllum	U	●	●	●		●	●	●		●		
Evenkiella	A	●					●					
Expressophyllum	A	●						●				
Falsicatenipora	J				●				●	●		
Fasciphyllum	O						●					
Favosipora	O	●								●		
Favosites	U	●	●	●	●	●	●	●	●	●	●	●
Fletcheria	O	●		●	●					●		
Fomitchevia	A						●					
Fossopora	V				●							
Goniophyllum	O	●		●								
Gissarophyllum	A						●					
Grabauphyllum	N			●								
Gukoviphyllum	O	●										
Gyalophyllum	O	●				●						
Halysites	U	●	●	●	●	●			●	●		
Hattonia	V									●		
Hedstroemophyllum	O	●					●	●		●		
Heliolites	U	●	●	●	●	●	●	●	●	●		
Nelioplasma	A						●					

		1	2	3	4	5	6	7	8	9	10	11
Helioplasmolites	A						●					
Helminthidium	O	●							●			
Hemiagetolites	A						●					
Hexismia	H			●			●	●		●		
Hillaepora	A						●					
Nolmophyllia	A						●			●		
Holmophyllum	U	●		●		●	●	●	●	●		
Holophragma	O	●		●				●				
Immenovia	A							●				
Implicophyllum	A						●					
Ketophyllum	O	●						●		●		
Kiaerites	O	●										
Kitakamiphyllum	J								●			
Kodonophyllum	U	●	●				●	●		●		
Koreanopora	A					●						
Kyphophyllum	O	●	●			●	●	●				
Laceripora	O	●					●	●				
Laminoplasma	O	●										
Lamprophyllum	O	●						●				
Leolasma	O											●
Loyolophyllum	V						●					
Lykocystiphyllum	O	●										
Maikottia	A		●				●					
Mastopora	O	●										
Mazaphyllum	V									●		
Medinophyllum	A						●					
Mesofavosites	O	●		●			●	●				
Mesosolenia	A	●					●	●				
Microconoplasma	A						●					
Microplasma	O	●	●					●		●		
Mictocystis	V									●		
Micula	A	●		●				●				
Miculiella	A	●					●	●				
Moyerolites	A							●				
Mucophyllum	V	?	●					●	●			
Multisolenia	U	●		●	●		●			●		
Multithecopora	O	●										
Neomphyma	A		●					●		●		
Neopaliphyllum	A						●	●				
Nodulipora	O	●										
Oliveria	N			●								
Pachypora	O	●										
Palaearaea	A						●					
Palaeocorolites	A						●	●				
Palaeocyathus	U	●		●			●			●		
Palaeofavosites	O	●		●	●	●	●	●				
Palaeophyllum	U	●	●	●	●		●	●		●		
Paliphyllum	A	●						●				
Parastriatopora	A	●				●	●		●	●		
Phaulactis	U	●		●			●	●		●		
Pilophylloides	A						●					
Pilophyllum	O	●				●		●		●		
Placocoenites	A	●					●					
Planalveolites	U	●		●			●			●		
Plasmopora	U	●		●			●	●		●		
Plicatomurus	A						●					
Porpites	O	●	●	●								
Proheliolites	A							●				
Propora	U	●		●	●	●	●	●	●	●		
Protaraea	O	●										
Protopilophyllum	A						●					
Ptychophyllum	N		?			●	●	●		●		
Pseudocryptophyllum	N			●								
Pseudophaulactis	A						●					
Pseudoplasmopora	A						●					
Pseudoplasmoporella	A						●					
Pycnactis	O	●	●			●		●				
Pycnolithus	O	●										
Pycnostylus	N	●		●						●		
Rhahdacanthia	O	●						●				
Rhabdocyclus	O	●	●				●					
Rhegmaphyllum	O	●										
Rhizophyllum	U	●	●	●		●	●		●	●		
Rhytidophyllum	O	●										
Romingeria	N	●		●				●				
Rukhinia	A	●					●					
Ryderophyllum	A		●				●					
Saaremolites	O	●										
Salairia	A						●					
Salairipora	A						●					
Salairophyllum	A		●		●		●					
Sapporipora	A					●	●	●				
Saucrophyllum	V			●								
Schedohalysites	V					●		●	●	●		
Schlotheimophyllum	O	●		●								
Scoliopora	O						●					
Scyphophyllum	A							●				
Shastaphyllum	H		●									
Solenihalysites	O	●										
Somphopora	A					●						
Soshkinolites	A						●					

TABLE 1—*Continued*

		1	2	3	4	5	6	7	8	9	10	11
Sparsisolenia	O	●										
Spongophylloides	O	●		●			●	●				
Spongophyllum	O	●				●			●	●	●	
Spumaeolites	A						●					
Squameofavosites	O	●					●	●		●		
Squameolites	A						●					
Stanleysmithia	O	●										
Stauria	O	●		●		●	●					
Stelliporella	O	●		●			●					
Stereoxylodes	O	●				?	●	●		●		
Stortophyllum	O	●					●	●				
Streptelasma	U	●		●			●	●		●	●	●
Striatopora	U	●		●			●	●		●		
Strombodes	O	●	?				●	●		●		
Stylopleura	N		●									
Subalveolitella	A	●					●					
Subalveolites	O	●					●					
Syringaxon	O	●	●	●								●
Syringolites	N	●		●								
Syringopora	U	●	●	●	●		●	●	●	●		
Syringoporinus	A							●		●		
Tabularia	A						●	●				
Taxopora	A						●					
Tenuiphyllum	A							●				
Thamnopora	U	●			●		●		●	●		
Thaumatolites	A							●				
Thecaspinellum	A						●	●				
Thecia	O	●		●	●			●				
Thecipora	A						●					
Tonkinaria	N		●									
Toquimaphyllum	N		●									
Trachypora	N	●		●								
Tryplasma	U	●	●	●			●	●	●	●		●
Weissermelia	O	●				●	●					
Wenlockia	O	●										
Wintunastraea	N		●									
Xiphelasma	O	●										
Yassia	V		?				●	●		●		
Zelophyllum	O	●	●			●		●				
Zeravschania	A						●					

Yassia enormis (Etheridge fil.) on the Siberian platform ; *Mucophyllum crateroides* Etheridge fil. in Tadzhikistan ; and in Australia the Asian species *Ptychophyllum* cf. *sibiricum* Ivanovskiy, *Cystiphyllum khantaikaense* (Zaprudskaya) and *Dentilasma honorabilis* Ivanovskiy (McLean, 1974*a*, 1975). A similarity between the Asian and Australian faunas was suggested by Hamada (1958), based largely on the occurrence of Schedohalysitidae in the region. Careful work on ontogeny of halysitids by Webby and Semeniuk (1969) sheds some doubt on the validity of Hamada's recognition of the Schedohalysitidae ; on the other hand, the geographic distribution of halysitid species is consistent with that of the genera, so that Hamada's interpretation is accepted here, pending further work on halysitid hystero-ontogeny.

Two recent reviews of the palaeobiogeography of Silurian corals (Kaljo and Klaamann, 1973 ; Leleshus, 1970, 1972) both suggest a progressive differentiation of faunas through the Silurian, leading to development of either two or four provinces in the Ludlow. Kaljo recognizes a European and an Asian province, the affinities of the American fauna being rather with the European than the Siberian area. Leleshus, on the other hand, concludes from an examination of the tabulates alone, that four provinces were developed, in North America, Europe, Asia and Australia.

It is probable that the unevenness of the available data is too great for a statistical approach such as that used by Leleshus ; the four provinces he suggests reflect rather the familiarity of authors with the faunas and literature of their own region, and the abundance of " endemic " genera, which will almost certainly prove more widespread ultimately, than a geographical pattern intrinsic to the corals. In the present state of our knowledge, " endemic " genera cannot be trusted as true indicators of provincialism. More reliable are groups which show a broader regional distribution.

Leleshus (1972) is of the opinion that the lack of differentiation of Silurian faunas is a function of time : " the Ludlovian provinces did not have time to form independent regions " (p. 74). The reason for this homogeneity is however not to be sought in terms of available time. The recent scleractinian faunas have developed as a result of the isolation of the Atlantic and Indo-Pacific provinces with the closing of the Tethys in the middle Miocene, a period of approximately 20 million years, only two-thirds of Silurian time. The real reason for Silurian distribution patterns as well as those of present seas is geographic. The present-day distribution is conditioned by the great meridional extensions of the Americas and the mass of Africa-Europe-Asia ; there is no possibility of migration from one area to the other. The Silurian geography was quite different from this, with a single large southern continent, a number of smaller land areas, and no great north-south obstructions to east-west migration of tropical faunas. The smaller land masses could act at best as a filter to migration, so that provincialism could only be weak.

The faunas recently described from western USA (Merriam, 1972, 1973) are in some respects similar to those from eastern Australia. *Arachnophyllum kayi* Merriam is very similar to *Zenophila walli* (Etheridge fil.) (they are at least congeneric) ; *Klamathastraea* Merriam is possibly a junior synonym of *Yassia* Jones (McLean, 1974*b*) ; and the Australian genus *Mucophyllum* occurs in California and Nevada,

TABLE 2

Geographical lists of genera according to the type locality of the type species. Genera which are potentially useful in provincial analysis are shown in italics.

Universal Fauna

Acanthohalysites
Alveolites
Arachnophyllum
Aulopora
Catenipora
Cladopora
Coenites
Cyathactis
Cystiphyllum
Entelophyllum
Favosites
Halysites
Heliolites
Holmophyllum
Kodonophyllum
Multisolenia
Palaeocyathus
Palaeophyllum
Phaulactis
Planalveolites
Plasmopora
Propora
Rhizophyllum
Streptelasma
Striatopora
Syringopora
Thamnopora
Tryplasma

Australia

Angullophyllum
Australophyllum
Coronoruga
Fossopora
Hattonia
Loyolophyllum
Mazaphyllum
Mictocystis
Mucophyllum
Saucrophyllum
Schedohalysites
Yassia

Japan

Falsicatenipora
Kitakamiphyllum

South America

Columnaxon

North America

Allotropiophyllum
Amsdenoides
Anisophyllum
Auloporella
Briantelasma
Camptolithus
Cannipora
Capnophyllum
Corrugopora
Craterophyllum
Denayphyllum
Diplophyllum
Ditoecholasma
Duncanella
Entelophylloides
Grabauphyllum
Hexismia
Oliveria
Ptychophyllum
Pseudocryptophyllum
Pycnostylus
Romingeria
Shastaphyllum
Stylopleura
Syringolites
Tonkinaria
Toquimaphyllum
Trachypora
Wintunastraea

Europe

Acanthocyclus
Acervularia
Adaverina
Alleynia
Angopora
Araeopoma
Carrandeophyllum
Calostylis
Cantrillia
Chonophyllum
Circophyllum
Cosmiolithus
Cyathophylloides
Cymatelasma
Dalmanophyllum
Densiphyllum
Desmidopora
Diplochone
Diploepora
Disphyllum
Dokophyllum
Endophyllum
Fasciphyllum
Favosipora
Fletcheria
Goniophyllum
Gukoviphyllum
Gyalophyllum
Hedstroemophyllum
Helminthidium
Holophragma
Ketophyllum
Kiaerites
Kyphophyllum
Laceripora
Laminoplasma
Lamprophyllum
Leolasma
Lykocystiphyllum
Mastopora
Mesofavosites
Microplasma
Multithecopora
Nodulipora
Pachypora
Palaeofavosites
Pilophyllum
Porpites
Protaraea
Pycnactis
Pycnolithus
Rhabdacanthia
Rhabdocyclus
Rhegmaphyllum
Rhytidophyllum
Saaremolites
Schlotheimophyllum
Scoliopora
Solenihalysites
Sparsisolenia
Spongophylloides
Spongophyllum
Squameofavosites
Stanleysmithia
Stauria
Stelliporella
Stereoxylodes
Stortophyllum
Strombodes
Subalveolites
Syringaxon
Thecia
Weissermelia
Wenlockia
Xiphelasma
Zelophyllum

Asia

Agetolites
Altaja
Amplexoides
Antherolites
Aphyllum
Aulocystella
Barrandeolites
Bogimbailites
Carinophyllum
Ceriaster
Chavsakia
Contortophyllum
Crassilasma
Cylindrostylus
Cymatella
Cystihalysites
Cystilasma
Cystipaliphyllum
Daljanolites
Dentilasma
Dinophyllum
Evenkiella
Expressophyllum
Fomitchevia
Gissarophyllum
Helioplasma
Helioplasmolites
Hemiagetolites
Hillaepora
Holomophyllia
Immenovia
Implicophyllum
Koreanopora
Maikottia
Medinophyllum
Mesosolenia
Microconoplasma
Micula
Miculiella
Moyerolites
Neomphyma
Neopaliphyllum
Palaearaea
Palaeocorolites
Paliphyllum
Parastriatopora
Pilophylloides
Placocoenites
Plicatomurus
Proheliolites
Protopilophyllum
Pseudophaulactis
Pseudoplasmopora
Pseudoplasmoporella
Rukhinia
Ryderophyllum
Salairia
Salairipora
Salairophyllum
Sapporipora
Scyphophyllum
Somphopora
Soshkinolites
Spumaeolites
Squameolites
Subalveolitella
Syringoporinus
Tabularia
Taxopora
Tenuiphyllum
Thaumatolites
Thecaspinellum
Thecipora
Zeravschania

though not elsewhere in the United States. The two areas concerned were, according to all reconstructions, separated then as now by the open sea ; it would therefore not be surprising to find faunal similarities on both sides of a proto-Pacific ocean, just as there are at the present time.

Brachiopod Provinces

In a number of important papers, a regional pattern in Silurian brachiopod faunas has been described (Cocks, 1972 ; Cocks and McKerrow, 1973 ; Boucot and Johnson, 1973). Of particular interest is the definition of the *Clarkeia* community, which has a restricted distribution in Africa and South America. This is considered to be a cold-water fauna by Cocks and McKerrow. Probable early Silurian (or latest Ordovician) glacial deposits are also known from the areas in which the *Clarkeia* community occurs (Bolivia and Argentina : Berry and Boucot, 1972 ; North Africa : Sougy and Lécorché, 1963, Destombes, 1968 ; South Africa: Cocks *et al.*, 1970). The distribution of these faunas appears somewhat anomalous for a supposed cold-water assemblage when plotted on a palaeogeographic map (see Cocks and McKerrow, 1973, text-fig. 3), as the most northerly locality, in the western Sahara, falls at 30°–40°S. The significance of this will be discussed later. No northern assemblages corresponding to the *Clarkeia* fauna have been recognized.

Synthesis

The observed distribution of Silurian coral occurrences is generally inconsistent with an expected equatorial distribution. Of the three palaeogeographic reconstructions reviewed, the best fit of the data is shown by the Rickard and Belbin model, on which all occurrences lie between 45°N and 45°S. Some of this restriction must be ascribed to the density of the reconstruction. The other two models show an anomaly confined chiefly to the northern hemisphere.

It could be argued that the near-universal distribution of coral faunas on the Creer and Smith *et al.* reconstructions points to widespread warm conditions during the Silurian, were it not for the presence in the southern hemisphere of the cold-water *Clarkeia* fauna. The distribution of corals in the southern area ties in well with the observed brachiopod distribution. It is perhaps significant that the apparently poor Silurian coral faunas of North Africa should occur north of the most northerly occurrence of the *Clarkeia* fauna. These occurrences lie just off the western coast of the southern continent of Gondwana ; the northward extension of the cold-water brachiopod fauna and the absence of corals in relatively low latitudes may have been due to a cold current which flowed northward along the western margin of Gondwanaland. This situation is analogous to that of the present-day Humboldt current off the west coast of South America, which has a pronounced cooling effect as far north as the equator itself.

In contrast to this situation are the observed data from the northern hemisphere, where no cold-water faunas have been defined ; instead, we find reef-building corals in areas immediately around the pole (Japan). It is quite illogical to expect that there was an Antarctic cold region without a similar Arctic one ; the explanation of the Asian situation must therefore be sought elsewhere.

The Rickard and Belbin model does not accord well with such a proposal. Firstly, the north African coral occurrences lie 20°–25° further south than on the other reconstructions, which alone would suffice to explain their impoverished nature, and the proximity of the cold-water brachiopod fauna. In addition, however, the N–S trend of the coastline has largely disappeared ; the localities of both the *Clarkeia* fauna and the corals would lie east of the influence of any north-flowing cold current. Similarly, though, the locale implied for the cold-water fauna may well have been too warm.

If we examine the areas of Gondwanaland, Euramerica, and Asia, it becomes apparent that, although the Euramerican and Gondwana land-masses have suffered marginal tectonism, their central portions have remained virtually unaffected since at least the Middle Palaeozoic. This is in complete contrast to the situation in Asia, which is almost surrounded by areas of substantial Tertiary movement, contains at least two large belts of great Mesozoic activity, and is divided into two by a very broad belt of Hercynian folding (this situation is well illustrated by Smith, Briden and Drewry, 1973, text-fig. 12). It follows that any consideration of the Asian area as a unit, even for Early Mesozoic times, and most certainly for the Mid-Palaeozoic, will lead to erroneous results. The distribution of corals and the absence of northern cold-water faunas suggests that none of the present land-masses was in the Arctic during the Silurian. The similarity of the Japanese faunas with those of Australia suggests that Japan at that time was much closer to Australia than shown on present reconstructions. Similarly, affinities between other faunas in Asia and those of Australia point to a position generally in the same area.

Conclusions

1. The distribution of the Silurian corals favours the reconstruction of Rickard and Belbin. This however is still subject to other conditions, notably that under (2) below, and the anomalously close positions of cold-water faunas in Mauritania and tropical ones in Algeria and Morocco.

2. The composite nature of the Asian continent makes it impossible to consider it a single unit, at least for the time interval under discussion. A final reconstruction will probably show Japan much nearer to the Australian area.

3. It is probable that none of the present continents lay in the Arctic area during the Silurian.

4. Faunal distribution in the southern hemisphere was probably influenced by a cold current which flowed northwards along the west coast of Gondwanaland.

5. Provincialism in corals during the Silurian was weak, largely due to the absence of substantial north-south trending geographical barriers.

References

Baldis, B. A. J., 1971. La Posición Estratigrafica de *Favosites argentinus* Thomas. *Ameghenian*a, 8, 77.

Berry, W. B. N., and Boucot, A. J. (eds), 1972. Correlation of the South American Silurian Rocks. *Geol. Soc. Amer., Spec. Pap.*, **133**.

Boucot, A. J., and Johnson, J. G., 1973. Silurian Brachiopods. In : Hallam, A. (ed.), *Atlas of Palaeobiogeography*. Elsevier, Amsterdam, p. 59.

Clarke, J. M., 1913. Fosseis Devonianos do Paraná. *Mon. Serv. geol. y mineral. do Brasil*, **1**, 1.

Cocks, L. R. M., 1972. The Origin of the Silurian *Clarkeia* Shelly Fauna of South America, and its Extension to West Africa. *Palaeontology*, **15**, 623.

Cocks, L. R. M., Brunton, C. H. C., Rowell, A. J., and Rust, I. C., 1970. The First Lower Palaeozoic Fauna Proved from South Africa. *Quart. J. geol. Soc. London*, **125**, 583.

Cocks, L. R. M., and McKerrow, W. S., 1973. Brachiopod Distributions and Faunal Provinces in the Silurian and Lower Devonian. In : Hughes, N. F. (ed.), Organisms and Continents Through Time. *Spec. Pap. Palaeont.*, **12**, 291.

Creer, K. M., 1973. On the Arrangement of the Landmasses and the Configuration of the Geomagnetic Field During the Phanerozoic. In : Tarling, D. H., and Runcorn, S. K. (eds), *Implications of Continental Drift to the Earth Sciences*. Acad. Press, London, vol. 1, 47.

Destombes, J., 1968. Sur la Nature Glaciaire des Sédiments du Groupe de 2^e Bari, Ashgill Supérieur de l'Anti-Atlas, Maroc. *C. r. Acad. Sci. Fr.*, sér. D, 684.

Goreau, T. F., and Goreau, N. I., 1959. The Physiology of Skeleton Formation in Corals. II. Calcium Deposition by Hermatypic Corals Under Various Conditions in the Reef. *Biol. Bull.*, **117**, 239.

Hamada, T., 1958. Japanese Halysitidae. *J. Fac. Sci. Tokyo Univ.*, (2), **11**, 91.

Hill, D., 1959. Distribution and Sequence of Silurian Coral Faunas. *J. Proc. Roy. Soc. N.S.W.*, **92**, 151.

Kaljo, D., and Klaamann, E., 1973. Ordovician and Silurian Corals. In : Hallam, A. (ed.), *Atlas of Palaeobiogeography*. Elsevier Amsterdam, **37**.

Lange, F. W., 1972. Silurian of Brazil. In : Berry, W. B. N., and Boucot, A. J. (see above), **33**.

Leleshus, V. L., 1970. Paleogeografiya Ordovika, Silura i Rannego Devona po Tabulyatomorfnym Korallam i Granitsy Siluriyskoy Sistemy. *Izvest. Akad. nauk SSSR*, geol. ser., **9**, **83**. English translation in : *Int. geol. Review*, 1971/73, **13**, 427.

Leleshus, V. L., 1972. *Siluriyskie Tabulyaty Tadzhikistana*. Akad. nauk Tadzh. SSR, Inst. geol., Izdat. " Donish ", Dushanbe.

McLean, R. A., 1974*a*. Cystiphyllidae and Goniophyllidae (Rugosa) from the Lower Silurian of New South Wales. *Palaeontographica*, A, **147**, 1.

McLean, R. A., 1974*b*. Chonophyllinid Corals from the Silurian of New South Wales. *Palaeontology*, **17**, 655.

McLean, R. A., 1975. Lower Silurian Rugose Corals from Central New South Wales. *J. Proc. Roy. Soc. N.S.W.*, **108**, 54.

Maury, C. J., 1929. Uma Zone de Graptolitos do Llandovery Inferior no Rio Trombetas, Estado do Para, Brasil. *Mon. Serv. geol. min. Brasil*, **7**, 1.

Merriam, C. W., 1972. Silurian Rugose Corals of the Klamath Mountains Region, California. *U.S. geol. Surv. prof. Pap.*, **738**, 1.

Merriam, C. W., 1973. Silurian Rugose Corals of the Central and Southwest Great Basin. *U.S. geol. Surv. prof. Pap.*, **777**, 1.

Pickett, J. W., and Jell, J. S., 1974. The Australian Tabulate Coral Genus *Hattonia*. *Palaeontology*, **17**, 715.

Scrutton, C. T., 1965. Periodicity in Devonian Coral Growth. *Palaeontology*, **7**, 552.

Scrutton, C. T., 1971. Palaeozoic Coral Faunas from Venezuela. I, Silurian and Permo-Carboniferous Corals from the Merida Andes. *Bull. brit. Mus. (Nat. Hist.)*, Geol., **20**, 183.

Smith, A. G., Briden, J. C., and Drewry, G. E., 1973. Phanerozoic World Maps. In : Hughes, N. F. (ed.), Organisms and Continents Through Time. *Spec. Pap. Palaeont.*, **12**, 1.

Sougy, J., and Lécorché, J. P., 1963. Sur la Nature Glaciaire de la Base de la Série de Garat el Hamoueïd (Zemmour, Mauritanie septentrionale). *C. r. Acad. Sci. Fr.*, **256**, **4471**.

Webby, B. D., and Semeniuk, V., 1969. Ordovician Halysitid Corals from New South Wales. *Lethaia*, **2**, 345.

Geological Survey of New South Wales,
Mining Museum,
36 George Street,
Sydney, N.S.W.

(Received 18.6.75)

Journal and Proceedings, Royal Society of New South Wales, Vol. 108, pp. 157–167, 1975

Some Early Cretaceous Organic-walled Microplankton from the Great Australian Basin, Australia

Roger Morgan

Abstract—Four new genera and seven new species of organic-walled microplankton are described. Two genera and five species are fossil dinoflagellate cysts, and two monospecific genera are of uncertain biological origin. The dinoflagellates *Diconodinium davidii*, *Spinidinium boydii* and *Bourkidinium granulatum* and the acritarch *Nummus monoculatus* are useful biostratigraphic forms in the marine part of the section. The dinoflagellates *Fusiformacysta salasii* and *Batiacasphaera macrogranulata* and the acritarch *Microfasta evansii* are useful biostratigraphic and palaeo-environmental indicators in the non-marine and transgressional part of the sequence.

The archeopyle problem in *Diconodinium* is discussed, and some specimens previously assigned to *D. multispinum* (Deflandre and Cookson) are redescribed. The generic description of *Batiacasphaera* is emended to expand the range of ornament types.

Introduction

Early Cretaceous microplankton of the Great Australian Basin are not well known despite the principally taxonomic papers of Cookson and Eisenack since 1958, and the principally biostratigraphic papers of Evans (1966*a*–*b*) and Burger (1973 and in press). With a few exceptions, the stratigraphic distributions of microplankton species are particularly poorly known. On the other hand, the stratigraphic distribution of many spore and pollen species are well known (Dettmann, 1963; Dettmann and Playford, 1969).

The purpose of the present contribution is to introduce seven new species which are considered important to the understanding of the microplankton palynostratigraphy of the Great Australian Basin, and to discuss their palaeoenvironmental significance briefly. A locality map of the boreholes mentioned is presented as Figure 1.

In quoting dimensions of the species described, the following convention is followed throughout: The first number is the minimum, the bracketed number the mean, and the third number the maximum dimension.

Systematic Palaeontology

Class Dinophyceae

Cyst-Genus *Diconodinium* Eisenack and Cookson 1960

Type species *Diconodinium multispinum* (Deflandre and Cookson, 1955 p. 257, Plate 1, Figure 5) Eisenack and Cookson, 1960 p. 3.

Diconodinium davidii sp. nov.

(Plate I, Figures 1a–b, 2a–d)

Description:

Cyst consists of a broadly subtriangular epitract bearing a long steeply conical, distally truncate apical horn, and a broadly rounded hypotract bearing a single strong, sharply pointed antapical horn slightly offset from the longitudinal axis. The cingulum is about 5 μ wide, and offset slightly at the sulcus. The autophragm bears a moderately dense cover of small solid spinulae or clavae about 1·0–1·5 μ high and about 1·0 μ thick. These are absent from the cingulum and rare on the sulcus area, but otherwise cover the entire autophragm. The spinulae or clavae may be randomly distributed but are more often, at least partly, aligned in rows to reveal traces of tabulation, and are always aligned in two rows along the margins of the cingulum. If aligned, the peritabular spinulae or clavae are larger and stouter than the intratabular ones. On some specimens, most of the clavae are peritabular with few or none intratabular. The archeopyle is type Ia or $\overline{\text{I}}$Pa. The former type results when only the lateral and apical sutures of the reflected 2a plate open, and the plate remains attached antapically to the 4″ reflected plate. Commonly, the lateral sutures of plate 4″ at least partly open, so that the operculum consists of a single piece (comprising plates 2a and 4″) that remains attached at, or close to, the cingulum.

Dimensions:

72 (83) 96 μ long and 41 (50) 57 μ broad (10 specimens measured).

Holotype :

Plate I, Figure 1 : 80 μ long and 47 μ broad. M.M.M.C. 2001.

Comparison :

This species is similar to *Diconodinium arcticum* Manum and Cookson which has shorter horns, less dense and finer ornament (minute granules up to 0·5 μ in diameter rather than spinulae or clavae 1·0–1·5 μ high and about 1μ in diameter) and is smaller (50–73 μ long, 32–53 μ broad rather than 72–96 μ long and 41–57 μ broad). *D. pusillum* Singh (1971) differs from the new species by having shorter horns, finer, sharply pointed spines 0·5 μ long and by being smaller (40 (47) 54 μ long and 28 (36·5) 43 μ broad). *D. firmum* Harland (1973) can be distinguished by its small size (36·0 (42·7) 50·0 μ long and 18·0 (29·3) 30 μ broad), solid (not hollow) apical horn, fine granulation (no size given), thin wall and broad cingulum. A precingular archeopyle may be present in *D. firmum*. *Diconodinium pelliferum* (Cookson and Eisenack, 1958) (85 μ long and 59 μ broad) and *Diconodinium dispersum* (Cookson and Eisenack, 1958) (64–90 μ long and 38–62 μ broad) are similar in size to *D. davidii* (72–96 μ long and 41–57 μ broad). Surface ornament in *D. pelliferum* consists of long (1·0–2·5 μ) sharply pointed spines, and in *D. dispersum* of long (2·0–3·0 μ) strongly capitate spines, while the new species has blunt non-capitate spinulae or clavae (1·0–1·5 μ long).

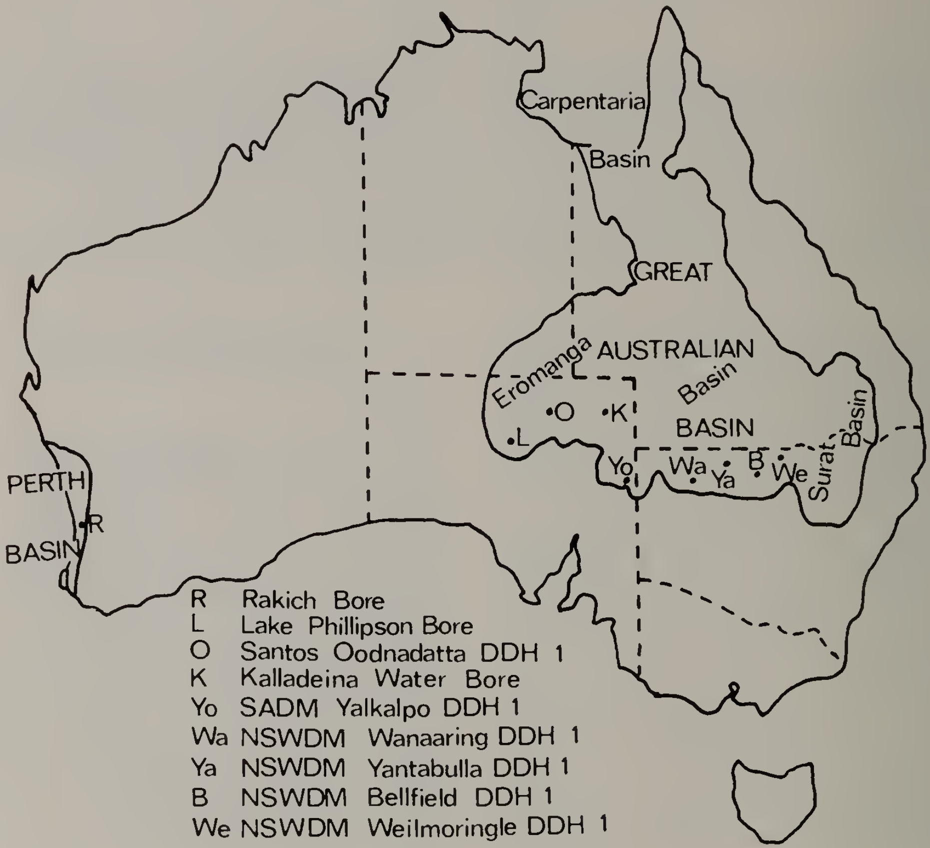

Fig. 1

The species most similar to *D. davidii* is *Diconodinium multispinum* (Deflandre and Cookson, 1955). The holotype of the latter species is very different from the described and figured specimen assigned to *Palaeohystrichophora multispina* by Cookson and Eisenack (1958) and subsequently transferred to *Diconodinium* by Eisenack and Cookson (1960). I have examined the latter specimen but not the holotype of *D. multispinum*. In general, the name seems to be applied to forms with the following features : broadly fusiform cyst having a narrow cingulum that divides the cyst approximately equally ; a short apical and a single antapical horn; autophragm bears a dense covering of small granulae or short spinulae (about 0·5 μ long and broad), that are rarely aligned. From this concept the new species differs by having longer horns and coarser, less dense ornament. Strictly, the name *D. multispinum* should be applied to the morphologically and time-stratigraphically distinct holotype. A new name would then be necessary for the forms assigned by Cookson and Eisenack (1958) to *Palaeohystrichophora multispina*. Taxonomic changes await study of the holotype.

The new species differs from most other described species of *Diconodinium* by the possession of an archeopyle, and from all species, other than those mentioned herein, by type of surface ornament, and by overall shape.

Distribution :

(Holotype locality is marked (H), paratype locality (P). This convention is followed throughout).

Upper *C. hughesii* subzone
  Santos Oodnadatta No. 1 ; 232·4 m, 244·0 m
  SADM DDH Yalkalpo No. 1 ; 99·5 m, 114·5 m
  NSWDM DDH Weilmoringle No. 1 ; 219·9 m (P)
  NSWDM DDH Bellfield No. 1 ; 158·0 m (H), 120·2 m
  Kalladeina Water Bore 1,101·1 m, 1,049·2 m
  NSWDM DDH Yantabulla No. 1 ; 122·0 m
  NSWDM DDH Wanaaring No. 1 ; 184·5 m
C. striatus subzone
  SADM DDH Yalkalpo No. 1 ; 89 m
  NSWDM DDH Bellfield No. 1 ; 59·8 m
  NSWDM DDH Yantabulla No. 1 ; 92·1 m
C. paradoxa zone
  Santos Oodnadatta No. 1 ; 164·7 m

Common in the upper *C. hughesii* subzone (Aptian) of Dettmann and Playford (1969), with occasional specimens in the *C. striatus* subzone and *C. paradoxa* (Albian) zone.

Cyst genus *Spinidinium* Cookson and Eisenack, 1962*b*

Type species *Spinidinium styloniferum* Cookson and Eisenack, 1962*b* p. 489, Plate I, Figures 1–5

Spinidinium boydii sp. nov.

(Plate I, Figure 3a–d)

Description :

Cyst is very broadly fusiform in dorsal-ventral view. The apical horn is broadly conical and distally truncate. A single, small broad, pointed antapical horn is present and is offset only slightly from the longitudinal axis. The sides are smoothly convex as there is no prominent cingular furrow. The surface ornament consists of relatively sparse solid granulae to truncate spinulae, (usually about 1–3 μ long and 0·5 μ thick) that are aligned in rows. Tabulation is defined by the alignment of the ornament, mostly peritabular with few intratabular granulae or spinulae. The cingulum and sulcus are always devoid of ornament. Alignment may define reflected plate outlines only weakly, with apparently random granulae or spinulae scattered over most of the periphragm, except for the cingulum and the sulcus. Both endophragm and periphragm are thin, and always separate at the base of the apical and the antapical horns. The archeopyle is intercalary, type Ia (2a only) ; the operculum is attached antapically.

Comparisons :

Spinidinium vestitum Brideaux 1971, differs from this species by having an angular pentagonal outline due to the much longer horns, and by bearing ornament consisting of cones and spines. Separation of the wall layers at the horns is absent in *S. vestitum*.

Spinidinium styloniferum Cookson and Eisenack, 1962*b* differs from this species by having more strongly developed horns, a deep cingular furrow, thicker wall layers, and much denser, stouter ornament.

Dimensions :

41 (49) 72μ long and 33 (42) 66 μ broad (10 specimens measured).

Holotype :

Plate I, Figure 3 ; 47 μ long and 37 μ broad. M.M.M.C. 2002.

Distribution :

Upper *C. hughesii* subzone
  Kalladeina Water Bore 1,101·1 m, 1,049·2 m, 1,036·1 m
  NSWDM DDH Yantabulla No. 1 ; 154·0 m
C. striatus subzone
  NSWDM DDH Weilmoringle No. 1 ; 99·1 m, 132·1 m
  NSWDM DDH Bellfield No. 1 ; 39·7 m, 101·3 m (H)
  Kalladeina Water Bore, 1,005·6 m, 988·2 m
  NSWDM DDH Yantabulla No. 1 ; 53·4 m
  NSWDM DDH Wanaaring No. 1 ; 95·5 m, 122·0 m
Lower *C. paradoxa* zone
  Kalladeina Water Bore, 886·0 m
  NSWDM DDH Wanaaring No. 1 ; 53·4 m

Ranges from upper *C. hughesii* subzone (Aptian) of Dettmann and Playford (1969), is very common in the *C. striatus* subzone, and rarely occurs in the *C. paradoxa* (Albian) zone.

Spinidinium styloniferum Cookson and Eisenack, 1962b
(Plate II , Figure 1a–e)

1962b *Spinidinium styloniferum* Cookson and Eisenack p. 489, Plate 1, Figures 1–5

Revised Description :

Cyst is thick walled, outline roughly pentagonal in dorsal-ventral view. The periphragm is drawn out into a broadly conical, distally truncate apical horn, a steeply conical, distally pointed left antapical horn, and a weakly developed right antapical horn. The cingulum is broad, divides the cyst into about equal parts, and is only offset slightly at the sulcus. The endophragm is approximately ellipsoidal ; the two wall layers separate slightly at the base of the horns. The periphragm bears many solid rod-like projections with broadly rounded distal ends. The rod-like ornament is occasionally 2·5–5·0 μ long and 1·0–1·5 μ diameter, but more commonly is 2·0–4·0 μ long and 0·5–1·0 μ in diameter. The ornament is closely spaced and aligned along the cingulum margins, and peritabular to the reflected plate areas. Some specimens have dense intratabular ornament as well ; all specimens lack ornament on the cingulum and sulcus. The archeopyle is intercalary, type Ia (2a only) elongate trapezoidal ; the archeopyle is attached along the antapical margin.

Dimensions :

43 (49) 62 μ long and 33 (40) 49 μ broad (10 specimens measured).

Holotype :

Plate II, Figure 1 ; 57 μ long and 43 μ broad. P 21271.

Type locality :

Rakich's bore, Caversham, Perth Basin between 350–355 ft., cuttings sample containing mixed Aptian-Albian assemblage.

Comments :

Recent re-examination shows that the holotype bears very coarse and dense ornamentation, the maximum size of which approximates that given above. Examination of other specimens on the slide containing the holotype and topotypic material shows that specimens with finer and less dense ornamentation are more typical. The angular outline, deep cingular furrow and presence of pericoels are constant features. No specimens exactly like the holotype have yet been observed from the Great Australian Basin, but frequent specimens identical with the less heavily ornamented specimens from the type locality do occur, often in association with specimens of *Spindinium boydii*.

Distribution :

C. striatus zone
NSWDM DDH Weilmoringle No. 1 ; 99·1 m, 132·1 m
NSWDM DDH Bellfield No. 1 ; 101·3 m, 59·8 m
C. paradoxa zone
Santos Oodnadatta No. 1 at 164·7 m

Occurs most commonly in the *C. striatus* (Aptian-Albian) subzone of Dettmann and Playford (1969), with occasional specimens into the *C. paradoxa* (Albian) zone.

Cyst-genus *Bourkidinium* gen. nov.
Type species *Bourkidinium granulatum* sp. nov.

Description :

Cysts are chorate, elongate ellipsoidal, and bear long, hollow, tubular processes which are restricted to the apex and antapex (probably associated with only the apical and antapical series' of reflected plates). The low relief surface ornament shows no evidence of a cingulum or tabulation. The archeopyle is apical, type A.

Comparison :

This genus differs from *Tanyosphaeridium* Davey and Williams, 1966 by having processes present only at the apex and antapex.

Stratigraphic occurrence :

Restricted to the ?Late Aptian and Early Albian of Australia.

Bourkidinium granulatum gen. et sp. nov.
(Plate II, Figure 2a–c)

Description :

Chorate cyst is elongate ellipsoidal and bears long, hollow, distally flared processes arranged in two groups, one at the apical, and the other at the antapical, end. The number of processes is variable, but there are always more in the antapical group (9–15) than in the apical group (4–7). The processes are 23–30 μ long, 1·0–2·5 μ in diameter, cylindrical or slightly tapering towards the distal end, which is strongly flared, slightly recurved with serrate margins, and 5–6 μ in diameter. The body, which is about 45 μ long and 25 μ in diameter, is densely granulate and lacks indications of a cingulum or tabulation. The archeopyle is apical, type A, and all, or all but one or two, of the apical group of processes are on the free operculum.

Comparison :

This species is easily recognized by the unusual distribution of the processes. In both *Tanyosphaeridium isocalamus* (Deflandre and Cookson, 1955) and *T. variecalamum* Davey and Williams, 1966, that have ellipsoidal bodies, the processes are distributed more or less uniformly on the cyst, and their distal ends are not widely expanded distally as in *Bourkidinium granulatum.*

Dimensions :

Central body 35 (46) 62 μ long and 20 (24) 29 μ broad, (10 specimens measured).

Holotype :

Plate II, Figure 2 central body 62 μ long and 29 μ broad. M.M.M.C. 2003.

Distribution :

C. striatus subzone
NSWDM DDH Wanaaring No. 1 ; 95·5 m
NSWDM DDH Weilmoringle No. 1 ; 133·6 m, 99·1 m (H)
NSWDM DDH Bellfield No. 1 ; 101·3 m, 59·8 m
SADM DDH Yalkalpo No. 1 ; 86·25 m
Low *C. paradoxa* zone
NSWDM DDH Wanaaring No. 1 ; 53·4 m

Restricted to the *C. striatus* subzone (Late Aptian or Early Albian) of Dettmann and Playford (1969) and lower *C. paradoxa* zone (Albian).

Cyst-genus *Fusiformacysta* gen. nov.

Type species *Fusiformacysta salasii* sp. nov.

Description :

Cysts are fusiform with bluntly rounded, tapered apical and single antapical horns. The autophragm is ornamented with low relief features (scabrate to punctoreticulate). Archeopyle is precingular, type 2P–?5P, and the operculum is free.

Comparison :

This genus is similar in shape to *Svalbardella* Manum 1960 and to *Palaeocystodinium* Alberti 1961. These genera differ from *Fusiformacysta* by being cavate and by possessing an intercalary rather than a precingular archeopyle. *Svalbardella* and *Palaeocystodinium* are restricted to the Uppermost Cretaceous and Tertiary, while *Fusiformacysta* is so far restricted to the earliest Cretaceous.

Stratigraphic occurrence :

Restricted to the Neocomian of Australia.

Fusiformacysta salasii gen. et sp. nov.

(Plate II, Figures 4a–c, 5a–b)

Description :

Cyst is fusiform with long conical apical and single antapical horns which have bluntly rounded tips. The horns are similar in size and shape, the antapical horn sometimes being shorter ; each is equal to about one quarter of the total cyst length. The autophragm shows no trace of tabulation. The cyst contains no inner body. The archeopyle is large, precingular, and formed by the loss of two to perhaps five individually separating reflected plates. The cyst is usually bent in the area near the archeopyle, so that the longitudinal axis is rarely straight.

Dimensions :

107 (123) 152 μ long and 33 (43) 51 μ broad (10 specimens measured).

Holotype :

Plate II, Figure 4 incomplete specimen 127 μ long and 51 μ broad. M.M.M.C. 2005.

Comparison :

This species differs from other fusiform cysts by having an autophragm, a large precingular archeopyle and a fine, uniform granulation.

Distribution :

Low *C. stylosus* zone
SADM DDH Yalkalpo No. 1 ; 211·46 m
Kalladeina Water Bore, 1,162·7 m, 1,168·2 m, 1,184·9 m
NSWDM DDH Wanaaring No. 1 ; 389·2 (H) (P)
NSWDM DDH Weilmoringle No. 1 ; 435·2 m

The species is rare in all localities, but occurs consistently low in the *C. stylosus* zone of Dettmann and Playford (1969) and is therefore early Neocomian in age.

Cyst-genus *Batiacasphaera* Drugg 1970

Type species *Batiacasphaera compta* Drugg 1970, p. 813–814, Figures 6 A–E, 7 A–B

Emended description :

Cysts subspherical to lenticular, with an angular apical archeopyle of type A. Ornament consists of positive elements which may be separate, or fuse to form rugulae or a reticulum. Membranous ornament and tabulation are absent.

Comparison :

This genus differs from *Canningia* Cookson and Eisenack, 1960 in that the latter exhibits antapical horns. The overall shape of

Batiacasphaera is similar to *Cassiculosphaera* Davey 1969, which has membranous reticulate ornament, *Cassidium* Drugg 1967, which has a tabulate rugulate wall, and *Chytroeisphaeridia* (Sarjeant, 1962) Downie and Sarjeant, 1964 emend Pocock 1972, which lacks ornamentation.

Batiacasphaera macrogranulata sp. nov.
(Plate II, Figure 3a–d)

Description :

In dorso-ventral view, specimens are subcircular in outline, lacking an apical protrusion. Autophragm bears a medium dense cover of low, flat, solid, granulae, that are about 1·5 μ in diameter, or has short rugulae formed by the coalescing of two or more adjacent granulae. The density of granulae is variable ; some specimens bear mostly granulae and few rugulae, while others bear almost entirely rugulae. The surface between the granulae or rugulae is psilate. The archeopyle is apical, type A, operculum free ; the six precingular reflected plates and the sulcal notch are distinguishable by the partial opening of the accessory archeopyle sutures. The sulcal notch is always offset from the midline, as the shape of the cyst is lenticular.

Dimensions :

49 (53) 60 μ long and 49 (55) 69 μ broad (10 specimens measured).

Holotype :

Plate II, Figure 3 ; 60 μ long and 69 μ broad. M.M.M.C. 2004.

Comparison :

The new species differs from *Batiacasphaera compta* Drugg 1970, which has fine reticulate to foveolate ornament, and from *Batiacasphaera baculata* Drugg 1970, which has fine granulae and rod-like tuberculae covering the surface.

Comment :

The new species is common in assemblages lacking other dinoflagellates or containing only a few other forms. With only superficial examination it may be misidentified as a damaged baculate spore.

Distribution :

C. stylosus zone
- SADM DDH Yalkalpo No. 1 ; 211·46 m
- Kalladeina Water Bore ; 1,162·7 m, 1,184·9 m
- NSWDM DDH Wanaaring No. 1 ; 348·0 m, 389·2 (H)
- NSWDM DDH Weilmoringle No. 1 ; 352·0 m, 435·2 m .

Occurs throughout the Neocomian *C. stylosus* zone of Dettmann and Playford (1969), and is the most frequent dinoflagellate in some samples.

Group Acritarcha Evitt

Acritarch genus *Microfasta* gen. nov.
Type species *Microfasta evansii* sp. nov.

Description :

A small, cylindrical ring-shaped acritarch whose diameter usually exceeds its width. The ring may be variously ornamented.

Stratigraphic occurrence :

Restricted to the Neocomian and Lower Aptian of Australia.

Microfasta evansii gen. and sp. nov.
(Plate III, Figures 2a–d, 3)

1960 Gen. et sp. indet. *FORM A* Eisenack and Cookson p. 10, Plate III, Figures 12–14

Description :

Band-like acritarch is made up of a series of long, hollow, cylindrical chambers running lengthways across the ring, and arranged side by side around the ring. The chambers are closed at both ends, and their walls are usually slightly crenulate and finely granulate. The sides of the ring, at which the chamber ends are closed, are usually thickened, and form solid edges. Frequently, the delicate cylindrical chambers are damaged, and only small fragments of the membrane adhere to the ring. In such cases ridges with small fragments of membrane mark the position of the pre-existing cylinder walls.

Dimensions :

Diameter 20 (30) 37 μ and width 6 (11) 12 μ (10 specimens measured).

Holotype :

Plate III, Figure 3 ; 30 μ in diameter and 12 μ wide. M.M.M.C. 2009.

Comment :

As stated by Eisenack and Cookson (1960), the biological affinities of this form are completely unknown. However, it is extremely distinctive and widespread in Australian Neocomian sediments containing limited microplankton assemblages.

Burger (in press) has expressed the opinion that these ring structures may be arranged in life to form long filaments with the heavy thickening marking the lines of fracture between adjacent rings.

Distribution :

C. stylosus zone
  NSWDM DDH Yantabulla No. 1 ; 274·2 m
  NSWDM DDH Wanaaring No. 1 ; 389·2 m, 348·0 m (H), 317·8 m
  SADM DDH Yalkalpo No. 1 ; 190·72 m, 202·30 m
Lower *C. hughesii* subzone
  NSWDM DDH Bellfield No. 1 ; 220·5 m
  NSWDM DDH Weilmoringle No. 1 ; 320·6 m
  NSWDM DDH Yantabulla No. 1 ; 247·7 m
  NSWDM DDH Wanaaring No. 1 ; 290·7 m
Lake Phillipson Bore, South Australia 26·8 m (P).

This species is widely distributed and common in the late *C. stylosus* zone (Neocomian) and early *C. hughesii* subzone (Neocomian–Aptian) of Dettmann and Playford (1969). Also recorded by Eisenack and Cookson (1960) from similar levels (Late Neocomian and Lower Aptian) of the Carnarvon, Carpentaria and Eromanga Basins, by Evans (1966*a*) in the Carpentaria and Surat Basins, and by Evans (1966*b*) from the Gippsland and Otway Basins, this species appears to be a very useful biostratigraphic marker. I have recently recorded this species from the same biostratigraphic level in the Perth Basin (unpubl.). In some samples, it is the dominant microplankton species.

Acritarch genus *Nummus* gen. nov.
Type species *Nummus monoculatus* sp. nov.

Description :

Lenticular fossil is single-walled, with a slight thickening around the margin in dorsal-ventral view. A subcircular to rounded angular pylome is located in an " intercalary " position, and most of the " ventral " wall is lost, apparently by disintegration.

Comparison :

This genus differs from *Cyclopsiella* Drugg and Loeblich 1967, by having a single wall layer instead of two, and by the " disintegrating " instead of solid, ventral wall. *Lecaniella* Cookson and Eisenack 1962*a*, *Paralecaniella* Cookson and Eisenack 1970, *Eyrea* Cookson and Eisenack, 1971 and *Epicephalopyxis* Deflandre 1935, all lack a pylome.

Stratigraphic occurrence :

Restricted to the Aptian of Australia.

Nummus monoculatus gen. et sp. nov.
(Plate III, Figures 1a–d, 4a–c)

Description :

Single walled fossil is lenticular in shape, with a slight thickening around the subcircular margin in dorsal-ventral view. A moderately large subcircular to rounded angular pylome is located in an " intercalary " position on the " dorsal " side, halfway between the margin and the centre of the fossil. The " dorsal " wall is of moderate thickness, and is granulo-punctate. The ventral wall is very thin, granulopunctate and generally almost completely disintegrated. Some specimens have most of the ventral wall intact, while others have small remnants of ventral wall clinging to the marginal thickening which marks the junction of dorsal and ventral sides. As most specimens are slightly compressed, the margins are usually folded in an irregular manner. A " cingulum " may be suggested beneath the pylome on the dorsal side by a fold, or by a line of slightly coarser ornament.

Dimensions :

35 (46) 55 μ long and 31 (39) 43 μ broad (10 specimens measured).

Holotype :

Plate III, Figure 1 ; 45 μ long and 41 μ broad. M.M.M.C. 2007

Comparison :

The new species differs from *Cyclopsiella elliptica* Drugg and Loeblich, 1967 and *Cyclopsiella vieta* Drugg and Loeblich, 1967 by having a single wall layer instead of two, and by having a disintegrating " ventral " wall.

Distribution :

Lower and mid *C. hughesii* subzone
  NSWDM DDH Yantabulla No. 1 ; 184·2 m
  NSWDM DDH Wanaaring No. 1 ; 290·7 m, 257·4 m (P)
  NSWDM DDH Weilmoringle No. 1 ; 284 m
  Santos Oodnadatta No. 1 ; 264·4 m, 256·8 m
  SADM DDH Yalkalpo No. 1 ; 180·71 m, 156·52 m, (H) 155·2 m, 148·30 m
C. striatus subzone
  NSWDM DDH Yantabulla No. 1 ; 53·4 m
  NSWDM DDH Wanaaring No. 1 ; 154·3 m
  SADM DDH Yalkalpo No. 1 ; 89 m, 86·25 m
Occurs rarely to very frequently in the early and mid *C. hughesii* subzone (Late Neocomian to Aptian) of Dettmann and Playford (1969), is absent from the late *C. hughesii* subzone, and occurs rarely, apparently reworked in the *C. striatus* subzone (Late Aptian or Early Albian).

Discussion

The sequence of microplankton (dinoflagellate and acritarch) floras that can be recognized along the southern margin of the Great Australian Basin lies outside the scope of the present contribution and will be discussed fully in a later paper. The biostratigraphic significance of the present species can be best evaluated when compared with the spore and pollen zones of Dettmann and Playford (1969). A summary is presented as Figure 2. The palaeoenvironmental evaluation of the present species rests in part on the work of Harris (1973).

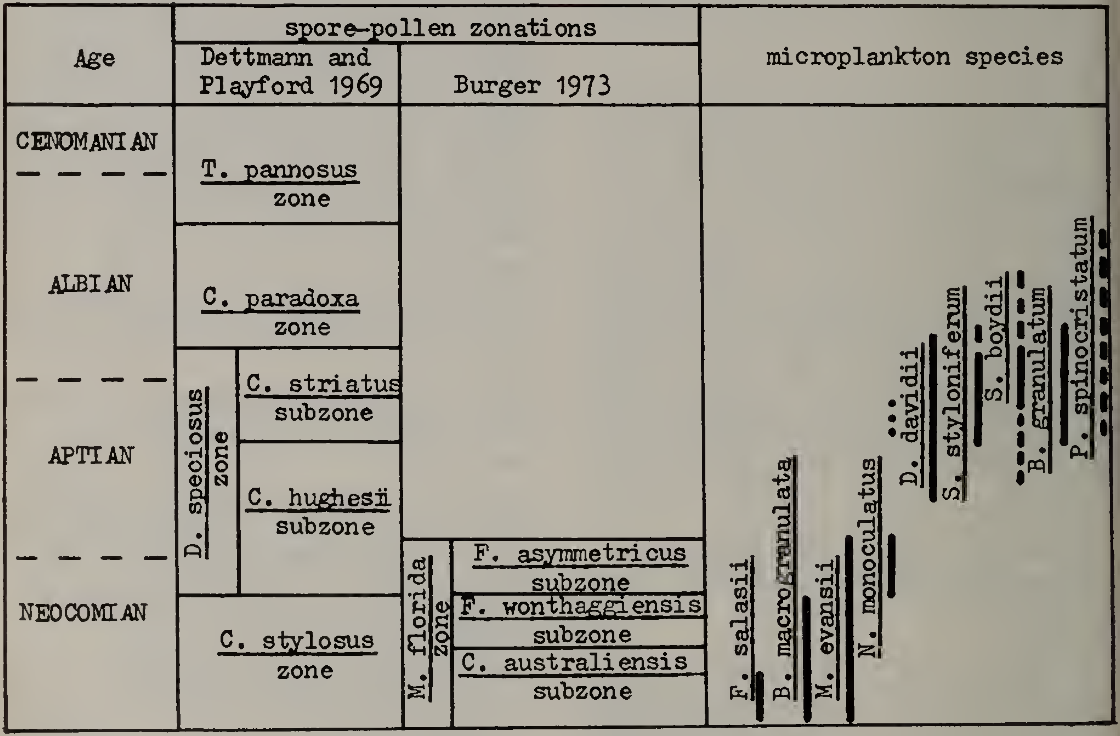

Fig. 2. Microfossil range chart

Fusiformacysta salasii is always rare, but it has a very restricted distribution close to the base of the Cretaceous and early in the *C. stylosus* spore-pollen zone. Because it occurs in rocks otherwise almost devoid of microplankton, its distribution may be largely facies-controlled. It does seem, however, to occur at a stratigraphically consistent level, within the limits of the spore-pollen zonation. All of the six samples in which it occurs have very low species diversity, but the dinoflagellate frequency with respect to other palynomorphs is variable. The species *Fusiformacysta salasii* is morphologically distinct from any cysts described from " marine " rocks. Acritarchs are rare in, or absent from, these samples. These features of the assemblages are considered by Harris (1973) to be typical of " non-marine " Tertiary assemblages. The lithological units with which *F. salasii* is associated (Lower Hooray sandstone in N.S.W. and Algebuckina Sandstone and lower Cadna-Owie Formation in S.A.) show mostly fluvial lithofacies, with some marine influence in the upper part of the Cadna-Owie Formation. There seems no doubt that *F. salasii* is a " non-marine " dinoflagellate in the sense of Harris.

Batiacasphaera macrogranulata occurs at five of its seven localities in association with *F. salasii*. The lithological units within which it is found (The Upper and Lower Hooray Sandstone in N.S.W., and the Algebuckina Sandstone and Cadna-Owie Formation in S.A.) show a gradation upwards from non-marine fluvial to transgressional lithofacies. The palynomorph assemblages in which it occurs have low species diversity, which increases in younger assemblages, and variable dinoflagellate frequency with respect to other palynomorphs. In the sense of Harris (1973), these features overlap the criteria for " non-marine " and " marginal marine " assemblages. I consider that *B. macrogranulata* is restricted to sediments having little or no marine influence. This species occurs at a number of different palynostratigraphic levels according to the spore-pollen zonation, hence, this species is probably more valuable as a facies rather than a biostratigraphic indicator.

Microfasta evansii occurs in Neocomian—Aptian samples from many basins in Australia, only in samples containing few microplankton. In the Great Australian Basin it occurs only once in the fluvial facies, is very common in the transgressional facies and occurs rarely in some samples in older levels of the overlying marine mudstone of the Wallumbilla Formation in N.S.W., and the Bulldog Shale in S.A. It occurs once with *F. salasii* and twice with *B. macrogranulata.* The assemblages in which it occurs feature low diversity (usually less than five microplankton species), few microplankton with respect to spores and pollen, presence of acritarchs, and the recurrence of constituent species in marine assemblages higher in the succession. These features are considered by Harris (1973) to be typical of his " marginal marine " assemblages. Thus I consider frequent *M. evansii* to be " marginal marine ", although the species can tolerate a range from " non-marine " fluvial to " marginal marine " environments. Support for this view is provided by other data on the distribution of this species. Evans (1966*a–b*) recorded the species (as gen. et sp. indet. *Form A* Eisenack and Cookson, 1960) from rocks in the Otway, Gippsland and Great Australian Basins, which contain few or no dinoflagellates. Evans (1966*b*) concludes that the environment is " aquatic ". I have seen specimens in the Carnarvon Basin (recorded by Eisenack and Cookson, 1960) and the Perth Basin of Western Australia, where the species is confined to Neocomian to Aptian rocks containing few other microplankton. The species is not recorded from marine palynomorph assemblages of the same age, which are frequently rich in dinoflagellates.

Nummus monoculatus occurs consistently in the early and mid *C. hughesii* spore-pollen zone, sometimes rarely, or to 30% of the microplankton, making it a good biostratigraphic indicator. It occurs in assemblages which have moderate microplankton diversity (5–30 species), low, variable microplankton content (4–24%) with respect to other palynomorphs, and more dinoflagellates than acritarchs, in both numbers and diversity. I consider such assemblages " marine ", although the low microplankton content suggests that the sample sites were never far from land.

" Marine " assemblages of the same age in Western Australia commonly have very high microplankton content (See Wiseman and Williams, 1974), high microplankton diversity, and many different species. These dissimilarities between Great Australian Basin marine palynomorph and megafaunal assemblages and those of the same age in Western Australia may be a product of geographic barriers, latitudinal differences, shallowness of the Great Australian Basin or a combination of these factors.

Diconodinium davidii is restricted to the upper *C. hughesii* and lower *C. striatus* spore-pollen zones. It is very frequent in the topmost part of the *C. hughesii* zone, and frequently comprises 20–40% of the microplankton. The base-range of this species is considered to be an excellent biostratigraphic datum, while the high frequency of the species in most samples makes it easy to recognize. Near the top of its range, in the *C. striatus* spore-pollen zone, the species is rare. This species is common in all the sections studied, and occurs in the " marine " rocks.

Spinidinium boydii ranges from the upper *C. hughesii* to lower *C. paradoxa* spore-pollen zones. It occurs rarely in many samples, but is very frequent in all " marine " samples from the middle and upper *C. striatus* spore-pollen zone, where it comprises 30–60% of the microplankton assemblage. The total range of the species is of little biostratigraphic value because it is so rare towards the extreme ends of its range; the interval over which the species is very common is of considerable stratigraphic value.

Spinidinium styloniferum is not common in the Great Australian Basin, and occurs rarely in " marine " assemblages throughout the *C. striatus* and *C. paradoxa* spore pollen zones, and is hence of little biostratigraphic value. It is however more common in samples that contain abundant specimens of *S. boydii.*

Bourkidinium granulatum, although always very rare, is very distinctive, and has been observed only in " marine " assemblages of the *C. striatus* and lower part of the *C. paradoxa* spore-pollen zones. It is tentatively used as a biostratigraphic indicator and is frequently associated with rare specimens of *Protoellipsoidinium spinocristatum* Davey and Verdier, 1971. The latter is recorded previously only from the early to late Albian of the Paris Basin, France by Davey and Verdier (1971, p. 47).

The present observations are thus in accord with Harris (1973) with respect to criteria that can be used for environmental conclusions. The new species described here are useful as biostratigraphic and palaeoenvironmental indicators at least in the Lower Cretaceous of the Great Australian Basin.

Acknowledgements

This article is published with the permission of the Under Secretary of Mines, N.S.W. and the Director of Mines, South Australia. A large part of the work was carried out as research toward the degree of Ph.D. at the University of Adelaide. Mr. T. A. Darragh and the Council of the National Museum of Victoria, Melbourne, kindly made many important specimens from their collection available for comparative study. For helpful comment and criticism, I am grateful to my supervisor, Dr. B. McGowran of the University of Adelaide, Dr. J. W. Pickett of the N.S.W. Department of Mines and Dr. D. Burger of the Bureau of Mineral Resources. I am especially thankful to Mr. W. K. Harris of the South Australian Department of Mines and Dr. L. E. Stover of Esso Production Research Company, who made many detailed suggestions concerning the manuscript.

References

Alberti, G., 1961. Zur Kenntnis Mesozoischer und alttertiäres Dinoflagellaten und Hystrichosphaerideen von Nord—und Mitteldeutschland sowie einigen anderen Europäischen Gebieten. *Palaeontographica A*, **116**, 1.

Brideaux, W. W., 1971. Palynology of the Lower Colorado Group Central Alberta, Canada. I: Introductory Remarks. Geology and Microplankton Studies. *Palaeontographica B*, **135**, 53.

Burger, D., 1973. Palynological Observations in the Carpentaria Basin, Queensland. *Bur. Min. Resour. Bull.*, **140**, 27.

Burger, D. (in press). Some Early Cretaceous Plant Microfossils from Queensland, Australia. *Bur. Min. Resour. Bull.*, **160**.

Cookson, I. C., and Eisenack, A., 1958. Microplankton from Australian and New Guinea Upper Mesozoic Sediments. *Roy. Soc. Vict., Proc.* **70** (1), 19.

Cookson, I. C., and Eisenack, A., 1960. Upper Mesozoic Microplankton from Australia and New Guinea. *Palaeontology*, **2** (2), 243.

Cookson, I. C., and Eisenack, 1962*a*. Some Cretaceous and Tertiary Microfossils from Western Australia. *Roy. Soc. Vict., Proc.*, **75**, 269.

Cookson, I. C., and Eisenack, A., 1962*b*. Additional Microplankton from Australian Cretaceous Sediments. *Micropalaeontology*, **8**, (4), 485.

Cookson, I. C., and Eisenack, A., 1970. Die Familie der Lecaniellaceae n. fam. Fossile Chlorophyta, Volvocales? *Neues Jahrb. Geol. Paläontol. Mh.*, 321.

Cookson, I. C., and Eisenack, A., 1971. Cretaceous Microplankton from Eyre No. 1 Bore, Core 20, Western Australia. *Roy. Soc. Vict., Proc.*, **84**, 217.

Davey, R. J., 1969. Non-calcareous Microplankton from the Cenomanian of England, Northern France and North America. Part I. *Bull. Br. Mus. nat. Hist. (Geol.)*, **17**, 103.

Davey, R. J., and Verdier, J. P., 1971. An Investigation of Microplankton Assemblages from the Albian of the Paris Basin. *Verhandel. Koninkl. Ned. Akad. Wetenschap., Afdel. Natuurk.*, Sect. I, **26** (2), 1.

Davey, R. J., and Williams, G. L., 1966. The Genus *Hystrichosphaeridium* and its Allies, in Studies on Mesozoic and Cainozoic Dinoflagellates. *Bull. Brit. Museum, Geol. Suppl.*, **3**, 53.

Deflandre, G., 1935. Considerations Biologique sur les Microorganisms d'origne Planctonique Conserves dans les Silex de la Craie. *Bull. Biol. Fr. Belg.*, **69**, 213.

Deflandre, G., and Cookson, I. C., 1955. Fossil Microplankton from Australian late Mesozoic and Tertiary Sediments. *Aust. J. mar. freshw. Res.*, **6** (2), 242.

Dettmann, M. E., 1963. Upper Mesozoic Microfloras from South-eastern Australia. *Roy. Soc. Vict., Proc.*, **77**, 1.

Dettmann, M. E., and Playford, G., 1969. Palynology of the Australian Cretaceous: A Review; in *Stratigraphy and Palaeontology*: Essays in honour of Dorothy Hill, 174, *Aust. Natl Univ. Press* (Canberra).

Downie, C., and Sarjeant, W. A. S., 1964. Bibliography and Index of Fossil Dinoflagellates and Acritarches. *Geol. Soc. Amer. Mem.*, **94**, 1.

Drugg, W. S., 1967. Palynology of the Upper Moreno Formation (Late Cretaceous-Paleocene) Escarpado Canyon, California. *Palaeontographica B*, **120**, 1.

Drugg, W. S., 1970. Some New Genera, Species, and Combinations of Phytoplankton from the Lower Tertiary of the Gulf Coast, U.S.A. *North. Amer. Paleontol. Convention Chicago, Proc. G*, 809.

Drugg, W. S., and Loeblich, A. R. Jr., 1967. Some Eocene and Oligocene Phytoplankton from the Gulf Coast, U.S.A. *Tulane Stud. Geol.*, **5**, 181.

Eisenack, A., and Cookson, I. C., 1960. Microplankton from Australian Lower Cretaceous Sediments. *Roy. Soc. Vict., Proc.*, **72** (1), 1.

Evans, P. R., 1966*a*. Contribution to the Palynology of Northern Queensland and Papua. *Bur. Min. Resour. Rec*: 1966/198 (unpubl.).

Evans, P. R., 1966*b*. Mesozoic Stratigraphic Palynology of the Otway Basin. *Bur. Min. Resour. Rec.* 1966/69 (unpubl.).

Harland, R., 1973. Dinoflagellate Cysts and Acritarchs from the Bearpaw Formation (Upper Campanian) of Southern Alberta, Canada. *Palaeontology*, **16** (4), 665.

Harris, W. K., 1973. Tertiary Non-marine Dinoflagellate Cyst Assemblages from Australia. *Spec. Publs. geol. Soc. Aust.*, **4**, 3.

Manum, S., 1960. Some Dinoflagellates and Hystrichosphaerids from the Lower Tertiary of Spitzbergen. *Nytt. Mag. Bot.*, **8**, 17.

Manum, S., and Cookson, I. C., 1964. Cretaceous Microplankton in a Sample from Graham Island, Arctic Canada, Collected during the Second "Fram" Expedition (1898–1902). With notes on Microplankton from the Hassel Formation, Ellef Ringnes Island. *Schrifter utgitt av det Norske Videnskaps—Akademi i Oslo I. Mat–Naturv. Klasse*, Ny Ser., **17**, 1.

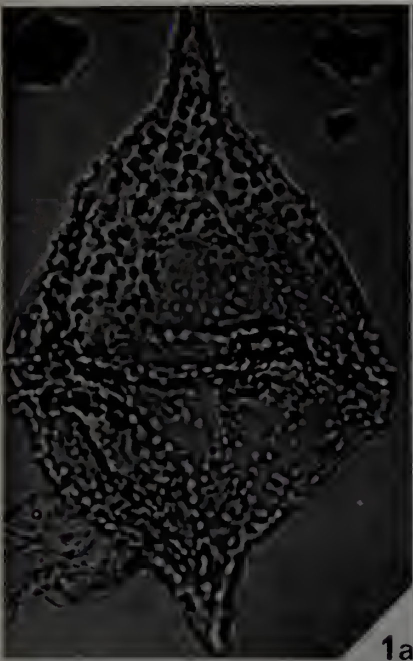
1a

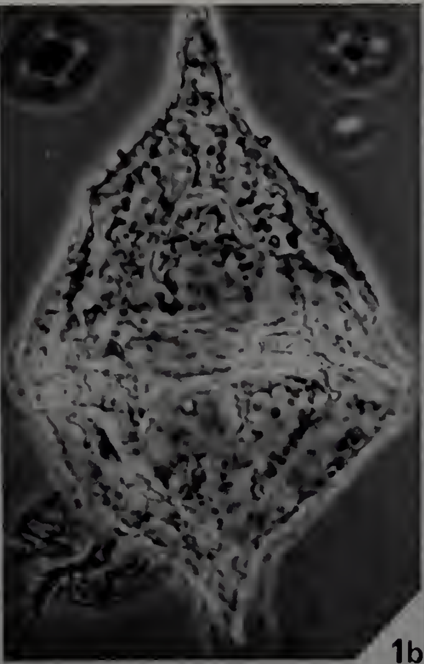
1b


2a


2b


3a

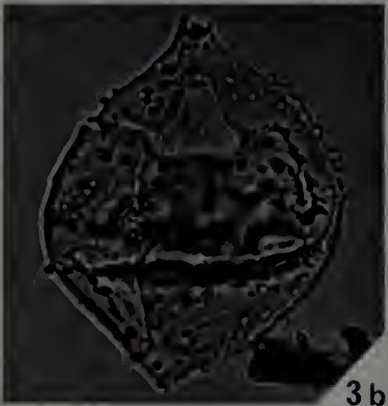
3b


2c


3c


3d

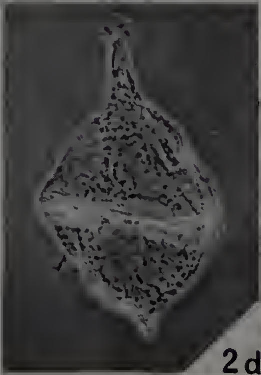
2d

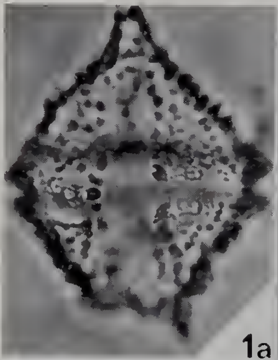
1a

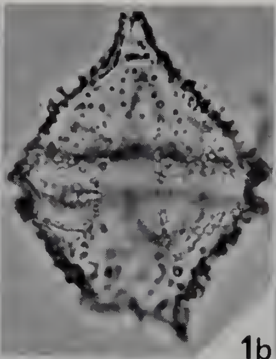
1b

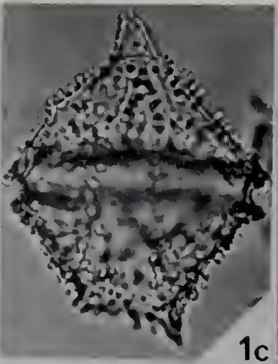
1c


1d


2 a


2 b


2 c


1e

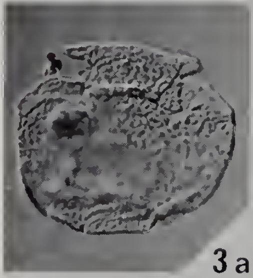
3 a


3 b


3 c


3 d

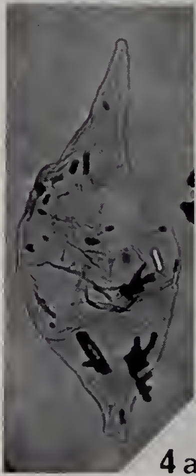
4 a


4 b

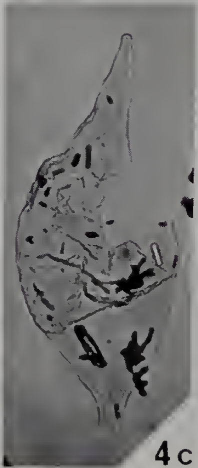
4 c


5a


5b


1a

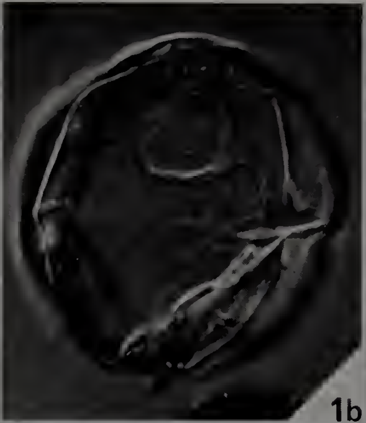
1b


4a


1c


1d

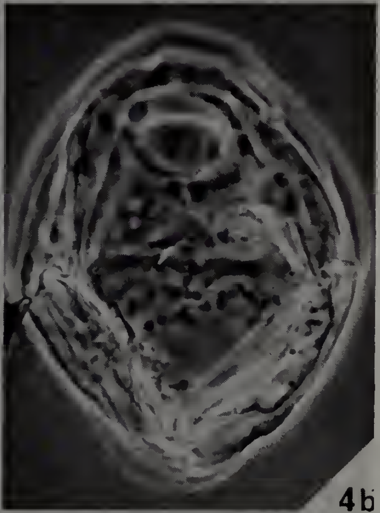
4b


2a


2b


2c

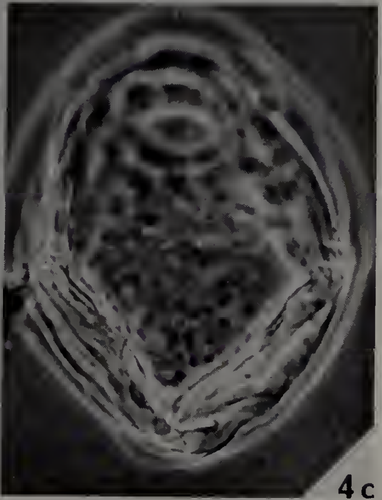
4c


2d

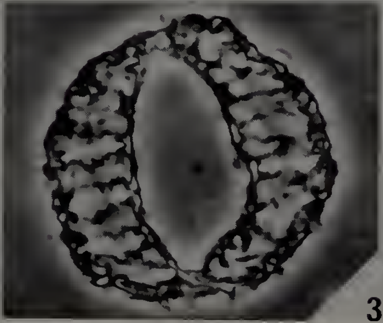
3

POCOCK, S. A. J., 1972. Palynology of the Jurassic Sediments of Western Canada Part 2. Marine Species. *Palaeontographica B*, **137**, 85.

SARJEANT, W. A. S., 1962. Microplankton from the Ampthill Clay of Melton, South Yorkshire. *Palaeontology*, **5**, 478.

SINGH, C., 1971. Lower Cretaceous Microfloras of the Peace River Area, North-western Alberta. *Res. Coun. Alberta, Bull.*, **28** (2), 301.

VEEVERS, J. J., HEIRTZLER, J. R. *et al.*, 1974. Initial Reports of the Deep Sea Drilling Project, Vol. 27 Washington (U.S. Government Printing Office), Vol. 27, p. 915.

WISEMAN, J. F., and WILLIAMS, A. J., 1974. Palynological Investigations of Samples from Sites 259, 261 and 263, Leg 27, see Veevers, Heirtzler, *et al.*, (1974).

Geological Survey of N.S.W.,
Mining Museum,
36 George Street,
Sydney, N.S.W. 2000.

(Received 22 January 1975)

EXPLANATION OF PLATES

Specimen repositories are shown as prefixed by a P (National Museum of Victoria, Melbourne) or M.M.M.C. (Mining Museum Microplaeontological Collection, Sydney). The geological localities of these specimens is shown in the taxonomic section by (H) for holotype and (P) for paratype.

PLATE I

FIGURES 1, 2.—*Diconodinium davidii* sp. nov. Figure 1, holotype in bright field (1a) and phase contrast (1b) showing the type Ia archeopyle ×1,000 M.M.M.C. 2000. Figure 2, paratype in interference contrast (2a–c) and phase contrast (2d) showing the coarse ornamentation and type Ia archeopyle ×400 M.M.M.C. 2001.

FIGURE 3.—*Spinidinium boydii* sp. nov. Holotype shown in bright field. Figure 3b shows the apical separation of periphragm and endophragm. ×1,000 M.M.M.C. 2002.

PLATE II

FIGURE 1.—*Spinidinium styloniferum* Cookson and Eisenack. Holotype in bright field ×1,000 P 21271.

FIGURE 2.—*Bourkidinium granulatum* gen. et. sp. nov. Holotype in bright field. ×400 M.M.M.C. 2003.

FIGURE 3.—*Batiacasphaera macrogranulata* sp. nov. Holotype in bright field ×400 M.M.M.C. 2004.

FIGURES 4, 5.—*Fusiformacysta salasii* gen. et. sp. nov. Figure 4. Holotype in bright field showing (4b) one detached precingular plate inside the autophragm. ×400 M.M.M.C. 2005. Figure 5. Paratype in bright field showing almost complete loss of precingular plate row. ×400 M.M.M.C. 2006.

PLATE III

FIGURES 1, 4.—*Nummus monoculatus* gen. et. sp. nov. Figure 1. Holotype in bright field (1a) and interference contrast (1b–d) showing traces of the " ventral " wall. ×1,000 M.M.M.C. 2007. Figure 4. Paratype in phase contrast showing (4b) the suggested " cingulum ". ×1,000 M.M.M.C. 2008.

FIGURES 2, 3.—*Microfasta evansii* gen. et. sp. nov. Figure 2. Holotype in bright field ×1,000 M.M.M.C. 2009. Figure 3. Paratype in phase contrast ×800 P 17895.

Journal and Proceedings, Royal Society of New South Wales, Vol. 108, pp. 168–188, 1975

The Functional Anatomy of Phacopid Trilobites : Musculature and Eyes*

K. S. W. CAMPELL

Mr. President, members and friends of the Society.

I first heard the name W. B. Clarke when, as a student studying a course entitled " Major Geological Problems ", I had to read a paper by W. H. Bryan on " The relationship of the Australian continent to the Pacific ocean—now and in the past ". This was the Clarke Memorial Lecture for 1944. It is a little dated now, but not all that much. It was good stuff, and like all good stuff it has grown old with dignity and grace. One hopes that contemporary students of geotectonics are encouraged to read it, for it provides a fine historical perspective. I count it a privilege to be allowed to follow in the train of the men and women who, in honouring the memory of W. B. Clarke, have made contributions of this kind to geological science in Australia.

Unlike most previous lecturers I am not attempting a subject of regional or global sweep, but rather I am going to the opposite extreme to examine some aspects of the functional biology of a family of fossils. In doing this I am conscious that I have Clarke's approval. He is justly remembered for his regional geological histories and his major work on " The Sedimentary Formations of New South Wales " in which he used fossil data to solve geological problems. But not only did he respect his fossils for their geological information content—he really loved them. What other explanation can there be for the fact that he sketched 2000 specimens before sending them off to Europe for professional attention ? And being a man of wide scientific and humane education as well as Christian conviction, who can doubt that he reflected long and hard upon the significance of the detail he was recording ? Tonight I would like to continue such reflection.

One is continually impressed by the extent to which uniformitarianism of a particularly narrow kind dominates studies of the functional anatomy of fossils. At its crudest the question is put in the form—Do related living organisms show soft anatomy comparable to that being postulated ? If the answer is negative, then the postulate is assumed to be incorrect. In this form the argument is obviously absurd. Animals in the past must have been uncannily like their living relatives for it to make sense, and evolution must have been a curiously restricted process, failing to produce new anatomy once a basic pattern was established. Uniformitarianism has to be applied in a much broader way, emphasis being placed on the application of physical and chemical principles to observed fossil structures, as well as on comparisons with particular anatomical structures in living forms. I suspect that if this is done the evolutionary process will be found to have produced a wealth of organisms utilizing methods and materials long since discarded, and we will abandon the tendency, so common at present, to force fossils into the categories established for recent organisms.

In support of this contention an examination of the trilobite family Phacopidae has been undertaken. Discoveries of several kinds in the past decade have made it possible to take a new look at the muscular, visual, alimentary, chemosensory and tactosensory systems of this group. Of these I will deal with the first two only.

The Musculature

Inferences about muscles in trilobites have usually been based on analogies with modern enrolling arthropods (e.g. Raymond, 1920). More recently, work by Cisne (1974, 1975) on pyritized specimens of *Triarthrus eatoni* Hall from the Ordovician of the United States of America, has shown vague structures that have been interpreted as pyrite deposited on the sites of decomposed muscle fibres. However such muscle traces are extremely rare, their interpretation is not always free from ambiguity, and there is no guarantee that results from one trilobite may be extrapolated to all.

In a different category is the evidence from muscle insertion sites preserved on trilobite

---

* The Clarke Memorial Lecture, delivered before the Royal Society of New South Wales, 10th July, 1975.

exoskeletons. For many years it has been known that the extrinsic limb muscles were attached either to apodemes on each segment or to flattened areas (especially in the axial region of the cephalon) corresponding with the original segmentation. However, the other muscle systems rarely show evidence of attachment. Eldredge (1971) has summarized the available information on attachment sites thought to be related to the suspension of the stomach and the movement of the hypostome in Phacopaceans. More recently I have attempted to show (Campbell, in press) that the apodemes on certain dalmanitids show evidence of the attachment of dorsal longitudinal muscles both in the cephalon and the pygidium, and that some of the muscle scars described by Eldredge may have served for the attachment of ventral longitudinal muscles also.

The discovery in the Middle Silurian of Dudley, England, of a specimen of *Eophacops musheni* (Salter) in which an extensive array of muscle scars is preserved, has provided the opportunity to check earlier reconstructions and to propose the presence of previously undescribed muscle systems. This specimen is preserved in mudstone that contains quantities of pyrite, and during preservation the dorsal surfaces of the exoskeleton have been slightly abraded. On immersion in liquid vast numbers of symmetrically spaced dark spots and lines appear. These are not situated on the external surface, and have nothing to do with so-called "ornament". In appearance they are all similar to the linear scars associated with the extrinsic limb muscle attachments in the glabella, and this is presumptive evidence that they are muscle scars. The only other possibility is that they represent sites of slight thinning, or even perforations of the exoskeleton associated with sensory structures. This is considered improbable because (a) detailed study of other specimens has produced no evidence of perforations, at least on the same scale; (b) they seem to be concentrated along furrows in the exoskeleton, such as the palpebral and interpleural furrows, whereas sensory organs are usually placed on the prominences; (c) the density of the clustering is not indicative of sensory structures; (d) they are excluded by the doublures, for example on the pygidium, which is unusual if they were sense-related; (e) they exhibit a remarkable bilateral symmetry. None of these points contradicts the view that they are muscle insertions, and in fact most of them positively support that view.

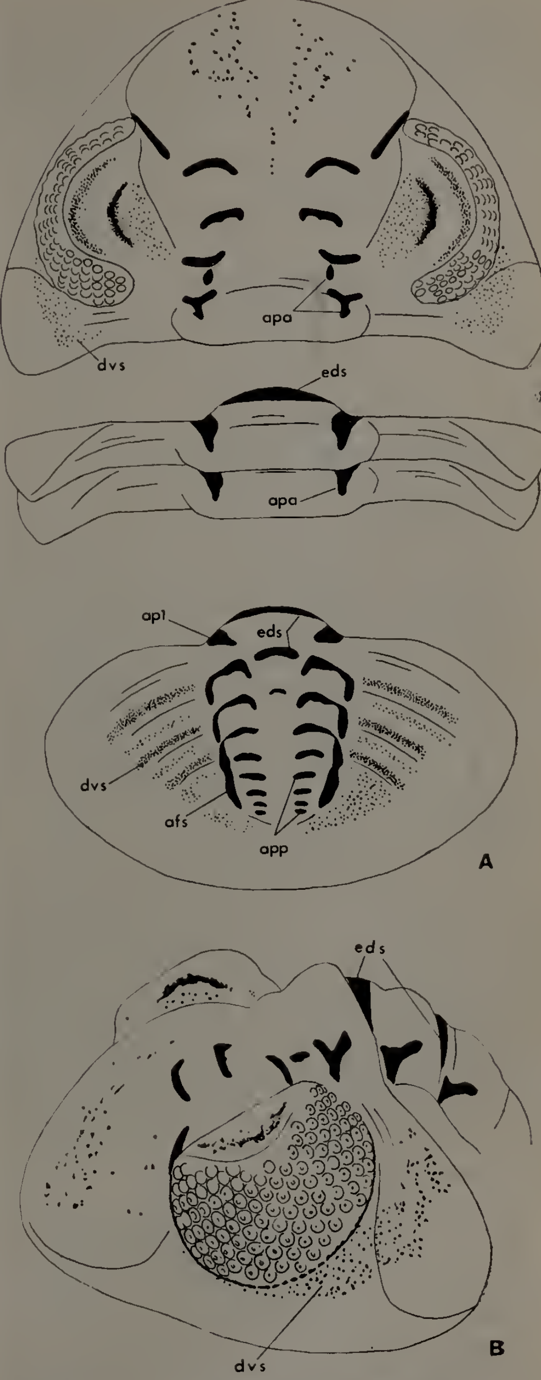

FIGURE 1 a, b.—Dorsal and lateral views of *Eophacops musheni* (Salter) showing muscle scars. Based on A28671 Sedgwick Museum, Cambridge. *a f s*=axial furrow scars; *a p a*=appendage posterior auxiliary scars; *a p* 1=first pygidial apodeme; *a p p*=posterior pygidial apodemes; *e d s*=external dorsal scars.

Assuming, then, the validity of this interpretation, it is possible to divide the scars into the following groups—those on (1) the lateral part of the axis, associated with the apodemes or apodemal pits ; (2) the median parts of the glabella ; (3) the median part of the anterior border and border furrow ; (4) the palpebral lobes and palpebral rims ; (5) the sub-ocular furrows ; (6) the lateral borders of the cephalon ; (7) the pleurae of both thorax and pygidium ; (8) the pygidial pseudo-half rings.

(1) Quite clear scars are present on the lateral parts of the glabella in addition to the occipital, 1p, 2p and 3p scars. In particular there is a large oblique one on the anterior slope of the faint depression that separates the lateral nodes of the occipital ring, and joins anteriorly with the occipital apodemal scar. Similar scars occur in similar positions on the thoracic rings. On the depression separating the node of the lateral part of 1p there is an obviously homologous scar, but it is rather more longitudinal in outline. Clearly these scars are where auxiliary muscles for the limbs were attached. They lie behind the apodemes for the corresponding segments and hence they are referred to as appendage posterior auxiliary scars (*apa* in Figure 1). It may be that the scars 2p and 3p turn back at their medial extremities because a scar of this series has joined the main scar.

Without knowing the points of insertion of the above muscles into the proximal segments of the appendages it is impossible to determine their precise functions, but clearly they served to rotate the proximal segments. The interesting point about these discoveries is that it is possible to interpret the development of nodes on the glabellar lobes and the thoracic rings as the result of muscle insertions, and presumably the strength of such nodes will be related to the activity of the associated muscles, thus offering an opportunity for a functional interpretation.

On the pygidium the appendage muscles show a most significant pattern. On the first segment there are apodemes and auxiliary muscle scars quite similar to those of the thorax. However, the second and third segments have transverse comma-shaped scars along the inter-ring furrows, turned back medially along the edge of the pseudo half-rings, and joined laterally to large scars in the axial furrow. This pattern gives a very distinctive appearance to this part of the pygidium, an appearance that can be seen on all members of the Phacopidae. It should be given more weight in the definition of the family. The most posterior segments retain the scars in the axial furrow but they become fused. The transverse scars become separated from them, lose their comma shape, and lie in the transverse furrows.

The medial part of the transverse scar is the homologue of the appendage posterior auxiliary scar of the thorax, and the lateral part is the homologue of the apodemal scar. There are no scars in the axial furrows of the thoracic segments, so presumably those on the pygidium must be left by muscles that have significance for that part of the skeleton only. Such muscles are most likely to be the ventral longitudinals. As soon as enrolment had begun, the line of action of such muscles attached at these scars would have been below the thoraco-pygidial fulcrum (see Figure 2), and hence they would have been effective. Appendage muscles may have been attached to them also, but it is significant that they do not extend to the most posterior part of the axial furrows, and hence this hypothesis is not favoured.

Although outrolling of the exoskeleton must have been assisted by the increase of pressure on the body fluids caused by contraction of the dorso-ventral muscles, dorsal longitudinal muscles would also have played a part. Insertion sites have been described in the faces of the apodemes of the related dalmanitids and hence they may be assumed to have been present in phacopids (Campbell, in press). There is no evidence of muscle scars in the ring furrows on the thorax as would be expected if those muscles occupied a broad band similar to that figured by Cisne (1974) for *Triarthrus*. They must have been narrow and restricted to the lateral part of the axis, attaching into the backs of the occipital and 1p apodemes in the cephalon, the front of the thoracic apodemes, and the front of the first (and possibly the second) apodemes of the pygidium.

(2) A group of small scars is arranged in a sub-triangular fashion on the anteromedian part of the frontal lobe of the glabella of almost all members of the Phacopacea. Their significance has been discussed by several authors and summarized by Eldredge (1971), who concluded that they were for the support of the anterior part of the digestive tract. Recent work on certain Devonian dalmanitids from America has shown that at least the anterior-most scars of this set are often associated with distortions of the exoskeleton. Presumably when the first layers of skeletal tissue had been deposited after a moult the muscles contracted with such force that the thin carbonate layers became per-

manently mis-shapen. It seems improbable that such force would be exerted by suspensory muscles, but in organism with a large pygidium like a dalmanitid, the longitudinal enrolling musculature would certainly be required to exert considerable force to overcome the inertia of the pygidium in water. It is of interest that the largest scars of this sort are towards the anterior end of the auxiliary field where the ventral longitudinal scars would be anchored (*cf.* Cisne, 1974, Figure 2).

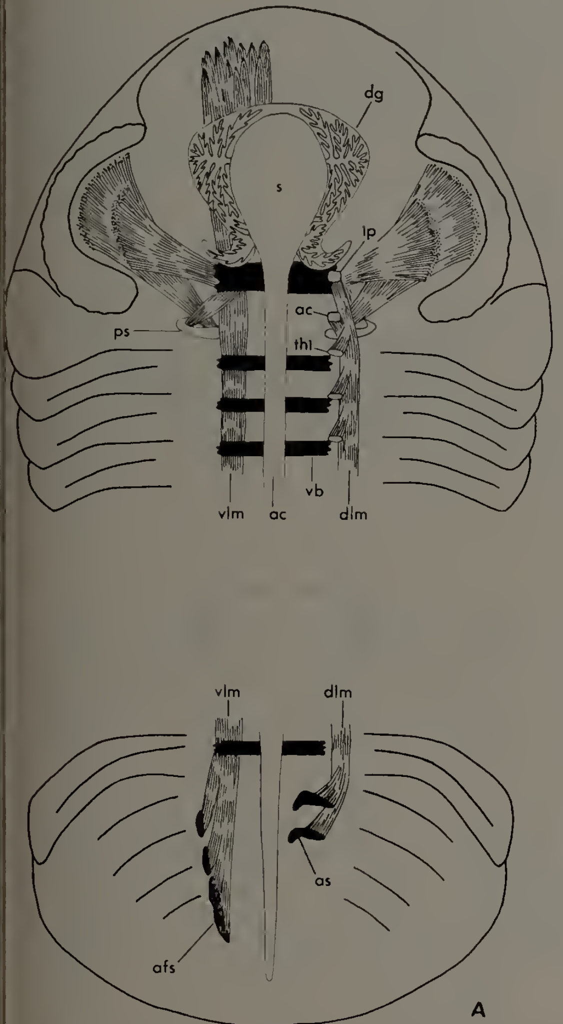

No distortion resulting from undue force has been observed by me in members of the Phacopidae, but this may be explained by the small absolute size of the specimens and the small size of their pygidia relative to those of the Dalmanitidae. They would have been much easier to enrol, a point that is emphasized by the relatively small size of the auxiliary scars themselves.

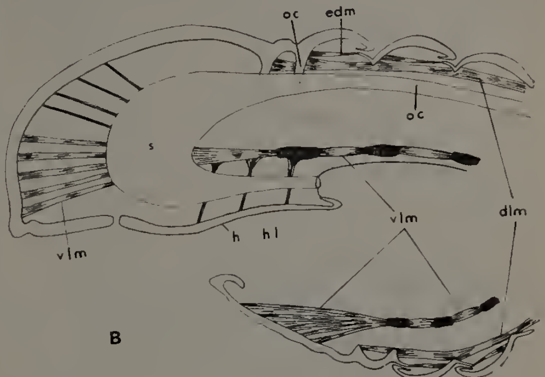

FIGURE 2 a, b.—(*a*) Muscles of the axial and palpebral regions of *Eophacops musheni* in dorsal aspect. Left side shows the ventral longitudinal and right side the dorsal longitudinal muscles. (*b*) Cut away lateral view of a generalized phacopid based on *Phacops rana* and *Eophacops musheni*. Symbols as in Figure 1 and as follows. *a c*= alimentary canal; *a s*=apodemal scar; *d g*= digestive gland; *d l m*=dorsal longitudinal muscle; *e d m*=external dorsal muscle; *h*=hypostome; *h l*=muscles for raising the hypostome; *o c*= occipital apodeme; *p s*=proximal segment of the occipital appendage; *s*=stomach; *s m*=muscles for suspension of the stomach; *th* 1=first thoracic apodeme; *v b*=ventral endoskeletal bar; *v l m*= ventral longitudinal muscle.

It is clear that some of the central scars serve to support the alimentary tract as previously indicated. As can be seen from Figure 2, the stomach is in such a position that without anterior and anterodorsal supporting muscles it could not possibly maintain its position. Such muscles are well known in living arthropods (see for example Hessler, 1964, Figure 12).

(3) Though they are not clearly seen on the specimen of *E. musheni*, members of the Phacopidae are known to have a row of scars along the anterior border furrow. These are well shown in *Paciphacops birdsongensis* (Delo) (see Campbell, in press, Plate XI, Figure 1c), and in *Phacops rana milleri* Stewart (see Eldredge, 1971, Plate XIII, Figure 5). These scars are always small, and are probably related to those discussed under (2) above. On the other hand, they may be for the attachment of the muscles that raised the hypostome. In this connection it should be noted that I have not been able to produce evidence of muscle scars on the cephalic doublure of any of the species studied. There is some evidence that the structures so inter-

preted by Eldredge are similar to the collars around perforations through the exoskeleton, and may be related to sensory structures or to tegumentary ducts. It is probable that the hypostomal muscles were attached to the ventral longitudinal muscles rather than the exoskeleton.

(4) The scars of the palpebral region form two clearly defined bands in the palpebral furrow and the furrow on the palpebral rim (see Plate A, Figure 2 ; and Figure 2). The scars are small and approximately equi-dimensional, but they are very closely packed, those in the palpebral furrow being almost entirely contiguous whereas the spacing of those on the rim furrow are a little less dense. There are also occasional scars scattered over the palpebral regions as a whole.

(5) All Phacopids have a furrow below the visual surface of the eye, and in *E. musheni* this furrow is covered with scars somewhat larger than those described above under (4), particularly in the area below lens files 8–14. Towards the front of the eye they form a continuous band, but towards the rear they form semi-discrete patches. Although this concentration of scars is particularly clear, other smaller ones spill down on to the neighboring cheek and join a band of scattered scars (6) that run back in an arc across the facial suture on to the lateral parts of the posterior border. This arc lies adaxially to the inner edge of the doublure.

So far as I am aware, none of the scars referred to in points 4–6 have been reported previously. Nothing of the kind was noted by Cisne (1974). Consequently it is necessary to glean new evidence to support a functional interpretation. Analogy with living arthropods suggests three possible interpretations of muscles in such lateral parts of the cephalon—extrinsic limb muscles of the specialized cephalic limb, musculature for the suspension of the cephalic ventral endoskeletal bar(s), dorso-ventral muscles that attach to the ventral membrane and operate to vary the turgor of the body fluids. The X-radiographs of Stürmer and Bergström show the presence of large proximal segments on at least the two posterior cephalic appendages, suggesting that these limbs had a specialized role in food-gathering. (Similar results have been obtained for *Triarthrus* by Cisne (1974, 1975), and for *Olenus* by Whittington (1975)). Such structures would presumably require specialized musculature additional to that inserted into the glabellar furrows in order to produce rotation. The length of the area of insertion along the palpebral region in species with large eyes, is sufficiently great to produce rotation in both clockwise and anticlockwise directions on the three posterior cephalic appendages. In *Limulus*, a primitive arthropod with complex limbs in the region of the mouth, the extrinsic muscles extend laterally well beyond the line of the apodemes into the region of the eye (Benham, 1885, Plate 76, Figure 1). During enrolment of a phacopid there would be a tendency for the ventral longitudinal muscles to pull the endoskeletal bar downwards (see Figure 2b), and hence it would be mechanically advantageous to have dorso-lateral support from the palpebral region. Evidence favouring this view again comes from *Limulus* which has the ventral endoskeletal bar supported laterally by a pair of muscles (Benham, 1885, muscles 58 and 59). Incidentally I see no need to postulate the presence of more than one endoskeletal bar in the cephalon of phacopids as Cisne has done for *Triarthrus*.

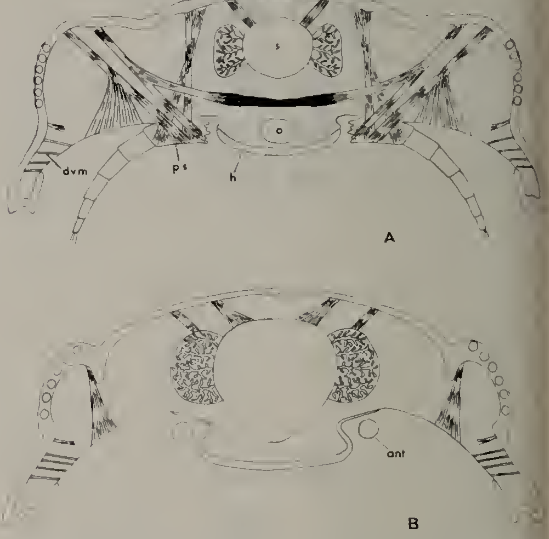

FIGURE 3 a, b.—Cross sections of the cephalon of a generalized phacopid based on *Phacops rana* and *Eophacops musheni*. The sections are across the posterior and anterior parts of the eyes respectively. The form of the digestive glands is hypothetical. Symbols as in previous figures and as follows. *a n t*= antenna ; *d v m*=dorso-ventral muscles : *o*=oesophagus.

Fortunately there is further evidence from the Hunsrück phacopids bearing on this problem. The so-called ommatidia of Stürmer and Bergström discussed below in the section on eyes, could reasonably be interpreted as pyritized tendon or muscle tissue. Cisne (1974) has shown that pyritization of this type can occur, and Bergström (pers. comm.) reports that he has seen it also in specimens of *Mimetaster* and *Cheloniellon* from the Hunsrückschiefer. The fact that in the phacopid material the striation in question is so intimately related to the eyes is consistent with the scars of the palpebral regions of *E. musheni*. In addition, one of the specimens of Stürmer and Bergström (WS613, Plate 18) shows a diffuse mass of tissue extending in a backwardly curved arc across the cephalon from eye to eye. This would correspond well with the predicted position of a support for a ventral endoskeletal bar. Moreover, in living forms the bar is sometimes supported by dorso-lateral and ventro-lateral muscles (see Hessler, 1964, Figs 11, 25, 28 for *Triops* and *Hutchinsoniella,* and Benham, 1885, for *Limulus*), and consequently it is within the bounds of uniformitarian argument to interpret the phacopid scars in this way.

On the other hand, the disposition of the scars on the lateral and posterior cephalic borders is not consistent with this interpretation, as the cross-section in Figure 3 shows. It is possible that these are the scars of dorso-ventral muscles that functioned in the same way as the pleural muscles discussed under (6) below. This opens the possibility that other dorso-ventral muscles were attached to some of the scars in the palpebral region, particularly those on the palpebral rim. However the scars on the subocular furrow are so strong, and so closely clustered that they may be better interpreted as supporting the ventral endoskeletal bar.

(6) Along the interpleural furrows of the pygidium there is a concentration of equidimensional scars that extend laterally to the line of the inner edge of the doublure where they stop abruptly. Some scars also occur on the posterior and/or anterior pleural bands. These scars are not so closely packed as those on the palpebral lobes. On the posterior half of the pygidium the scars of the various segments begin to mingle. There are a few scattered scars posterior to the axis.

Comparable scars on the thorax are difficult to observe, but there appear to be some on the posterior pleural bands lateral to the fulcral points and there may be a few more on the anterior bands medial to the fulcral points.

By analogy with living arthropods there are two possible functions for these muscles—lateral suspension of the ventral endoskeletal bars, or suspension of the ventral membranes. As has been shown above, strong ventral musculature must have existed in the phacopids, but it is probable that these muscles were attached directly to the dorsal exoskeleton in the axial furrows. Thus there would not have been any ventral endoskeletal bars in the pygidium. On the other hand, the wide spread of these scars and their termination along the line of the doublure are consistent with the alternative view that they were for the dorso-ventral musculature.

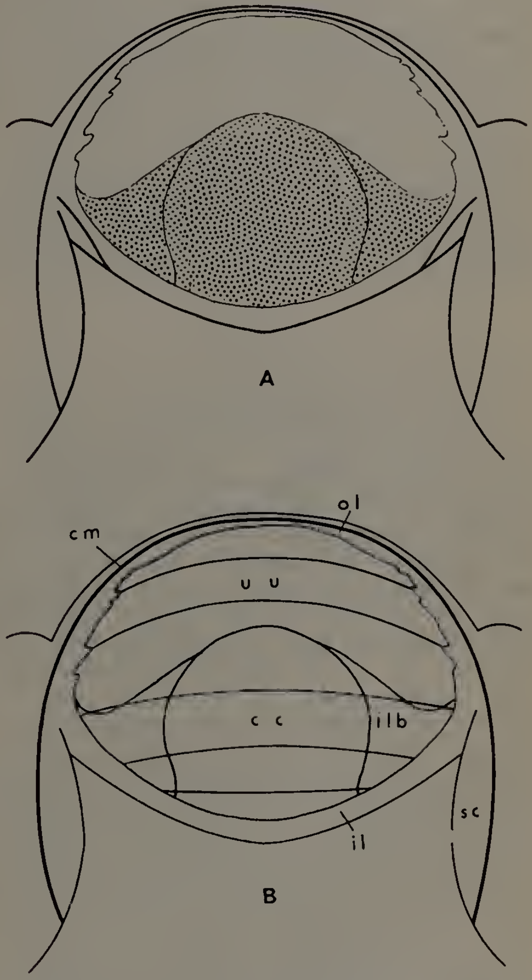

FIGURE 4 a, b.—Reconstructed sections through a lens of *P. rana milleri* showing the various lens elements and lamination. *c c*=central core; *c m*=corneal membrane; *i l b*=intralensar bowl; *i l*=inner layer; *o l*=outer layer; *s c*=sclera.

(7) The presence of external dorsal muscles has been postulated by Hupé (1953) on the grounds of their presence in living arthropods, and the obvious maximal flexing efficiency of muscles inserted in that position, but it has been difficult to demonstrate their existence. Öpik (1937) recorded the presence of paired

scars in the pygidium of *Reraspis plautini* which he regarded as the insertion sites of extensors, but their paired nature suggests that they are likely to be extrinsic limb muscle scars. Whittington and Campbell (1967) described non-silicification of the anterior edges of the half-rings in species of *Proetus*, and this may represent a variation in composition of skeletal tissue where the external dorsal muscles as well as arthrodial membranes were inserted. *E. musheni* shows arcuate scars in the anterior edges of the pygidial pseudo-half rings, which structures are common to all members of the Phacopacea and many other trilobites. In addition the leading edges of the half-rings on the thorax show dark discoloration of the same type, indicating that similar soft tissues were attached there also. I take this as very strong support for the existence of external dorsal muscles.

THE EYES

Introduction

The compound eyes of the Phacopacea have excited interest for almost 140 years (Quenstedt, 1837) and recently they have been subjected to considerable analytical treatment especially by Clarkson (see Clarkson, 1975, for summary and bibliography). In particular, the visual fields have been inferred from external morphology found in members of the group; thin and polished sections have provided data on lens structure and on the possible positions of the light receptors, and a certain amount of speculation on the physiology of the eye has ensued. By and large it has been concluded that the Phacopacea had ommatidial eyes of the apposition type; that the fields of view of the whole eyes usually cover horizontal arcs of 120° to 170° (though the angle is reduced to a few tens of degrees in some late genera such as *Cryphops*), and vertical angles of 20° to 40°; that the internal structure of the lenses varies from genus to genus and may be indicative of systematic relationship; and that the eyes may be sexually dimorphic.

The main contentions of this lecture are that the eye structure has more in common with reduplicated ocelli than with compound eyes; that although the internal structures of the lenses vary from species to species, there is nevertheless a basic pattern common to all, and that this pattern is necessary because of the highly birefringent nature of the calcite of which they are composed; and that the eyes are definitely sexually dimorphic.

Internal Structure of Lenses

The internal structures of the lenses of *Paciphacops logani*, *Paciphacops birdsongensis*, *Phacops rana*, *Eophacops musheni* and *Reedops deckeri* have been examined in polished section and by immersion in high refractive index liquids. *P. birdsongensis* has also been examined in partially silicified material, and specimens of *R. deckeri* in which some of the intralensar structures are replaced by a ferruginous substance that outlines the structure with great clarity, have also been available. Finally, thin sections of *P. rana* have been prepared for observation in polarized light.

In all these types of preservation the following elements have been observed: (a) an outer layer or corneal membrane; (b) an upper unit; (c) a central body or core, termed the proximal nucleus by Clarkson (1969) and the subcorneal lens by Towe (1973); (d) an intralensar bowl; and (e) a basal layer. The fact that they are present in such different modes of preservation indicates that they are original structures and are not the result of diagenetic changes. In summary the lens elements are as follows.

(1) An outermost layer, referred to by Clarkson (1967) as the corneal membrane, covers the whole external surface of the lens and penetrates the interlensar sclera. In some specimens of *P. rana* the detail of this layer is visible and it is seen to be composite. The most prominent feature is a dark layer which is partially or completely covered by a clear layer, and penetrates the entire depth of the sclera. This dark layer is seen at high magnifications to consist of a number of laminae. The overlying clear layer joins the sclera around its margins. Forming a continuous film across the lens surface beneath the dark layer is another clear layer which is usually thinnest axially and thickens to two or three times its axial value peripherally. This thickening in some specimens is achieved by a series of ragged interdigitations with the 'upper unit' of the lens which is described below. This clear layer is apparently continuous with a thin basal layer of similar appearance around the base of the entire lens. The orientation of the carbonate in all these layers is not completely clear because the thickness of the sections makes interference between the adjacent layers so great that it is difficult to make unambiguous observations. However, I suspect that the microcrystalline carbonate forming them has random crystallographic orientation.

(2) An upper unit of variable thickness consisting of calcite with its C-axes oriented as

shown on Figure 6. This unit shows distinct lamination with the laminae having a lesser curvature than the lens surface. Notice that the orientation of the C-axes changes in a regular manner so that over most of the upper unit they remain at 80°–90° to the surface of the lamina in which they occur. The laminae may be formed of organic material. Though it has not been possible to confirm this by direct determination, the presence of organic material in other parts of trilobite exoskeletons as well as other calcified arthropods (Dalingwater, 1973) supports this hypothesis. Further, the cloudy appearance of the lenses in thin section is caused by patches of dark material, more or less irregularly distributed but showing some banding. These patches have not been introduced into the lenses after death, but probably result from decomposition of the organic layers. Variation in the refractive index within the corneal lenses of living arthropods by chemical variation of the layers, is a well-known phenomenon, though this is probably not their function in phacopid eyes.

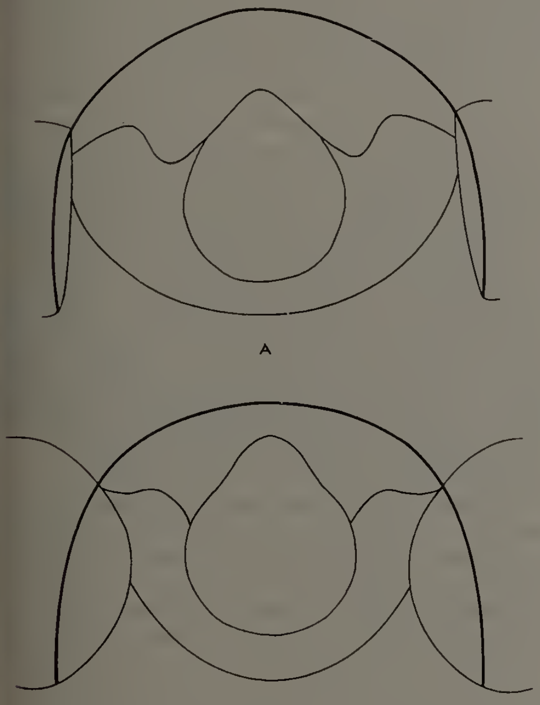

FIGURE 5 a, b.—Diagrammatic sections of the lenses of the two morphs of *Paciphacops raymondi* (Delo) from the Haragan Formation, Oklahoma. Drawn from polished surfaces. Further details in Campbell (in press).

(3) An ellipsoidal to pyriform central core that varies in size and position, is enveloped in a layer that is formed of unusually clear calcite. In some species it is in contact with the basal layer of the lens, and in others it is well above the basal layer (see Figure 5). The central part of the core has a dirty appearance due to inclusions. Overall, the calcite of the core (including its envelope) is oriented with its C-axis parallel with the lens axis. In species from the Early Devonian Haragan Formation the envelope and the corneal membrane are preferentially replaced by iron compounds.

(4) The intralensar bowl is formed of calcite with many inclusions. It is sometimes preferentially dissolved during diagenesis. Its calcite is in optical continuity with that of the central core. This unit and the central core are both crossed by laminae similar to those described for the upper unit.

(5) The basal layer can usually be traced around the lens into the lower layers of the corneal membrane. This is also apparently composed of clear, randomly oriented, microcrystalline calcite.

It was suspected that the different lens components would vary their refractive indices by substituting various elements in the calcite lattice. The three possible substituting elements are Fe, Mn and Mg. Microprobe scanning failed to show traces of the first two, and the variation in Mg is so small that it would have no effect on the refractive index (Figure 6).

Sub-lensar Structures

Clarkson (1967*b*) in his discussion of the physiology of *Phacops* eyes assumed that ommatidia existed, and that given the orientation of the lens axes and the sublensar alveoli, such ommatidia would have been short and of apposition type. More recent work by Stürmer and Bergström (1973) on pyritized specimens from the Hunsrückschiefer, has suggested that there were extremely long ommatidia extending from the eyes to some indefinite area beneath the glabella. Clarkson (1973) has already given reasons for not accepting this interpretation, and with these I am in agreement. Dr Bergström has generously lent me the relevant radiographs and the following features of the structures in question are apparent in them. (a) They are not disposed along the optic axes of the lenses. This is not simply to be explained as a result of post-mortem deformation because they could never have been along the lens axes without crossing one another, and yet in most specimens they have a more or less regular radial pattern. Moreover, the optic axes of the upper rows of lenses of many phacopids intersect the axial furrow and hence the ommatidia could not have passed beneath the glabella. (b) They appear to form a planar set and not a block of rays as they should if they were developed behind all lenses. This can scarcely be explained by pyritization of the surface set of ommatidia only, because of the similarity between specimens and the fact that considerable thicknesses of other tissues are pyritized. (c) As Clarkson has pointed out, the rays extend beyond the palpebral regions in some specimens. Bergström (pers. comm.) now believes that the rays may be exite filaments from some of the cephalic appendages, and there is little doubt that such structures are visible on some specimens. Clarkson has suggested that they may be parts of a caecal system. In my view, some of them may be interpreted as tendons or muscle fibre bundles (see above). But there is now little support for the view that they are ommatidia.

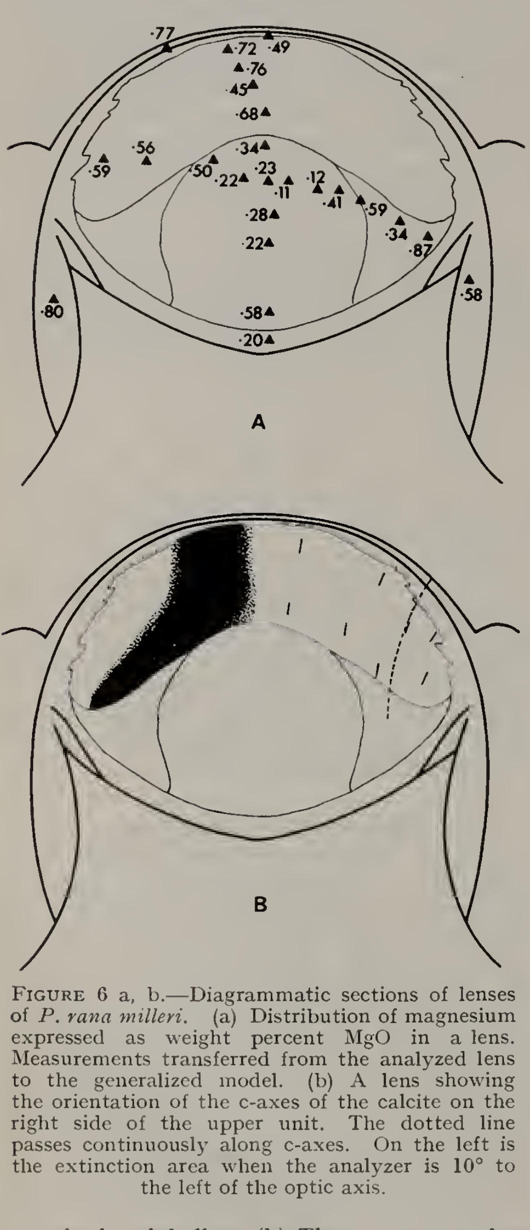

Figure 6 a, b.—Diagrammatic sections of lenses of *P. rana milleri*. (a) Distribution of magnesium expressed as weight percent MgO in a lens. Measurements transferred from the analyzed lens to the generalized model. (b) A lens showing the orientation of the c-axes of the calcite on the right side of the upper unit. The dotted line passes continuously along c-axes. On the left is the extinction area when the analyzer is 10° to the left of the optic axis.

The only other observed sublensar structures that may have a bearing on this problem are those figured by Clarkson (1967*b*, Text-Fig. 1; 1969, Text-Fig. 2, 3). These are rare thin-walled cylindrical structures with their walls apparently continuous with the inner edges of the corneal membrane embedded in the sclera. The cylinders are approximately 2·5 times the height of the lens surmounting them. Clarkson (p. 606–607) regarded these structures as the equivalents of the crystalline cones found below the corneal lenses of most modern ommatidial eyes, though he did countenance the possibility that they were the membranes in which the ' photoreceptive organs ' were contained.

Another feature that has a bearing on this problem is the fact that (Clarkson, 1967*b*) in some parts of the eye the cylinder of sclera has its axis at an angle to the optic axis of the lens situated within it. This is a peculiar arrangement if there were long ommatidia behind the lenses, as the ommatidial axes would be expected to be coincident with both the optic axes of the lenses and the axes of the scleral cylinders.

Thus the observed structures do not lead one to infer ommatidia or any other kind of sublensar structure that can be directly related to modern arthropods. The interpretation of this region of the eye is dependent on indirect evidence, some of which will now be considered.

Indirect Evidence Bearing on the Nature of the Visual Units

Apposition compound eyes are the most common type of eye in living arthropods. They occur in a wide variety of diurnal forms from fast flying insects to slow-moving benthic marine crustaceans, and in different parts of this wide range they exhibit some distinctive structural adaptations. Consequently a discussion on the relevance of modern forms to the interpretation of phacopid eyes should concentrate on slow-moving aquatic animals.

It is known that the effectiveness of modern compound and ocellar eyes depends on a number of factors including the diameter of the lenses, the capacity of the lens to produce a good focus, the size of the receptors with respect to the size of the Airy disc associated with the focus, and the position of the receptor surface with respect to the focal plane of the lens. In addition, apposition eyes require small interommatidial angles and this, coupled with the multiplicity of their lenses, permits them to have much smaller lenses than ocellar eyes without loss of sensitivity. Assuming that phacopid eyes obeyed similar principles, it should be possible to determine if they approximate more closely to ommatidial or ocellar eyes.

The high double refraction of calcite makes it an unlikely substance to use in a lens system. Apposition eyes depend on focusing a beam of light on the end of a small rhabdom, the crystalline cone usually acting merely as a spacing element, thus making the best use of the acuity conferred by the lens. The lens of a phacopid is a very complex structure, and although attempts have been made to show that a beam parallel with the optical axis would be focused at an appropriate point (Clarkson and Levi-Setti, 1975), no discussion of the behaviour of an oblique beam has been attempted. Moreover, these authors suggest that the ordinary and extraordinary rays would focus in different planes. There is the additional problem that their lens model may be incorrect (see below). Hence there is as yet no evidence from the dioptric system for or against the apposition hypothesis.

The diameter of the corneal lenses in apposition eyes of slow-moving aquatic arthropods is rarely greater than 0·2 mm. For example, in specimens of *Limulus* with eyes approx 10 mm long the largest lenses are only 0·2 mm in diameter, and this only in animals that are many times the size of a phacopid. Although *Limulus* and *Phacops* eyes are comparable in shape, it is not uncommon for the lenses in a *Phacops* eye about 10 mm long to be up to 0·7 mm in diameter (Clarkson, 1966*b*), and eyes only 4·5 mm long frequently have lenses up to 0·4 mm. Consequently phacopid lenses are three times greater in diameter than the largest of those in ommatidial eyes, and they are an order of magnitude larger than most.

It may be argued that the large diameter of phacopid lenses increased sensitivity, and that this was necessary because the animals were adapted to dark conditions or to nocturnal habits. The former proposition may be ignored because the geological evidence is that most of them lived in clear shallow water, but the latter proposition may well be true. However, I can find no examples of living species in which the lens diameter is unusually large either because of the generally dark conditions or nocturnal habits (see for example Doflein, 1904 ; Welsh

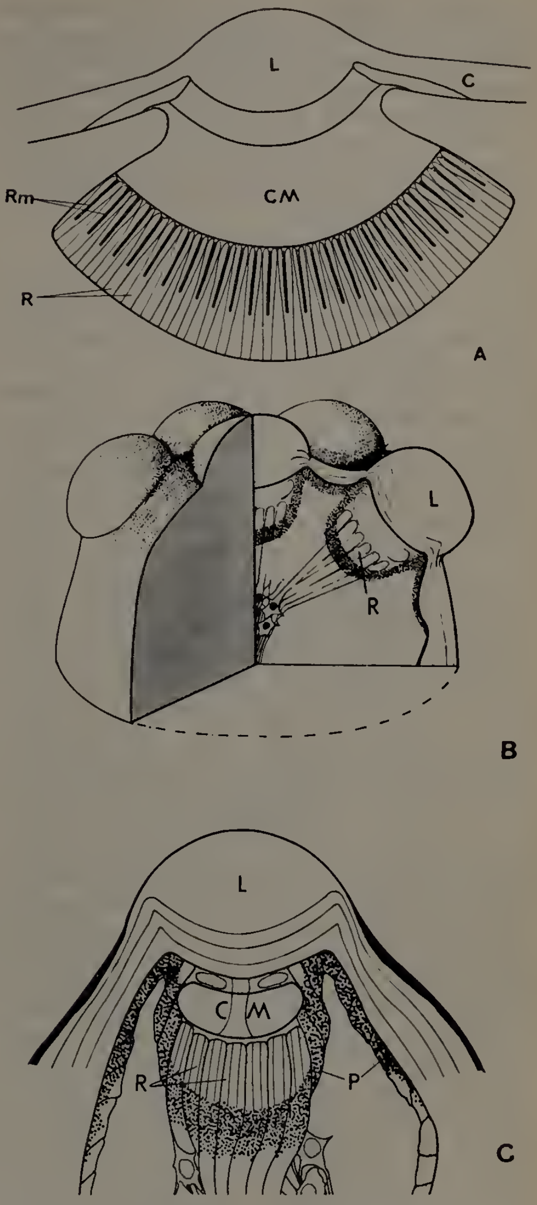

FIGURE 7 a-c.—Reconstruction of an ocellus of the larva of the sawfly *Perga* based on the work of Meyer-Rochow (1974). (b, c) Reconstruction of an ocellar eye of the larva of the ant-lion *Euroleon* modified from the work of Jockusch (1967). *C*=cuticle ; *C M*=corneagenous material ; *R*=rhabdoms ; *Rm*=rhabdomeres.

and Chace, 1937). The deep sea Brachyura described by Doflein (1904) have corneal facets 35–100 μ in diameter, and there seems to be no systematic variation of lens size with total eye size. These values are no different from those of Brachyura from shallow water environments. Consequently the large lens diameters are not likely to be explained in terms of operation under dark conditions.

For an eye of given size and curvature, and lenses approximately in contact with one another laterally, increase in lens diameter automatically increases the interommatidial angles. Increase in curvature of the eye surface without increase in size also increases the interommatidial angles. In most ommatidial eyes, even in slow moving crustaceans, these angles are usually 4–8°. In *Limulus*, Waterman (1954) records interommatidial values between 4–15°, the high values being confined to the region of high curvature at the posterior of the eye. Over the area of greatest lens concentration in the eye of *Phacops rana milleri* " the longitudinal axial (interommatidial) angles average 6°, but they increase anteriorly to 14°, and posteriorly where the curvature is extreme, to 20°. Latitudinal axial angles are about 3° in the region of maximum concentration, increasing upwards to 14° ; in other parts of the visual field they average 10° (Clarkson, 1966*b*, p. 470). Other phacopids have somewhat smaller angles, but still large in comparison even with *Limulus*. In almost all phacopids the sclera between the lenses is thick, and in *P. rana* it is especially so. As a result the interommatidial angles could be considerably reduced while maintaining the lens size, simply by closer packing. In this respect, therefore, if the eyes are ommatidial, they do not make optimum use of the space they occupy.

Evolutionary trends in phacopids are towards reduction in the number of units in the eye, whereas in ommatidial compound eyes the trend towards better eyes invariably has involved an increase in the number of facets and reduction in the interommatidial angles. It is difficult to conceive of phacopid eyes with two or three lenses being ommatidial.

Finally, nothing is known about rhabdom size in phacopids, and this factor cannot be used in the present argument.

Consequently, on balance, the indirect evidence suggests that the characters of the optic units in phacopid eyes are not those associated with ommatidia. On the contrary, if ommatidîa lay behind the facets it would seem to be impossible for even the best of them to resolve objects subtending small angles at the eye.

An Alternative Hypothesis

If the eyes are not ommatidial the only alternative by analogy with living forms is that they are ocellar. Of course, they may be of a type which has no modern analogue, a view which is lent some credence by the fact that the lenses are composed of calcite, a substance not used in living arthropod eyes.

Lindström (1901, p. 31–34) considered that the trilobites *Harpes*, *Harpides* and possibly *Trinucleus* had 1–3 ocelli, but phacopid eyes were not considered to be of this type. He referred to them as " aggregate eyes ", a special category. In living arthropods compound ocelli are not common, and where they occur they are usually in aggregates of up to six units. They are most common in the larval stages, though a group of three ocelli is common in many adult insects. The arrangement of the units is not always in a regular geometrical pattern. However, even in larvae the lenses reach a diameter of 0·35 mm, which is many times larger than the largest ommatidial lenses, but comparable with those of phacopids. The structure of the lenses varies from group to group, but in essence they are formed of several layers with differing refractive index contained within a corneal and a basal membrane. The lens of the sawfly *Perga* is in many respects like the lens of a phacopid (Meyer-Rochow, 1974, Fig. 13). It is strongly biconvex and consists of a basal unit like the intralensar bowl, and an upper unit which is apparently homogeneous. The differences between this and a phacopid are probably the result of the use of calcite in the phacopid lens.

The sublensar structures in ocelli also vary considerably, but basically they consist of transparent corneagenous tissue immediately below the lens, and below that a layer of retinula cells the upper surface of which lies approximately at the focal plane of the lens. The transparent tissue and the retinula layer are encompassed by a pigmented layer (see Jockusch, 1967, Fig. 3 ; Meyer-Rochow, 1974, Figs 4, 14, 15). One interesting feature of these structures in the antlion *Euroleon nostras* figured by Jockusch, is that in relative depth they are comparable with the sublensar cones described by Clarkson for *Phacops fecundus* and *Reedops cephalotes*. This suggests the possibility that there was transparent tissue occupying the space within the scleral lumen, and the distal edges of the retinula cells formed a surface as shown in

Figure 8. It is interesting that the larva of *Euroleon* with six ocelli in its array has fewer retinula cells per ocellus than *Perga*, which has only one ocellus. Presumably this simply means that each ocellus in a multi-element eye is required to scan a smaller part of the field, and one would therefore expect *Phacops* with its multitude of lenses to resemble *Euroleon*, as it would if the reconstruction in Figure 8 is correct. Such an arrangement offers an explanation of the divergence between the axis of the scleral cylinder and the optic axis of the lens—they would not need to be coincident if the retinula cells were close to the base of the lens. (A further advantage of this pattern is discussed below.) Also, since these sublensar units are so short they would in no way obstruct the muscle bundles attached to the ventral surface of the palpebral furrow and the palpebral rim.

For such an interpretation to be valid, however, it would be necessary to show that the focal plane of the lens at each locus is approximately in the position predicted. The only way of approaching this problem is by ray-tracing. This can be done with some accuracy for *Phacops rana* using the lens model outlined above and making certain minimal assumptions about the refractive indices of the various lens layers and the proposed corneagenous layer.

Using a lens model based upon the features described above, my two colleagues R. A. Eggleton and L. Belbin have computed ray paths for *P. rana*. Some simplifications of the model have been used but these are not regarded as significantly affecting the dioptrics. Thin layers of organic material with a refractive index of 1·50 have been placed in the upper unit. They have almost no effect on the ray path. It is considered possible that their function from an optical point of view was to separate the layers of calcite so that the orientation of the c-axes in successive layers could change in the manner shown in Figure 6. From a morphological point of view they represent growth layers. Similar layers occurred in the intralensar bowl and the central core, where the c-axis has a constant direction, but they would not have had any effect on the ray path unless they occurred in great numbers. There is no adequate evidence for this, and so they have been ommitted from the model. A second simplification is that the c-axes in the upper unit are considered to be normal to the surfaces of the layer in which they are found whereas they are apparently at 75–90° to the surfaces. The refractive indices of sea water and the sublensar organic material have been taken as 1·33 and 1·35 respectively. Since the lens has been determined to be almost pure $CaCO_3$, calcite refractive indices have been used appropriately for ordinary and extraordinary rays.

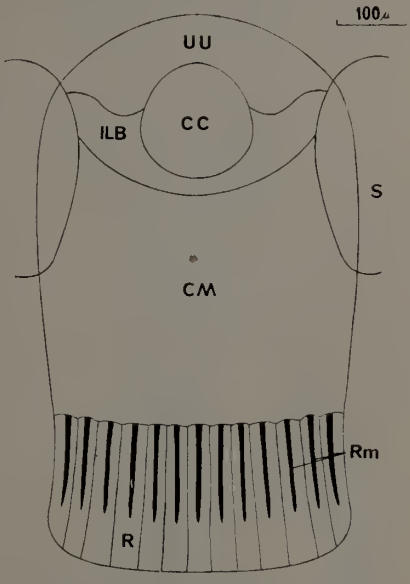

FIGURE 8.—Diagrammatic reconstruction of an optical unit of a phacopid trilobite. (Same symbols as Figure 7.)

For the ordinary rays from a parallel beam of light parallel with the optic axis, the focal length of the lens is approximately 1·6 times, and for the extraordinary rays approximately 1·65 times, the lens thickness. Given the imperfections of the model and the approximations involved, these foci are sufficiently close to be considered as coincident. Similar beams incident at 10° and 20° to the optic axis also produce approximately coincident foci for the two rays, though the definition of the foci is rather poorer than that of the rays parallel with the axis. All rays focus approximately in the same plane (see Figure 9).

It is concluded from these data that the lens model is reasonably accurate. In particular, the coincidence of the ordinary and extraordinary rays is regarded as remarkable, and an improvement over the model used by Clarkson and Levi-Setti. To check that the crystallographic orientations used are really significant, other models with different orientations were also tested, but they either did not produce a focus or there was a poor focus at a remote focal plane.

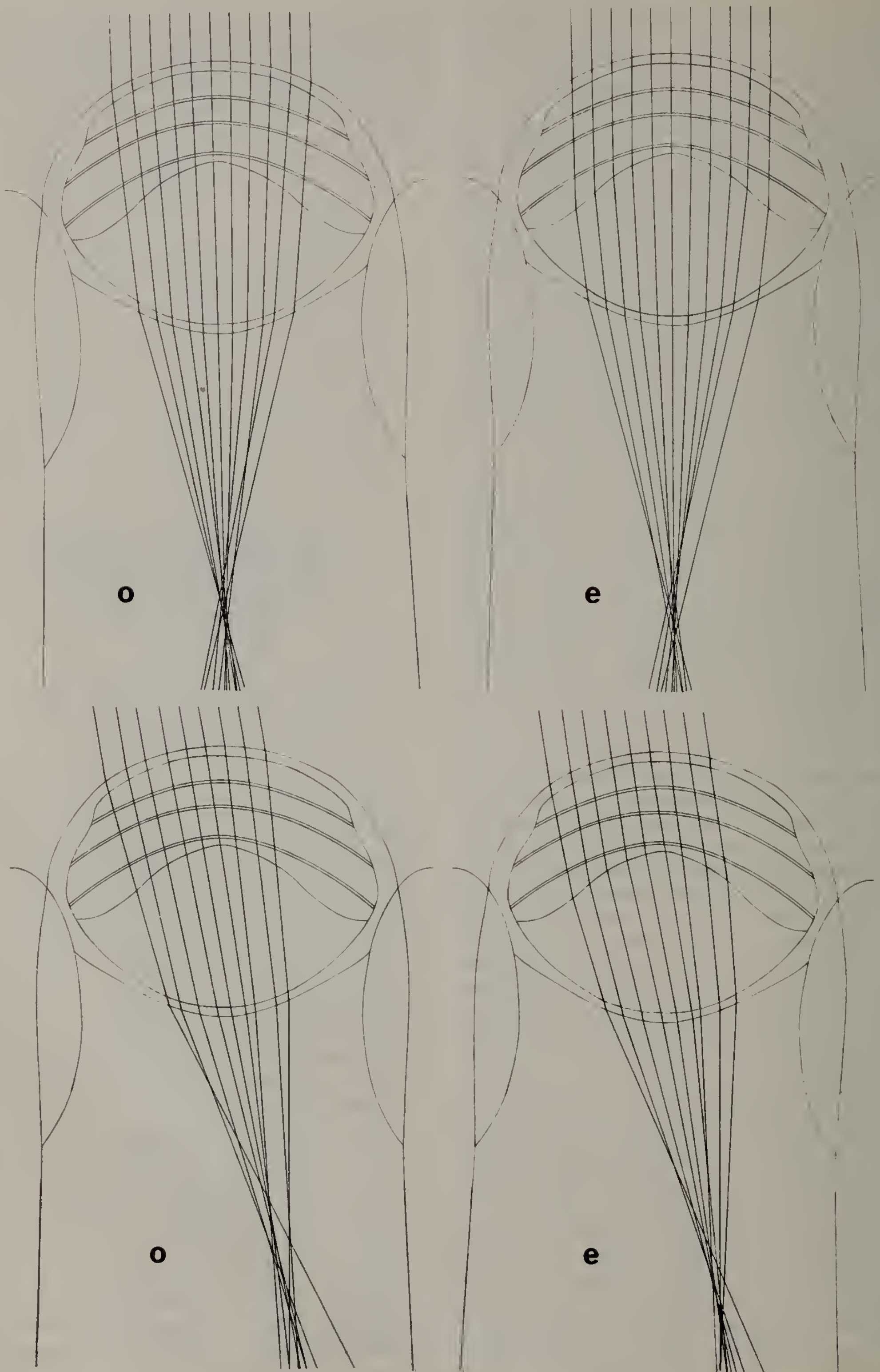
o
e
o
e

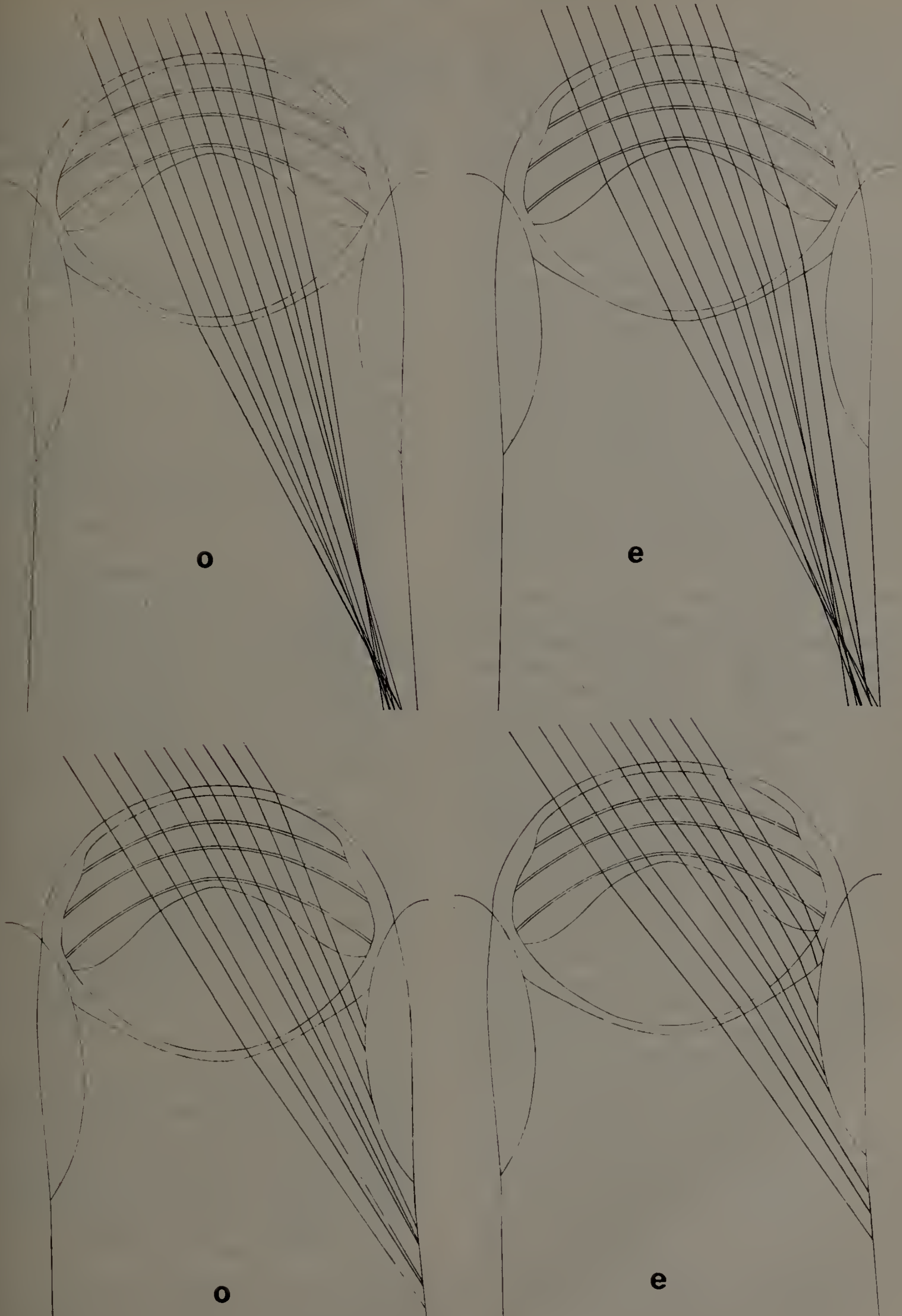

FIGURE 9.—Computer simulated ray paths through the lens model used in Figure 6. Transverse lines in the upper unit represent laminations. Some paths are obviously displaced, probably because of the method of digitizing the lens elements in 5° units. The four pairs of figures show the ordinary and extraordinary rays incident respectively at angles of 0°, 10°, 20° and 30° to the optic axis of the lens.

It may be reasonably be assumed that the focal plane of the lens defines the upper surface of the retinula layer. That this is not concave is a matter for some surprise because the rhabdoms would be expected to be oriented approximately parallel with the light beam. However this may be the result of slight errors in the model and in the calculation of the ray paths.

The depths of the sublensar capsules in the species where Clarkson has observed it are approximately the same relative to the size of the lenses—*viz* 1·5–2·0 times the lens thickness. This indicates that the scleral lumen and most of the sublensar capsule would have been occupied by the transparent corneagenous layer. It seems probable to me that short rhabdoms occupied the bottom of the capsule, the basal membrane of which was the basal layer of the visual unit in the same manner as in *Euroleon*. However, the possibility that the rhabdoms lay beneath the basal membrane of the capsule cannot be disregarded.

As can be seen from Figure 9, light incident at angles greater than about 22° will impinge on the walls of the sublensar capsule or the sclera before reaching a focus. This gives the lens a relatively narrow field of vision in comparison with the ocellar lens of *Perga*, but it is quite consistent with the interocellar angles referred to above. Although the total angle of vision of each lens is 45–50°, the focus is good only in a relatively small foveal region. The amount of light reaching a laterally placed rhabdom will depend on the angle of incidence of the light, but it might be expected that as little as 30% of the incident light in a beam will focus on any given rhabdom. Thus although the data are not good enough to produce precise figures, it would be surprising if high acuity and high sensitivity occurred outside a small group of centrally situated rhabdoms, and this effectively restricts acute vision to directions within a few degrees (10° at the most) of the optic axis. Under these circumstances the overlap of acute vision between neighbouring visual units will be small. It should be noted that in the ommatidial eye of *Limulus*, although the total visual angle is approximately 50° the acceptance angle (i.e. the angle of 50% sensitivity) is only ±6° (Kirschfeld and Reichardt, 1964, p. 49), and in *Limulus* the interommatidial angles are not greatly different from the interocellar angles in *P. rana*. According to the above authors the large overlap of the visual fields of adjacent ommatidia in *Limulus* is effectively reduced by a lateral inhibition system. In the case of *P. rana* effective reduction of acute vision would be produced by the quality of the dioptrics.

The fact that some sort of focus is achieved even at the margins of the retinula suggests a reason for the asymmetry of the scleral lumen with respect to the optic axis of the lens, in the visual units near the periphery of the eye. This effect was noted by Clarkson (1967 ; 1969). As is shown in the horizontal section in Figure 10*a*, the asymmetry has the effect of increasing the

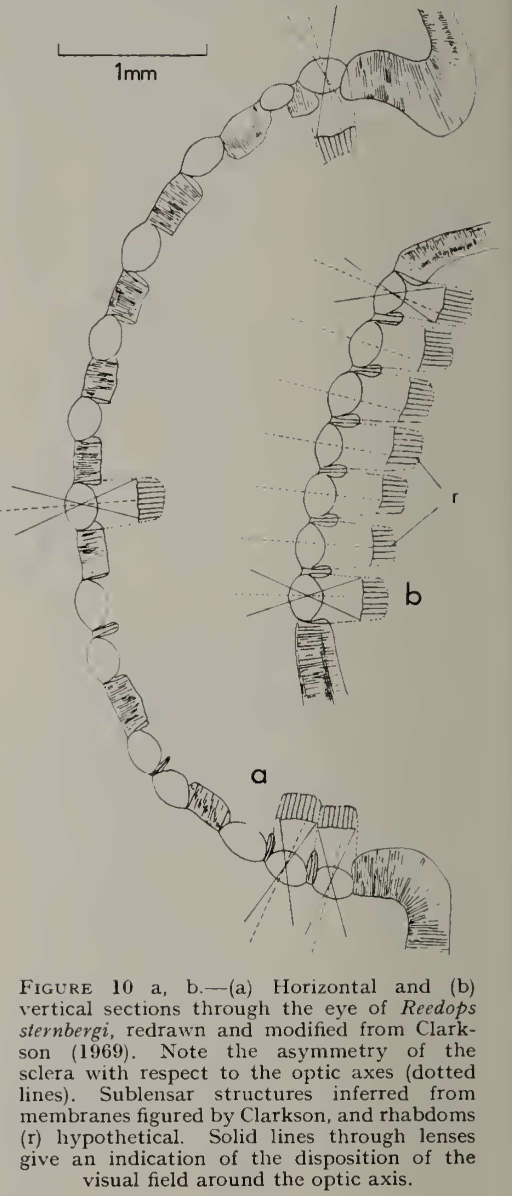

FIGURE 10 a, b.—(a) Horizontal and (b) vertical sections through the eye of *Reedops sternbergi*, redrawn and modified from Clarkson (1969). Note the asymmetry of the sclera with respect to the optic axes (dotted lines). Sublensar structures inferred from membranes figured by Clarkson, and rhabdoms (r) hypothetical. Solid lines through lenses give an indication of the disposition of the visual field around the optic axis.

field of vision of the eye at the anterior and posterior ends, though the quality of the images at the limits of the field would have been relatively poor. Also as noted by Clarkson, vertical sections of the eyes of most species show the sclera disposed horizontally, and the sclera bounding the upper edge of the lens projecting further inwards than that bounding the lower edge. This results in a far greater asymmetry than that in the horizontal sections, and is best illustrated by sections of *Reedops sternbergi* given by Clarkson (1969, Text-Fig. 4). Such an arrangement is possible only because the vertical inter-axial (interommatidial) angles are much smaller than the corresponding horizontal ones, and hence the vertical field is well covered by many lenses. It is not surprising, therefore, to find that the higher lenses in each file are positioned in the sclera so that the effective field of vision is greater above the horizontal than below it (see Figure 10*b*).

The Functioning of a Phacopid Eye

Thus a case can be made for considering that each lens in a phacopid eye was at the apex of an ocellus-like structure. No living organism, however, has anything comparable with the total eye complexity shown by phacopids, and so it is now necessary to try to determine what advantage this complexity confers. To do this it is necessary to examine the function of known ocellar eyes.

Pure ocellar (or stemmatal) vision is found in living arthropods among slow-moving terrestrial or aquatic adults, or in the larval stages of forms which change to ommatidial vision in the quick-moving adults. What advantage is it then for a slow moving organism to have ocellar vision ? Meyer-Rochow (1974, p. 1588) has shown that the " little stemmata of sawflies are capable of polarization sensitivity, motion detection and form and colour perception ", and this achieved with a single lens on each side of the head. Moreover, because of the design of the lens, the total visual field is about 200° with a 50% value of 140°. On the other hand acceptance angles of individual centrally situated rhabdoms have been determined by ray tracing methods to be as low as 3·6° whereas those towards the periphery are up to 16·4°. Experimental work gives somewhat larger values. Mean acceptance angles for all rhabdoms are approximately $11{\cdot}5 \pm 5{\cdot}1°$ in the light adapted and $13{\cdot}8 \pm 6{\cdot}8°$ in the dark adapted state. The mean apertural angle is 40°+. High resolution is restricted to the axial part of the receptor system, the resolution values falling off rapidly towards the limits of the retinula. Nevertheless angles as low as 4° can be resolved.

Forms with compound ocelli such as the larvae of tiger-beetles, ant-lions, cabbage caterpillars and the like, with up to six lenses in each array, have also been studied in detail. Jockusch (1967) has described the most regular of these, the small domed eyes of the antlion larva (*Euroleon nostras*). A diagrammatic section is shown in Figure 7*b*. The individual units are separated by thick pigmented bands which are continued around the bases of each group of rhabdoms. Mean acceptance angles for all rhabdoms are approximately 16° but the total apertural angle is approximately 47°, a value much less than that given above for *Perga*. The angle between the optic axes of adjacent ocelli is approximately 60°, and this together with the apertural angle above gives each aggregate eye a cone shaped field with an apical angle of approximately 170°. However, because of the high interocellar angle not all points within this cone are efficiently scanned while the eye is stationary, so that some movement of the animal is required to cover the field with acute vision. Without behavioural studies it is not possible to determine the capacity of these eyes for movement and form perception, and no measurements of their acuity are available. However, assuming that each ocellus had comparable acuity to those of *Perga*, it would seem that the increase in number of ocelli increases the acuity of the eye over the whole field but it does not expand the size of the field.

In other organisms the ocelli are not arranged in geometrical fashion but are spread more or less randomly along each side of the head. Details of the fields and acuities of these eyes have not been available to me.

If the conclusion that the phacopid visual units are ocellus-like is correct, there is no known living form with the ocelli arranged in a comparable geometrical pattern. What then is the significance of the phacopid pattern ? Clarkson has proposed that it is an adaptation to movement perception. Longitudinal movement was detected only because the visual field is divided into vertical strips which are the result of organization of the lenses into vertical files, and latitudinal movement perception is possible because the slight vertical curvature of the visual surface produces continuously changing elevations in the successive lens axes in each vertical file.

This interpretation is almost certainly correct as far as it goes, but it leaves two points without satisfying explanations.

(a) The Phacopina with schizochroal eyes is related to the Cheirurina with holochroal eyes (Moore, 1959), and probably developed from it. Holochroal eyes have lenses without intervening sclera and their facet diameters and " interommatidial angles " are comparable with those of apposition eyes of living arthropods. These are known to function well as movement detectors, their efficiency being attested by the fact that they are found in a large number of distantly related groups. Is it reasonable to suppose, therefore, that schizochroal eyes conferred some special advantage for movement detection rather than a capacity of some other kind ?

(b) Some schizochroal eyes have only a few lenses and these are often irregularly arranged so that they cannot have functioned in the manner indicated for multi-element forms. Eye reduction occurred independently several times in the Phacopina between the Late Silurian and the Late Devonian. Examples are *Denkmannites* (Late Silurian), *Prokops* (Early Devonian), *Reedrops* (Early-Middle Devonian), and *Cryhops* (Late Devonian). It is often suggested that eyes of this type were degenerate and that animals bearing them lived in the deeper and darker parts of the sea (see Clarkson 1967*a* for summary). This interpretation is faced with some real difficulties. Forms with reduced eyes are found in shallow water deposits with large-eyed species in circumstances indicating that they have not been transported (Chlupâć, 1966, p. 126). The lenses in species with reduced eyes are invariably directed anterolaterally, the direction covered by the densest lens array in multi-facetted species, and hence the direction of most acute vision. This suggests that reduced eyes were still functional. The little evidence available (there has been no detailed work yet) on lens structure suggests that lenses in reduced eyes are comparable with those in large eyes. Nor can the irregularity of the arrangement of the small number of lenses be regarded as indicative of degeneracy, for groups of ocelli are often irregular in modern organisms (e.g. the larvae of tiger beetles, Friedericks, 1931) while being highly functional. Of course the rhabdoms and nerves could have been degenerate, but that cannot be checked, and such a view should not be invoked without strong support from some other source. We are left, therefore, with functional reduced eyes that could not have formed visual strips or measured elevations by engaging successive lenses in a vertical file.

The ocellar hypothesis provides the possibility of another explanation. The very similar biochemical and neurophysiological properties of ocelli and compound eyes, and the fact that they occur at different ontogenetic stages of the same organisms suggests that they are under the control of the same genes. It is interesting to note therefore that although the trilobite family Cheiruridae is predominantly holochroal, some of its members, e.g. *Holia* and *Acanthoparypha*, have multi-element eyes with larger lenses than normal and some features in common with schizochroal eyes (Whittington and Evitt, 1954). It may be that this is an example of an abrupt change in gross eye morphology resulting from a small genetic change. As indicated above the Phacopina may have been derived from the Cheirurina, and schizochroal eyes may have resulted from a similar change.

If this is the reason for the large number of lenses, it is then possible to offer a reasonable explanation for eye reduction. Essentially this depends on the fact that the field of vision and the range over which the vision is acute can be extended by increasing the number of rhabdoms behind each lens and improving their response. Each optic unit in a large eye would have a number of rhabdoms, and the amount of information received would have been enormous, requiring a very complex nervous system. Consequently, it would be expected that in eyes with a large number of lenses, each visual unit would have had relatively few rhabdoms, acute vision being restricted to a small number of them near the centre of the retinula. Eyes with only a few visual units would be expected to have more rhabdoms distributed over a surface of slightly greater diameter, and lens and sublensar designs that would permit the expansion of the visual field. In addition the size of the " focal fovea " over which there was high resolution would be expected to be larger.

We are still left with the problem of complete blindness. It is not the result of life in the deep sea. Erben (1958) has suggested that accidental eye reduction took place in well-lighted environments and animals bearing reduced eyes were preadapted to live in dark or semi-dark environments, and hence were more successful than forms with normal eyes. This explanation may be thought to account for the occurrence of reduced eyes with normal ones in shallow-water deposits. However, it really is no explanation at all—it depends on an unexplained accident. If, on the other hand, eye reduction is adaptive, as suggested above, it may be possible to explain not only the repetition of reduction in the family, but also the repetition of blindness. The general habit of phacopids with large eyes may be inferred with confidence from the studies of the sensory and limb structures in such species as those described by Stürmer and Bergström (1973) and Miller (1975). They must have been active epifaunal carnivorous animals. Nothing is known of the limbs of blind phacopids but a good deal is known of their gross morphology. Many have depressed exoskeletons with acutely angled profiles on the front of the glabella, and the entire dorsal surface is without macro-ornament.

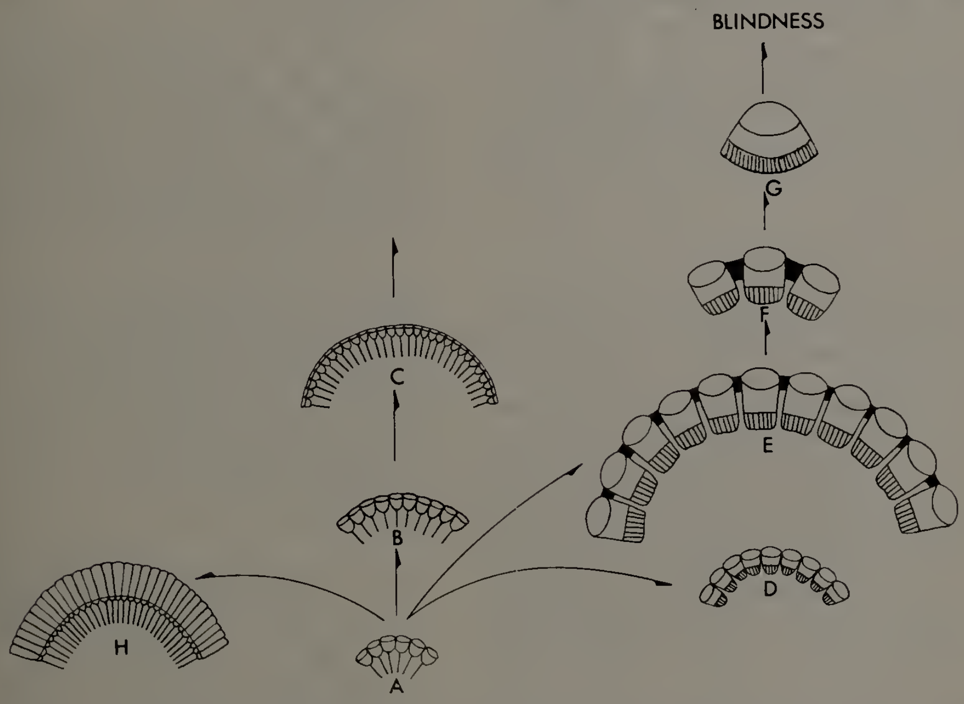

Figure 11.—Suggested evolution of some trilobite eye types. A–C, represents the evolution of the holochroal type with gradual reduction in lens size, increase in lens numbers and increase in eye size. D, the abortive development of the *Acanthropharya* eye type. E–G, the schizochroal type with gradual reduction in lens numbers and increase in the number of rhabdoms per lens, and decrease in rhabdom size. H, one of several other modifications described by Clarkson, in this case the elongate calcite prism lenses of *Asaphus*.

Most of these types are preserved in muddy sediments. All these features are consistent with a shallow burrowing mode of life, whether it be burrowing in mud or in a dense mat of weed on the bottom. Note that although some genera with reduced eyes have a similar gross morphology (e.g. *Denkmannites* which includes both sighted and blind species (Schrank, 1973)), there are others that are little different from contemporaneous species with normal eyes. *Eocryphops*, for example, is highly ornamented and similar to contemporaneous species of *Phacops*.

However, it is clear that burrowing beneath the sediment or beneath an organic mat does not provide the complete answer because there are genera with reduced eyes (such as *Eocryphops*) and others that are blind (such as *Trimerocephalus*), containing species that are highly ornamented and have glabellae with steep front walls. In fact these species are in many respects quite similar to *Phacops*. Such animals may have lost their sight as a result of a change to detritus feeding. Instead of ploughing in the mud, they may have dug shallow vertical burrows, processing the excavated mud for food as did the blind cryptolithids (Campbell, 1975*b*). The loss of sight in such forms would have been accompanied by the compensating development of olfactory and tactile sensory capacities to a high level.

In summary, then, the explanation of blindness is that :

(*a*) The number of lenses was reduced in some species as a result of the increase in the number of rhabdoms per visual unit. This reduction took place in several environments.

(*b*) Species with few lenses could more easily lose their eyes than those with many lenses.

(*c*) Some such species adopted a semi-burrowing habit, became smooth, flat and blind, whereas others became deposit feeders that were never completely buried and hence retained their high profiles and strong dorsal ornament.

The last hypothesis, unlike many others in this field, is capable of being tested. It is scarcely conceivable that either of the above burrowing types could function with exites as large as those figured by Stürmer and Bergström for large-eyed *Phacops* sp. Appendage-bearing blind phacopids should be sought. Burrows are not uncommonly preserved particularly in muddy rocks, but careful observation is needed to distinguish them. And finally, scanning electron microscopy of the surfaces of blind forms should be carried out to see if the surface sensory structures are consistent with the habitat indicated.

One other interesting point is that since both the outer and inner covering layers on the lenses have a randomly oriented micro-crystalline structure, light entering and leaving the system will be effectively depolarized. Light passing through seawater becomes polarized in various planes depending on the angle of elevation of the sun, but it would become largely depolarized on reflection from the objects in the field of vision of the trilobite. It would not be expected that an organism of this kind would have any use, such as navigation, for polarized light, and hence depolarization would be an advantage. Light from a depolarized parallel incident beam having passed through the upper unit would remain unpolarized because of the radial arrangement of the c-axes of the crystals in this layer. Passage through the central core and the optically continuous intralensar bowl would not repolarize the light because the originally parallel beam would enter it from a variety of directions as a result of the focusing effect of the upper unit. The reason for the thin inner lens layer with its randomly oriented c-axes is therefore obscure.

Sexual Dimorphism of Eyes

Many phacopid species show dimorphism of many characters. This has been known for many years (Girty, 1899) and the eye dimorphism of both European and American species has been commented upon by Clarkson (1966, 1969), Selwood and Burton (1969), Eldredge (1972, 1973) and Campbell (1968, in press). Many species are represented by two eye types at a single locality, and some are represented by three. A good example of the former is *P. raymondi* Delo, and of the latter *P. birdsongensis* Delo. Morphs are most easily distinguished by the number of lens files and the number of lenses per file as is shown by the counts of the lenses of *P. raymondi* given in Figure 12. There may be other differences as well. Size and structure of the lenses, thickness and height of the sclera, and height of the eye on the cheek are dimorphic in some species but not in others. Moreover some species, such as *P. rana* show no eye dimorphism.

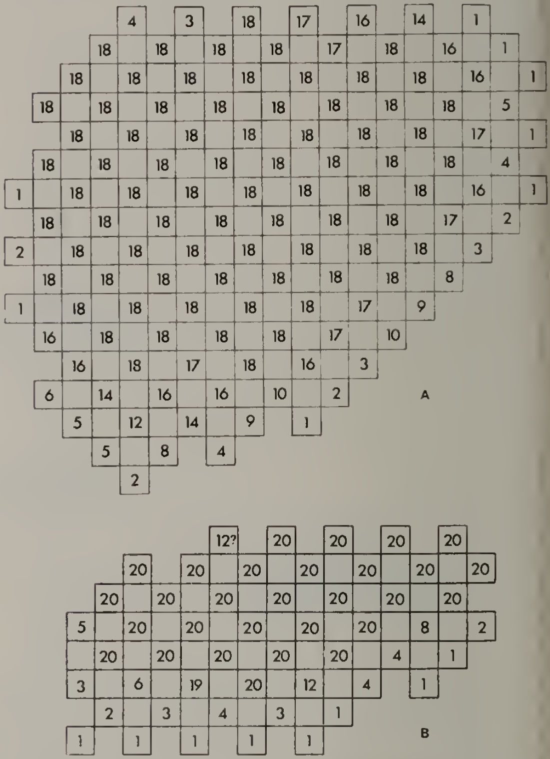

FIGURE 12 a, b.—Pattern of lenses in the two morphs of *Paciphacops raymondi* from the Lower Devonian Haragan Fm. of Oklahoma. (a) shows the lens distribution in eighteen specimens of the large-eyed morph and (b) in twenty specimens of the small-eyed morph. Further details in Campbell (in press).

The significance of this is not understood, but a clue may be obtained from a study of *P. raymondi*. The large-eyed morph has large perforations through most of the glabellar tubercles, but the small-eyed morph does not. These perforations were probably the sites of tactile or chemosensory structures. Thus other sensory structures as well as eyes are dimorphic, and it seems reasonable to conclude that the morphs had different habits, perhaps of scavenging or detritus feeding. No attempts have yet been made to examine the optical properties of the lenses of a pair of morphs, but this is obviously desirable.

Acknowledgements

During the preparation of this lecture I have enjoyed the assistance of numerous colleagues. Dr. R. A. Eggleton and Mr L. Belbin produced the computer simulation of ray paths through the lenses ; Dr. N. Ware did the electron microprobe analyses ; Messrs D. J. Holloway and G. R. Harper prepared the text figures and L. Seeuwen the photographs. Professor G. A. Horridge, Dr. Simon Laughlin and Dr. V. B. Meyer-Rochow have discussed neurobiological problems and have suggested many references to the literature. Professor Horridge also criticized a draft of the text on the eyes, and suggested many improvements. To all these gentlemen I wish to express my thanks.

References

Benham, W. B. S., 1885. Description of the Muscular and Endoskeletal Systems of *Limulus*. *Trans. zool. Soc. London*, **11** (2), 314.

Campbell, K. S. W., 1968. Trilobites of the Henryhouse Formation, Oklahoma. *Bull. Okla. geol. Surv.*, **115**, 1.

Campbell, K. S. W., 1975*b*. The Functional Morphology of *Cryptolithus* Fossils and Strata, **4**, 65.

Campbell, K. S. W. (in press). Trilobites of the Haragan, Bois D'Arc and Frisco Formations. *Bull. Okla. geol. Surv.*

Chlupáč, I., 1966. The Upper Devonian and Lower Carboniferous Trilobites of the Moravian Karst. *Sb. geol. ved. paleontol.*, **7**, 1.

Cisne, J., 1974. Trilobites and the Origin of Arthropods. *Science*, **186**, 13.

Cisne, J., 1975. Anatomy of *Triarthrus eatoni* (Trilobita) . . . Results of a Radiographic Study. *Fossils and Strata*, **4**, 45.

Clarkson, E. N. K., 1966*a*. Schizochroal Eyes and Vision of Some Silurian Acastid Trilobites. *Palaeontology*, **9** (1), 1.

Clarkson, E. N. K., 1966*b*. Schizochroal Eyes and Vision in Some Phacopid Trilobites. *Palaeontology*, **9** (3), 464.

Clarkson, E. N. K., 1967*a*. Environmental Significance of Eye-reduction in Trilobites and Recent Arthropods. *Mar. Geol.*, **5**, 367.

Clarkson, E. N. K., 1967*b*. Fine Structure of the Eye in Two Species of *Phacops* (Trilobita). *Palaeontology*, **10** (4), 603.

Clarkson, E. N. K., 1969. On the Schizochroal Eyes of Three Species of *Reedops* (Trilobita : Phacopidae) from the Lower Devonian of Bohemia. *Trans. Roy. Soc. Edinb.*, **68** (8), 183.

Clarkson, E. N. K., 1973. The Eyes of *Asaphus raniceps* Dalman (Trilobita). *Palaeontology*, **16** (3), 425.

Clarkson, E. N. K., 1975. The Evolution of the Eye in Trilobites. *Fossils and Strata*, **4**, 7.

Clarkson, E. N. K., and Levi-Setti, R., 1975. Trilobite Eyes and the Optics of Des Cartes and Huygens. *Nature*, **254**, 663.

Dalingwater, J., 1975. Trilobite Cuticle Microstructure and Composition. *Palaeontology*, **16** (4), 827.

Doflein, F., 1904. Brachyura. *Wiss. Ergebn. dt. Tiefsee-Exped. Valdivia*, **6**, 1.

Eldredge, N., 1971. Patterns of Cephalic Musculature in the Phacopina (Trilobita) and their Phylogenetic Significance. *J. Paleont.*, **45**, 52.

Eldredge, N., 1972. Systematics and Evolution of *Phacops rana* (Green, 1832) and *Phacops iowensis* Delo, 1935 (Trilobita) from the Middle Devonian of North America. *Bull. Am. Mus. nat. Hist.*, **147**, 45.

Eldredge, N., 1973. Systematics of Lower Middle Devonian Species of the Trilobite *Phacops* Emmrich in North America. *Bull. Am. Mus. nat. Hist.*, **151**, 285.

Erben, H. K., 1958. Blinding and Extinction of Certain Proetidae (*Tril.*). *J. palaeont. Soc. India*, **3**, 82.

Friederichs, H. F., 1931. Beiträge zur Morphologie und Physiologie der Sehorgane der Cicindeliden (Col.). *Z. Morph. Ökol. Tiere*, **21**, 1.

Girty, G. H., 1899. Preliminary Report on Paleozoic Invertebrate Fossils from the Region of the M'Alester Coal Field, Indian Territory. *U.S. Geol. Surv., 19th Ann. Rept.*, 1897–1898, 539.

Hessler, R. R., 1964. The Cephalocarida, Comparative Skeletomusculature. *Mem. Conn. Acad. Arts. Sci.*, **16**, 1.

Hupé, P., 1953. Trilobites *in* Piveteau, J., (Ed.), *Traité de Paléontologie*, Masson et Cie, Paris, **44**.

Jockusch, B., 1967. Bau und Funktion eines Larvalen Insektenauges—Untersuchungen am Ameisenlöwen (*Euroleon nostras* Fourcroy, Planip., Myrmel.). *Z. vergl. Physiol.*, **56**, 171.

Kirschfeld, Von K., and Reichardt, W., 1964. Die Verarbeitung Stationärer optischer Nachrichten im Komplexauge von *Limulus*. *Sonderdruck. aus " Kybernetik "*, **2**, 43.

Lindström, G., 1901. Researches on the Visual Organs of the Trilobites. *K. Svenska Vetensk—Akad. Handl.*, **34**, 1.

Meyer-Rochow, V. B., 1974. Structure and Function of the Larval Eye of the Sawfly, *Perga*. *J. Insect Physiol.*, **20**, 1565.

Miller, J., 1975. Structure and Function of Trilobite Terrace Lines. *Fossils and Strata*, **4**, 155.

Moore, R. C. (Ed.), 1959. *Treatise on Invertebrate Paleontology, Part O, Arthropoda I.* Geol. Soc. Am. and Univ. Kansas Press, Kansas.

Quenstedt, A., 1937. Beitrage zur Kenntnis der Trilobiten, mit besonderen Rucksicht auf ihr bestimmte Gliederzahl. *Arch. Naturgesch.*, **3**, 337.

Schrank, Von E., 1973. *Denckmannites caecus* n.sp., ein blinder Phacopidae aus dem höchsten Thüringer Silur. *Z. geol. Wiss.*, **1**, 347.

Selwood, E. B., and Burton, C. J., 1969. Possible Dimorphism in Certain Devonian Phacopids (Trilobita), *in* Westermann, G. E. G. (Ed). *Sexual Dimorphism in Fossil Metazoa and Taxonomic Implications*, E. Schweizerbartsche Verlagsbuchhandlung, Stuttgart, Page 196.

Stürmer, W., and Bergström, J., 1973. New Discoveries on Trilobites by X-rays. *Paläont. Z.*, **47**, 104.

Waterman, T. H., 1954. Directional Sensitivity of Single Ommatidia in the Compound Eye of *Limulus*. *Proc. natn. Acad. Sci. Wash.*, **40**, 258.

Welsh, J. H., and Chace, F. A., 1937. The Eyes of Deep-sea Crustaceans: I. Acanthephyridae. *Biol. Bull.*, **72**, 55.

Whittington, H. B., 1975. Anatomy and Mode of Life of *Olenoides serratus*, Burgess Shale, British Columbia. *Fossils and Strata*, **4**.

Whittington, H. B., and Campbell, K. S. W., 1967. Silicified Silurian Trilobites from Maine. *Bull. Mus. Comp. Zool.*, **135** (9), 447.

Whittington, H. B., and Evitt, W. R., 1954. Silicified Middle Ordovician Trilobites. *Mem. geol. Soc. Am.*, **59**.

Department of Geology,
Australian National University,
Canberra, A.C.T.

(Received 30.7.1975)

Explanation of Plate A

Eophacops musheni (Salter) from the Middle Silurian of Dudley, England. Specimen A28671, Sedgwick Museum, Cambridge, England. Specimen photographed under glycerine. Figures 1–3 are ×6·5 approx.; Figures 4–6 are ×8·5 approx.

Explanation of Plate B

All scale units 0·2 mm.

Figures 1–6.—*Phacops rana milleri* Stewart, horizon and locality unknown. 36856 Australian National University Collection. 1–3. Oblique section through three lenses photographed (1) in unpolarized light; (2) in cross polarized light with the plane of polarization of the analyzer parallel with the vertical edge of the plate; (3) in cross polarized light with the plane of polarization of the analyzer at 20° to the left. Note the layering of the lenses in (1), and the patterns of extinction of the various lens units in (2) and (3). 4. Vertical section through two lenses photographed in plane polarized light. Scale unit is 0·2 mm. 5, 6. A lens photographed in cross polarized light, with the polarization plane of the analyzer parallel with the optic axis of the lens in (6) and at 10° to the right in (5).

Figure 7.—*Phacops rana* Green from the Silica Shale, Ohio. 11215 Australian National University Collection. A single lens photographed in plane polarized light. The central core is well shown.

Explanation of Plate C

Figures 1, 2.—The eyes of the two morphs of *Paciphacops raymondi* (Delo) ×4·7 and ×9. Haragan Formation, Lower Devonian, Oklahoma.

Figures 3–5.—Three partly silicifed specimens of *Paciphacops birdsongensis* (Delo), all ×16 approx. Ross Formation, Lower Devonian, Tennessee. (3) shows lenses from which the upper unit has been removed, but the intralensar bowl and central core are still present. Arrow indicates a hollow central core. (4) shows an individual with the corneal membranes removed, and the upper unit is removed medially to reveal the tip of the central core. (5) shows lenses on the left with the intralensar bowl still present and the cavity for the base of the core, and sites on the right from which all the lenses have been removed. On all these specimens the sclera has been removed by natural weathering.

Figure 6.—The eye of a large-eyed morph of *Paciphacops birdsongensis* (Delo) ×9 approx. Birdsong Shale, Lower Devonian, Tennessee. This specimen has the original exoskeletal material present.

1

2

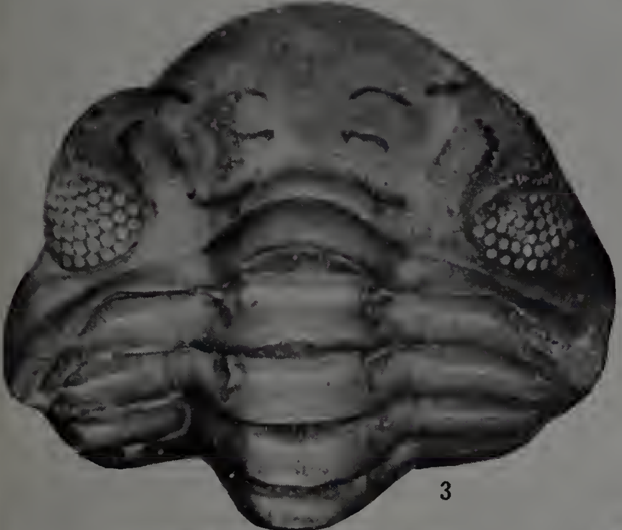

3

4

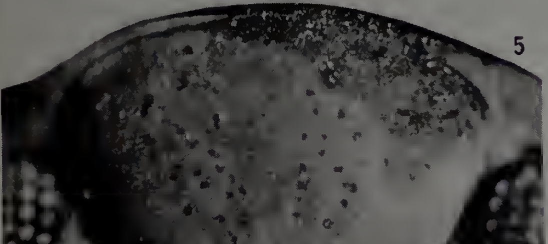

5

6


1

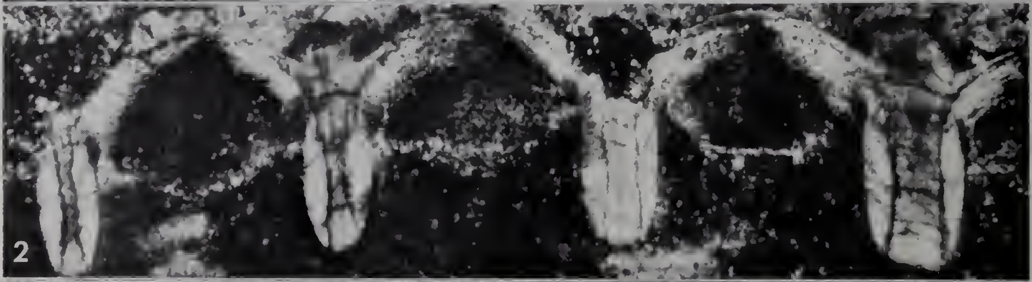
2

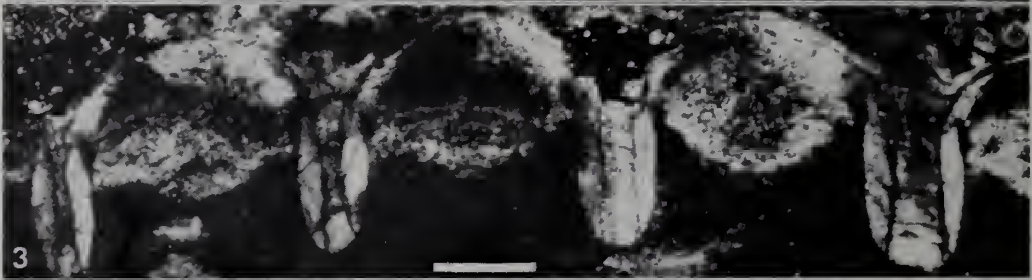
3

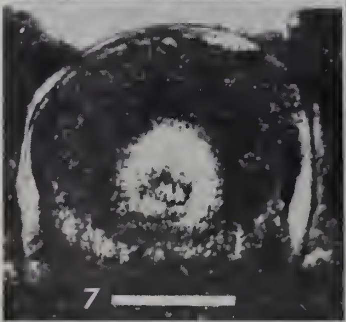
7


4

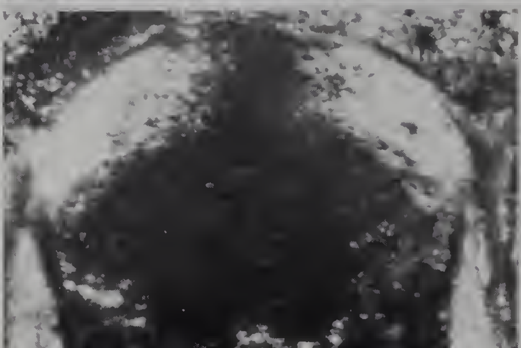
6

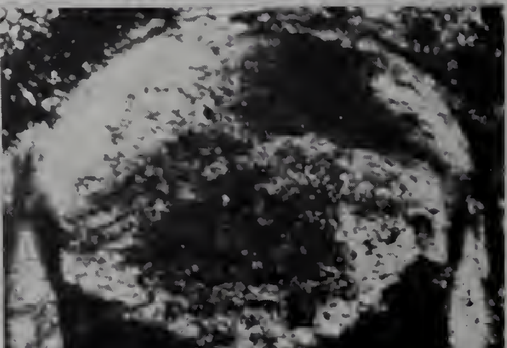
5

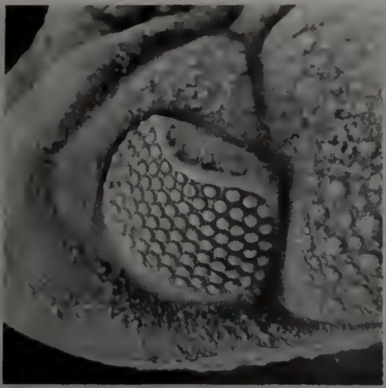

1

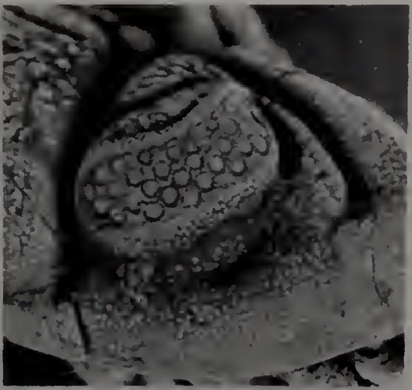

2

3

4

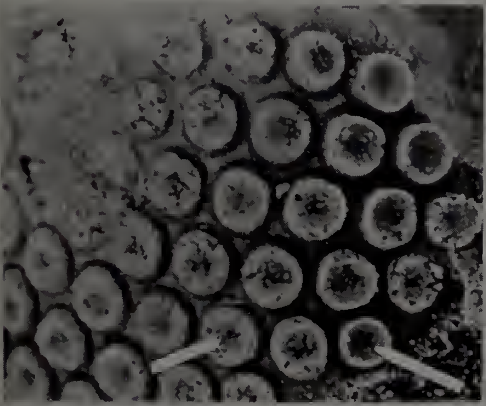

5

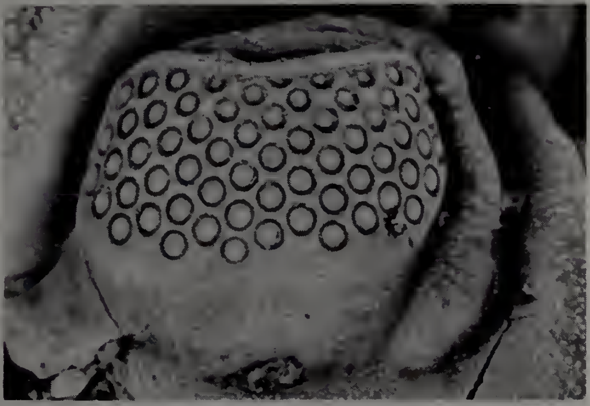

6

Journal and Proceedings, Royal Society of New South Wales, Vol. 108, pp. 189–202, 1975

Bud Failure of Stonefruits—Some Changes in Development and Chemical Composition of the Flower Buds of Peach

(*Prunus persica* L. Batsch)

H. D. R. Malcolm

Abstract—Because the failure of reproductive buds of peach increases in their developmental stages from differentiation to bud-burst, its incidence appears to relate neither to stage of development nor to chilling. Measurements of bud volume, weight, water, respiration and the contents of nitrogen, sugar, protein and amino acids showed that only respiration increased whilst most others decreased following intermediate fluctuation with the onset of failure.

Introduction

In New South Wales bud drop of peach occurs from March to October ; there being appreciable variation between cultivars and seasons. In average years on the Murrumbidgee Irrigation Areas (MIA) about half the flower buds of Elberta peach, for example, fail to develop but in some seasons as many as 90 per cent may fail (Lenz, 1963). Saikia *et al.* (1967) found 80–90 per cent bud failure to be common in some almond cultivars grown in the United States.

Extensive bud failure has often been attributed to insufficient winter chilling (e.g. Black, 1955 ; Weinberger, 1967). Such failure either from abscission, or necrosis without abscission, may be observed in early autumn and thereafter increases in severity until flowering. The incidence may vary widely between trees of the same cultivar growing in adjacent orchards, possibly because of some within-tree nutrient competition ; and between trees of different cultivars which differentiate varying proportions of vegetative and flower buds (Lenz, 1963). Kester (1968) reported that some bud failure in almond is hereditary and non-transmissible. Abscission associated with a virus infection has also been suggested (Saikia *et al.*, 1967). Apart from observation that bud failure occurs most commonly in late winter, very little is known of its association with climatic factors, or the degree of proneness to failure of buds at different stages of development.

Although development of buds and shoots of some peach cultivars in particular environments has been studied, for example the Anzac and Pullar's Cling cultivars by Barnard and Read (1932) in Victoria, and the Lovell peach cultivar by Chandler and Tufts (1933) in the United States, it was necessary to document the seasonal development of the particular cultivars used in this study. Further, the nature of any disruption of metabolism in the buds may be revealed by following changes in some of their chemical components. The onset of rest of buds in autumn is generally accompanied by a decrease in the proportion of water to dry weight and an accompanying decrease in respiration rate (Kosseva *et al.*, 1968 ; Kozlowski, 1964). When visibly active growth resumes, the water content increases and respiration rate rises ; both changes almost certainly reflect change in enzyme content. Karapetyan (1967) reported seasonal change in carbohydrate content of the buds of almond and peach, and this in turn may be related to bud failure prevalent in trees with low starch content early and low sugar content late in the season.

Nitrogen content is reported to increase considerably in the flower buds of peach during bud burst (Radu, 1960) and about one-third to one-half of the nitrogen in buds is translocated back into the shoots before flower abscission (Murneek, 1930). Denny *et al.* (1965) found aspartic acid predominant amongst the total amino acids of peach leaves and that arginine, glutamic acid, and alanine were the predominant free amino acids. These changes would be expected in the general sequence involved during bud development from initiation to flower emergence.

This paper discusses the development of shoots and flower buds of a typical peach variety (King Edward) grown in the orchard of the Macquarie University, Sydney. Data are also given of low-temperature requirements for breaking of rest of this cultivar and of two others, one in the same orchard and the other grown on the MIA. The study was undertaken to examine these changes and make comparisons between healthy (viable) and failure-prone (abscissing) flower buds. The three peach cultivars compared were Edward VII, commonly called King Edward (KE) a cultivar very similar to Watt's Early; Blackburn (BB), another freestone type grown in the mid-coastal regions of N.S.W. (Holbeche, 1966); and Golden Queen (GQ) the main clingstone cultivar grown inland for processing (Malcolm, 1965). Experience of commercial growers has indicated that the chilling requirements of these three cultivars increase in the order KE, BB and GQ. Some incidence of bud failure was suspected but not definitely known in KE and BB, whereas GQ was known to be prone to bud failure.

Materials and Methods

Mature 15-year-old trees of the KE and BB cultivars were available in the University orchard, but to include GQ for comparison under similar conditions three-year-old trees of each cultivar, potted and adequately fertilized, were grown in the University glasshouse. Two orchards in the MIA were selected to study gross samples of GQ buds, one at Yanco where very little bud failure was known to occur and the other at Stoney Point where bud failure was a long recognized problem.

Generally, whole branches were cut from the trees to provide samples for analyses, and taken to the laboratory where buds and shoots were removed, measured, weighed, and frozen. The frozen samples were dried to a constant weight on a Vertis freeze-drier, thus providing data on moisture content and material for chemical analyses free from enzyme action. Temperatures in the orchards and glasshouses were recorded continuously.

Shoot growth, and chilling: Periodicity of shoot growth was studied by measuring five new terminal shoots on each of four trees from the time they commenced to elongate in early spring. To assess termination of rest in winter, shoots similar to those being measured were cut periodically and placed with their cut ends immersed in water in an incubator maintained at 22°C. About 5 mm of wood was cut from the immersed ends of the shoots after five days to maintain water uptake, and the number of flower buds which had opened after a further five days was recorded. The chilling requirements of these shoots were taken to have been satisfied when at least 40 per cent of the buds had opened.

Bud failure and histology: Samples of bud primordia and flower buds were harvested at all stages of growth and development. They were separated into viable and failure-prone, the viable buds being those firmly attached to the twigs whereas the failure-prone buds were only loosely attached, could easily be removed, and showed browning around the periphery of the abscission zone at the base of the bud. They were fixed in FAA (formalin: acetic acid: ethanol: water—5 : 5 : 68 : 27) dehydrated through an ethanol/tertiary butyl alcohol/paraffin oil series, infiltrated with wax under vacuum, and embedded according to the method of Johansen (1940). Serial sections were then cut at 8–10 μm thickness on a Spencer rotary microtome, and stained in aniline blue and safranin, using the method of Conn *et al.* (1960).

Respiration

The ends of sections of fresh shoots (10–15 cm long) with intact buds were coated with molten paraffin wax and placed in a respiration chamber at 22°C. Oxygen consumed by the shoots and buds was monitored by a calibrated Mackereth oxygen electrode connected to a 10 mV recorder (Mancy and Westgarth, 1962). After a constant rate of oxygen consumption was attained the shoots were removed from the chamber and the buds were excised at their abscission layers. The wounds on the shoots were coated with paraffin wax, and the shoots were then returned to the chamber and left until a constant rate of oxygen uptake was again indicated. Oxygen consumed by the buds was calculated from the difference between the two rates.

Sugar

Sugar was extracted from freeze-dried buds, leaves, and shoots, in 75 per cent ethanol in an Ultra Turrax homogenizer. The homogenate was centrifuged for 10 minutes at 2,500 rpm, the supernatant decanted, dried in a rotary vacuum evaporator, and finally taken up in 4 ml 10 per cent isopropanol. Total sugar was determined by Benedict's Test (Harper, 1967) using glucose and fructose standards at 535 nm in a spectrophotometer. Total sugar was separated into components by chromatography on Whatman No. 1 paper in n–butanol: acetic acid; water (12 : 3 : 5) followed by phenol: water (4 : 1). Chromatograms were developed by both the silver nitrate/sodium hydroxide method of Trevelyan *et al.* (1950) and by aniline phthalate spray (Smith, 1958).

Chemical tests for glucose, fructose, sucrose, and ribose were made by the methods of Harper

(1967). Similar tests for reducing sugars were made following invertase treatment, and also by the Seliwanoff test (Oser, 1965). Further identification of the sugars was made by gas-liquid chromatography (GLC).

Nitrogen

Total nitrogen in the buds was determined by the micro-Kjeldahl method described by Oser (1965) in which duplicate 0·2 g samples of ground and freeze-dried buds were analysed.

Amino Acids

Ground freeze-dried samples (each 1 g DW buds) were extracted first by boiling for three minutes in 100 ml 80 per cent ethanol and allowing to stand for 10 minutes, the supernatant decanted, and then a further 100 ml boiling 20 per cent ethanol added to the residue. After a further 10 minutes the two supernatants were combined, and reduced under vacuum to about 50 ml (Smith, 1958). The concentrated aqueous extracts were washed with 100 ml acetone containing 1·0 ml 10N HCL, followed by 100 ml ether to remove salts, chlorophyll, and fats (Cassidy, 1957). The extracts were finally evaporated to dryness under vacuum and the residues taken up in 0·5 ml 10 per cent isopropanol. Aliquots (each 20 µl) of the extracts were separated on Whatman No. 1 chromatography paper (25×25 cm), ascending in two dimensions in standard solvents followed by development with ninhydrin. The developed spots were cut out and eluted in 10 per cent isopropanol, following which the coloured solutions were compared with standards in a spectrophotometer at wavelengths of 450 and 570 nm (Moore and Stein, 1948).

Protein

One-gram samples of freeze-dried buds were extracted by grinding in 6·0 ml sucrose/phosphate buffer pH 7·0 at 0°C (Evans *et al.*, 1963), to which one per cent Polycar AT (an inert cross-linking insoluble form of polyvinylpyrrolidone) was added to remove tannins and anthocyanins and to prevent precipitation of the proteins (Jaarsveld and Meynhardt, 1967). The homogenates were later centrifuged for 30 minutes at 10,000 g and 5°C. The supernatant was decanted, a portion used to determine the total soluble protein by the Lowry-Folin method (Oser, 1965), and the remainder subjected to acrylamide gel electrophoresis (Rogers, 1965). The Rf values of the stained protein bands were calculated by measurement against a lighted opalescent screen, photographed, and later scanned at 600 nm in a densitometer. Further extracts for comparison were run through a DE–32 cellulose column eluted with 0·02M tris-buffer containing a NaCl salt concentration gradient from 0–1M. The absorbance of each 5 ml fraction collected was read in a spectrophotometer at 280 nm. Approximate molecular weights of the main protein fractions were calculated following fractionation on Sephadex G–100 and on polyacrylamide gels (Anon, 1968 ; Hedrick and Smith, 1968).

Comparative levels of 14 mineral nutrients in buds and leaves were determined using the techniques and equipment described by Leece (1967) for routine leaf analyses.

Results

Shoot growth : The growth record for KE in the University orchard during the 1967–68 season showed that the terminal shoot underwent two periods of elongation. The growth rate accelerated as daily temperatures increased during spring, but decreased after mid-October, when flower bud initiation began. A second shoot elongation accompanied the initiation of axillary buds but this ceased at the end of December long before flower primordia were visible. Unfolding of leaf buds on the shoots did not appear to be closely related to shoot elongation.

Flower initiation : Most flower buds appeared to be initiated as lateral buds of a central vegetative bud. They were borne only in the axils of leaves on current season's shoots, singly or in pairs, and sometimes in threes. Triplet bud formation, that is, a central leaf bud with a reproductive bud on either side (Plate Id) was observed in the central region of vigorous shoots. These vigorous shoots attained a diameter of 3–8 mm by the time bud differentiation began. Often a third reproductive bud arose below the central leaf bud.

Of all three cultivars (KE, BB and GQ), irrespective of location, branches which produced weak shoot growth also produced predominantly single flower buds. When these buds are clustered around the tips of the shoots, a characteristic commonly referred to by growers as " tip-bearing ", it causes poor fruit yields. Such buds initiated immediately behind the shoot tip appear to develop directly into flower buds. On more vigorous shoots, however, 5–10 mm diameter, where these single buds immediately below the tips are commonly reproductive, further single buds borne in the basal regions on those shoots are invariably vegetative. Despite similar patterns of shoot development found for all three cultivars in their respective orchards, only KE and BB were similar to their orchard-grown counterparts when grown in the glasshouse, whilst all three cultivars differed in times of their individual stages of development.

Bud growth and differentation : A detailed study was made of growth of buds of KE, the sequence of growth and the histology of development of the buds is described in Table 1. It is representative of the pattern of development of the buds in the three cultivars studied. Increase in diameter of shoots, especially of one-year-old wood, continued for some two to three months after extension growth had ceased. That is, until about time of bud differentiation. Following this, there appeared to be no correlation between stage of bud development and incidence of failure until differentiation was complete. Abscission was most severe at bud burst, that is, during their expansion and following maturation. On KE this occurred only shortly after completion of differentiation, but on GQ bud burst occurred some two months after differentiation (Plate IIj). When compared with orchard temperature records this corresponded with the completion of sufficient exposure to low temperature or chilling.

TABLE I

Summary of Shoot and Bud Growth

Stage of Shoot Growth	Growth and Histology of the Buds	Reference Plate
Flowering, closely followed by vegetative growth on one-year-old woody shoots. These shoots slowly increased in diameter but not in length	No primordia found in the axils of the leaves	Nil
(i) Initiation of reproductive buds began just before the second flush of the vegetative growth	Late October—Accessory meristems under the prophylls on either side of the vegetative bud in the leaf axil	Plate II a
(ii) Number of leaves increased until about time of fruit ripening	November—The bud scales developed rapidly to enclose the growing point	Plate II b
(iii) Shoot tips continued elongation until about the end of December	Early Jan.—The growing point of the bud became rounded in contrast to the elongated vegetative buds	Plate II c and d
(iv) Side shoots on the one-year-old wood also ceased growth	Early Feb.—the growing point enlarged and became flattened at the top	
(v) Bud differentiation. The growth of the reproductive buds was sufficiently advanced so that triplet bud formations, that is, a vegetative bud with a reproductive bud on either side were clearly visible in the axils of the leaves on the longer shoots	February–March. The sub-apical initial cells became more organized and meristematic, the growing point more flattened, and calyx lobes began to form around the periphery. The reproductive and vegetative buds were clearly distinct in macroscopic appearance	Plate II e (see also Plate Ia)
(vi) Defoliation (leaf-fall)	Late March–Early April. Corolla, androecium, and gynoecium initials arose rapidly in that order	Plate II f
(vii) Reduced rate of bud expansion with onset of winter conditions	May–June. The gynoecium grew rapidly from the protuberance on the receptacle. Stamens differentiated into filaments and anthers. A locule formed in the ovary. Spore mother cells differentiated in the anthers	Plate II g and h
(viii) and (ix) The buds began to expand rapidly. Pink petals showed through the tips of the bud scales in what is known as the " pink " stage pre-flowering.	Early July. Two ovules differentiated in the ovary and pollen in the anthers	Plate II i
	Mid July. One ovule matured in the ovary and the flower was ready to open	Plate II j

Bud abscission and necrosis : In the University orchard, bud failure was greatest on KE and BB in 1967, and on GQ at Stoney Point in 1969 (Table 2). Many of the buds died *in situ* and did not absciss due to necrosis of their flower initials (Plate Ib). Trees growing in the relatively warmer conditions in the University glasshouse were most subject to this form of bud failure. In the more usual type of failure abscission layers formed at the bases of the peduncles (Plate Ia and b), and buds were later shed because of tissue rupture in these layers. A variation of this type of failure occurred when cambial activity caused an abscission layer to be formed in the cortex of the shoot well below the point of attachment of the bud (Plate Ic). When flower buds died but did not absciss, early growth of the associated vegetative bud resulted (Plate Ie) ; but where there was no associated vegetative bud further growth often arose from a meristem which developed at the base of the necrotic bud receptacle.

Chilling requirement: When shoots were taken from the orchard and incubated, the buds of KE opened after only 50 hours, and those of BB after 380 hours of cumulative chilling below 7°C. Shoots taken from GQ in the glasshouse, however, did not flower until they were given additional chilling in a cold-room at 2°C, their total then being 716 hours. In the MIA orchards, the total chilling received easily exceeded this amount in each year (Table 2).

Table 2

Mean Percentage Bud Failure of the Three Peach Cultivars, KE, BB and GQ, and Hours of Low Temperature in Winter

Cultivar and Location	Per cent Necrotic Bud Failure 1969	Per cent Bud Abscission 1969	Per cent Total Bud Failure 1969	Per cent Total Bud Failure 1968	Per cent Total Bud Failure 1967	Chilling-hours Below 7°C		
						1969	1968	1967
KE Orchard	2·5	5·0	7·5	Nil	9·5	420	630	310
KE Glasshouse	25·5	15·5	41·0	56·5	+	156*	50*	+
BB Orchard	4·5	13·5	18·0	9·5	19·5	420	630	310
BB Glasshouse	27·0	15·3	42·3	47·0	+	156*	50*	+
GQ Orchard	2·5	54·0	56·5	+	+	975	1023	898
GQ Glasshouse	90·0	Nil	90·0	100	+	159*	50*	+

* heated in winter. + = no data.

Under glasshouse conditions where less chilling was experienced than in the orchard, more triple-bud formations were found on the shoots of BB than on KE. However, with the shortest chilling requirement, KE differentiated more buds per shoot than the other two varieties.

For the three cultivars studied there was an inverse relationship between the duration of the vegetative growth preceding bud differentiation and the chilling requirement of the cultivar. The length of time required for the further development of flower buds from differentiation to bud burst, was in proportion to this chilling requirement.

Bud growth: There was a rapid rise in dry weight of KE buds in both 1967 and in 1968 (Figure 1) shortly after differentiation, then only a slow increase from early March to mid-May possibly associated with leaf-fall. This was followed by a reduction in dry weight before a final rapid increase at bud burst. Some 30 to 45 per cent of the dry matter of the buds to time of leaf-fall was therefore lost before bud burst.

The water content of the KE buds remained relatively constant from March to July. The decreasing proportion of water during the autumn was attributed to a slight fall in actual water per bud and lagging behind the increasing dry matter; when the dry matter then decreased the water changed only slightly, resulting in an increased proportion of water. Bud size, regardless of cultivar, did not affect these overall patterns. The much smaller increase in both fresh weight and moisture-dry weight ratio of GQ buds in the Stoney Point orchard when compared with the GQ buds in the Yanco orchard just before bud burst (Figure 2) was associated with a high percentage failure (Table 3).

Respiration: Respiration rates during early bud growth and dormancy were about 300 to 400 μl oxygen per gram dry weight per hour (Figure 3). Assuming a mean respiration of 365 μl O_2/gDW/hr for KE buds, for example in the April to June period, the loss of weight would have been equivalent to about 14 mg carbohydrate. Since the actual loss in bud dry weight during this period was 16 mg, assuming no further import of carbohydrate from the twig in dormancy, most of this loss could be caused by respiration.

The failure-prone GQ buds from the Stoney Point orchard had a lower respiration rate than the Yanco orchard buds in April and May. However, the rate for Stoney Point GQ buds then increased markedly during the winter, long before bud burst, and at a time when both dry weight and water content increased slowly.

Bud sugar: The mean sugar content of shoots of the three cultivars is shown in Table 4.

TABLE 3

Volume, Dry Weight, and Failure of Buds of the Three Cultivars

Cultivar, Orchard and Year	Apparent Volume in Mid-June (cm³)	Dry Weight in Mid-June (mg)	Per cent Failure	
			By Abscission	By Necrosis
KE–Macquarie 1967	0·023	22	7·5	2·0
KE–Macquarie 1968	0·043	25	0·0	0·5
BB–Macquarie 1969	0·085	25	13·5	4·5
GQ–Yanco 1969	0·065	23	4·0	1·5
GQ–Stoney Pt. 1969	0·053	19	54·0	2·5

Shoots with few flower buds had low sugar content, indicating a relationship between carbohydrate metabolism and number of buds per shoot. There was, however, no difference in composition of the sugar in the two types of shoot. Not only was this found to consist of glucose plus fructose in the ratio of approximately 2 : 1 in extracts of the shoots, but also in relatively pure exudates from glands on the leaves. A considerable amount of sugar was exuded by leaf glands of BB and GQ trees growing in the glasshouse. The concentration of the exuded sugar was considerably higher, about 2·0 M, than the calculated 0·25 M in shoots, buds, and in discs cut from leaves. No sucrose was detected in any of the analyses. Sugar in the buds of GQ in both the Yanco and Stoney Point orchards continued to increase from leaf-fall through dormancy until bud burst (Figure 4).

TABLE 4

Sugar in the Peach Shoots

Sample (All Buds Removed Before Extraction)	Sugar Content (Per cent of Fresh Weight)	Number of Flower Buds Formed per cm Length of Shoot
GQ shoots with many buds	1·02	2·0
GQ shoots with few buds	0·49	0·2
BB shoots with many buds	0·84	1·2
BB shoots with few buds	0·57	0·3
KE shoots with many buds	2·00	2·2
KE shoots with few buds	1·79	0·6

Nitrogen : Nitrogen was lowest in the KE buds in the University orchard in both 1967 and 1968 (Figure 5) at time of differentiation, thereafter increasing to a maximum at bud burst. Nitrogen increased more rapidly in April-May 1968, but fell more slowly than in 1967. Fewer analyses were made on GQ than on KE. Similarly Stoney Point GQ buds accumulated nitrogen earlier in dormancy than the Yanco orchard GQ buds. The Yanco buds also accumulated metabolites more rapidly on approach to bud burst than did the Stoney Point buds.

Amino acids : The concentrations of six out of eight major amino acids found in the KE buds increased around time of differentiation (Figure 6a). Only aspartic and glutamic acids decreased in parallel with total nitrogen. The amides of these two acids, asparagine and glutamine, each increased about three-fold at the same time. Arginine was the predominant amino acid, both at differentiation and at bud burst. There was a general reduction in content of amino acid about time of leaf-fall, which at that stage corresponded with the general rise in total bud nitrogen. The quantities of all eight major amino acids increased sharply at bud burst, the same pattern being found in the GQ buds at Yanco in 1969 as in the KE buds in the University orchard in 1968 (Figure 6, a–b). Traces of serine, glycine, cysteic acid, lysine, threonine, valine and the leucines were also found, but mainly at bud burst ; their quantities being insufficient for accurate measurement.

Soluble : protein : Soluble protein in the KE buds increased sharply around time of differentiation, the increase occurring earlier in 1967 than in 1968 (Figure 7). Concentration of bud protein fell generally during late autumn and early winter, but rose again well before bud burst. A similar sequence was found for GQ which had a correspondingly higher level of protein in viable than in failure-prone buds.

Three major fractions of soluble protein of approximate molecular weights 100×10^3, 26×10^3, and $4 \cdot 4 \times 10^3$ respectively, differed in extracts of viable and abscissing buds of the BB cultivar (Figure 8). There was more protein of MW 26×10^3 (Fraction 2) and less of MW 100×10^3 (Fraction 1) in abscissing than in viable buds. Both the total soluble protein, and the number of fractions separated on

TABLE 5

Mineral Nutrients in the Leaves and Flower Buds

Orchard	Sample	Time	Mineral Nutrients													
			S %	Ca %	Mg %	Na %	K %	Cl %	N %	P %	Fe ppm	Mo ppm	Mn ppm	Cu ppm	Zn ppm	B ppm
Stoney Pt.	leaves	Feb.		2·20	0·74	0·01	2·54	0·11	2·58	0·17	—	—	37	12	22	54
Yanco ..	leaves	Feb.		3·22	0·88	0·01	2·54	0·02	2·58	0·16	—	—	24	17	19	59
Stoney Pt.	buds	Sept.		0·83	0·32	0·01	1·41	0·10	3·28	0·50	216	0·50	27	285*	52	71
Yanco ..	buds	Sept.		0·73	0·30	0·02	2·03	0·07	3·19	0·40	262	0·26	36	17	42	56
Stoney Pt.	buds at bud-burst	Oct.	0·118	1·50	0·22	0·01	0·61	0·10	1·65	0·23	275	0·36	19	19	26	87
Yanco ..		Oct.	0·140	1·06	0·26	0·01	0·62	0·25	2·16	0·21	216	0·04	24	25	38	62

* High level thought largely due to application of a copper oxychloride spray five days prior to bud sampling.

polyacrylamide gels, increased most between initiation and differentiation of the buds than in the later stages of development when some further fractions appeared. Some of these fractions were absent from extracts of the abscission-prone buds.

Mineral nutrients : There was a gross difference between levels of only one of the 14 nutrients compared (Table 5), molybdenum being much higher in the buds where the incidence of failure was high.

Discussion

Differences in growth between the three cultivars appeared to be correlated with the duration of exposure to low temperature required to break their dormancy. This determined not only the length of the dormant period but also whether growth activity, expressed as expansion of the flower buds, commenced in late winter or early spring. Between 600 and 900 hours exposure below 7°C is reported necessary for most peach cultivars grown commercially in the United States (Anon, 1941). However, the duration of active shoot extension may also be restricted despite wide differences in the times of commencement of growth. There is therefore a period of vegetative growth limited by the requirement for winter chilling. If the period of decreased bud expansion related to " deep organic dormancy " (Weinberger, 1967) is prolonged because of insufficient chilling, there is excessive bud failure and restricted spring growth. This was very much the effect recorded for GQ grown in the glasshouse. Knowledge of relative stages of extension growth and chilling requirements of cultivars thus assists in determining times of initiation and differentiation of the buds. Stages of development in differentiation, however, appear to parallel closely the early findings of both Barnard and Read (1932) and Chandler and Tufts (1933), and more recently Stadler and Strydom (1967).

The first mature vegetative growth apparently provides the photosynthetic activity necessary to support the early development of the fruit, and the second flush of growth supports expansion of the fruit following pit-hardening. This may explain too, why the sugar secreted by leaf glands ceases after the first growth flush (Malcolm, 1970) ; it probably then being diverted into the expanding fruit. Hladik (1967) showed that bud failure may result when leaf area is inadequate to support both fruit and new bud growth. If this is so, relatively fewer flower buds would be expected on the trees following a heavy crop year.

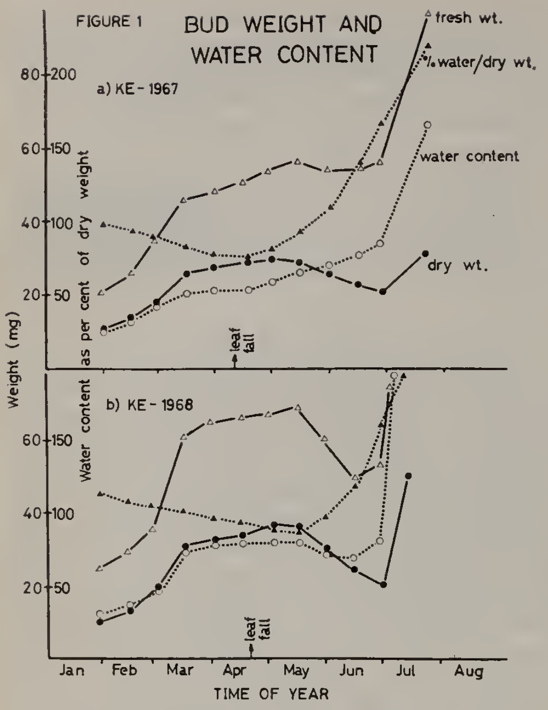

FIGURE 1.—Bud weight and water content.

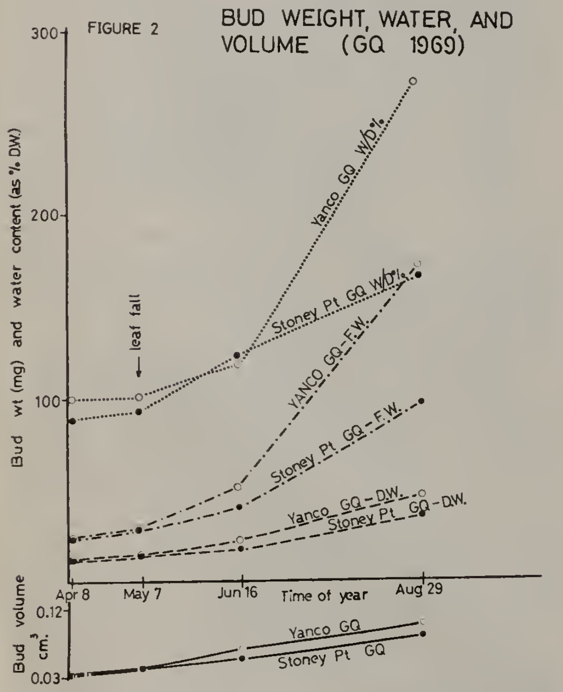

FIGURE 2.—Bud weight, water and volume (GQ 1969).

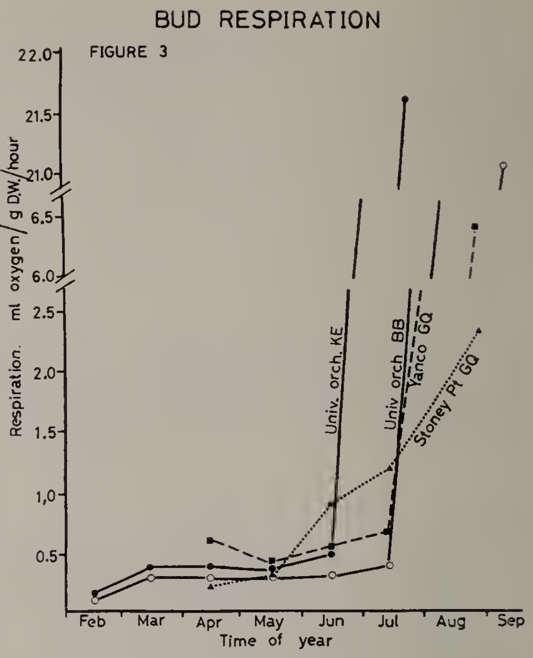

FIGURE 3.—Bud respiration

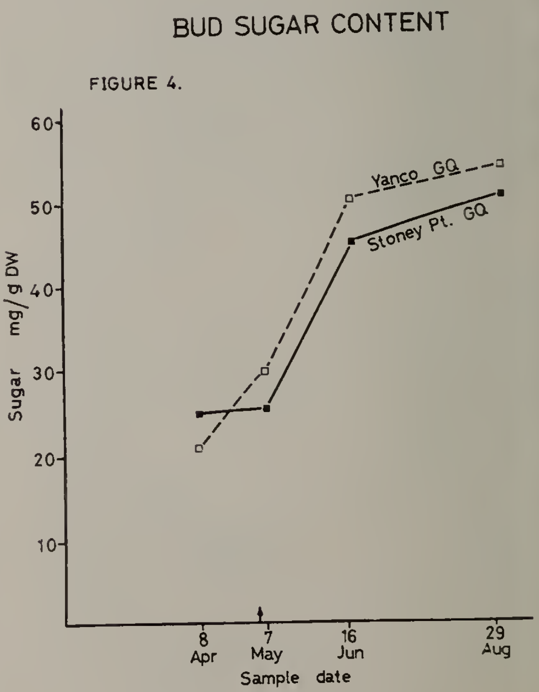

FIGURE 4.—Bud sugar content.

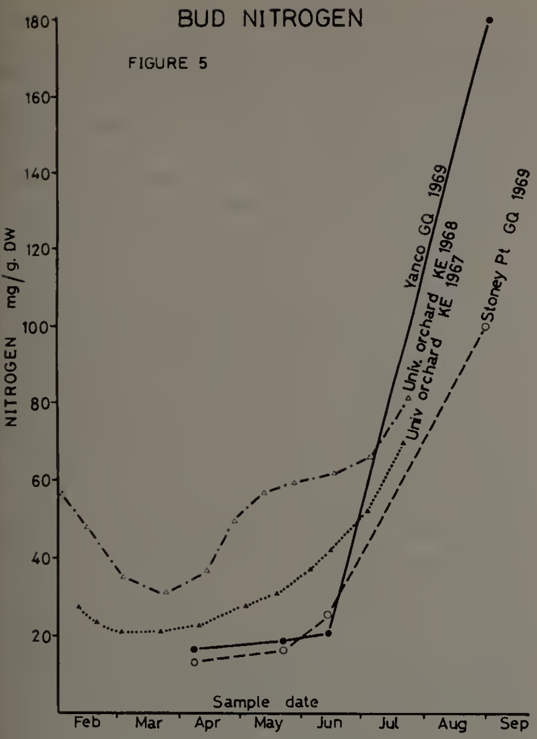

FIGURE 5.—Bud nitrogen.

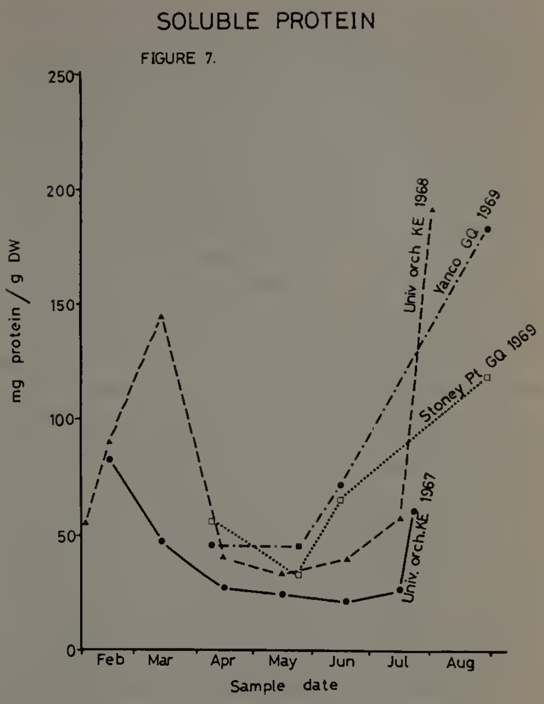

FIGURE 7.—Soluble protein in the buds.

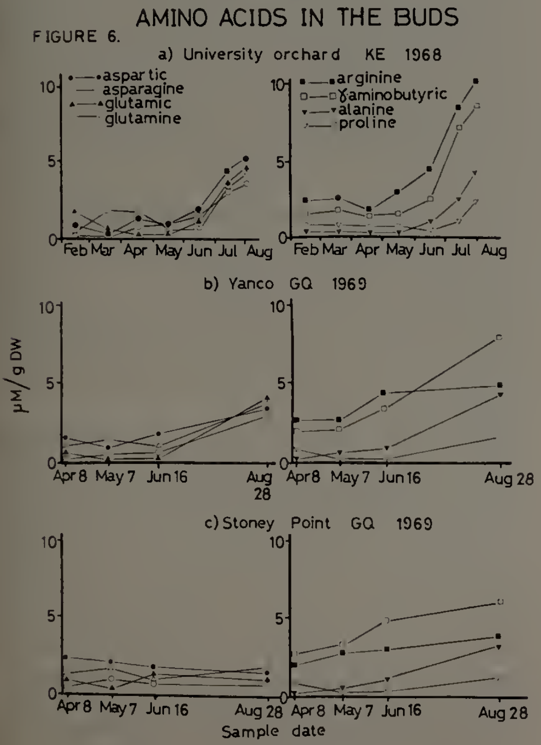

FIGURE 6.—Amino acids in the buds.

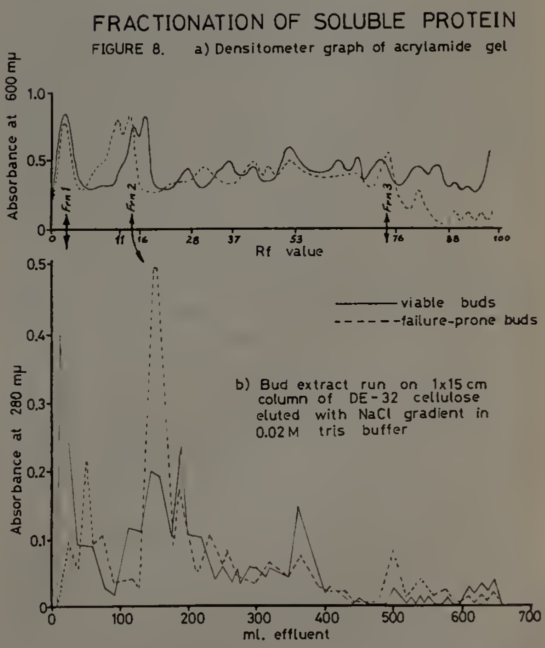

FIGURE 8.—Fractionation of soluble protein from buds.

Although the incidence of bud failure during the three seasons of this study was not exceptionally high, both abscission and necrosis of buds were recorded in each year from April onwards—that is, shortly after commencement of differentiation of the basic flower parts. The reproductive buds which were initiated at distinctly different times on the three cultivars, all reached differentiation at much the same time in March. Thereafter the only major processes to be completed before flowering were the relatively prolonged differentiation and development of the pollen and ovule. It may well be that a certain degree of chilling is essential for this process. Any delay in this, and its associated balance of growth substance, would almost certainly explain poor flowering and fruit set (Luckwill, 1963). Necrosis and abscission, which often occur before differentiation of the ovule, would then appear more dependent upon other metabolic processes taking place in the buds. A relationship between bud failure and chilling was evident on both KE and BB in the University orchard in 1967 and 1969. In those years there was less chilling than in 1968 when the bud failure was only slight.

The usual form of bud abscission is well documented in the literature and the abscission layer formation is common to many fruits and leaves. The other form of abscission, however, originating in the cortex of the shoot is unusual and may be associated with virus infection. Trees in the orchard at Stoney Point where this form of abscission was prevalent, were shown by plant pathologists of the N.S.W. Department of Agriculture to be infected by Prunus necrotic ringspot and greasy sunken mottle viruses. Most of the failure observed in this study, however, involved abscission of the buds and only a minor proportion was necrotic and did not absciss. Failure to break dormancy as a consequence of inadequate chilling could not be greatly implicated because the evidence suggests that the chilling experienced under the respective orchard conditions was more than adequate.

The extent to which buds absciss or die varies greatly within cultivars in different years, suggesting also some disruption of metabolism not associated with the above factors ; a condition akin to but not as stable as that described by Kester (1968) as " genetic ".

Total nitrogen in GQ buds in mid-June, 1969, was about 20 mg/g DW at Yanco and about 25 mg/g DW at Stoney Point. The soluble protein plus the amino acids, included because they are sparingly soluble in aqueous buffer, only amounted to about 75 mg/g DW of the Yanco buds and 70 mg/g DW of the Stoney Point buds. This protein plus amino acids would thus account for about 11 mg and 10 mg (55 and 40 per cent) of the total nitrogen in the GQ buds from the Yanco and Stoney Point orchards respectively. These amounts are in close agreement with the 42 per cent soluble organic nitrogen in the stems of dormant peach reported by Davidson and Shive (1935). That is, about half of the nitrogen in the buds was unaccounted for and was presumably associated with other nitrogenous components such as nucleic acids, nucleotides, and insoluble protein. Sugar contributed 51 mg/g and 46 mg/g (5·1 and 4·6 per cent) towards the dry weights of the Yanco and Stoney Point GQ buds respectively. At this time, starch content of the buds would be expected to be relatively low.

Twenty per cent of the contents of the buds was therefore unaccounted for by the analyses made in this study. Fats and waxes comprised about 15 per cent (as a residue of methanol extraction) and there was in addition insoluble cellulose and similar compounds. Although changes in the more important labile metabolites were studied, interpretation of the data was limited by uncertainty concerning the remainder. Despite these limitations it was clear that while the apparent volume of the buds increased markedly throughout the whole period of winter rest the dry weight increased only slightly. This increase in dry weight continued until about six to eight weeks prior to bud burst, indicating inflow of nutrients into the buds for some time after leaf-fall. Such inflow of nutrients should have been similar in the two GQ orchards but the buds were relatively smaller on the trees at Stoney Point when compared with buds at a similar stage of development at Yanco. Saikia *et al.* (1967), however, found that loss of viability in small buds of almond was accompanied by a decrease in the fresh weight, but this was in turn caused by anatomical abnormalities in the eumeristems in late summer.

Respiration rates of the abscissing buds did not show the 10- to 20-fold increase found in the normal buds preceding bud burst. Kosseva *et al.* (1968) found a similar pattern of change for buds of *Rosa damascena* L. which were undergoing abscission. In their study single buds of about 0·25 g FW respired at 0·15 mg CO_2/hr at onset of abscission (equivalent to a reduction from 308 to 96 μl CO_2/g FW/hr). When the respiration rates of the GQ buds at Yanco were compared with those of the GQ buds at Stoney Point in April a similar difference was found although no appreciable bud abscission had occurred in either orchard at that time. The same ratio between the respiration rates was again found at bud burst when the incidence of failure was high in the Stoney Point orchard. Such a rapid increase in the rate of respiration at bud burst is obviously related to the expansion of viable buds and their probable increase of enzymes in comparison with the slower rates of increase in buds destined to fail

There was little difference between the concentrations of sugars in the GQ buds at Yanco and at Stoney Point. The composition of the sugar, however, conflicts with the report of El-Mansy and Walker (1966) that fructose is the main sugar in peach. Glucose was the predominant sugar not only in the flower buds but also in the leaves, the total sugar being made up of glucose plus fructose. This finding supports Baldwin's (1963) report that peach buds contain both glucose plus fructose, but no sucrose. Because less sugar was found in twigs which supported few reproductive buds compared with twigs with many buds, it is also possible that some conversion of starch to sugar is associated with the increased meristematic activity. The rapid accumulation of sugar in buds following leaf-fall supports the data of Barnard and Read (1932) and Dowler and King (1966), and almost certainly is the result of transformation of starch to sugar in response to low temperature (Barker, 1936). GQ buds in the Stoney Point orchard increased in respiration rate earlier than the buds at Yanco which could further be ascribed to this change if the appearance of the necessary enzymes could be explained.

All of the eight major amino acids found in the buds in this study have been reported by Durzan (1968) to increase in concentration at bud burst. Arginine and its analogue γ–aminobutyric acid were the predominant amino acids found, which agrees with the data of Taylor (1967). Some amino acids even at low concentrations are capable of inhibiting plant growth and causing specific morphological alterations. Significantly, many of these inhibitory amino acids have been related to aspartic acid metabolism (Dunham and Bryan, 1969). It appears possible that some small protein fractions present in failure-prone but lacking in viable buds could be composed of these inhibitory amino acids.

The main changes in the chemical components associated with buds destined to fail in the spring were, therefore, a higher rate of respiration from about two months preceding bud burst, a lower concentration of soluble protein and amino acids, and a relatively slow increase of aspartic and glutamic acids and their amides. Certain protein fractions also diminished in the failing buds, and of these, the fraction of high molecular weight around 100×10^3 was reduced, possibly by hydrolysis, at the onset of bud failure. This does not, however, explain the large amount of protein of molecular weight around 26×10^3 associated with abscissing buds unless it includes the aspartic and glutamic acids and their amides. Neither could its presence be attributed solely to virus, although the involvement of virus with bud failure is suspect. The same fractions were found in both viable and abscissing buds of all three cultivars studied. The changes in chemical composition specific to buds about to absciss may be summarized therefore as, early burst in respiration, slow increase in sugar, low nitrogen, low level of soluble protein, and low amino acid content, all of which could cause, or be caused by, retarded growth of the buds.

Leaf analyses, at a vegetative phase of growth around time of differentiation before bud failure was evident, failed to reveal any significant difference between mineral nutrition of trees and their proneness to bud failure. Some differences in mineral elements have been reported in association with imbalance of growth regulating substance such as indoleacetic acid by Ben-Yehoshua and Biggs (1970). Changes in concentration of some growth regulating substances are also known to be associated with bud failure of peach (Malcolm, 1972), and they may further be linked with changes in enzyme activity as suggested by Krupnikova (1967). The relatively high level of molybdenum in the buds prone to failure defies explanation unless the increase in metabolism in viable buds at bud-burst results in its transport out of those buds to other parts of the trees.

Summary

The reproductive buds of peach are initiated in spring during a temporary decrease in the rate of vegetative growth, possibly in response to some internal nutritional diversion. The buds need a certain amount of chilling for breaking their "rest" but this is usually adequate and unrelated to their failure. Prolonged chilling delays flowering and shortens the period for vegetative growth. Failure of the buds, from either abscission or necrosis, can occur at any stage of their development its incidence being mild up to differentiation then increasing in severity up to bud-burst.

Volume, weight and the contents of nitrogen and sugar in the flower buds all increase from

initiation until mid-winter when there is a transient decrease followed by a rapid increase. Respiration also increases from this stage on approach of bud-burst. Failure-prone buds show an earlier increase in rate of respiration than normal buds and a slower rise thereafter, and levels of nitrogen, protein, sugar and particularly aspartic and glutamic acids and their amides are lower.

Acknowledgements

The assistance of Miss J. S. Railton and Mr. G. J. Rich during this study is gratefully acknowledged, and the Chemistry Branch of the New South Wales Department of Agriculture for the analyses of mineral nutrients.

References

Anon, 1941. Effects of Climatic Factor : on Growing Plants. In Climate and Man Yearbook of the United States Department of Agriculture. (Eds.), Hildreth, A. C., Magness, J. R., and Mitchell, J. W.

Anon, 1968. Sephadex. Instructions for the Gel Filtration Kit. Jan. 1968–1. Pharmacia Fine Chemicals, Uppsala, Sweden.

Baldwin, J. G., 1963. Dormancy in Deciduous Fruit Trees and Vines. *Proc. 2nd Aust. Fruit Res. Conf.*, 9 : 3 : 1. Published by CSIRO Melbourne.

Barker, J., 1936. Analytic Studies in Plant Respiration. *Proc. Roy. Soc. Biol.*, **119**, 453.

Barnard, C., and Read, F. M., 1932. Studies on Growth and Fruit Bud Formation. IV. Apricot and Peach. *J. Vict. Dept. Agric.*, **30**, 28.

Ben-Yehoshua, A., and Biggs, R. H., 1970. Effects of Iron and Copper ions in Promotion of Selective Abscission and Ethylene Production by Citrus Fruit and the Inactivation of Indoleacetic Acid. *Plant Physiol.*, **45** (5), 604.

Black, M. W., 1955. The Problem of Prolonged Rest in Deciduous Fruit Trees. *Rept. 13th Intl. Hort. Congr. London*, 1122.

Cassidy, H. G., 1957. *Technique of Organic Chemistry Vol. X. Fundamentals of Chromatography.* Interscience Publishers Inc. N.Y. Arnold Weissberger, Ed.

Chandler, W. H., and Tufts, W. P., 1933. Influence of the Rest Period on Opening of Buds on Fruit Trees in Spring and on Development of Flower Buds of Peach Trees. *Proc. Amer. Soc. Hort Sci.*, **30**, 180.

Conn, H. J., Darrow, M. A., and Emmel, V. M., 1960. *Staining Procedures. The Biological Stain Commission.* Williams and Wilkins Co., Baltimore, U.S.A.

Davidson, O. W., and Shive, J. W., 1935. Determination of the Nitrogenous Fractions in Vegetative Tissues of the Peach. *Plant Physiol.*, **10**, 73.

Denney, A., Walker, D. R., and Norton, R. A., 1965. A Study of Selected Biochemical Constituents in Certain Prunus Species. *Proc. Amer. Soc. Hort. Sci.*, **89**, 140.

Dowler, M. W., and King, F., 1966. Seasonal Changes in Starch and Soluble Sugar Content of Dormant Peach Tissues. *Proc. Amer. Soc. Hort. Sci.*, **89**, 80.

Dunham, V. L., and Bryan, K., 1969. Synergistic Effects of Metabolically Related Amino Acids on the Growth of a Multicellular Plant. *Plant Physiol.*, **44** (11), 1601.

Durzan, D. J., 1968. Nitrogen Metabolism of Picea Glauca. I. Seasonal Changes of Free Amino Acids in Buds, Shoot Apices and Leaves, and the Metabolism of Uniformly Labelled ^{14}C–L–arginase by Buds During the Onset of Dormancy. *Can. J. Bot.*, **46** (7), 909.

El-Mansy, H. I., and Walker, D. R., 1966. Biochemical Changes Occurring in Apricot and Peach Buds During their Rest Period. *Proc. 17th Intl. Hort. Congr. Md.* **1**, Abstr., 510.

Evans, W. J., Woodham, A. A., Carney, W. B., Dechary, J. M., and Altschul, A. M., 1963. Fractionation of Particulate Proteins of the Peanut Cotyledon. *Proc. Seed Protein Conf. New Orleans*, 218.

Harper, H. H., 1967. *A Review of Physiological Chemistry.* 11th Edn. Lange Medical Publications, Los Altos, California.

Hedrick, J. L., and Smith, A. J., 1968. Size and Charge Isomer Separation and Estimation of Molecular Weights of Proteins by Disc Gel Electrophoresis. *Arch. Biochem. Biophys.*, **126**, 155.

Hladik, F., 1967. Fertility as a Factor Influencing the Growth and Productivity of Peach Trees. I. The Influence of Fertility on the Growth and on the Differentiation of Flower Buds. Ved. PR. Ovocnarske vyzk ustav ovacnarsky. *Holo Vousich*, **3**, 51.

Holbeche, J. A., 1966. Peach and Nectarine Growing. *N.S.W. Dept. Agric. Hort. Bull.* H121.

Jaarsveld, P. P. van, and Meynhardt, J. T., 1967. The Effect of Carbowax on the Activity of Indoleacetic Acid Oxidase from Peach Leaf Tissue. *Sth. Afr. J. Agr. Sci.*, **10** (4), 901.

Johansen, D. R., 1940. *Plant Microtechnique.* McGraw-Hill, London.

Karapetyan, K. A., 1967. Dynamics of Changes in the Carbohydrates in the Buds of the Almond and Peach in Connection with their Frost Resistance. *Biol. Zh. Arm.*, **20** (8), 58.

Kester, D. E., 1968. Noninfectious Bud Failure, a Nontransmissible Inherited Disorder in Almond. I. Pattern of Phenotype and Inheritance. *Proc. Amer. Soc. Hort. Sci.*, **92**, 7.

Kosseva, D., Zolotovich, G., and Decheva, R., 1968. Study on Flower Buds of *Rosa Damascena* Mill. in Conjunction with their Falling Off. *Rastenevod. Nauki*, **5** (2), 31.

Kozlowski, T. T., 1964. *Water Metabolism in Plants.* Harper, New York.

Krupnikova, T. A., 1967. Enzyme Activity Affected by Zinc Deficiency. (Transl.) Mikroelem. Biosfere Ikh. Primen. Sel, Khoz. Med. Sib. Dal'nego Vosloka, Dokl. Sib. Kouf. 2nd 1964, (Publ. 1967), pp. 318 (Russian).

Leece, D. R., 1967. Leaf Analysis as a Guide in Diagnosing Malnutrition in Peach Trees. (*Prunus persica* L. Batsch) M.Sc.Agr. thesis. The University of Sydney.

Lenz, F., 1963. Flower Initiation and Development of Stonefruit Varieties in the Murrumbidgee Irrigation Areas. *Proc. 2nd Aust. Fruit Res. Conf. Orange and Terrigal, N.S.W.*, **9** (13), 1.

Luckwill, L. C., 1963. Some Aspects of the Physiology of Reproduction in the Apple. *Proc. 2nd Aust. Fruit Res. Conf. Orange and Terrigal, N.S.W.*, **4**, 1.

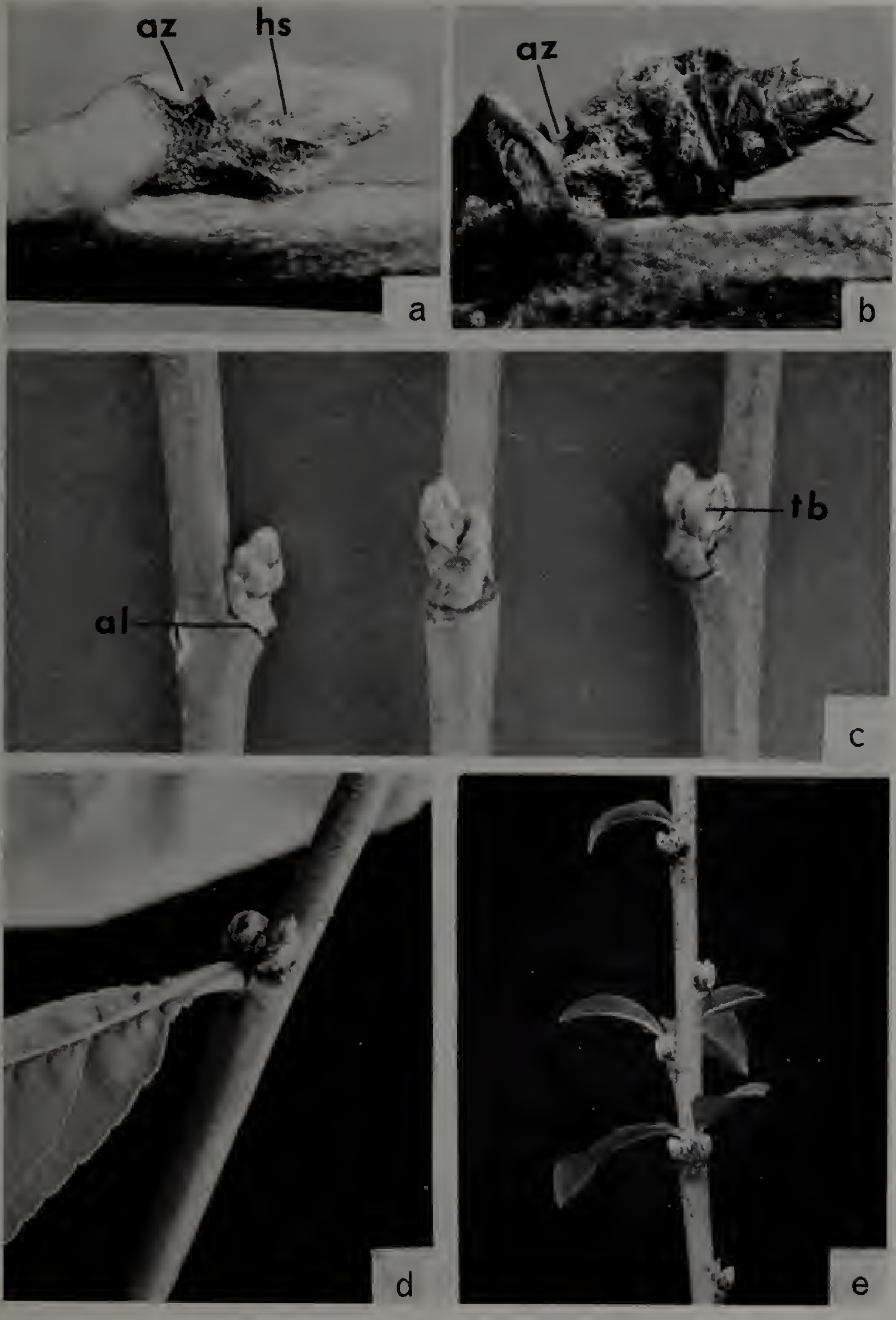

Plate I (a, b.)—Abscission zone at base of bud peduncle. (c) Unusual abscission zone in shoot cortex. (d) Vegetative bud with reproductive buds on either side. (e) Necrotic flower buds and early shoots of vegetative bud growth.

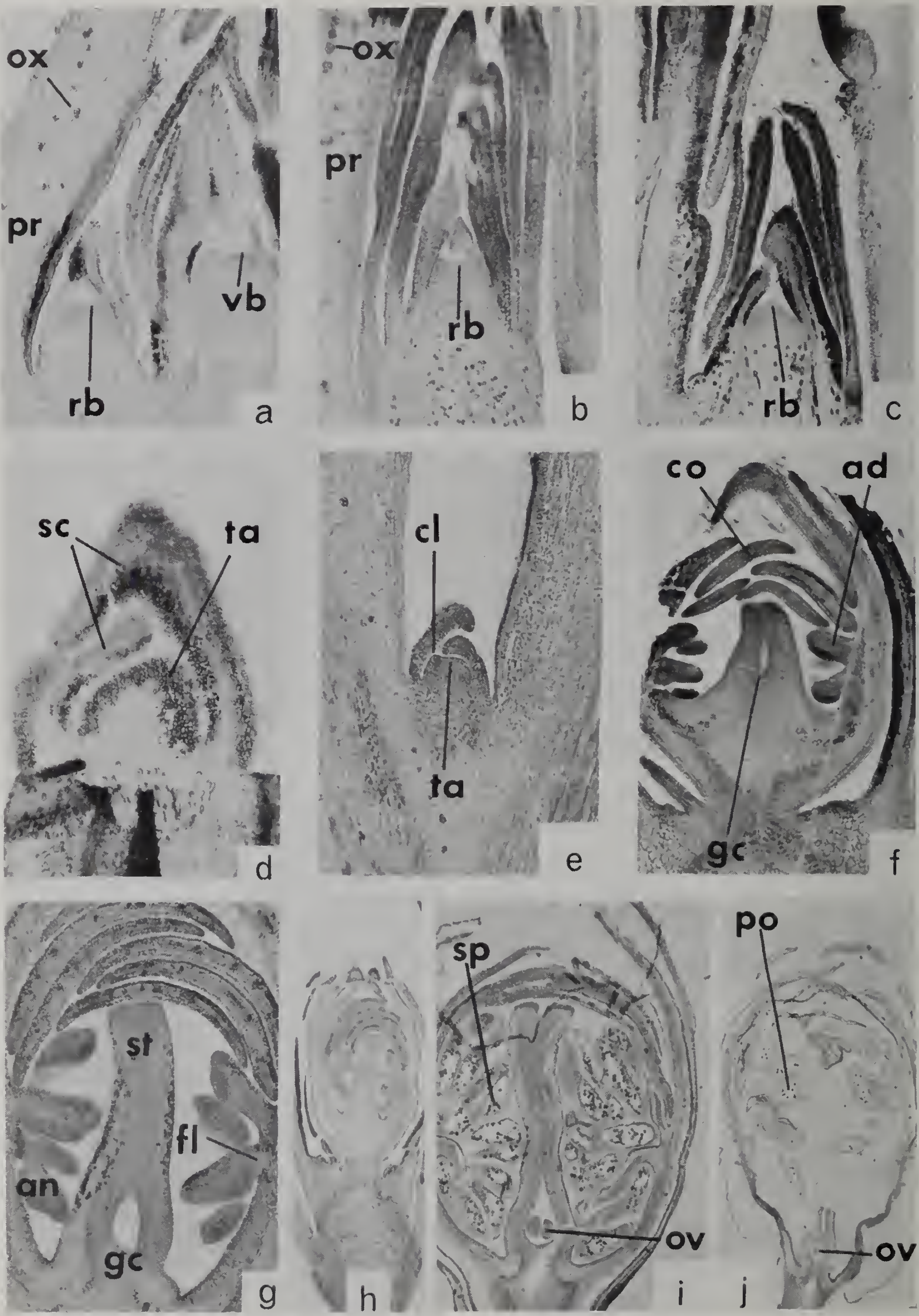

Plate II—Development of the bud in histological section. a–j (see separate descriptions)—Ref. Table 1.

MALCOLM, H. D. R., 1965. The Golden Queen Peach. *Agric. Gaz. N.S.W.*, **76** (3), 143.

MALCOLM, H. D. R., 1970. On the Physiology of the Shoot System of Peach with Special Reference to Bud Failure. Ph.D. thesis. Macquarie Univesrtiy.

MALCOLM, H. D. R., 1972. Some Growth Substances Associated with Bud Failure of Peach. In :— Plant Growth Substances 1970. D. J. Carr (Ed.), *Proc. 7th Intl. Conf. Springer-Verlag*, Berlin.

MANCY, K. H., and WESTGARTH, W. C., 1962. A Galvanic Cell Oxygen Analyzer. *Journ. W.P.C.F.*, **34** (10), 1037, Asheville, Carolina, U.S.A.

MOORE, S., and STEIN, W. H., 1948. Photometric Ninhydrin Method for Use in the Chromatography of Amino Acids. *J. Biol. Chem.*, **176**, 367.

MURNEEK, A. E., 1930. Quantitative Distribution and Seasonal Fluctuations of Nitrogen in Apple Trees. *Proc. Amer. Soc. Hort. Sci.* **27**, 228.

OSER, B. L. (Ed.), 1965. *Hawk's Physiological Chemistry*. 14th Edn. McGraw-Hill, New York.

RADU, I. F., 1960. Translation. :—Changes in Total Nitrogen During the Vegetative and Dormant Periods of Apple, Pear, Apricot and Peach Trees. *Lucr. sti. Inst. Cerc. Hort-vitic.*, 1959–60, 1961.

ROGERS, L. J., 1965. A Simple Apparatus for Disc Electrophoresis. *Biochem. Biophys. Acta.*, **94**, 324.

SAIKIA, B. N., KESTER, D. E., and BRADLEY, M. V., 1967. Dormant Vegetative Buds in Normal and Bud-failure Forms of Almond. (*Prunus amygdalus* Batsch). *Proc. Amer. Soc. Hort. Sci.*, **89**, 150.

SMITH, I. (Ed.), 1958. *Chromatographic and Electrophoretic Techniques*. William Heinemann. Medical Books Ltd., London.

STADLER, J. D., and STRYDOM, D. K., 1967. Flower Bud Development of Two Peach Cultivars in Relation to their Winter Chilling Requirements. *Sth. Afric. Journ. Agric. Sci.*, **10** (3), 831.

TAYLOR, B. K., 1967. Storage and Mobilization of Nitrogen in Peach Trees : A Review. *J. Aust. Inst. Agric. Sci.*, **33** (1), 23.

TREVELYAN, W. E., PROCTOR, D. P., and HARRISON, G. S., 1950. Detection of Sugars on Paper Chromatograms. *Nature.*, London, **166**, 44.

WEINBERGER, J. H., 1967. Studies on Flower Bud Drop in Peaches. *Proc. Amer. Soc. Hort. Sci.*, **91**, 78.

N.S.W. Dept. of Agriculture,
Biological and Chemical Research Institute,
P.M.B. 10, Rydalmere,
N.S.W. 2116. Australia.

(Received 3.2.75)

EXPLANATION OF PLATE I

(a) A " single " flower bud from which the outer glabrous scales have been removed to show the hairy inner scales (hs) and abscission zone (az). (Approx. 3 × natural size). (b) A typical necrotic " single " flower bud from which the scales have been removed. (Approx. 3 × natural size). (c) Lateral shoots bearing flower buds below which an abnormal abscission zone (az) has formed into the cortex of the shoot. This abscission causes loss of the whole triplet bud (tb). (Approx. natural size). Photograph courtesy of Dr. P. F. Kable. (d) A " triplet " bud formation in the axil of a mature leaf. Note the relatively small vegetative bud situated between the two flower buds. (Approx. natural size). (e) Necrotic flower buds in the " triplet " bud formation causing early growth of the central vegetative bud. (Approx. $\frac{1}{2}$ natural size).

EXPLANATION OF PLATE II

(a) Longitudinal section through the bud primordia in the axil of a leaf on the KE cultivar in late October, 1966. The central vegetative bud (vb) can be seen to the right of the photograph, with the primordium of the reproductive bud (rb) to its left, the two being covered by the prophyll (pr) shown on the far left. Note the oxalate crystals (ox) in the cells of the prophyll. Magnification ×55. (b) A KE reproductive bud primordium in late November. Note the bud-enclosing prophyll (pr) on the right of the photograph. Magnification ×55. (c) A KE reproductive bud primordium in early January, 1967. Magnification ×55. (d) A KE reproductive bud in early February, 1967, with all but two of the scale initials (sc) removed. Note the characteristic dome shape of the tunica (ta) indicating onset of differentiation. Magnification ×55. (e) A KE reproductive bud in late March, 1967. Calyx lobes (cl) have begun to appear around the periphery of the now " flattened " tunica (ta). Magnification ×20. (f) A longitudinal section through a differentiating KE reproductive bud in late April, 1967. Note that within one month, the corolla (co), androecium (ad) and gynoecium (gc), have differentiated. Magnification ×55. (g) A longitudinal section through a KE reproductive bud in early May, 1967. Note the increase in bud size, the enlarged gynoecium (gc) with its elongated style (st) and the androecium differentiating into filaments (fl) and anthers (an). Magnification ×55. (h) A KE bud section in early June, 1967. Note that little differentiation of the flower initials has occurred during the past month. Magnification ×20. (i) A KE bud section in early July, 1967. In the past month rapid differentiation of the flower initials has taken place, and the bud has increased in size. Tetrads of spores (sp) have differentiated in the anthers, and two ovules (ov) have differentiated in the ovary. The style has also further elongated. Magnification ×20. (j) A KE bud section on July 19, 1967. The bud has enlarged considerably on approach of bud burst. Pollen (po) has formed in the anthers and filaments have formed (broken away in the sectioning). A single ovule is shown in the ovary, the other having degenerated. The bud differentiation is now complete. Magnification ×8.

Report of Council for the Year Ended 31st March, 1975

Meetings and Lectures :

LOCATION : Large Hall, Science House, 157 Gloucester Street, Sydney:

April 4th : Annual General Meeting, *Presidential Address :* Floppy Rulers and Light Pens, *Dr. J. P. Pollard, Australian Atomic Energy Commission.*

May 1st : Some Little Publicised Aspects of the Design of the Sydney Opera House, *Mr. Peter Hall, Architect.*

June 5th : Basic Drawings for Fine Art, Industry and Social Communication, *Mr. Arthur J. Murch, Artist.*

July 3rd : Adaptations of Cattle to Tropical Environments, *Professor N. T. M. Yeates, Professor of Livestock Production, University of New England.*

August 7th : Conservation of Marine Resources, *Dr. K. Radway Allen, Chief, Division of Fisheries and Oceanography, CSIRO.*

September 4 : Symposium, Students' Attitudes in Contemporary Educational Institutions, *Prof. A. G. Mitchell, Macquarie University* ; *Mr. B. Coles, President, Sydney University Union ; Mrs. B. Bowen, Principal, Killara High School.*

October 2 : The Formation of Petroleum, *Dr. J. Taylor, Assistant Chief, CSIRO Division of Mineralogy.*

November 6 : Food Additives, *Mr. John Neuhaus, Assistant Government Analyst, Division of Analytical Laboratories, Lidcombe.*

December 4 : Designing a New-Generation Aircraft Landing System, *Mr. H. C. Minnett, Chief, Division of Radiophysics, CSIRO.*

LOCATION : Lecture Theatre 2, School of Chemistry, University of Sydney:

August 15 : Liversidge Lecture for 1974—Chance and Design : An Historical Perspective of the Chemistry of Oral Contraceptives, *Professor A. J. Birch, Dept. of Organical Chemistry, Research School of Chemistry, Australian National University.*

Attendances at these meetings totalled 519.

Annual Dinner : The Annual Dinner, held in the Reception Hall, Sydney Opera House, was attended by 93 members and guests. The guest speaker was Prof. B. R. Williams, Vice-Chancellor and Principal of the University of Sydney, his address being entitled, " Science, Wisdom and the Good Society."

Awards.—The following Awards for 1974 were made : James Cook Medal : Sir Marcus Oliphant ; The Edgeworth David Medal : Dr. A. W. Snyder ; Clarke Medal : Dr. C. H. Tyndale-Biscoe ; Walter Burfitt Prize : Dr. B. Robinson ; Olle Prize : Mr. David A. Gray ; The Liversidge Research Lectureship : Prof. A. J. Birch.

The Society's Medal was not awarded.

Summer Schools.—Two highly successful Summer Schools, held during January 1975, were attended by more than 120 Fifth Form students. The one organized around the theme " Chemistry and the Consumer " was held at Macquarie University, the other entitled " The Earth's Environment in the Universe ", was held at Science House and included visits to CSIRO Radiophysics Laboratories, Epping, the University of Sydney, Fleurs Observatory at Kemps Creek and Sydney Observatory.

Membership.—Membership at 31st March, 1975, was—Life Members 10, Members 374, Associates 30.

Publications.—Volume 107 of the Journal and Proceedings was published in two parts during the year. A grant of $500 was received from the National Library of Australia towards the cost of publishing a subject index. This index was prepared by Mr. A. F. Day and covers the four years of the Transactions of the Philosophical Society of New South Wales as well as the first fifty years of the Journal and Proceedings of The Royal Society of New South Wales.

Library.—2,690 items were received and processed. These comprised periodicals on exchange from some 354 societies and institutions, donations and periodicals purchased. Two hundred and fifty-nine members, societies and organizations used the library facilities during the year. The re-cataloguing of the library was commenced during the year.

Finance.—Due to increasing costs and loss of revenue from Science House, the year has been a most difficult one financially, the deficit for the year being $10,742. Council does not expect any improvement until after the new Science House is well established. A grant of $1,750 was received from the Government of New South Wales. Originally this was made in lieu of printing the Journal but now falls far short of this expenditure, which currently is approaching $8,000 a year.

New Science House.—During the year Science House Pty. Ltd., the company jointly formed by the Society and the Linnean Society of New South Wales purchased a building at the northern end of Clarence Street for the purpose of establishing a Science Centre to replace the existing Science House. Alterations to the building are expected to begin during the first half of the coming year.

Acknowledgements.—Council wishes to acknowledge the excellent work carried out during the year by the Executive Secretary, Mrs. V. Lyle, the Assistant Librarian, Mrs. G. Proctor, and all concerned with the organization of the Summer Schools and monthly lectures.

Honorary Treasurer's Report

There was a deficit for the period of $10,742 as against a deficit for the previous year of $5,293 resulting in a net additional deficit of $5,449 made up as follows :

	$	$
Increase in general interest		2,538
Increase in sale of back numbers		1,905
Increase in members subscriptions and application fees		547
Increase in donations received		483
Increase in summer school surplus		91
Sale of centenary volume and subject index		144
Reduction in rentals		1,348
		7,056
Less		
	$	
Reduction in science house surplus	3,370	
Reduction in sale of reprints	327	
Reduction in subscriptions to journal	469	
Reduction in sale " Sydney Opera House Commemorative Issue "	1,153	
Increase in salary costs	2,561	
Increase in printing costs	3,295	
Increase in general expenses	272	
Library recataloguing	1,058	
		12,505
Total decline		$5,449

Last financial year an amount of $28,420 was set aside to be written off over a three year period with the present year being the second year of this budget plan. The reason for this approach is that the loss of income from Science House was thereby to be made available for general operating expenses of the Society. The present deficit includes a heavy component resulting from the nearly doubling of our printing expenses for the Journal, although this was fortunately offset by the sale of back issues—a " windfall " item which cannot be anticipated in our coming budget.

We enter the third year of our budget plan with $12,385 available (15% more than the current year). However, by the end of the three year period, cash flow is not expected from Science House Pty. Ltd. as was anticipated. The management of our remaining cash reserves in the present inflationary climate, becomes a critical task for the Council in the coming years and some cutting back in expenses seems inevitable as our reserves would otherwise only take us to 1977.

Report of the South Coast Branch of the Royal Society of New South Wales

Officers :

President : B. Clancy

Secretary : G. Doherty

Council representative : G. Doherty

No meetings of the South Coast Branch were held during the year.

Financial Statement, 1974 :

Previous Balance	$118.13
Accumulated interest	$4.15
Present Balance	$122.28

G. Doherty,
Secretary.

31st March, 1975.

Report of New England Branch of the Royal Society of New South Wales for 1974

Officers for 1974

Chairman	H. G. Royle
Secretary-Treasurer	T. O'Shea
Committee	R. L. Stanton N. T. M. Yeates D. H. Fayle N. H. Fletcher
Branch Representative on Council	R. L. Stanton

The following meetings were held :

3rd May, 1974 : The Nature and Significance of Fossil Evidence Concerning the Separation of the Continents During Geological Time, *Professor D. Hill, F.R.S. Emeritus Professor of Geology, University of Queensland.*

20th September, 1974 : The Ecology of Worm Populations, *Dr. J. W. Pickett, Geological Survey of N.S.W. President, Royal Society of N.S.W.*

15th October, 1974 : Alcohol and the Breathalyser, *Dr. P. Carroll, University of New South Wales.*

21st November, 1974 : Man's Future in the Light of His Past Evolution, *Professor G. Ledyard Stebbins, University of California.*

Financial Statement :

Balance at Commercial Banking Company of Sydney Limited, University of New England Branch, 29th March, 1974	$273.34	
Credit—Interest to 25th June, 1974	$4.96	
Interest to 30th December, 1974	$4.82	$283.12
Debit—Advertising	$7.00	$7.00
Balance at 31st March, 1975		$276.12

Rod Gould,
Secretary-Treasurer.

31st March, 1975.

THE ROYAL SOCIETY OF NEW SOUTH WALES
BALANCE SHEET – 28TH FEBRUARY 1975

1974 $			$
	RESERVES		
12,123	Library reserve – note 1		10,478
453,971	Resumption reserve		453,971
205	LIBRARY FUND – note 1		5,214
—	LONG SERVICE LEAVE FUND – note 1		806
26,696	ACCUMULATED FUNDS		16,793
492,995	NET FUNDS		$487,262
	Represented by:		
	CURRENT ASSETS		
675	Cash at bank and in hand	6,304	
205	Cash at bank – library fund – note 1	214	
—	Debtors for subscriptions – note 2	—	
892	Other current debtors and prepayments	1,394	
30,318	Short term deposits	7,320	
32,090			15,232
	Less		
	CURRENT LIABILITIES		
674	Sundry creditors & accruals	6,316	
128	Subscriptions paid in advance	366	
6	Life members subscriptions – current portion	6	
808			6,688
31,282	NET CURRENT ASSETS		8,544
	Add		
	FIXED ASSETS – note 4		
1,868	Furniture and office equipment	2,208	
2	Lantern	2	
13,600	Library	13,600	
16	Pictures	15	
15,486			15,825
	INVESTMENTS – note 5		
9,680	Commonwealth bonds and inscribed stock	9,680	
12,123	Short term deposits	11,284	
—	Loan secured by mortgage	20,000	
21,803			40,964
	ASSOCIATED CORPORATIONS – note 3		
1	Shares	1	
424,490	Advances and loans – unsecured	421,990	
424,491			421,991
	TRUST FUNDS – note 6		
7,000	Commonwealth bonds and inscribed stock	7,000	
3,036	Short term deposits	3,396	
10,036			10,396
503,098			497,720
	Less		
	NON-CURRENT LIABILITIES		
10,035	Trust funds – note 6	10,396	
68	Life members subscriptions – non-current portion	62	
10,103			10,458
$492,995	NET ASSETS		$487,262

INCOME AND EXPENDITURE ACCOUNT FOR YEAR ENDED 28TH FEBRUARY 1975

1974 $		$	$
(5,041)	NET SURPLUS (DEFICIT) for period before bad debts		(10,953)
	Add		
—	REDUCTION in provision for bad debts		641
(5,041)			(10,312)
	Less		
175	INCREASE in provision for bad debts	—	
77	SUBSCRIPTIONS written off	430	
252			430
(5,293)	NET SURPLUS (DEFICIT) for period		(10,742)
	Add		
—	DONATIONS to library fund		5,009
17,162	INTEREST on compensation investment		—
—	TRANSFER from library reserve – note 1		1,645
37,367	ACCUMULATED FUNDS brought forward from 1974		26,696
49,236	FUNDS AVAILABLE		22,608
	Less		
—	TRANSFER to library fund – note 1	5,009	
17,162	TRANSFER to resumption reserve	—	
3,224	TRANSFER to library reserve	—	
—	TRANSFER to long service leave fund – note 1	806	
2,154	CENTENARY VOLUME – stock written off	—	
22,540			5,815
$26,696	ACCUMULATED FUNDS – 28th February 1975		$16,793

The above account and the balance sheet are to be read in conjunction with the notes attached.

J.P. POLLARD
Honorary Treasurer

J.W. PICKETT
President

AUDITOR'S REPORT TO THE MEMBERS

1. In our opinion a) the attached Balance Sheet and Income and Expenditure Account, together with the notes thereon, have been properly drawn up so as to correctly show the state of the Society's affairs at 28th February 1975 and the deficit for the year ended on that date.

   b) the accounting and other records have been properly kept in accordance with the Rules of the Society.

2. We have satisfied ourselves that the Society's Commonwealth Bonds and Inscribed Stock are properly held and registered.

65 York Street
Sydney

HORLEY & HORLEY
Chartered Accountants
Registered under the
Public Accountants
Registration Act 1945
as amended

2nd April 1975

THE ROYAL SOCIETY OF NEW SOUTH WALES

NOTES ON ACCOUNTS - 28TH FEBRUARY, 1975

1. MOVEMENTS IN PROVISIONS AND RESERVES

(i) LIBRARY RESERVE

1974 $			
8,898	Balance at 1st March 1974		12,1[illegible]
	Add		
3,225	From accumulated funds re sale of assets in previous periods		—
12,123			12,1[illegible]
	Less		
	Transferred to accumulated funds re		
—	Library recataloguing	1,058	
—	Typing & printing subject index	1,087	
—		2,145	
	Less		
—	Donation towards printing subject index	500	
—			1,645
$12,123	Balance at 28th February 1975		$10,478
	Represented by:		
$12,1[illegible]	Short term deposits		$10,478
	(See also note 5)		

(ii) LIBRARY FUND

1974 $		
—	Balance at 1st March 1974	205
	Add	
205	Donations	5,009
$ 205	Balance at 28th February 1975	$5,[illegible]14
	Represented by:	
205	Cash at bank	[illegible]4
—	Loans to associated corporations	[illegible],000
$ 205		$[illegible],[illegible]14
	(See also note 3)	

(iii) LONG SERVICE LEAVE FUND

1974 $		
—	Balance at 1st March, 1974	—
	Add	
—	Amount included in accumulated funds at 28th February, 1974 transferred	764
—	Interest	4[illegible]
$ —	Balance at 28th February 1975	$806
	Represented by:	
$ —	Short term deposits	$806
	(See also note 5)	

[illegible]. DEBTORS FOR SUBSCRIPTIONS

1974 $		
830	Owing by members	190
	Less	
830	Reserve for bad debts	190
$—		$—

3. ASSOCIATED CORPORATIONS

The Society is currently planning a joint venture with the Linnean Society for the establishment of a Science Centre for New South Wales and to facilitate this a company, Science House Pty. Limited, has been formed in which each Society has a 50% interest.

Advances and loans to the company have been made for an indefinite period on an interest free basis. No terms of repayment have been arranged. No material repayments are anticipated prior to 28th February 1976.

1974 $		
$424,490	Total amount advanced	$421,990
	Representing:	
424,490	Resumption reserve	416,990
—	Library fund	5,000
$424,490		$421,990

4. FIXED ASSETS

The basis adopted for the valuation of fixed assets is:

Furniture and office equipment	- cost less depreciation
Lantern	- cost less depreciation
Library	- 1936 valuation
Pictures	- cost less depreciation

5. INVESTMENTS

1974 $		
9,680	General funds	29,680
12,123	Library reserve	10,478
—	Long service leave fund	806
$21,803		$40,964

6. TRUST FUNDS

	Clarke Memorial	Walter Burfitt Prize	Liversidge Bequest	Olle Bequest
Capital	$3,600	$2,000	$1,400	$—
Revenue				
Income for period	249	139	97	122
Less				
Expenditure	—	168	18	60
	249	(29)	79	62
Balance from 1974	810	800	370	1,056
	$1,059	$ 771	$ 449	$1,117

DETAILED INCOME & EXPENDITURE ACCOUNT FOR YEAR ENDED 28TH FEBRUARY, 1975

1974 $		$	$
	INCOME		
3,440	Membership subscriptions - ordinary		3,551
9	- life members		6
159	Application fees		135
3,608			3,692
1,794	Subscriptions to journals		1,325
1,750	Government subsidy		1,750
7,152	Total membership & journal income		6,767
3,370	Science house management - share of surplus		—
3,334	Interest on general investments		5,872
254	Sale of reprints		—
2,818	Sale of back numbers		4,723
1,602	Sale of "Sydney Opera House Commemorative Issue"		449
—	Sale of centenary volume		129
—	Sale of subject index		15
23	Donations - general		6
—	- printing subject index		500
6	Summer school surplus		97
18,559	TOTAL INCOME		18,558
	Less		
	EXPENDITURE		
500	Accountancy		750
500	Advertising		95
103	Annual social		518
110	Audit		110
—	Branches of the society		46
154	Cleaning		167
164	Depreciation		199
76	Electricity		121
81	Entertaining		48
144	Insurance		163
83	Legal expenses		—
315	Library purchases		315
—	Sale of reprints		73
—	Library recataloguing		1,058
76	Miscellaneous		261
343	Postages & telegrams		427
	Printing - Vol 106, Parts 1 - 2 "Sydney Opera House Commemorative Issue"	640	
	- Vol 106, Parts 3 - 4	1,432	
	- Vol 10[illegible], Parts 1 - 4	5,344	
	- Subject index	1,087	
	- Binding	125	
	- Postages	699	
6,032			9,327
617	Printing, general & stationery		861
6,406	Rent		5,058
12[illegible]	Repairs		150
6,749	Salaries and superannuation		9,310
338	Telephone		454
23,600	TOTAL EXPENDITURE		29,511
$([illegible],041)	NET SURPLUS (DEFICIT) FOR YEAR		$(10,953)

Members of the Society, April, 1975

A list of members of the Society to April, 1974 is included in Volume 107. During the year ended 31st March, 1975 the following elections were made to the Society by Council.

Honorary Membership

Bullen, Keith Edward, D.Sc., F.R.S., F.A.A., Emeritus Professor of Applied Mathematics, University of Sydney, 2000 (1946 : P3).

Le Fevre, Raymond James Wood, D.Sc., F.R.S., F.A.A., Emeritus Professor of Chemistry : 6 Aubrey Road, Northbridge, 2063 (1947 : P4 : President, 1961).

Life Membership

Ida Alison Browne, William Millership and Kathleen Margaret Sherrard were granted life membership.

The following were elected Members of the Society :

Barry, Jerard Michael, B.Sc., Australian Atomic Energy Commission, p.r., 209 Botany Street, Kingsford, N.S.W. 2032 (1974).

Baynes, Peter Bruce, B.A. (Hons.), International House, P.O. Box 1799, Wollongong, N.S.W. 2500 (1974).

Baynes, Rosalind, International House, P.O. Box 1799, Wollongong, N.S.W. 2500 (1974).

Bowen, Betty Brunsdon, B.A., Dip.Ed., 12 Crown Street, Harris Park, Parramatta, N.S.W. 2150 (1974).

Broinowski, Stefan Morrell, 20 Thornton Street, Darling Point, N.S.W. 2027 (1974).

Chisholm, John Morrison, B.Sc. (Hons.), 4 Margaret Place, Lane Cove, N.S.W. 2066 (1974).

Chowdhury, Nazmul Karim, B.Sc., 5/170 Nelson Street, Annandale, N.S.W. 2038 (1974).

Clark, Betty, 7 Clarence Street, Bankstown, N.S.W. 2200 (1974).

Coles, Bernard Anthony, B.A. LL.B. (Sydney), 113 Norfolk Road, Epping, N.S.W. 2121 (1974).

Coppell, William George, M.A. (Hons.), Ph.D., Adv.Dip. Tchg., 12 Lynwood Close, Pennant Hills, N.S.W. 2120 (1974).

Dolanski, Joseph, B.Sc., c/- Mining Museum, 36 George Street, Sydney, N.S.W. 2000 (1974).

Donnelly, Dorothy May, B.A. (Sydney), Dip.Lib. (Univ. N.S.W.), 10 Oak Street, Ashfield, N.S.W. 2131 (1974).

Downes, Peter Michael, 8 Lavoni Street, Mosman, N.S.W. 2088 (1974).

Duffy, Kevin William, 5a Glendale Road, Turramurra, N.S.W. 2074 (1974).

Edwards, Robert John, B.Sc., Grad.Dip., 2/20 Redall Street, Manly, N.S.W. 2095 (1974).

Emery, Hilary Mary Myvanwy, B.Sc., 234 Bay Terrace, Wynnum, Q'ld. 4178 (1974).

Esplin, Trevor Thomas, 5 Waverton Avenue, Waverton, N.S.W. 2060 (1974).

Hampton, Alan Stacey, A.R.I.B.A., 39 Jindabyne Street, French's Forest, N.S.W. 2086 (1974).

Hockley, John James, B.Sc. (Hons.), Ph.D., Dip.Ed., 244 Ware Street, Fairfield, N.S.W. 2165 (1974) (P : 1).

Jenkins, Christopher James, B.Sc. (Hons.), Blundell Court, Sidney Sussex College, Cambridge, England (1974).

Jez, Joseph, F.R.A.I.A., A.R.I.B.A., Suite 6–19/21 Forsyth Street, Glebe, N.S.W., 2037 (1974).

King, Harold Marflet, 20 Beaumont Road, Killara, N.S.W. 2071 (1974).

Lowe, Stephen Paul, B.Sc. (Hons.), 14 Wattle Avenue, Macquarie Fields, N.S.W. 2564 (1974).

Loxton, John Harold, B.Sc. (Hons.), M.Sc. (Melb.), Ph.D. (Cantab.), School of Mathematics, University of New South Wales, P.O. Box 1, Kensington, N.S.W. 2033 (1974).

Lyons, Michael Thomas, Dip.Tech. (Sci.) (N.S.W.I.T.), M.Chem. (Univ. N.S.W.), 677 Kingsway, Gymea, N.S.W. 2227 (1974) (P : 1).

McGillivray, Allan James George, J.P., A.I.A.P., 28 McMahon Street, Willoughby, N.S.W. (1974).

McLean, Ross Alastair, B.Sc., Ph.D., Institute of Sedimentary and Petroleum Geology, Geological Survey of Canada, 3303–33rd Street, N.W., Calgary, Alberta, Canada (1974) (P : 1).

Malcolm, Harvey Donald Robert, M.Sc. (Syd.), Ph.D. (Macq.), 61 Union Street, North Sydney, N.S.W. 2060 (1974).

Post, Wendy Louise, 41 Reina Street, North Bondi, 2026 (1974).

Reid, Donald Anthony, Richmond Street, Woodenbong, N.S.W. 2476 (1974).

Rickwood, Peter Cyril, B.Sc., (Hons.) (London), Ph.D. (Cape Town), A.R.I.C., F.G.S., School of Applied Geology, University of New South Wales, P.O. Box 1, Kensington, N.S.W. 2033 (1974).

Talbot, William Reginald, 8 Paradise Avenue, Roseville, N.S.W. 2069 (1974).

Thirsk, Olive Ruth, Dip.Arch. (The Polytechnic), A.R.I.B.A., A.R.A.I.A., 6 The Grosvenor, 3 Wyuna Road, Point Piper, N.S.W., 2027 (1974).

Wasson, Robert James, B.A. (Hons.), 17 Greendale Street, Greenwich, N.S.W. 2065 (1974).

The following resignations were received :

John Percival Brown
Gilbert James Butland,
Charles Alexander Menzies Gray
Allan MacColl
Charles Edward Marshall
Peter Joseph O'Halloran
Alex Reichel
George Seddon
Robert William Upfold

The following names were written off under Rule XVIII :

Bruce Ian Cruikshank
Robert Henry Goodwin
Ernest Kokot
Daryl John McCarthy
Morris Behan McCullagh
Peitro Majstrenko
Patrick Arthur Price
Harold Walter Read
Jill Mina Rhodes
Stanley Arthur South
Stephen Sydney Sampson
Ann Ruth Smith
Glennie Forbes Smith
Eric Leslie Stevens
Frances Wheelhouse

Associate Membership

The following were elected to Associate Membership by the Council :

Anderson, Christopher William, P.O. Box 30, Chatswood, N.S.W. 2067 (1974).
Baggs, Allison Joan, 4 De Villiers Avenue, Chatswood, N.S.W. 2067 (1974).
Benson, James Montgomery, 27 Junction Road, Wahroonga, N.S.W. 2076 (1974).
Black, Lesley Faye, 39 Cummins Street, Broken Hill, N.S.W. 2880 (1974).
Caracciolo de Vietri, Maximilian Francesco, 181 Carrington Road, Coogee, N.S.W. 2034 (1974).
Cartmill, John Andrew, 15 Glendower Avenue, Eastwood, N.S.W. 2122 (1974).
Ferrero, Edward, 56 Arterial Road, St. Ives, N.S.W. 2075 (1974).
Hudson, Robert Alan, 36 The Esplanade, Sylvania, N.S.W. 2224 (1974).
Humphries, David, 183 Bath Road, Kirrawee, N.S.W. 2232 (1974).
Johnson, Brian David, B.A. (Hons.), 139 Adderton Road, Carlingford, N.S.W. 2118 (1974).
Johnston, Michael, 87 Sherwood Street, Revesby, N.S.W. 2212.
Lindley, Ian David, South Oxley, Gilmore, N.S.W. 2697 (1974).
King, Thelma, 20 Beaumont Road, Killara, N.S.W. 2071 (1974).
McCaul, Kenneth Bruce, 16 Challis Avenue, Dulwich Hill, N.S.W. 2203 (1974).
McCulloch, Ian, 537 Willarong Road, Caringbah, N.S.W. 2229 (1974).
Molloy, Peter David, B.A., 16 Merriwa Street, Gordon, N.S.W. 2072 (1974).
Mory, Arthur John, Box 3930 Falls Road, Somersby, N.S.W. 2250 (1974).
Murch, Ria Mavis, 109 Palmgrove Road, Avalon Beach, N.S.W. 2107 (1974).
Perry, Andrew Graham, 10 Calga Avenue, Roseville Chase, N.S.W. 2069 (1974).
Pitt, Michael Charles, 51a Clanville Road, Roseville, N.S.W. 2069 (1974).
Porritt, Patricia May, 23 Rothwell Road, Turramurra, N.S.W. 2074 (1974).
Rose, John Graham, 302 Alfred Street, Cromer, N.S.W. 2099.
Sebel, Aliza Joy, 5 Iluka Road, Clifton Gardens, N.S.W. 2088 (1974).
Symon, Julian, 10 Weonga Road, Dover Heights, N.S.W. 2030 (1974).
Wallis, Helen Nancy, 16 Linkmead Avenue, Clontarf, N.S.W. 2093 (1974).

The following resignation was received from Associate Membership :

Ada M. Brown.

Hilary Mary Myvanwy Emery transferred to Membership and Joseph Moldavan was written off under Rule 56.

Obituary

Joseph James FALLON (1949) (Deceased 26.4.71).
Russell GRIFFIN (1952).
William John KIRCHNER (1920).
Daniel George MOYE (1944).
John Henry PRIESTLEY (1961).

Section of Geology

Meetings and Lectures

Location : Small Hall, Science House.

19th April, 1974 : Office Bearers for 1974/75 were elected :
Chairman : Mr. J. M. Chisholm
Honorary Secretary : Miss W. L. Post
Address : THE MOUNT MORGAN MINE (QUEENSLAND) : A " COMPLETE " ORE DEPOSIT—Associate Professor L. J. Lawrence

21st June, 1974 : *Address :* THE MICRO-STRUCTURE OF OPALS—R. A. Ball and A. S. Mallin

Location : School of Applied Geology, University of New South Wales.

22nd August, 1974 : *Address:* THE EXPERIMENTAL DEVELOPMENT OF A SULPHUR ISOTOPE GEO-THERMOMETER—Mrs. Suzanne Doolan

Location : School of Earth Sciences, Macquarie University.

25th October, 1974 : *Address :* SEVEN GEOLOGICAL PARADOXES FROM THE RED SEA REGION—Dr. Lloyd Hamilton

Location : Small Hall, Science House.

21st March, 1975 : *Address :* BOUGAINVILLE : AN INTEGRATED REVIEW—Mr. R. A. Creelman

A total of 67 members and visitors attended these meetings. The Council decided at its meeting on 29th February, 1975 that the activities of the Section should be suspended until further notice.

INDEX

AUSTRALASIAN MEDICAL PUBLISHING CO. LTD.
71-79 ARUNDEL ST., GLEBE, N.S.W., 2037
1975

THE ROYAL SOCIETY OF NEW SOUTH WALES

The Society originated in the year 1821 as the Philosophical Society of Australasia. Its main function is the promotion of Science through the following activities: Publication of results of scientific investigation through its Journal and Proceedings; the Library; award of Prizes and Medals; liaison with other Scientific Societies; Monthly Meetings; and Summer Schools. Special meetings are held for the Pollock Memorial Lecture in Physics and Mathematics, the Liversidge Research Lecture in Chemistry, and the Clarke Memorial Lecture in Geology.

Membership is open to any interested person whose application is acceptable to the Society. The application must be supported by two members of the Society, to one of whom the applicant must be personally known.

Membership categories are:

Full members: $15 p.a. plus $3 application fee.

Associate members (spouses and persons under the age of 25 years): $5 per annum plus $1 application fee or $8.50 p.a. to receive the Journal plus $1 application fee.

Absentee members: $10.50 p.a. plus $3 application fee.

Subscription to the Journal, which is published in four Parts per year, for non-members is $A17 p.a. plus postage (and bank charges for overseas subscriptions).

For application forms for membership and enquiries *re* subscriptions, enquire from

The Executive Secretary,
The Royal Society of New South Wales,
Science House,
157 Gloucester Street,
Sydney, 2000, N.S.W.

The Society welcomes manuscripts of research (and occasional review articles) in all branches of science, art, literature and philosophy, for publication in the Journal and Proceedings.

Manuscripts will be accepted from both members and non-members, though those from the latter should be communicated through a member. Manuscripts should be sent to the Honorary Editorial Secretary at the above address.

THE ROYAL SOCIETY OF NEW SOUTH WALES SYDNEY
FOUN. 1821. INC. 1881

Contents

Chemistry :

Geology :

Palaeontology :

Plant Physiology :

AUSTRALASIAN MEDICAL PUBLISHING CO. LTD.
71-79 ARUNDEL ST., GLEBE, N.S.W., 2037
1975